Small molecule activation by ruthenium phosphine and N-heterocyclic carbene complexes

Jazzar, Rodolphe

Award date:
2003

Awarding institution:
University of Bath

Small molecule activation by ruthenium phosphine and N-heterocyclic carbene complexes.

Submitted by Rodolphe Fouad René Jazzar

For the degree of PhD

of the University of Bath

2003

COPYRIGHT

Signed.....

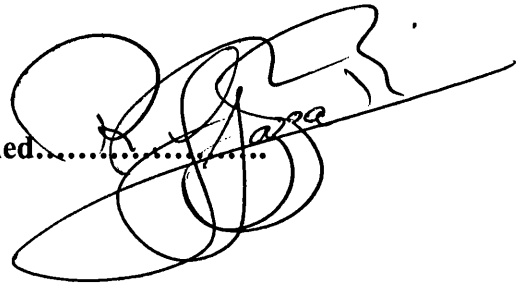

ProQuest LLC
789 East Eisenhower Parkway
P.O. Box 1346
Ann Arbor, MI 48106-1346

"(To a student)
Dear Miss ---

I have read about sixteen pages of your manuscript ... I suffered exactly the same treatment at the hands of my teachers who disliked me for my independence and passed over me when they wanted assistants ... keep your manuscript for your sons and daughters, in order that they may derive consolation from it and not give a damn for what their teachers tell them or think of them. ... There is too much education altogether."

Einstein, Albert
(1879-1955)

Acknowledgements

I would like to thank my supervisor Dr Mike Whittlesey for his support and his encouragement during these last three years. It was a real pleasure to work under the supervision of such a dedicated and motivated scientist.

I would like to thank particularly Dr Stuart Macgregor from Heriot-Watt University for all the computational studies which are reported in this thesis and for those which are still currently ongoing. Also Dr. Mary Mahon for her help and support in running and solving the X-ray structures reported here, as well as all the inorganic section staff for their help and support in various problems I encountered throughout these last three years.

Special thanks go to Dr M. Hargreaves and M. Varrone for their help, support and more importantly their friendship all throughout these last years and hopefully for the years to come.

Many thanks to: S. Richards and M. Edwards for their work and dedication in collaborative research projects.

S. Douglas and B. Paine who are currently working on the follow up of this project for being enjoyable people to work with, to J. Goicoechea for hours of agreeable music taste and to Dr S. Kirkham for interesting NMR discussions. Also to the project students I had the opportunity to supervise in the lab: P. Bhatia, M. Chilvers, and S. Chatwin who taught me how hard and rewarding it can be to teach and to supervise.

Finally it is hard to go through three years of research without the support of friends and relatives. So I would like to thank them all, but as it is impossible to name them all, I will just name a few. All the members of my family (Rudolf, Claudine, Jean-Michel, Audrey et Cristelle) who although far away remained part of my day to day life and to:

K. Grezil	V. Piccio	L. Bosch	S. Saman.	C. Papageorgiou
S. Ferrer	L. Borello	A. Speck	A. Rifat	L. Apostolico
M. Lunn	N. Patmore	S. Ushiroda	D. Robinson	and so on....

And as all that would not have been possible without funding, EPSRC is gratefully thanked. Finally, acknowledgment is made to Johnson Matthey plc for their kind loan of ruthenium starting materials.

Small molecule activation by ruthenium phosphine and N-heterocyclic carbene complexes.

Rodolphe Fouad René Jazzar

Abstract

The first part of the thesis concerns the ruthenium catalysed coupling of alkenes and aromatic ketones (Murai reaction). High-temperature in-situ IR spectroscopy has been used to study the mechanism of this reaction which is catalysed by $Ru(PPh_3)_3(CO)H_2$. An inverse dependence of formation of the coupled alkene-ketone product is observed upon varying the concentration of CH_2=$CHSi(OEt)_3$, although a linear dependence is found with CH_2=$CHSiR_3$ (R = Me, Ph). An unexpected humped dependence is seen upon changing the concentration of ketone, maximising at [ketone]:[alkene] = 2:1. Alternative catalysts for the Murai reaction have been probed. Their reactivity follows the order $Ru(PPh_3)_3$(*o*-$C_6H_4C(O)CH_3$)H > $Ru(PPh_3)_3(CO)(C_2H_4)$ >> $Ru(PPh_3)_2(CO)$(*o*-$C_6H_4C(O)CH_3$)H. Two related ortho-metallated catalysts have also been prepared; their reactivity shows the importance of the stereochemistry of the substituents.

The second part of the thesis concerns the reactivity of a range of ruthenium N-heterocyclic carbene (NHC) complexes. Thermolysis of $Ru(PPh_3)_3(CO)H_2$ with 1,3-bis(2,4,6-trimethylphenyl)imidazolin-2-ylidene (IMes) leads to unprecedented C-C activation of an sp^2-sp^3 hybridised C-C bond of the carbene. C-H activation has also been observed under milder conditions. The mechanisms of these reactions have been probed by deuterium labelling studies, DFT calculations and use of alternative P/As precursors. Reaction of $Ru(AsPh_3)_3(CO)H_2$ with IMes affords $Ru(IMes)_2(CO)(S)H_2$ (S = EtOH, H_2O) upon attempted crystallisation. These two compounds act as precursors for a range of bis NHC ruthenium compounds with Ru-OH, Ru-SH, Ru-SR, Ru-OCOR, Ru-FH and Ru-ClH linkages. Many of these compounds have been crystallographically characterised.

Abbreviations

PPh_3	Triphenyl phosphine
PCy_3	Tricyclohexyl phosphine
PMe_3	Trimethyl phosphine
$P(C_6F_5)_3$	Tripentafluorobenzene phosphine
$P(OPh)_3$	Triphenyl phosphite
dppe	1,2-bis(diphenylphosphino)ethane
dppp	1,2-bis(diphenylphosphino)propane
dmpe	1,2-bis(dimethylphosphino)ethane
$AsPh_3$	Triphenyl arsine
Arphos	1-diphenylarsino-2-diphenylphosphinoethane
Ph	Phenyl
Cp	Cyclopentadienyl
Cp^*	Pentamethylcyclopentadienyl
COD	cyclooctadiene
NHC	N-heterocyclic carbene
IAd	1,3-bis(1-adamantyl)imidazolin-2-ylidene
IPr	1,3-bis(2,6-di-isopropylphenyl)imidazolin-2-ylidene
IMes	1,3-bis(2,4,6-trimethylphenyl)imidazolin-2-ylidene
ITol	1,3-bis(4-methylphenyl)imidazolin-2-ylidene
ICy	1,3-bis(cyclohexyl)imidazolin-2-ylidene
ADMET	Acyclic Diene Metathesis
CM	Cross Metathesis
RCM	Ring Closing Metathesis
ROMP	Ring Opening Metathesis Polymerisation
TON	Turn over number
TOF	Turn over frequency
NMR	Nuclear Magnetic Resonance
δ	Chemical Shift
ppm	Parts per million
J	Coupling constant
Hz	Hertz
IR	Infra-Red
CIR	cylindrical internal reflectance
υ	Frequency
cm^{-1}	Wavenumbers
h	hours
min	minutes
mol	moles
mmol	millimoles
g	grams
mg	milligrams
mL	millilitres
μL	microlitres
Å	Angstroms

NB: ^1H NMR spectra were recorded at either 400 or 300 MHz; $^{31}P\{^1H\}$ and ^{19}F NMR spectra correspond to 121 MHz and 376 MHz respectively.

Table of Contents

Part 1.

- o -

Part 2.

- o -

Chapter 7. Experimental

- o -

Appendix

Crystallographic data (available on CD).

- o -

PART 1.

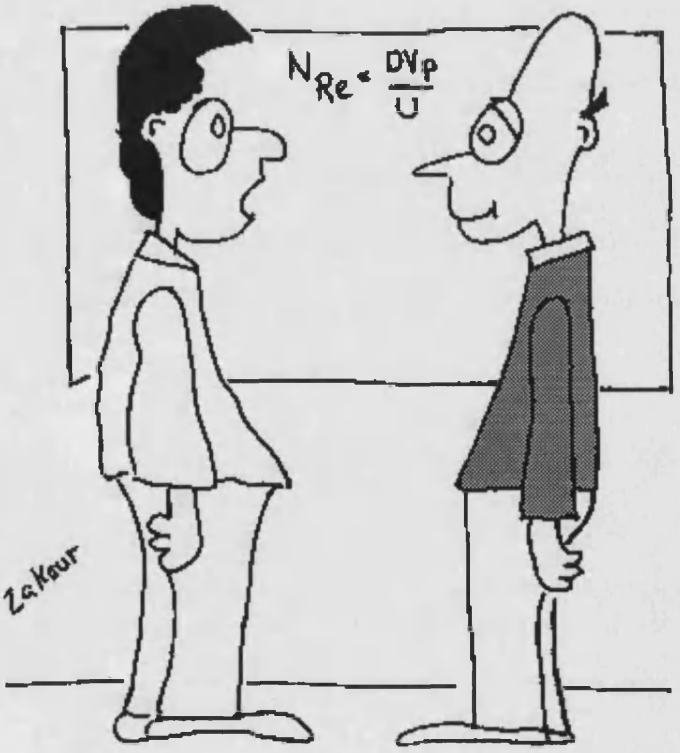

After years of extensive research, I have concluded beyond any doubt that I need more grants!

Chapter 1.

Introduction to C-H bond activation and its applications in homogeneous catalysis.

1.1. Introduction.

Homogeneous catalysis is nowadays a relatively mature field of chemistry in which numerous and diverse reactions are being explored, coupled with informative studies of mechanism and theory. In comparison to the fields of heterogeneous catalysis and biocatalysis, homogeneous catalysis has grown dramatically but remains, however, a relatively untapped resource whose importance cannot be overestimated. As industry becomes more oriented toward speciality chemicals, methods to catalyse functional group transformations, polymerisations, hydrocarbon activations and inductions of asymmetry will be increasingly in demand. Among the variety of bonds to be activated, the synthetic utility of cleaving C-H bonds has long been recognised in chemistry and selective activation of specific types of C-H bonds is by all means one of the fastest growing areas of modern chemistry due to its attractive applications in industry, medicine and research. As shown in **Figure 1.1.** a large variety of C-H bonds have been shown to be activated catalytically by transition metal complexes.[1]

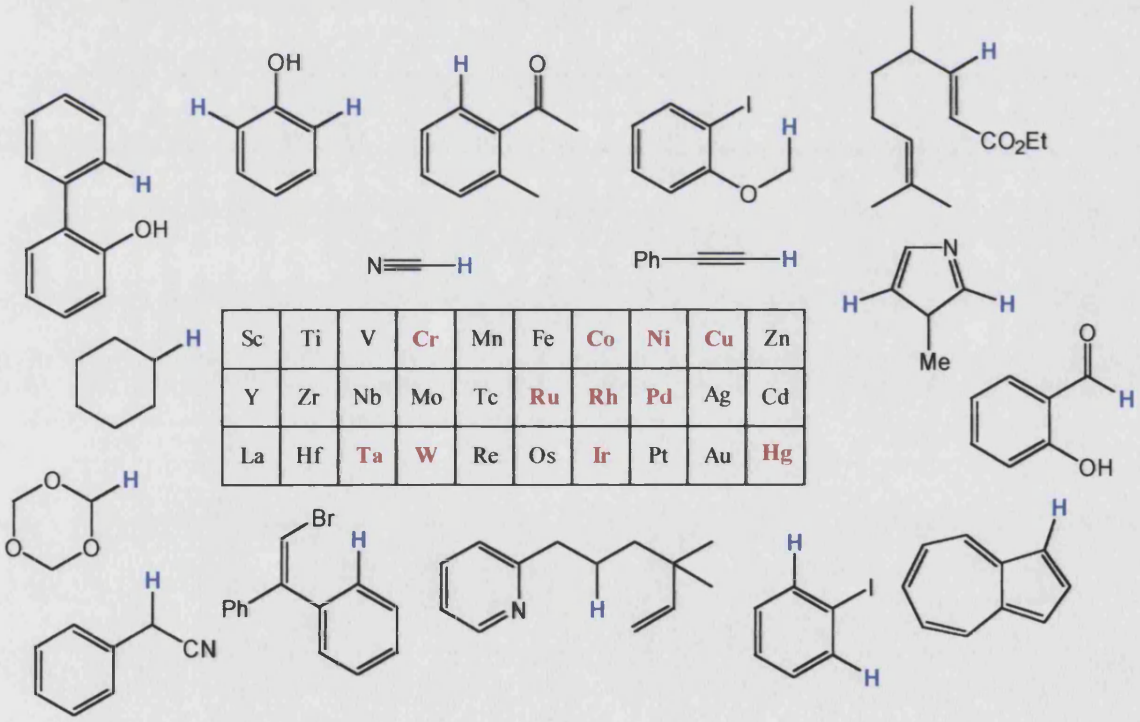

Figure 1.1. - *A diverse range of C-H activations that are catalysed by transition metal complexes.*

In this introduction, a brief overview of metal promoted C-H bond activation in homogeneous media will be described both from a stoichiometric and a catalytic point of view. It is certainly not intended to be a definitive and detailed review of the subject, as this area has been thoroughly described in major reviews and articles.[1]

1.1.1. Early examples of C-H activation.

The first metal-containing systems which were capable of activating C-H bonds including Fenton's reagent (hydroxylation) and mercury salts (direct mercuration), were discovered as early as the end of the nineteenth century. Initial pioneering work reported during the 1930s, described the electrophilic auration of arenes[2] and a radical chain auto-oxidation of hydrocarbon initiated by metal derivative.[3]

The development of this field really started in the 1960s with the discovery by Kleiman and Dubeck of C-H bond cleavage in azobenzene by a Cp_2Ni complex,[4] and was rapidly followed by C-H activation of sp^3 hybridized carbon atoms.[5] In 1969, the first activation reactions of C-H bonds in alkanes were discovered.[6] It was found that platinum(II) salts catalyse the H-D exchange between methane or its analogues and D_2O at 100°C, and that $Co(PPh_3)H_3$ induces deuteration of methane by D_2 at room temperature. Since then, extensive research efforts have been reported on the cleavage of C–H bonds by low-valent metal-complexes which have been shown to proceed via an oxidative addition mechanism to form either alkyl and aryl derivatives.[7] In contrast later development have demonstrated that high oxidation state metals proceed via formation of organometallic species.[8] Although there are fewer examples of C-H activation by high oxidation state metal complexes, the investigations of their properties really started at the end of the 1980s and has grown significantly since.[9]

1.1.2. Stoichiometric C-H activation.

1.1.2.1. C-H bond activation by transition metal complexes.

Selective functionalisation of alkanes by transition metal complexes has been a target for inorganic chemists for over 30 years and has been described as one of the 'Holy Grails' of chemistry.[10] Synthetic organic chemistry is now at such a level of sophistication that practically any target molecule may be synthesised by using a multitude of known reagents and reactions. Hydrocarbons are typically the most inexpensive and most abundant of all organic chemicals, yet saturated hydrocarbons are not readily employed in organic transformations toward the formation of more valuable products such as alcohols, ketones and acids due to their inherent lack of reactivity. It is then challenging from various points of view, to find routes from these basic materials to more commercially viable products.

C–H bond cleavage or 'activation' can be thought of as arising from weakening of the C–H σ-bond prior to rupture which can be induced by coordination with a metal centre. However, C–H bonds are extremely strong (BDE (C–H) in $CH_4 \approx 400$ kJ mol^{-1}), kinetically inert (high lying HOMO and LUMO) and non polar. Investigations of the reactions of metal complexes with hydrocarbons in homogeneous median as led to the classification of four general types of processes **[Scheme 1.1.]**. Reaction **(a)** represents the most common type of reaction, in which oxidative addition occurs at vacant coordination site on the metal centre. Reaction **(b)** show a homolytic or radical process, while the reaction **(c)** describe the reversible addition of a R-H bond to a M=X bond where X can either be heteroatom containing ligand or an alkylidene ($M=CR_2$). Finally reaction **(d)** represents the use of an electrophilic metal centre to break the R-H bond, for which two reaction pathways have been proposed, one involving a concerted mechanism via so-called σ-bond metathesis and one which proceeds via an oxidative addition pathway.

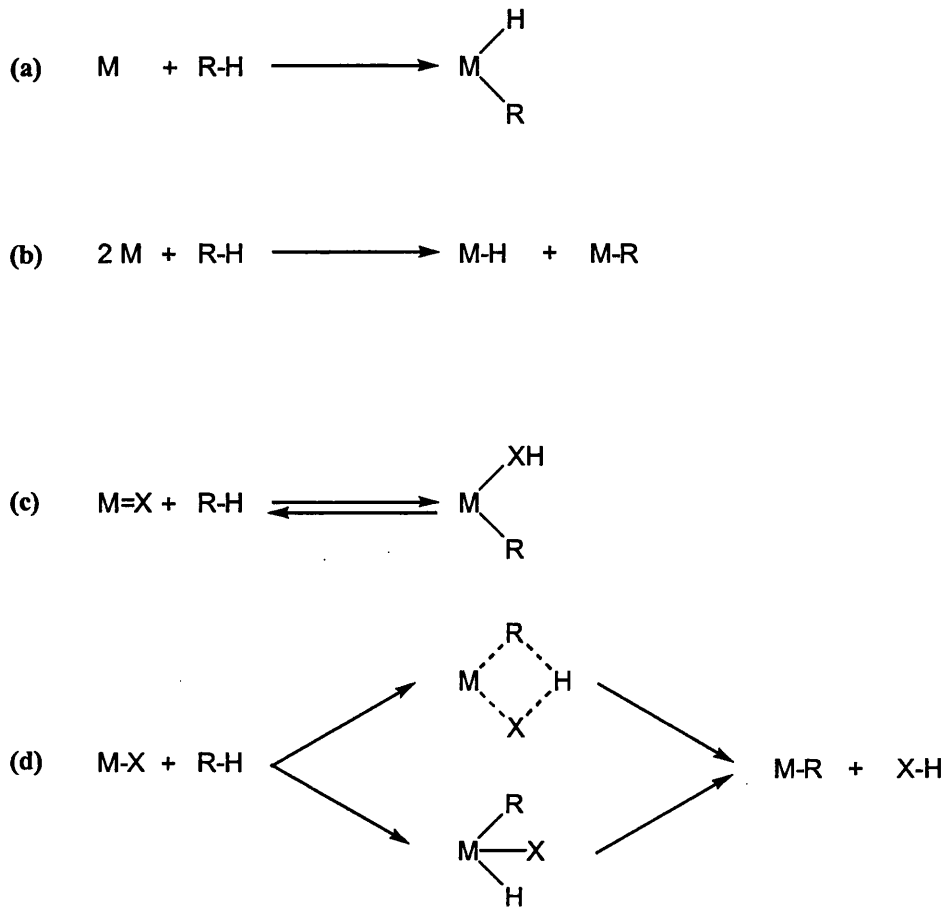

Scheme 1.1. - *Mechanisms for R-H (R = aryl, alkyl, alkenyl) activation by transition metal complexes.*

1.1.2.2. Kinetic selectivity versus thermodynamic selectivity.

Stoichiometric C-H bond activation is nowadays a relatively well studied process and a considerable number of examples have been reported in the literature in the last two decades. Due to their possible direct applications to catalysis, numerous processes have been thoroughly studied from a mechanistic, thermodynamic and kinetic point of view. Therefore several systems have been used to investigate the C-H bond activation and two types of selectivity have been considered. Kinetic selectivity, which describes the rate at which a certain type of bond reacts, and thermodynamic selectivity, which describes the energetic preference for cleavage of a particular type of bond.[1a] The main features of these distinct types of selectivity can be seen in **Figure 1.2.** which represents a diagram of the change in free energy (ΔG) as a function of the reaction of a metal fragment with two different hydrocarbons RH and R'H.

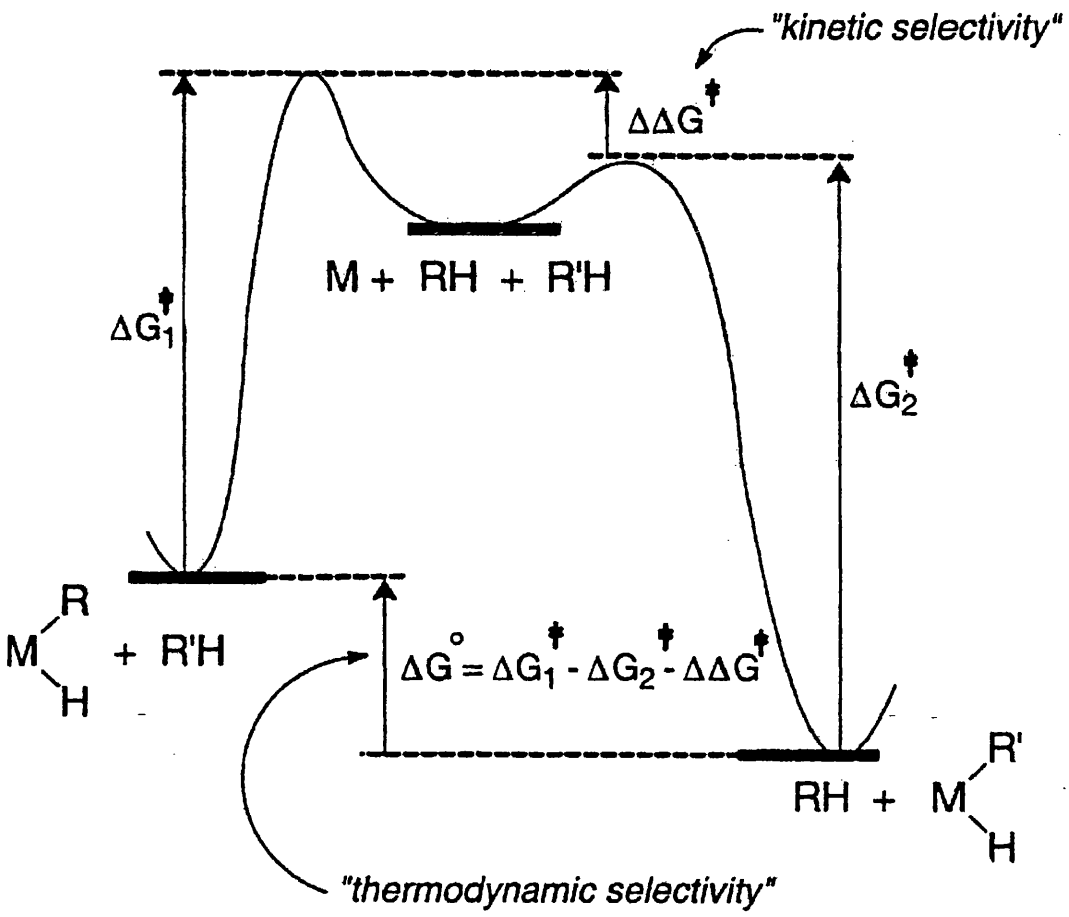

Fig. 1.2. – *Free energy diagram showing kinetic vs. thermodynamic selectivity.*[1a]

1.1.2.3. Examples of stoichiometric C-H activation.

Among all the types of C-H bonds studied, alkane C-H activation remains by far the most interesting and challenging area of research. Crabtree et al. reported the first well characterised reaction of an alkane with an homogeneous transition metal complex upon addition of cyclopentane to $[Ir(PPh_3)_2H_2]^+$ to give cyclopentadienyl-iridium.[11] In a major advance, Bergman et al. described in 1982 the direct formation of an alkylmetal species from a simple alkane **[Scheme 1.2.]**[12] upon photochemical dissociation of H_2 from (η^5-C_5Me_5)$Ir(PMe_3)H_2$ and oxidative addition of pentane to the resulting coordinatively unsaturated intermediate (η^5-C_5Me_5)$Ir(PMe_3)$.

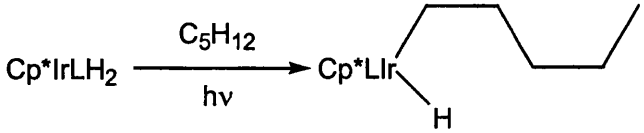

Scheme 1.2.

Stoichiometric C-H activation has been used thoroughly in the study of various catalytic reactions. One such example was demonstrated by Suggs et al., who isolated the first stable acylrhodium (III) hydride, proposed as an intermediate in the mechanism for the hydroacylation reactions [**Scheme 1.3.**].[13]

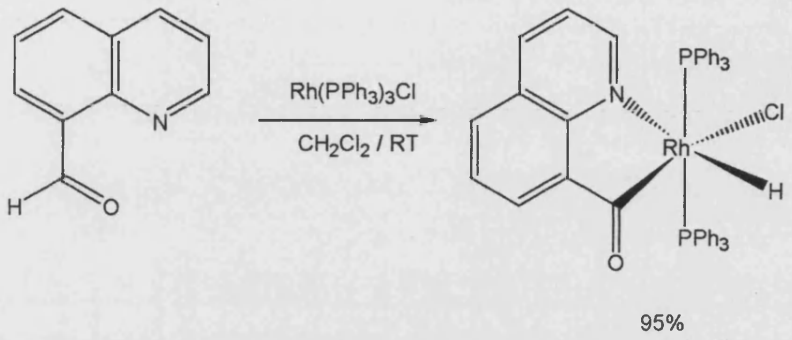

Scheme 1.3.

Very much work has been reported in the study of C-H bond activation of alkanes, and benzene by $Cp^*Ir(PMe_3)(R)H$ complexes (R = alkyl, C_6H_5) [**Scheme 1.4.**].[14] These extensive studies have uncovered the kinetic selectivity and the thermodynamic selectivity of this system, while calorimetric experiments designed to obtain the absolute Ir-C bond strength have shown the strong thermodynamic preference for benzene activation suggested by the large difference in the Ir-C_6H_5 vs. Ir-C_6H_{11} bond strengths (125 kJ mol^{-1}).

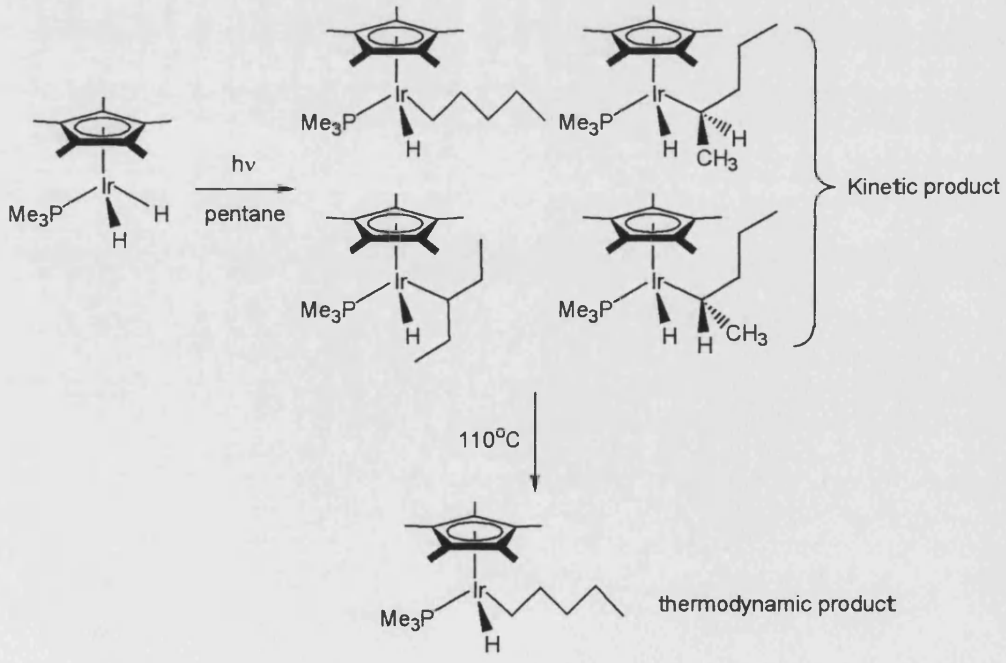

Scheme 1.4.

1.1.3. Catalytic C-H activation.

By comparison to stoichiometric C-H bond activation, transition metal-catalyzed functionalisation of C-H bonds still remains a relatively untouched field of chemistry.[15] One of the major problems to be overcome in developing catalytic C–H bond activation reactions for producing functionalised organic molecules is that the C–H bond of the product (alcohol, ketone, etc.) is likely to be more reactive than that of the starting alkane. This combined with low yields, low selectivity and poor catalyst turnover numbers have restricted synthetically useful and commercially viable examples of catalytic C–H bond activation. Nevertheless, a number of examples have been reported and some interesting research is currently being developed mainly with the intention of forming C-C bonds through direct C–H bond cleavage. These have been shown to be very promising with good selectivity and high yields of products.

1.1.3.1. Catalytic dehydrogenation of alkanes and arenes.

In 1979, Crabtree et al. reported the first example of stoichiometric dehydrogenation of alkanes using an iridium-phosphine complex.[11] Related work was then extended by Baudry and Ephritikhine into the first example of a catalytic conversion of alkanes with respect to a transition metal complex.[16] Their work showed that a rheniums polyhydride complex catalyses dehydrogenation of cycloalkanes to cycloalkenes in the presence of *tert*-butylethene, which act as a sacrificial hydrogen acceptor **[Scheme 1.5.]**. Although only 9 turnover were achieved, this result remains pioneering in the field.

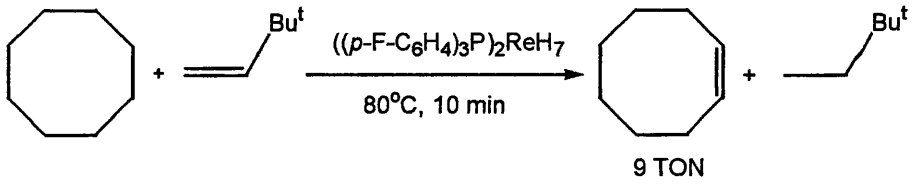

Scheme 1.5.

In 1990 a notable advance was achieved in the dehydrogenation of alkanes by Saito et al.[17] They reported the first example of efficient alkane dehydrogenation in the absence a sacrificial hydrogen acceptor under thermal conditions, using $RhCl(PPh_3)_3$ as a catalyst.

In 1997, Gupta and Goldman found a highly efficient dehydrogenation of cyclodecane to cyclodecene using an iridium PCP complex **[Scheme 1.6.]**.[18] In this case, 360 turnovers were achieved in 24 h.

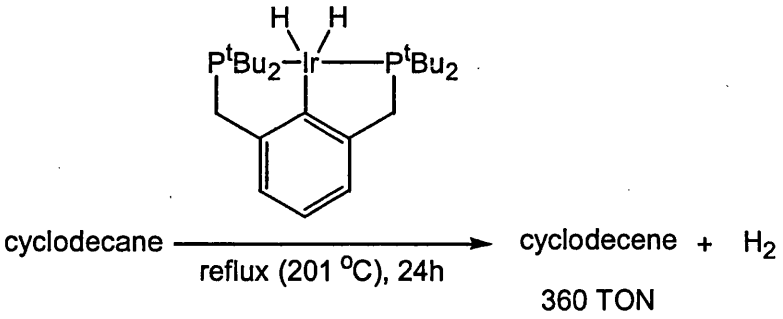

Scheme 1.6.

Catalytic dehydrogenation of alkanes and arenes has found applications in dehydrogenative silylation. Among the many examples reported,[19] Tanaka et al. have reported the platinum-catalysed *ortho* selective silylation of aromatic aldimines with hexamethyldisilane. **[Scheme 1.7.]**.[20]

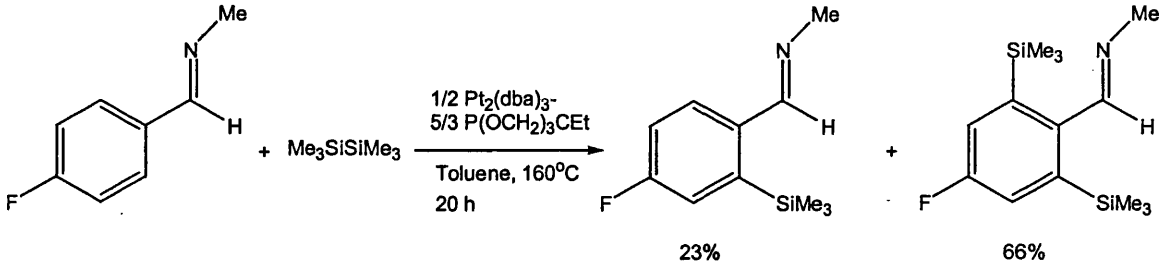

Scheme 1.7.

1.1.3.2. Catalytic hydroacylation with aldehydes.

Decarbonylation of aldehydes by $RhCl(PPh_3)_3$ is at the origin of hydroacylation,[21a] and was first observed by Sakai et al. in the intramolecular hydroacylation of enals. However, use of a stoichiometric amount of rhodium complex was required and the yield of product was low (30%).[21b] This process was improved by Miller et al., who devised catalytic methods to the cyclised ketone product **[Scheme 1.8.]**.[21c]

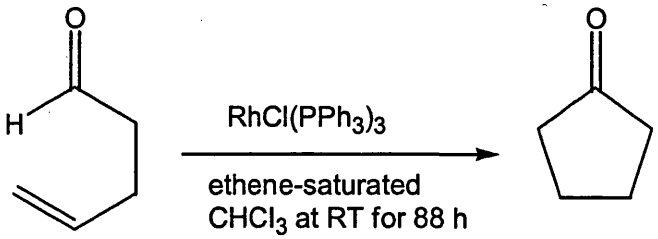

Scheme 1.8.

This process has been extended to several organic syntheses, such as the intramolecular hydroacylation of unsaturated aldehydes[22] to allow resolution of racemic enals.[23] Further work by Miller et al. described the first example of intermolecular hydroacylation of an aldehyde with an alkene giving ketones **[Scheme 1.9.]**.[24]

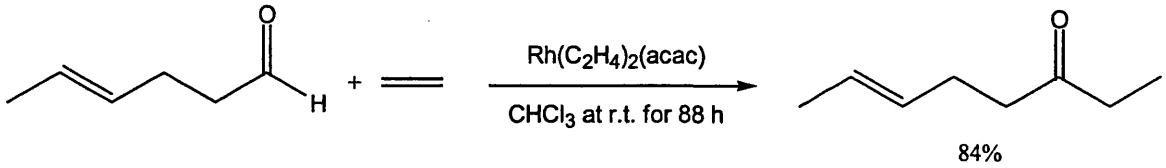

Scheme 1.9.

Extension of this process to alkyne C-H bonds affords α,β-unsaturated ketones **[Scheme 1.10.]**. Both aliphatic and aromatic alkynes are applicable to the reaction and, in the case of unsymmetrically substituted alkynes, the regioselectivity depends upon the steric bulkiness of the alkyl substituents. This was first published in 1990[25] and has since been further developed by a range of authors.[26]

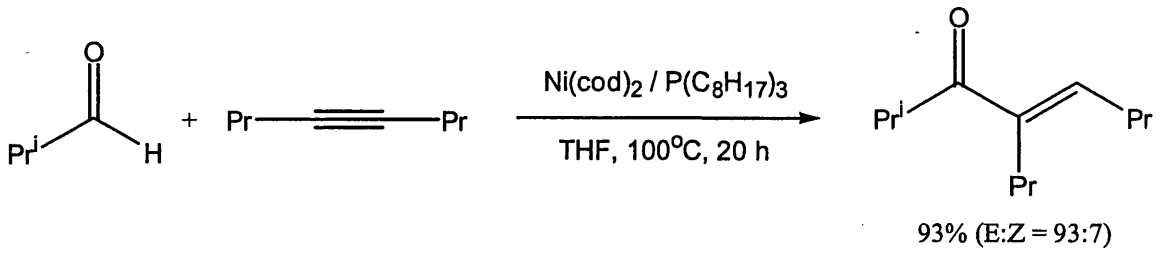

Scheme 1.10.

1.1.3.3. Michael addition and aldol reactions.

Murahashi et al. have reported the $Ru(PPh_3)_4H_2$-catalysed addition of activated nitriles to aldehydes, ketones and α,β-unsaturated carbonyl compounds **[Scheme 1.11]**.[27]

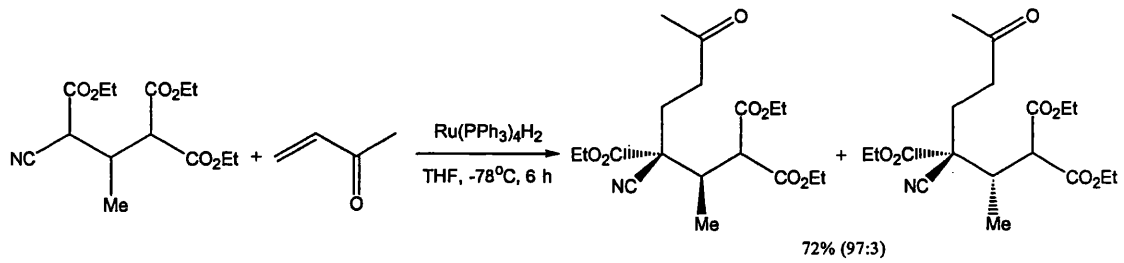

Scheme 1.11.

Ito et al. reported that the rhodium-catalysed Michael addition of α-cyano carboxylates to α,β-unsaturated carbonyl compounds can be made asymmetric **[Scheme 1.12]**.[28] This Michael reaction takes place in high chemical and optical yields even with low catalyst loading (0.1 – 1 mol%), and it was shown that the *trans*-chelating chiral bisphosphines (TRAP) are more effective than *cis*-chelating bisphosphines.

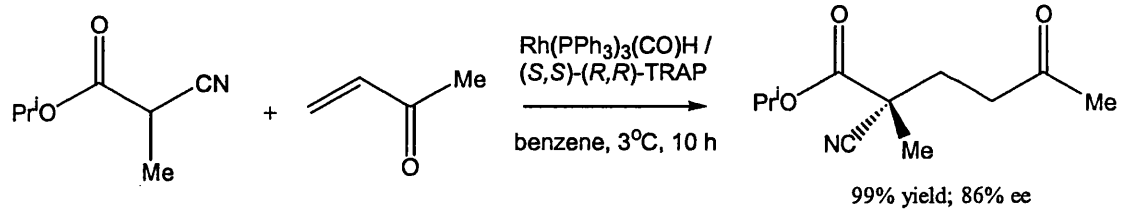

TRAP = 2,2"-bis[1-(diphenylphosphino)ethyl]-1,1"-biferrocene

Scheme 1.12.

1.1.3.4. Addition to carbon-carbon multiple bonds.

Trost et al. have reported the palladium-catalysed addition of C-H bonds in active methylene compounds to allenes **[Scheme 1.13.]**.[29] With allenes having electron-withdrawing groups (F, Cl, Br, CF_3 and OCF_3) on the phenyl substituents, addition takes place predominantly at the internal carbon atom. In contrast, terminal attack is favoured for allenes having an electron-donating group (CH_3 and OCH_3) on the methyl.

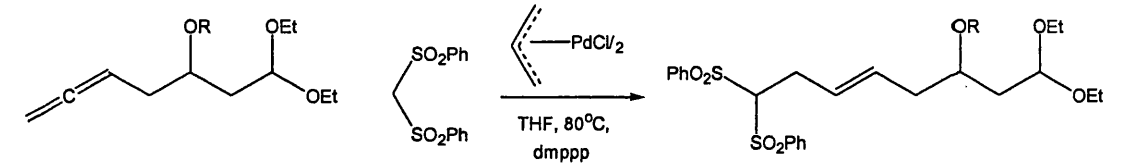

dmppp = 1,3-bis(di-(2-methoxylphenyl)-phosphino)propane

TBDPS =

R = TBDPS (Y = 64%) : E / Z = 100/0

R = H (Y =71%) : E/Z = 75/25

Scheme 1.13.

1.1.3.5 Catalytic carbon–carbon bond formation through direct C–H bond cleavage.

Catalytic carbon-carbon formation through direct cleavage of a C-H bond is of wide interest. This process has mainly been investigated via insertion of carbon monoxide and isocyanides into a C-H bond,[47] addition of a C-H bond to a carbon-carbon double bond[35] or triple bond[38] and via coupling of C-H bonds with carbon monoxide and alkenes.[31] These represent some of the few examples of interest from a synthetic viewpoint as they show interesting selectivity and efficiency.

1.1.3.5.1. Addition of C-H bonds to carbon-carbon double bonds.

Catalytic additions of carbon-hydrogen bonds to alkenes constitutes one of the most efficient and cheap ways to selectively functionalize C-H bonds. It was first reported by Yamazaki et al.[30] in 1978 who catalytically synthesised diphenylmethyl phenyl ketone in good yield from diphenylketene in the presence of $Rh_4(CO)_{12}$ under a CO atmosphere **[Scheme 1.14.]**.

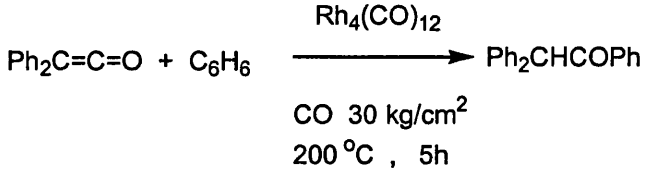

Scheme 1.14.

Later the same rhodium catalyst was also found to be effective for the synthesis of styrenes via dehydrogenative vinylation of benzene with ethene **[Scheme 1.15.]**.[31]

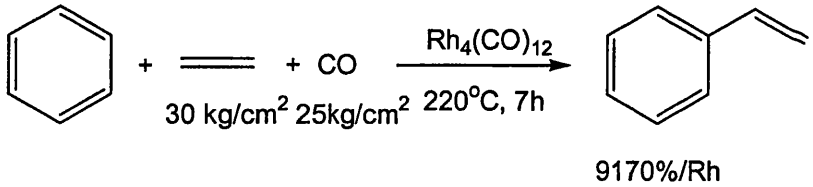

Scheme 1.15.

Addition of an sp^3 hybridised C-H bond adjacent to a nitrogen atom in dimethylamine to 1-pentene is catalysed by a tungsten amide complex to give N-methyl-N-(2-methyl-pentyl)amine **[Scheme 1.16.]**.[32]

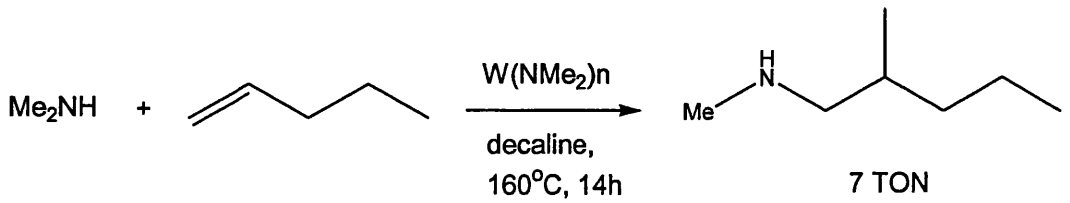

Scheme 1.16.

The α C-H bonds of ether oxygen are added to *tert*-butylethene in the presence of a catalytic amount of $Ir(P^iPr_3)_2H_5$ under mild conditions (50°C) **[Scheme 1.17.]**.[33]

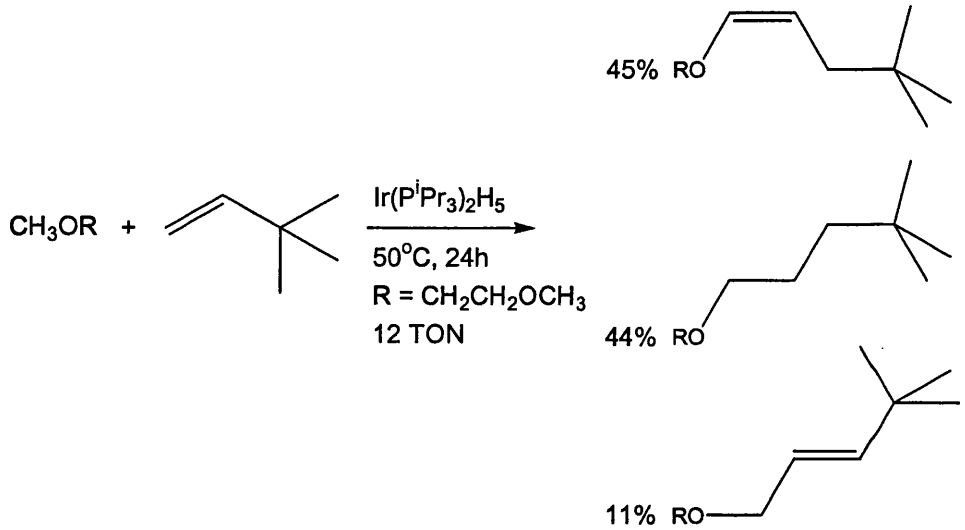

Scheme 1.17.

Heteroatom directed ethylation of the benzene ring in phenol is catalysed by ruthenium(II)-phosphite complexes. The alkylation takes place at the position *ortho* to the hydroxyl group exclusively, and the corresponding 1:2 addition product is the major product **[Scheme 1.18.]**.[34]

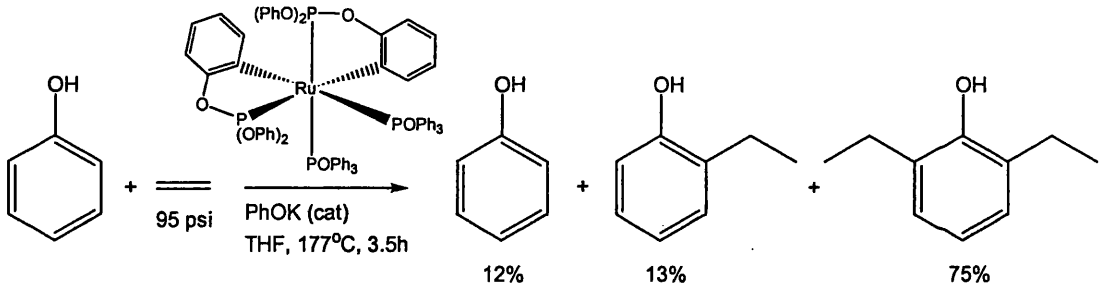

Scheme 1.18.

In 1989, the first example of catalytic asymmetric C–H/alkene coupling was reported by Jordan et al.[35] They reported the α alkylation of picoline via C–H bond

cleavage reaction with the aid of a chiral tetrahydroindenyl-zirconium complex **[Scheme 1.19.]**.

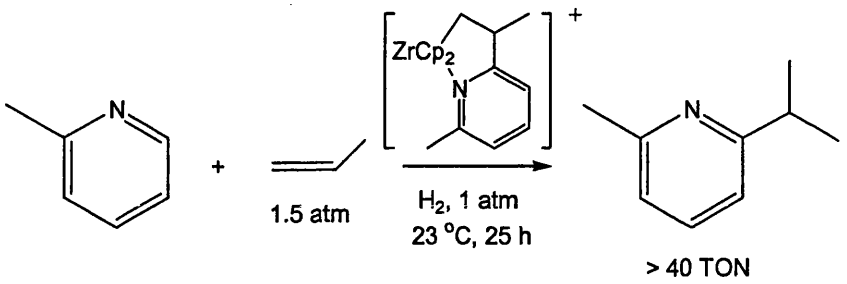

Scheme 1.19.

1.1.3.5.2. Addition of C-H bonds to carbon-carbon triple bond.

Various methods have been reported in the literature for the preparation of substituted styrenes[36,37] among which the Heck reaction remains one of the best studied methods.[37] One major drawback of this method is due to the use of halocarbons which are indispensable to the C-C bond formation.

Pioneering work by Yamazaki et al.[38] has shown the possibility of overcoming this problem by direct addition of otherwise unreactive C-H bonds, through C-H activation. Their work on the coupling of aromatics and heteroaromatics with alkynes **[Scheme 1.20.]** has shown that site selectivity is possible depending on the substituents on the aromatic ring. For example with R = CH_3, activation at the *meta* position is preferred while with R = F, reaction occurs predominantly at the *ortho* position. The authors propose that this selectivity arises from an inductive effect of the electronegative atoms.

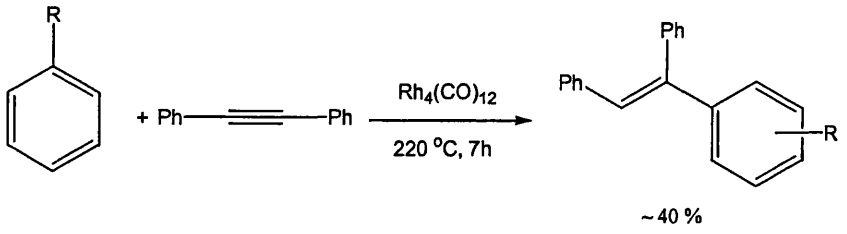

Scheme 1.20.

This work has been extended by others to allow the use of azobenzene in rhodium and cobalt catalysed reactions,[39] while it was shown that $Ru(PPh_3)_3(CO)H_2$ catalyses the *ortho*-selective addition of C-H bonds in aromatic ketones **[Scheme 1.21.]**.[40]

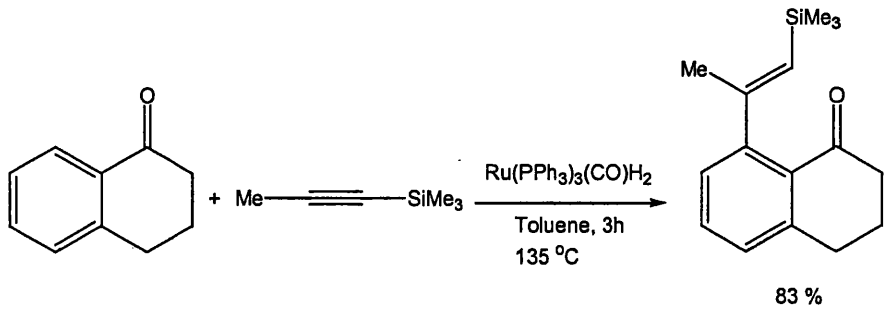

Scheme 1.21.

1.1.3.5.3. Insertion of carbon monoxide and isocyanide into the C-H bond.

Several examples of transition metal-catalysed insertions of carbon monoxide and isocyanide into C-H bonds are known. The carbonylation of a C-H bond to give aldehydes requires photochemical conditions. Eisenberg et al. have used iridium,[43] rhodium[44] and ruthenium[45] complexes to produce benzaldehyde from benzene. This method has been extended by Tanaka et al. and these authors have demonstrated that under CO, benzene reacted photochemically to afford a mixture of benzaldehyde, benzylalcohol and benzoic acid **[Scheme 1.22.]**.[46]

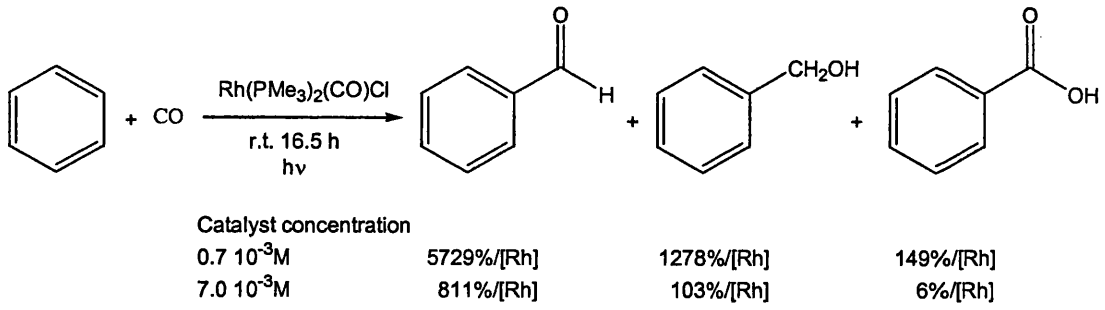

Scheme 1.22.

The isoelectronic isocyanides have generally been used as alternatives to CO. In 1986, Jones et al. reported that a low-valent ruthenium phosphine complex catalysed intramolecular insertion of an isocyanide into an sp^3 hybridised C-H bond under thermal conditions **[Scheme 1.23.]**.[47] This work represented a new route for the synthesis of indoles.

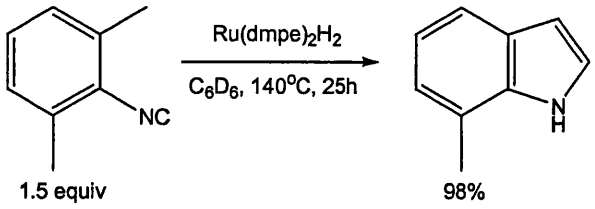

Scheme 1.23.

1.1.4. C-H bond activation in the presence of CO and alkenes.

Moore et al. reported the first example of the highly selective carbonylation of aromatic ketones with the aid of $Ru_3(CO)_{12}$ as a catalyst **[Scheme 1.24.]**.[41] This reaction affords linear pyridyl ketones with various terminal alkenes.

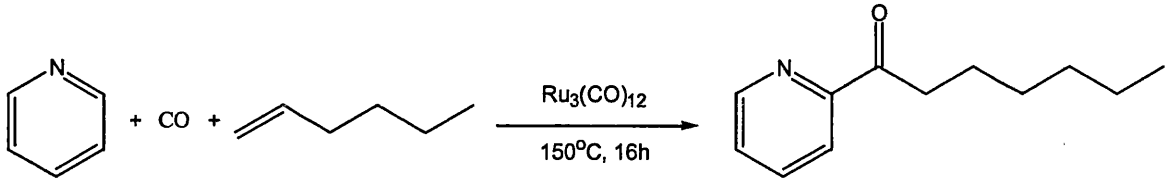

Scheme 1.24.

This reaction was thoroughly studied by Murai et al.[42f] **[Scheme 1.25.]** who considerably extended the scope of this reaction.[42a-i] In fact a large variety of *N*-heteroaromatic substrates **[Figure 1.3.]** and alkenes[42l] **[Figure 1.4.]** have been applied in this process.

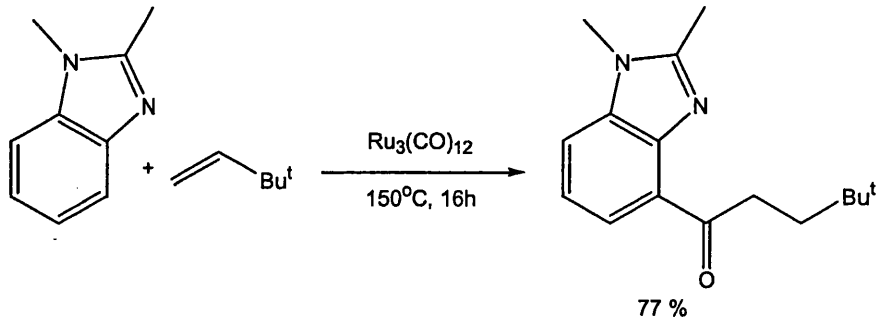

Scheme 1.25.

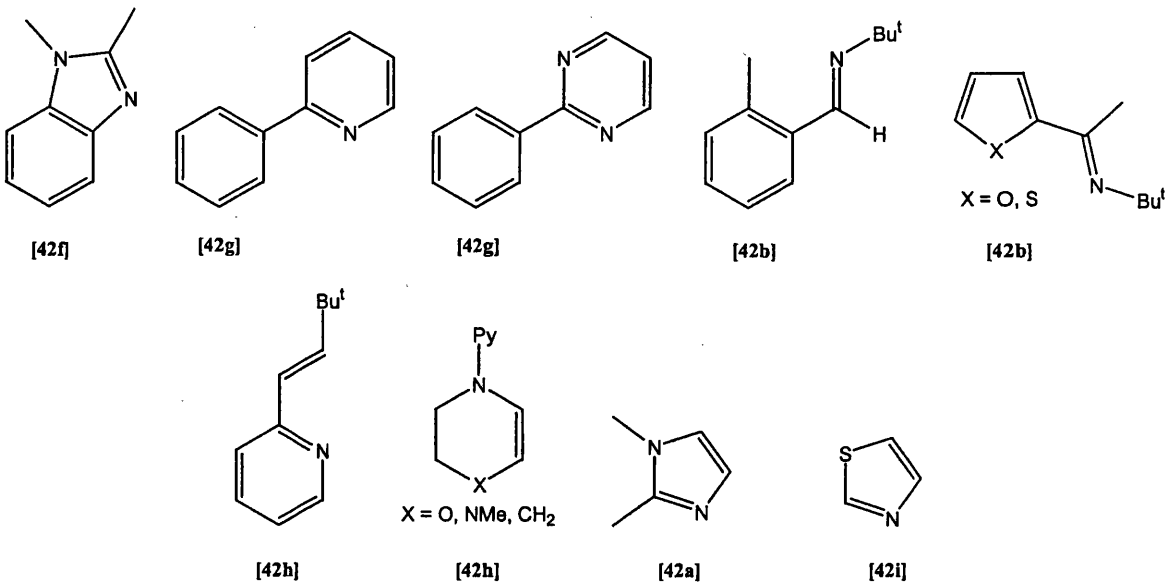

Figure 1.3.

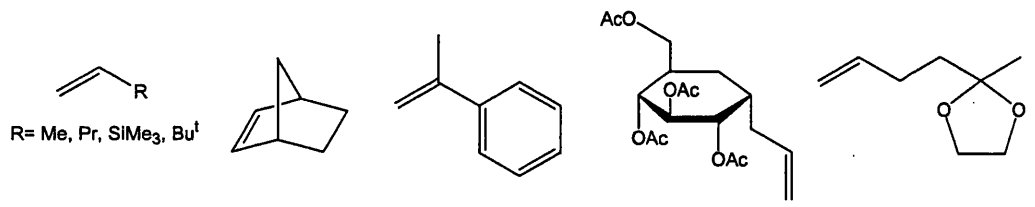

Figure 1.4.

The most recent advances in this area have been under the same reaction conditions as reported for the acylation of *N*-heteroaromatic compounds **[Scheme 1.26.]**. Ru-catalysed intramolecular cyclocoupling of ketones (or aldehydes) with alkenes (or alkynes) occurs in the presence of CO gas and leads to γ-butyrolactones.[42j] The reaction, which is best described by **Figure 1.5.**, represents the first example of the catalytic synthesis of heterocycles via an intermolecular carbonylative [2 + 2 +1] cycloaddition.

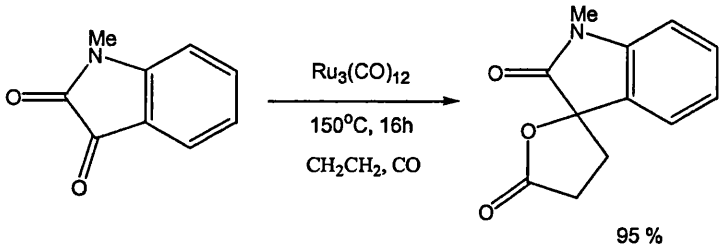

Scheme 1.26.

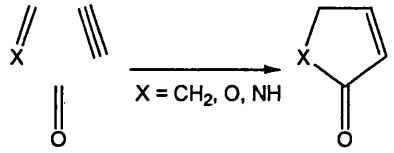

Figure 1.5.

1.1.5. Ruthenium catalysed *ortho*-C-H activation of ketone

In 1993, Murai et al.[48] reported the first highly efficient and selective example of an aromatic C–H/alkene coupling reaction. The reaction of aromatic ketones with alkenes, in the presence a ruthenium catalyst gives the corresponding *ortho* alkylated compounds in high yields, up to a quantitative yield in most cases **[Scheme 1.27.]**.

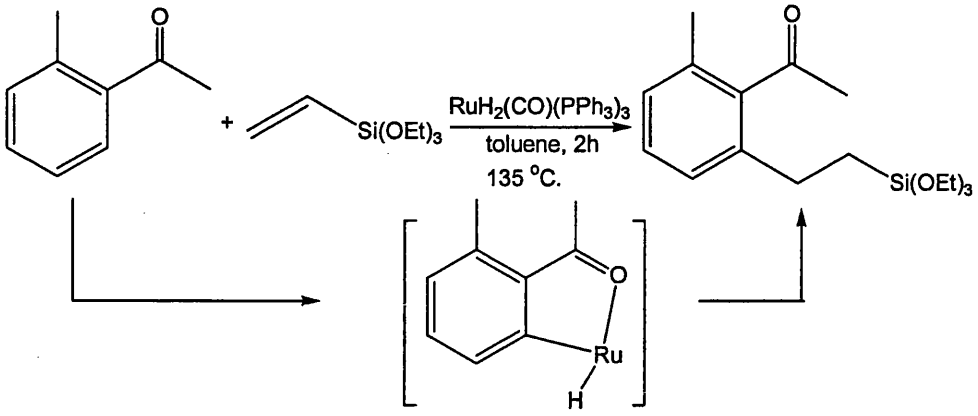

Scheme 1.27.

The C-C bond formation occurred exclusively at a position *ortho* to the ketone carbonyl group, and was proposed to involve coordination of the *ortho* carbonyl group to the ruthenium **[Scheme 1.27.]**.[49] One of the most important findings in their studies is that C-H bond cleavage is not the rate determining step as a rapid equilibrium exists prior to the reductive elimination step, leading to C-C bond formation **[Scheme 1.28.]**.

The biggest limitation to the reaction comes from the types of substituents that are present on the alkene, as electron-donating and electron withdrawing groups showed no reactivity **[Figure 1.6.]**.

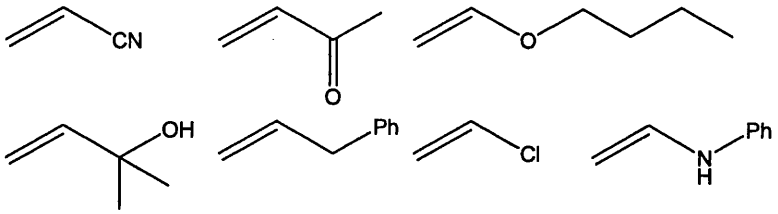

Figure 1.6. - *Alkenes that do not undergo C–H/alkenecoupling under the Murai conditions.*

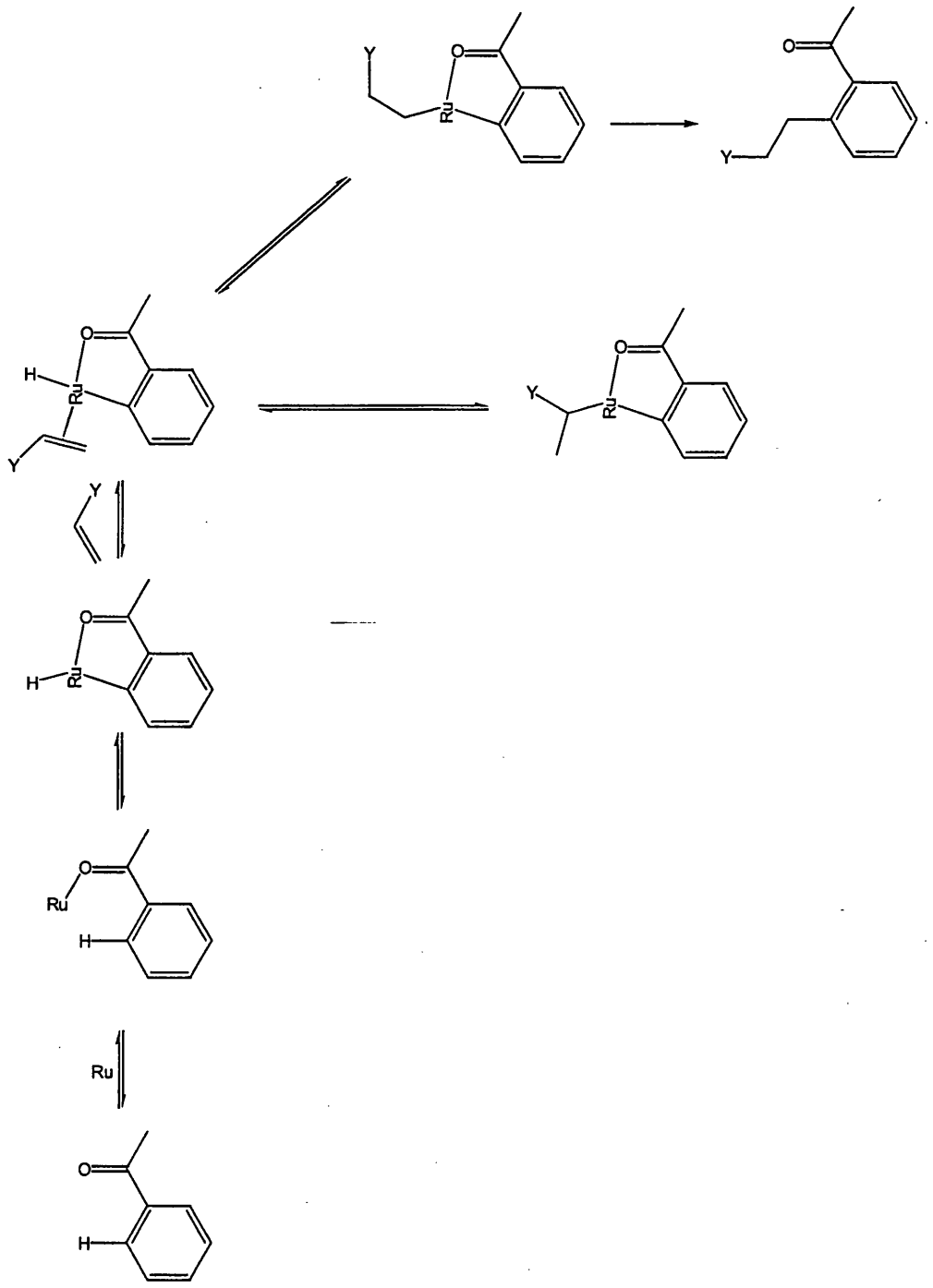

Scheme 1.28.

Functional group compatibility and the effect of substituents on the site-selection have been systematically studied in the reaction of various acetophenones.[51] Functional groups such as NMe_2, OMe, F, NEtC(O)Me, CO_2Et, and CN were found to be tolerated under the conditions of the reaction **[Figure 1.7.]**.

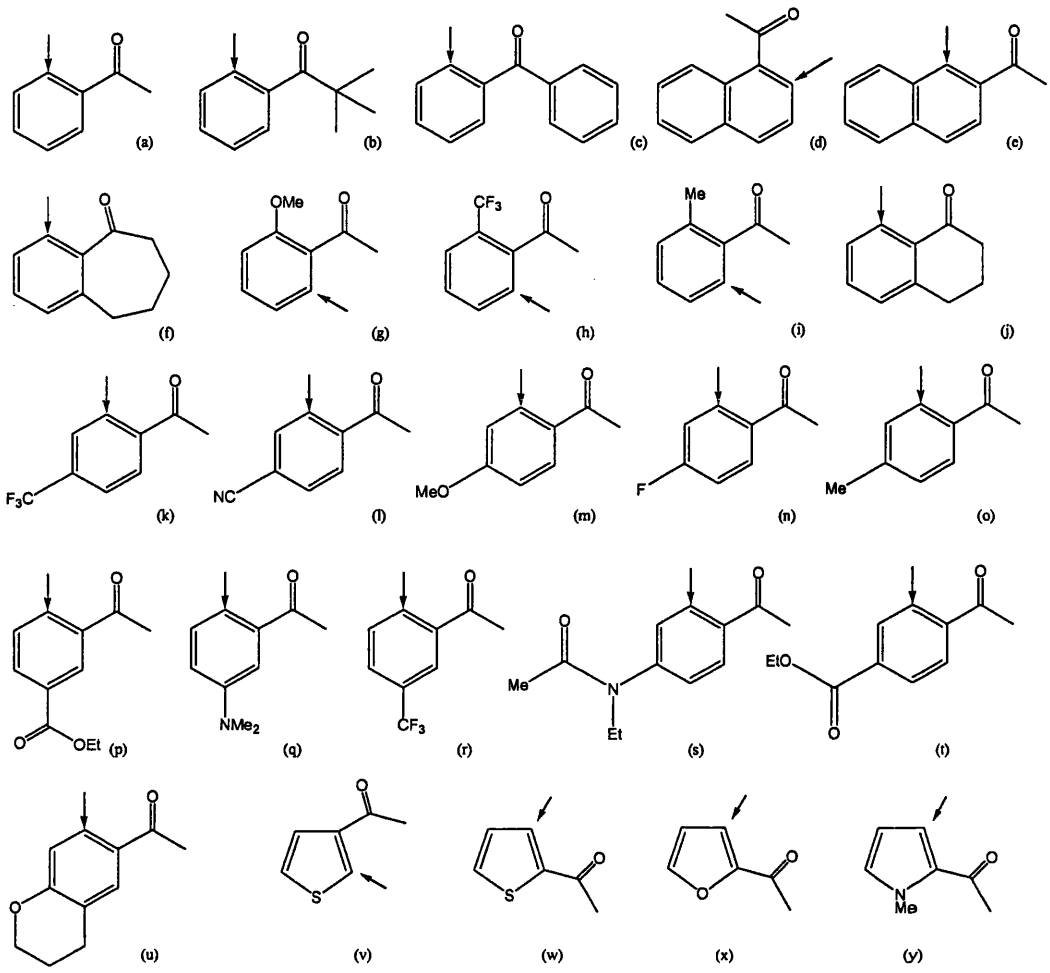

Figure 1.7. - *The variety of aromatic and heteroaromatic compounds found to be reactive in the Murai reaction. The arrows show the position of C–C bond formation.*

Interestingly in the cases of *meta*-substituted acetophenones (**Figure 1.7.**: (p), (q), (r), (s), (t)), where two different reaction sites are present at the *ortho* position, the site selectivity is found to be controlled by steric factors. When *m*-methoxy-acetophenone is reacted with triethoxyvinylsilane, the reaction takes place at the much-congested *ortho* positions suggesting that the heteroatoms assist in bringing the ruthenium closer to the C–H bond **[Scheme 1.29.]**. As shown in **Figure 1.8.**, similar results were found for various groups at the *meta* position.

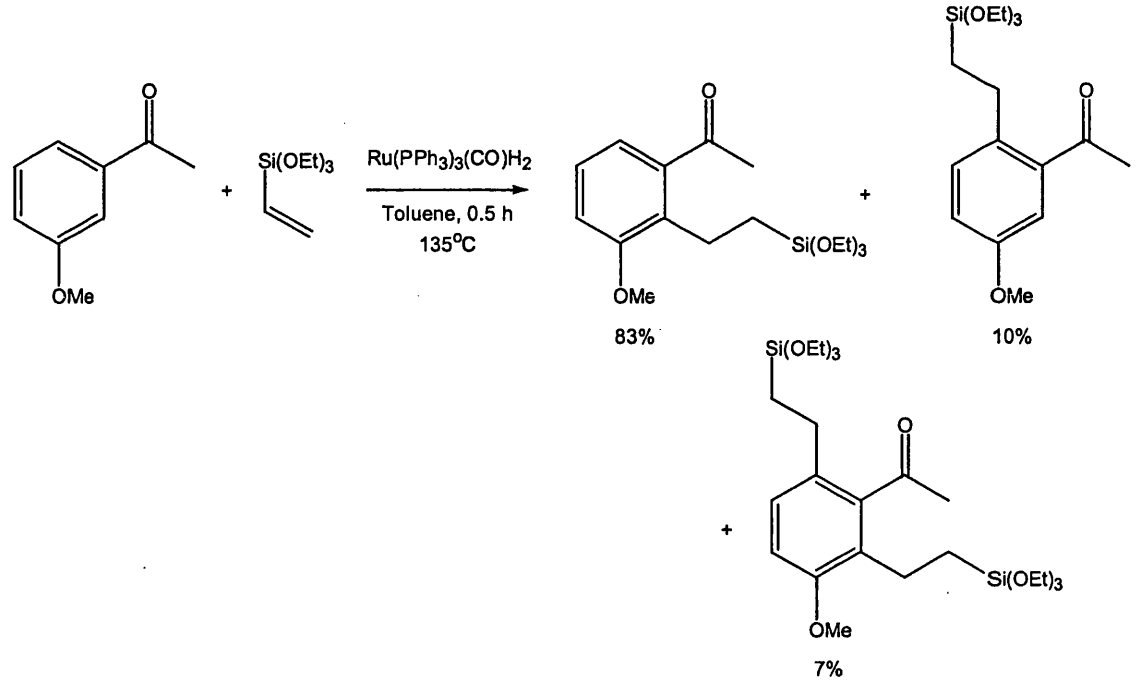

Scheme 1.29.

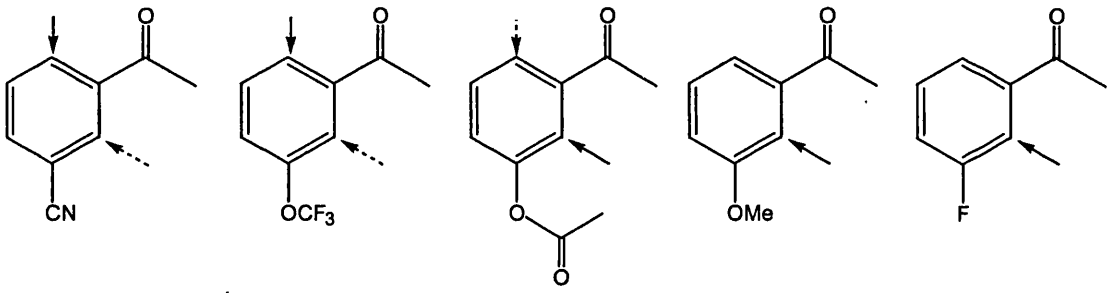

Figure 1.8. - *A variety of the meta substituted phenyl ketones that undergo preferential ortho C–C bond formation according to the nature of the meta substituted groups.*

Woodgate et al. extended this methodology to the synthesis of natural products using $Ru(PPh_3)_3(CO)_2$ as a catalyst **[Scheme 1.30.]**.[52]

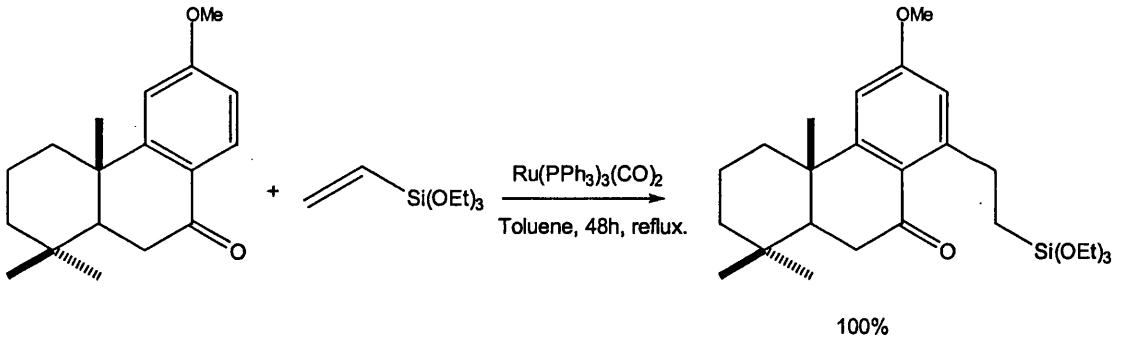

Scheme 1.30.

Grigg & Sevic showed that the reaction of acetylpyridines with triethoxyvinylsilane gave coupling *ortho* to the acetyl group which corresponds to the more electron-deficient aromatic ring.[53] In the case of 3-benzolpyridine, C-H bond insertion into the more electron deficient pyridine ring was observed **[Scheme 1.31.]**.

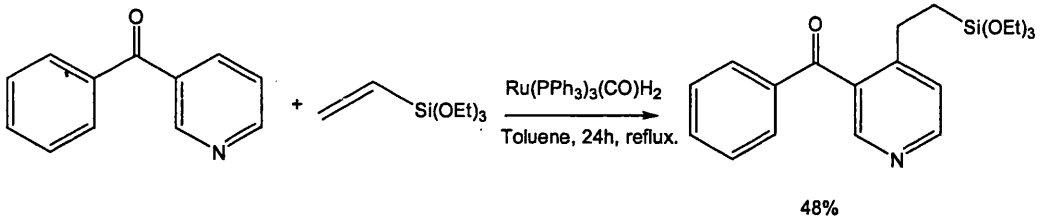

Scheme 1.31.

This C–H/alkene coupling was applied to polymer chemistry in the copolymerisation of acetophenones (which have two free *ortho* C–H bonds) and α,ω-dienes using $Ru(PPh_3)_3(CO)H_2$ as the catalyst.[54] The findings showed that substituted acetophenones with an electron-donating group exhibit higher reactivities and that this step growth polymerisation gives a high molecular weight polymer. This implies that each step proceeds virtually quantitatively **[Scheme 1.32.]**.

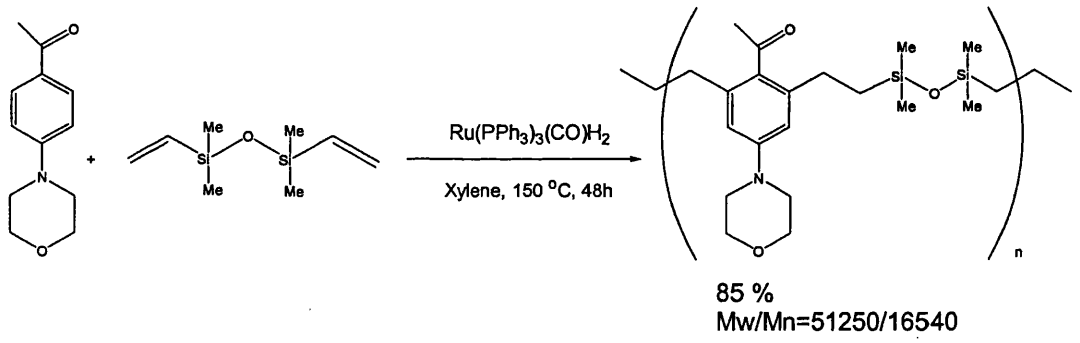

Scheme 1.32.

Trost et al. reported similar results for the addition of conjugated esters to alkenes under identical conditions **[Scheme 1.33.]**.[50]

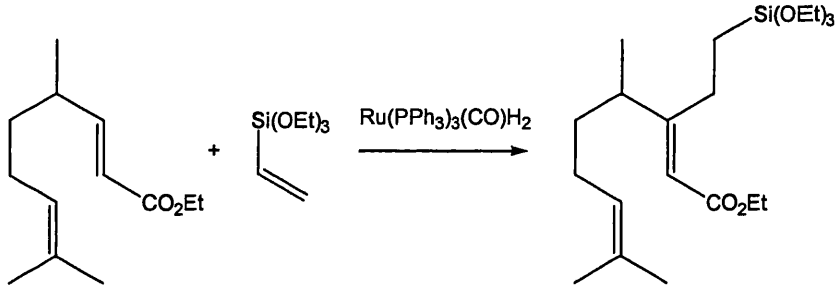

Scheme 1.33.

Nitrogen functionalities can also work as the directing group, with formation of the expected insertion product **[Scheme 1.34.]**. A minor product is the vinylic product formed in 10% yield.[1a,55] In reactions of aromatic imines, $Ru_3(CO)_{12}$ is the superior catalyst even though this complex is ineffective for the reactions of aromatic ketones. As shown in **Scheme 1.35.** depending on the steric hindrance of the aromatic imines the reactivity could be tuned to generate preferentially the vinylic side product. It is proposed that this is due to steric repulsion between the methyl group **[Scheme 1.35.]** and to the oxygen in the dihydrooxazine ring. Moreover as shown in **Scheme 1.36.** similar work was achieved using a Rh precursor.[56]

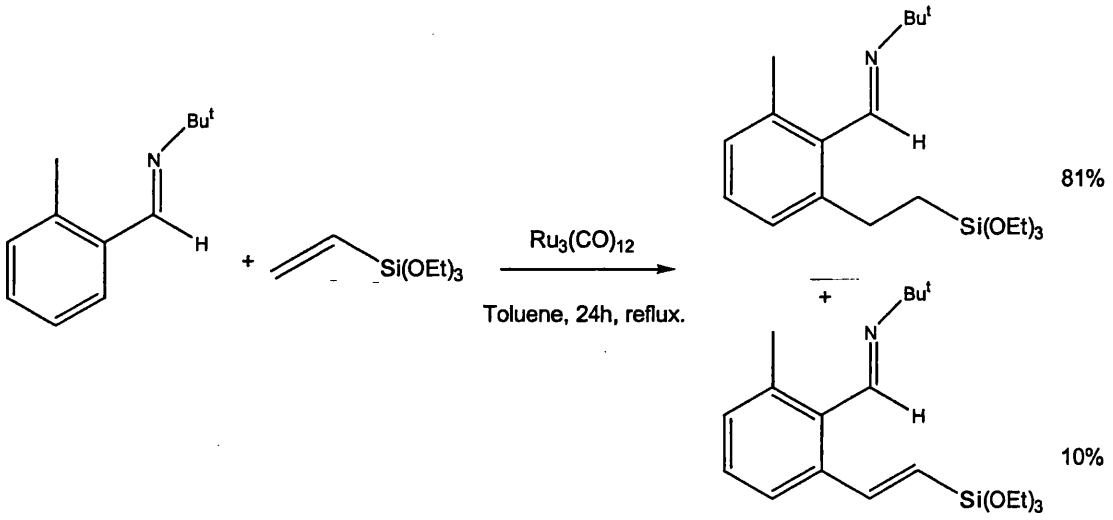

Scheme 1.34.

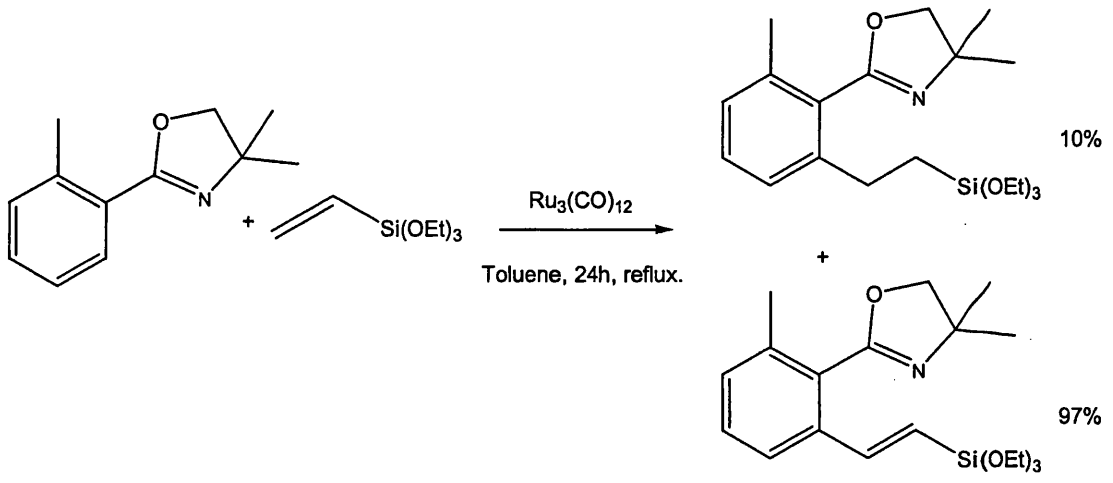

Scheme 1.35.

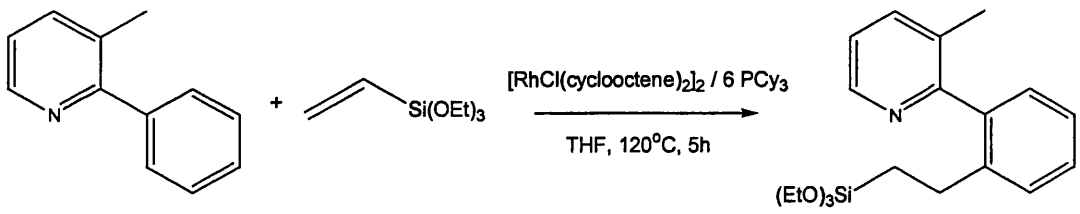

Scheme 1.36.

The Murai process was extended to alkenic C-H bonds at the β-position of conjugated enones **[Scheme 1.37.]**.[57] Acyclohexenes exhibit high reactivities and the presence of an oxygen atom at the allylic position of the 6-membered ring seems to increase the reactivity of the enones.

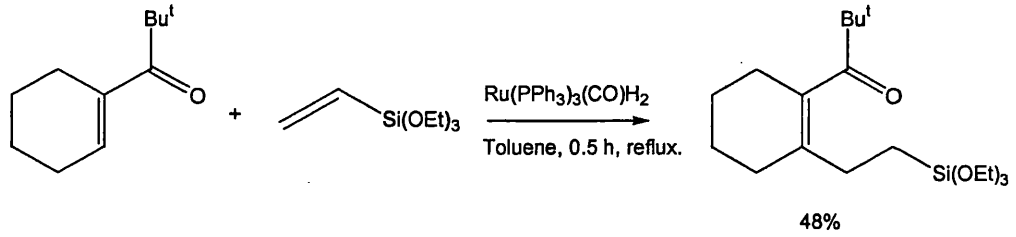

Scheme 1.37.

1.2. Conclusion.

Of all the catalytic reactions involving C-H activation described in this chapter, very few showed a combination of high regioselectivity and high conversion under mild conditions.

The reaction described by Murai comes closest to being the most useful from a synthetic point of view; this discovery is considerable as alkylated aromatic compounds such as 2'-methyl-6'-[2-(triethoxysilyl)ethyl]acetophenone **[Figure 1.9.]**, are difficult to prepare by other, more conventional organic methods. These methods are either not applicable to acyl substituted aromatic compounds or, as in the case of Friedel-Crafts acylation of alkylbenzenes, yield the *para*-substituted isomer as the major product. Finally other techniques involving the electrophilic alkylation of benzenes cannot be applied to electrodeficient acylbenzenes.[57] An other important aspect of this reaction is that C–C bond formation occurred exclusively at the terminal carbon of the alkene and acyl group addition is more favourable at the less hindered side of the double bond.

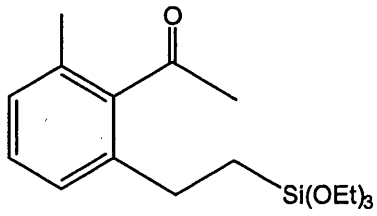

Figure 1.9.

One of the major drawbacks of the Murai reaction is the need for forcing conditions (such as the high temperature) along with restrictions on reactive substituents present on the alkene. The rational development of alternative catalysts to $Ru(PPh_3)_3(CO)H_2$ which (a) may function to lower temperature and (b) allow access to other types of alkenes can only come about through a complete understanding of the reaction mechanism.

1.3. References

1. **(a)** Bergman, R. G. *Science*, **1984**, *223*, 902. **(b)** Crabtree, R. H. *Chem. Rev.*, **1985**, *85*, 245. **(c)** Crabtree, R. H. *Chem. Rev.*, **1995**, *95*, 987. **(d)** Shilov, A. E.; Shul'pin, G. B. *Chem. Rev.*, **1997**, *97*, 2879. **(e)** Kakuishi, F.; Murai, S. "*Topics in Organometallic Chemistry*", ed. S. Murai, Springer-Verlag, Berlin, **1999**, 47. **(f)** Dyker, G. *Angew. Chem. Int. Ed.*, **1999**, *38*, 1698. **(g)** Trost, B. M.; Toste, F. D.; Pinkerton, A. B. *Chem. Rev.*, **2001**, *101*, 2067. **(h)** Ritleng, V.; Sirlin, C.; Pfeffer, M. *Chem. Rev.*, **2002**, *102*, 1731. **(i)** Labinger, J. A.; Bercaw, J. E. *Nature*, **2002**, *417*, 507.
2. Karash, M.S.; Isbell, H. C. *J. Am. Soc.*, **1931**, *53*, 3053.
3. Haber, F.; Willstatter, R. *Ber. Dtsh. Chem. Ges.*, **1931**, *64B*, 2844.
4. Kleiman, J. P.; Dubeck, M. *J. Am. Chem. Soc.*, **1963**, *85*, 1544.
5. Chatt, J.; Davidson, J. M. *J. Chem. Soc.*, **1965**, 843.
6. Gol'dshleger, N. F.;Tyabin, M. B.; Shilov, A. E.;Shteinman, A. A. *Zh. Fiz. Kim.*, **1969**, *43*, 2174.
7. **(a)** Baudry, D.; Ephritikhine, M.; Felkin, H. *J. Chem. Soc., Chem. Commun.*, **1980**, 1243. **(b)** Crabtree, R. H.; Mihelcic, J. M.; Quirk, J. M. *J. Am. Chem. Soc.*, **1979**, *101*, 7738. **(c)** Janowicz, A. H.; Bergman, R. G. *J. Am. Chem. Soc.*, **1982**, *104*, 2214. **(d)** Jones, W. D.; Feher, F. J. *Organometallics*, **1963**, *2*, 562. **(e)** Green, M. L. H. *J. Chem. Soc.*, Dalton trans., **1986**, 2469.
8. **(a)** Shul'pin, G. B.; Shilov, A. E.; Kitaigoroskii, A. N.; Zeile-Krevor, J. V. *J. Organomet. Chem.*, **1980**, *201*, 319. **(b)** Shul'pin, G. B.;Nizova, G. V.; Shilov, A. E. *J. Chem. Soc., Chem. Commun.*, **1983**, 671. **(c)** Serdobov, M. V.; Nizova, G. V.; Shul'pin, G. B. *J. Organomet. Chem.*, **1984**, *265*, C12. **(d)** Watson, P. L. *J. Am. Chem. Soc.*, **1983**, *105*, 6491.
9. **(a)** Groves, J. T.; Nemo, T. E.; Myers, R. C. *J. Am. Chem. Soc.*, **1979**, *101*, 1032. **(b)** Barton, D. H. R., Gastiger, M. J.; Motherwell, W. B. *J. Chem. Soc., Chem. Commun.*, **1983**, 41.
10. Arndtsen, B. A.; Bergman, R. G.; Mobley, T. A.; and Peterson, T. H. *Acc. Chem. Res.*, **1995**, *28*, 154
11. Crabtree, R. H.; Mihecic, J. M.; Quirk, J. M., *J. Am. Chem. Soc.*, **1979**, *101*, 7738
12. Janowicz, A. H.; Bergman R.G., *J. Am. Chem. Soc.*, **1982**, *104*, 352
13. Suggs, J.W. *J. Am. Chem. Soc.*, **1978**, *100*, 640.

14. **(a)** Wax, M. J.; Stryker, J. M.; Buchanan, J. M.; Kovac, C. A.; Bergman, R. G. *J. Am. Chem. Soc.*, **1984,** *106*, 1121. **(b)** Nolan, S. P.; Hoff, C. D.; Stoutland, P. O.; Newman, L. J.; Buchanan, J. M.; Bergman, R. G.; Yang, G. K.; Peters, K. S. *J. Am. Chem. Soc.*, **1987,** *109*, 3143. **(c)** Buchanan, J. M.; Stryker, J. M.; Bergman R. G. *J. Am. Chem. Soc.*, **1986,** *108*, 1537.

15. **(a)** Periana, R. A.; Taube, D. J.; Gamble, S.; Taube, H.; Satoh, T.; Fujii, H. *Science*, **1998**, *280*, 560. **(b)** Waltz, K. M.; Hartwig, J. F. *Science*, **1997**, *277*, 211. **(c)** Chen, H.; Hartwig, J.F. *Angew. Chem. Int. Ed.*, **1999**, *38*, 3391. **(d)** Ishiyama, T.; Tkagi, J.; Hartwig, J. F.; Miyaura, N. *Angew. Chem.. Int. ed.*, **2002**, *41*, 3056.

16. Baudry, D.; Ephritikhine, M.; Felkin, H.; Holmes-Smith, R. *J. Chem. Soc. Chem. Commun*, **1983**, 788

17. **(a)** Fujii, T.; Saito, Y. *J. Chem. Soc. Chem. Commun.*, **1990**, 161. **(b)** Fujii, T.; Higashino, Y.; Saito, Y. *J. Chem. Soc. Chem. Commun.*, **1993**, 517.

18. **(a)** Xu, W-W.; Rosini, G.P.; Gupta, M.; Jensen, C.M.; Kaska, W.C.; Krogh-Jespersen, K.; Goldman, A. S. *Chem. Commun.*, **1997**, 2273.**(b)** Jensen, C. M. *Chem. Commun.*, **1999**, 2443.

19. **(a)** Gustavson, W. A.; Epstein, P. S.; Curtis, M. D. *Organometallics*, **1982**, *1*, 884. **(b)** Ushimaru, Y.; El Sayed, A. M. M.; Tanaka, M. *Organometallics*, **1993**, *12*, 2065. **(c)** Djurovich, P. I.; Dolich, A. R.; Berry D. H.; *J. Chem. Soc. Chem. Commun.*, **1994**, 1897. **(d)** Sakahura, T.; Tokunaga, Y.; Sodeyama, T.; Tanaka, M. *Chem. Lett.*, **1987**, 2375. **(e)** Ishikawa, M.; Okazaki, S.; Naka, A.; Sakamoto, H.; *Organometallics*, **1992**, *12*, 4987. **(f)** Ishikawa, M.; Naka, A.; Oshita, J. *Organometallics*, **1993**, *12*, 4987.

20. Williams, N. A.; Uchimaru, Y.; Tanaka, M. *J. Chem. Soc. Chem.Commun.*, **1995**, 1129.

21. **(a)** Tsuji, J.; Ohno, K. *Synthesis*, **1969**, 157. **(b)** Sakai, K.; Ide, J.; Oda, O.; Nakamura, N. *Tetrahedron Lett.*, **1972**, 1287. **(c)** Lochow, c. F.; Miller, R. G., J. *Am. Chem. Soc.*, **1976**, *98*, 1281.

22. Larock, R. C.; Oertle, K.; Potter, G. F. *J. Am. Chem. Soc.*, **1980**, *102*, 190.

23. **(a)** James, B. R.; Young, C. G. *J. Chem. Soc. Chem. Commun.*, **1983**, 1215. **(b)** James, B. R.; Young C. G. *J. Organomet. Chem.*, **1985**, *285*, 321. **(c)** Taura, Y.; Tanaka, M.; Funakoshi, K.; Sakai K. *Tetrahedron Lett.*, **1989**, *30*, 6349. **(d)** Taura, Y.; Tanaka, M.; Wu, X-M.; Funakoshi, K.; Sakai, K. *Tetrahedron*, **1991**, *47*, 4879. **(e)** Wu, X-M.; Funakoshi, K.; Sakai, K. *Tetrahedron Lett.*, **1992**, *33*, 6331. **(f)**

Barnhart, R. W.; Wang, X.; Noheda, P.; Bergens, S. H.; Whelan, J.; Bosnich, B. *J. Am. Chem. Soc.*, **1994**, *116*, 1821. **(g)** Barnhart, R. W.; Wang, X.; Noheda, P.; Bergens, S. H.; Whelan, J.; Bosnich, B. *Tetrahedron*, **1994**, *50*, 4335. **(h)** Barnhart, R. W.; McMorran, D. A.; Bosnich, B. *Chem. Commun.*, **1997**, 589.

24. Vora, K. P.; Lochow, C. F.; Miller, R. G. *J. Organomet Chem.*, **1980**, *192*, 257.

25. Tsuda, T.; Kiyoi, T.; Saegusa, T. *J. Org. Chem.*, **1990**, *55*, 2554.

26. **(a)** Lee, H.; Jun, C-H. *Bull. Korean Chem. Soc.*, **1995**, *16*, 1135 (b) Kokubo, K.; Matsumasa, K.; Miura, M.; Nomura, M. *J. Org. Chem.*, **1997**, *62*, 4564.

27. **(a)** Naota, T.; Taki, H.; Mizumo, M.; Murahashi, S-I. *J. Am. Chem. Soc.*, **1989**, *111*, 5954. **(b)** Murahashi, S-I.; Naota, T.; Taki, H.; Mizumo,M.; Takaya, H.; Komiya, S.; Mizuho, Y.; Oyasato, N.; Hiraoka, M.; Hirano, M.; Fukuoka, A. *J. Am. Chem. Soc.* **1995**, *117*, 12436. **(c)** Murahashi, S. -I.; Naota, T. *Bull. Chem. Soc. Jpn.*, **1996**, *69*, 1805.

28. **(a)** Sawamura, M.; Hamashima, H.; Ito, Y. *J. Am. Chem. Soc.*, **1992**, *114*, 8295. **(b)** Sawamura, M.; Hamashima, H.; Ito, Y. *Tetrahedron*, **1994**, *50*, 4439.

29. Trost, B. M.; Gerusz, V. J. *J. Am. Chem. Soc.*, **1995**, *117*, 5156.

30. Hong, P.; Yamazaki, H.; Sonogashira, K.; Hagihara, N. *Chem. Lett.*, **1978**, 535.

31. **(a)** Hong, P.; Yamazaki, H. *Chem. Lett.*, **1979**, 1335. **(b)** Hong, P.; Yamazaki, H. *J. Mol. Catal.*, **1984**, *26*, 297.

32. Nugent, W. A.; Ovenall, D. W.; Holmes, S. J.; *Organometallics*, **1983**, *2*, 161.

33. Lin, Y.; Ma, D.; Lu, X. *Tetrahedron Lett.*, **1987**, *28*, 3249.

34. Lewis, L. N.; Smith, J. F. *J. Am. Chem. Soc.*, **1986**, *108*, 2728.

35. Rodewald, S.; Jordan, R. F. *J. Am. Chem. Soc.*, **1994**, *116*, 4491.

36. Collman, J. P.; Hegedus, L. S.; Norton, J. R.; Finke, R. G. *Principles and Applications of Organotransition Metal Chemistry*. **1987**, University science books California.

37. Heck, R. F. *Palladium reagents in organic syntheses*. **1985**, Academic Press, London.

38. **(a)** Hong, P.; Cho, B-R.; Yamazaki, H. *Chem. Lett.*, **1979**, 339. **(b)** Yamazaki, H.; Hong, P.; *J. Mol. Catal.*, **1983**, *21*, 133. **(c)** Hong, P.; Cho, B-R., Yamazaki, H. *Chem. Lett.*, **1980**, 507.

39. **(a)** Hallbritter, G.; Knoch, F.; Wolski, A.; Kisch, H. *Angew. Chem. Int. Ed. Engl.*, **1994**, *33*, 1603. **(b)** Aulwurm, U. R.; Melchinger, J. U.; Kisch, H. *Organometallics*, **1995**, *14*, 3385.

40. Kakuishi, F.; Yamamoto, Y.; Chatani. N.; Murai S. *Chem. Lett.*, **1995**, 681.

41. Moore, E. J.; Pretzer, W. R.; O'Connell, T. J.; Harris, J.; La Bounty, L.; Chou, L.; Grimmer, S. S. *J. Am. Chem. Soc.*, **1992**, *114*, 5888.

42. **(a)** Chatani, N.; Fukuyama, T.; Kakiuchi, F.; Murai, S. *J. Am. Chem. Soc.*, **1996**, *118*, 493. **(b)** Chatani, N.; Kakiuchi, F.; Murai, S. *J. Org. Chem.*, **1997**, *62*, 5647. **(c)** Fukuyama, T.; Chatani, N.; Kakiuchi, F.; Murai, S. *Organometallics*, **1997**, *16*, 3615. **(d)** Ishii, Y.; Chatani, N.; Kakiuchi, F.; Murai, S. *Tetrahedron Lett.*, **1997**, *38*, 7565. **(e)** Fukuyama, T.; Chatani, N.; Kakiuchi, F.; Murai, S. *J. Am. Chem. Soc.*, **1998**, *120*, 11522. **(f)** Chatani, N.; Ie, Y.; Kakiuchi, F.; Murai, S. *J. Org. Chem.*, **1997**, *62*, 2604. **(g)** Chatani, N.; Ishii, Y.; Ie, Y.; Kakiuchi, F.; Murai, S. *J. Org. Chem.*, **1998**, *63*, 5129. **(h)** Chatani, N.; Fukuyama, T.; Tatamidani, H.; Y.; Kakiuchi, F.; Murai, S. *J. Org. Chem.*, **2000**, *65*, 4039. **(i)** Tobisu, M.; Chatani, N.; Asaumi, T.; Amako, K.; Ie, Y., Fukumoto, Y.; Murai, S. *J. Am. Chem. Soc.*, **2000**, *122*, 12663.

43. **(a)** Fisher, B. J.; Eisenberg, R. *Organometallics*, **1983**, *2*, 764. **(b)** Kunin, A. J.; Eisenberg, R. *J. Am. Chem. Soc.*, **1986**, *108*, 535.

44. Kunin, A. J.; Eisenberg R. *Organometallics*, **1988**, *77*, 2124.

45. Gordon E. M.; Eisenberg R. *J. Mol. Catal.*, **1988**, *45*, 57.

46. **(a)** Sakakura, T.; Tanaka, M. *Chem. Lett.*, **1987**, 249. **(b)** Sakakura, T.; Tanaka, M. *J. Chem. Soc. Chem. Commun.*, **1987**, 758. **(c)** Sakakura, T.; Tanaka, M. *Chem. Lett.*, **1987**, 1113. **(d)** Sakakura, T.; Sasaki, K.; Tokunaga, Y.; Wada, K.; Tanaka, M. *Chem. Lett.*, **1988**, 155. **(e)** Sakakura, T.; Sodeyama, T.; Sasaki, K.; Wada, K.; Tanaka, M. *J. Am. Chem. Soc.*, **1990**, *112*, 7221.

47. **(a)** Jones, W. D.; Kosar, W. P. *J. Am. Chem. Soc.*, **1986**, *108*, 5640. **(b)** Hsu, G. C.; Kosar, W. P.; Jones, W. D. *Organometallics*, **1994**, *13*, 385.

48. Murai, S.; Kakuishi, F.; Sekine, S.; Tanaka, Y.; Kamatani, A.; Sonoda, M.; Chatani, N. *Nature*, **1993**, *366*, 529.

49. **(a)** Murai, S.; Kakuishi, F.; Sekine, S.; Tanaka, Y.; Kamatani, A.; Sonoda, M.; Chatani, N. *Pure Appl. Chem.*, **1994**, *66*, 1527. **(b)** Kakiushi, F.; Sekine, S.; Tanaka, Y.; Kamatani, A.; Sonoda, M.; Chatani, N.; Murai, S. *Bull. Chem. Soc. Jpn.*, **1995**, *68*, 62. **(c)** Murai, S.; Kakuishi, F.; Chatani, N. *Pure Appl. Chem.*, **1997**, *69*, 589.

50. Trost, B. M.; Imi, K.; Davies, I. W. *J. Am. Chem. Soc.*, **1995**, *117*, 5371.

51. Murai, S.; Kakuishi, F.; Sonoda, M.; Chatani, N. *J. Organomet. Chem.*, **1995**, *504*, 151.

52. **(a)** Harris, P. W. R.; Woodgate, P. D. *J. Organomet. Chem.*, **1996**, *506*, 339. **(b)** Harris, P. W. R.; Woodgate, P. D. *J. Organomet. Chem.*, **1997**, *530*, 211.

53. Grigg, R.; Savic, V. *Tetrahedron Lett.*, **1997**, *38*, 5737.

54. **(a)** Guo, H.; Tapsak, M. A.; Weber, W. P. *Macromolecules*, **1995**, *28*, 4714. **(b)** Guo, H.; Wang, G.; Tapsak, M. A.; Weber, W. P. *Macromolecules*, **1995**, *28*, 5686. **(c)** Lu, P.; Paulasaari, J. K.; Weber, W.P. *Macromolecules*, **1996**, *29*, 8583. **(d)** Wang, G.; Guo, H.; Weber, W. P. *J. Organomet. Chem.*, **1996**, *521*, 531.

55. **(a)** Kakuichi, F.; Sato, T.; Yamaushi, M.; Chatani, N.; Murai, S. *Chem. Lett.*, **1999**, 19. **(b)** Chatani, N.; Asaumi, T.; Yorimitsu, S.; Ikeda, T.; Kakiushi, F.; Murai, S. *J. Am. Chem. Soc.*, **2001**, *123*, 10935.

56. Kakuishi, F.; Sonoda, M.; Chatani, N.; Murai, S. *Chem. Lett.*, **1996**, 111.

57. Kakuishi, F.; Tanaka, Y.; Sato, T.; Chatani, N.; Murai S. *Chem. Lett.*, **1995**, 679.

58. **(a)** "*Advanced Organic Chemistry*", ed by March, J.; 4th ed., J. Wiley-Interscience. **1992.** **(b)** "*Comprehensive Organic Synthesis*", ed by Trost, B. M.; Fleming I.; Heathcock, C. H. Pergamon Press, Oxford, U.K. (1991).

Chapter 2.

Kinetic study of the Murai reaction: ruthenium catalyzed C-H/alkene coupling.

2.1. Introduction.

2.1.1. Mechanistic aspects of C-H/alkene coupling.

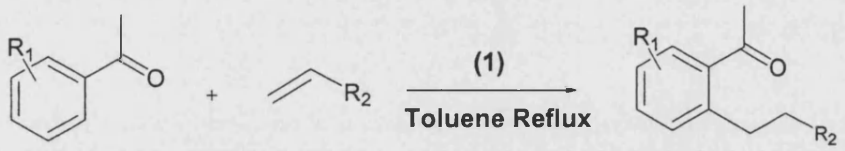

(61) **(60)** **(62)**

Scheme 2.1.

We have seen in **Chapter 1** that most of the work reported by Murai et al.[1-8] and others[9-12] on the reaction shown in **Scheme 2.1** has focused on exploring the range of reactive substrates. In fact in only a few cases have mechanistic aspects of the reaction been probed.[3b, 4, 13-15] Preliminary studies[3, 15] with respect to the reaction mechanism of the ruthenium-catalysed C-H/alkene coupling have revealed that initial hydrogenation of the alkene with **(1)** gives a zero-valent species such as $Ru(CO)(PPh_3)_3$, and deuterium labelling experiments [**Scheme 2.2.**]. have demonstrated that a complete scrambling occurred among the two *ortho* positions of the ester and the three vinylic positions of the vinylsilane even though no coupling product was obtained.

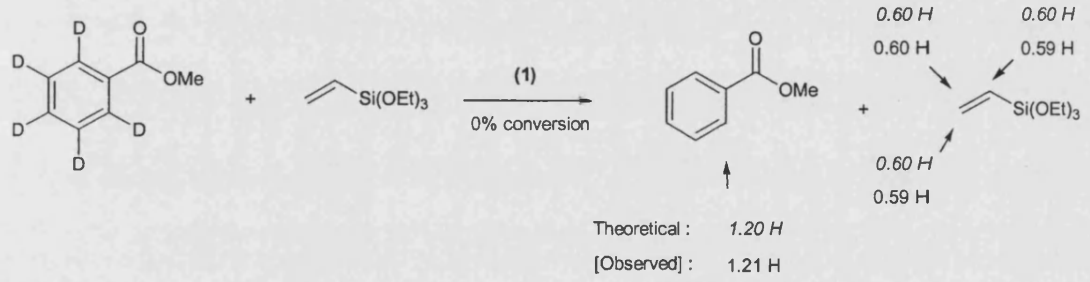

Scheme 2.2.

Further mechanistic studies for obtaining informations with respect to the rate determining step have been measured by means of experimental ^{13}C kinetic isotope effects (KIEs) at natural abundance in the reaction of ketones and aromatic esters.[16] If C-C bond formation step is rate determining, the relative intensity of the *ortho*-carbon in the starting material should be increased compared with those at natural abundance. It was found that the KIE of *ortho* carbon was 1.033 in ester and 1.023 in ketones (generally 1.00 in aromatic carbons), suggesting that facile C-H bond cleavage occurs in both the ketone at the *ortho* position, and the silyl alkene at the terminal and axial position. On the basis of these studies

determining in both aromatic esters and ketones. Moreover since H/D exchange occurred only at the *ortho* position, chelation assistance is critically important in C-H bond activation by the ruthenium metal centre. This, added to the fact that C-C bond formation occurs only at the position *ortho* to the ketone, strongly suggested formation of an *ortho* metallated ruthenium ketone complex.

Finally, DFT calculation conducted by Matsubara et al. probed computationally the reaction of benzaldehyde with ethene catalyzed by three- and four-coordinate complexes $Ru(CO)(PH_3)_n$ (n = 2, 3) as active species.[17,18] These calculations have shown that the *ortho*-CH bond of benzaldehyde selectively adds to ethene, due to the existence of an unusual metallacycle d^6 five-coordinate complex intermediate stabilized by a CH agostic interaction **[Figure 2.1 (a)]**. In fact, the CH bond cleavage was shown to proceed in two steps during which the energy barrier is lowered significantly by the existence of the stable agostic intermediate. Subsequent alkene insertion into the RuH bond (insertion into Ru-C is less energetically favourable) and CC bond formation follows and was shown to proceed through a metallacycle intermediate **[Figure 2.1., (b)]** again stabilised by an agostic interaction. Finally it was demonstrated that the CC bond formation step, which has an activation energy of 113 kJ/mol, was rate-determining.

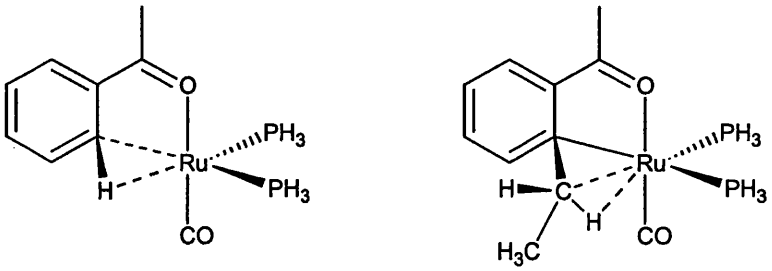

Figure 2.1.

On the basis of these observations by both Murai and Matsubara, a proposed mechanism was suggested **[Scheme 2.3.]**. In a first step, activation of the catalyst precursor by alkene is proposed to afford the catalytically active species. The second step consists of the subsequent *ortho* metallation of the active species with a ketone group, finally proceeding through to C-C bond formation and decomplexation to afford the final product.

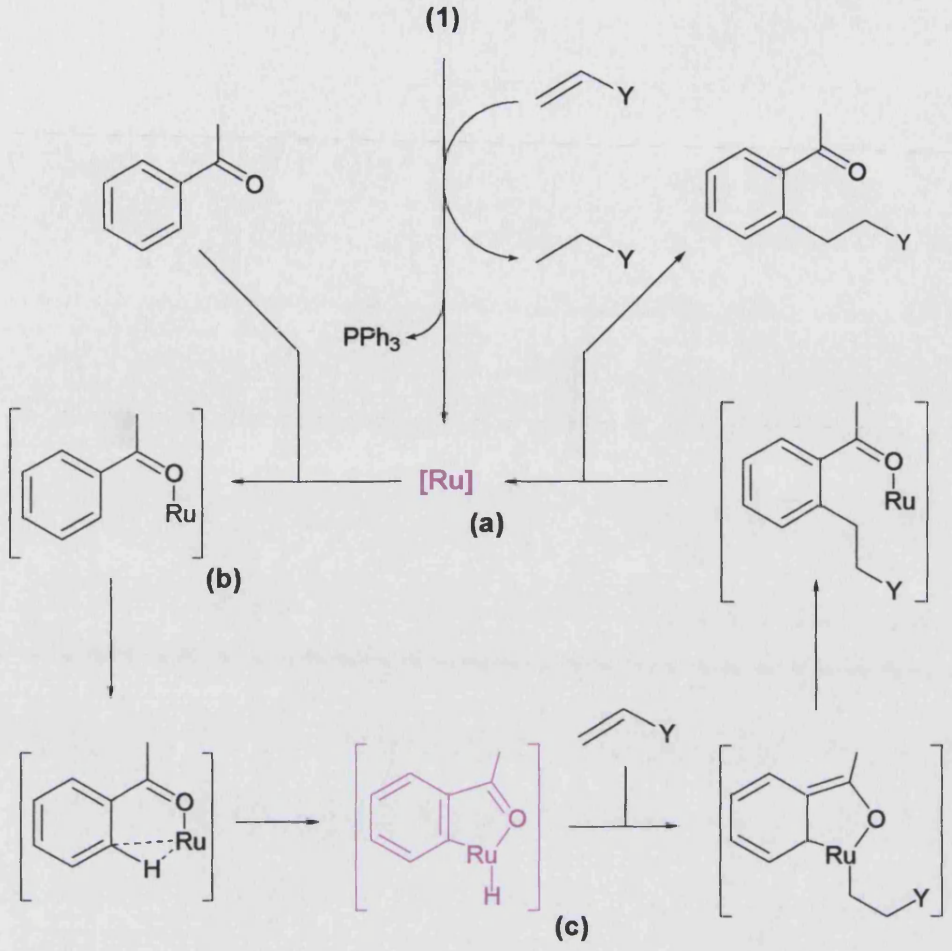

Scheme 2.3. - *Proposed mechanism for the Murai reaction.*

2.1.2. Cylindrical internal reflectance: a method for *in-situ* catalytic studies.

As for the Murai reaction, a complete understanding of mechanistic detail is missing from many industrially and biologically important catalytic reactions that require high pressures and/or high temperatures. As most of the steps in a catalytic cycle are by definition fast, it is not easy to establish either the structure of the catalytically active species (which is likely to be present only at very low concentrations) or how this or any other intermediate interacts with organic substrates in the stoichiometric steps along the reaction pathway. One solution is to break the catalytic cycle down into a series of component reactions and to study them individually. However, the crux is to study these reactions under the "real catalytic conditions" so that any species that are observed are known to be truly involved in the catalytic cycle.

The problem then is to find a spectroscopic tool to allow such observations to be made. Such a sensitive monitoring system should:

- Examine the desired reaction under truly *in-situ* conditions.
- Be able to deal with reactions in extreme conditions, such as very absorbing solutions or strongly corrosive solvents.
- Not alter initial reaction parameters.

The reaction we are interested in studying involves metal carbonyl species and ketone substrates, which exhibit strong characteristic infra-red chromophores, between ca. 2000-1600 cm^{-1}. For example, **(1)** shows a terminal Ru-CO band at 1942 cm^{-1} and 2'-methylacetophenone displays a strong C=O vibration at 1690 cm^{-1}. More crucially, since the reaction only proceeds upon heating, the measurements will have to be carried out at high temperature.

An analytical system meeting these requirements has already been successfully used to study a number of metal catalysed high-pressure reactions. The key tool for this work involves FTIR coupled to a high-pressure cylindrical internal-reflectance infrared cell[19] (CIR). Originally developed by W. R. Moser for homogeneous transition metal catalysed reactions, the CIR cell is a relatively new method for the infrared analysis of chemical reactions and allows direct observation of reaction intermediates in a chemical reaction under conditions of both high temperature, and if required, high pressure. The power of this technique has been shown by the work of Haynes and Maitlis in Sheffield[20] in elucidating the kinetics of the complete catalytic cycles of rhodium and iridium catalysed carbonylation of methanol in the Mosanto and CATIVA processes. A combination of high pressure/temperature IR plus NMR studies and independent synthesis has helped to establish the structure of reaction intermediates and determine kinetic data of key steps of oxidative addition of MeI and migratory insertion to afford metal acyl species. **[Figure 2.2.]**. The rhodium and iridium pathways have been shown to be very similar, but crucially different in the nature of the rate-determining step. In the rhodium case, the oxidative addition of CH_3I to the intermediate $[Rh(CO)_2I_2]^{2-}$ is the slow step, but in the iridium reaction, migratory addition of CO is rate-determining step. These results have proven to be fundamental to the introduction and commercialisation of the new CATIVA iridium/iodide catalysed system.

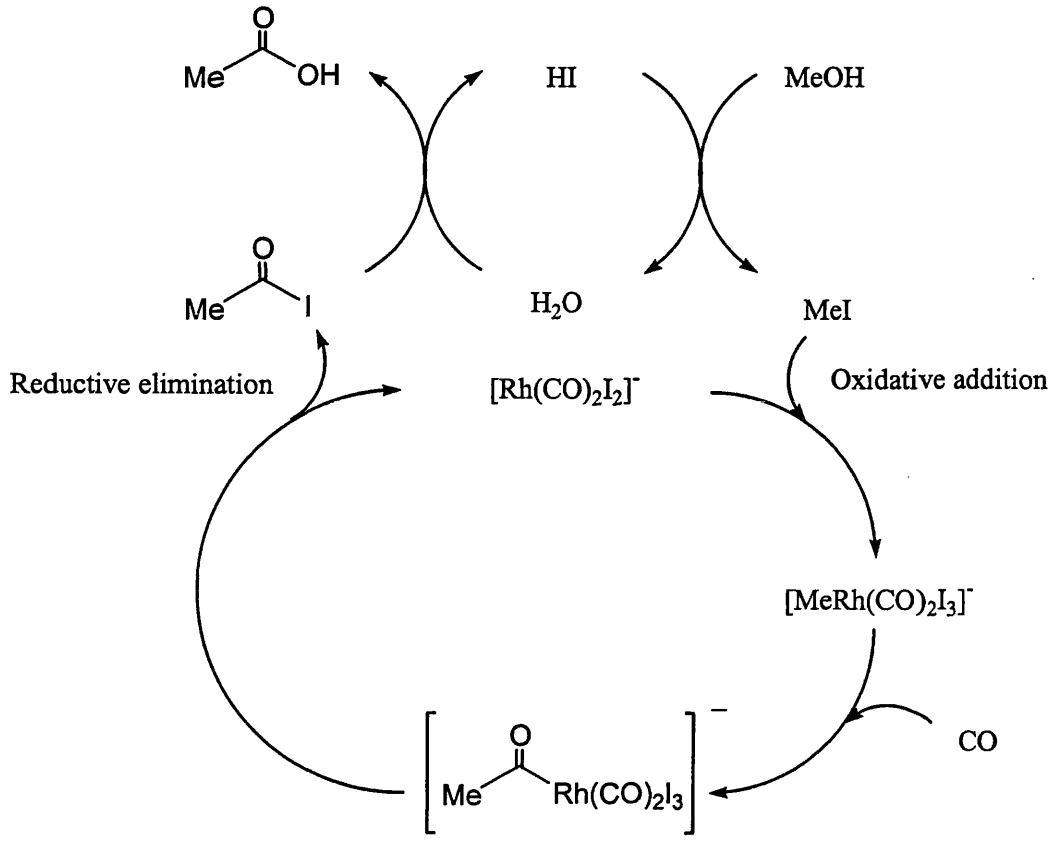

Figure 2.2. - *Rhodium and iodide-catalysed carbonylation of methanol.*

Optical system.

The CIR cell used in our studies **[Figure 2.4.]**, comprises a plug flow reactor, fitted with a CIR crystal (a ZnSe crystal rod with polished 45° conical ends) through which the IR beam emitted by a Nicolet Protégé 460 FTIR spectrometer was transmitted. As illustrated in **Figure 2.3.**, the infrared beam was directed into a set of convex mirrors and is redirected onto the 45° angle of the CIR rod. As the beam passes along the rod, 10 internal reflections at the rod-solution interface leads to a modulation of the IR intensity by solvent and solute absorption. The resulting IR spectrum is similar to that obtained in a conventional transmission experiment but with a very short effective pathlength (ca. 10-15 μm), which means that reliable quantitative measurement can be performed.

The cell has a low volume (400μl) and was equipped with a heating jacket allowing measurements to be made up to 250 °C **[Figure 2.4.]**. A feature that will be vital to us later in the project is the ability of the cell to take gas pressures of up to 1500 psi. The cell was

coupled to an IR spectrometer with rapid scan facilities, up to 35 scans per second at 16 cm^{-1} resolution.

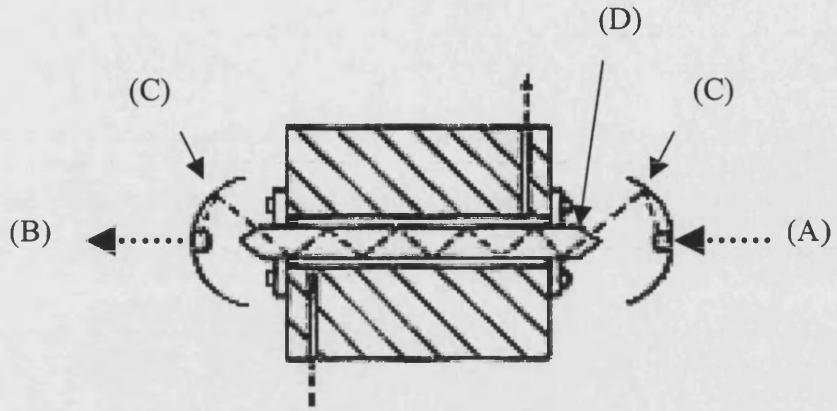

Figure 2.3. - *Cylindrical internal reflectance crystal cell. (A) incident infrared beam, (B) emitted beam directed toward detector, (C) focusing mirrors, (D) cylindrical internal reflectance crystal of either ZnSe, ZnS, Si, Ge.*

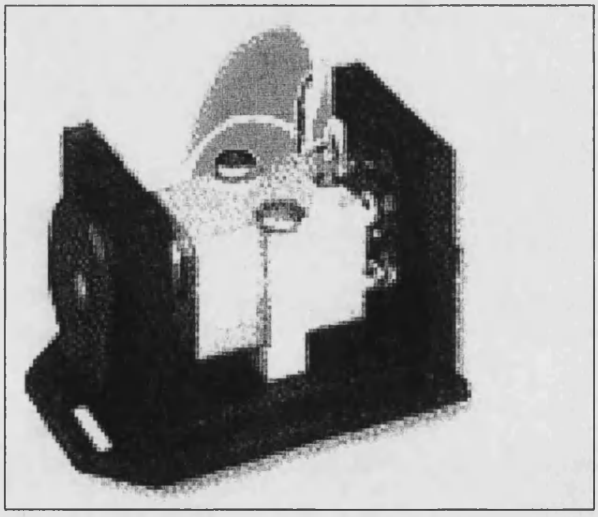

Figure 2.4. - *Plug flow CIR cell equipped with thermostated heating block, high-pressure gas inlet and effluent lines.*

Advantages and disadvantages.

The CIR reactors have demonstrated that they lead to truly *in-situ* results, they are able to provide analysis in strongly absorbing solvents such as water or acetic acid, lead to analyses that show no path-length dependence on pressure and little on temperature, and are exceptionally easy to run and to obtain instantaneous analyses as the reaction parameters are altered. The CIR reactors have shown a few disadvantages, as the fact that the small diameter crystal used in a low-volume reactor are fragile, especially ZnSe and are to be mounted and heated carefully. The studies of reactions with a pH > 12, is also undesirable as the crystal becomes etched, leading to loss of IR signal.

2.2. Results and discussion.

The work described in this chapter focuses on the reaction of **(1)** with a range of silyl substituted alkenes and several phenyl ketone derivatives over a range of temperatures The influence of the -SiR_3 group attached to the alkene on the kinetics of the reaction was studied by variation of R from OEt **(60a)**, Me **(60b)** and Ph **(60c)** **[Scheme 2.4.]**. Study of the ketone influence has proved to be complex due to the difficulty in finding ketones suitable for the IR measurement; changes in ν_{CO} between starting ketone **(61)** and product **(62)** were needed that allowed the two compounds to be differentiated by IR. Both 2-methylacetophenone **(61a)** and 4-fluoroacetophenone **(61b)** have proved to be suitable for IR study, leading to the study of mono and di C-C bond formation with **(61a)**, and **(61b)** respectively.

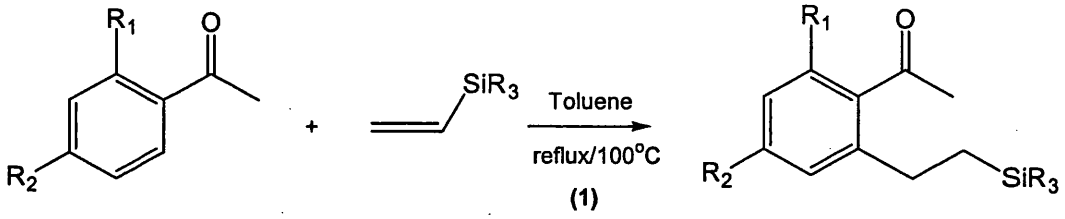

R_1 = Me, R_2 = H **(61a)**

R_1 = H, R_2 = F **(61b)**

R = OEt **(60a)**

R = Me **(60b)**

R = Ph **(60c)**

R = OEt, R_1= Me, R_2 = H **(62a)**

R = Me, R_1= Me, R_2 = H **(62b)**

R = Ph, R_1= Me, R_2 = H **(62c)**

R = OEt, R_1= $CH_2CH_2SiOEt_3$, R_2 = F **(62d)**

R = Me, R_1= $CH_2CH_2SiMe_3$, R_2 = F **(62e)**

Scheme 2.4. - *C-H bond functionalisation of phenyl ketones with various silyl-substituted alkenes leading to C-C coupling.*

2.2.1. Preliminary studies.

The IR spectrum of a toluene solution of **(1)** (9.9 x 10^{-5} mol) and **(60a)** (9.9 x 10^{-4} mol) shows a single carbonyl stretching band at 1941 cm^{-1} at room temperature. Upon heating to 100°C, this band decreased in intensity and a new CO band appeared at 1918 cm^{-1}. Complete conversion to this product was seen at 373 K within 10 minutes; no further changes were observed at 135°C over an additional 60 minutes **[Scheme 2.5.]**. However, when a toluene solution of **(1)** (9.9 x 10^{-5} mol) and 2'-methylacetophenone (9.9 x 10^{-4} mol) was heated to 135°C, no reaction was observed **[Scheme 2.5.]**.

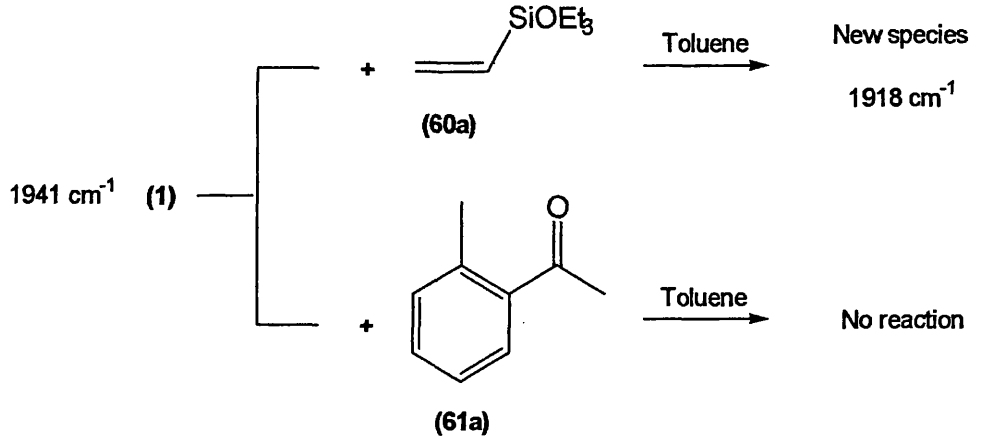

Scheme 2.5.

Finally a toluene solution of **(1)** (9.9 x 10^{-5} mol) was reacted with both **(60a)** and **(61a)** (both at 9.9 x 10^{-4} mol) in toluene at 100°C to afford **(62a)** **[Scheme 2.6.]**. The IR spectra recorded at regular intervals (every 30s) showed progressive formation of **(62a)** and decay of **(61a)** in the region of the IR spectrum associated with the ketone absorptions **[Scheme 2.6., Spectra 2.1.]**. This is shown in **Figure 2.5.** as a plot of the initial species at 1689 cm^{-1} and of the final species at 1702 cm^{-1}. Similarly in the Ru-CO region of the spectrum, decay of the carbonyl band for **(1)** is observed along with growth of a new band at 1910 cm^{-1}. Changes in the Ru-CO region of the IR spectrum, occur prior to those in the ketone region. This is associated with initial activation of **(1)** which is necessary to generate the active catalyst species which then functionalises **(61a)**.

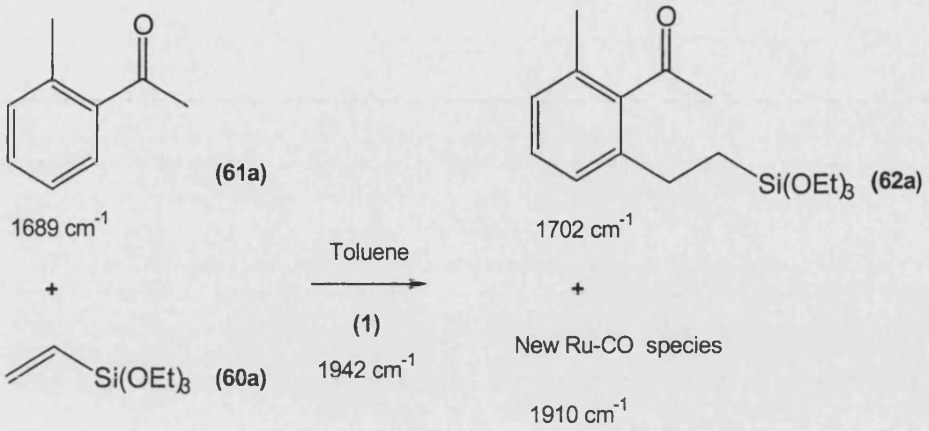

Scheme 2.6.

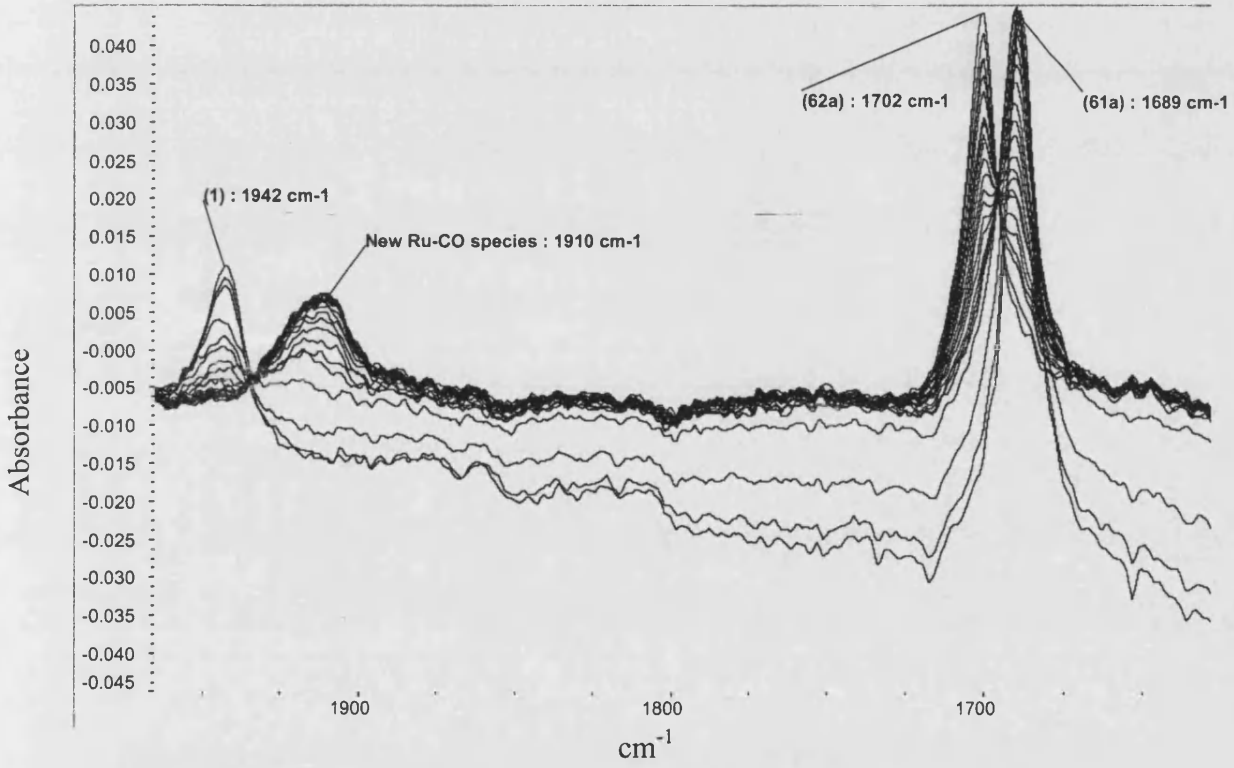

Spectra 2.1. - *Change in the IR spectra during the reaction of* ***(1)*** *with* ***(60a)*** *and* ***(61a)*** *and* ***(62a)****, in toluene at 100 °C.*

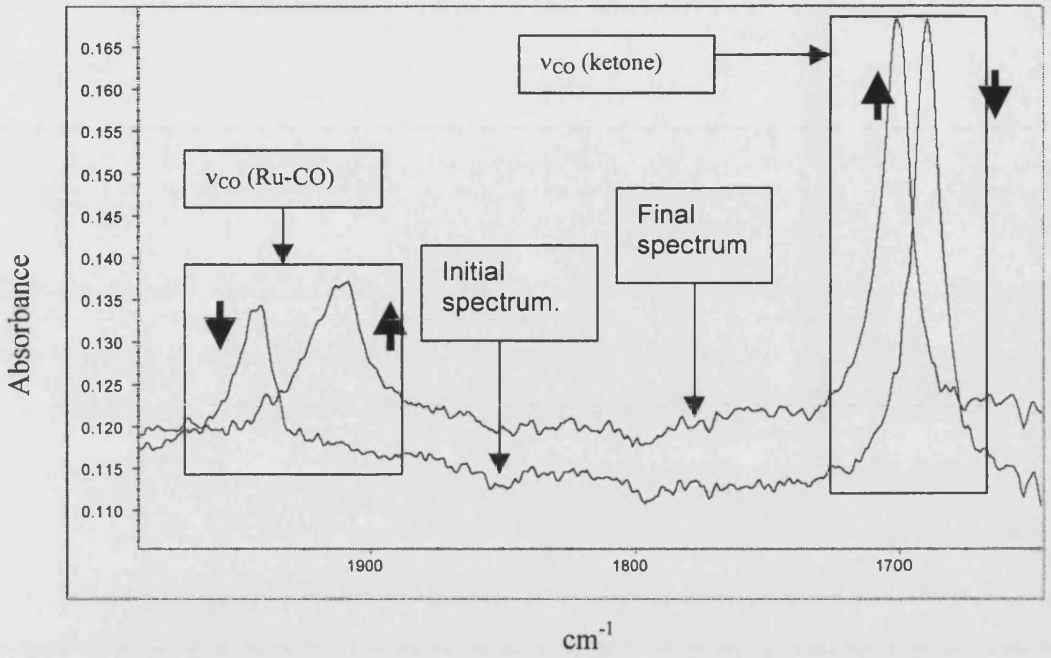

Figure 2.5. - *Initial and final IR spectrum from reaction of* ***(60a)*** *with* ***(61a)*** *and* ***(1)*** *at 100°C in toluene.*

2.2.2. Kinetic model applied to the Murai reaction.

These initial investigations resulted in direct kinetic analysis of the Murai reaction. In fact direct analysis of the several spectra generated by a sequential recording of the IR spectra during the reaction resulted in the possible quantification of the concentration by means of the analysis of the intensity of the observed IR signals. This was achieved using the Beer-Lambert law ($A = \varepsilon l [X]$). This equation readily simplifies when considering that l and ε remains constant for a known compounds under the experiment conditions ($A = k [X]$). Therefore, for a set compound the concentration is directly proportional to the absorbance, which extends to any time (t) of the reaction. Therefore it is possible to plot the concentration versus (t) and to deduce the rate constant of the process.

The variation of the intensity of the peaks in the Ru-CO region of the IR spectra **[Spectra 2.2.]** can be plotted as a function of time. The resulting graph is shown in **Graph. 2.1.**; ((a) shows the first order decay in the concentration of **(1)** at 1941 cm^{-1}, and (b) for the growth in the concentration of the Ru-CO new product at 1910 cm^{-1}. These results show that the rate of formation of the new ruthenium species is similar to the rate of decay of **(1)** (k_{obs}(growth) = 4.35 x 10^{-3} s^{-1}; k_{obs}(decay) = 4.48 x 10^{-3} s^{-1}). (**NB:** The rate of the reaction was calculated by plotting Ln[intensity] as a function of time. The intensity was defined as

follow: Intensity = $|A_t - A_\infty|$ with A_t= being the absorbance at a time t and A_∞ the absorbance at t infinity.)

On the same analytical basis the variation of the intensity of the peaks in the ketone region resulted in a series of plots as shown in **Spectra 2.3.** for the carbonyl peaks of **(61a)** and **(62a).** As seen before, this variation readily converted to a plot of the variation in intensity versus time as shown in **Graph. 2.2.** ((d) for the decay of **(61a)**, and (c) for the growth of **(62a)**). These two curves fit to an exponential function and the log plot shows that the decrease in the concentration in **(61a)** matches the growth in concentration of **(62a)** (k_{obs}(growth) = 1.41x 10^{-3} s^{-1}; k_{obs}(decay) = 1.31 x 10^{-3} s^{-1}).

It is interesting to note that the rate constant for depletion of **(1)** is approximately 3 times faster than the rate constant for the loss of **(61a)**. This in turn shows that activation to give the catalytically active species is not the rate determining step, a point which has already been suggested by various authors.[21,22] Moreover, we observed that full conversion of **(1)** to the new Ru-CO species occurs prior to any C-C coupling product being observed, and that the IR band of this new species (1910 cm^{-1}) remains until the end of the reaction suggesting that this species is possibly the active catalyst of the reaction.

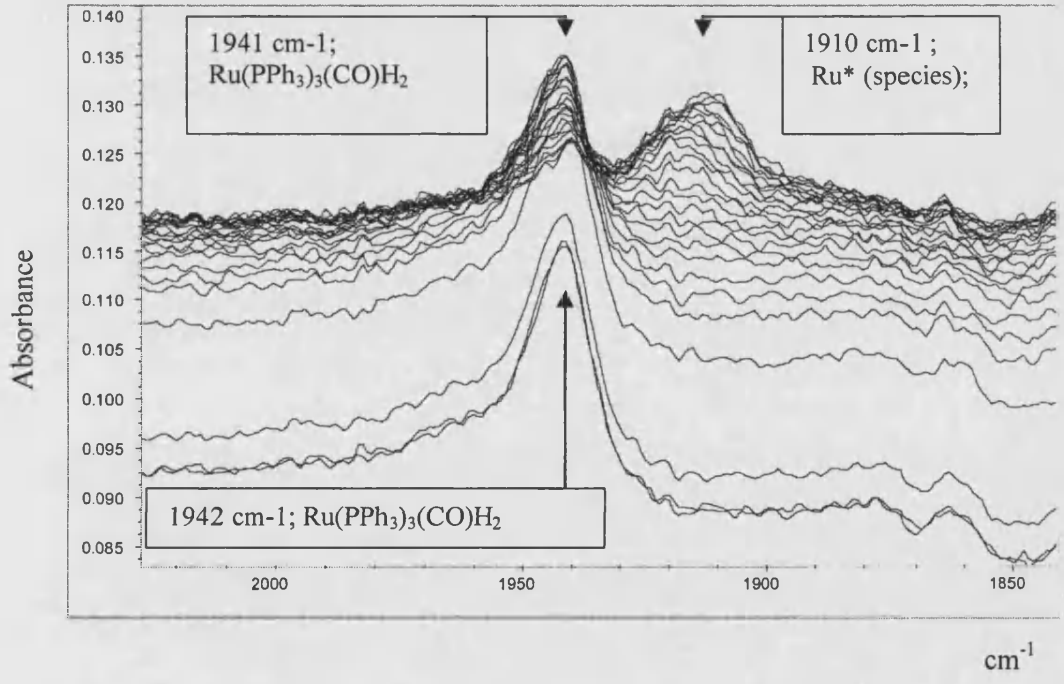

Spectra 2.2. - *IR spectra of the ruthenium carbonyl region.*

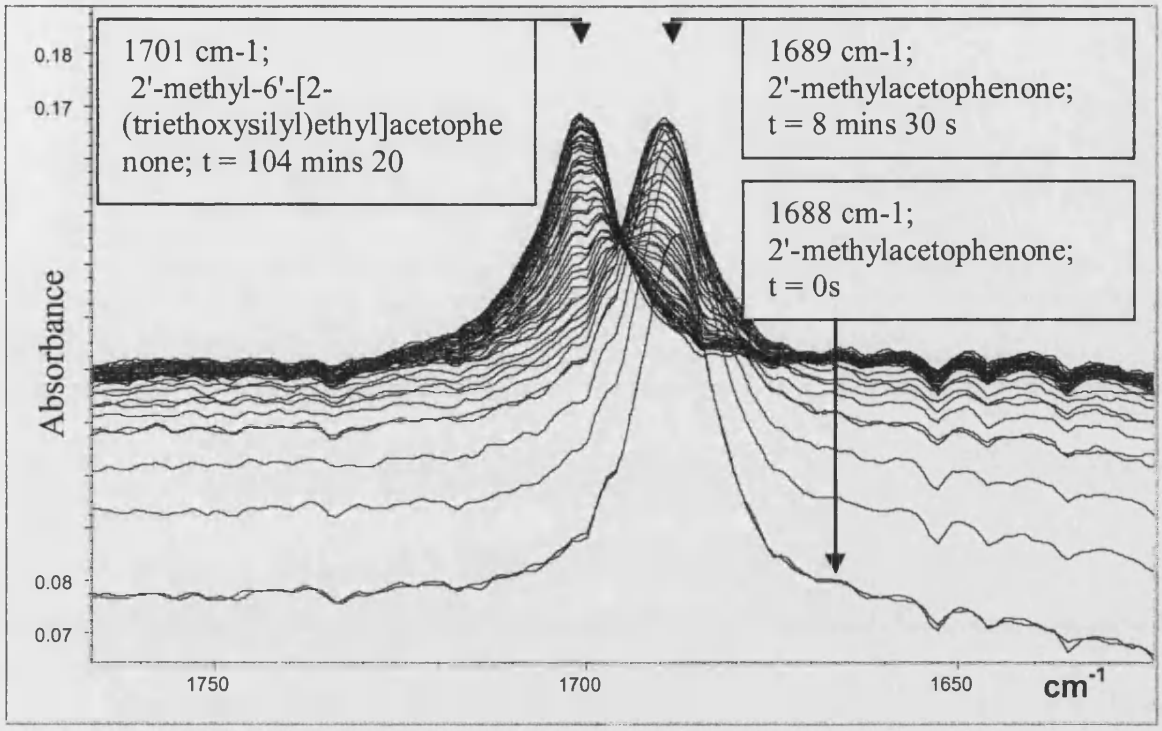

Spectrum 2.3. - *IR spectra showing changes in concentration of* ***(61a)*** *and* ***(62)*** *with time.*

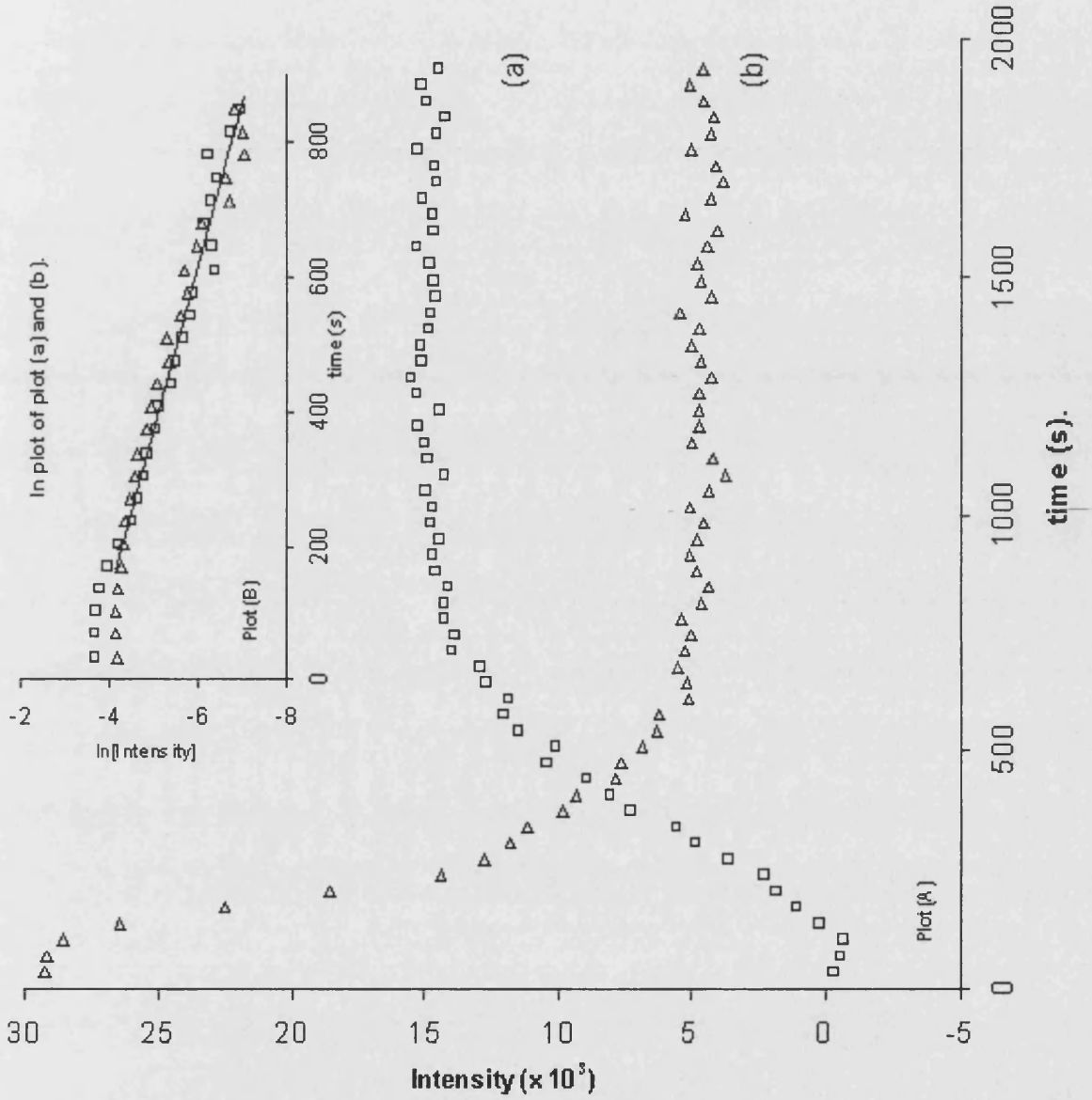

Graph. 2.1. *Plot (A): Variation in concentration of* ***(1)*** *curve (a), and of the* ***Ru-CO*** *curve (b).*

Plot (B): Determination of the rate constant.

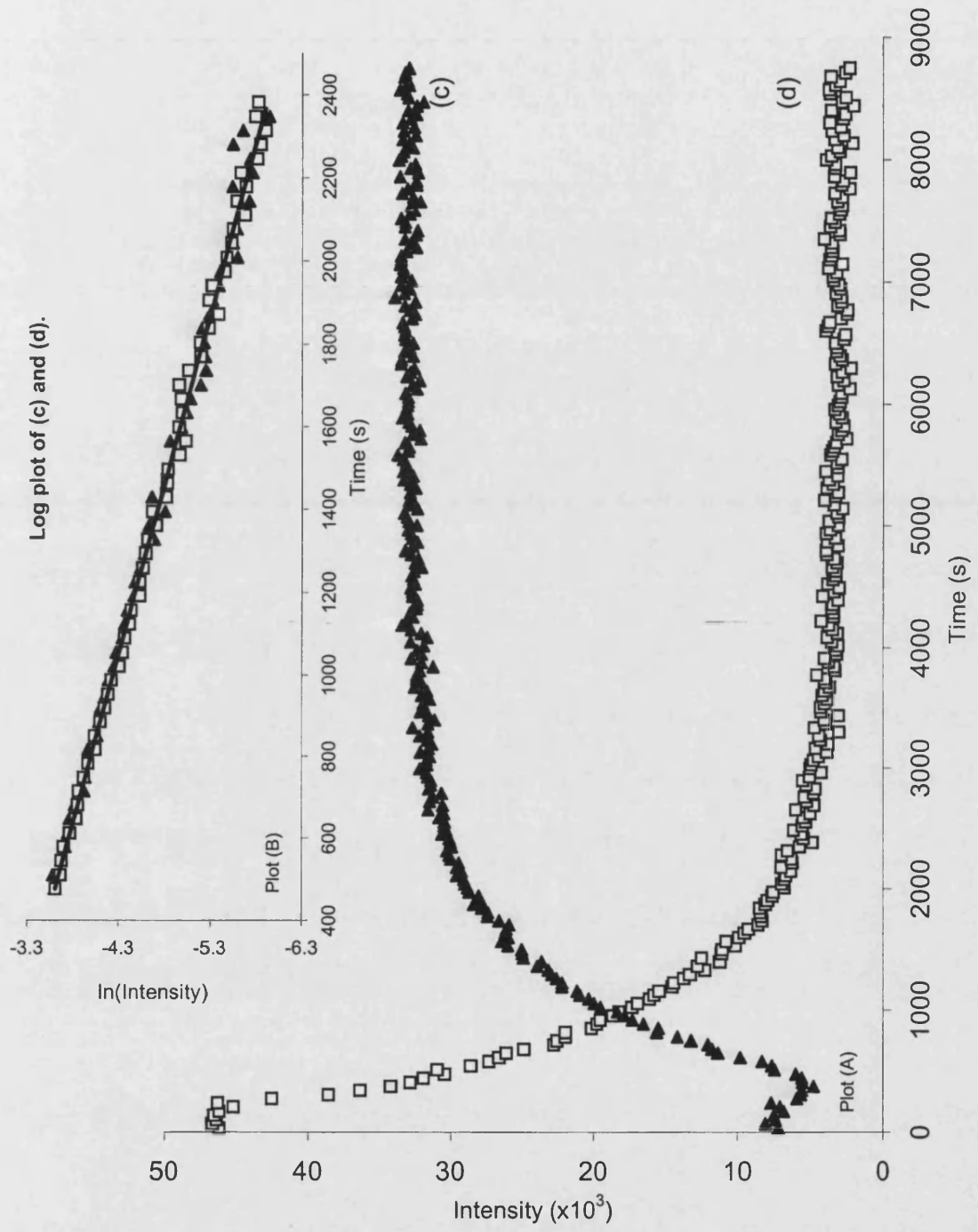

Graph 2.2. *Plot (A): Plotting the variation in intensity of the **(61a)** curve (d), and of **(62a)** curve (c).*

Plot (B): Determination of the rate constant.

2.2.3. Influence of the nature of the alkene and ketone upon the IR signals of the Ru-CO species.

When toluene solutions of **(1)** were reacted with CH_2=$CHSiR_3$ (R= OEt **(60a)**, Me **(60b)**, Ph **(60c)**) **[Table 2.1., Run 1, 3, 5]** at 100 °C and followed by IR, rapid depletion of the band due to **(1)** at 1941 cm^{-1} was observed. New species appeared depending on the nature of the alkene substrate with absorption bands at 1918 cm^{-1} (R = OEt, Run 1), 1920 cm^{-1} (R = Me, Run 3) and 1925 cm^{-1} (R = Ph, Run 5) **[Figure 2.7.]**. A close look at the observed rate constants for Runs 1, 3, and 5 **[Table 2.1]** shows that the k_{obs} of reaction (decay and formation) is largely influenced by the nature of the alkene. These can be scaled down as k_{obs} **(60b)** > k_{obs} **(60c)** > k_{obs} **(60a)**, which implies a faster reaction of **(1)** with **(60b)** rather than with **(60a)**.

This observed reactivity of **(1)** with vinylsilane alkenes **(60a-c)** suggests that the newly formed species is alkene dependant. On the basis of reported work,[22] it would seem rational to suspect a $Ru(PPh_3)_2(CO)$(alkene) species to be formed. Nevertheless the observed IR bands (1918, 1920, and 1925 cm^{-1}) are inconsistent with the formation of a Ru(0) species[23,24] and are more in line with Ru(II) species.[25] Therefore we must conclude that although the final product of these reactions is not a $Ru(PPh_3)_2(CO)$(alkene) species, alkene must somehow be involved in the nature of this species.

In a similar way, when repeated under the same reaction conditions but by using an equimolar mixture of **(61a)** and CH_2=$CHSiR_3$ **[Table 2.1., Run 2, 4, 6]**, depletion of **(1)** was observed and new species appeared which showed an absorption band at 1910 cm^{-1} (Run 2), 1920 cm^{-1} (Run 4), and 1925 cm^{-1} (Run 6) **[Figure 2.7.]**. The rate of growth of these new species was found to be fairly similar, and to be independent of the nature of the ketone. In fact when comparing Run 3 to 4 and 5 to 6, it appears that a similar species is observed independently to the presence of **(61a)** **(NB:** the peculiarity observed in Run 1 / 2 is discussed in **Chapter 2.2.9.**). Finally addition of **(61a)** to the reaction mixture resulted in a decrease of the rate of formation of these new species.

These measurements point out that the product species is unaffected by the presence of ketone if the alkene is either CH_2=$CHSiMe_3$ or CH_2=$CHSiPh_3$. However peculiar behaviour is observed in the case of CH_2=$CHSi(OEt)_3$, point which will be reviewed later in this chapter on the basis of further observations.

Finally the fact that k_{obs} of product formation (or loss) is slowed down when ketone, and alkene is introduced simultaneously into the system suggests that the observed rate for this overall process is the rate determining step **[Figure 2.6.]**.

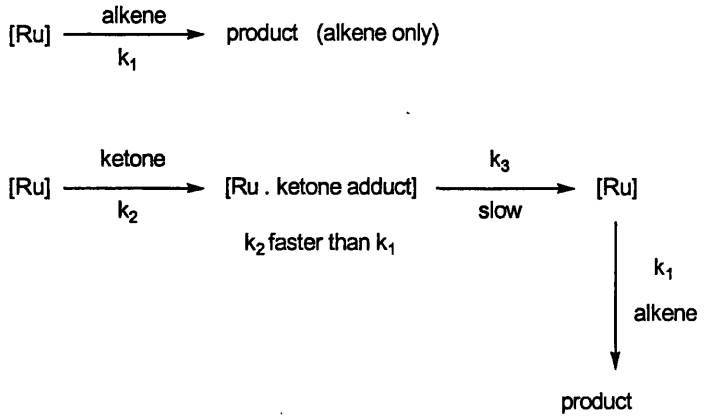

k_3 (breakdown of ketone adduct) is rate determining step

Figure 2.6.

Run	(1) with:	IR Band of (1)	Heating at 100 °C	IR band of final Ru species	k_{obs} (s^{-1})
1	(60a)	1941 cm^{-1}	⇒	1918 cm^{-1}	3.50 x 10^{-3}
2	(60a) + (61a)	1941 cm^{-1}	⇒	1910 cm^{-1}	1.25 x 10^{-3}
3	(60b)	1941 cm^{-1}	⇒	1920 cm^{-1}	4.35 x 10^{-3}
4	(60b) + (61a)	1941 cm^{-1}	⇒	1920 cm^{-1}	1.31 x 10^{-3}
5	(60c)	1941 cm^{-1}	⇒	1926 cm^{-1}	3.75 x 10^{-3}
6	(60c) + (61a)	1941 cm^{-1}	⇒	1925 cm^{-1}⇒	1.28 x 10^{-3}

Table 2.1. - *Reaction of (1) with various alkenes (60a - c) and/or (61a).*

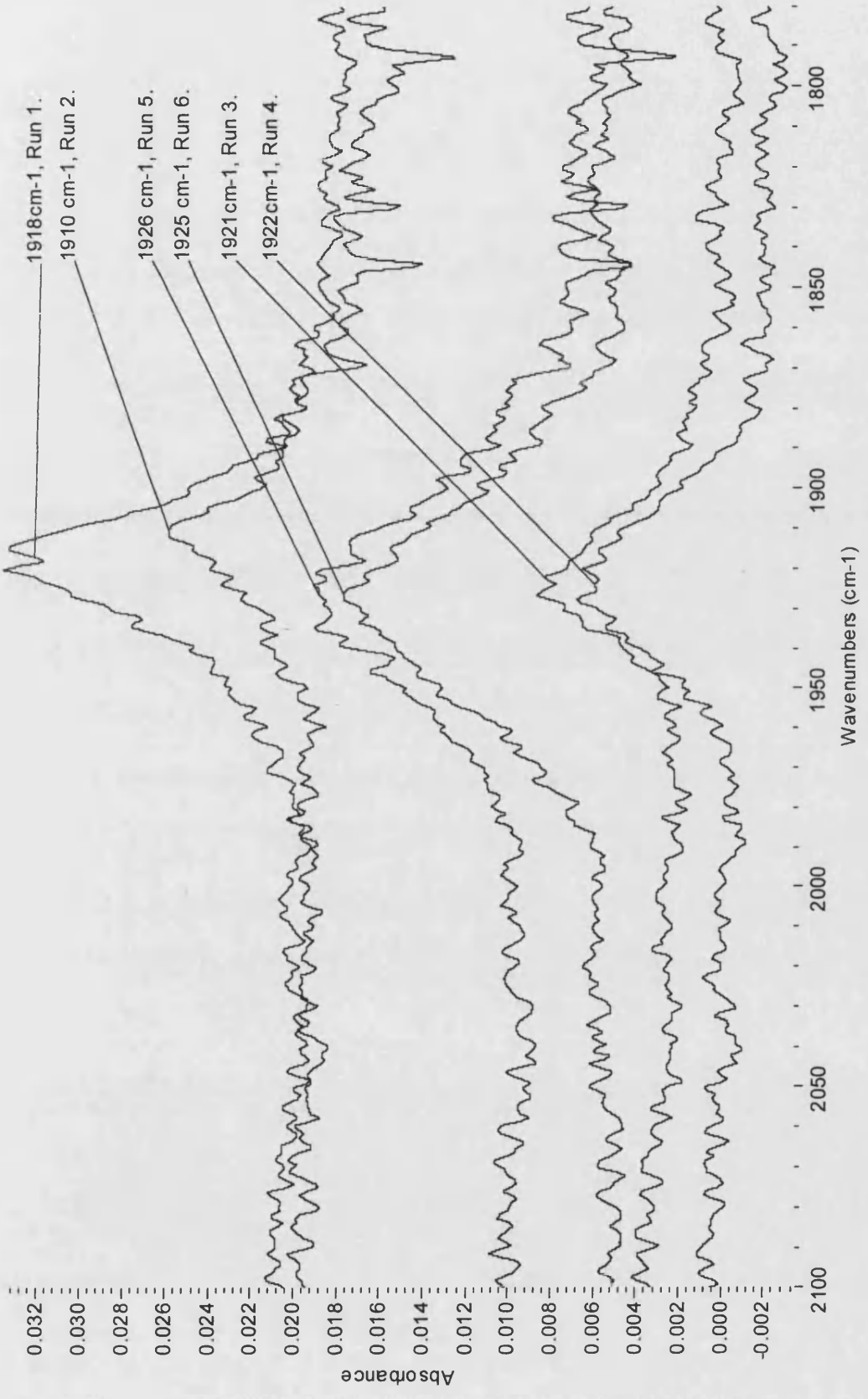

Figure 2.7. - *New absorption band seen for the new ν(Ru-CO) species seen in runs 1, 2, 3, 4, 5, 6.*

2.2.4. Influence of alkene on the rate of formation of C-C coupling product.

The kinetic measurements reported in this section (by means of k_{obs}), come from monitoring the carbonyl bond for the ketone and the C-C coupled product.

2.2.4.1. Influence of the concentration of (60a).

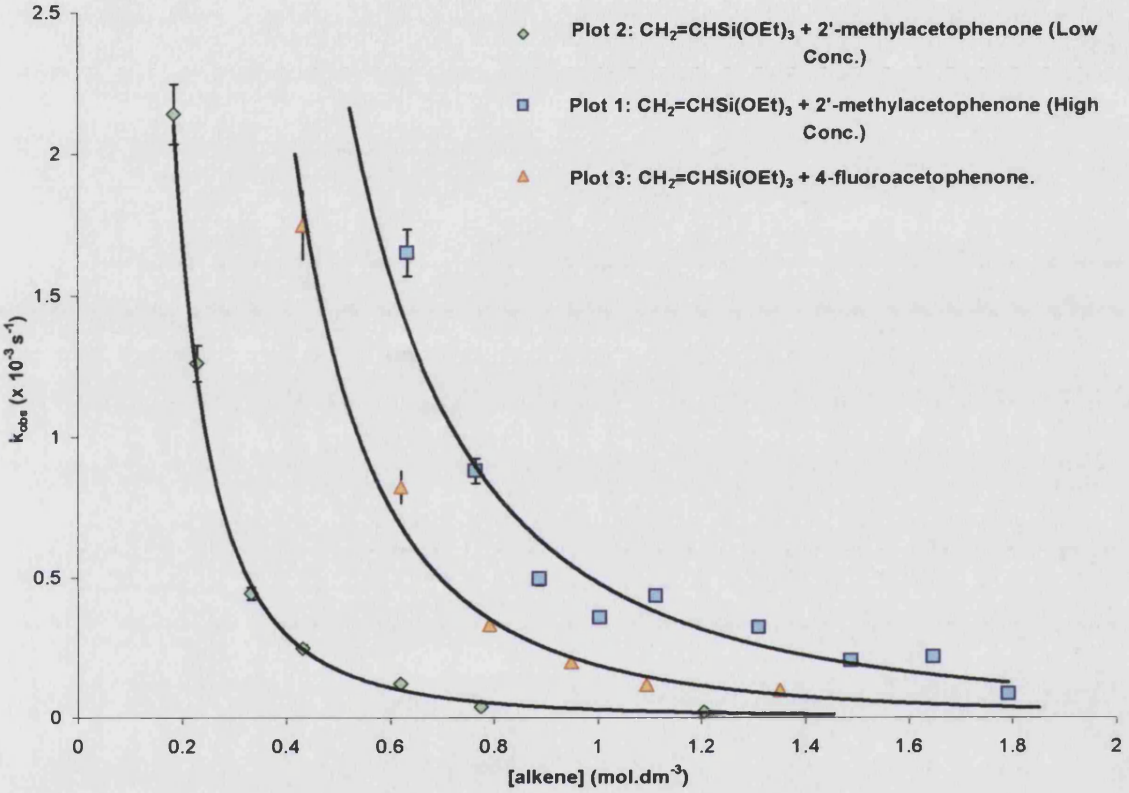

Graph 2.3. - *Plot of k_{obs} vs [60a].*

When first examined, a relatively concentrated mixture was used with **(1)** (9.9×10^{-5} mol), **(61a)** (9.9×10^{-4} mol), and **(60a)** ($0.3 - 4 \times 10^{-3}$ mol) in 2 ml of toluene, which resulted in Plot 1 on **Graph. 2.3.**. Surprisingly as the concentration of **(60a)** increased, the rate of the reaction rapidly decreases approaching a very slow conversion at high concentration. To probe whether this inhibition was the result of high concentrations giving a highly viscous solution, analogous measurements on a dilute mixture were performed. Thus using concentrations of **(1)** / **(60a)** / **(61a)** of respectively $5\ 10^{-5}$ mol / $0.5\text{-}2\ 10^{-3}$ mol / $0.5\ 10^{-3}$ mol in 2 ml of toluene gave the variation with alkene concentration show in Plot 2, **Graph 2.3.** i.e. the same pattern as seen for the higher concentration system. The inhibitory effect was seen to be independent of the nature of the ketone used; the same trend was observed using **(61b)** instead of **(61a)** **[Graph 2.3., Plot 3].**

Preliminary evidence from NMR studies suggests that the retardation, certainly at high concentrations of **(60a)**, arises from a side reaction between **(1)** and **(60a)** **[See Chapter 2.2.9.]**.

2.2.4.2. Effects on k_{obs} of varying the concentration of (60b) and (60c).

The influence of the alkene concentration was further investigated by means of the silyl substituted alkene derivatives **(60b)** and **(60c)**. A plot showing the observed rate constants for formation of 2'-methyl-6'-[2-(trimethyl)ethyl]acetophenone **(62b)** as a function of the concentration of **(60b)** is shown in Plot 2, **Graph. 2.4.** A plot of k_{obs} versus **[60b]** is linear and gives a second order rate constant for reaction of 8.5×10^{-3} $dm^3.mol^{-1}.s^{-1}$. When **(60b)** was replaced by **(60c)**, the variation of k_{obs} with [alkene] was also linear **[Graph 2.4., Plot 3]**, but now the second order rate constant k_1 is approximately 3 times slower at 3.3×10^{-3} $dm^3.mol^{-1}.s^{-1}$

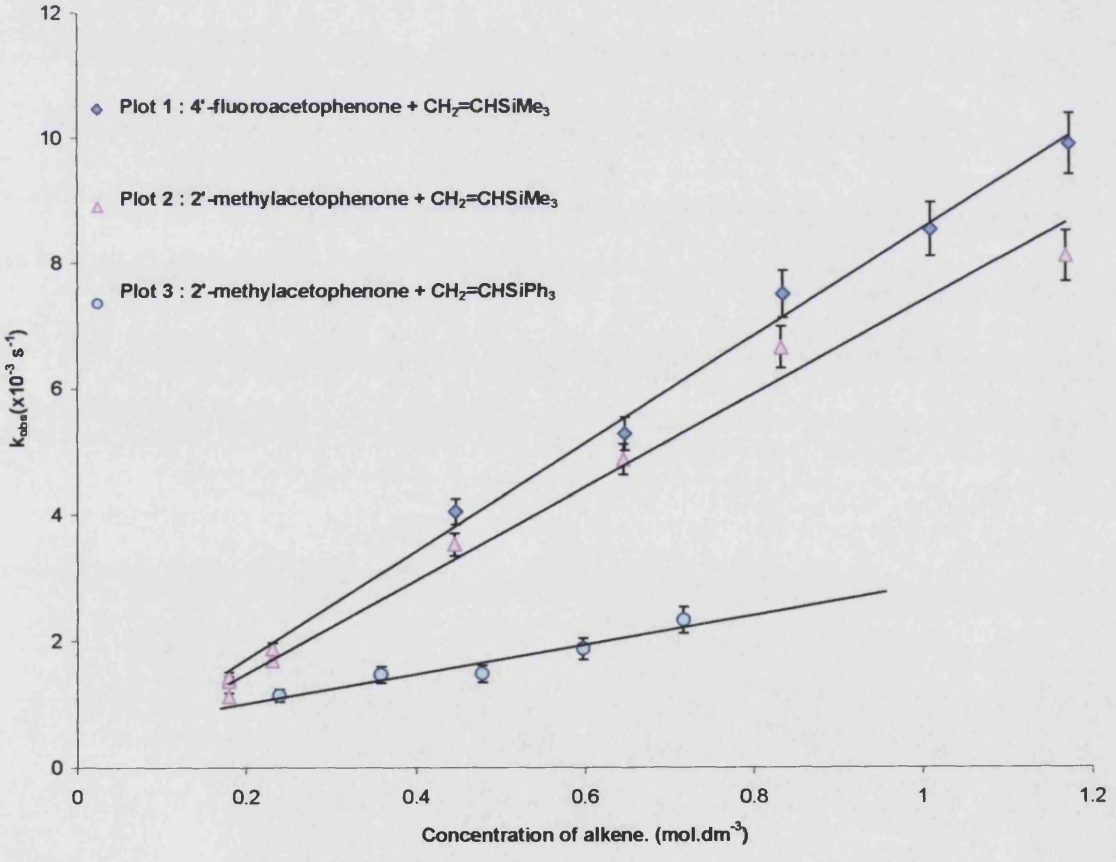

Graph. 2.4. - *Variation of **[60b]** or **[60c]** with **(61a)** or **(61b)** and **(1)**.*

When the ketone was changed from **(61a)** to **(61b)** and the value of the rate constant monitored as a function of **[60b]** (varied from 0.4 - 1.1 mol.dm^{-3}) a clear variation of k_{obs} was seen with a second order rate constant of 7.4 10^{-3} dm^3.mol^{-1}.s^{-1} **[Graph 2.4., Plot1]**. This value is with experimental errors of that in Plot 2 **[Graph 2.4.]** suggesting that the rate of reaction of **(60b)** with ketone is independent of the nature of the ketone. The smaller value of k_1 for **(60c)** may reflect either a steric or electronic effect or a combination of both.

2.2.5. Effect of ketone concentration on rate of formation of C-C coupling product.

2.2.5.1. Influence of the concentration of (61a)

Following the same pattern, varying the concentration **(61a)** from (0.18 to 1.2 mol.dm^{-3} with a ratio of **(1)** / **(60a)** of (5 x 10^{-5} mol / 0.5 x 10^{-3} mol) in 2 ml of toluene resulted in **Graph. 2.5.**. As seen from **Graph 2.5.**, a peculiar influence of the concentration of **(61a)** on k_{obs} is observed. In fact, as the concentration of ketone increased, the rate was found to increase linearly up to a maximum and then decrease linearly. Interestingly the maximum rate occurs at an alkene : ketone ratio of 1 : 2.

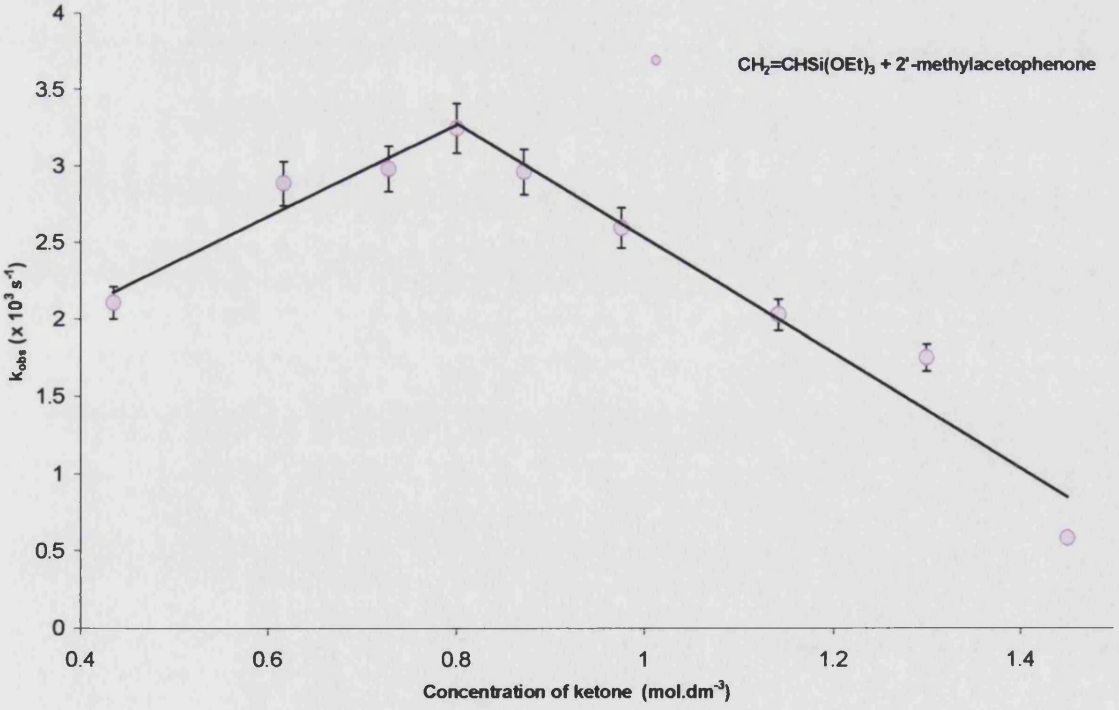

Graph. 2.5. - *Variation of [61a] with (60a) and (1).*

2.2.5.2. Variation of the concentration of (61a) or (61b) with (60b) or (60c).

To probe whether this unexpected influence of ketone concentration was peculiar to the use of **(61a)**, we changed the alkene to both **(60b)** and **(60c)**. The resulting trends are shown in **Graph 2.6.** (Plot 1 for **(60b)** and Plot 2 for **(60c)).** In both cases the rate dependence for the conversion of ketone showed no major change in the profile already seen with **(60a)**. Again, maximum rates are achieved with a ratio of alkene to ketone of 1:2.

Upon changing from **(61a)** to **(61b)** an apparent linear variation of k_{obs} with [ketone] was seen using **(60b)**. However, 4-fluoroacetophenone can undergo C-C coupling at the two available sites *ortho* to the ketone group. Thus the data in Plot 3 **[Graph 2.6.]** is not comparable to that in either Plot 1 or 2.

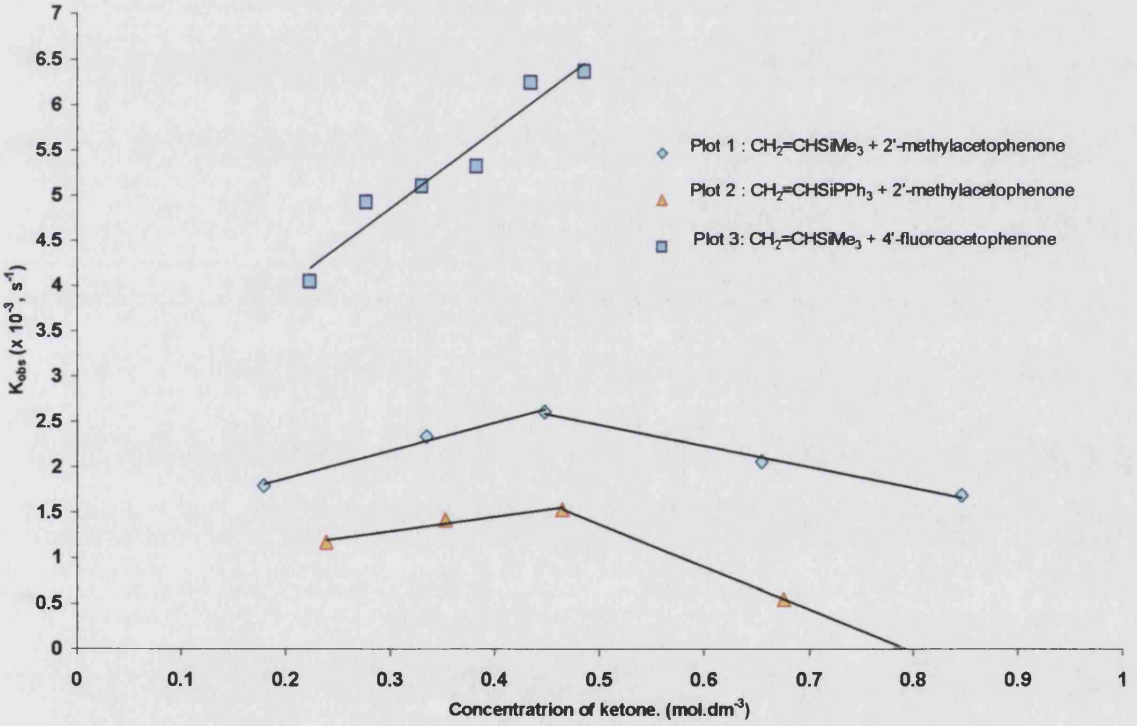

Graph. 2.6 - *Kinetic effect of the concentration of the **(61a)** or **(61b)** the rate of the Murai reaction using **(60b)**, or **(60c)** with **(1)**.*

2.2.6. Influence of the catalyst concentration.

In order to improve our understanding of the chemistry of the Murai reaction, the effect of varying the concentration of **(1)** on the rate of the C-C coupling product was investigated. The concentration of catalyst precursor was varied from 0.01 $mol.dm^{-3}$ to 0.05 $mol.dm^{-3}$, keeping the concentration of the ketones and alkenes substrates constant (0.5 x 10^{-3} mol). As expected the rate of conversion of ketone was found to be linearly dependent on the concentration of the ruthenium complex **[Graph. 2.7.]**.

When using **(60b)** with either **(61a) [Graph 2.7., Plot 2]** or **(61b) [Graph 2.7.,** Plot 3**]** a first order dependence of the reaction upon the concentration of catalyst was observed which passes through the origin. However although a linear dependence of the rate is observed using **(60a)** and **(61a) [Graph 2.7., Plot 1]**, it does not appear to be strictly first order with a highly negative intercept. Analysis of Plot 1, shows that excess of **(1)** must be introduced into the system before any reaction is observed. This observation suggests that **(1)** is being consumed by some side reaction **[See Chapter 2.2.9.]** rather than performing catalysis.

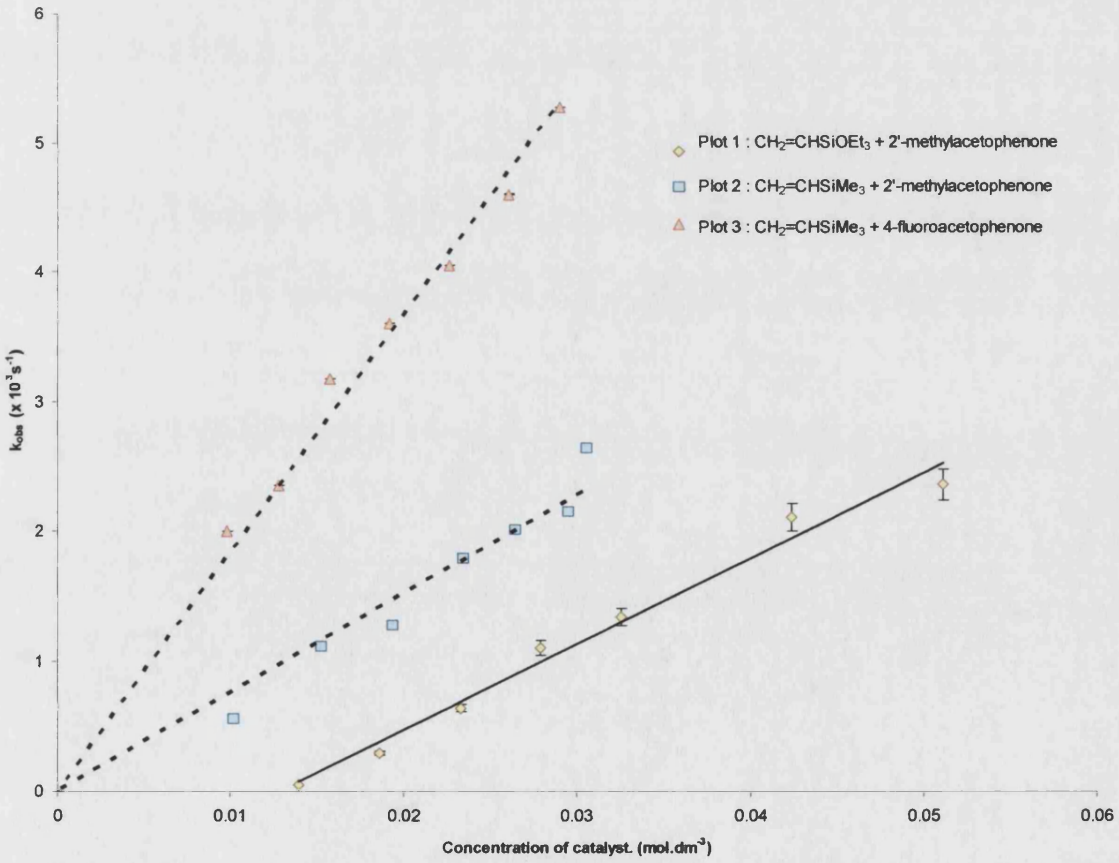

Graph. 2.7. - *Kinetic effect of the concentration of (1) on the rate of the Murai reaction.*

2.2.7. Influence of triphenylphosphine concentration.

It has been suggested by various authors[3,21,22] that free triphenylphosphine must be produced during the reaction of **(1)** with the alkene substrate to produce the active catalyst, **[Scheme 2.7.]**. Therefore we looked at the effect of adding free triphenylphosphine to the reaction mixture.

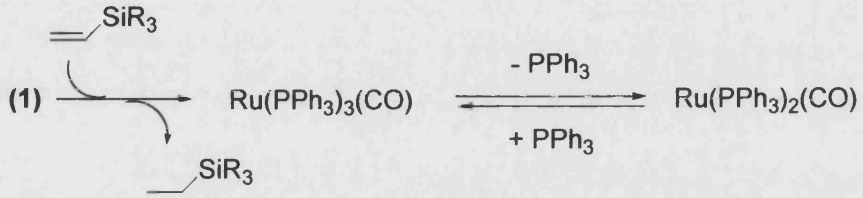

Scheme 2.7.

As seen from **Graph 2.8.** addition of triphenylphosphine to the reaction mixture resulted in a non linear decrease of the rate of the reaction. This inhibition of k_{obs} upon addition of PPh_3 suggests that the proposed loss of phosphine from the catalyst precursor does occur during the first step of the reaction. Nevertheless the non-linear behaviour implies that at higher concentration of PPh_3, other coordinatively unsaturated species may also be undergoing trapping by phosphine.

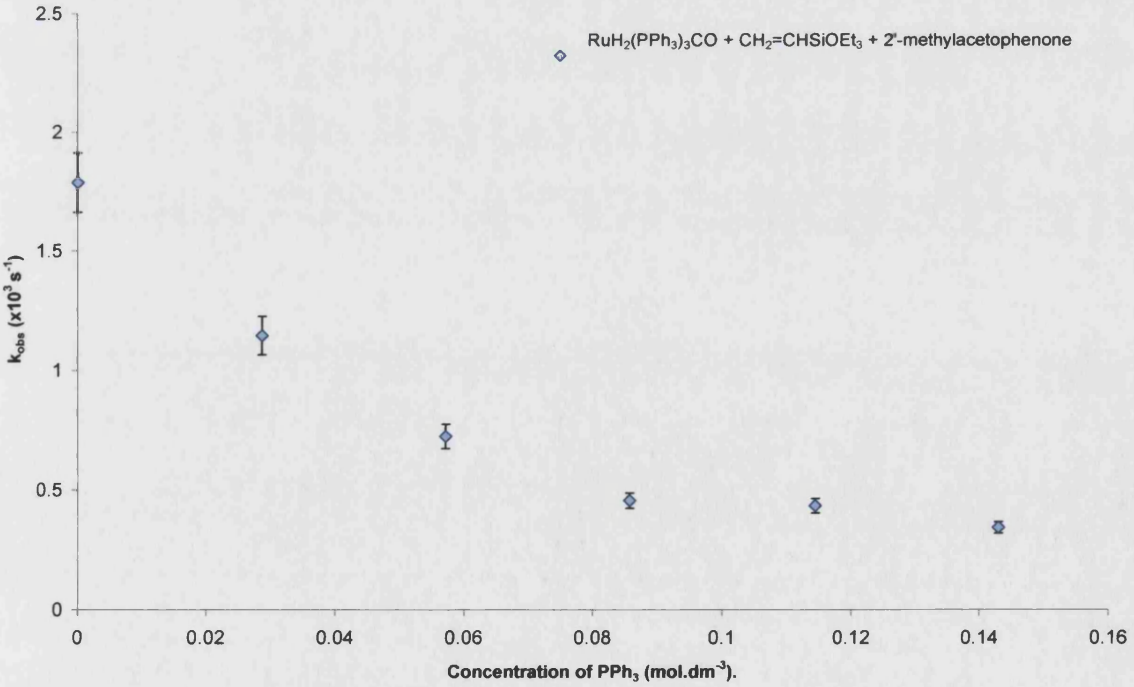

Graph. 2.8. - *Kinetic effect of the concentration of triphenylphosphine on the rate of the Murai reaction.* ***[(1) / (60a) / (61a) :*** *5×10^{-5} mol / 0.5×10^{-3} mol / 0.5×10^{-3}]*

2.2.8. Temperature effects on the Murai reaction.

In order to gain more insight into the reaction mechanism the activation parameters of the reaction were considered. This study was achieved by varying the temperature from 358 K to 403 K for a solution consisting of **(1)** ($9.9\ 10^{-5}$ mol) with either **(61a)**, or **(61b)** ($0.18\ 10^{-3}$ mol) and either **(60a)**, **(60b)**, or **(60c)** ($0.18\ 10^{-3}$ mol) in 2 ml of toluene.

In each case the rate of the reaction was found to proceed as expected, with k_{obs} increasing as a function of the temperature as demonstrated in **Graph 2.9.**

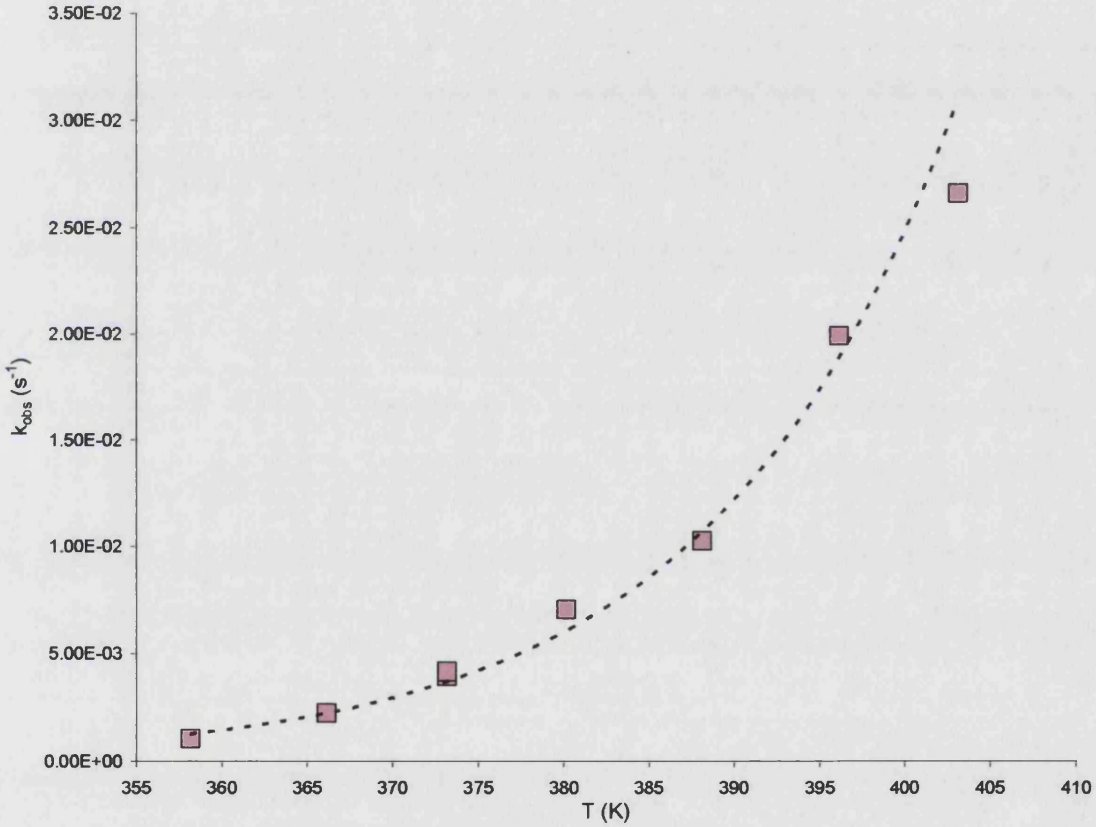

Graph. 2.9. *Example of the observed variation of the rate constant depending on the reaction temperature represented here for* ***(60b)*** *with* ***(61b).***

The activation parameters where calculated using the Arrhenius equation:

$$k = A \cdot e^{-Ea/RT}$$

where: k is the rate constant for the reaction.
A the pre-exponential factor.
E_a energy of activation.
R = 8.31433 (gas constant).
T the temperature in Kelvin.

A plot of $\{\ln(k_{obs})$ vs $1/T\} \Leftrightarrow \{ \ln (k_{obs}) = (- E_a / RT) + \ln A$ gives a straight line of slope $-E_a / RT$ from which is derived the E_a of the reaction (E_a = (slope) . R) as shown in **Graph 2.10.** and **Graph 2.11.** The activation energies for all the reactions are summarised in **Table 2.2.**

Since the activation energy is a function of the free energy of the reaction, it was possible to deduce the enthalpy and entropy of activation of the reaction **[Table 2.2.]** by plotting $\ln (k_{obs} / T)$ vs $1 / T$ (Eyring equation) **[Graph 2.12.]**.

$$\ln (k / T) = - (\Delta H^{\neq} / RT) + \ln (K / h) + (\Delta S^{\neq} / R)$$

where: **k** is the rate constant for the reaction.
$\Delta H^{\neq}$ the enthalpy of activation ($kJ.mol^{-1}$)
$\Delta S^{\neq}$ the entropy of activation ($J.mol^{-1}.K^{-1}$)
R = 8.31433 gas constant. **K** = 1.38×10^{-23} JK^{-1} (Boltzman constant)
T the temperature in Kelvin. **h** = 6.6×10^{-34} (Planck constant)

The activation parameters of the reaction extracted from the temperature dependence experiments on the reactivity of 2'-methylacetophenone towards CH_2=$CHSiR_3$ (R= OEt, Me, Ph) and $Ru(PPh_3)_3(CO)H_2$ were found to be very similar. The activation parameters for various sets of alkenes and ketones were deduced. At this stage it is not certain to what extent these relate to a particular step in the reaction. Therefore further investigations are required in order to assert these to a step of the reaction **[Table 2.2.]**.

Alkene	Temperature, K	$10^3 k_{obs}$ (s^{-1})	Ea ($kJ.mol^{-1}$)	$\Delta H^{\neq}$ ($kJ.mol^{-1}$)	$\Delta S^{\neq}$ ($J.mol^{-1}.K^{-1}$)
Triethoxyvinylsilane	358	0.314			
+	373	1.44			
2'-methylacetophenone	380	1.78			
	388	1.94			
	396	3.01			
	403	3.72	58.4	55.3	156.0
Trimethylvinylsilane	358	0.709			
+	366	1.23			
2'-methylacetophenone	373	1.88			
	380	2.85			
	388	4.26			
	403	5.83	69.2	66.1	122.0
Triphenylvinylsilane	358	0.48			
+	366	0.77			
2'-methylacetophenone	373	1.42			
	388	1.98			
	403	4.10	60.3	57.1	149.8
Triethoxyvinylsilane	358	0.56			
+	366	0.81			
4-fluroacetophenone	373	1.95			
	380	2.63			
	388	3.17			
	396	9.71			
	403	10.50	81.3	78.2	71.1
Trimethylvinylsilane	358	1.05			
+	366	2.25			
4-fluoroacetophenone	373	4.05			
	380	7.05			
	388	10.30			
	396	19.90			
	403	26.60	86.1	82.9	90.8

Table 2.2. - *Activation parameters for the Murai reaction.*

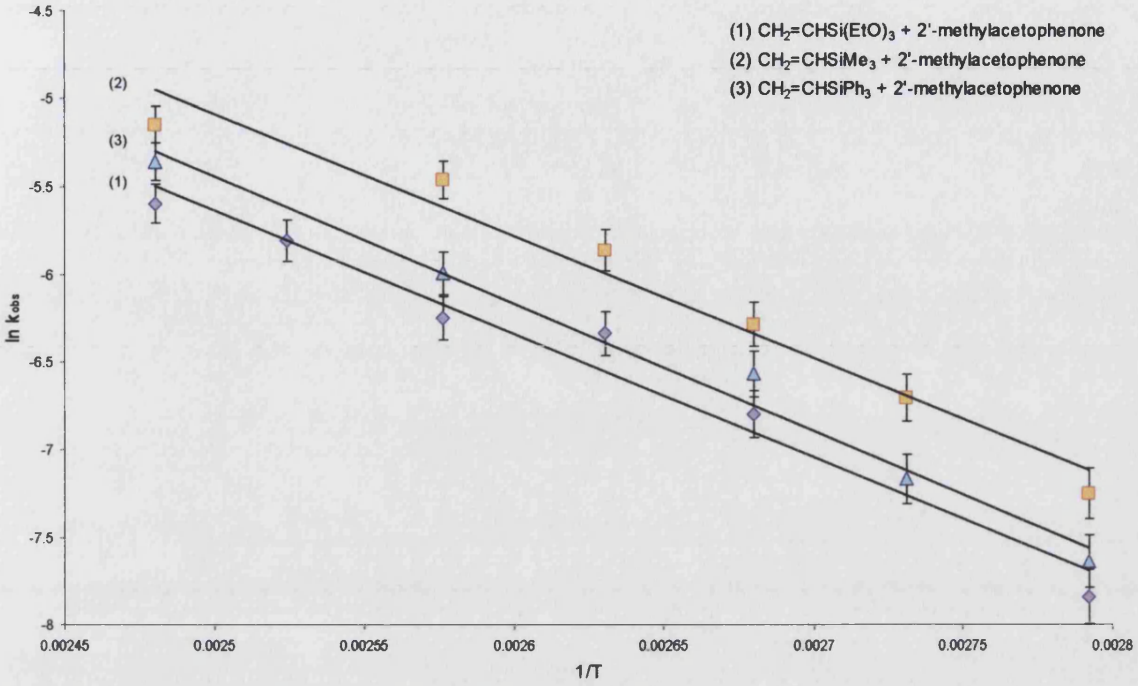

Graph. 2.10. - *Plot of ln(k_{obs}) vs 1/T for* ***(61a)*** *with* ***(60 a - c)***

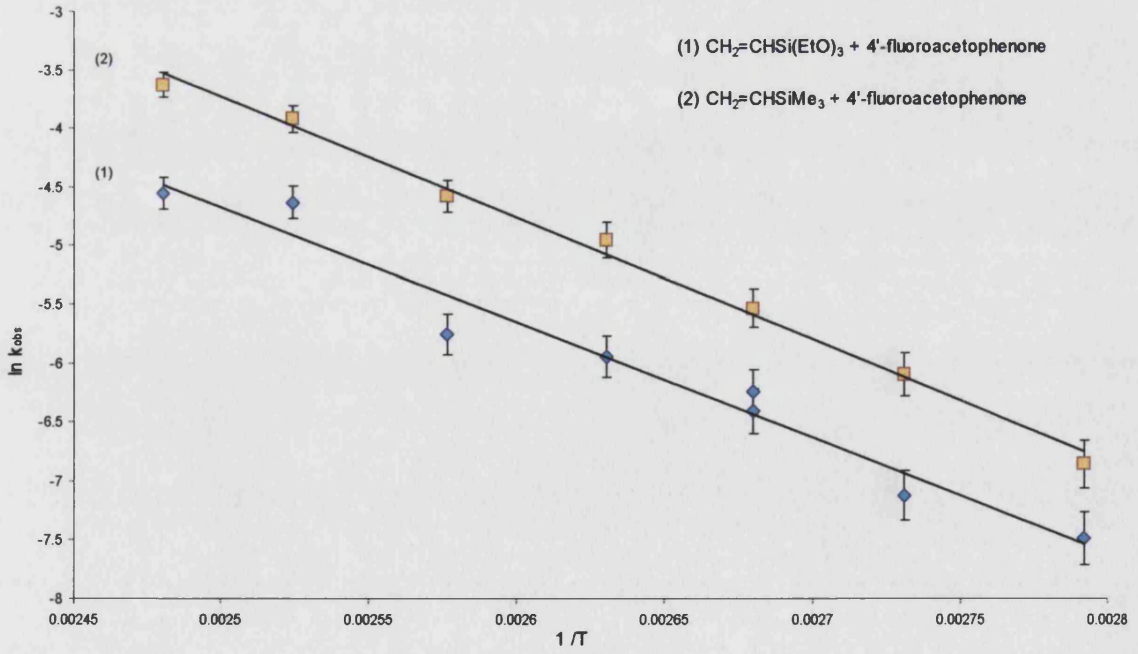

Graph. 2.11. - *Plot of ln(k_{obs}) vs 1/T for* ***(61b)*** *with* ***(60 a, b).***

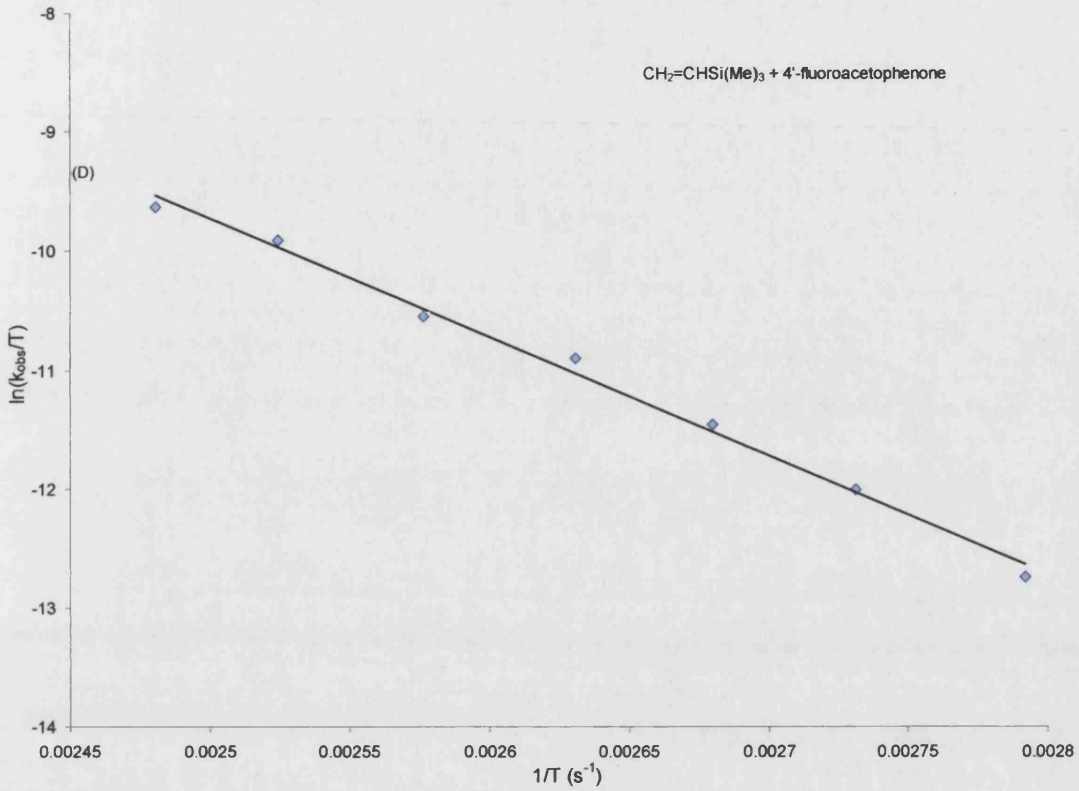

Graph. 2.12. - *Plot of ln(k_{obs}) vs 1/T for* ***(60a)*** *with* ***(61 b)***

2.2.9. NMR investigation of the reaction of (1) with (60a)

In order to understand the surprising reactivity seen between **(1)** and CH_2=CHSi(OEt)$_3$ **(60a)**, NMR investigations on this reaction were conducted. The reaction of **(1)** with a 2 fold excess of **(60a)** was carried out at 120 °C. After 5 min, the $^{31}P\{^1H\}$ spectrum of the resulting solution showed formation of two new species, one showing a singlet at 50.9 ppm and the other displaying a doublet and triplet at 52.8 and -34.7 ppm (J_{PP} = 15.8 Hz). These two species were assigned to $Ru(CO)_2(PPh_3)_3$ **(3)** (on the basis of independent synthesis) and $Ru(PPh_3)_2(PPh_2(o\text{-}C_6H_4))(CO)H$ **(23) [See Chapter 3.2.2.1.] [Scheme 2.8.]**. After one hour **(3)** was dominant and full conversion was observed after 5 hours.

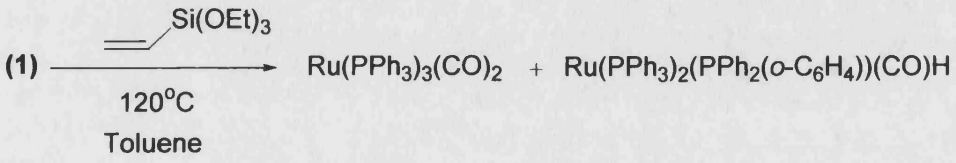

Scheme 2.8.

The importance of the concentration of **(60a)** was probed by reacting **(1)** with a 20 fold excess of **(60a)** resulting in the full conversion of **(1)** into **(3)** after two hours at 120 °C. Furthermore, the formation of another species displaying a singlet at 56.6 ppm was observed after 5 hours. This proved to be $Ru(CO)_3(PPh_3)_2$ **(4)** **[Scheme 2.9.]**.

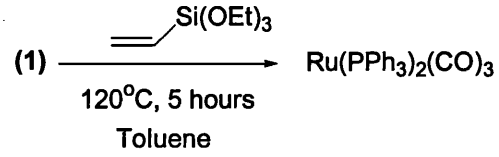

Scheme 2.9.

On the basis of these observations we propose that decarboxylation of the ethoxy group of the **(60a)** must occur, leading to formation of the catalytically less active **(3)** and **(4)** **[See Chapter 3.2.1.5.]**. In order to verify the possibility of decarboxylation of the ethoxy moiety by the species formed upon reaction of **(1)** with an alkene, we decided to react **(1)** in ethanol under one atmosphere of ethene at 120 °C for 2 hours which resulted in complete conversion of **(1)** into **(4)** **[Scheme 2.10.]**.

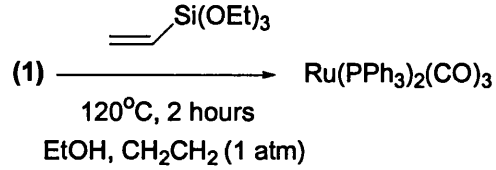

Scheme 2.10.

Finally the side reaction described in **Scheme 2.10.** was probed under catalytic conditions by reacting a 1:10:60 mixture of **(1)** / **(60a)** / **(61a)** at 120°C. After 1 hour partial formation of **(62a)** was observed along with **(3)** and **(4)** (detected by $^{31}P\{^1H\}$ NMR) **[Scheme 2.11.]**. **NB:** Formation of **(3)** was also observed when reacting a 1:10:10 mixture of **(1)** / **(60a)** / **(61a)**.

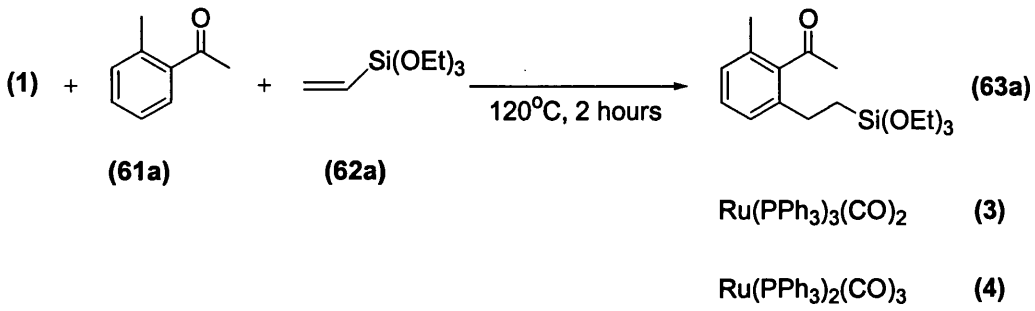

Scheme 2.11.

Decarboxylation of alcohols has been observed previously, such as decarboxylation of EtOH by $Ru(PPh_3)_3(H_2)H_2$.[25] Decarboxylation of alkenes with alkoxysilyl substituents have been reported by Komiya et al who proposed a mechanism for the reactions involving the cleavage of C-O, Si-O and OC-CH_n bonds as key steps.[26] Finally Hiraki et al. have observed the formation of di- and tricarbonylruthenium(0) species from **(1)** via decarboxylation of methyl benzoates.[22]

2.3. Conclusion.

Although the IR study of the catalytic addition of aromatic carbon-hydrogen bonds to alkenes with the aid of ruthenium complexes proved initially to be more complicated than our first expectations, our work has proven the viability of the FTIR / CIR technique to study such a catalytic process, leading to an important determination of kinetics.

We have observed the strong inhibition of the reaction in the presence of high concentrations of PPh_3, and **(60a)**. In the case of **(60a)** it has been shown that a side reaction occurs between **(1)** and **(60a)**, proceeding via decarboxylation of the ethoxy moiety leading to formation of un-reactive $Ru(PPh_3)_3(CO)_2$ and $Ru(PPh_3)_2(CO)_3$. Meanwhile the PPh_3 inhibition is consistent with the proposed loss of PPh_3 during the Murai reaction.

Kinetic experiments on the dependence of silyl alkene's concentration such as CH_2CHSiR_3 has shown the reaction to be first order in alkene concentration when R = Me and Ph. Moreover the importance of the R group on the silyl alkene has been observed leading to a side reaction in the case of **(60a)** and a lower activity of R = Ph relatively to R = Me.

We have observed a peculiar influence in ketone concentration which is found to be independent of the type of alkene used, leading to the observation of a two step process. In a first step a linear increase of the rate of the reaction upon addition of ketone is observed, followed by an inhibition step when a ratio of ketone to alkene equal to 2:1 is reached. We have not been able to determine whether this inhibition is due to a competition process between alkene / ketone coordination or to a side reaction between the ketone and the active catalytic species. At this point, further studies are required to try to fully understand this unusual kinetic data.

The reaction has shown to be first order in catalyst precursor and finally the activation parameters of the overall process have been determined.

This study represents the first kinetic insight in the Murai reaction and is followed by synthetic observations in **Chapter 3**.

2.4. Reference.

1. Kakuishi, F.; Murai, S. "*Topics in Organometallic Chemistry*", ed. By S. Murai, Springer-Verlag, Berlin, **1999**, 47.
2. Murai, S.; Kakuishi, F.; Sekine, S.; Tanaka, Y.; Kamatani, A.; Sonoda, M.; Chatani, N. *Nature*, **1993**, *366*, 529.
3. **(a)** Murai, S.; Kakuishi, F.; Sekine, S.; Tanaka, Y.; Kamatani, A.; Sonoda, M.; Chatani, N. *Pure Appl. Chem.*, **1994**, *66*, 1527. **(b)** Kakiushi, F.; Sekine, S.; Tanaka, Y.; Kamatani, A.; Sonoda, M.; Chatani, N.; Murai, S. *Bull. Chem. Soc. Jpn.*, **1995**, *68*, 62. **(c)** Murai, S.; Kakuishi, F.; Chatani, N. *Pure Appl. Chem.*, **1997**, *69*, 589. **(d)** Kakiuchi, F.; Sato, T.; Igi, N.; Chatani, N.; Murai, S. *Chem. Lett.*, **2001**, 386.
4. Fuji, N.; Kakiuchi, F.; Yamada, A.; Chatani, N.; Murai, S. *Bull .Chem. Soc. Jpn.*, **1998**, *71*, 285.
5. Murai, S.; Kakiuchi, F.; Sonoda, M.; Chatani, N. *J. Organomet. Chem.*, **1995**, *504*, 151.
6. **(a)** Kakiuchi, F.; Sato, T.; Yamaushi, M.; Chatani, N.; Murai, S. *Chem. Lett.*, **1999**, 19. **(b)** Chatani, N.; Asaumi, T.; Yorimitsu, S.; Ikeda, T.; Kakiushi, F.; Murai, S. *J. Am. Chem. Soc.*, **2001**, *123*, 10935.
7. Kakuishi, F.; Sonoda, M.; Chatani, N.; Murai, S. *Chem. Lett.*, **1996**, 111.
8. Kakuishi, F.; Tanaka, Y.; Sato, T.; Chatani, N. Murai S. *Chem. Lett.*, **1995**, 679.
9. **(a)** Guo, H.; Tapsak, M. A.; Weber, W. P. *Macromolecules*, **1995**, *28*, 4714. **(b)** Guo, H.; Wang, G.; Tapsak, M. A.; Weber, W. P. *Macromolecules*, **1995**, *28*, 5686. **(c)** Lu, P.; Paulasaari, J. K.; Weber, W.P. *Macromolecules*, **1996**, *29*, 8583. **(d)** Wang, G.; Guo, H.; Weber, W. P. *J. Organomet. Chem.*, **1996**, *521*, 531.
10. Grigg, R.; Savic, V. *Tetrahedron Lett.*, **1997**, *38*, 5737.
11. **(a)** Harris, P. W. R.; Woodgate, P. D. *J. Organomet. Chem.*, **1996**, *506*, 339. **(b)** Harris, P. W. R.; Woodgate, P. D. *J. Organomet. Chem.*, **1997**, *530*, 211.
12. Trost, B. M.; Imi, K.; Davies, I. W. *J. Am. Chem. Soc.*, **1995**, *117*, 5371.

13. Matsubara, T.; Koga, N.; Musaev, D. G., Morokuma, N., K. *J. Am. Chem. Soc.*, **1998**, *120*, 12692.

14. Matsubara, T.; Koga, N.; Musaev, D. G., Morokuma, N., K. *Organometallics*, **2000**, *19*, 2318.

15. Kakiuchi, F.; Murai, S. *Acc, Chem. Res.*, **2002**, *35*, 826.

16. Kakiuchi, F.; Ohtaki, H.; Sonoda, M.; Chatani, N.; Murai, S. *Chem. Lett.* **2001**, 918.

17. Matsubara, T.; Koga, N.; Musaev, D. G.; Morokuma, K. *J. Am. Chem. Soc.*, **1998**, *120*, 12692.

18. Matsubara, T.; Koga, N.; Musaev, D. G.; Morokuma, K. *Organometallics*, **2000**, *19*, 2318.

19. Moser, W. R.; Cnossen, J. E.; Wang, A. W.; Krouse, S. A.; *J. Catal.*, **1985**, *95*, 21.

20. **(a)** Maitlis, P. M.; Haynes, A.; Sunley, G. L.; Howard, M. J. *J. Chem. Soc., Dalton Trans.*, **1996**, 2187. **(b)** Ghaffar, T.; Adams, H.; Maitlis, P. M.; Sunley, G.J.; Baker, M. J.; Haynes, A. *Chem. Commun.*, **1998**, 1023.

21. Kawano, H.; Tanak, R.; Fujikawa, T.; Hiraki, K.; Onishi, M. *Chem. Lett.* **1999**, 401.

22. Hiraki, K.; Kira, S.; Kawano, H. *Bull. Chem. Soc. Jpn.*, **1997**, *70*, 1583.

23. Bohanna, C.; Estruelas, M. A.; Lahoz, F. J.; Onate, E.; Oro, L. A. Sola, E. *Organometallics*, **1995**, *14*, 4825.

24. Van Der Sluys, L.S.; Kubas, G. J.; Caulton, K. G. *Organometallics*, **1991**, *10*, 1033.

25. Van Der Sluys, L. S.; Kubas, G. J.; Caulton, K. G. *Organometallics*, **1991**, *10*, 1033.

26. Komiya, S.; Srivastava, R. S.; Yamamoto, A.; Yamamoto, T. *Organometallics*, **1985**, *4*, 1504.

Chapter 3.

Synthetic investigation of the Murai reaction.

3.1. Introduction

As seen in **Chapter 2** it was proposed that the remarkable regioselectivity for the position α to the ketone group in the Murai reaction is due to coordination of the carbonyl group to the ruthenium (so-called 'chelation assistance') to give intermediate **(b)** **[Scheme 3.1]**.[1] The *ortho* C-H bond sits in close proximity to the metal centre and can be easily activated to give the *ortho* metallated complex **(c)**. The importance of species such as **(b)** and **(c)** in the catalytic cycle has been reinforced by density functional calculations.[2,3]

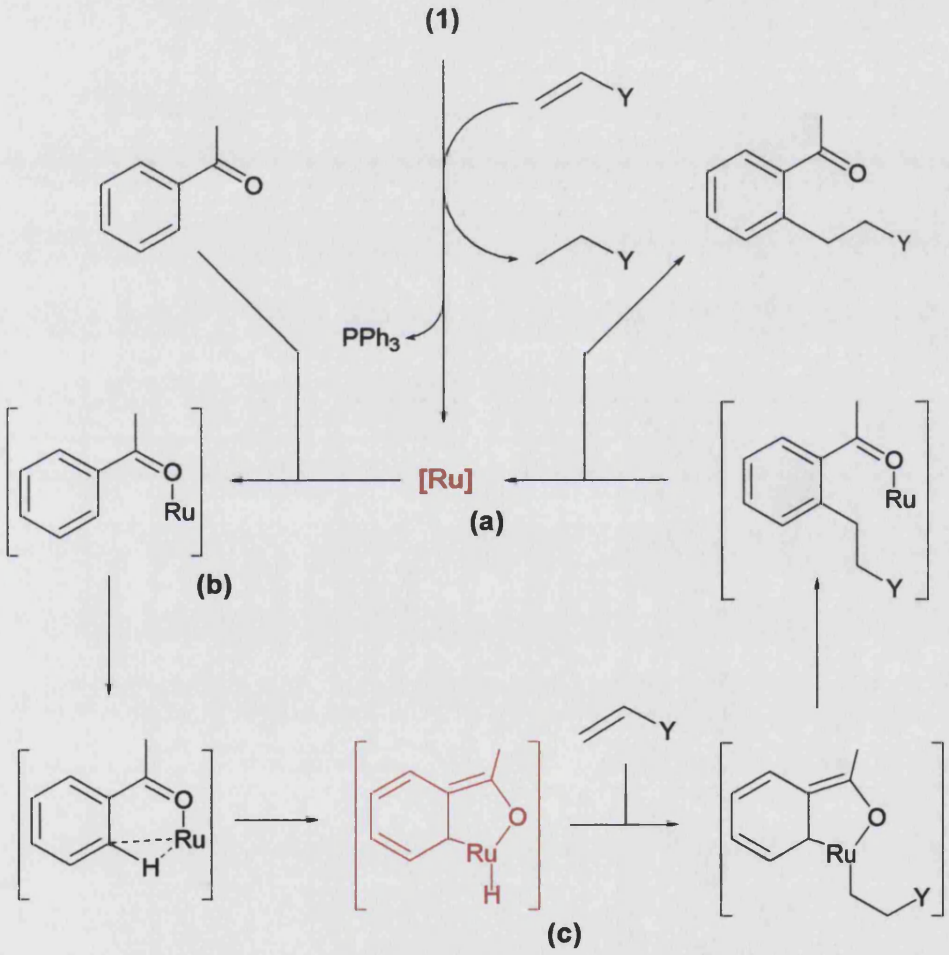

Scheme 3.1. - *Proposed mechanism for the Murai reaction.*

Other features of the above mechanistic cycle are of interest. In the first step, hydrogenation of the alkene by **(1)** yields a coordinatively unsaturated fragment **(a)**, which may be the 16-electron species $Ru(PPh_3)_3(CO)$. This would presumably be rapidly trapped by alkene to afford a ruthenium(0) alkene complex.

Fragmentation of $Ru(CO)(PPh_3)_3$(alkene) must occur in the next step of the cycle to provide a vacant coordination site for binding of the ketone and subsequent C-H activation, although it is not clear what other ligands are attached to ruthenium in this catalytically active species. The density functional studies have shown that the energies of activation for the *ortho-*, *meta-* and *para* C-H bonds in benzaldehyde by $Ru(PH_3)_3(CO)$ are remarkably similar and that only the 14-electron species $Ru(PH_3)_2(CO)$ displays preference exclusively for the *ortho* site.[2,3] This provides support for $Ru(PH_3)_2(CO)$ as a reasonable candidate as the active species for the Murai reaction.

In order to assess these observations and postulated mechanism, a synthetic approach has been used by several research groups,[4-7] leading to major observations. It has been shown by Weber et al. that **(1)** reacts with $(CH_2CH)_2SiMe_2$ in the presence of a stoichiometric amount of styrene to give the zero-valent ruthenium alkene complex $Ru(PPh_3)_2(CO)[\eta\text{-}(CH_2{=}CH)SiMe_2]$ **(7) [Scheme 3.2.]**.[4]

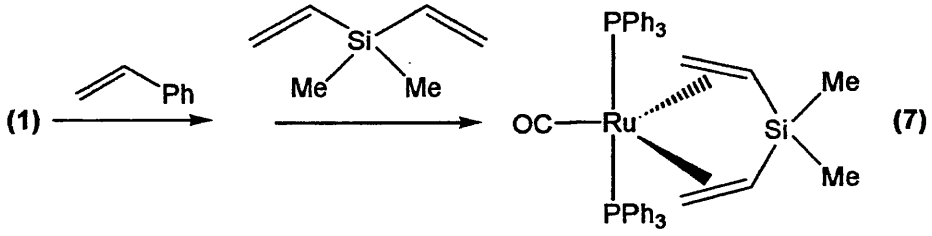

Scheme 3.2.

Further work by these authors later demonstrated that **(1)** reacts with a stoichiometric amount of styrene followed by *o*-acetylstyrene to give the alkene complex $[Ru(PPh_3)_2(CO)\{CH_3C(O)C_6H_4CH{=}CH_2\}]$ in which both the C=O and C=C groups are bonded to the metal centre **[Scheme 3.3.]**.[5]

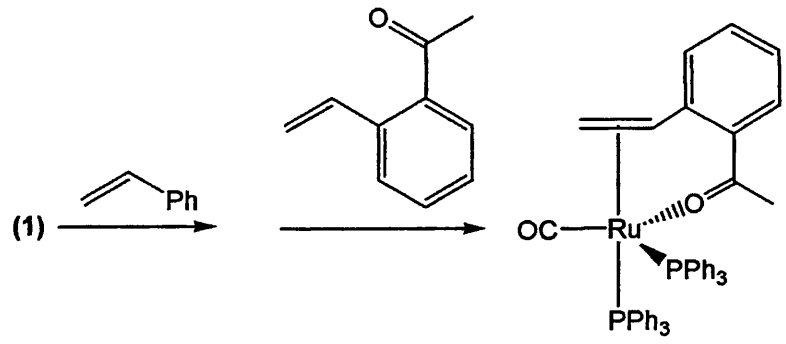

Scheme 3.3.

In contrast to high temperatures required for Murai catalysis with **(1)**, Chaudret and co-workers have recently reported that $Ru(PCy_3)_2H_2(H_2)_2$ (6) acts as a precursor for the coupling of ethene with acetophenone or benzophenone at room temperature.[6] The *ortho*metallated species $Ru(PCy_3)_2(o\text{-}C_6H_4C(O)X)(L)H$ (X = CH_3 or C_6H_5, L = H_2 or CO) have been directly prepared from $Ru(PCy_3)_2H_2(H_2)_2$ and also function as catalysts in the case of L = H_2, but not if L = CO **[Scheme 3.4.]**.

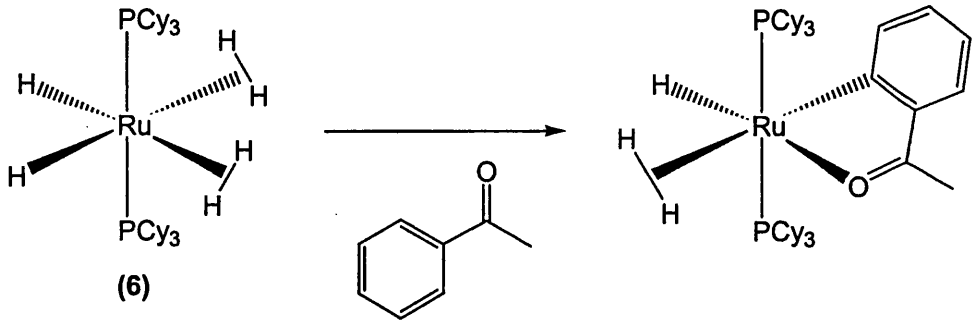

Scheme 3.4.

In a later example, Drouin et al. have reported that the *ortho* metallated Ru(1,4-bis(dicyclohexylphosphino)butane)(CO)[$OC(C_6H_4)(Ph)$]H shows modest activity but improved stability over the PCy_3 systems, which were unstable at elevated temperatures **[Scheme 3.5.]**.[7] Thus, 58% conversion of benzophenone to 2-ethylbenzophenone is found after 22 h at 60°C under 260 psi of ethene.

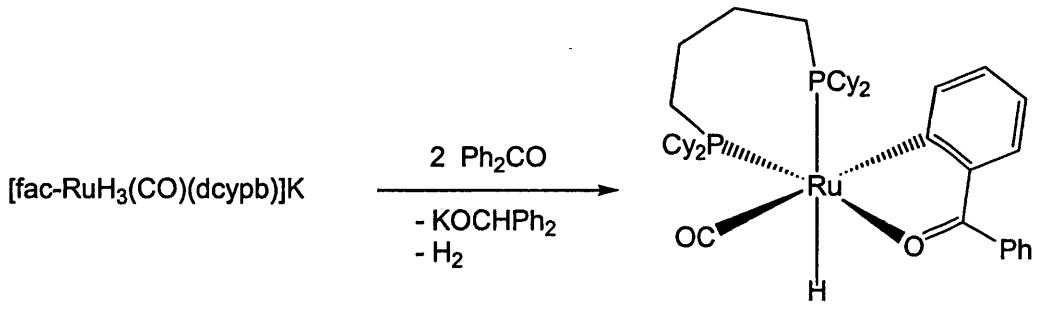

dcypb = 1,4-bis(dicyclohexylphosphino)butane

Scheme 3.5.

We were interested in examining the catalytic activity of similar *ortho* metallated species with triphenylphosphine ligands in order to make direct comparisons with species proposed to be on the Murai catalytic pathway. In this chapter, we report the synthesis and reactivity of compounds related to possible intermediates in the proposed mechanism **[Scheme 3.1.]**, as well as to discuss in more detail this mechanism in light of our NMR observations and collaborative density functional calculations.

3.2. Results and discussion.

3.2.1. Synthesis and reactivity of species directly related to the Murai reaction.

3.2.1.1. Synthesis of $Ru(PPh_3)_3(CO)(\eta^2\text{-}C_2H_4)$ (12)

The stoichiometric reaction of **(1)** with CH_2=$CHSi(OEt)_3$ in toluene at 135°C has been reported to give triethoxyethylsilane, but there has been no attempt to establish the fate of the remaining 16-electron ruthenium fragment.[1] When we used ethene rather than CH_2=$CHSi(OEt)_3$, ethane was produced upon reaction with **(1)** in toluene at 120°C and a yellow microcrystalline solid was isolated which has been identified as $Ru(PPh_3)_3(CO)(\eta^2\text{-}C_2H_4)$ **(12) [Scheme 3.6.]**.

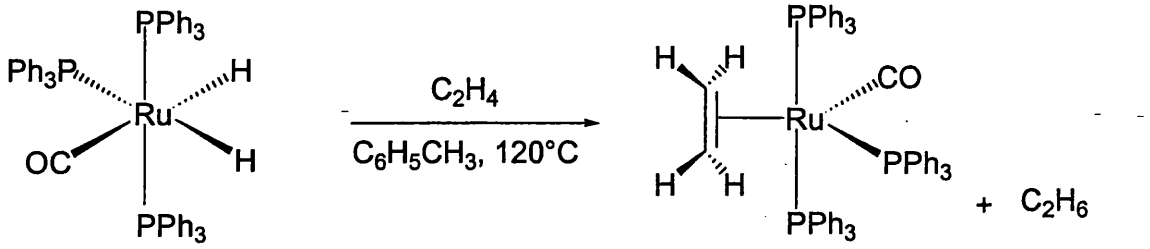

Scheme 3.6.

The complex showed a single band in carbonyl region at 1854 cm^{-1}, consistent with a zero-valent ruthenium species. The $^{31}P\{^1H\}$ NMR spectrum of **(12)** in d^8-toluene at 298 K showed a broad singlet at δ 48.4, indicating that the complex is rapidly fluxional **[Spectrum 3.1., (a)]**. This was confirmed by the room temperature ^1H NMR spectrum **[Spectrum 3.2., (a)]**, which exhibited a single broad ethene resonance at δ 1.79. Cooling to 203 K led to sharpening of the $^{31}P\{^1H\}$ NMR spectrum into a doublet and a triplet (J_{PP} = 9.7 Hz) **[Spectrum 3.1., (c)]**, while decoalescence of the ethene resonance was seen in the proton NMR spectrum leading to two peaks in a 1:1 ratio at 1.33 and 2.34 ppm, although these were still quite broad **[Spectrum 3.2., (b)]**. These VT experiments suggested that **(12)** is stereochemically nonrigid at room temperature, analogous to other Ru(0) ethene complexes such as $Ru(\eta^2\text{-}C_2H_4)(CO)_2(P^tBu_2Me)_2$[8a] and $Ru(\eta^2\text{-}C_2H_4)(CO)_2(d^tbpe)$.[8b] Moreover both the $^{31}P\{^1H\}$ and ^1H NMR spectrum indicate that **(12)** oscillates between two structural configurations as shown in **Scheme 3.7.**. The ethene ligand is only weakly bound and was readily lost upon subjecting the compound to vacuum.

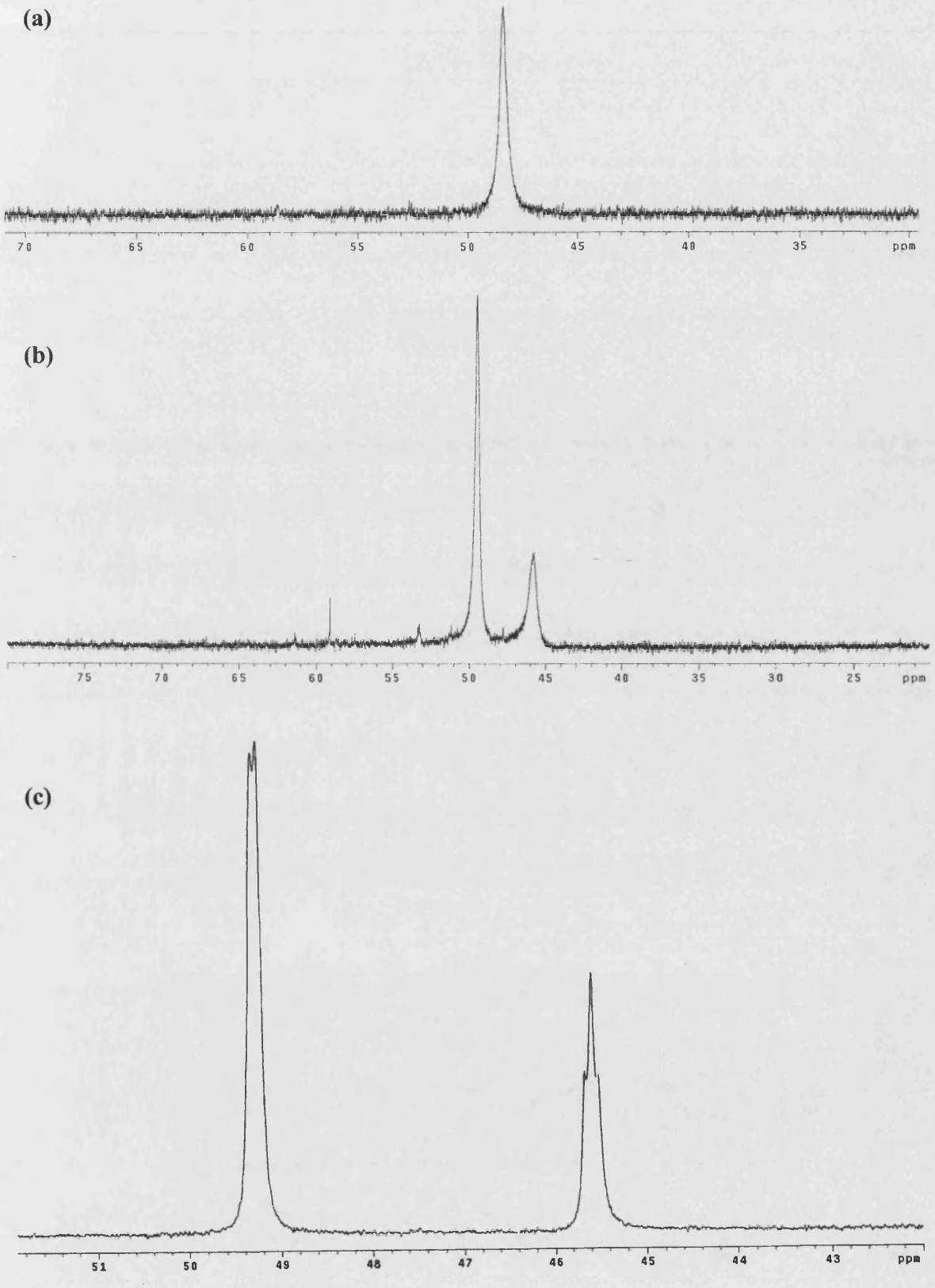

Spectrum 3.1. - *Variable temperature $^{31}P\{^{1}H\}$ spectrum of (12) with:* ***(a)*** *298 K;* ***(b)*** *253K;* ***(c)*** *203K*

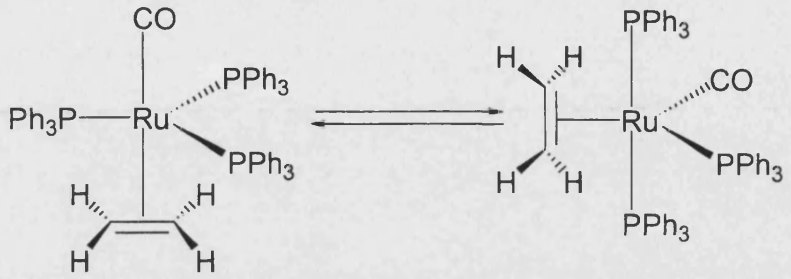

Scheme 3.7.

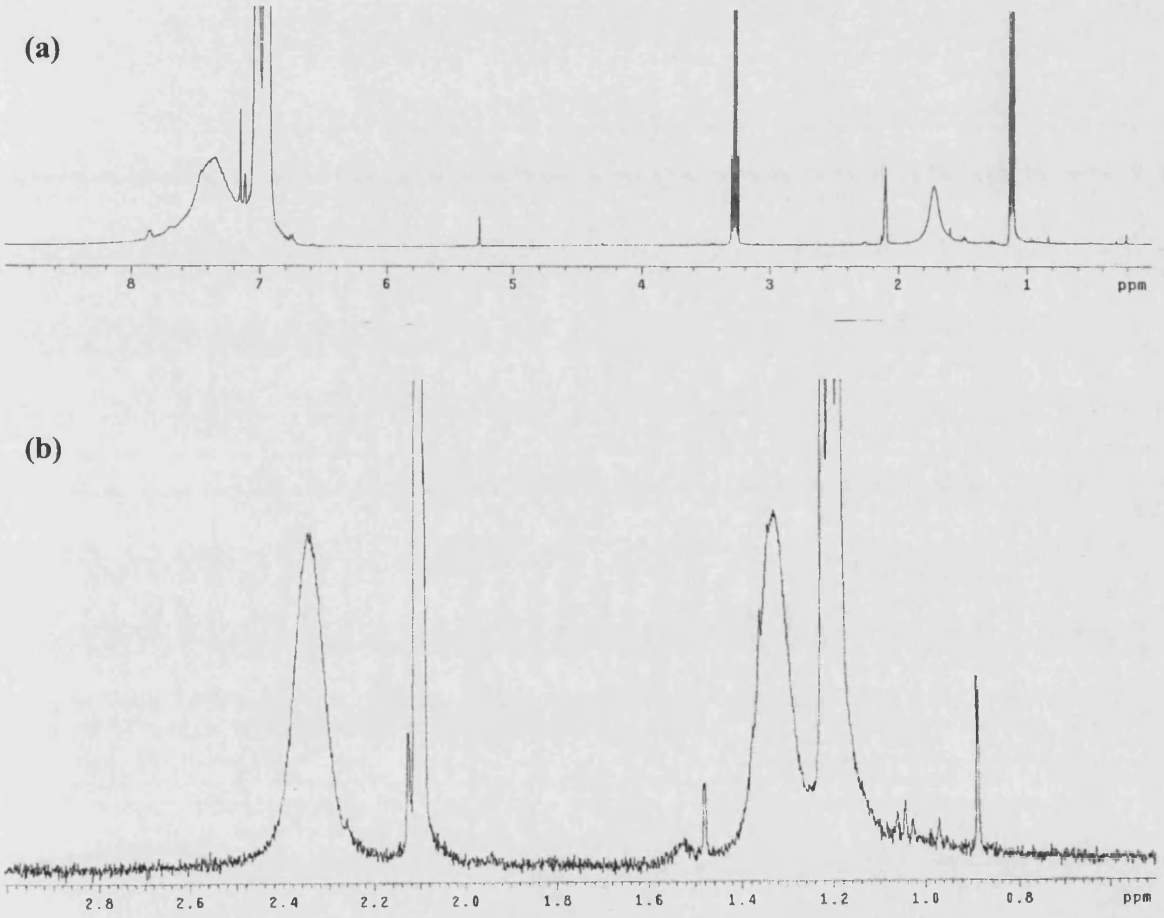

Spectrum 3.2. - *Variable temperature ^1H spectrum of* ***(12)*** *with:* ***(a)*** *298 K,* ***(b)*** *203 K.*

For such a simple compound, it is surprising that **(12)** has not previously been structurally characterized, although its lability in losing ethene may be an influential factor in this. The solid state structure of **(12)** was determined by X-ray crystallography and is shown in **X-Ray 3.1**. Selected bond distances and angles are given in **Table 3.1.**.

The geometry at the ruthenium centre is a distorted trigonal bipyramid with the coordinated ethene ligand in the equatorial plane along with the CO and one PPh_3 group, consistent with well-established notion that the best σ-donor groups occupy axial positions and the best π-acceptors lie in the equatorial plane.[9] For the same reasons, the Ru-P(2) bond length is shorter than both Ru-P(1) and Ru-P(3). These two axial phosphines bend away from the equatorial PPh_3 group {P(1)-Ru-P(3), 103.06(7)°; P(2)-Ru-P(3), 102.14(6)°} so that the (*trans*) P(1)-Ru-P(3) angle is only 153.79(7)°. The five atoms Ru, P(3), C(55), C(56) and C(57) define a good plane with a maximum deviation of 0.03 Å from planarity. The C(55)-C(56) bond length of 1.451(11) Å together with the reduction of the angles around carbon indicate significant back-bonding from Ru to C π* and contribution from a metallacyclopropane structure.[10] However as seen in **Table 3.2.** the Ru-C and C-C bond lengths can be compared with those reported for similar ruthenium π-complexes,[11,12] as well as with those reported for platinum π-complexes of vinylsilanes and vinylsiloxanes.[13,14] The **Ru-CO** (1.972(11) Å) bond is longer than observed in $Ru(PPh_3)_2(CO)((CH_2CH)_2SiMe_2)$ (1.848(12) Å) and in $Ru(P(CH_3)_2(C_6H_5))_2(CO)(CH_2CH_2)Cl_2$ (1.831 (12) Å) indicating less back bonding from the ruthenium to the carbon carbonyl in **(12)**.[4,15]

Selected Bond Lengths	**[Å]**		
Ru(1)-C(57)	1.972(11)	P(1)-C(7)	1.841(7)
Ru(1)-C(55)	2.213(10)	P(1)-C(1)	1.847(7)
Ru(1)-C(56)	2.199(8)	P(2)-C(25)	1.835(7)
Ru(1)-P(1)	2.3498(19)	P(2)-C(31)	1.844(7)
Ru(1)-P(2)	2.3825(19)	P(2)-C(19)	1.862(7)
Ru(1)-P(3)	2.4148(18)	P(3)-C(37)	1.838(7)
O(1)-C(57)	1.395(10)	P(3)-C(49)	1.841(8)
C(55)-C(56)	1.451(11)	P(3)-C(43)	1.855(7)
P(1)-C(13)	1.833(7)		

Selected Bond Angles	[°]		
C(57)-Ru(1)-C(55)	164.6(3)	C(55)-Ru(1)-P(2)	96.30(18)
C(57)-Ru(1)-C(56)	126.4(3)	C(56)-Ru(1)-P(2)	86.7(2)
C(55)-Ru(1)-C(56)	38.4(3)	P(1)-Ru(1)-P(2)	153.79(7)
C(57)-Ru(1)-P(1)	83.4(2)	C(57)-Ru(1)-P(3)	104.6(2)
C(55)-Ru(1)-P(1)	90.55(18)	C(55)-Ru(1)-P(3)	90.62(19)
C(56)-Ru(1)-P(1)	83.1(2)	P(1)-Ru(1)-P(3)	103.06(7)
C(56)-Ru(1)-P(3)	129.0(2)	O(1)-C(57)-Ru(1)	176.5(9)
C(57)-Ru(1)-P(2)	83.4(2)	P(2)-Ru(1)-P(3)	102.14(6)

Table 3.1. - *Selected bond lengths [Å] and angles [°] for $Ru(PPh_3)_3(CO)(C_2H_4)$.*

Compounds	**C-C [Å]**	**Ru-C [Å]**	**[Ref]**
$Ru(PPh_3)_2(CO)((CH_2CH)SiMe_2)$	1.41(2) / 1.37(2)	2.208(12) / 2.220(11) 2.85(12) / 2.308(12)	**[4]**
$RuH_2\{(\eta^4\text{-}HSiMe_2(CH{=}CHMe)\}(PCy_3)_2$	1.394(9)	2.316(6) / 2.269(6)	**[15]**
$Ru(P(CH_3)_2(C_6H_5))_2(CO)(CH_2CH_2)Cl_2$	1.376(19)	2.214(4)	**[16]**
$[CpRu(\eta^2\text{-}C_2H_4)(dippe)][BPh_4]$	1.43(2)	2.25(1) / 2.20(1)	**[17]**

Table 3.2. - *Selected bond lengths [Å] for π-complexes.*

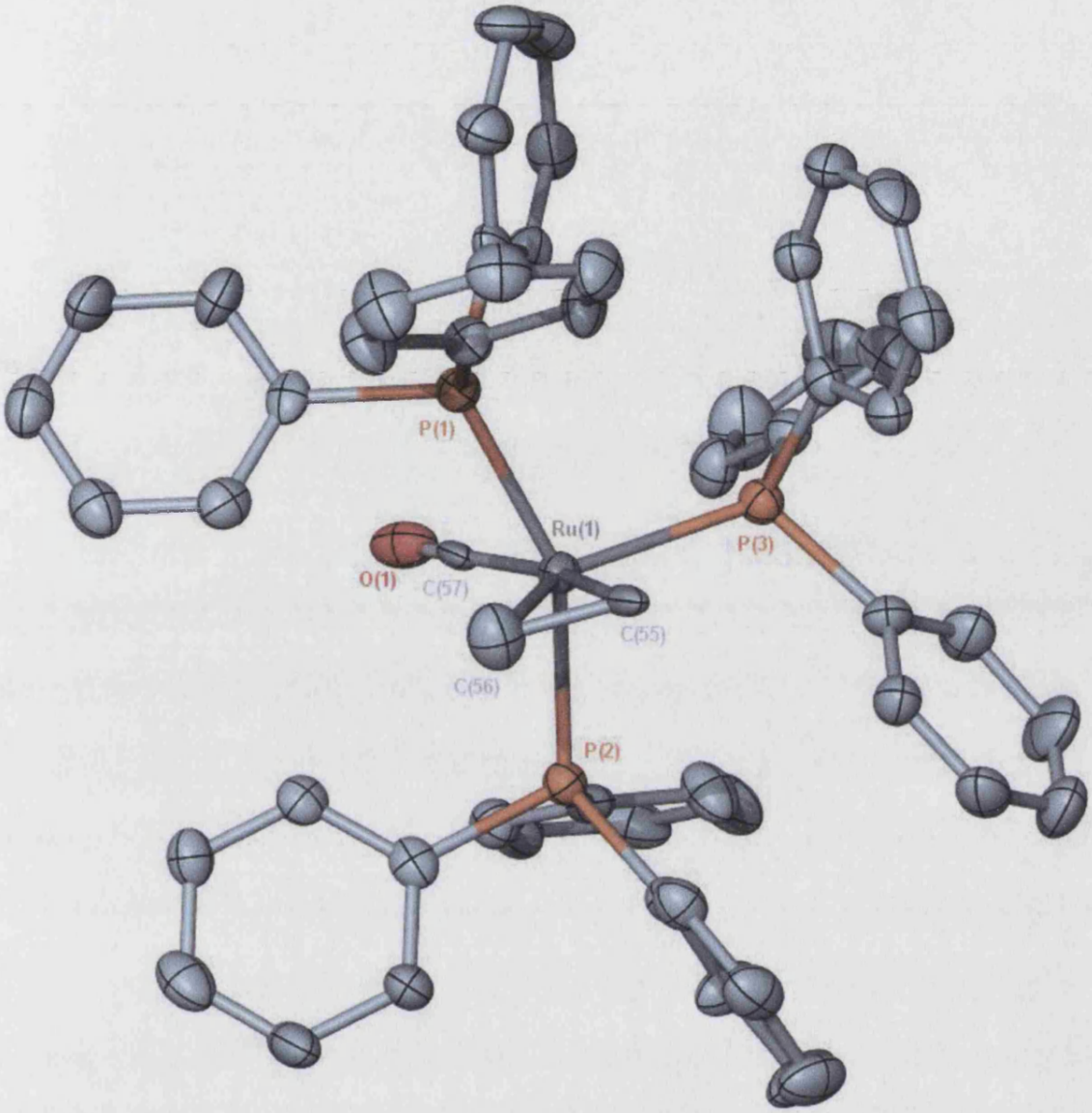

X-Ray 3.1. - *X-ray structure of* ***(12)****. Thermal ellipsoids are set at the 50% probability level. Hydrogen atoms have been omitted for clarity.*

3.2.1.2. Synthesis of $Ru(PPh_3)_2(CO)(\eta^4\text{-}(CH_2{=}CH\text{-}CH{=}CH_2))$ (13)

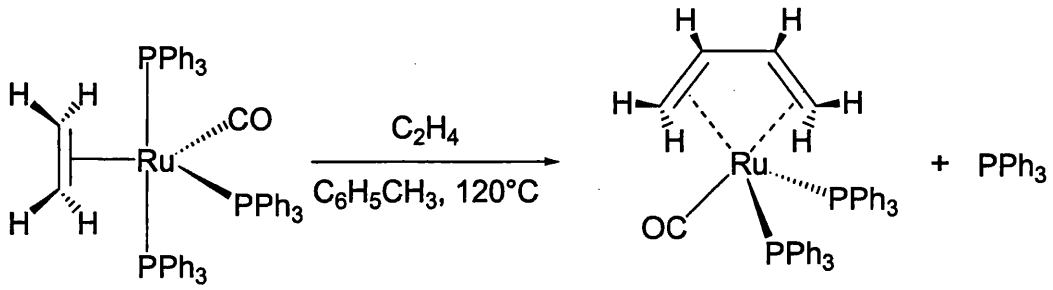

Scheme 3.8.

Complex **(12)** reacted further with ethene to produce the butadiene complex $Ru(PPh_3)_2(CO)(\eta^4\text{-}(CH_2{=}CH\text{-}CH{=}CH_2))$ **(13) [Scheme 3.8.]**. This was isolated as a light orange solid upon precipitation from cold hexane and showed a single band in the carbonyl region at 1902 cm^{-1}, consistent with a zero-valent ruthenium species. The $^{31}P\{^1H\}$ NMR spectrum of **(13)** in d^8-toluene at 298 K showed two broad singlets at δ 60.7 and 47.8 indicating that the complex is rapidly fluxional **[Spectrum 3.3.]**. This was confirmed by the room temperature ^1H NMR spectrum **[Spectrum 3.4., (a)]**, which exhibited 5 single broad resonances at δ 5.34, 5.00, 2.19, 1.22, and -0.74 and integrating in a 1:1:1:1:2 ratio. Cooling to 273 K led to sharpening of the four signals at lower field, while decoalescence of the resonance at δ -0.74 was seen leading to two broad quartet peaks in a 1:1 ratio at -0.74 and -0.86 ppm. Warming to 353 K led to the coalescence of the signals at δ 5.34 and 5.00 to a broad signal at δ 5.11 ppm, coalescence of the signals at δ 2.19 and 1.22 to a broad resonance at δ 1.55, and sharpening of the signal at δ -0.74 to a broad triplet at δ -0.75 (J_{HP} = 7.2 Hz) **[Spectrum 3.4., (c)]**. Although the $^{13}C\{^1H\}$ NMR spectrum of **(13)** supported the coordination of butadiene, it proved difficult to determine the exact structure of **(13)** in solution.[18-20] **NB**: The VT NMR data suggest the possibility of three rapidly inter-converting structures probably based around a piano stool type of structure.[19]

The structure of **(13)** was confirmed by the ^1H NMR shift of related diene complexes as shown in **Figure 3.1.**, as well as by reaction of **(1)** with butadiene gas, which resulted in the formation of **(13)**.

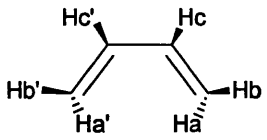

Compound	Ha	Ha'	Hb	Hb'	Hc	Hc'	[Ref]
$Ru(Sb^iPr)3(CH_2CH\text{-}CH{=}CH_2)_2$	0.03	0.03	1.67	1.67	4.10	4.10	[18]
$Ru(PPh_3)_3(CH_2{=}CH\text{-}CH{=}CH_2)$	-0.55	-0.55	2.08	2.08	4.4	4.4	[19]
$Os(PiPr_3)_2(CO)(CH_2{=}CH\text{-}CH{=}CH_2)$	-1.07	-0.77	1.64	1.71	4.56	5.05	[20]
$Os(PiPr_3)_2(CO)(CH_2{=}CH\text{-}CH{=}CHPh)$	-0.22	-0.22	1.32	1.94	5.03	5.16	[20]

Figure 3.1.

In order to understand whether or not this C-C bond formation from two molecules of ethene was restricted to ethene, we investigated the reactivity of **(1)** with styrene. At this point, we become aware of the studies of Hiraki et al. who had reported reaction of styrene with **(1)** to afford $Ru(PPh_3)_2(CO)(PhCH{=}CH_2)_2$, and of **(1)** with 1,3-dienes to afford $Ru(PPh_3)_2(CO)(\eta^4\text{-}1,3\text{-dienes})$ complexes.[21] Their work on diene chemistry confirmed the nature of **(13)** but C-C bond formation between two molecules of styrene was not observed to generate a diene complex.

On the basis of the work described by Bohanna et al.[20] for the formation of $Os(P^iPr_3)_2(CO)(CH_2{=}CH\text{-}CH{=}CHPh)$ it is possible to devise a possible mechanism for the formation of **(13) [Scheme 3.10.]**.

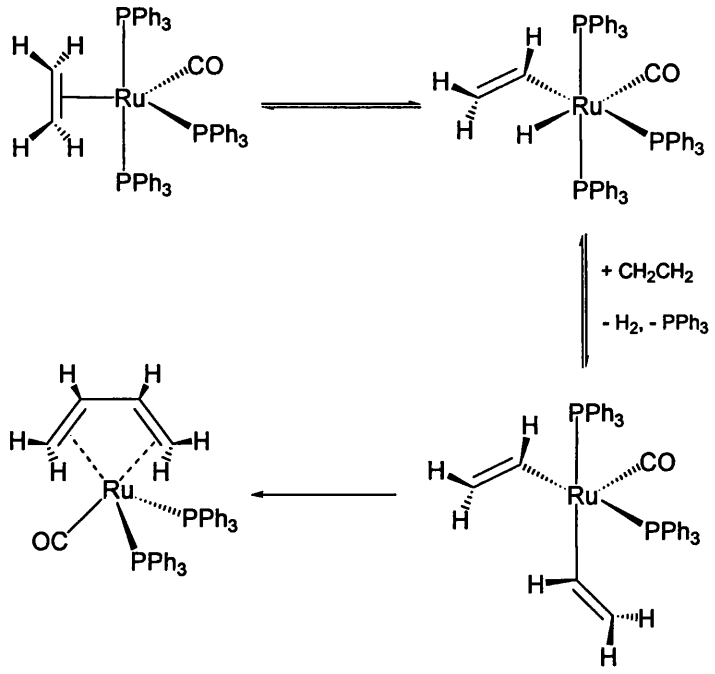

Scheme 3.10. - *Proposed mechanism for the formation of (13).*

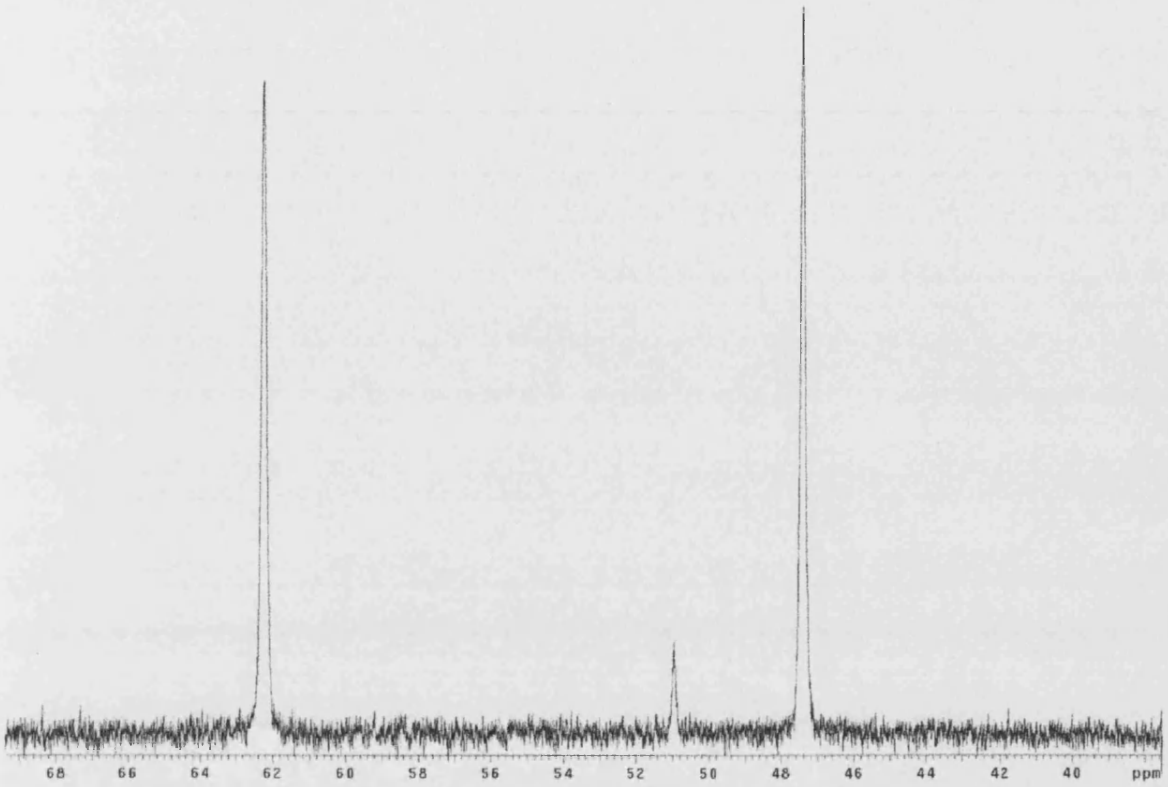

Spectrum 3.3. - *$^{31}P\{^{1}H\}$ NMR spectrum of* ***(13)***.

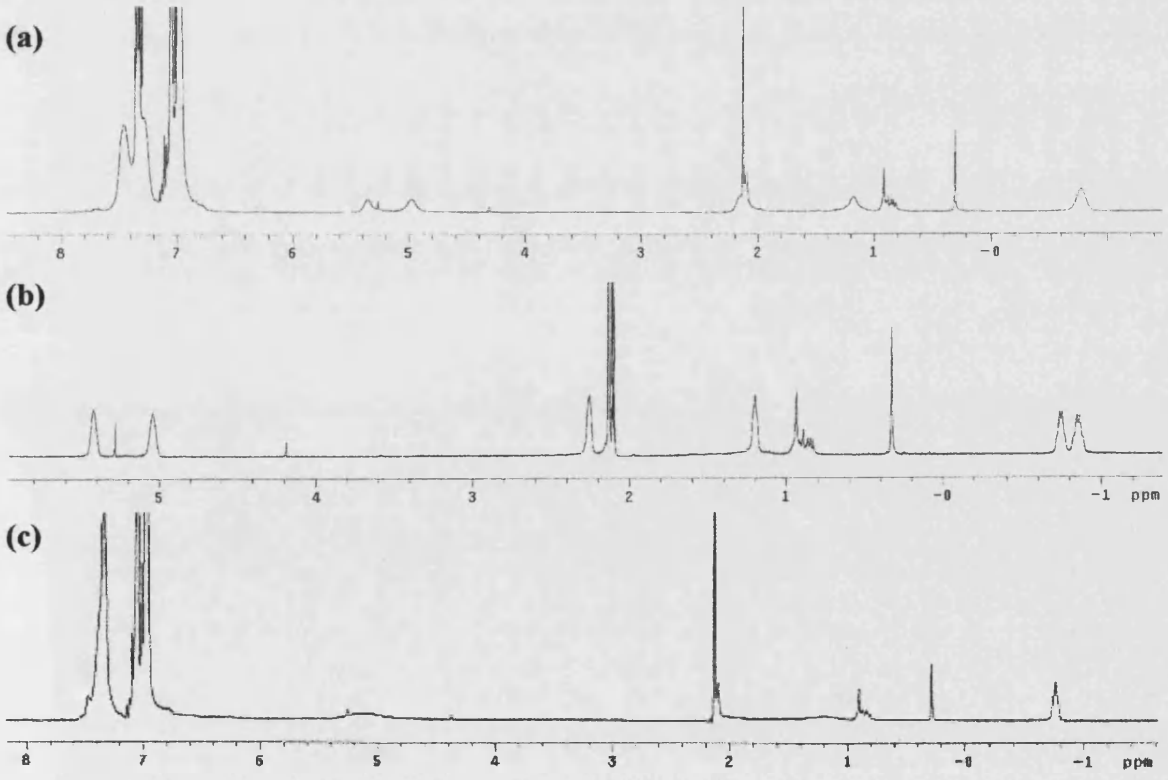

Spectrum 3.4. - *Variable temperature ^{1}H NMR spectra of* ***(13)*** *at:* ***(a)*** *298 K;* ***(b)*** *273 K; (c) 353 K.*

3.2.1.3. Synthesis of $Ru(PPh_3)_3(C_6H_4C(O)CH_3)H$ (14) and $Ru(PPh_3)_3(p\text{-}CH_3O\text{-}C_6H_4C(O)CH_3)H$ (15)]

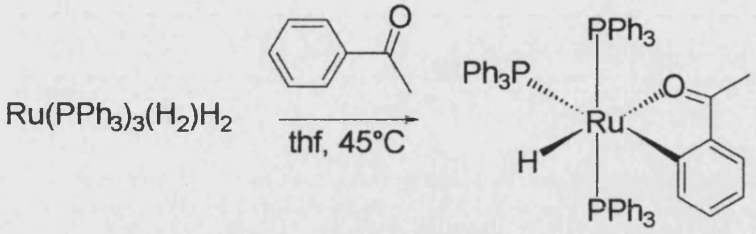

Scheme 3.11.

Reaction of the labile dihydrogen dihydride complex $Ru(PPh_3)_3(H_2)H_2$ **(6)** with acetophenone at 45°C gave the orange *ortho* metallated complex $Ru(PPh_3)_3(C_6H_4C(O)CH_3)H$ in high yield **[Scheme 3.11.]**. The IR spectrum of **(14)** showed two bands at 1940 and 1574 cm^{-1} assigned to ν_{RuCO} and ν_{CO} respectively. The $^{31}P\{^1H\}$ NMR spectrum displayed a doublet and a triplet (J_{PP} = 31.1 Hz), while the proton spectrum showed a high field hydride signal at -15.42 ppm split into a doublet of triplets (J_{PH} = 26.0 Hz, J_{PH} = 13.2 Hz) and a singlet for the methyl group of the *ortho* metallated ketone at 1.36 ppm **[Spectrum 3.5.]**. The poor solubility of the complex both in aromatic solvents (C_6D_6, $C_6D_5CD_3$) and d^8-thf prevented satisfactory $^{13}C\{^1H\}$ NMR data from being recorded.

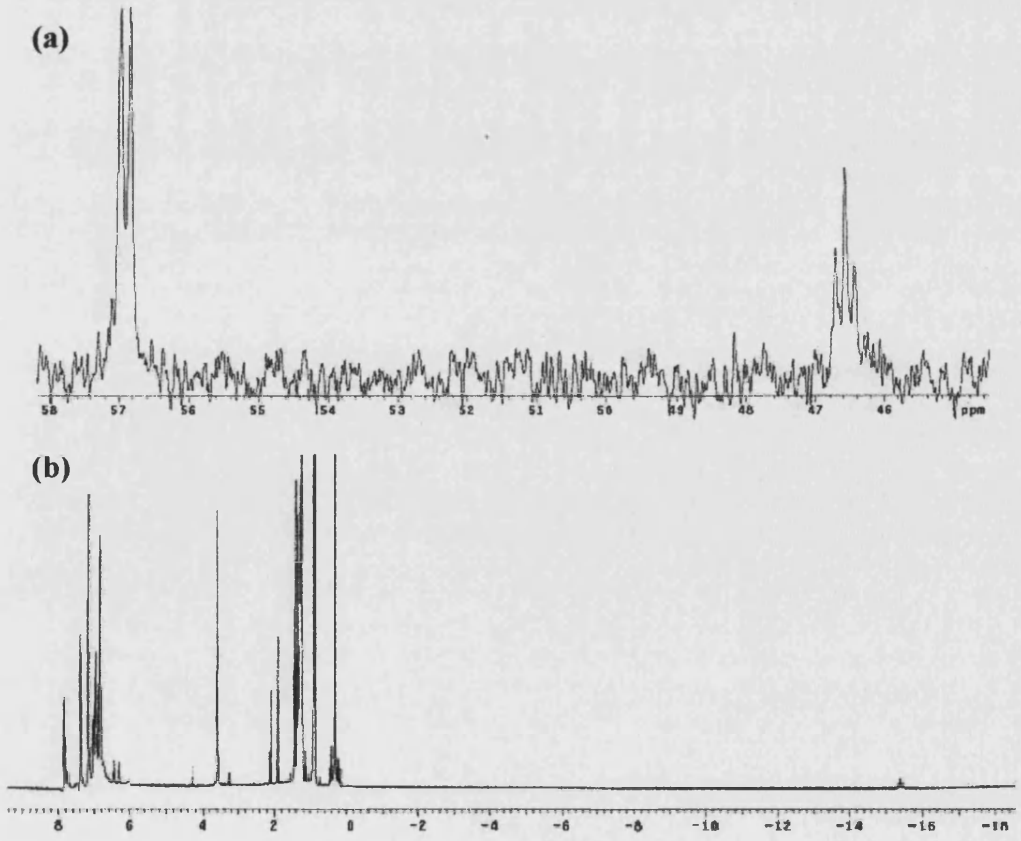

Spectrum 3.5. - *Spectrum of (14): (a) $^{31}P\{^1H\}$; (b) ^1H.*

The solid state structure of **(14)** was determined by X-ray crystallography and is shown in **X-Ray 3.2**. Selected bond distances and angles are given in **Table 3.3.**.

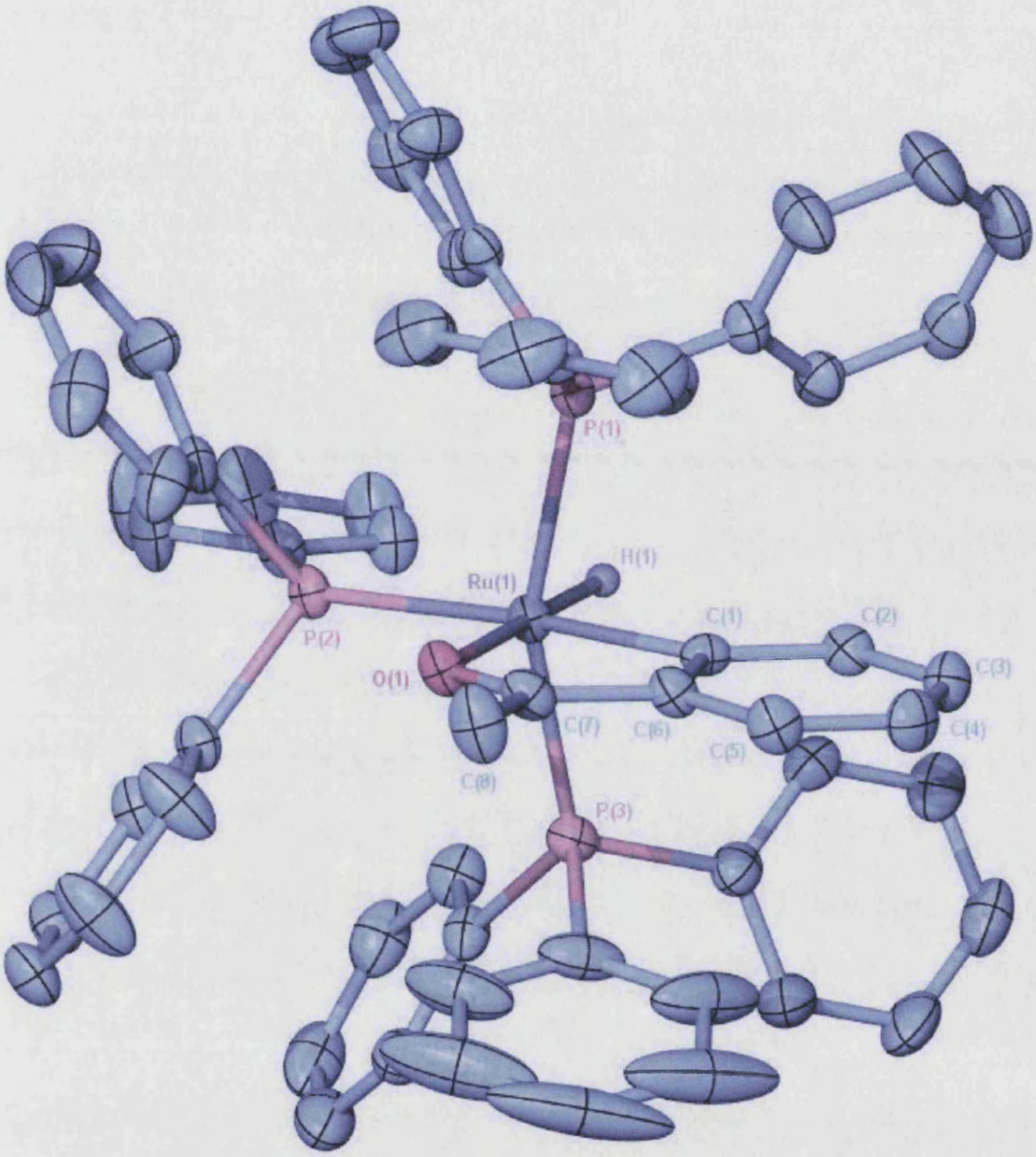

X-Ray 3.2. - *X-ray structure of* ***(14)****. Thermal ellipsoids are set at the 50% probability level. Hydrogen (apart from hydrides) atoms have been omitted for clarity.*

The coordination geometry around ruthenium is distorted from an octahedron with a compressed P(1)-Ru-P(3) angle of 158° resulting from the steric bulk of the PPh_3 group in the equatorial plane. In comparison to the Ru-O bond distances in the related *ortho* metallated complexes $Ru(PPh_3)_2(CO)(C_6H_4C(O)CH_3)Cl$ and $Ru(PMe_2Ph)_2(CO)(C_6H_3CH_3C(O)C_6H_4CH_3)Cl$ (2.125(8) Å and 2.093(10)/2.136(11) Å respectively), the Ru-O bond

length in **(14)** is considerably longer (2.211(2) Å) due to its position *trans* to hydride rather than *trans* to chloride **[Table 3.4.]**.[22,23] Nevertheless **(14)** is in within range for this type of *ortho* metallated compounds as shown in **Table 3.4.**.

Selected Bond Lengths	**[Å]**		
Ru(1)-C(1)	2.115(3)	C(7)-C(8)	1.507(5)
Ru(1)-P(1)	2.3223(9)	Ru(1)-O(1)	2.211(2)
Ru(1)-P(2)	2.3563(9)	Ru(1)-P(3)	2.3259(9)
O(1)-C(7)	1.251(4)	C(1)-C(2)	1.417(5)
C(1)-C(6)	1.428(4)	C(2)-C(3)	1.377(5)
C(3)-C(4)	1.394(5)	C(4)-C(5)	1.373(5)
C(5)-C(6)	1.401(5)	C(6)-C(7)	1.448(5)
Selected Bond Angles	**[°]**		
C(1)-Ru(1)-O(1)	76.68(10)	C(1)-Ru(1)-P(1)	83.49(9)
O(1)-Ru(1)-P(1)	94.46(6)	C(1)-Ru(1)-P(3)	82.00(9)
O(1)-Ru(1)-P(3)	97.19(6)	P(1)-Ru(1)-P(3)	158.76(3)
C(1)-Ru(1)-P(2)	168.12(9)	O(1)-Ru(1)-P(2)	91.48(6)
P(1)-Ru(1)-P(2)	98.57(3)	P(3)-Ru(1)-P(2)	98.82(3)
O(1)-C(7)-C(8)	118.5(3)	O(1)-C(7)-C(6)	119.1(3)

Table 3.3. - *Selected bond lengths [Å] and angles [°] for* $Ru(PPh_3)_3(o\text{-}C_6H_4C(O)CH_3)H$.

Compounds	**Ru-C_6H_4**	**Ru-OC**	**[Ref]**
$Ru(PPh_3)_2(CO)(C_6H_4C(O)CH_3)Cl$	2.07(2)	2.125(8)	**[22]**
$Ru(PMe_2Ph)_2(CO)(C_6H_3CH_3\,C(O)C_6H_4CH_3)Cl$	2.044(17) / 1.987(19)	2.093(10) / 2.136(11)	**[23]**
Ru(dcypb)(CO)[OC(C_6H_4)(Ph)]H	2.144(2)	2.056(3)	**[7]**
$Os(P^iPr_3)_2(C_6F_4C(O)CH_3)H_3$	2.103(4)	2.141(3) Å	**[24]**

Table 3.4. – *Selected bond length in ortho metallated ketone complex of ruthenium.*

In the same manner as already seen for **(14)**, **(5)** reacted with *p*-methoxy-acetophenone to afford the deep orange $Ru(PPh_3)_3(p\text{-}CH_3O\text{-}C_6H_4C(O)CH_3)H$ **(15)**. The IR spectrum of **(15)** showed three bands at 1973, 1946, and 1580 cm^{-1} assigned to ν_{RuCO}, ν_{RuH} and ν_{CO} respectively. As with **(14)**, the poor solubility of the complex prevented any satisfactory NMR data from being recorded.

3.2.1.4. Synthesis of $Ru(PPh_3)_2(CO)(C_6H_4C(O)CH_3)H$ (16) and $Ru(PPh_3)_2(CO)(p\text{-}CH_3O\text{-}C_6H_4C(O)CH_3)H$ (17)

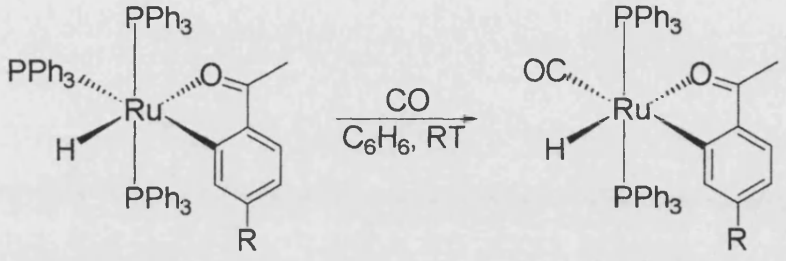

(14) R = H
(15) R = OMe

(16) R = H
(17) R = OMe

Scheme 3.12.

Upon reaction of **(14)** with CO at room temperature, rapid loss of the equatorial PPh_3 group occurred to give $Ru(PPh_3)_2(CO)(C_6H_4C(O)CH_3)H$ **(16)** in good yield **[Scheme 3.12.]**. The hydride ligand in **(16)** appeared as a triplet at δ -14.29 (J_{PH} = 21.2 Hz) in the ^1H NMR spectrum **[Spectrum 3.6.]**, while the $^{13}C\{^1H\}$ NMR spectrum showed two low field triplets at δ 202.9 (J = 14.9 Hz) and 204.9 (J = 12.8 Hz), assigned to the metallated carbon and carbonyl ligands respectively on the basis of ^1H-$^{13}C\{^1H\}$ HMQC and HMBC experiments. The IR spectrum displayed three bands at 1932, 1899 and 1583 cm^{-1} assigned to $\nu_{Ru\text{-}H}$, ν_{CO} and $\nu_{Ru\text{-}O=C}$ respectively.

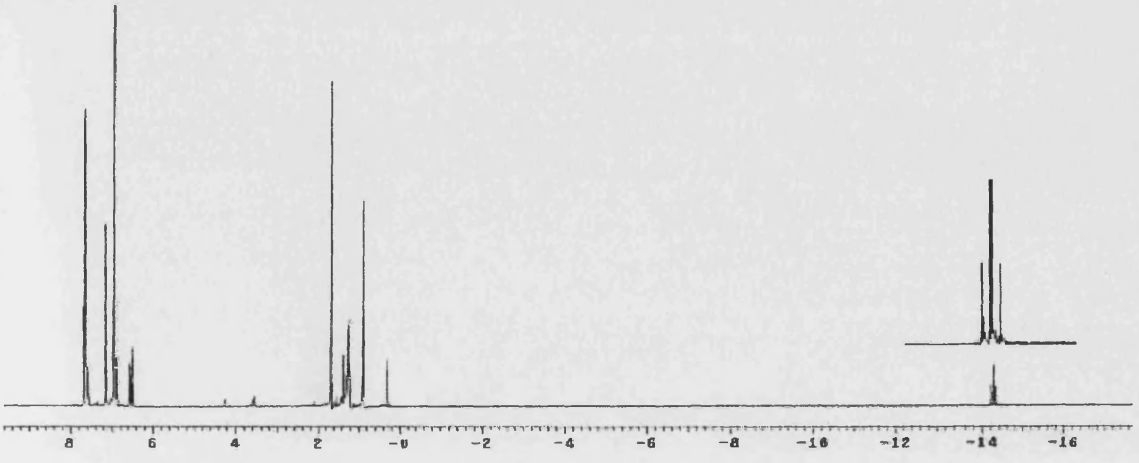

Spectrum 3.6. - *^1H NMR spectrum of (16).*

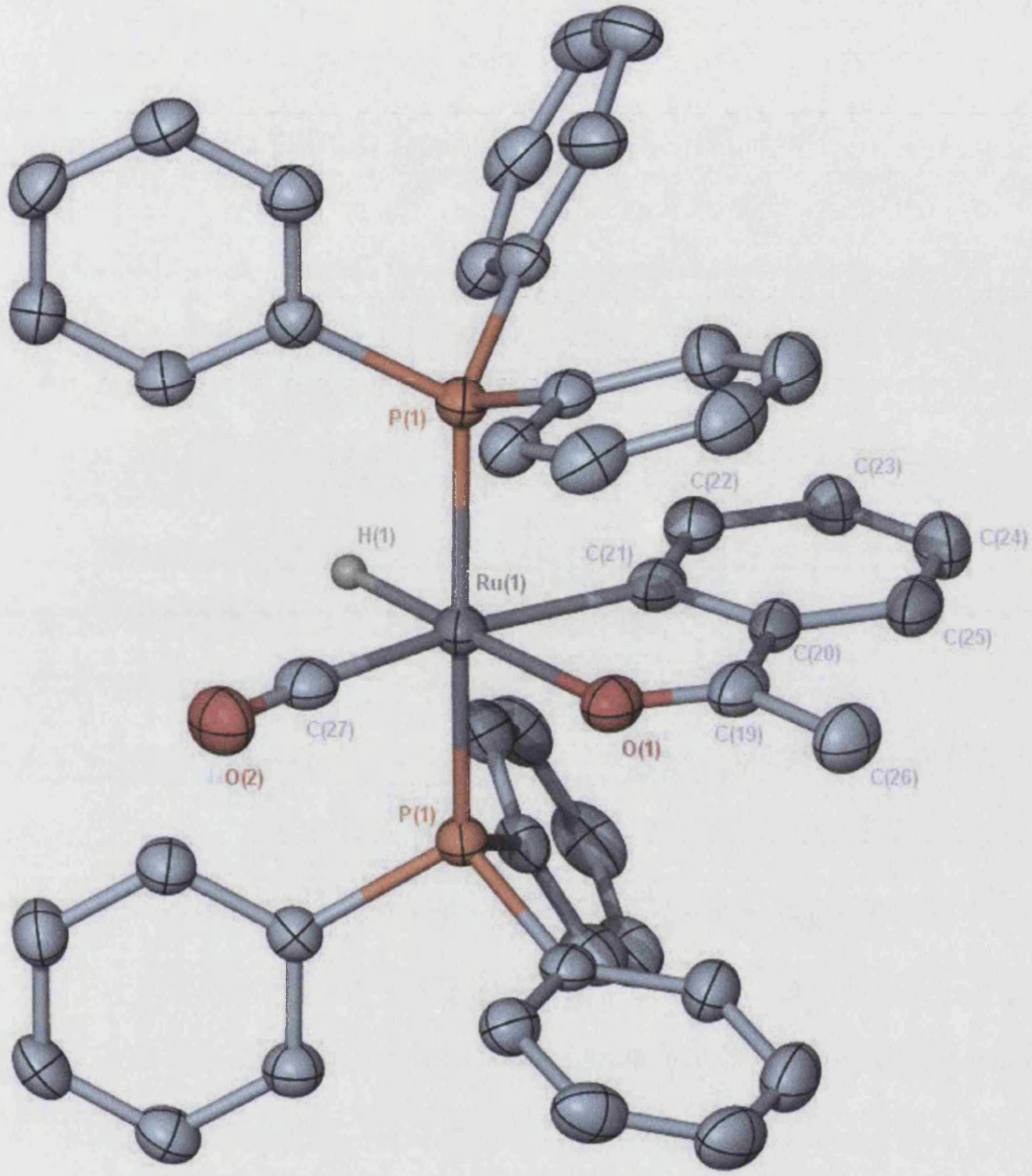

X-Ray 3.3. - *X-ray structure of* ***(16)****. Thermal ellipsoids are set at the 50% probability level. Hydrogen (apart from hydrides) atoms have been omitted for clarity.*

Selected Bond Lengths	**[Å]**		
Ru(1)-C(27)	1.890(5)	Ru(1)-C(21)	2.120(5)
Ru(1)-O(1)	2.188(3)	Ru(1)-P(1)	2.3191(8)
Ru(1)-P(1)#1	2.3191(8)	P(1)-C(13)	1.823(3)
P(1)-C(1)	1.836(3)	O(1)-C(19)	1.241(6)
O(2)-C(27)	1.153(6)	C(19)-C(26)	1.507(7)
C(19)-C(20)	1.462(7)	C(20)-C(21)	1.439(6)
C(20)-C(25)	1.400(7)	C(22)-C(23)	1.394(7)
C(21)-C(22)	1.391(7)	C(24)-C(25)	1.385(8)
C(23)-C(24)	1.388(7)		
Selected Bond Angles	**[°]**		
C(27)-Ru(1)-C(21)	168.4(2)	C(27)-Ru(1)-O(1)	91.42(17)
C(21)-Ru(1)-O(1)	76.94(16)	C(27)-Ru(1)-P(1)	92.97(2)
C(21)-Ru(1)-P(1)	87.67(2)	O(1)-Ru(1)-P(1)	92.82(2)
C(27)-Ru(1)-P(1)#1	92.97(2)	C(21)-Ru(1)-P(1)#1	87.67(2)
O(1)-Ru(1)-P(1)#1	92.82(2)	P(1)-Ru(1)-P(1)#1	171.70(4)
C(19)-O(1)-Ru(1)	116.2(3)	O(1)-C(19)-C(20)	118.8(4)
C(22)-C(21)-Ru(1)	132.8(4)	C(20)-C(21)-Ru(1)	112.9(3)
O(2)-C(27)-Ru(1)	173.7(4)		

Table 3.5. - *Selected bond lengths [Å] and angles [°] for* $Ru(PPh_3)_2(CO)(o\text{-}C_6H_4C(O)CH_3)H$

Although we were only able to obtain relatively mediocre quality crystals, the solid state structure of **(16)** was determined by X-ray crystallography as shown in **X-Ray 3.3**. Selected bond distances and angles are given in **Table 3.5.**. The presence of the relatively small CO ligand in the equatorial plane relaxes the steric strain on the *trans* phosphine groups to give a P(1)-Ru-P(1) angle of 171°.

Similarly **(15)** reacted with CO to afford $Ru(PPh_3)_2(CO)(p\text{-}CH_3O\text{-}C_6H_4C(O)CH_3)H$ **(17)**. The ^1H NMR spectrum showed the hydride ligand in **(17)** appeared as a triplet at δ -14.44 (J_{PH} = 22.0 Hz), while the $^{13}C\{^1H\}$ NMR spectrum showed two low field triplets at δ 205.2 (J = 14.4 Hz) and 208.5 (J = 13.9 Hz), assigned to the metallated carbon and carbonyl ligands respectively. The IR spectrum displayed three bands at 2024, 1917 and 1626 cm^{-1} assigned to $\nu_{Ru\text{-}H}$, ν_{CO} and $\nu_{Ru\text{-}O=C}$ respectively.

The structure of **(17)** was determined by X-ray crystallography **[X-Ray 3.4.]** Selected bond distances and angles are given in **Table 3.6.**. Very little difference is seen in the structure for **(16)** and **(17)**. Nevertheless elongation of the $Ru\text{-}C_{phenyl}$ is observed in **(17)** relatively to **(16)** (2.120(5) vs 2.105(2)Å), accompanied by a shortening of the Ru-O bond (2.188(3) vs 2.2041(14)Å). This effect might be result from the increase in delocalisation of electron around the *ortho*metallated phenyl ring in **(17)** brought about by the oxygen of the methoxy moiety.

Selected Bond Lengths	**[Å]**		
Ru(1)-H(99)	1.559(15)	Ru(1)-C(46)	1.895(2)
Ru(1)-C(4)	2.105(2)	Ru(1)-O(1)	2.2041(14)
Ru(1)-P(2)	2.3216(5)	Ru(1)-P(1)	2.3381(5)
O(1)-C(2)	1.251(3)	O(3)-C(46)	1.148(3)
C(1)-C(2)	1.502(3)	C(2)-C(3)	1.446(3)
C(3)-C(8)	1.410(3)	C(3)-C(4)	1.422(3)
C(4)-C(5)	1.398(3)	C(5)-C(6)	1.393(3)
C(6)-C(7)	1.403(3)	C(7)-C(8)	1.377(3)
Selected Bond Angles	**[°]**		
C(46)-Ru(1)-C(4)	176.57(8)	O(1)-C(2)-C(3)	119.33(18)
C(46)-Ru(1)-O(1)	99.86(7)	C(4)-Ru(1)-O(1)	76.73(7)
P(2)-Ru(1)-P(1)	171.197(19)	C(3)-C(4)-Ru(1)	113.74(15)
C(2)-O(1)-Ru(1)	114.73(13)		

Table 3.6. - *Selected bond lengths [Å] and angles [°] for* $Ru(PPh_3)_2(CO)(p\text{-}CH_3O\text{-}C_6H_4C(O)CH_3)H$.

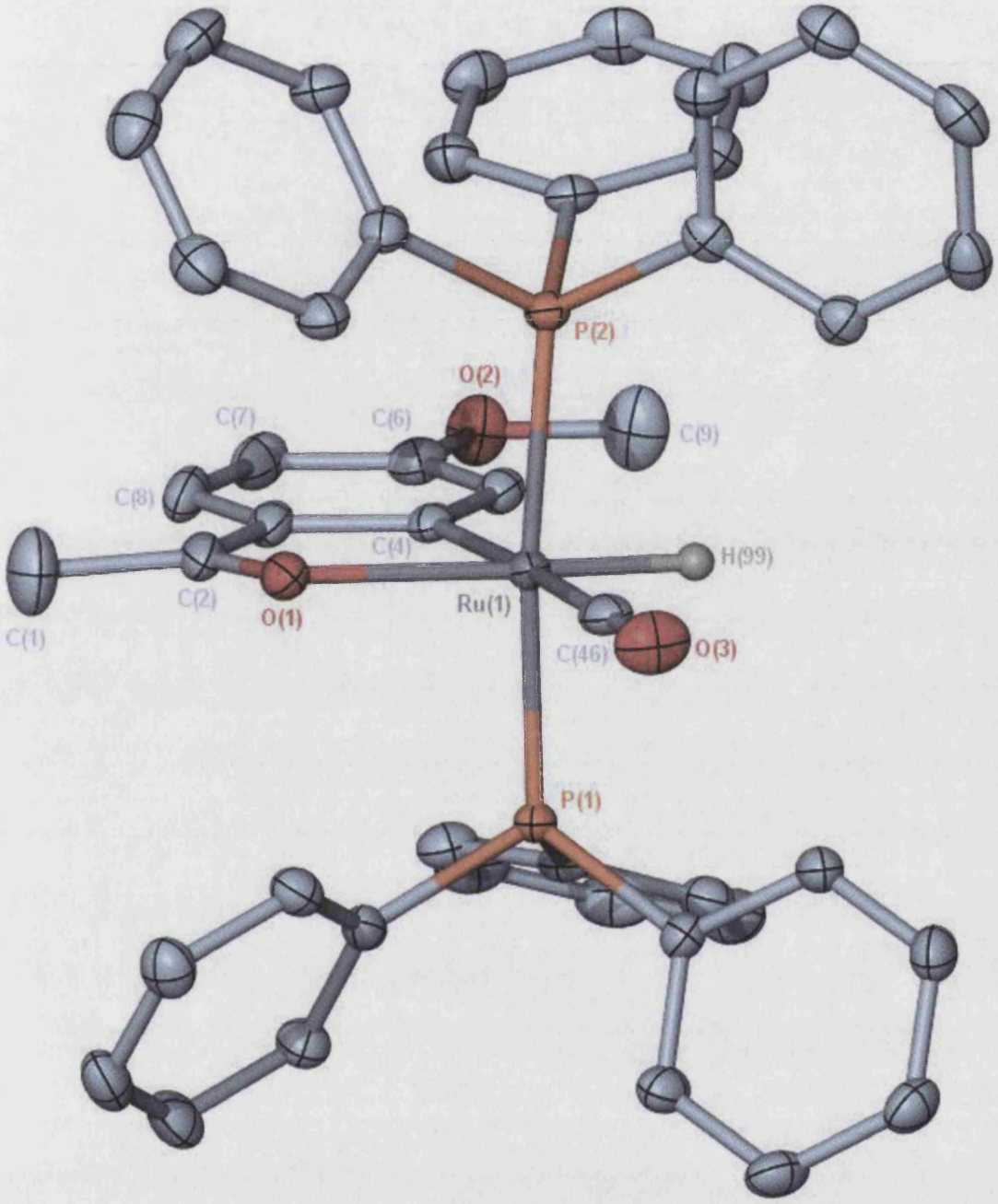

X-Ray 3.4. - *X-ray structure of* ***(17)****. Thermal ellipsoids are set at the 50% probability level. Hydrogen (apart from hydrides) atoms have been omitted for clarity.*

3.2.1.5. Synthesis of $Ru(PPh_3)_2(Me_2SO)(C_6H_4C(O)CH_3)H$.

Reaction of **(14)** with Me_2SO at room temperature resulted in the rapid loss of the equatorial PPh_3 and formation of $Ru(PPh_3)_2(Me_2SO)(C_6H_4C(O)CH_3)H$ **(21)** in good yield **[Scheme 3.8.]**.

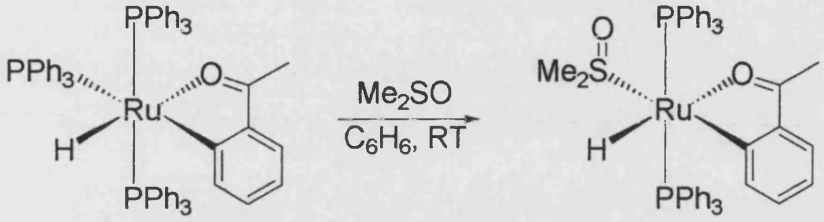

Scheme 3.13.

The proton NMR spectrum displayed a triplet hydride resonance at δ -15.30 (J_{PH} = 24.6 Hz) while a singlet was observed for the coordinated Me_2SO ligand at δ 2.09 **[Spectrum 3.7.]**. The $^{13}C\{^1H\}$ NMR spectrum showed two low field triplets at δ 206.4 and 195.2 (J = 15.8 Hz), assigned to the metallated carbon and Ru-O=C respectively on the basis of ^1H-$^{13}C\{^1H\}$ HMQC and HMBC experiments. The IR spectrum displayed two bands at 1971 and 1571 cm^{-1} assigned to ν_{Ru-H} and $\nu_{Ru-O=C}$ respectively.

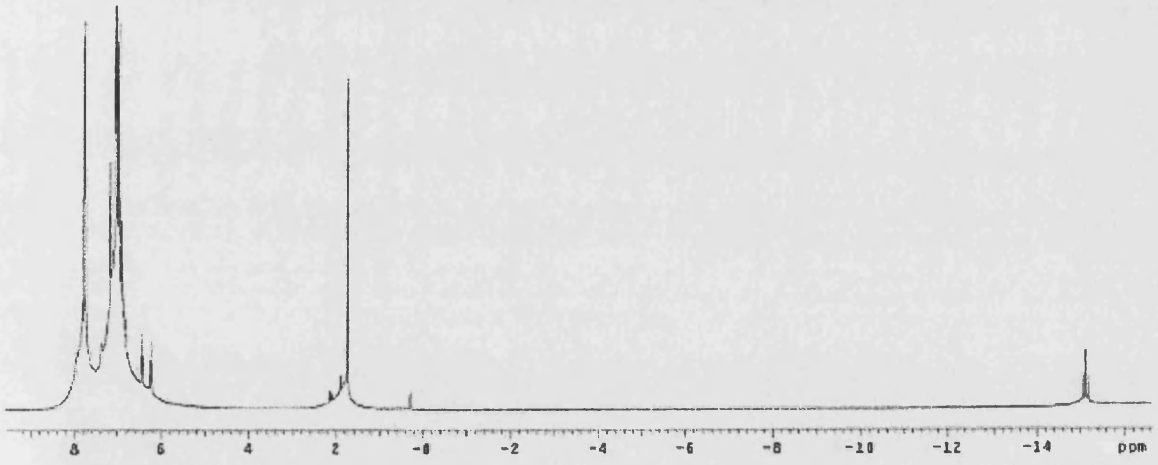

Spectrum 3.7. - *^1H NMR spectrum of $Ru(PPh_3)_2(Me_2SO)(C_6H_4C(O)CH_3)H$).*

The structure of **(21)** was elucidated by X-ray crystallography **[X-Ray 3.5.]** Selected bond distances and angles are given in **Table 3.5.**. The structure shows that the Me_2SO ligand is sulfur-bound and occupies an equatorial site with a Ru-S bond distance of 2.3083(11) Å. The P-Ru-P angle of 157.7° is close to that found in **(16)**. The Ru-C bond lengths to the sp^2 *ortho* metallated carbon on the aromatic ring in **(14 - 17)** and **(21)** are all

very close (2.100(5)-2.120(5) Å) and thus essentially independent of the *trans* ligand (PPh_3, CO or DMSO).

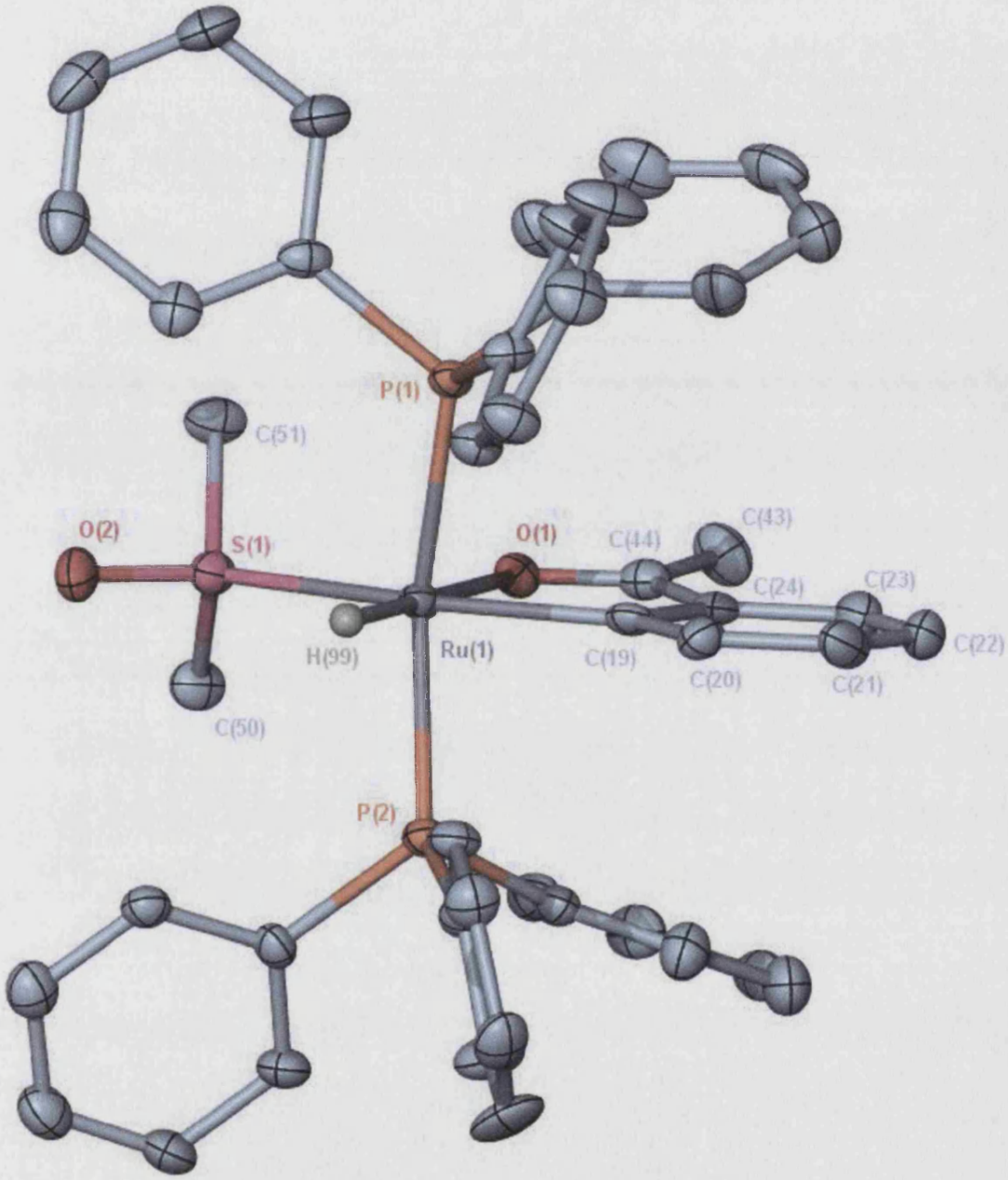

X-Ray 3.5. - *X-ray structure of* ***(21)****. Thermal ellipsoids are set at the 50% probability level. Hydrogen (apart from hydrides) atoms have been omitted for clarity.*

Selected Bond Lengths	**[Å]**		
Ru(1)-O(1)	2.183(3)	Ru(1)-C(19)	2.100(5)
Ru(1)-P(1)	2.3143(12)	Ru(1)-S(1)	2.3083(11)
S(1)-O(2)	1.477(4)	Ru(1)-P(2)	2.3229(12)
S(1)-C(51)	1.802(5)	S(1)-C(50)	1.788(5)
O(1)-C(44)	1.244(6)		
Selected Bond Angles	**[°]**		
C(19)-Ru(1)-O(1)	77.64(15)	O(1)-Ru(1)-S(1)	86.78(9)
C(19)-Ru(1)-S(1)	164.41(14)	C(19)-Ru(1)-P(1)	83.28(12)
O(1)-Ru(1)-P(1)	96.55(9)	S(1)-Ru(1)-P(1)	98.57(4)
O(1)-Ru(1)-P(2)	98.20(9)	C(19)-Ru(1)-P(2)	83.59(12)
P(1)-Ru(1)-P(2)	157.66(4)	S(1)-Ru(1)-P(2)	98.93(4)
C(44)-O(1)-Ru(1)	114.6(3)		

Table 3.7. - *Selected bond lengths [Å] and angles [°] for* $Ru(PPh_3)_2(Me_2SO)(C_6H_4C(O)CH_3)H$.

3.2.1.6. Catalytic activity of (12-17) and (21) for Murai chemistry.

As shown in the proposed catalytic cycle at the start of the chapter, Murai and co workers suggest that a $Ru(C_6H_4C(O)CH_3)H$ species is an intermediate on the way to ketone-alkene coupling. As seen already in **Chapter 1** this postulate is based on the high regioselectivity observed in the C-C coupling, which can only be rationalised by *ortho* metallation of the ketone substrate with the ruthenium centre. This postulate is reinforced by several observations on the catalytic activities of *ortho*-metallated species.[5-7] Interestingly, two conflicting ideas have been suggested in the literature as to the other ligands attached to the metallated complex. It was first suggested by Trost et al.[25] that CO must be first lost from complex **(1)** during the reaction **[Scheme 3.14.]** affording $Ru(PPh_3)_3$ as a catalytic species in the reaction. Alternatively, several observations points out loss of PPh_3 rather than CO, affording $Ru(PPh_3)_2(CO)$ as active species. Support for the CO

exclusion originated from the observed inhibition of the Murai reaction by CO gas,[25] and was acknowledged in a recent publication by Chaudret et al.[6b] who demonstrated that whereas $Ru(PCy_3)_2(C_6H_4C(O)CH_3)(H_2)H$ exerted catalytic activity, the carbonyl complex $Ru(PCy_3)_2(CO)$ $(C_6H_4C(O)Ph)H$ remained catalytically inert.

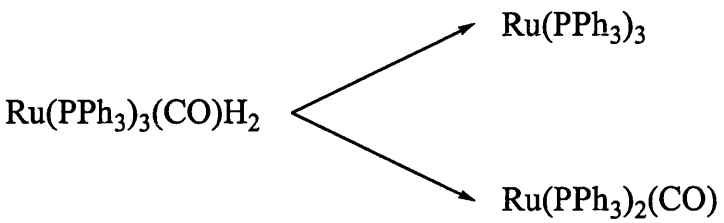

Scheme 3.14. -

Nevertheless, most of these reported examples have been far from being true comparisons with the Murai system, due to the use of different types of ligand around the ruthenium centre. Therefore true comparative data is needed to realistically assess the importance of Ru *ortho*-metallated complexes on the pathway to C-C coupling. Complexes **(16)** and **(17)** represent direct comparisons to the proposed intermediates. Moreover, variations of the ligand *cis* to the hydride in **(14)**, **(16)** and **(21)** from the weakly coordinated PPh_3 and DMSO to the strongly coordinated CO ligand provides an interesting assessment on the importance of this coordination site.

In order to assess the catalytic activity of complexes **(12-17)** and **(21)** relative to $Ru(PPh_3)_3(CO)H_2$, we chose to study the reaction of 2'-methylacetophenone with triethoxyvinylsilane, which were identified by Murai as the most reactive substrates **[Scheme 3.15.]**.[1] Blocking of the second *ortho* position on the ketone by a methyl group also removed the potential for a double insertion reaction. The results are summarised in **Table 3.8.** and include measurements on $Ru(PPh_3)_3(CO)H_2$ which were performed for direct comparison.

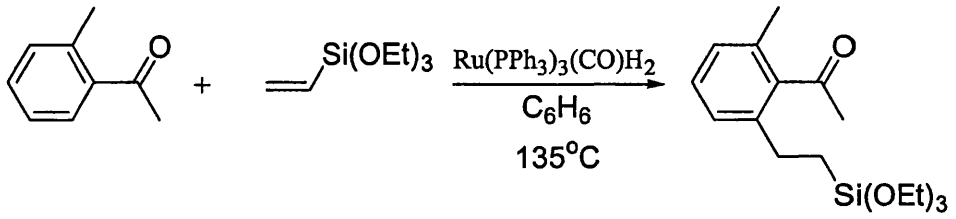

Scheme 3.15.

This study was conducted in refluxing toluene solution (5 mol% catalyst loading) and the extent of the C-C coupling reaction analysed by GC. Complexes **(16, 17)** and **(21)**

proved inferior to **(1)**, with the carbonyl complexes **(16, 17)** showing essentially zero catalytic activity in agreement with Chaudret's studies on $Ru(PCy_3)_2(CO)(o\text{-}C_6H_4C(O)CH_3)H$. These measurements suggest that CO binds too strongly in the coordination site that is important for catalysis to occur. The tris-phosphine complex $Ru(PPh_3)_3(o\text{-}C_6H_4C(O)CH_3)H$ produced a higher yield of product compared to $Ru(PPh_3)_3(CO)H_2$ over shorter periods of time, although the catalytic activity ultimately plateaued off leading to lower overall conversion after 2 h. It is not yet clear why this is the case, but we assume that the high temperature used for the reaction coupled to the poor thermal stability of **(14)** resulted in degradation of the catalyst over time.

Catalyst	Reaction Time (min)	Coupling product %	TON	TOF (TON/h)
(1)	60	66		
	120	96	48	24
(12)	120	44	21	10
(13)	120	13	6-7	
(14)	30	62		
	60	71		
	120	76	42	21
(21)	***30***	***12***		
	60	***16***		
	240	***22***	***11***	***3***
(16)	120	4		
(17)	120	0-2		

Table 3.8. - Catalytic coupling of 2'-methylacetophenone with triethoxyvinysilane

The catalytic study was extended to **(12, 13)** in order to assess the importance of a Ru^0 alkene complex (generated in a first step of the reaction) on the reaction pathway. Although **(12)** proved active for the reaction, a lower yield of product was found by comparison to **(1)**. This in turn suggests that although a Ru^0 alkene complex might be

formed on the pathway to C-C bond formation the low activity of this later does not place it directly on the way and **(12)** should therefore be considered more like a side product of the reaction. Similarly **(13)** showed really poor activity for the reaction; the formation of a fairly stable diene complex might explain some of the limitations observed by Murai and co-workers in the use of diene compounds.[1] Nevertheless the formation of ethene and a conjugated diene complex such as **(12)** and **(13)** indicate unambiguously that **(1)** reacts with an alkene to give the highly reactive ruthenium(0) species $Ru(PPh_3)_2(CO)$. However, this point will be discussed further in **Chapter 3.3.** on the basis of further insight into the catalytic cycle described later in this chapter.

We have investigated the effect of replacing the PPh_3 ligands in **(1)** by $AsPh_3$, bidentate ligands such as dppp and arphos and changing the phosphine for the N-heterocyclic carbene ligand IMes (= 1,3-bis-(2,4,6-trimethylphenyl)imidazol-2-ylidene). Neither $Ru(PPh_3)_2(CO)_2H_2$ nor $Ru(PPh_3)(dppp)(CO)H_2$ proved active for the Murai reaction, the latter presumably due to the fact that it undergoes very rapid intramolecular activation of one of the dppp phenyl rings.[26] Hope for better activity using the weakly coordinating arsine ligand $AsPh_3$ or the bidentate mix phosphine-arsine arphos proved unsuccessful; although $Ru(AsPh_3)_3(CO)H_2$ showed some activity, it was poor. No activity was observed using $Ru(PPh_3)(arphos)(CO)H_2$. Finally, although Murai reported similar catalytic activity for $Ru(PPh_3)_2(CO)_3$ and $Ru(PPh_3)_3(CO)_2$ to that seen for **(1)** but over a longer reaction time (6.5 hr vs. 2 hr),[1] we were unable to repeat these observations even under similar reaction conditions and only poor activity for $Ru(PPh_3)_3(CO)_2$ was observed.

Finally in anticipation of better activity, we looked at mixed phosphine N-heterocyclic carbene complexes of ruthenium and were able to synthesise $Ru(IMes)(PPh_3)_2(CO)H_2$, which displayed comparable activity to **(1)** under similar conditions **[Chapter 5]**. Nonetheless, the activity of this carbene complex was not optimized and there is now evidence of deactivation pathways from C-C / C-H cleavage to suggest that this precursor may not exhibit higher overall catalytic activity.

3.2.2. *In situ* NMR investigations of the C-C coupling process: a new insight on the Murai reaction.

3.2.2.1. Investigation of the Murai reaction step by step.

In 2000, Hiraki et al. reported studies on the reaction of **(1)** with styrene and *m*-$CF_3C_6H_4C(O)CH_3$ **[Scheme 3.16.]**.[21] Their results showed the formation of a series of isomeric *ortho*-metalled ketone complexes (shown in **Scheme 3.16.**) which were formed at 70 °C during the reaction. Initially the *cis*-phosphine complex **(22a)** was formed, which readily converted to the *trans* phosphine isomer **(22b)** at this temperature. This finally isomerised to a second *trans* phosphine isomer with hydride *trans* to the activated aryl ring **(22c)**. None of these species were isolated and only poorly characterised by NMR due to their facile interconversion.

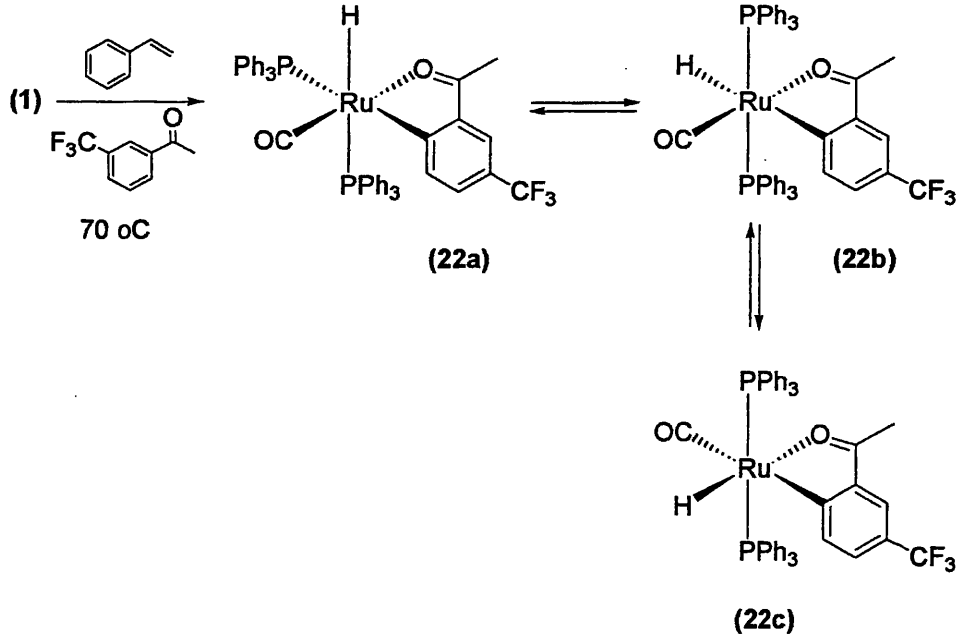

Scheme 3.16. - *Observed C-H/alkene coupling reaction between (1) and 3'-(trifluoromethyl)acetophenone promoted by styrene.*

In light of these interesting results, we decided to follow the reaction of **(1)** with alkene and 2'-methylacetophenone in detail by NMR to look for similar isomeric species.

Reaction of a 1:1 mixture of **(1)** with trimethylvinylsilane at 60 °C for 10 hours resulted in formation of a stoichiometric amount of trimethylethylsilane and the metallated complex $Ru(PPh_3)_2(o\text{-}C_6H_4PPh_2)(CO)H$ **(22)** **[Scheme 3.17.]**. **(22)** displayed two

phosphorus signals, a doublet at δ 52.8 (P_a) and a triplet at δ -34.7 ppm (P_b, J_{PP} = 15.8 Hz), and a characteristic hydridic proton at δ -8.27 (J_{HP} = 26.5 Hz, J_{HP} = 83.4 Hz) **[Spectrum 3.12.]**. complex **(22)** was described by Hiraki et al. as a side product in the reaction of **(1)** and triethoxyvinylsilane.[21]

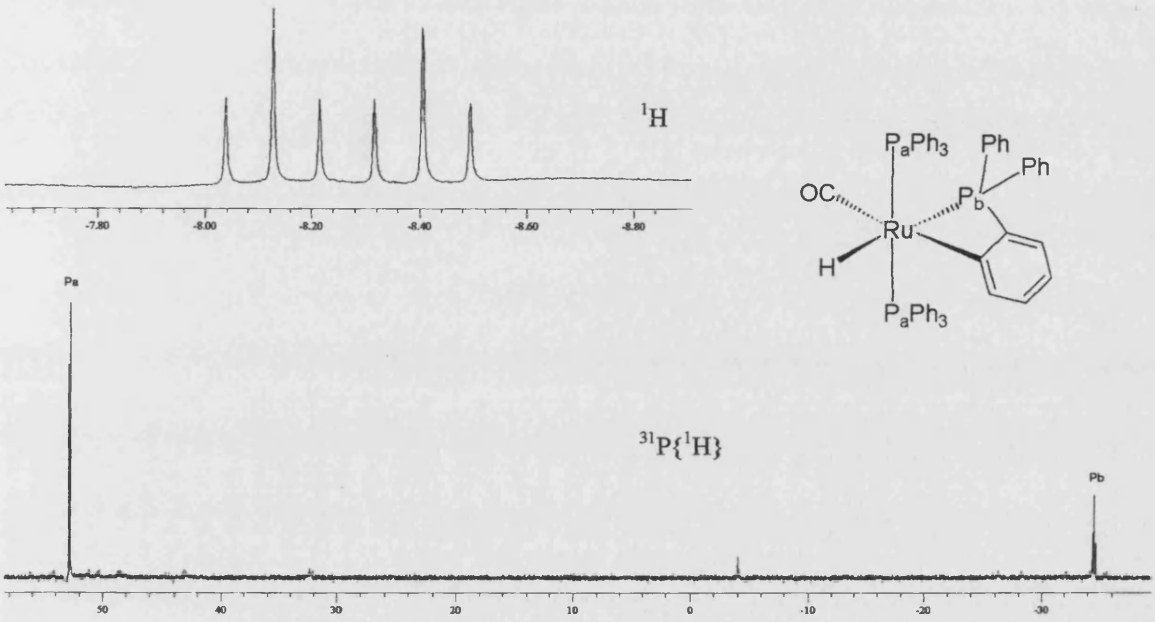

Spectrum 3.12. - *^{1}H NMR and phosphorous spectra of (22).*

The resonance from P_b, the phosphorus atom of the *ortho*-metallated phosphine ligand, is at much lower frequency than the signal from any of the other triphenylphosphine complexes that we have prepared. This low frequency shift for the phosphorus atom of an *ortho*-metallated triphenylphosphine is in the opposite direction to those found for metallated phosphites,[27] and phosphines where a five-membered ring is formed[28] but in the same sense as that found in the phosphorus atoms of the metallated phosphines in $Fe(PMe_3)_3(CH_2PMe_2)H$,[29] $Cr(PMe_3)_3(CH_2PMe_2)H$[30] and $Ru(PPh_3)_2(o\text{-}C_6H_4PPh_2)(CH_2CH_2)H$.[19]

Addition of acetophenone to **(22)** at room temperature resulted in rapid formation of *cis*-$Ru(PPh_3)_2(CO)(C_6H_4C(O)CH_3))H$ **(23) [Scheme 3.17.]**. **(23)** displayed two doublet phosphorus resonances at δ 40.0 and δ 36.5 (J_{PP} = 18.5 Hz), while the hydridic proton appeared as a doublet of doublets at δ -5.84 (J_{HP} = 24.4 Hz, J_{HP} = 92.9 Hz) **[Spectrum 3.13.]**. The *ortho* metallated acetophenone moiety displayed a broad doublet for the methyl group of the *ortho* metallated ketone at δ 1.76 (J_{HP} = 1.7 Hz), while the remaining protons on the phenyl ring of the ketone were assigned on the basis of a ^{1}H COSY spectrum.

$^{31}P\{^{1}H\}$-^{1}H HETCOR spectroscopy indicates correlation between the ketone protons and phosphorus in **(23)**.

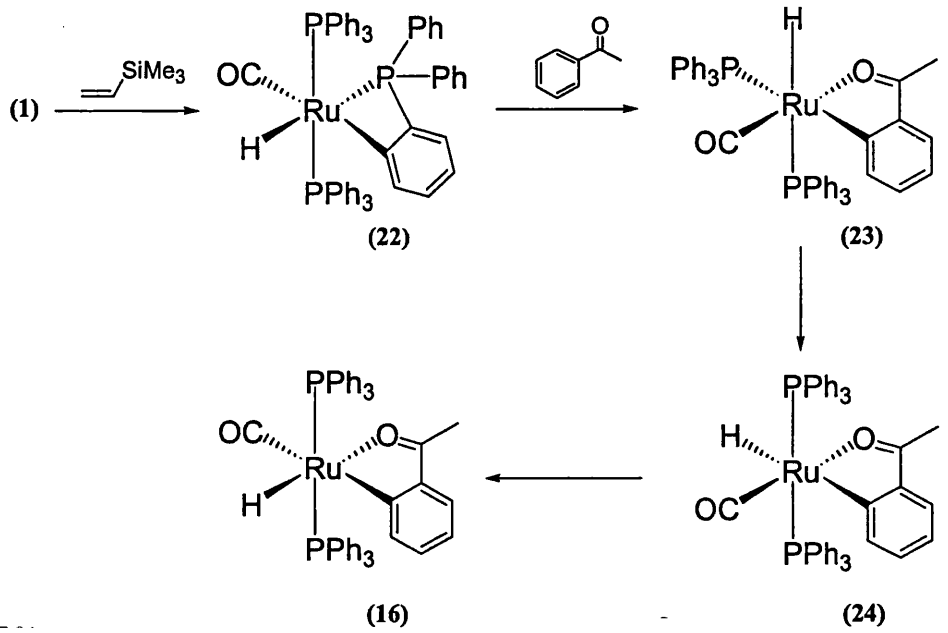

Scheme 3.17. - *Observed C-H/alkene coupling reaction between (1) and acetophenone promoted by trimethylvinylsilane.*

In solution, thermal isomerisation of **(23)** readily occurred within days at room temperature to afford the *trans* phosphine isomer *trans*-$Ru(PPh_3)_2(CO)(C_6H_4C(O)CH_3))H$ **(24)**, which in turn isomerised to **(16)**. **(24)** displayed a triplet signal at -3.26 ppm (J_{HP} = 22.4 Hz), while the methyl resonance was seen as a singlet at 1.98 ppm. On the basis of the $^{31}P\{^{1}H\}$-^{1}H HETCOR and ^{1}H COSY spectroscopy, the protons on the phenyl ring of the ketone were unambiguously assigned.

The relative rate of isomerisation of *cis*-phosphines complexes based on **(23)** into *trans* phosphine isomers similar to **(24)** and **(16)** has been observed to be dependent on the type of ketone used. In fact with 4-fluoroacetophenone up to 5 days were necessary, whereas bonded acetophenone converted within 2 days and 2-methylacetophenone within 24 hr. It is not yet quite clear why this is the case and further work in this regard is needed.

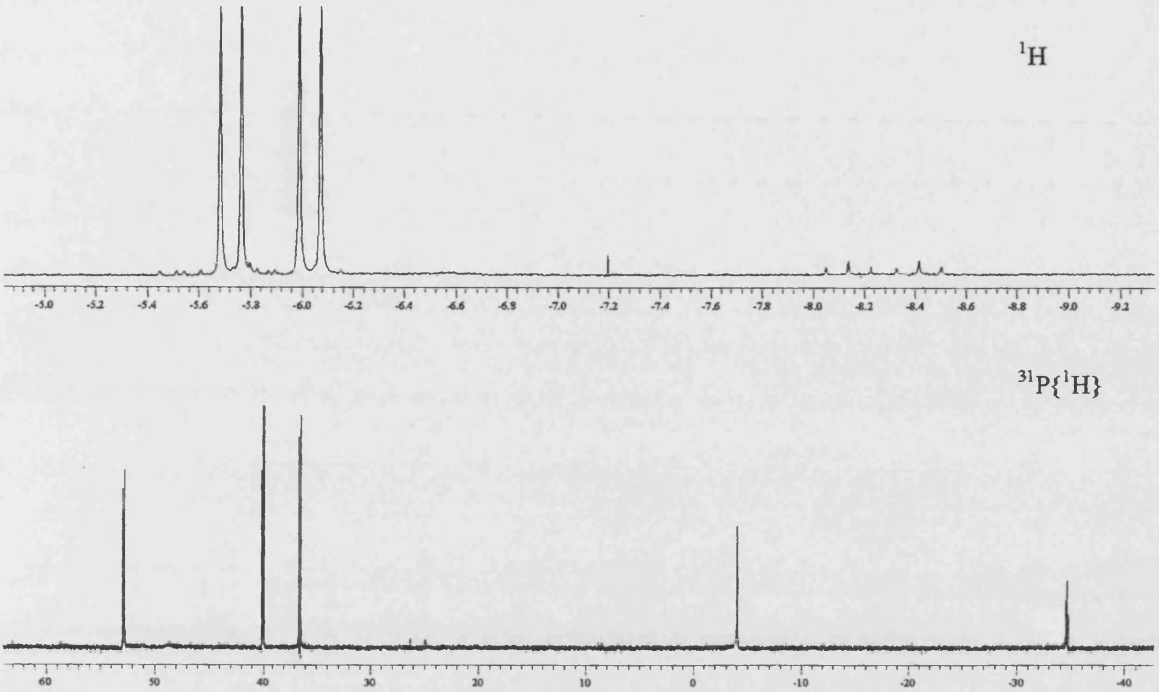

Spectrum 3.13. – ^{1}H and $^{31}P\{^{1}H\}$ NMR spectra of **(23)**.

As the reactivity of **(16)** toward the Murai chemistry had been studied, we set out to investigate the reactivity of the isomers **(23)** and **(24)**. Addition of 2 equivalents of trimethylvinylsilane to a C_6D_6 solution of **(23)** in a Youngs resealable NMR tube resulted in formation of 2-(trimethyl-ethyl-silane)acetophenone, and 2,6-di(trimethyl-ethyl-silane) acetophenone (both characterised by ^{1}H NMR spectroscopy) within hours at room temperature. Addition of 2 equivalents of trimethylvinylsilane to a Youngs NMR tube containing a mixture of **(24)** and **(16)** in C_6D_6 resulted in formation of **(62)** (mono and di substituted) only upon heating. **(24)** decomposed around 70°C, whereas **(16)** (as already observed previously), did not react readily and up to 5 days at this temperature were necessary to afford minute amount of **(A)** and **(B)**. These interesting results suggest the importance of considering isomers of **(16)** such as **(23)** and **(24)** as possible candidates on the pathway to the C-C coupling.

In the light of these results, DFT calculations were performed by Dr Stuart Macgregor (Heriot-Watt University) in order to assess the relative energies of the 7 possible isomers for the 6-coordinate *ortho* metallated species **[Figure 3.3.]**, as well as for the 5-coordinate *ortho* metallated species **[Figure 3.4.]** species. The dissociation energies of the PH_3 ligands are indicated by the pointed arrows in **Figure 3.3.**. As seen in **Figure 3.3.** an energy minimum is reached for a species **(c)** isostructural to **(23)**. A similar species stabilised by an agostic interaction reported by Morokuma et al. **[Figure 3.3., (a)]**,[3] has

been shown to be a stable intermediate on the pathway to C-C bond formation. Furthermore as shown in **Figure 3.2.** the energy of dissociation of the PH_3 phosphines on this zero-energy species is a minimum for the phosphine *trans* to the hydride, leading to the formation of another zero energy 5-coordinate *ortho* metallated species **[Figure 3.3., species 7]**. A different route is suggested by Morokuma involving dissociation of the phosphine *trans* to the *ortho* metallated carbon to afford stable complex **(b) [Figure 3.2.]**. These two different routes remain to be probed but indicate complexes isostructural to **(36)** as possible intermediates on the pathway to C-C bond formation.

Morokuma et al.

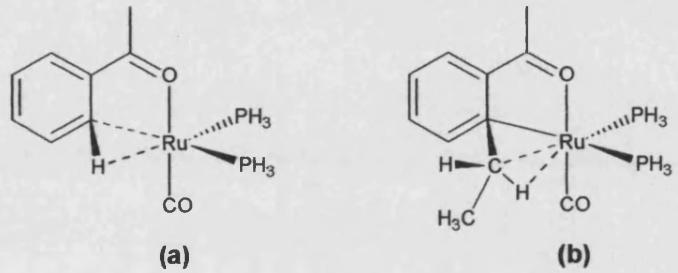

Macgregor et al.

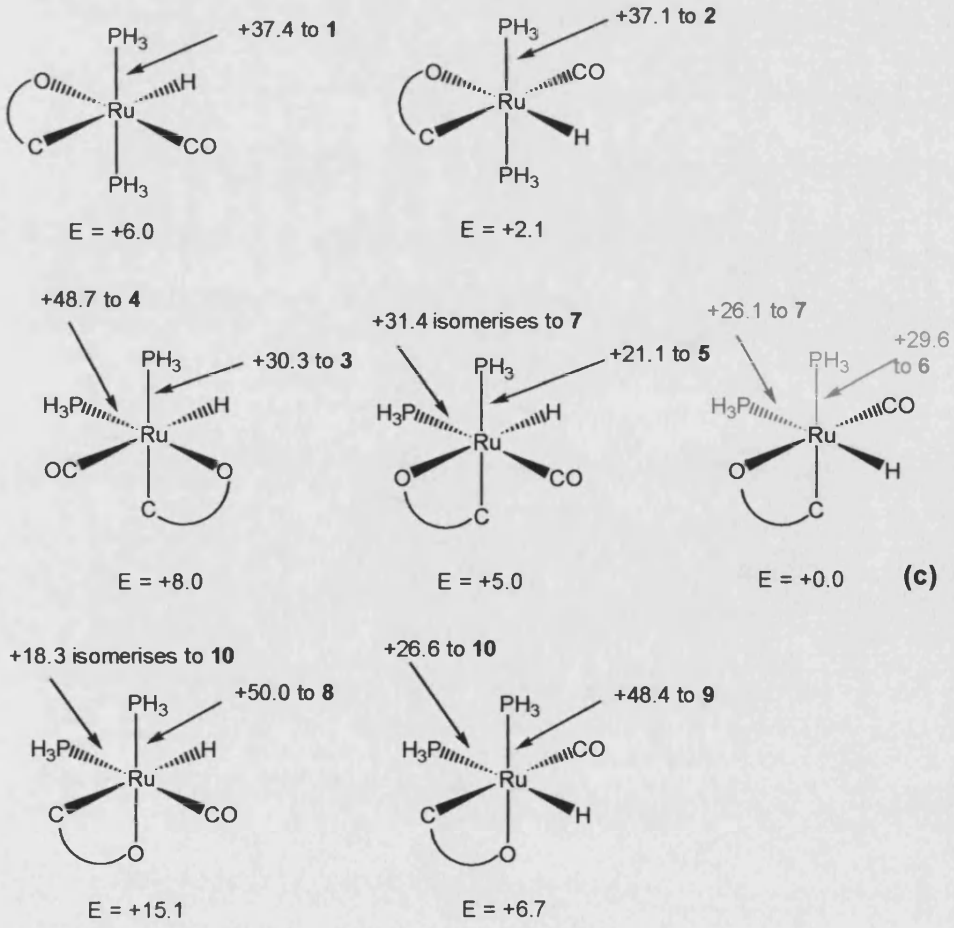

Figure 3.2. - *Relative energies of the various 6-coordinate species.*

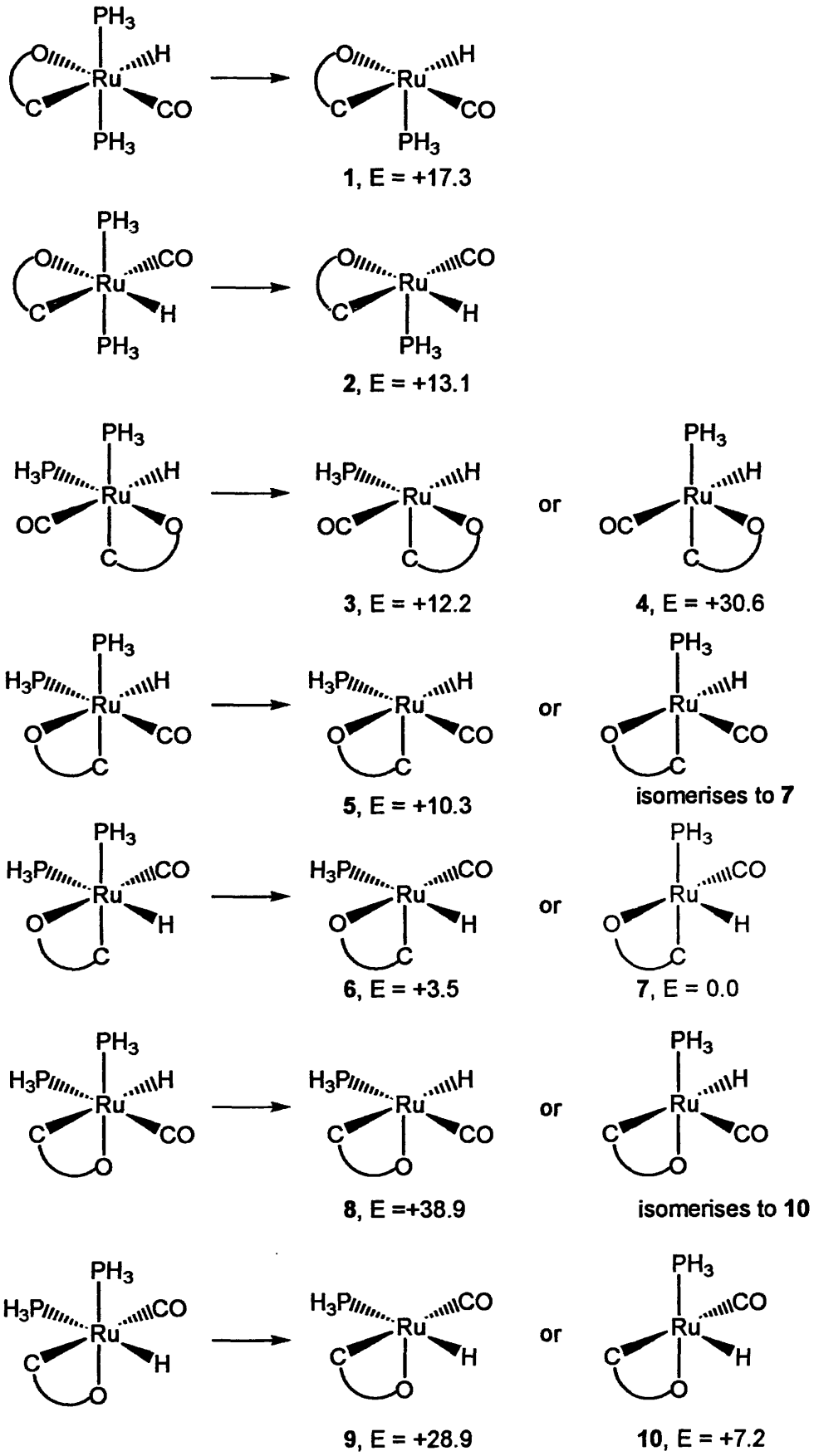

Figure 3.3. - *Relative energies of the various 5-coordinate species.*

3.2.2.2. Investigation of the reactivity of (12).

Although **(12)** proved to be moderately active for catalysing the Murai reaction we decided to investigate its a reactivity with a stoichiometric amount of 2-methylacetophenone. **(12)** slowly reacted with 2-methylacetophenone at 100 °C to afford 2-methyl-6-ethyl-acetophenone and the *ortho*-metallated complex **(22)** **[Scheme 3.18.]**. This surprising result suggests that **(12)** plays a key role in the Murai reaction. Moreover, it demonstrated that if a Ru^0 species was to be formed during the Murai reaction it would subsequently react with the ketone substrate to afford the C-C coupling product and **(22)**, which we have seen to be highly reactive towards ketones.

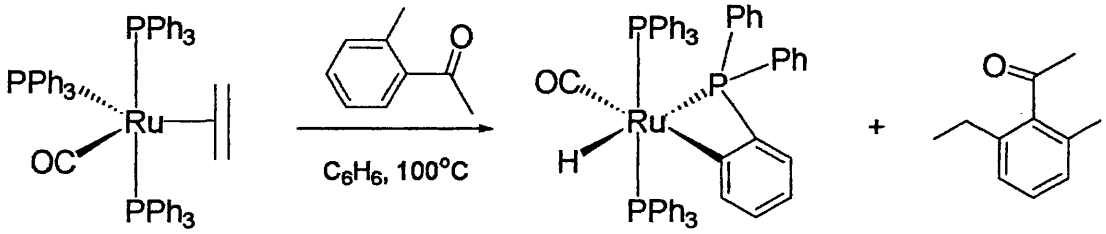

(12) **(22)**

Scheme 3.18.

3.2.2.3. Investigation of the reactivity of (14).

The stoichiometric reaction of **(14)** with ethene showed rapid formation of free PPh_3 (observed by $^{31}P\{^1H\}$ NMR) along with a single species with a $^{31}P\{^1H\}$ resonance at 58.5 ppm attributed to $Ru(PPh_3)_2(o\text{-}C_6H_4C(O)CH_3)(CH_2CH_2)H$ **(25)** **[Scheme 3.19.]**. The NMR spectrum of this species showed a triplet hydride resonance at δ -13.91 (J_{HP} = 21.2 Hz), a singlet resonance at δ 2.03 attributed to the acetophenone methyl group and a broad triplet a δ 2.86 (J_{HP} = 3.2 Hz). These 3 signals integrated 1:3:4 respectively. The broad triplet was attributed to coordinated ethene, (this signal disappeared upon using CD_2CD_2 instead of ethene) **[Spectrum 3.14.]**. Over a longer reaction time (10 hours at room temperature) and excess ethene, **(14)** reacted further to form the *ortho*metallated complex $Ru(PPh_3)_2(o\text{-}C_6H_4PPh_2)(CH_2CH_2)H$[19] and the C-C coupling product 2,6-diethyl-acetophenone. $Ru(PPh_3)_2(o\text{-}C_6H_4PPh_2)(CH_2CH_2)H$ was previously described by Cole-Hamilton et al. upon reaction of $Ru(PPh_4)H_2$ with ethene. It displays a characteristic doublet of triplets hydride at δ - 6.5 (J_{HP} = 70.0 Hz, J_{HP} = 24.0 Hz) in the ^1H spectrum, and a doublet and a triplet at δ 50.2 and -38.4 (J = 15.8 Hz) in the $^{31}P\{^1H\}$ NMR spectrum. In

the absence of an exess of ethene, **(22)** decomposed to several products which could not be analysed, along with a mixture of 2-ethyl-acetophenone and 2,6-diethyl-acetophenone.

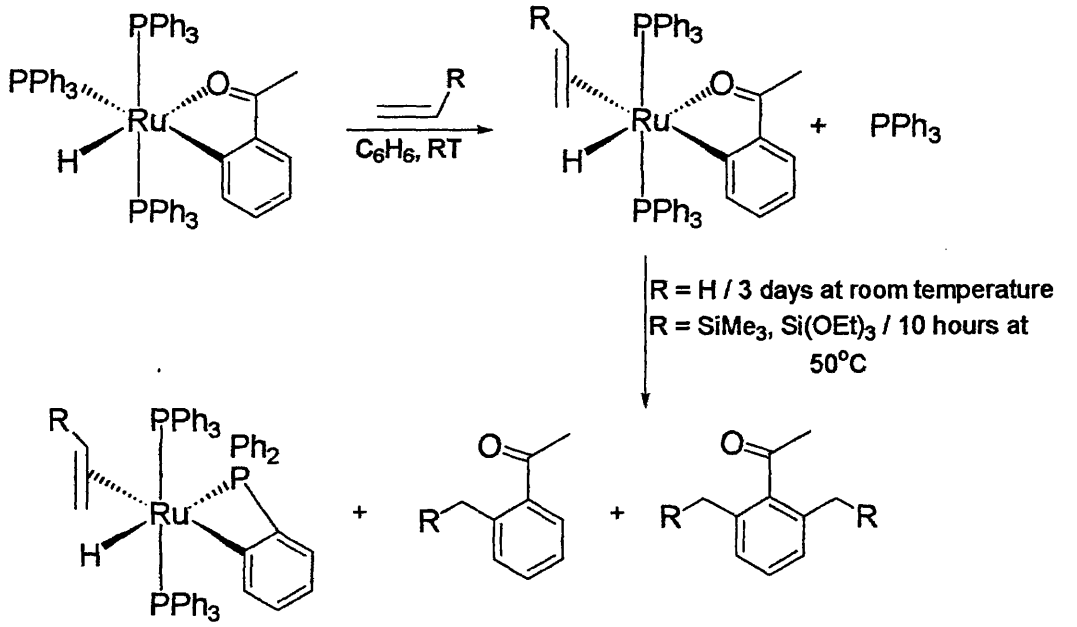

Scheme 3.19.

It is important to note that an identical process was observed when using R = $SiMe_3$ and $SiOEt_3$ although their reactivity was not investigated in any detail. Nevertheless formation of the C-C coupling product was observed in both cases along with decomposition of the ruthenium complex.

3.2.3. Synthesis and reactivity of complexes similar to Hiraki's complexes.

3.2.3.1. Synthesis of *cis-N,H*-$Ru(PPh_3)_2(CO)(NC_4H_3C(O)CH_3)H$ (19).

Upon reaction of **(1)** with the free pyrrolyl phosphine $P(Py)_2(NC_4H_3C(O)CH_3)$ at reflux, we were surprised to find formation of *cis-N,H*-$Ru(PPh_3)_2(CO)(NC_4H_3C(O)CH_3)H$ **(19)** as a result of the degradation of the phosphine ligand **[Scheme 3.20.]**. The complex was formed cleanly but in a low yield.

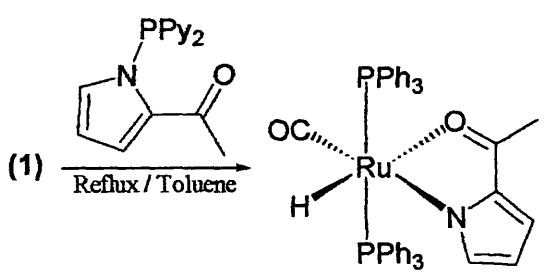

Scheme 3.20.

The ^{1}H NMR spectrum of **(19)** displayed a triplet hydride at δ -13.91 (J_{PH} = 20.0 Hz) **[Spectrum 3.14.]**, while the $^{13}C\{^{1}H\}$ NMR spectrum showed one low field triplet at δ 204.9 (J = 13.0 Hz) and a broad singlet at 188.5, assigned to the carbonyl and Ru-O=C groups respectively on the basis of ^{1}H-$^{13}C\{^{1}H\}$ HMQC and HMBC experiments. The IR spectrum displayed three bands at 2037, 1927, and 1535 cm^{-1} assigned to ν_{Ru-H}, ν_{CO} and $\nu_{Ru-O=C}$ respectively.

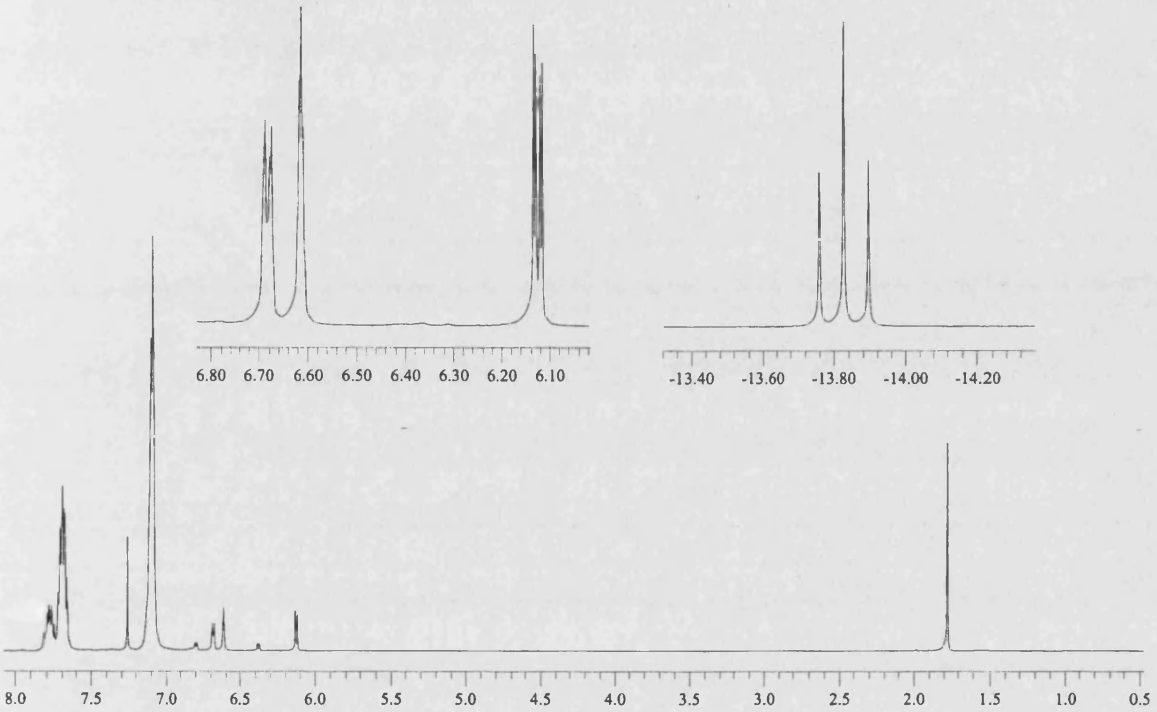

Spectrum 3.14. - ^{1}H NMR spectrum of **(19)**.

The structure of **(19)** was determined by X-ray crystallography **[X-Ray 3.6.]** Selected bond distances and angles are given in **Table 3.9.**.

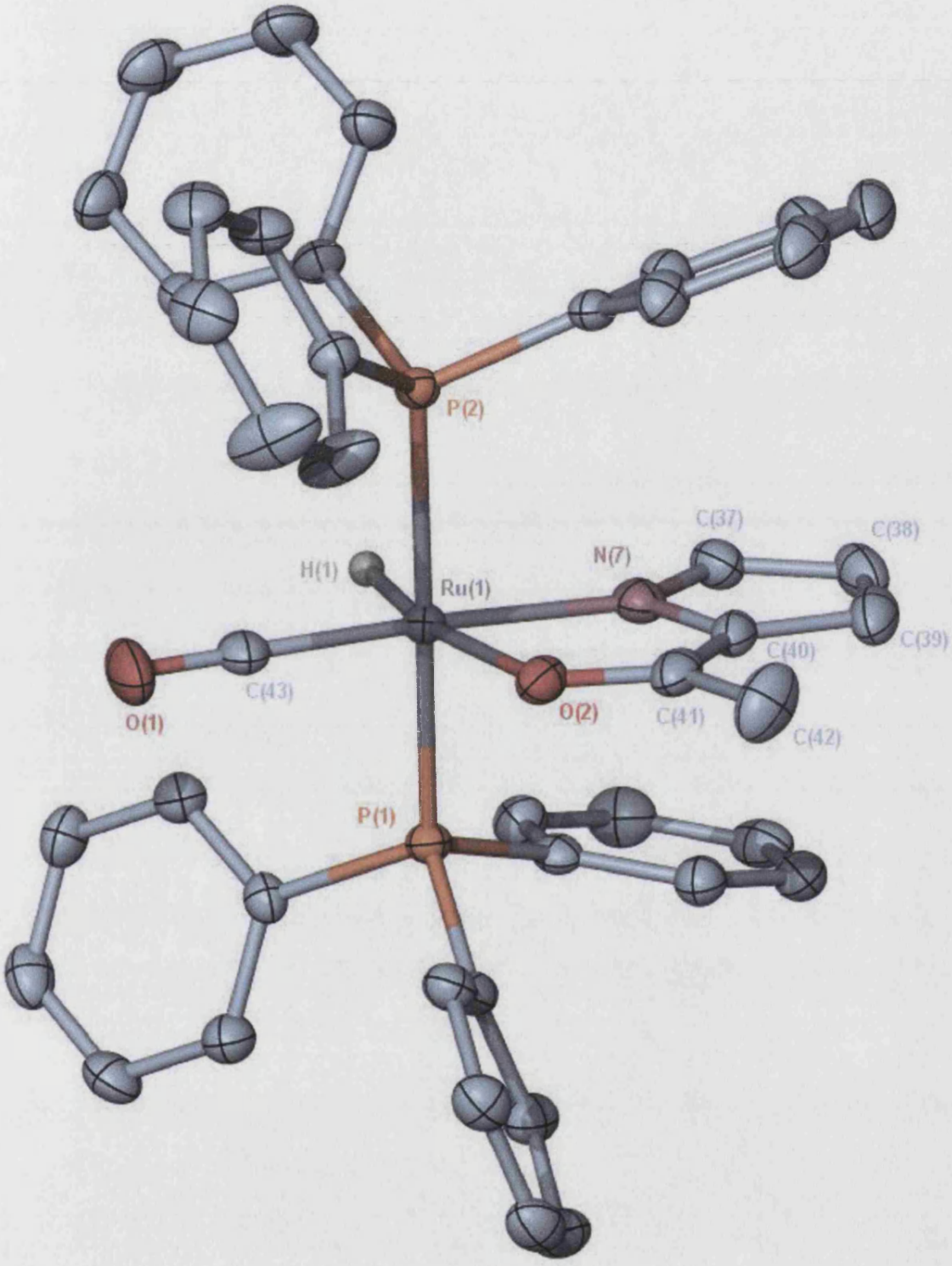

X-Ray 3.6. - *X-ray structure of* ***(19)****. Thermal ellipsoids are set at the 50% probability level. Hydrogen (apart from hydrides) atoms have been omitted for clarity.*

Selected Bond Lengths	**[Å]**		
Ru(1)-C(43)	1.834(3)	Ru(1)-N(7)	2.118(2)
Ru(1)-O(2)	2.212(2)	Ru(1)-P(1)	2.3496(7)
Ru(1)-P(2)	2.3598(7)	O(1)-C(43)	1.154(4)
O(2)-C(41)	1.273(4)	N(7)-C(37)	1.336(4)
N(7)-C(40)	1.387(4)	C(37)-C(38)	1.395(5)
C(38)-C(39)	1.388(5)	C(39)-C(40)	1.418(4)
C(40)-C(41)	1.404(4)	C(41)-C(42)	1.490(4)
Selected Bond Angles	**[°]**		
C(43)-Ru(1)-N(7)	174.84(12)	C(43)-Ru(1)-O(2)	99.14(12)
N(7)-Ru(1)-O(2)	75.96(9)	C(43)-Ru(1)-P(1)	91.43(9)
N(7)-Ru(1)-P(1)	87.71(6)	O(2)-Ru(1)-P(1)	98.06(5)
C(43)-Ru(1)-P(2)	90.78(9)	N(7)-Ru(1)-P(2)	90.73(6)
O(2)-Ru(1)-P(2)	88.76(5)	P(1)-Ru(1)-P(2)	172.41(3)
C(41)-O(2)-Ru(1)	113.84(19)	O(2)-C(41)-C(40)	119.2(3)
N(7)-C(40)-C(41)	117.4(3)	C(40)-N(7)-Ru(1)	113.63(18)

Table 3.9. - *Selected bond lengths [Å] and angles [°] for cis-Ru(PPh$_3$)$_2$(CO)(NC$_4$H$_3$C(O)CH$_3$)H*

3.2.3.2. Synthesis of *trans-N,H*-Ru(PPh$_3$)$_2$(CO)(NC$_4$H$_3$C(O)CH$_3$)H. (20)

In order to investigate the formation of **(19)**, we decided to attempt an alternative synthesis using a route analogous to that described for the formation of **(16)** and **(17)**. Reaction of **(5)** with acetyl pyrrole at 45°C in THF afforded the *trans-N,H*-Ru(PPh$_3$)$_3$(NC$_4$H$_3$C(O)CH$_3$)H **(18)** complex which was characterised by IR and NMR spectroscopy **[Scheme 3.21.]**. Surprisingly when **(18)** was reacted with CO, instead of forming **(19)** as expected, we obtained *trans-N,H*-Ru(PPh$_3$)$_2$(CO)(NC$_4$H$_3$C(O)CH$_3$)H **(20)** in which the hydride was *trans* to the pyrrole nitrogen **[Scheme 3.21.]**.

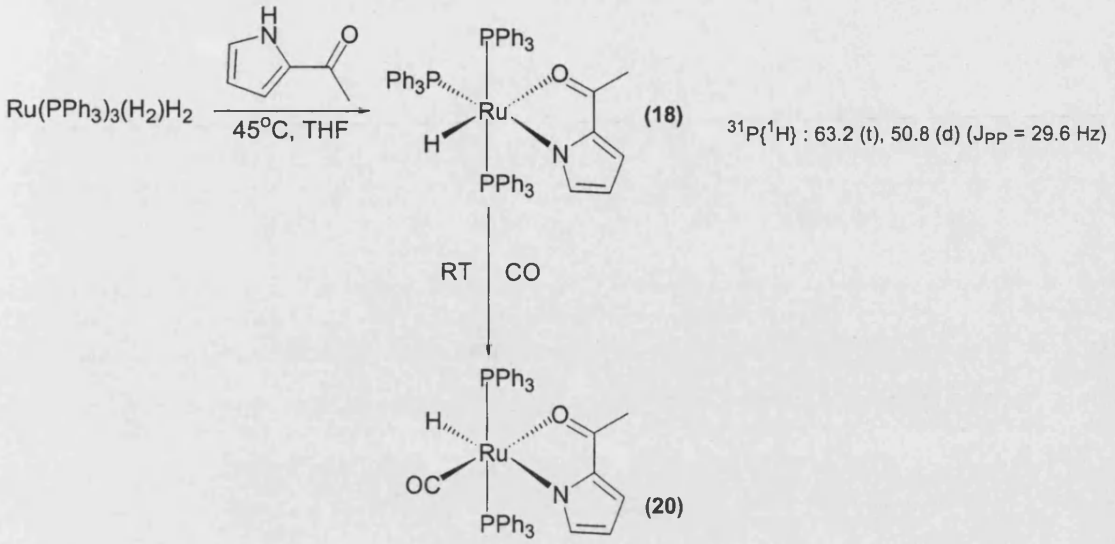

Scheme 3.21.

The hydride ligand in **(20)** appeared as a triplet at δ -9.39 (J_{PH} = 20.8 Hz) in the ^{1}H NMR spectrum **[Spectrum 3.15.]**, while the $^{13}C\{^{1}H\}$ NMR spectrum showed a low field triplet at δ 207.1 (J = 13.5 Hz) and a broad singlet at 188.2, assigned to the carbonyl and Ru-O=C respectively using 2D NMR methods. The IR spectrum displayed three bands at 1962, 1917, and 1536 cm^{-1} assigned to ν_{Ru-H}, ν_{CO} and $\nu_{Ru-O=C}$ respectively. The structure of **(20)** was determined by X-ray crystallography to confirm the geometry **[X-Ray 3.7.]** Selected bond distances and angles are given in **Table 3.10.**.

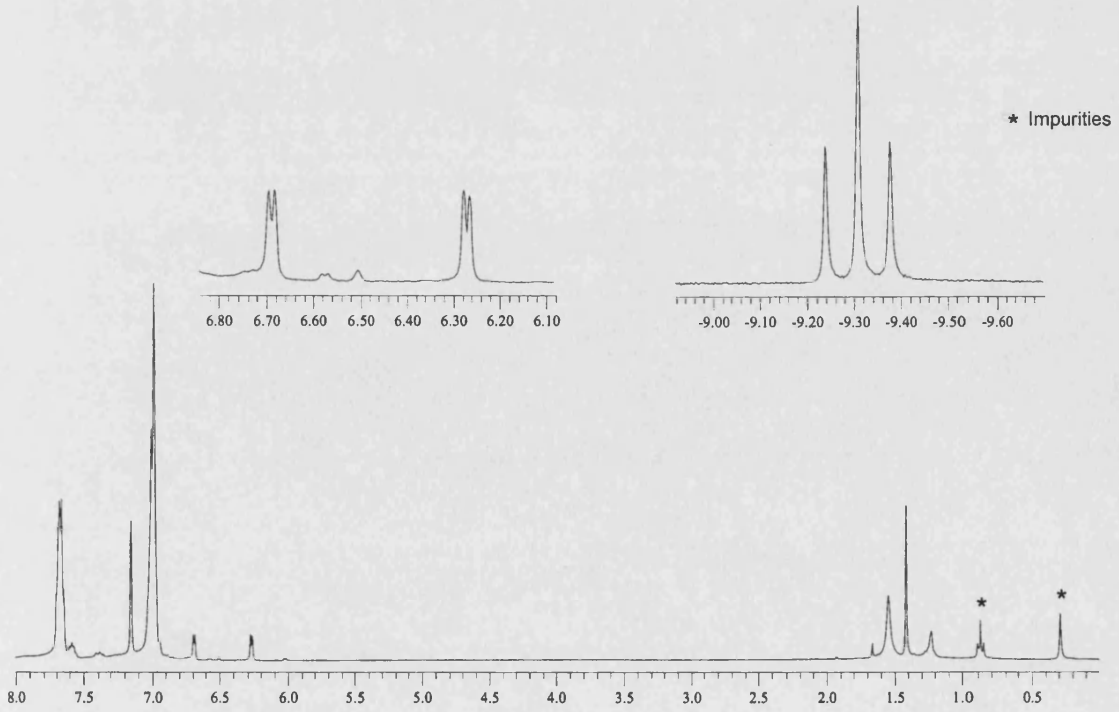

Spectrum 3.15. – *^{1}H NMR spectrum of (20).*

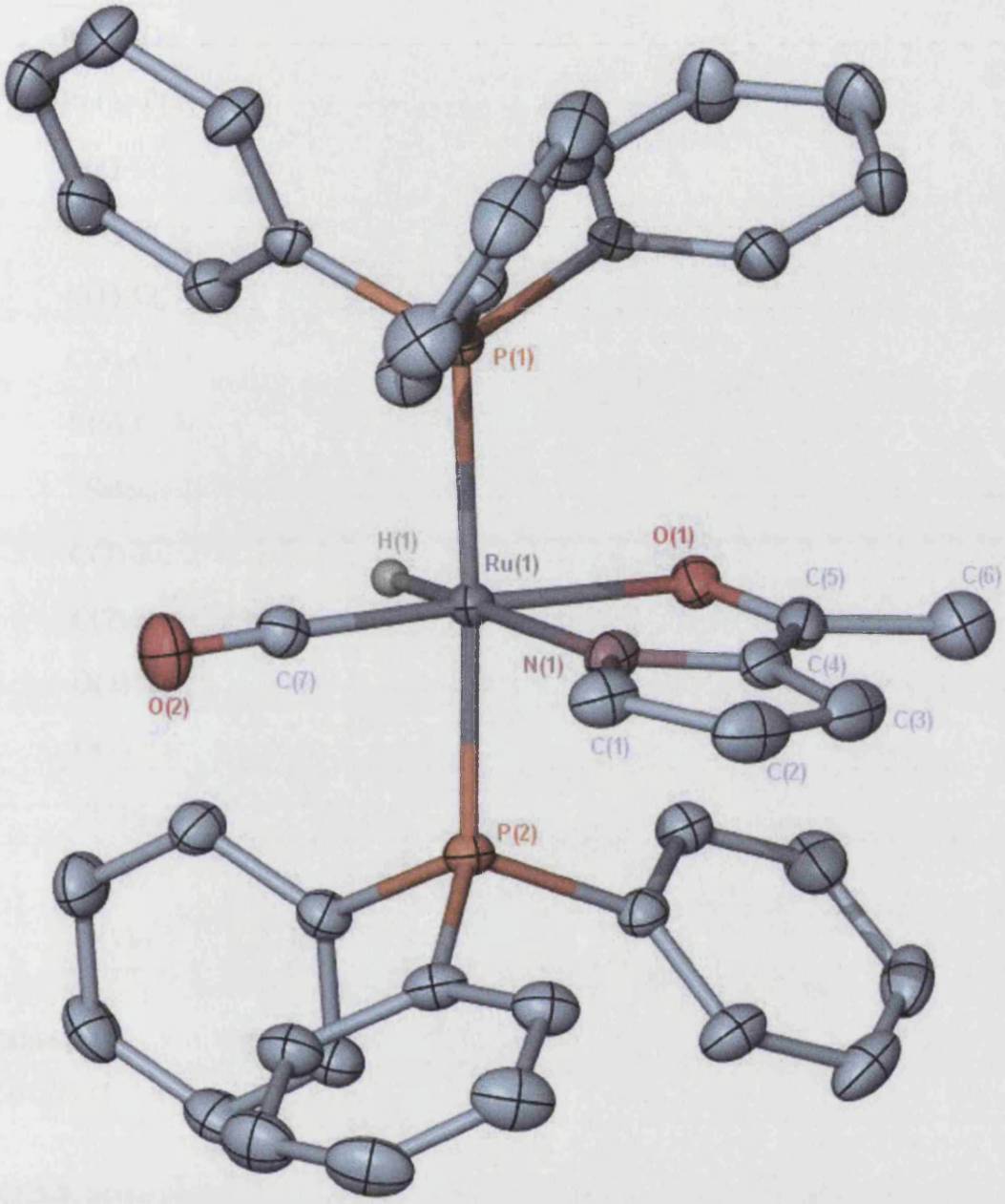

X-Ray 3.7. - *X-ray structure of* ***(20)****. Thermal ellipsoids are set at the 50% probability level. Hydrogen (apart from hydrides) atoms have been omitted for clarity.*

Selected Bond Lengths	**[Å]**		
Ru(1)-O(1)	2.1391(14)	Ru(1)-C(7)	1.815(2)
Ru(1)-P(1)	2.3319(4)	Ru(1)-N(1)	2.1551(19)
O(1)-C(5)	1.281(3)	Ru(1)-P(2)	2.3404(5)
N(1)-C(1)	1.338(3)	O(2)-C(7)	1.155(3)
C(1)-C(2)	1.423(4)	N(1)-C(4)	1.392(3)
C(3)-C(4)	1.415(3)	C(2)-C(3)	1.375(4)
C(5)-C(6)	1.500(3)	C(4)-C(5)	1.398(3)
Selected Bond Angles	**[°]**		
C(7)-Ru(1)-O(1)	176.65(7)	O(1)-Ru(1)-N(1)	76.58(6)
C(7)-Ru(1)-N(1)	100.59(8)	C(7)-Ru(1)-P(1)	91.57(6)
O(1)-Ru(1)-P(1)	90.51(4)	N(1)-Ru(1)-P(1)	95.46(5)
O(1)-Ru(1)-P(2)	88.91(4)	C(7)-Ru(1)-P(2)	89.42(7)
P(1)-Ru(1)-P(2)	171.47(2)	N(1)-Ru(1)-P(2)	92.69(5)
C(4)-N(1)-Ru(1)	111.62(14)	N(1)-C(4)-C(5)	116.67(19)
O(1)-C(5)-C(4)	119.74(19)	C(5)-O(1)-Ru(1)	114.74(14)

Table 3.10. - *Selected bond lengths [Å] and angles [°] for trans-Ru(PPh$_3$)$_2$(CO(NC$_4$H$_3$C(O)CH$_3$)H*

3.2.3.3. Structural analysis of (19) and (20).

Comparison of the two isomeric complexes **(19)** and **(20)** reveals some minor changes in the bond lengths and angles of the metallated ketone ring **[Figure 3.4.]**. As expected significant lengthening of the Ru-X bond *trans* to hydride is observed. Thus in **(19)**, the Ru-O distance of 2.212(2) Å compared to the Ru-O bond length of 2.1391(14) Å in **(20)** in which the Ru-O is *trans* to CO. Noticeable also is the difference in the Ru-CO distances 1.834(3) Å when *trans* to N in **(19)**, 1.815(2) Å and when *trans* to O in **(20)**. Finally very little difference is observed within the metallated acetopyrrole moiety **[Figure 3.4.]**.

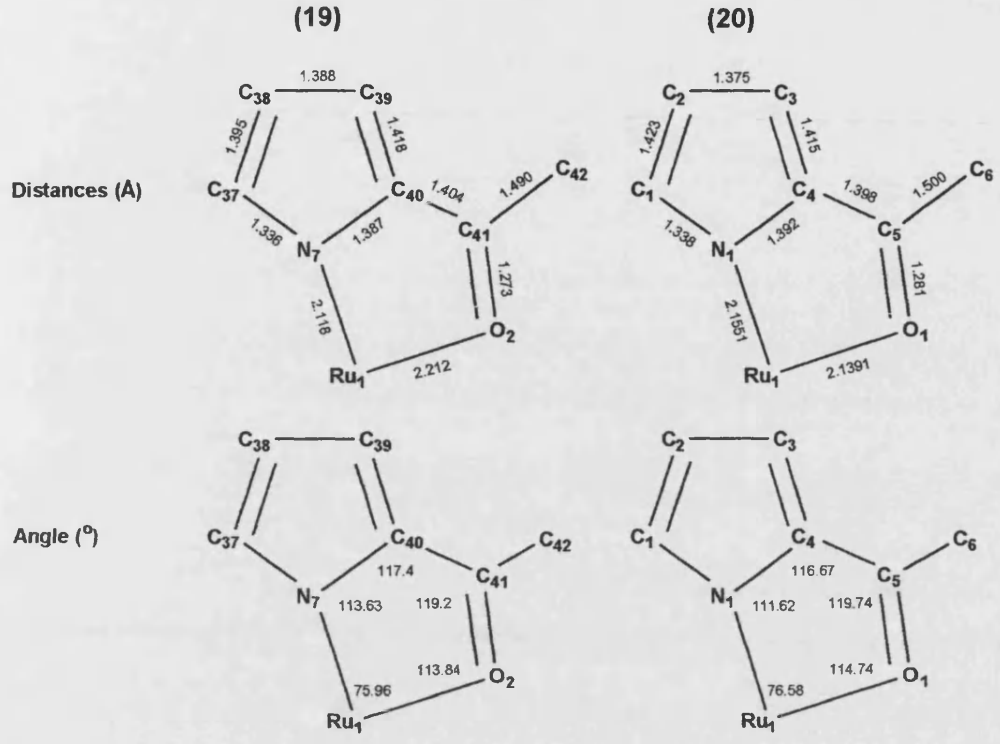

Figure 3.4. – *Selected bond distances and angles in (19) and (20).*

3.2.3.4. Thermal isomerisation of (20) into (19).

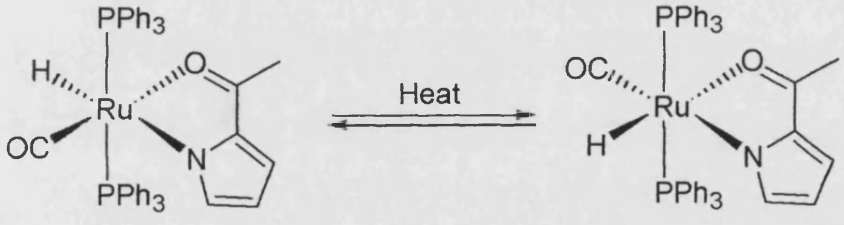

(20) **(19)**

Scheme 3.22. - *Isomerisation of (20) into (19).*

Comparable to the process observed in interconverting **(23)**, **(24)** and **(16)**, thermolysis of **(20)** produced **(19)** **[Scheme 3.22.]**. This process was followed using ^{1}H NMR spectroscopy looking at the hydride region as shown in **Spectra 3.16.** This was used to yield a plot of the concentration versus time **[Graph 3.1.]** and then a plot of ln[concentration] of either **(19)** or **(20)** versus time resulted in a straight line indicative of a first order process. This experiment was repeated at different temperatures in order to investigate the influence of temperature on the rate of isomerisation **[Graph 3.1.]**.

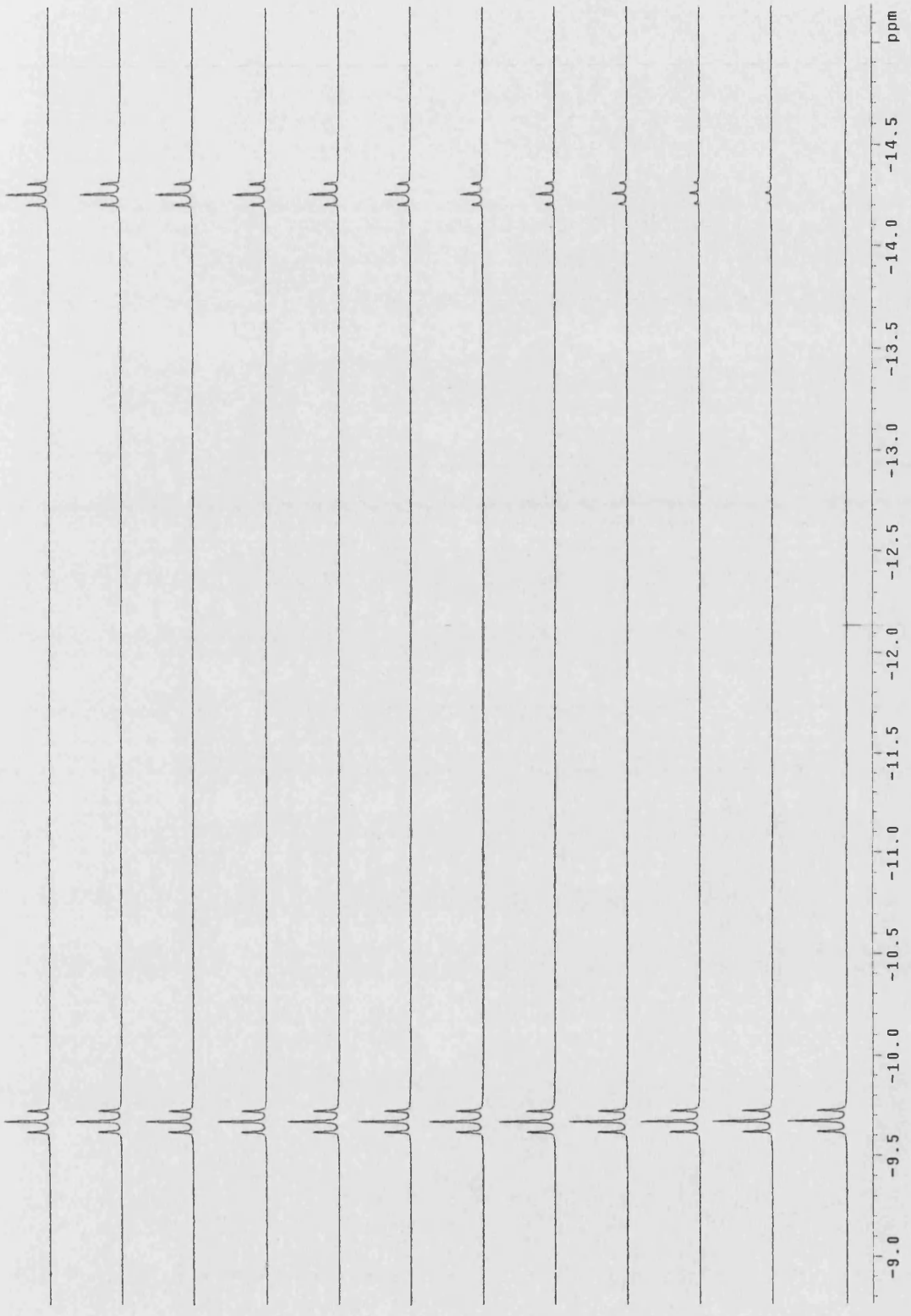

Spectra 3.16. - *Selected ^{1}H NMR spectra of the reaction described in* ***Scheme 3.16.***.

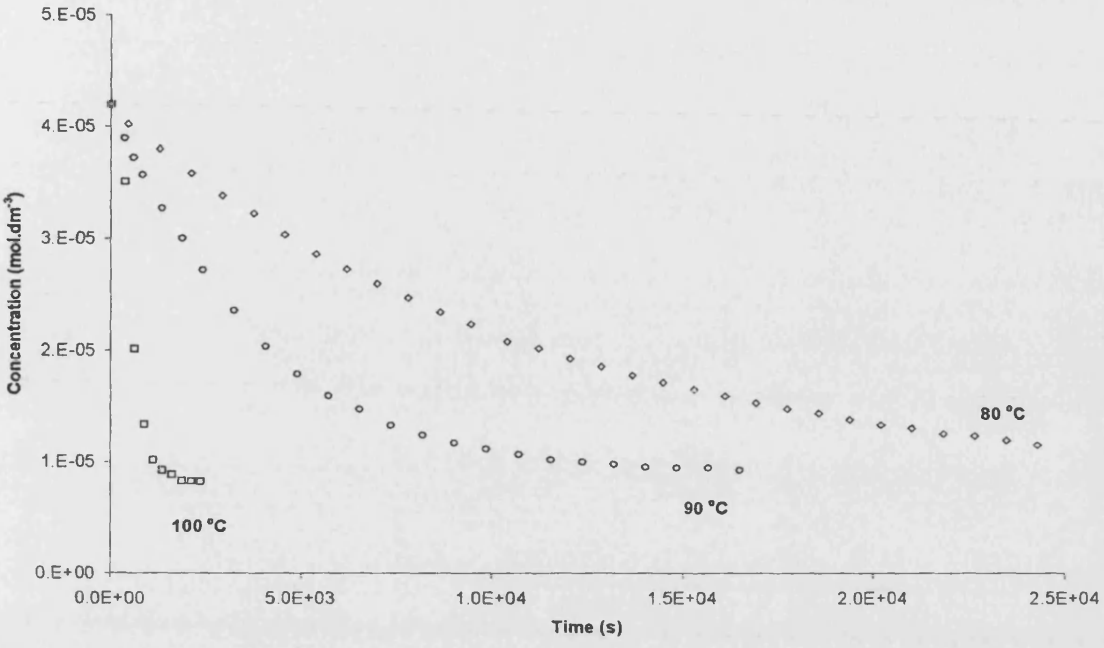

Graph 3.1. - *Plot of the concentration of* ***(20)*** *versus time for the reaction in* ***Scheme 3.22.***.

The rate constant at a set of temperatures **[Table 3.11.]** could be derived from the slope by plotting - *ln*[concentration] versus time **[Graph 3.2.]**. Out of the rate constants observed at typically 80, 90, 100 °C **[Table 3.11.]**, we were able to plot the Arrhenius plot and consequently deduce the energy of activation for the isomerisation. It is important to notice the large positive value observed for $\Delta S^{\ddagger}$ indicating a dissociative reaction.

Temp K	k_{obs} (x 10^5) s^{-1}	E_a $kJ.mol^{-1}$	$\Delta H^{\ddagger}$ $kJ.mol^{-1}$	$\Delta S^{\ddagger}$ $J.mol^{-1}.K^{-1}$
353	9.48	189	186	201
358				
363	23.3			
368				
373	304			

Table 3.11. - *Rate constants, E_a, $\Delta H^{\ddagger}$ and $\Delta S^{\ddagger}$ for the isomerisation of* ***(20)*** *into* ***(19)***.

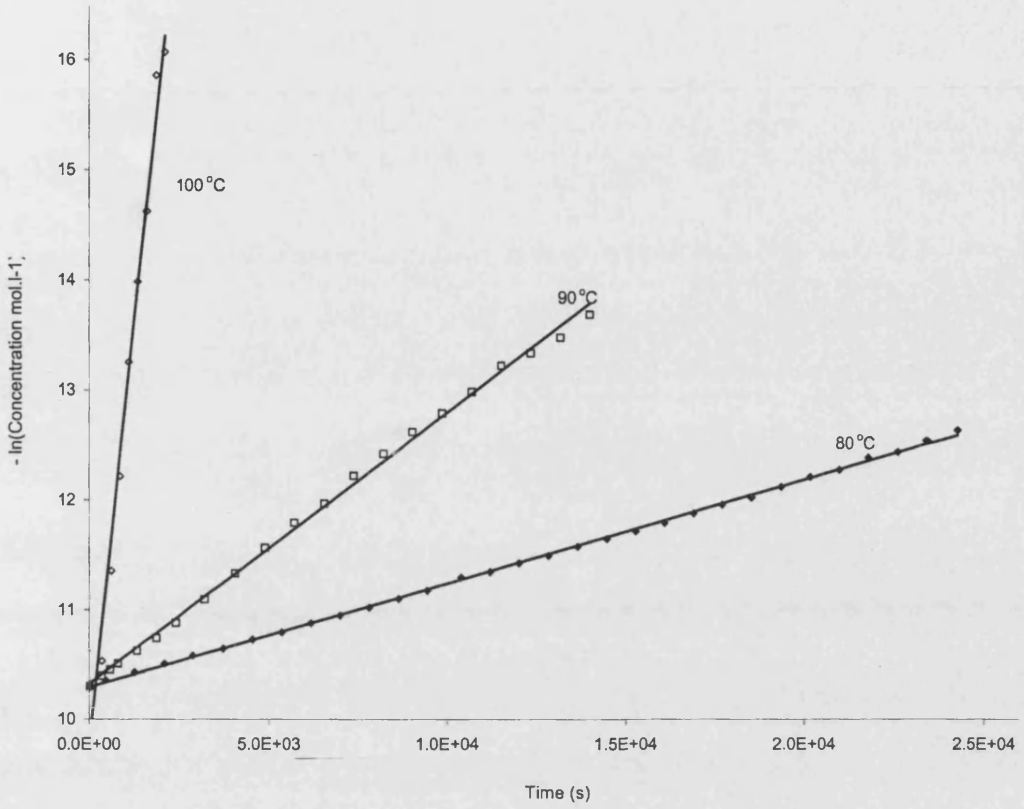

Graph 3.2. - *Plot of - ln[19] versus time.*

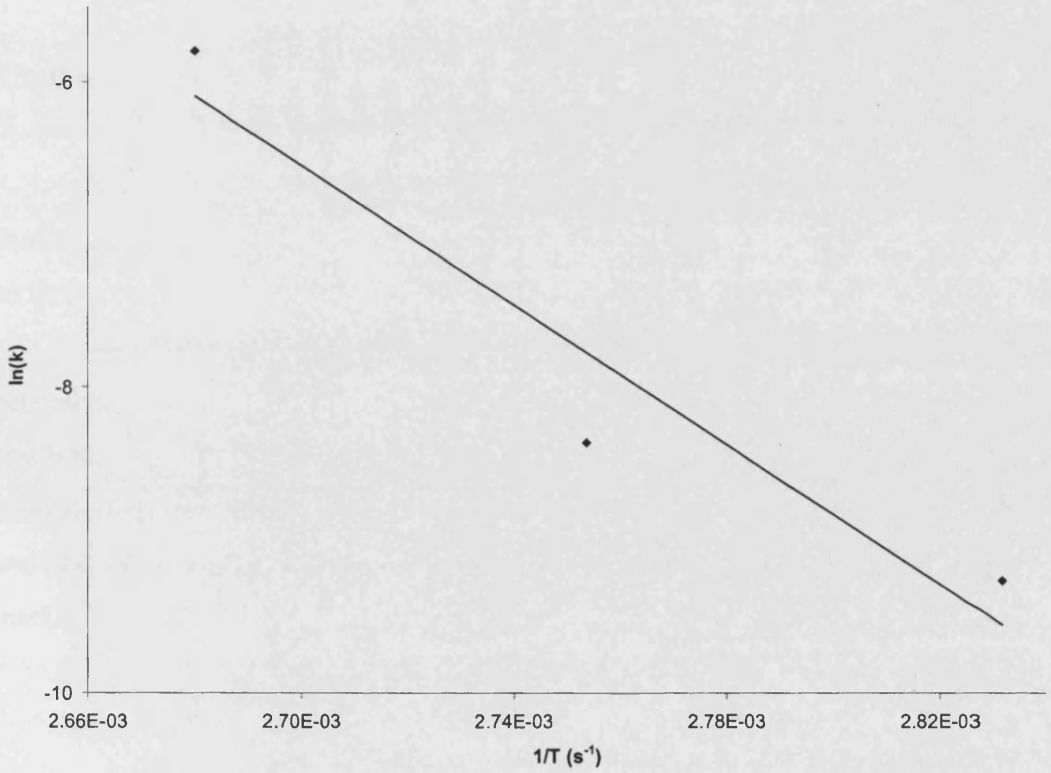

Graph 3.3. - *Arrhenius plot for the reaction in* ***Scheme 3.22.***.

3.2.3.5. About the formation of (20).

Although the mechanism of formation of **(20)** in the reaction of **(1)** with the pyrrolyl-phosphine ligand was not probed, decomposition of these ligands is not unusual. The P-N bond in N-pyrazolyl phosphines has been shown to be highly reactive towards protic ROH molecules. This has been demonstrated by Ros et al. who reported the MeOH promoted intramolecular decomposition of the P-N bond of the coordinated pyrazolyl phosphine ligand in $Ru(PPh_2(Me_2Pz))(p\text{-cymene})Cl_2$, to afford the structurally characterised $[Ru(PPh_2OH)(Me_2HPz)(p\text{-cymene})(PPhOH]Cl$.[31]

3.2.3.6. Reactivity of (19) and (20) toward C-C coupling.

Due to the evident similarities between **(19)** and **(20)** and the *ortho*-metallated ketone species already studied, we decided to investigate whether or not the isomerisation resulted in a major change in the reactivity of these *ortho*-metallated species. Using the same conditions as stated before in **3.2.1.5.**, no reaction was observed using **(19)** as the ruthenium precursor for up to 10 days at 135°C, whereas use of **(20)** as a catalyst resulted in 23 % conversion after 2 hours at 135°C.

3.3. Discussion of the mechanism of C-C coupling.

It is possible to draw some conclusions on the proposed mechanism from our studies and to postulate a more advanced mechanism on the basis of the observations made so far.

As shown in **Scheme 3.23.** it was proposed by various authors[1-5, 21] that initial activation of **(1)** by the alkene substrate generates the active catalytic species in the reaction. Our work in this respect has shown that when there is activation of **(1)** by the alkene substrate, it produces one equivalent of the corresponding alkane via hydrogentaion and the $16e^-$ ruthenium species $Ru(PPh_3)_3(CO)$. This fact is demonstrated by the different reactivity observed when **(1)** is reacted with either ethene or trimethylvinylsilane **[Scheme 3.23.]**. In the first case use of the ethene afforded **(12)**, whereas in the later case formation of the *ortho*-metallated phosphine complex **(22)** was observed.

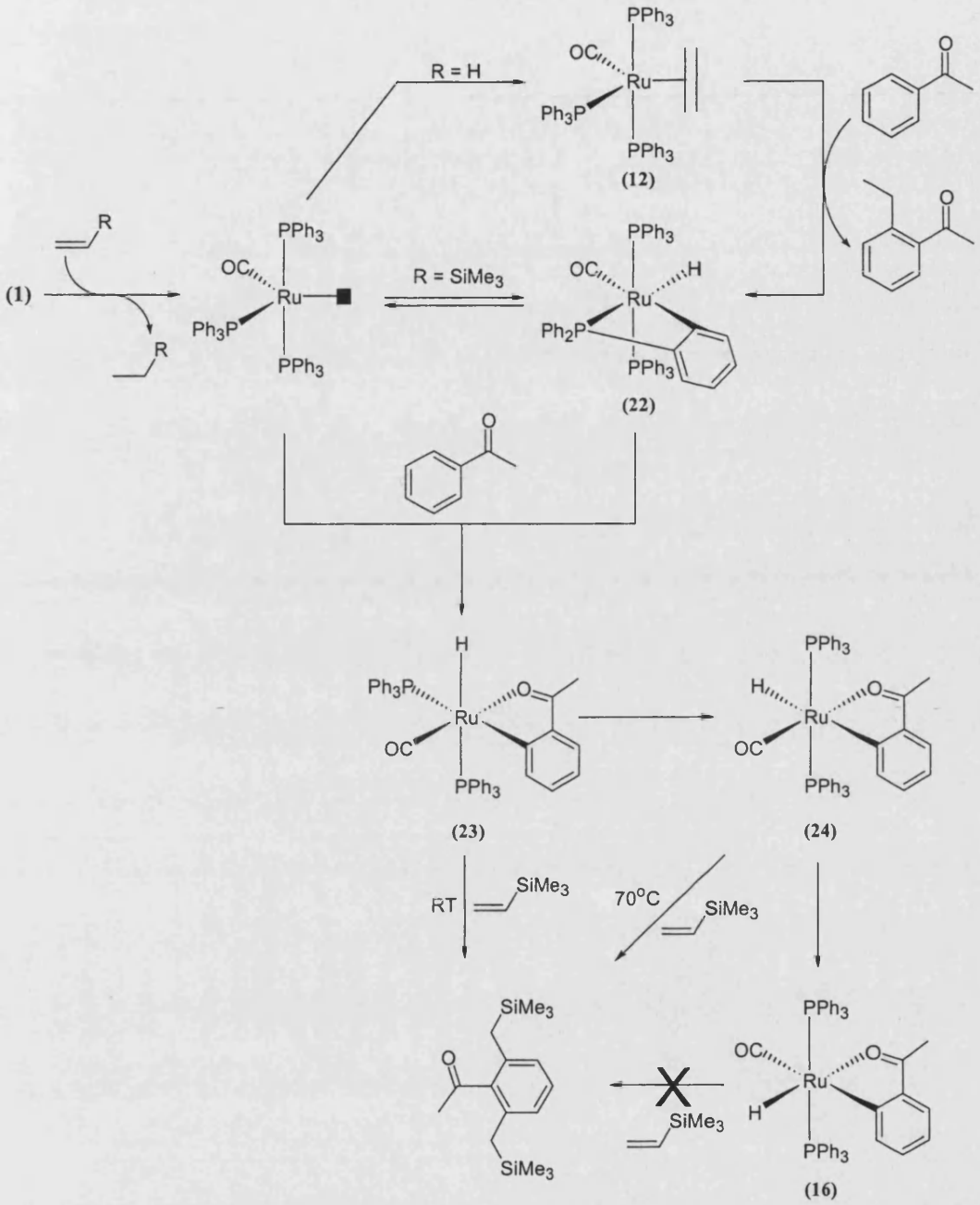

Scheme 3.23.

Due to the highly regiospecificity of the Murai reaction, it was proposed that the C-C bond coupling reaction must occur via an *ortho*-metallated ketone complex similar to complex **(16)**. We have demonstrated the poor catalytic activity of this species as well as that of similar complexes including **(14)** and **(21)**. Moreover, we have observed that these complexes have a relatively high thermal stability which can in turn explain their poor catalytic activity. In fact benzene solutions of either **(16)** or **(19)** did not decompose over days at 140°C and furthermore, a benzene solutions of these complexes under 1 atm of ethene did not show any reaction even after days at 135 °C. Therefore it is possible on the

basis of our work to eliminate *ortho*-metallated complexes with a stereochemistry such as **(16)** as being on the pathway to C-C bond formation.

Similarly to Hiraki's work we have been able to observe and characterise complexes structurally related to **(16)** such as **(23)** and **(24)**, and upon addition of trimethylvinylsilane to a mixture of **(23)**, **(24)**, and **(16)** we have observed at room temperature formation of the C-C coupling product following rapid reaction **(23)**. Moreover we have seen that although **(19)** is inactive for C-C coupling, its isomer **(20)** displays moderate reactivity for C-C bond formation. These results suggest that *ortho*-metallated complexes with a stereochemical arrangement of ligands as in **(23)** may actually be on the pathway to C-C activation. The question of the isomer has been examined in colaboration with Dr S. A. Mcgreggor as already described and with agrees with this postulate.

3.4. Conclusions.

Although our results do not provide definitive evidence for or against the coordination of a CO ligand in metallated species on the Murai pathway, we believe that our work in this area has been as close as possible to the reaction conditions reported by Murai.

All the evidence we have so far point to $Ru(PPh_3)_2(CO)$ as being the active catalytic species of the C-C coupling and do not corroborate Trost et al postulate of CO exclusion from the ruthenium catalytic species during the reaction.

These authors on the basis that the catalytic reaction is strongly inhibited in the presence of a CO atmosphere, propose a highly coordinatively unsaturated $Ru(PPh_3)_3$ stabilised by solvents molecules as active species of the reaction.

It is appreciable, on the basis of our work as much as on the basis of reported work in this area, that a highly coordinatively-unsaturated ruthenium species might be the active species. However one has to be careful when considering the importance of introducing a foreign material such as CO into a catalytic reaction.

In fact it is well known that ruthenium(0) species are converted into $Ru(PPh_3)_2(CO)_3$ in the presence of CO and PPh_3, in addition we have seen in **Chapter 2** that **(22)** reacted rapidly with CO at room temperature to afford $Ru(PPh_3)_3(CO)_2$ and

Finally the $Ru(PPh_3)_2(CO)$ moiety is very rigid, owing to the push-pull effect of electron between the PPh_3 and CO ligands, and is not likely to dissociate CO easily.

Following the same way of thinking, our work in this area contradict the postulate proposed by Chaudret et al.[6] of any complexes such as $Ru(PCy_3)_2(C_6H_5C(O)CH_3)(H_2)H$ to be true intermediates in the catalytic cycle postulated by Murai. Although we appreciate that $Ru(PCy_3)_2(C_6H_5C(O)CH_3)(H_2)H$ is a catalyst precursor for the Murai reaction, it is very unlikely that a dihydrogen complex is being formed during the reaction.

3.5. References.

1. **(a)** Murai, S.; Kakiuchi, F.; Sekine, S.; Tanaka, Y.; Kamatani, A.; Sonoda, M.; Chatani, N. *Nature*, **1993**, *366*, 529. **(b)** Murai, S.; Kakiuchi, F.; Sekine, S.; Tanaka, Y.; Kamatani, A.; Sonoda, M.; Chatani, N. *Pure Appl. Chem.* **1994**, *66*, 1527. **(c)** Kakiuchi, F.; Sekine, S.; Tanaka, Y.; Kamatani, A.; Sonoda, M.; Chatani, N.; Murai, S. *Bull. Chem. Soc. Jpn.*, **1995**, *68*, 62. **(d)** Murai, S.; Chatani, N.; Kakiuchi, F. *Pure Appl. Chem.* **1997**, *69*, 589.
2. Matsubara, T.; Koga, N.; Musaev, D. G., Morokuma, N., K. *J. Am. Chem. Soc.*, **1998**, *120*, 12692.
3. Matsubara, T.; Koga, N.; Musaev, D. G., Morokuma, N., K. *Organometallics*, **2000**, *19*, 2318.
4. Paulasaari, J.K.; Moiseeva, N.; Bau, R.; Weber, W.P. *J. Organomet. Chem.*, **1999**, *587*, 299.
5. Lu, P.; Paulasaari, J.; Jin, K.; Bau, R.; Weber, W. P. *Organometallics*, **1998**, *17*, 584.
6. **(a)** Guari, Y.; Sabo-Etienne, S.; Chaudret, B. *Eur. J. Inorg. Chem.* 1999, 1047. **(b)** Guari, Y.; Sabo-Etienne, S.; Chaudret, B. *J. Am. Chem. Soc.*, 1998, 120, 4228.
7. Drouin, S. D.; Amoroso, D.; Yap, G. P. A.; Fogg, D. E. *Organometallics,* **2002**, *21*, 1042.
8. **(a)** Ogasawara, M.; Macgregor, S. A.; Streib, W. E.; Folting, K.; Eisenstein, O.; Caulton, K. G. *J. Am. Chem. Soc.*, **1996**, *118*, 10189. **(b)** Gottschalk-Gauding, T.; Huffman, J. C.; Gerard, H.; Eisenstein, O.; Caulton, K. G. *Inorg. Chem.*, **2000**, *39*, 3957.
9. Rossi, A. R.; Hoffmann, R. *Inorg. Chem.*, **1975**, *14*, 365.
10. **(a)** Wong, W.-K.; Chiu, K. W.; Statler, J. A.; Wilkinson, G.; Motevalli, M.; Hursthouse, M. B. *Polyhedron* **1984**, *3*, 1255. **(b)** Helliwell, M.; Vessey, J. D.; Mawby, R. J. *J. Chem. Soc., Dalton Trans.*, **1994**, 1193.
11. **(a)** Schmid, H., Ziegler, M. L. *Chem. Ber.*, **1976**, *109*, 132. **(b)** Bennet, M. A.; Jonhson, R. N.; Tomkins, I. B.; *J. Am. Chem. Soc.*, **1974**, *96*, 61.
12. de C. T. Carrondo, M. A. A. F.; Chaudret, B. N.; Cole-Hamilton, D. J.; Skapski, A. C.; Wilkinson, G. *J. Chem. Soc., Chem. Commun.*, **1978**, 463.
13. Chandra, G.; Lo, P. Y.; Hitchcock, P. B.; Lappert, M. F. *Organometallics*, **1987**, *6*, 191.

14. Lewis, L. N.; Colborn, R. E.; Grade, H.; Bryant Jr, G. L.; Sumpter, C. A.; Scott, R. A. *Organomettallics*, **1995**, *14*, 2202.

15. Delpech, F.; Sabo-Etienne, S.; Donnadieu, B.; Chaudret, B.; *Organometallics*, **1998**; *17*, 4926.

16. Brown, L. D.; Barnard, C. F.; Daniels, J. A.; Mawby, R. J.; Ibers, J. A. *Inorg. Chem.*, **1978**, *17*, 2932.

17. de los Rios, I.; Jimenez Tenorio, M.; Padilla, J.; Puerta, M. C.; Valerga, P.; *Organometallics*, **1996**, *15*, 4565.

18. Werner, H.; Grunwald, C.; Laubender, M.; Gevert, O. *Chem. Berg.*, **1996**, *129*, 1191.

19. Cole-Hamilton, D. J.; Wilkinson, G. *Nouv. Jour. Chim.*, **1976**, *1*, 141.

20. Bohanna, C.; Estruelas, M. A.; Lahoz, F. J.; Onate, E.; Oro, L. A. Sola, E. *Organometallics*, **1995**, *14*, 4825.

21. Hiraki, K., Ishimoto, T., Kawano, H.; *Bull. Chem. Soc. Jpn.*, **2000**, *73*, 2099.

22. McGuiggan, M. F.; Pignolet, L. H. *Inorg. Chem.*, **1982**, *21*, 2523.

23. Dauter, Z.; Mawby, R. J.; Reynolds, C. D.; Saunders, D. R. *J. Chem. Soc., Dalton Trans.*, **1985**, 1235.

24. Barrio, P.; Castarlenas, R.; Esteruelas, M. A.; Lledos, A.; Maseras, F.; Onate, E.; Tomas, J.; *Organometallics*, **2001**, *20*, 442.

25. Trost, B. M.; Imi, K.; Davies, I. W. *J. Am. Chem. Soc.*, **1995**, *117*, 5371..

26. Kawano, H.; Tanaka, R.; Fujikawa, T.; Hiraki, K.; Onishi, M. *Chem. Lett.*, **1999**, 401.

27. **(a)** Stewart, R. P.; Benedict, J. J.; Isbrandt, L. *Inorg. Chem.*, **1976**, *15*, 2013. **(b)** Preece, M. Robinson, S. D.; Wingfield, J. N. *J. Chem. Soc. Dalton.*, **1976**, 613. **(c)** Stewart, R. P.; Isbrandt, L.; Benedict, J. J. *Inorg. Chem.*, **1975**, *14*, 2933.

28. **(a)** Gill, D. F.; Mann, B. E.; Shaw, B. L. *J. Chem. Soc., Dalton.*, **1973**, 270. **(b)** Bennett, M. A.; Johnson, R. N.; Tomkins, I. B. *Inorg. Chem.*, **1975**, *14*, 1908.

29. Rathke, J. W.; Muetterties, E. L. *J. Am. Chem. Soc.*, **1975**, *97*, 3272.

30. Karsh, H. H.; Klein, H. F.; Schmidbauer, H. *Angew. Chem. Int. Ed. Engl.*, **1975**, *14*, 637.

31. Tribo, R.; Pons, J. Yanes, R.; Piniella, J. F.; Alvarez-Larena, A.; Ros, J. *Inorg. Chem. Comm.*, **2000**, *3*, 545.

PART 2.

"Humanity needs practical men, who get the most out of their work, and, without forgetting the general good, safeguard their own interests. But humanity also needs dreamers, for whom the disinterested development of an enterprise is so captivating that it becomes impossible for them to devote their care to their own material profit.
Without doubt, these dreamers do not deserve wealth, because they do not desire it. Even so, a well-organized society should assure to such workers the efficient means of accomplishing their task, in a life freed from material care and freely consecrated to research."

Curie, Marie
(1867-1934)

Chapter 4.

Introduction to N-heterocyclic carbene chemistry.

4.1. Introduction.

As outlined in **Chapter 3**, both **(1)** and $Ru(PCy_3)_2(H_2)_2H_2$[1] show activity for the Murai reaction but under very different conditions (135°C vs. 30°C). However the advantage of lower temperature is offset by a longer reaction time (2 hr vs. 24 hr). Thus, $Ru(PPh_3)_2(PCy_3)(CO)H_2$ might be an interesting target molecule. Unfortunately, mixed phosphine complexes are difficult to synthesise cleanly. Therefore in order to investigate the catalytic activity of other candidates for the Murai reaction, we decided to focus our study on complexes displaying structural similarities to $Ru(PPh_3)_3(CO)H_2$, but where the reactivity was tuned by substitution of one triphenylphosphine ligand by an N-heterocyclic carbene ligand. The decision to use these ligands as possible substitutes for phosphines was prompted by their characteristics, which will now be described in this chapter.

The chemistry of stable carbenes is one of the fastest growing areas in both coordination and catalytic chemistry, with numerous reviews and articles available in the literature on this subject. Therefore, we only intend to give here a brief overview of the properties and synthesis of carbene ligands, along with a few examples of their main applications in coordination and catalytic chemistry.

4.1.1. Stable carbenes.

Carbenes are neutral molecules containing a divalent carbon atom. They only have six valence electrons, two non-bonding, making them electron deficient and highly reactive species. The electronic configuration gives rise to two different arrangements depending on whether the non-bonding electrons are paired or unpaired. Singlet carbenes have their non-bonding electrons paired, whereas triplet carbenes have their electrons in different orbitals with parallel spins **[Figure 4.1.]**.

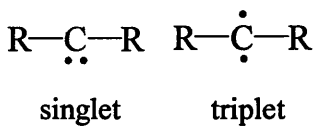

Figure 4.1 - *Representation of singlet and triplet carbenes.*

In triplet carbenes, there is a linear geometry with an sp-hybridisation around the carbene centre and two non-bonding degenerate p_x and p_y orbitals. Singlet carbenes have a

bent geometry which do not allow this degeneracy, due to the sp^2 hybridisation of the carbene centre.

In the singlet case, the two non-bonding electrons can distribute themselves amongst the two different types of orbitals (both in unused sp^2 hybrid or σ orbital, or one in σ and one in p_π) and their placement defines the electronic state of the molecule **[Fig 4.2.]**.

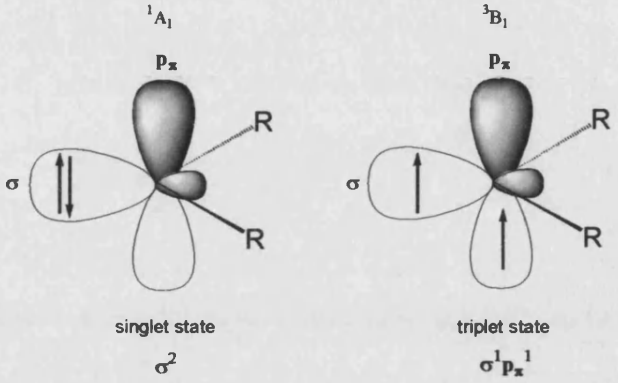

Figure 4.2. - *Representation showing the electron occupancy in the σ and p_π-orbitals.*

Wanzlick *et al.* suggested that there is an increase in stability of the singlet state whenever the substituents in the vicinal position provide σ-acceptor π-donor character.[3-4] In this position, the substituents are responsible for stabilising the carbene lone pair by creating a negative inductive effect, thus filling the empty p-orbital on the carbene carbon atom **[Figure 4.3.]**.

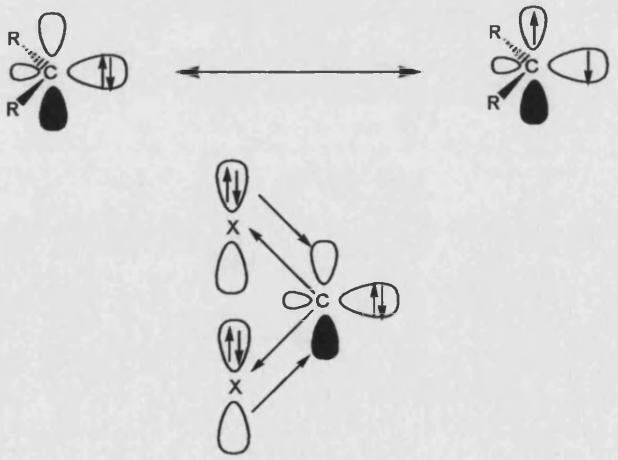

Figure 4.3. - *σ-acceptor and π-donors vicinal to the carbene-carbon atom stabilize the singlet state of carbenes.*

4.1.2. Stable Singlet Carbenes.

Stable N-heterocyclic carbenes **(NHC)** were first observed in 1961 by Wanzlick and co-workers, although none of these carbenes were ever isolated.[4] They recognised that carbenes with electron rich amino substituents at the 2 and 5 position are capable of stabilising the carbene centre, by enhancing the carbon atom's nucleophilicity and thermodynamic stability.[2-4] At that time the final product was isolated as a dimer. **[Scheme 4.1.]**

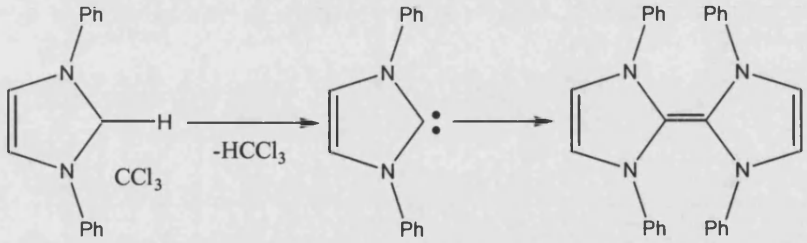

Scheme 4.1.

Based on this concept, the field of NHC chemistry really developed since the first successful synthetic attempts by Igau et al.[5] and Arduengo et al.[6]. In 1991 through the development of a new synthetic route, 1,3-bis(1-adamantyl)imidazolin-2-ylidene (IAd) was isolated and fully characterised **[Scheme 4.2.]**.[6-8] The X-ray structure of IAd can be simplified to a strongly bent singlet carbene (R-C-R = 100 - 110°), with a rather short N-C: bond (1.32-1.37 Å) showing some aromatic stabilisation of the ring. Arduengo and co-workers showed that this carbene was remarkably stable (a sealed sample in thf solution showed no decomposition after 7 years!), with a melting point of 240°C.

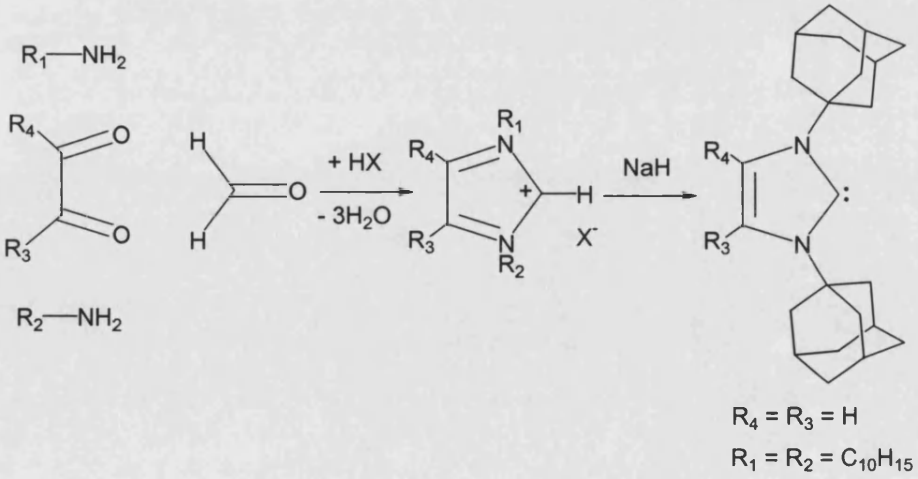

Scheme 4.2. *Synthesis of 1,3-bis(1-adamantyl)imidazolin-2-ylidene.*

Their work started a renaissance of the rich chemistry of these nucleophilic carbenes and in the last decade numerous variations of the basic imidazol-2-ylidene skeleton have appeared showing different steric and electronic effects. Cyclic diaminocarbenes were originally considered to be the only stable type of carbene due to the nitrogen providing good π-donor/σ-acceptor character, which combined with steric bulk and some aromatic character prevented dimerization.[9,10] New generations of NHC ligands go from having basic functionalised aryl on the N position **[Figure 4.4.]**, to more sophisticated NHCs with N groups designed for specific purposes **[Figure 4.5.]**.

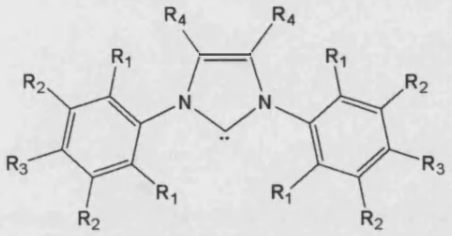

IMes[11] R_1, R_3 = Me, R_2, R_4 = H

IPr[12] R_1 = $CHMe_2$, R_2, R_3, R_4 = H

IMes-Cl[13] R_1, R_3 = Me, R_2 = H, R_4 = Cl

Figure 4.4.

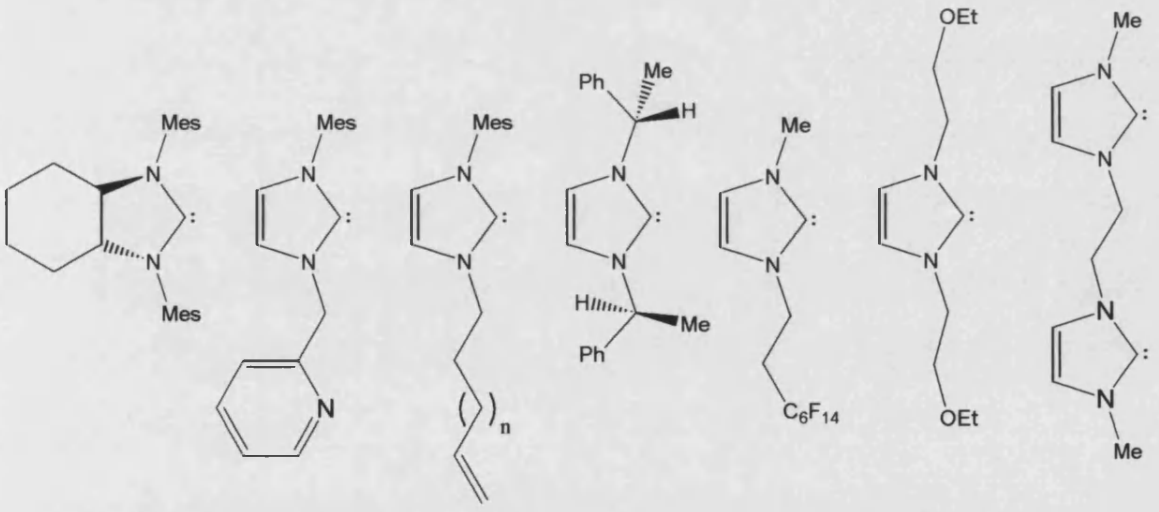

(a)[14] (b)[15] (c)[16] (d)[17] (e)[18] (f)[17] (g)[17]

Figure 4.5.

Later, imidazolidin-2-ylidenes, saturated, more electron-rich and non-aromatic versions of the imidazolin-2-ylidenes were isolated **[Figure 4.6., (a)]**.[19,20] Isolation of six-membered tetrahydropyrimid-2-ylidenes[21,22] **[Figure 4.6., (b)]** and of acyclic structures[23, 24] **[Figure 4.6., (c)]** came as an extension to this family of diaminocarbenes since they still posses two nitrogens vicinal to the carbene but lack the 6π-electron conjugation.

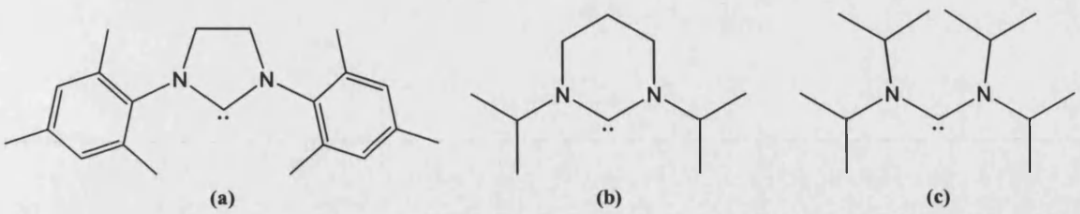

Figure 4.6.

The next generation of carbenes has demonstrated the tolerance of π-donor substituents such as alkoxy and alkylsulfido groups as shown in **Figure 4.7.**.[25]

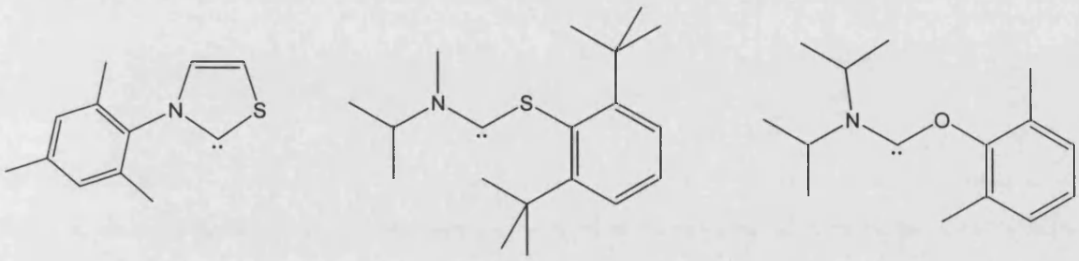

Figure 4.7.

4.1.3. Synthesis of NHCs.

Generally the synthesis of NHCs starts from *N-N'*-disubstituted azolium salts, which are commonly deprotonated with potassium *tert*-butoxide using thf as the solvent **[Scheme 4.3.]**.[6]

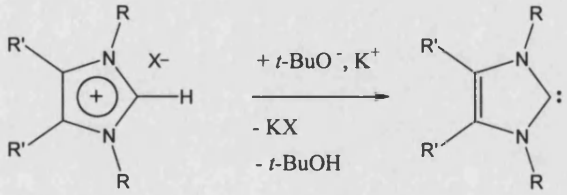

Scheme 4.3. - *Deprotonation of imidazolium salts using potassium tert-butoxide.*

These *N-N'*-disubstituted azolium salts, precursors to the free carbene, are generally accessible by two routes (i) and (ii), which complement each other. These methods have already been thoroughly reviewed in major reviews and articles and will not be explained in detail here.[26]

(i) nucleophilic substitution at the imidazole heterocycle **[Scheme 4.4.]**.

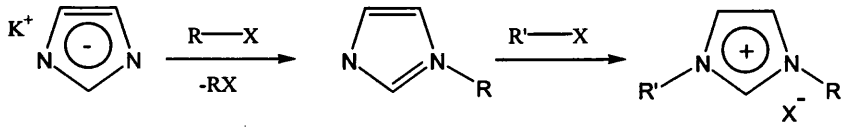

Scheme 4.4. - *Nucleophilic substitution synthesis.*

Imidazolium salt that can be prepared by this procedure, which involve alkylation of imidazole, are easy to obtain and often used for metal complex synthesis.[27-30] The main drawback of this route arises from the formation of elimination by-products when secondary and tertiary halides are used.

(ii) a multi-component reaction, building up the heterocycle with the desired substituents in one step **[Scheme 4.5.]**.[37-40]

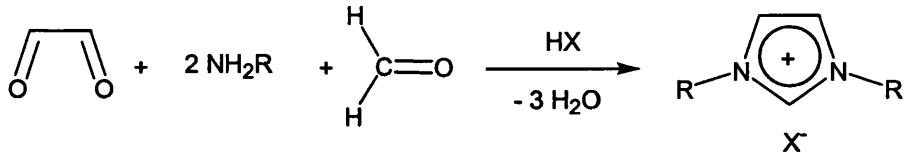

Scheme 4.5. - *Multi-component synthesis.*

In order to introduce other substituents at the 1- and 3- positions of the imidazolium salt the reaction of primary amines with glyoxal and formaldehyde in the presence of acid can be used.[31-33] Variation of the amine allows the preparation of imidazolium salt libraries which can be diversified by changing the anion of the imidazolium salt using different acids.[34] This method was extended to the use of chiral amines in the preparation of C_2-symmetric imidazolium salts.[35] A two step version of this synthesis has been shown to proceed via the synthesis of the bisimine in a first step, followed by subsequent ring closure with formaldehyde and an acid.[36, 37]

4.2. Transition metal chemistry involving NHCs.

Due to their rather unusual properties, the use of NHCs as ligands in coordination chemistry has been well documented in a number of recent reviews and articles.[35,38] The first examples of NHC complexes were reported in 1968 by Wanzlick and Schönherr[39] and by Öfele **[Figure 4.8.; (a), (b)]**.[40] Nowadays their application to coordination chemistry goes across the whole periodic table from the alkali metals (Li[41-44], Na[44], K[44]) **[Fig 4.8.; (c)]**, alkaline-earth metals (Be[47], Mg[45], Ca[46], Sr[46], Ba[46]), to both ends of the transition metal series (e.g. Ti[49, 51], Ta[49], Cr[53, 54, 48, 51], Re[55, 57, 56], Ru[58, 50, etc], Rh[35, 52, 59-61], Pd[62, 63], Au[64]) **[Fig 4.8.; (d)]**. A few examples of their application in rare earth metals chemistry have also been reported (Sm[65], Eu[66], U[67]) **[Figure 4.8.; (e)]**.

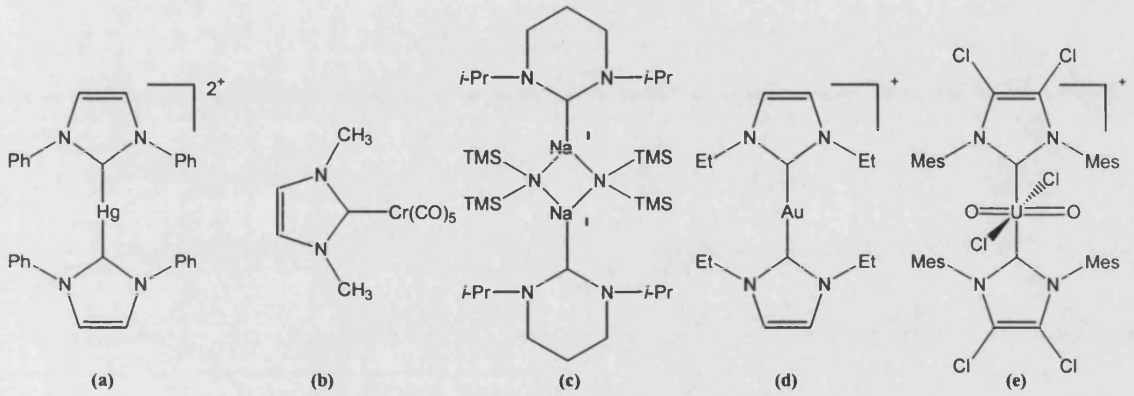

Figure 4.8. - *Examples of metal coordinated NHC ligands.*

Several synthetic methods have been reported for the synthesis of carbene-transition metal complexes.[26] Mainly four routes have been used: the *in situ* deprotonation of ligand precursors, the elimination of small molecules from a neutral ligand precursors, the complexation of the free, pre-isolated NHCs and the cleavage of electron-rich alkenes.

4.2.1. *In situ* deprotonation of ligand precursors.

The *in situ* complexation of the ligand has the advantage of not having to prepare and isolate the free carbene and has found its main applications in cases where the carbene is hardly stable or difficult to handle.[68] *In situ* deprotonation combined with phosphine substitution was reported as a convenient route to the synthesis of ruthenium-alkylidene complexes **[Scheme 4.6.]**.[69]

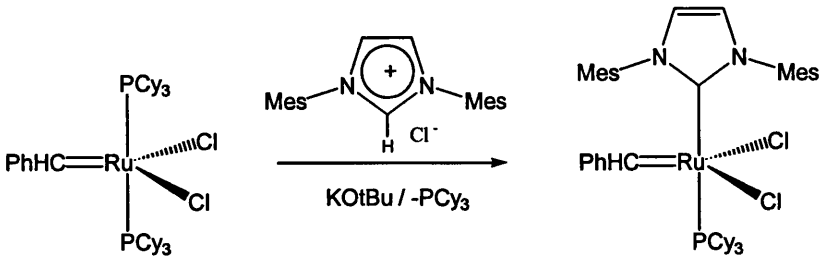

Scheme 4.6.

4.2.2. Elimination of small molecules from neutral ligand precursors.

This method was first used in 1961 by Wanzlick et al.[4] to prepare imidazolin-2-ylidenes and proceeded via elimination of an alcohol from a neutral 2-alkoxy-1,2-dihydro-1*H*-imidazole leading to the formation of the free carbene. In a variation of this method, a palladium(II) complex with allyl-substituted NHCs was reported through elimination of dimethylamine **[Scheme 4.7.]**.[70]

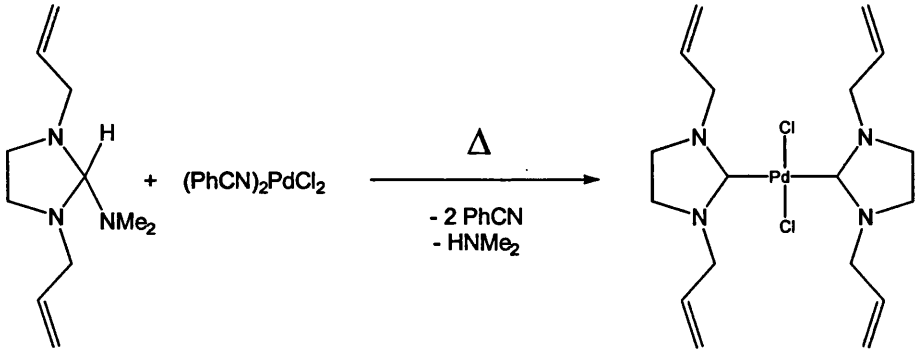

Scheme 4.7.

4.2.3. Complexation of the preformed free NHC.

Since the isolation of the first stable structurally characterised NHC by Arduengo et al.,[6] the use of free NHCs in the preparation of carbene complexes has experienced rapid development. Various methods have been shown to be suitable for the formation of NHC complexes, such as cleavage of dimeric complexes,[71] and exchange with coordinated ligands such as phosphine,[72] CO,[73] solvent,[74], etc...[75]. The ligand exchange provides an easy route to the synthesis of carbene complexes and has been widely used. In the Grubbs alkene metathesis catalyst, both phosphines can be exchanged for various NHCs without affecting the benzylidene moiety **[Scheme 4.8.]**.[76]

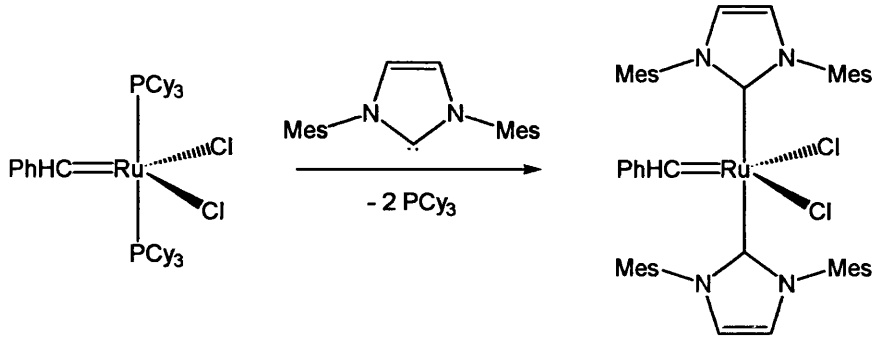

Scheme 4.8.

4.2.4. Cleavage of electron rich alkenes.

Electron rich alkenes are subject to thermal cleavage by various electrophilic transition metal complexes due to their nucleophilicity. These electron rich alkene or tetraaminoethene derivatives were first observed by Wanzlick et al.[4] and have been synthesised by several methods such as dimerisation of nonstable NHCs[77a] and deprotonation of imidazolidinium salts with Grignard reagents.[77b] Heating of tetraaminoethenes in the presence of a metal precursor such as metal carbonyl, has been shown to afford the corresponding NHC complex **[Scheme 4.9.]**.[78]

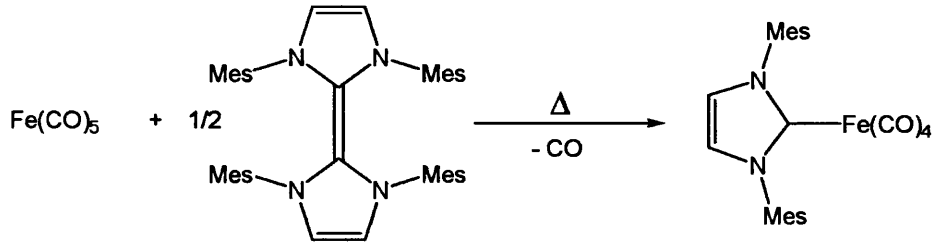

Scheme 4.9.

4.3. Properties of NHC ligands.

While it is possible to view NHCs as being *Fischer*-type carbenes, the M-C bonds in N-heterocyclic carbene complexes are much longer (2.1 Å cf. < 2 Å) than in the Fischer systems due to lack of π-back donation. While the lone pair of electrons on the carbon mimics σ-donating ligands such as P, N or O and could be considered as phosphine analogues, the real strength and versatility of NHC ligands rests in how they differ from these. The coordinating lone pair of electrons in NHCs is "harder" and more basic than a phosphine lone pair. The formally vacant p-orbital at the carbene centre has the potential to function as a weak π-acceptor, but has different directional character than P-X σ*-bonds

on a phosphine. NHCs have a different steric profile to phosphines. This has been defined by Nolan using two angles (A_L, A_H). The steric profile of phosphines is described by the cone angle (Θ) **[Figure 4.9.]**.

NHCs give an enhanced thermal stability to the M-C bond compared to phosphines. This is due to the thermal sensitivity of the latter, which under high temperatures, can undergo P-C bond degradation and therefore potential deactivation of any catalyst.[79]

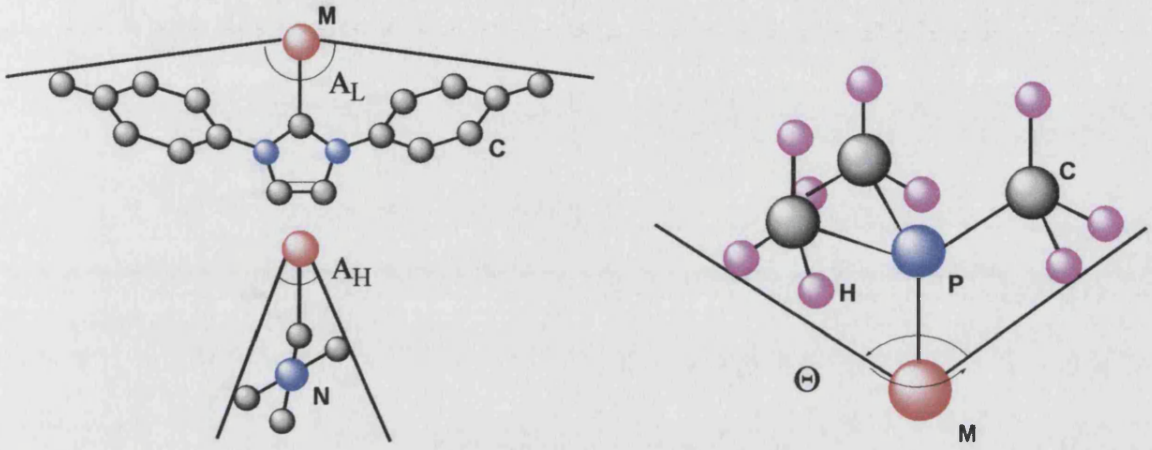

Figure 4.9. - *Determination of two steric parameters (A_L and A_H) associated with carbene ligands (left) and the cone angle (Θ) in phosphines (right).*

Work has been done to underline some of the major differences in the chemistry of NHCs in comparison to phosphine ligands. A comparison of IR carbonyl frequencies in *trans*-Rh(CO)L_2Cl] **[Table 4.1.]**[80] highlights the differences in electron donation from NHC and phosphine ligands. This is compatible with more electron density being on the metal centre and shows that NHC ligands are better electron donors than phosphines.

Nolan has demonstrated that the steric and electronic properties of the carbene can be readily modulated depending on the side arm substituents (N-R). This changes the susceptibility of the carbene towards direct substitution. For example, IMes coordinates more strongly to a Cp*RuCl fragment than does PCy_3 (by 5 kcal mol^{-1}).[81] Calorimetric measurements have established that carbene donor strength follows the order ICy > ITol > IMes > IPr, while steric bulk follows the inverse pattern (IPr > IMes > ITol > ICy) **[Scheme 4.10.; Figure 4.10.]**.

***trans*-[Rh(CO)L_2Cl] L**	**Absorption frequency (cm^{-1})**
1,3-Dimethylyimidazolin-2-ylidene	1924
1,3-Dicyclohexyl-imidazolin-2-ylidene	1929
PCy_3	1939
PMe_3	1957
PPh_3	1983
$P(C_6F_5)_3$	2003
$P(OPh)_3$	2018

Table 4.1.

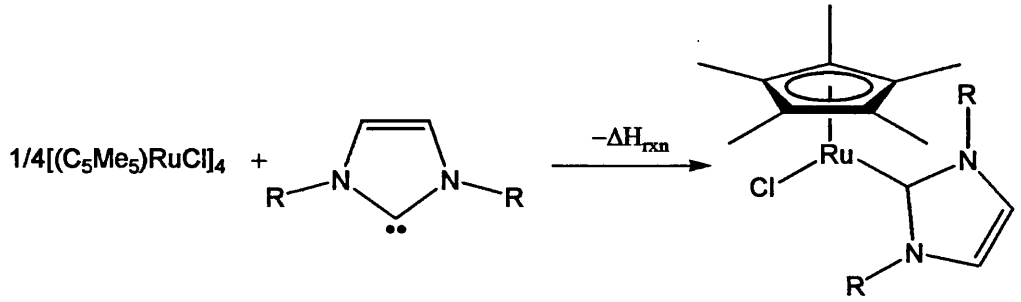

Scheme 4.10.

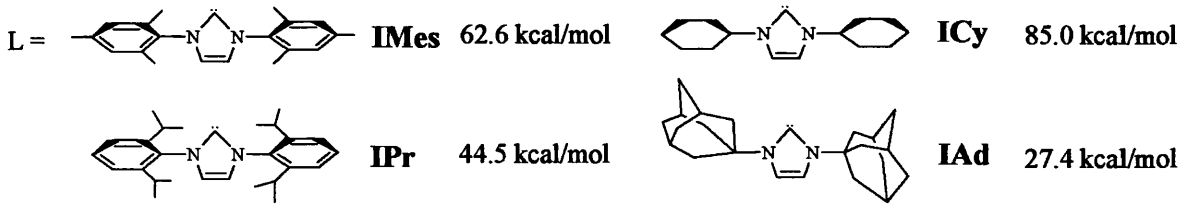

Figure 4.10. - *Calorimetric measurements (ΔHrxn [kcal/mol]) for the reaction according to* ***Scheme 4.10.***

4.4. Applications of NHCs in homogeneous catalysis.

As mentioned earlier, NHCs are remarkably stable and have unique chemical properties. Over the last two decades the catalytic activity of NHC metal complexes has been thoroughly investigated, and is well documented in a number of reviews and articles.[82-91] Because they are considered as phosphine mimics, their applications have mainly been devoted to improve already existing catalytic processes involving phosphines. In fact phosphines are widely used in controlling selectivity and reactivity in homogeneous catalysis[92] but they are often air and water-sensitive. As seen previously, phosphine or phosphite ligands are thermally sensitive; to prevent this degradation from affecting catalyst activity excess phosphine is often used to ensure catalyst stability.

NHCs provide a possible answer to this problem as they are strongly electron rich, bulky, resistant to oxidising agents and form stable bonds with metals. This has led to NHCs finding applications in a range of catalytic reactions including: hydroformylation of alkenes;[82] hydrogenation of alkenes[83,84] and dihydroamino acids;[85] hydrosilylation reactions;[86,87] copolymerisation of ethene and CO;[88] polymerization of alkynes;[89] cyclopropanation of alkenes[90] and furan synthesis.[91] Among the many examples reported, two of the most interesting examples of NHC and phosphine comparison are the **Heck reaction** and the **alkene metathesis**.

4.4.1. Alkene Metathesis.

In recent years, the alkene metathesis reaction **[Figure 4.11.]** has developed rapidly, largely through the work of Grubbs.

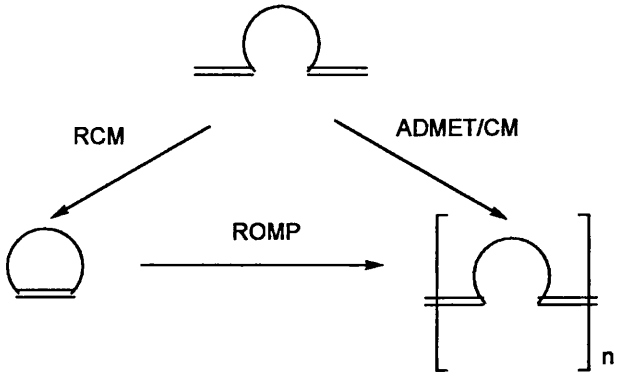

Figure 4.11. - *Alkene metathesis involving RCM (Ring Closing Metathesis), ROMP (ring opening metathesis polymerisation, ADMET (Acyclic Diene Metathesis), CM (Cross Metathesis).*

Alkene metathesis provides a route to unsaturated molecules that are often challenging or impossible to prepare by any other means. It developed rapidly with the discovery of the high catalytic activity of ruthenium (II) phosphine complexes **[Figure 4.12., (a)]**.[93,95] Further developments showed that the substitution of PPh_3 with the more electron-donating and sterically more demanding PCy_3 **[Figure 4.12., (b)]** was accompanied with a significant increase in the stability and performance of the complex.[94-96] A new generation of catalyst arose with the substitution of PCy_3 with NHCs such as IMes **[Scheme 4.8.]**.[82,76] Nevertheless, although NHCs are considered as even more electron-donating than trialkylphosphines, the catalytic performance of $Ru(IMes)_2(=CHPh)Cl_2$ proved to be comparable to that of **(b)**.

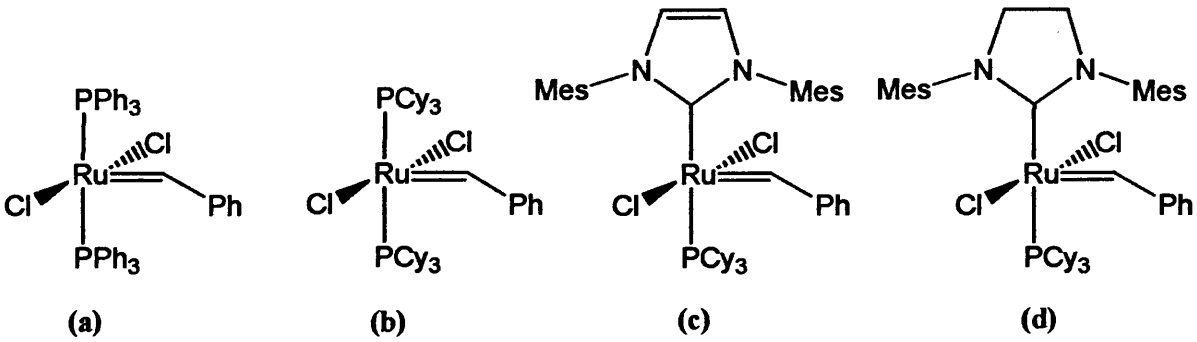

(a) (b) (c) (d)

Figure 4.12.

Recent mechanistic studies showed that the key insight was that $(PCy_3)_2Cl_2Ru=CHPh$ forms a highly active intermediate during the catalytic cycle. This has allowed further advances in the design of catalyst precursors of higher activity. These investigations showed that phosphine was a necessary ligand for the reaction to proceed, as it provided enough electron density on the metal to stabilise the active catalytic fragment and remained a ligand weak enough not to suppress the dissociative pathway.[97] A new generation of precursors based on the use of NHCs led to the synthesis of a mixed phosphine/carbene complex **(c)**.[72,98] This has proved to be a good compromise between the coordinating and electronic properties of carbene ligands, and the lability of phosphine ligands and has led to extensive applications in metathesis reactions.[99]

As seen in **Figure 4.13.**, further improvements were made by using imidazolidin-2-ylidene (IMes-H) as a substitute to IMes, complex **(d)**. This displayed catalytic activities greater than the performance of the molybdenum-imido system which was considered as intrinsically more active than late-transition metal systems.[100] Remarkably, **(d)** remains effective at loadings as low as 0.05 mol % for RCM (ring closing metathesis) reactions and

0.1 10^{-3} mol % (monomer: catalyst = 1 000 000) for ROMP (ring opening metathesis polymerisation). [101,102] The greater stability of **(d)** arises from the poor dissociation tendency of the IMes-H due to thermodynamic reasons.

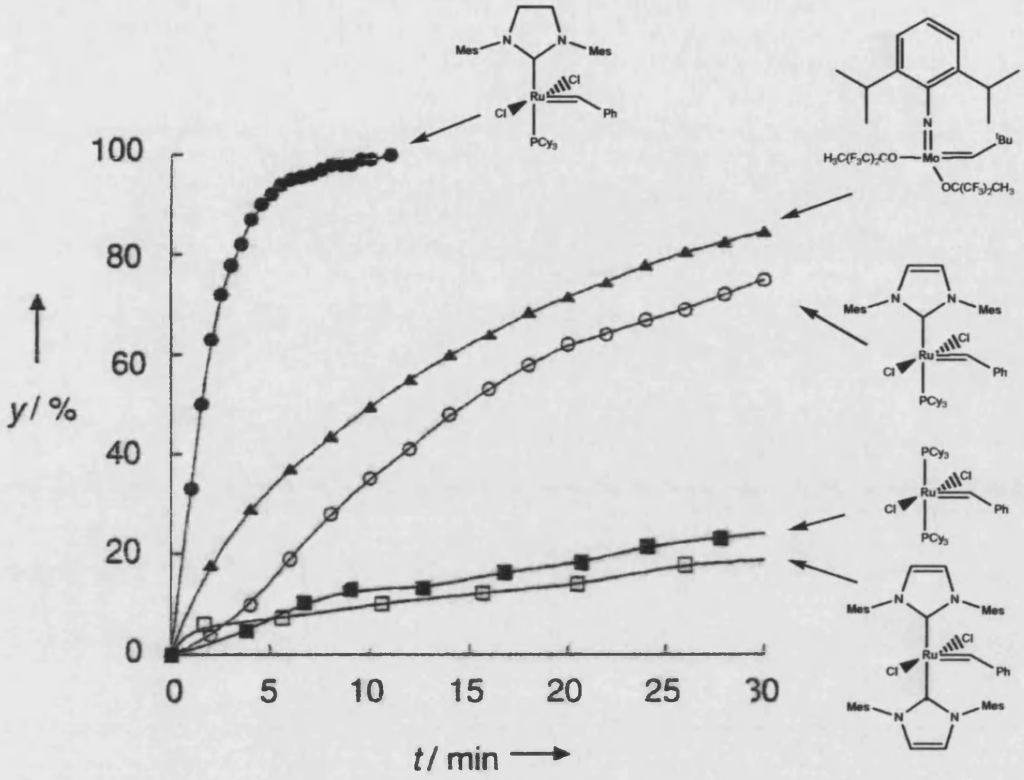

Figure 4.13. - *ROMP of 1,5-cyclooctadiene (y = yield of polyoctadienamer).*

4.4.2. Heck and Suzuki type reactions.

Other successful examples of catalysts containing NHC ligands are found in palladium- and nickel-catalysed carbon-carbon bond formations. The catalyst development with these metals has focused on Heck type reactions **[Scheme 4.12.].**[103] In fact due to their electron-donating properties NHCs have been found to facilitate the oxidative addition of aryl halides, whereas their sterically demanding properties have shown in various cases to result in acceleration of the catalysis.[104]

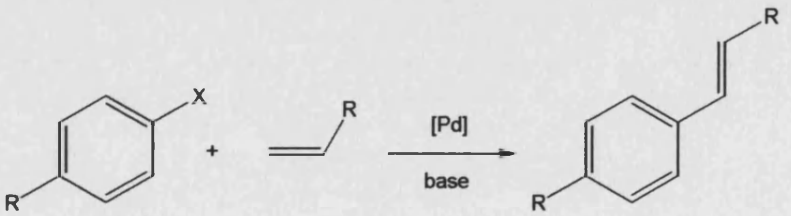

Scheme 4.12.

Recently Herrmann *et al.* have made use of stable palladium carbene complexes **(a)** and **(b) [Figure 4.14.]** for a range of C-C bond forming reactions such as Heck reactions and Suzuki coupling **[Figure 4.15.]**.[105]

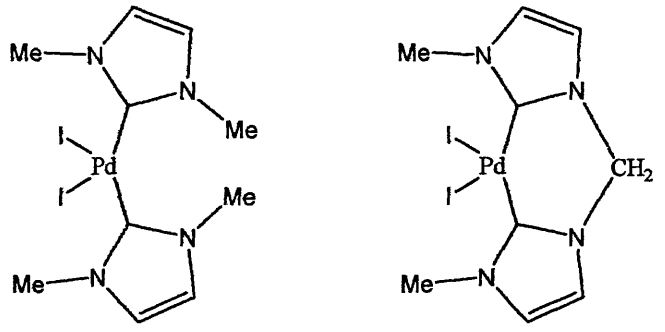

Figure 4.14. - *Pd catalysts for the Heck reaction and Suzuki coupling.*

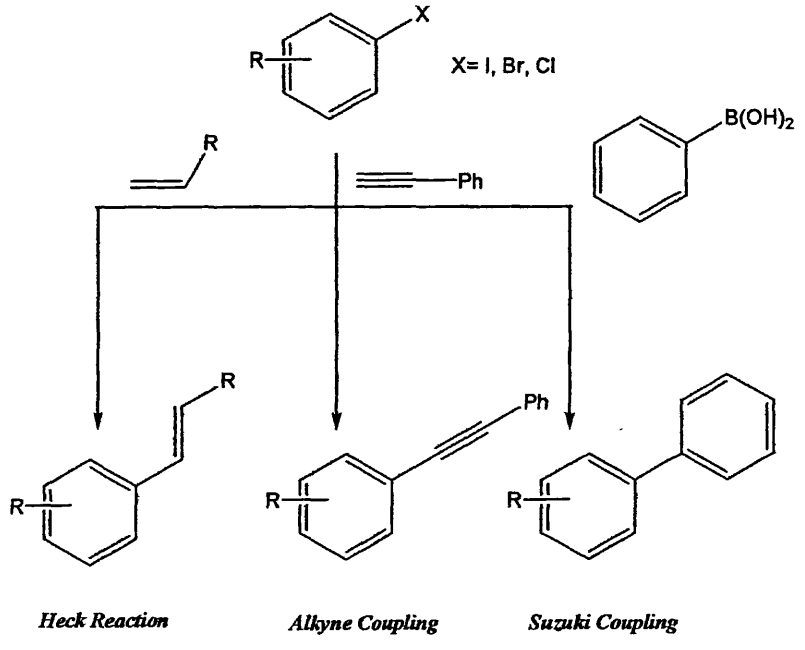

Figure 4.15.

As shown in **Figure 4.16.** although the conversion with the carbene free catalyst is greater other a longer period of time, the activity of the mono substituted carbine complex is higher. These results constitute primary results; and clearly demonstrate the influence of carbene complexes on Heck type reactions.[75a]

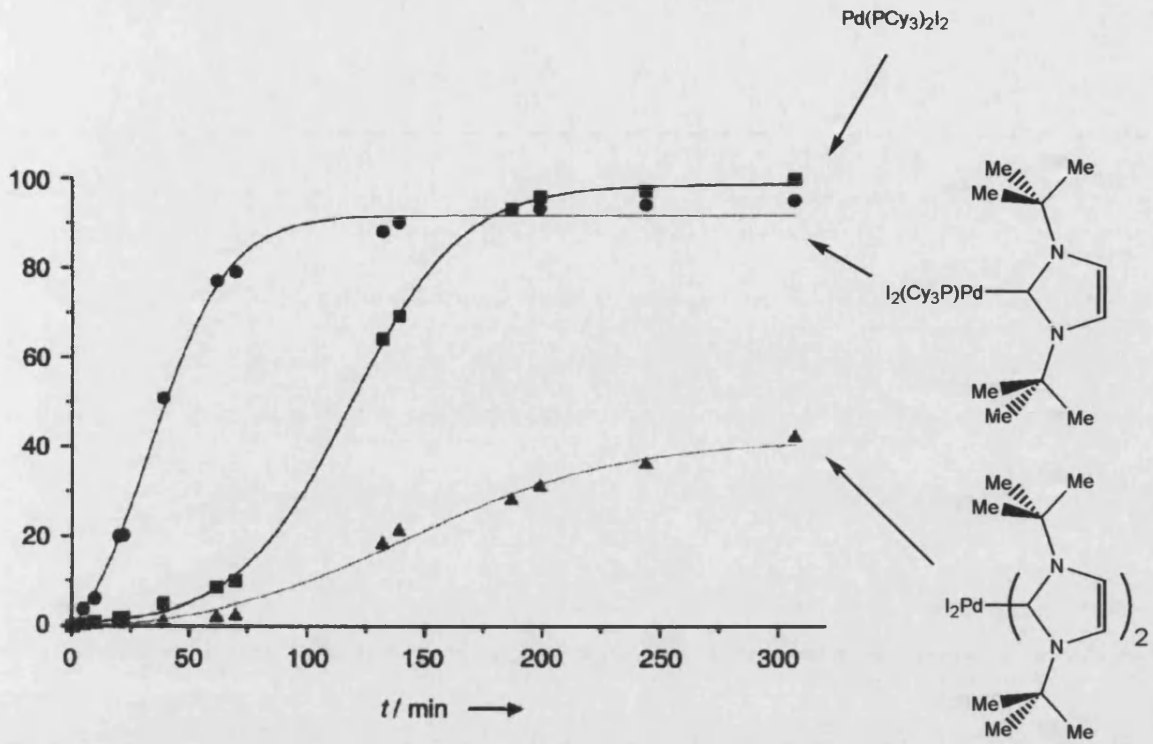

Figure 4.16. - *Influence of the ligands on the reactivity of Pd(II) catalysis in Suzuki type reaction. (Reported for the reaction of 4-chloro toluene and boronic acid.)*[75a]

4.5. Conclusions.

In this chapter we have demonstrated the unique properties of NHCs and their multiple applications in homogeneous catalysis. These ligands, since their isolation by Arduengo et al., have grown from being viewed as highly unstable intermediates to widely used compounds. Their application to coordination chemistry has been shown with most metals of the periodic table, and has resulted in major advances in catalytic processes such as alkene metathesis and Heck coupling reactions.

These new generations of catalysts have been demonstrated to be exceptionally stable toward heat, oxygen and moisture. Moreover, they proved to be rather resistant towards the attack of nucleophiles or electrophiles at the divalent carbon and, as demonstrated by theoretical calculations, carbene dissociation is unfavoured relative to phosphine.

It is on the basis of these observations that we decided to investigate the catalytic activity for Murai chemistry of the analogue of **(1)** bearing mixed carbene / phosphine ligands. Investigation of this area of research has led to the results reported in **Chapters 5** and **6**.

4.6. References.

1. Guari, Y.; Sabo-Etienne, S.; Chaudret, B. *J. Am. Chem. Soc.*, **1998**, *120*, 4228.
2. Wanzlick, H.-W.; Esser, F.; Kleiner, H-J. *Chem. Ber.*, **1963**, *96*, 1208.
3. Wanzlick, H.-W. *Angew. Chem. Int. Ed. Engl.*, **1962**, *1*, 75.
4. Wanzlick, H.-W.; Kleiner, H-J. *Angew Chem.*, **1961**, *73*, 493.
5. Igau, A.; Grutzmacher, H.; Baceiredo, A.; Bertand, G. *J. Am. Chem. Soc.*, **1998**, *110*, 6463.
6. Arduengo, A. J., III; Harlow, R. L.; Kline, M. *J. Am. Chem. Soc.*, **1991**, *113*, 361
7. Arduengo, A. J., III. *Acc. Chem. Res.*, **1999**, *32*, 913.
8. Bourissou, D.; Guerret, O.; Gabbaï, F. P.; Bertrand, G. *Chem. Rev.*, **2000**, *10*, 39.
9. Hahn, F. E.; Wittenbecher, L.; Le Van, D.; Frohlich, R. *Angew. Chem. Int. Ed.*, **2000**, *39*, 341.
10. Heinemann, C.; Muller, T.; Apeloig, Y.; Schwarz, H. *J. Am. Chem. Soc.*, **1996**, *118*, 2023.
11. Arduengo, A. J., III; Dias, H. V. R.; Harlow, R. L.; Kline, M. *J. Am. Chem. Soc.*, **1992**, *114*, 5530.
12. Arduengo, A. J., III; Krafczyk, R.; Schmuter, R.; Craig, H. A.; Goerlich, J. R.; Marshall, W. J. Unverzagt, M. *Tetrahedron*, **1999**, *55*, 14523.
13. Arduengo, A. J., III; Davidson, F.; Dias, H. V. R.; Goerlich, J. R.; Khasnis, D.; Marshall, W. J.; Prakasha, T. K. *J. Am. Chem. Soc.*, **1997**, *119*, 12742.
14. Lee, S.; Hartwig, J. F. *J. Org. Chem.*, **2001**,*66*, 3402.
15. Gründemann, S.; Kovacevic, A.; Albrecht, M.; Faller, J. W.; Crabtree, R. H. *J. Am. Chem. Soc.*, **2002**, 124, 10473.
16. Furstner, A.; Ackermann, L.; Gabor, B.; Goddard, R.; Lehmann, C. W.; Mynott, R.; Stelzer, F.; Thiel, O. R. *Chem. Eur. J.*, **2001**, 7, 3236.
17. **(a)** Herrmann, W. A.; Elison, M.; Fischer, J.; Kocher, C.; Artus, G. R. J. *Chem. Eur. J.* **1996**, *2*, 772. **(b)** Herrmann, W. A.; Kocher, C.; Goossen, L. J.; Artus, G. R. J. *Chem. Eur. J.* **1996**, *2*, 1627.
18. Xu, L.; Chen, W.; Bickley F. J.; Steiner, A.; Xiao, J. *J. Organomet. Chem.*, **2000**, 598, 409.
19. Denk, M. K.; Thadani, A.; Hatano, K.; Lough, A. J. *Angew. Chem. Int. Ed. Engl.*, **1997**, *36*, 2607.

20. Arduengo, A. J.,III; Goerlich, J. R.; Marshall, W. J. *J. Am. Chem. Soc.*, **1995**, *117*, 11027.

21. Alder, R. W.; Blake, M. E.; Bortolotti, C.; Bufali, S.; Butts, C. P.; Linehan, E.; Oliva, J. M.; Orpen, A. G.; Quayle, M. *Chem. Commun.*, **1999**, 241.

22. Alder, R. W.; Blake, M. E.; Bortolotti, C.; Bufali, S.; Butts, C. P.; Linehan, E.; Oliva, J. M.; Orpen, A. G.; Quayle, M. *Chem. Commun.*, **1999**, 1049.

23. Alder, R. W.; Allen, P. R.; Murray, M.; Orpen, A. G.; Quayle, M. *Angew. Chem. Int. Ed. Engl.*, **1996**, *35*, 1121.

24. Alder, R. W.; Blake, M. E. *Chem. Commun.*, **1997**, 1513.

25. Alder, R. W.; Butts, C. P.; Orpen, A. G. *J. Am. Chem. Soc.*, **1998**, *120*, 11526.

26. Herrmann, W. A.; Weskamp, T.; Böhm, V. P. W. *Adv. Organomet. Chem.*, **2002**, *48*, 1.

27. Fourmari, P.; de Cointet, P.; Laviron, E. *Bull. Soc. Chim. Fr.*, **1968**, 2438.

28. Chan, B. K. M.; Chan, N. H.; Grimmett, M. R. *Aust. J. Chem.* **1977**, *30*, 2005.

29. Haque, M. R.; Rasmussen, M. *Tetrahedron*, **1994**, *50*, 5535.

30. Grimmett, M. R. *Imidazole and Benzimidazole Synthesis;* Academic Press: London, **1997**.

31. Herrmann, W. A.; Kocher, C.; Gooβen, L. J.; Artus, G. R. J. *Chem. Eur. J.*, **1996**, *2*, 1627.

32. Arduengo, A. J., III; US 5077414, **1991**.

33. Herrmann, W. A.; Gooβen, L. J.; Spiegler, M. J. *Organomet. Chem.*, **1997**, *547*, 357.

34. Bohm, V. P. W.; Weskamp, T; Gstottmayr, C. W. K.; Herrmann, W. A. *Angew. Chem. Int. Ed Engl.*, **2000**, *39*, 1602.

35. Herrmann, W. A.; Gooβen, L. J.; Kocher, C.; Artus, G. R. J. *Angew. Chem. Int. Ed. Engl.*, **1996**, *35*, 2805.

36. Bildstein, B.; Malaun, M.; Kopacka, H.; Wurst, K.; Mitterbdck, M.; Ongania, K. H.; Opromolla, G.; Zanello, P. *Organometallics.*, **1999**, *18*, 4325.

37. Huang, J.; Nolan, S. P. *J. Am. Chem. Soc.*, **1999**, *121*, 9889.

38. **(a)** Weskamp, T.; Böhm, V. P. W.; Herrmann, W. A. *J. Organomet. Chem.*, **2000**, *600*, 12. **(b)** Jafarpour, L.; Nolan, S. P. *J. Organomet. Chem.*, **2001**, *17*, 617. **(c)** Jafarpour, L.; Nolan, S. P. *Adv. Organomet. Chem.*, **2001**, *46*, 181.

39. Wanzilck, H. –W.; Schonherr, H. –J. *Angew. Chem. Int. Ed. Engl.*, **1968**, *7*, 141.

40. Öfele, K. *J. Organomet. Chem.*, **1968**, *12*, P42.

41. Arduengo, A. J., III '96 ORCHEM (Bad Nauheim, Germany) "Nucleophile Carbene: Gestern, heute and morgen", **1996**.

42. **(a)** Boche, G.; Hilf, C.; Harms, K.; Marsch, M.; Lohrenz, J. C. W. *Angew. Chem., Int. Ed. Engl.*, **1995**, *34*, 4. **(b)** Hilf, C.; Bosold, F.; Harms, K.; Lohrenz, J. C. W.; Marsch, M.; Schimeczek, M.; Boche, G. *Chem. Ber.*, **1997**, *130*, 1201. **(c)** Hilf, C.; Bosold, F.; Harms, K.; Marsch, M.; Boche, G. *Chem. Ber.*, **1997**, *130*, 1213.

43. A 1,2-migration reaction has recently been observed with N-borane imidazol-2-ylidenes: **(a)** Wacker, A.; Pritzkow, H.; Siebert, W. *Eur. J. Inorg. Chem.*, **1998**, 843. **(b)** Wacker, A.; Pritzkow, H.; Siebert, W. *Eur. J. Inorg. Chem.*, **1999**, 789.

44. Alder, R. W.; Blake, M. E.; Bortolotti, C.; Bufali, S.; Butts, C. P.; Linehan, E.; Oliva, J. M.; Orpen, A. G.; Quayle, M. J. *J. Chem. Soc., Chem. Commun.*, **1999**, 241.

45. Arduengo, A. J., III; Dias, H. V. R.; Davidson, F.; Harlow, R. L. *J. Organomet. Chem.*, **1993**, *462*, 13.

46. Runte, O. Dissertation, Technische Universitat Munchen, 1997.

47. Herrmann, W. A.; Runte, O.; Artus, G. *J. Organomet. Chem.*, **1995**, *501*, C1.

48. Öfele, K.; Herrmann, W. A.; Mihalios, D.; Elison, M.; Herdtweck, E.; Scherer, W.; Mink, J. *J. Organomet. Chem.*, **1993**, *459*, 177.

49. Herrmann, W. A.; Öfele, K.; Elison, M.; Kuhn, F. E.; Roesky, P. W. *J. Organomet. Chem.*, **1994**, *480*, C7.

50. **(a)** Weskamp, T.; Schattenmann, W. C.; Spiegler, M.; Herrmann, W. A. *Angew. Chem., Int. Ed. Engl.*, **1998**, *37*, 2490. **(b)** Weskamp, T.; Kohl, F. J.; Hieringer, W.; Gleich, D.; Herrmann, W. A. *Angew. Chem., Int. Ed. Engl.*, **1999**, *38*, 2416. **(c)** Weskamp, T.; Kohl, F. J.; Herrmann, W. A. *J. Organomet. Chem.*, **1999**, *582*, 362. **(d)** Ackermann, L.; Furstner, A.; Weskamp, T.; Kohl, F. J.; Herrmann, W. A. *Tetrahedron Lett.*, **1999**, *40*, 4787.

51. Öfele, K.; Herberhold, M. *Z. Naturforsch.*, **1973**, *28b*, 306.

52. Kocher, C.; Herrmann, W. A. *J. Organomet. Chem.*, **1997**, *532*, 261.

53. Lappert, M. F.; McCabe, R. W.; Mac Quitty, J. J.; Pye, P. L.; Riley, P. I. *J. Chem. Soc., Dalton Trans.*, **1980**, 90.

54. **(a)** Voges, M. H.; Romming, C.; Tilset, M. *Organometallics.*, **1999**, *18*, 529. **(b)** Abernethy, C. D.; Clyburne, J. A. C.; Cowley, A. H.; Jones, R. A. *J. Am. Chem. Soc.*, **1999**, *121*, 2329.

55. Liu, C. Y.; Chen, D. Y.; Lee, G. H.; Peng, S. M.; Liu, S. T. *Organometallics*, **1996**, *15*, 1055.

56. **(a)** Liu, S. T.; Hsieh, T. Y.; Lee, G. H.; Peng, S. M. *Organomet*allics, **1998**, *17*, 993. **(b)** Ku, R. Z.; Huang, J. C.; Cho, J. Y.; Kiang, F. M.; Reddy, K. R.; Chen, Y. C.; Lee, K. J.; Lee, J. H.; Lee, G. H.; Peng, S. M.; Liu, S. T. *Organomet*allics, **1999**, *18*, 2145.

57. Xue, W. M.; Chan, M. C. W.; Su, Z. M.; Cheung, K. K.; Liu, S. T.; Che, C. M. *Organomet*allics, **1998**, *17*, 1622.

58. Öfele, K.; Herrmann, W. A.; Mihalios, D.; Elison, M.; Herdtweck, E.; Priermeier, T.; Kiprof, P. *J. Organomet. Chem.*, **1995**, *498*, 1.

59. Enders, D.; Gielen, H.; Raabe, G.; Runsink, J.; Teles, J. H. *Chem. Ber.*, **1997**, *130*, 1253.

60. Doyle, M. J.; Lappert, M. F.; Pye, P. L.; Terreros, P. *J. Chem. Soc., Dalton Trans.*, **1984**, 2355.

61. Herrmann, W. A.; Gooβen, L. J.; Spiegler, M. *Organometallics*, **1998**, *17*, 2162.

62. Green, J. C.; Scurr, R. G.; Arnold, P. L.; Cloke, F. G. N. *Chem. Commun.*, **1997**, 1963.

63. **(a)** Green, M. J.; Cavell, K. J.; Skelton, B. W.; White, A. H. *J. Organomet. Chem.*, **1998**, *554*, 175. **(b)** Mc Guinness, D. S.; Green, M. J.; Cavell, K. J.; Skelton, B. W.; White, A. H. *J. Organomet. Chem.*, **1998**, *565*, 165. **(c)** Mc Guinness, D. S.; Cavell, K. J.; Skelton, B. W.; White, A. H. *Organometallics*, **1999**, *18*, 1596. **(d)** Albert, K.; Gisdakis, P.; Rosch, N. *Organomtallics*, **1998**, *17*, 1608.

64. **(a)** Lee, K. M.; Lee, C. K.; Lin, I. J. B. *Angew. Chem. Int. Ed. Engl.*, **1997**, *36*, 1850. **(b)** Wang, H. M. J.; Chen, C. Y. L.; Lin, I. J. B. *Organometallics*, **1999**, *18*, 1216.

65. Arduengo, A. J., III; Tamm, M.; McLain, S. J.; Calabrese, J. C.; Davidson, F.; Marshall, W. J. *J. Am. Chem. Soc.*, **1994**, *116*, 7927.

66. **(a)** Schumann, H.; Glanz, M.; Winterfeld, J.; Hemling, H.; Kuhn, N.; Kratz, T. *Angew. Chem., Int. Ed. Engl.*, **1994**, *33*, 1733. **(b)** Schumann, H.; Glanz, M.; Winterfeld, J.; Hemling, H.; Kuhn, N.; Kratz, T. *Chem. Ber.*, **1994**, *127*, 2369.

67. Oldham, W. J. Jr.; Oldham, S., M.; Scott, B. L.; Abney, K. D.; Smith, W. H., Costa, D. A. *Chem. Commun.*, **2001**, 1348.

68. Luger, P.; Ruban, G. *Acta. Crystallogr. Sect. B.*, **1971**, *27*, 2276.

69. **(a)** Morgan, J. P.; Grubbs, R. H. *Org. Lett.*, **2000**, *2*, 3153. **(b)** Jafarpour, L.; Nolan, S. P. *Organometallics*, **2000**, *19*, 2055.

70. Chamizo, J. A.; Morgado, J.; Bernes, S. *Trans. Met. Chem.* **2000**, *25*, 161.

71. **(a)** Herrmann, W. A.; Goossen, L. J.; Artus, G. R. J.; Kocher, C. *Organometallics*, **1997**, *16*, 2472. **(b)** Prinz, M.; Grosche, M.; Herdtweck, E.; Herrmann, W. A. *Organometallics*, **2000**, *19*, 1692. **(c)** Kuhn, N.; Kratz, T.; Blaser, D.; Boese, R. *Inorg. Chim. Acta.*, **1995**, *238*, 179.

72. **(a)** Scholl, M.; Trnka, T. M.; Morgan, J. P.; Grubbs, R. H. *Tetrahedron Lett.*, **1999**, *40*, 2247. **(b)** Weskamp, T.; Kohl, F. J..; Hieringer, W.; Gleich, D.; Herrmann, W. A. *Angew. Chem. Int. Ed. Engl.*, **1999**, *38*, 2416. **(c)** Weskamp, T.; Kohl, F. J.; Herrmann, W. A. *J. Organomet. Chem.*, **1999**, *582*, 362.

73. **(a)** Kuhn, N.; Kratz, T.; Boese, R.; Blaser, D. *J. Organomet. Chem.*, **1994**, *479*, C32. **(b)** Kuhn, N.; Kratz, T.; Boese, R.; Blaser, D. *J. Organomet. Chem.*, **1994**, *470*, C8.

74. Herrmann, W. A.; Ofele, K.; Elison M.; Kuhn, F. E.; Roesky, P. W. *J. Organomet. Chem.*, **1994**, *480*, C7.

75. **(a)** Ofele, K.; Herrmann, W. A.; Mihalios, D.; Elison, M.; Herdtweck, E.; Sherer, W.; Mink, J. *J. Organomet. Chem.*, **2001**, *617-618*, 616. **(b)** Arduengo, A. J., III; Gamper, S. F.; Calabrese, J. C.; Davidson, F. *J. Am. Chem. Soc.*, **1994**, *116*, 4391.

76. Weskamp, T.; Schattenmann, W. C.; Spiegler, M.; Herrmann,W. A. *Angew. Chem. Int. En.*, **1998**, ST 2490.

77. **(a)** Wanzlick, H. -W.; Schikora, E. *Angew. Chem.*, **1960**, *72*, 491. **(b)** Lemal, D. M.; Kawano, K. I. *J. Am. Chem. Soc.*, **1962**, *84*, 1761.

78. **(a)** Lappert, M. F. *J. Organomet Chem.*, **1988**, *358*, 185. **(b)** Cetinkaya, B.; Dixneuf, P.; Lappert, M. F. *J. Chem. Soc., Chem. Comm.*, **1973**, 206. **(c)** Cetinkaya, B.; Dixneuf, P.; Lappert, M. F. *J. Chem. Soc., Dalton Trans.*, **1974**, 1827. **(d)** Lappert, M. F.; Pye, P. L. *J. Chem. Soc., Dalton Trans.*, **1977**, 2172. **(e)** Hitchcock, P. B.; Lappert, M. F.; Pye, P. L. *J. Chem. Soc., Dalton Trans.* **1978**, 826. **(f)** Hitchcock, P. B.; Lappert, M. F.; Thomas, S. A.; Thorne, A. J.; Carty, A. J.; Taylor, N. J. *J. Organomet. Chem.*, **1986**, *315*, 27. **(g)** Macomber, D. W.; Rogers, R. D. *Organometallics*, **1985**, *4*, 1485. **(h)** Delgado, S.; Moreno, C.; Macazaga, M. J. *Polyhedron*, **1991**, *10*, 725. **(i)** Hitchcock, P. B.; Lappert, M. F.; Pye, P. L. *J. Chem. Soc., Dalton Trans.*, **1977**, 2160. **(j)** Lappert, M. F.; Pye, P. L. *J. Chem. Soc., Dalton Trans.*, **1977**, 1283. **(k)** Lappert, M. F.; Pye, P. L.; McLaughlin, G. M. *J.*

Chem. Soc., Dalton Trans., **1977**, 1272.

79. Petz, W. *J. Organomet. Chem.*, **1979**, *172*, 415.

80. Kocher, C.; Herrmann, W. A. *J. Organomet. Chem.*, **1997**, *532*, 261.

81. Huang J.; Shanz H-J.; Stevens E. D.; Nolan S. P. *Organometallics*, **1999**, 18, 2370.

82. Weskamp, T. Schattenmann, W. C.; Speigler, M.; Herrmann, W. A. *Angew. Chem. Int. Ed. Engl.*, **1999**, *38*, 262.

83. Lappert, M. F. In *Transition Metal Chemistry*; Muller, A., Diemann, E., Eds.; Verlag Chemie: Weinheim, **1981**, 87.

84. Trzeciak, A. M.; Ziolkowski, J. J. *Abstracts of Papers XX Colloquy on Organometallic Chemistry, Germany-Poland* (Halle-Wittenberg), **1996**, 11.

85. Lappert, M. F. *Transition Metal Chemistry*; Muller, A.; Diemann, E., Eds; Verlag Chemie: Heidelberg, **1981**.

86. Hill, T. E.; Nile, T. A. *J. Organomet. Chem.*, **1977**, *137*, 293.

87. Herrmann, W. A.; Gooβen, L. J.; Kocher, C.; Artus, G. R. J. *Angew. Chem., Int. Ed. Engl.*, **1996**, *35*, 2805.

88. Gardiner, M. G.; Herrmann, W. A.; Reisinger, C. P.; Schwarz, J.; Spiegler, M. *J. Organomet. Chem.*, **1999**, *572*, 239.

89. Ku, R. Z.; Chen, D. Y.; Lee, G. H.; Peng, S. M.; Liu, S. T. *Angew. Chem., Int. Ed. Engl.*, **1997**, *36*, 2631.

90. Cetinkaya, B.; Özdemir, I.; Dixneuf, P. H. *J. Organomet. Chem.*, **1997**, *534*, 153.

91. Cetinkaya, B.; Özdemir, I.; Bruneau, C.; Dixneuf, P. H. *J. Mol. Catal. A.*, **1997**, *118*, L1.

92. Petz, W. *Angew. Chem. Int. Ed. Engl.*, **1975**, *14*, 367.

93. Nguyen, S. T.; Johnson, L. K.; Grubbs, R. H. *J. Am. Chem. Soc.*, **1992**, *174*, 3974.

94. Nguyen, S. T.; Grubbs, R. H.; Ziller, J. W. *J. Am. Chem. Soc.*, **1993**, *115*, 9858.

95. Schwab, P.; France, M. B.; Ziller, J. W.; Grubbs, R. H. *Angew. Chem. Int. Ed.*, **1995**, *34*, 2039.

96. Schwab, P.; Grubbs, R. H.; Ziller, J. W. *J. Am. Chem. Soc.*, **1996**, *118*, 100.

97. Dias, E. L.; Nguyen, S. T.; Grubbs, R. H. *J. Am. Chem. Soc.*, **1996**, *119*, 3887.

98. Huang, J.; Stevens, E. D.; Nolan, S. P.; Petersen, J. L. *J. Am. Chem. Soc.*, **1999**, *121*, 2674.

99. **(a)** Ackermann, L.; Furstner, A.; Weskamp, T.; Kohl, F. J.; Herrmann, W. A. *Tetrahedron Lett.*, **1999**, 40, 4787. **(b)** Frenzel, U.; Weskamp, T.; Kohl, F. J.; Schattenmann, W. C.; Nuyken, O.; Herrmann, W A. *J. Organomet. Chem.*, **1999**,

586, 263. **(c)** Hamilton, J. G.; Frenzel, U.; Kohl, F. J.; Weskamp, T.; Rooney, J. J.; Herrmann, W. A.; Nuyken, O. *J. Organomet. Chem.* **2000**, *606*, 8. **(d)** Furstner, A.; Thiel, O. R.; Ackermann. L.; Schanz, H. -J.; Nolan, S. P. *J. Org. Chem.*, **2000** *65*, 2204. **(e)** Furstner, A.; Thiel, O. R.; Kindler, N.; Bartkowska, B. *J. Org. Chem.* **2000**, *65*, 7990. **(f)** Jafarpour, L.; Huang, J.; Stevens, E. D.; Nolan, S. P. *Organometallics*, **1999**, *13*, 5416. **(i)** Huang, J.; Schanz, H. -J.; Stevens, E. D.; Nolan, S. P. *Organometallics*, **1999**, *18*, 5375. **(k)** Schanz, H.-J.; Jafarpour, L.; Stevens, E. D.; Nolan, S. P. *Organometallics*, **1999**, *18*, 5187. **(l)** Ackermann, L.; Eltom, D.; Furstner, A. *Tetrahedron*, **2000**, *56*, 2195. **(m)** Benningshoft, J. C. J.; Blaauw, R. H.; van Ginkel, A. E.; Rutjes, F. P. J. T.; Fraanje, J.; Goubitz, K.; Schenk, H.; Hiemstra, H. *Chem. Commun.*, **2000**, 1465. **(n)** Bourgeois, D.; Mahuteau, J.; Pancrazi, A.; Nolan, S. P.; Prunet, J. *Synthesis*, **2000**, 869. **(o)** Briot, A.; Bujard, M.; Gouverneur, V.; Nolan, S. P.; Mioskowski, C. *Org. Lett.*, **2000**, *2*, 1517. **(p)** Itoh, A.; Mitsukara, K.; Ishida, N.; Uneyama, K. *Org. Lett.*, **2000**, 2, 1431. **(q)** Frenzel, U.; Nuyken, O.; Kohl, F. J.; Schattenmann, W. C.; Weskamp, T.; Herrmann, W. A. *Polym. Mater. Sci. Eng.*, **1999**, *80*, 135.

100. Schrock, R. R.; Feldman, J.; Cannizzo, L. F.; Grubbs, R. H. *Macromol.*, **1987**, *20*, 1169.

101. Furstner, A.; Theil, O. R.; Blanda, G. *Org. Lett.*, **2000**, *2*, 3731.

102. **(a)** Bielawski, C. W.; Grubbs, R. H. *Angew. Chem. Int. Ed. Engl.*, **2000**, *39*, 2903. **(b)** Chatterjee, A. K.; Grubbs, R. H. *Org. Lett.*, **1999**, *1*, 175. **(c)** Chatterjee, A. K.; Morgan, J. P.; Scholl, M.; Grubbs, R. H. *J. Am. Chem. Soc.*, **2000**, *124*, 3783. **(d)** Lee, C. W.; Grubbs, R. H. *Org. Lett.*, **2000**, *2*, 2145. **(e)** Garber, S. B.; Kingsbury; J. S.; Gray, B. L.; Hoveyda, A. H. *J. Am. Chem Soc.*, **2000**, *122*, 8168. **(f)** Hyldtoft, L.; Madsen, R. *J. Am. Chem. Soc.*, **2000**, *122*, 8444. **(g)** Efremov, I.; Paquette, L. A. *J. Am. Chem. Soc.*, **2000**, *122*, 9324. **(h)** Limanto, J.; Snapper, M. L. *J. Am. Chem. Soc.*, **2000**, *122*, 8071. **(i)** Maynard, H. D.; Okada, S. Y.; Grubbs, R H. *Macromol.*, **2000**, *33*, 6239. **(j)** Smulik, J. A.; Diver. S. T. *Org. Lett.*, **2000**, *2*, 2271. **(k)** Wright, D. L.; Schulte, J. P.; Page, M. A. *Org. Lett.* **2000**, *2*, 1847.

103. **(a)** Mizoroki, T.; Mori, K.; Ozaki, A. *Bull. Chem. Soc. Jpn.*, **1971**, *44*, 581. **(b)** Heck, R. F.; Nolley, J. P. *J. Org. Chem.*, **1972**, 2320. **(c)** Shibasaki, M.; Vogl, E. M. *J. Organomet Chem.*, **1999**, *576*, 1. **(d)** de Meijere, A.; Meyer, F. E. *Angew. Chem. Int. Ed. Engl.*, **1994**, *33*, 2379.

104. Sturmer, R. *Angew. Chem. Int. Ed. Engl.*, **1999**, *38*, 3307.

105. **(a)** Swartz, J.; Bohm, V. P. W.; Gardiner, M. G.; Grosche, M.; Herrmann, W. A.; Hieringer, W.; Raudaschl-Sieber, G. *Chem. Eur. J.*, **2000**, *6*, 1773. **(b)** Herrmann, W. A.; Reisinger, C. -P.; Spiegler, M. *J. Organomet. Chem.*, **1998**, *557*, 93. **(c)** Gardiner, M. G.; Herrmann, W. A.; Reisinger, C. -P.; Schwartz, J.; Speigler, M. *J. Organomet. Chem.*, **1999**, *572*, 239.

Chapter 5.

C-C and C-H activation of N-heterocyclic carbene complexes of ruthenium.

5.1. Introduction.

As mentioned in **Chapter 4** we decided to investigate the catalytic activity of an carbene (NHC) derivative of **(1)** towards the Murai reaction. Our initial work focused on the synthesis of $Ru(PPh_3)_2(IMes)(CO)H_2$ **(26)** where the reactivity of **(1)** was modified by substitution of one triphenylphosphine ligand by a molecule of the well-known NHC bis(1,3-(2,4,6-trimethylphenyl)imidazol-2-ylidene) (IMes, **25**). During the thermolysis of **(1)** with IMes we observed sequential formation of **(26)**, and $Ru(PPh_3)(IMes)_2(CO)H_2$ **(29)**. Persistent heating at 110 °C resulted in activation of a C-C bond in one of the mesityl rings of the carbene ligand. There was no evidence for the C-H activation of IMes. Nevertheless this process could be detected upon treatment of **(26)** with alkene. After finding these very interesting results, we decided to try to uncover more on these rather surprising C-C and C-H bond activation reactions. Our work was aimed at providing some mechanistic information on both the C-C and the C-H activation reactions, as well as probing the reacivity of bidentate phosphine derivatives of **(26)** such as $Ru(dppp)(IMes)(CO)H_2$ **(27)** and $Ru(arphos)(IMes)(CO)H_2$ **(28)** towards C-C and C-H activation reactions. Very little was done to investigate the solution reactivity of **(26)** and **(30)**, and only their reactivity toward CO insertion was considered. The reactivity of **(26)** toward the Murai reaction has already been described in **Chapter 3** and thus will not be described in any further detail in this chapter.

5.1.1. Introduction to C-C and C-H bond activation.

A wide range of functional groups can be activated by transition metal complexes, and metal-catalyzed reactions of alkenes,[1] ketones,[2] amines,[3] aldehydes[4] and alcohols[5] have made a great contribution to the recent growth of organic synthesis.[6] More intriguingly, transition metal complexes have been shown to activate relatively inert bonds, such as hydrocarbons (C-H and C-C),[7] molecular nitrogen (N≡N),[8a,b] and molecular hydrogen (H-H).[8c,d] Although the activation of these inert classes of molecules has been observed, examples of these activations still remain rare, and in some cases are still seen as a challenge for synthetic inorganic chemists. In fact transition metal complex activation of C-H and C-C bonds in homogeneous processes is an active field of research as it can lead to the design of new selective and efficient processes for the functionalisation of hydrocarbons.

5.1.2. Introduction to intramolecular C-H bond activation.

In **Chapter 1** C-H bond activation in stoichiometric and catalytic reactions was described in some detail. We do not intend to discuss this area in more detail, but we will rather try to give the reader an overview of the field of intramolecular C-H activation, as well as some reported examples of intramolecular C-H activation in NHC complexes. Intramolecular C-H activation is nowadays a relatively well understood process which has been extensively reviewed both mechanistically and kinetically.[9,16] With many examples reported for various ligands such as PR_3 (R= C_6H_5,[10] C_6H_{10},[11]), diazobenzene,[12] or NHCs,[13] the rapid growth of the chemistry of cyclometallated complexes has led to many applications in organic synthesis, catalysis, and asymmetric reactions.[14]

5.1.2.1. Mechanistic aspect.

Similarly to standard C-H activation, there are three generally accepted mechanisms of intramolecular C-H bond cleavage: oxidative addition, electrophillic substitution, and so-called muticentered pathways **[Scheme 5.1.]**.[15] Specific metals tend to show one particular type of reactivity. For example Ti, Zr, Hf, Ta and Th have been shown to proceed via a nucleophilic route; Re, Fe, Ru, Os, Rh and Pt via an electrophilic process and Co and Pd via a multicentered route.[16a]

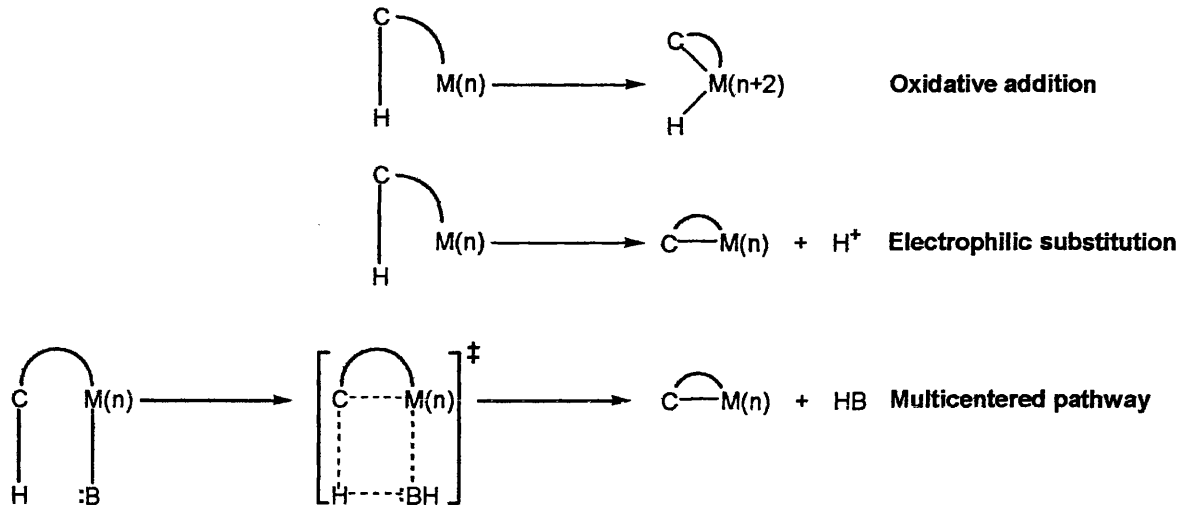

Scheme 5.1.

Another point in cyclometalation by any metal centre is the question of aromatic vs. aliphatic C-H bond activation.[17, 18] In fact aromatic C-H bond activations are more commonly observed than for aliphatic or benzylic C-H groups. Two theories have been proposed by Crabtree et al.[19] The first postulate is based on kinetic arguments, and proposes that arene groups can bond more easily to a metal centre in an η^2 fashion,[20] followed by oxidative addition. The second postulate originates from thermodynamic observations and proposes that the reactivity is driven by the strength of the bond being formed i.e. M-C(Aryl) > M-C(alkyl) > M-C(benzyl). Further work[19b] showed that intramolecular and more genrally C-H bond activation is driven by thermodynamic factors rather than by kinetic factors.

The first well characterised nucleophilic thermolytic intramolecular C-H activation, was reported in 1985 by Jones et al. **[Scheme 5.2.]**.[21] The reaction proceeded via reductive elimination of benzene, but although full conversion was observed in cyclohexane, reaction in benzene leads to a mixture of starting material and products. This observation was attributed to the existence of an equilibrium between the starting material and the product. C-H activation and subsequent formation of a hydride moiety was proved not to be the rate determining step. Moreover the cyclometalation was found to be thermodynamically triggered, and kinetically unfavoured.

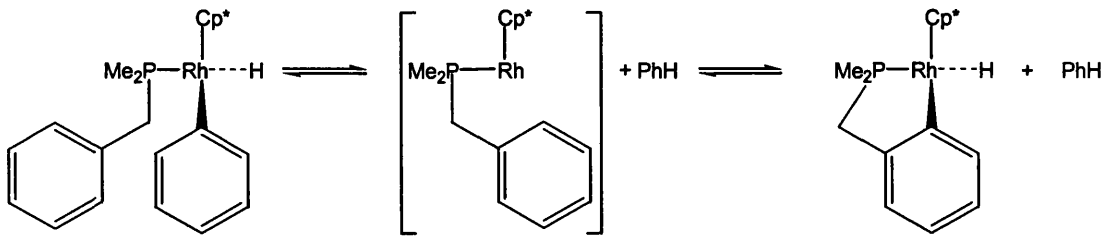

Scheme 5.2.

The existence of an electrophilic pathway to intramolecular C-H activation, was first demonstrated by Cope et al.[22,23] in their study of the reactivity of cyclopalladated compounds. Further investigation by Ryabov et al.[24] of the mechanistic and kinetic aspects of this reaction **[Scheme 5.3.]** showed that cyclopalladation must occur in the plane of a 14-electron palladium intermediate.

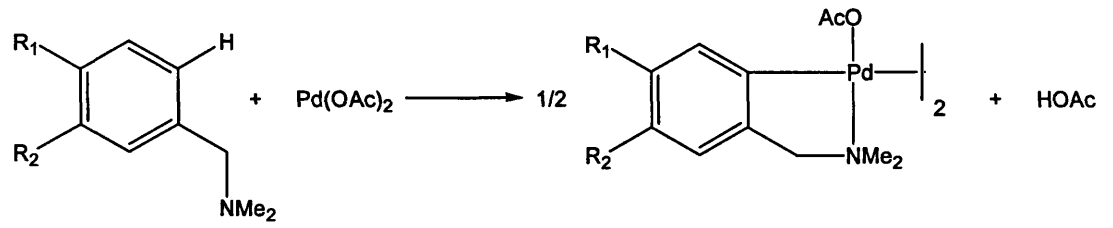

Scheme 5.3.

Although multi-centred pathways to intra-molecular C-H activation have not been directly observed, it has been proposed as a possible route in several intra-molecular reactions.[25] For examples as shown in **Scheme 5.4.**, the C-H bond activation of titanium (or zirconium) complexes cannot be realised by oxidative addition or reductive elimination due to the absence of a readily eliminating group. This suggests formation of a six-valent intermediate species, through a multi-centred transition state in which formation of the new M-C bond occurs at the same time that the leaving group-metal is being formed.

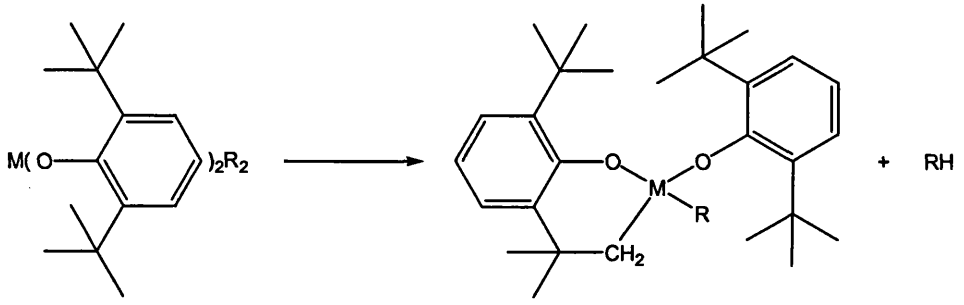

Scheme 5.4.

5.1.2.2. Further examples of intramolecular C-H bond activation.

In many reported examples of intramolecular C-H activation, the process is driven by a donor atom such as N, P or As. For example in 1990, Rabinovich et al. reported reversible intramolecular C-H activation of $W(PMe_3)_6$ **[Scheme 5.5.]**.[26] Similar intramolecular C-H activation has been observed in numerous phosphorus complexes, such as in the case of $Ru(PPh_3)_4H_2$[27] or $Ir(PPh_3)(Cp^*)(Me)_2$.[28]

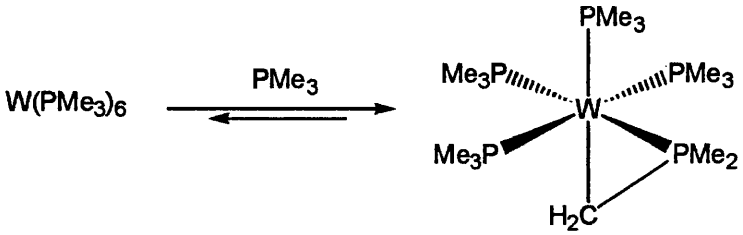

Scheme 5.5.

In a very nice example reported by Albrecht et al., transcyclometalation occurs with late transition metals through intramolecular C-H activation **[Scheme 5.6.]**.[29]

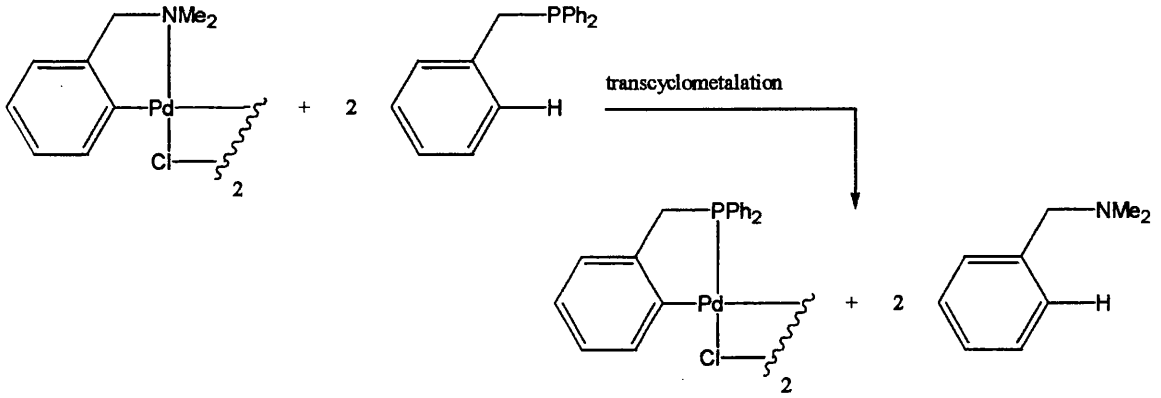

Scheme 5.6.

A remarkable example of reversible intramolecular C-H activation has been reported by Chaudret et al.[30] **[Scheme 5.7.]**. A mechanistic investigation of this process has shown that it is accompanied by proton transfer and facilitated by an agostic interaction between the C-H bond and the ruthenium centre.

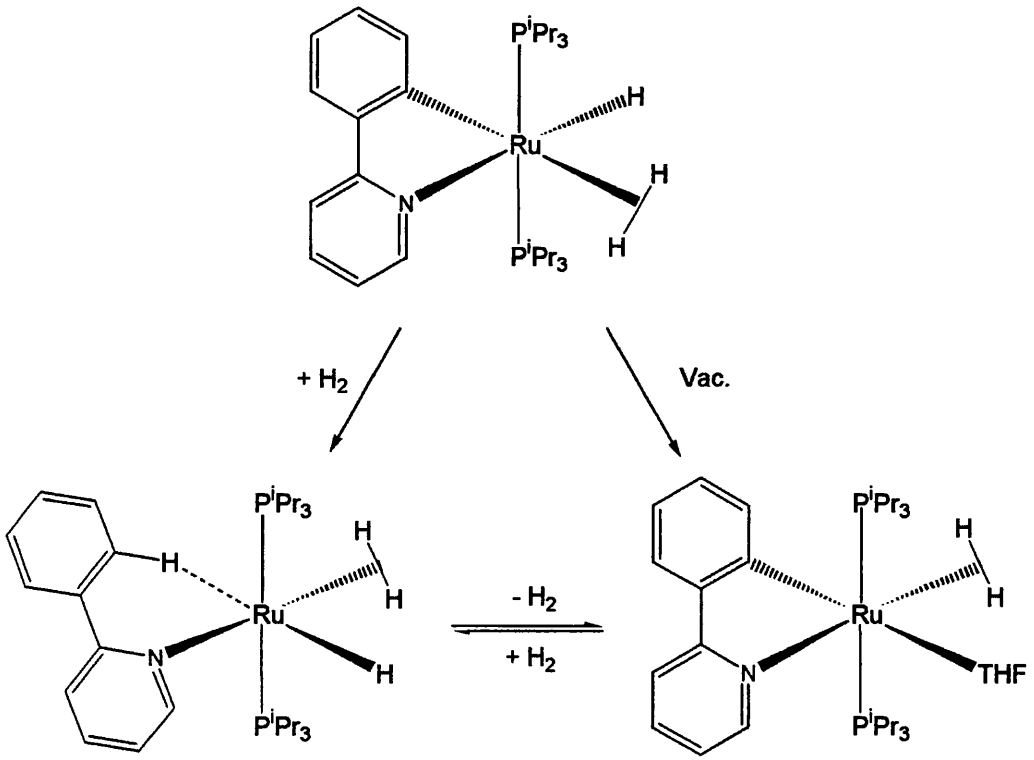

Scheme 5.7.

Finally carbene ligands have been shown in several examples not to be as passive as initially proposed. In 2002 Danapoulos et al. reported intramolecular C-H activation of NHC complexes of Rh and Ir **[Scheme 5.8.]**.[13b]

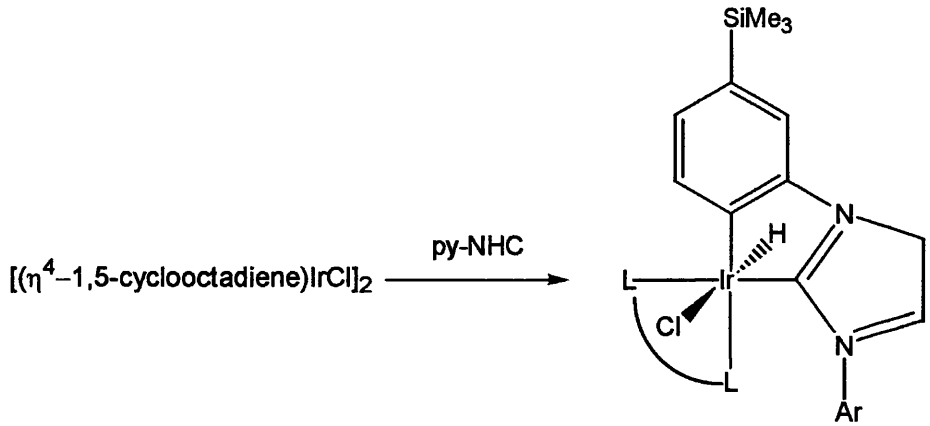

py-NHC = 1-[(2-(6-trimethylsilyl)pyridyl]-3-[(2,6-di-iso-propyl)phenyl]imidazol-2-ylidene

Scheme 5.8.

5.1.3. Introduction to C-C Bond activation.

As seen in **Chapter 1**, much work has been done in the field of C-H activation and homogeneous C-H bond activation is relatively well studied both synthetically and mechanistically. By comparison, C-C bond activation by homogeneous transition metals complexes still remains rare and poorly studied, with the exception of strained C-C bonds. Their robust nature cannot be understood from a thermodynamic point of view as C-H bonds are thermodynamically more stable than C-C bonds (BDE C-H = 440 kJ mol^{-1}, BDE C-C = 356 kJ mol^{-1}), but several factors, mainly kinetic, make C-H bond activation generally favoured over C-C bond activation.

Two routes have been described for C-C bond cleavage, one involving a β-elimination pathway and one an oxidative addition step.

5.1.3.1. β-carbon elimination.

The use of σ alkyl metal complexes provides an interesting route to C-C activation, as the bond between the β- and the γ- carbon of these complexes can be cleaved in a β-carbon elimination pathway **[Scheme 5.9.]**. Although examples of C-C bond cleavage via this process are quite rare, there are various examples reported in the literature.

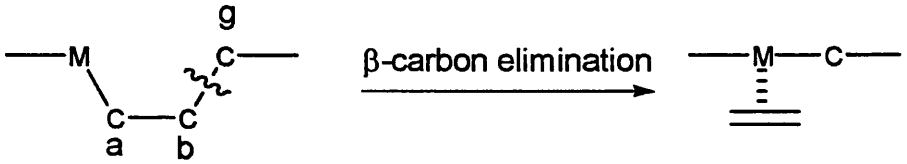

Scheme 5.9.

One of the first examples was reported by Watson et al.[31] They observed that thermal decomposition of a lutetium-isobutyl complex having a vacant coordination site led to a methyl complex and generation of propene by β-carbon elimination **[Scheme 5.10.]**.

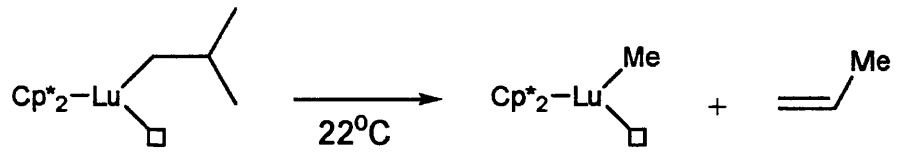

□ : vacant site

Scheme 5.10.

Another well known example occurs during the Ziegler-Natta[32] polymerization of propene. The role played by β-carbon elimination during this process was identified by Teuben et al.[33] who showed that during propene oligomerization mediated by cationic d^0 complex of Zr and Hf **[Scheme 5.11.]**, a methyl group is transferred from the growing chain to the metal during termination, therefore regenerating the methyl complex.

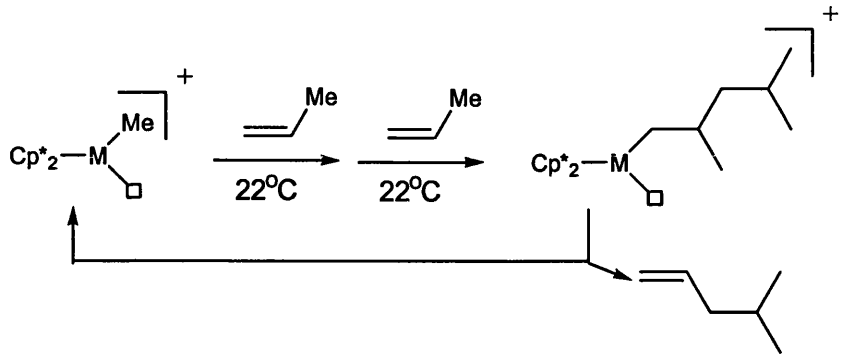

Scheme 5.11.

In one of the latest examples reported,[34] reversible migratory insertion/β-carbon elimination occurs between the coordinated alkyne and the bound alkyl group of an alkyl-niobium(alkyne) complex **[Scheme 5.12.]**.

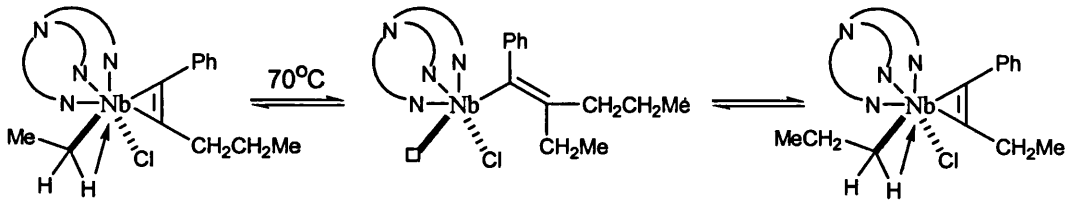

Scheme 5.12.

Few examples of β-carbon elimination in late metal systems have been reported. In one example by Bergman et al.[35] warming of a solution of an oxaruthenacycle led to the formation of methane and a cyclic enolate complex through β-methyl elimination **[Scheme 5.13.]**.

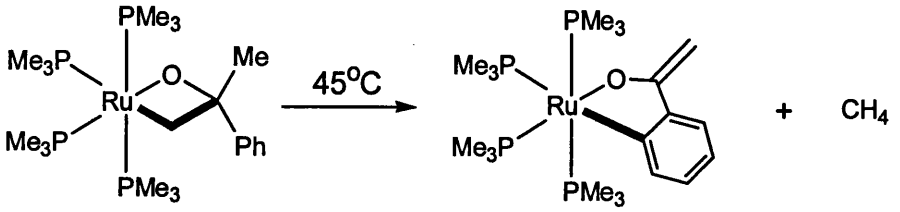

Scheme 5.13.

In a later example by these authors,[36] thermolysis of a ruthenacyclobutane produces a π-allyl complex in a reversible process. The reaction involves β-methyl transfer from the central carbon of the ligand to the metal through formation of a 16-electron intermediate **[Scheme 5.14.]**.

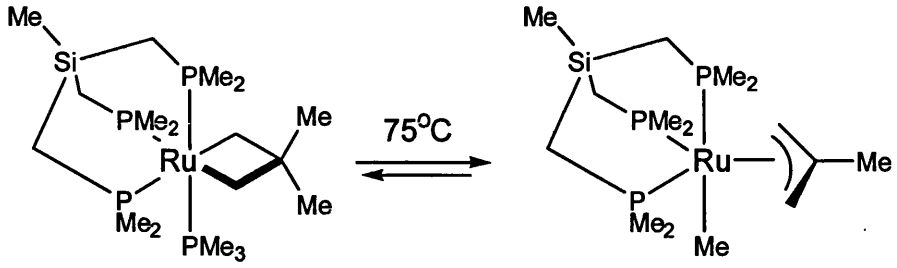

Scheme 5.14.

5.1.3.2. Oxidative addition.

The factors which account for the inactivity of C-C bonds toward oxidative addition by a transition metal can generally be attributed to three reasons;

(i) The generally easier approach of the metal centre to C-H bonds neighbouring the C-C bond.

(ii) A significantly higher activation barrier for C-C versus C-H activation

(iii) Thermodynamic factors in that although C-H bonds have a higher dissociation energy than C-C bonds they form an M-H bond via oxidative addition which is considerably stronger than the M-C bonds in alkyl complexes.[37]

The C-C σ bond is thermodynamically stable (dissociation energy of ≅ 356 kJ/mol) and by comparison, the M-C bond (293 kJ/mol) is lower in energy, thus making the oxidative addition of a C-C bond to a metal form at the expense of a more stable C-C bond. Furthermore, the constrained directionality of the C-C σ -orbital, by comparison to a C=C or a C-H bond **[Figure 5.1.]**, makes the approach of the metal centre to the C-C bond rather difficult. For example, in the C=C double bond, the π-orbitals of the double bond are oriented sideways allowing a facile interaction with the metal **[Figure 5.1.]**. In the case of a C-H bond as proposed by Crabtree et al,[38] the oxidative addition begins with an end-on

approach prior to a side-on coordination. This process can easily be understood by looking at the nature of the C-H bond which consists of a σ orbital connecting the carbon to the hydrogen along the bond axis **[Figure 5.1.]**. Therefore the hydrogen has its electron in a spherical 1s orbital and no substituents at its periphery allowing a facile approach to the metal centre. In contrast, the σ-orbital in a C-C bond lies along the bond axis **[Figure 5.1.]**, which forces a high directionality into the approach of the metal centre to the C-C bond, and furthermore quaternary carbon atoms bond to several ligands at their periphery making the steric bulk around the C-C bond an additional barrier to the oxidative addition.

All these factors contribute to making the kinetic barrier towards the oxidative addition of a metal to a C-C bond relatively high, thus making the C-C bond considerably more inert than a C-H bond.

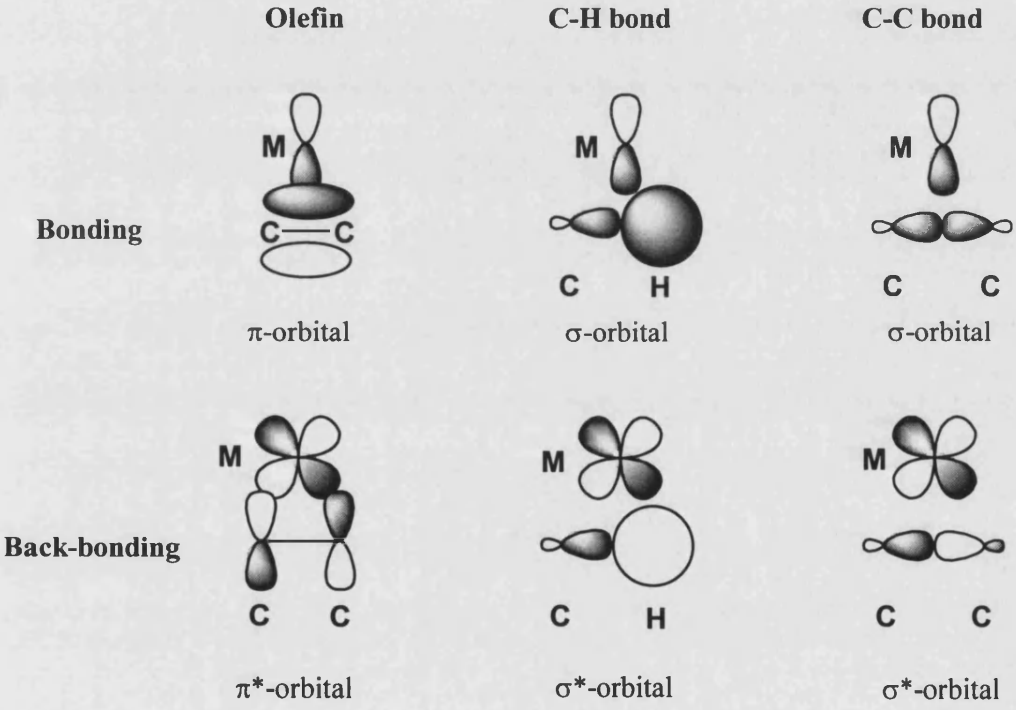

Figure 5.1.

Nevertheless C-C bond activation is not impossible as testified by several stable alkyl metal complexes.[39] A number of promoting strategies have been adopted to enhance reactivity, such as relief of ring strain, the attainment of aromaticity or addition of thermodynamic promoters. For example, addition of H_2 to the system may result in CH_4 elimination following the C-C activation step, making the whole process thermodynamically more favourable even in the case of a strong C-C bond.

5.1.3.2.1. Metal insertion into a strained C-C bond.

The use of strained alkanes such as cyclopropane or cyclobutane in C-C activation systems represents an advantage kinetically as well as thermodynamically. This increase in reactivity is mainly due to the relief in structural strain in the ring, but structural factors in the ring also make the C-C bond more accessible to the metal centre. In fact the orbitals connecting the carbon atoms in C_3 and C_4 rings are bent out compared to the linear C-C bond, thus increasing their kinetic accessibility. This bend out of the orbitals can be explained by the fact that orbitals in the C-ring are largely p in character and therefore can be seen as similar to the HOMO and LUMO in C=C **[Figure 5.2.]**.

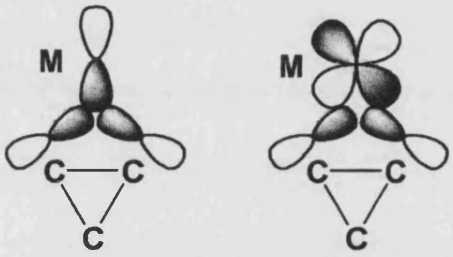

Figure 5.2.

The first example of metal promoted C-C activation of strained systems was reported by Tiper et al.[40] in 1955 **[Scheme 5.15.]**, who observed insertion of $PtCl_2$ into the C-C bond of cyclopropane in the presence of pyridine. This work was extended to a large variety of three[41, 45] and four[42] membered ring derivatives, through extensive use of late transition metal complexes containing Pt,[43] Rh,[44, 48] Fe,[45] Ni,[46] Ir,[47] and Co.[48]

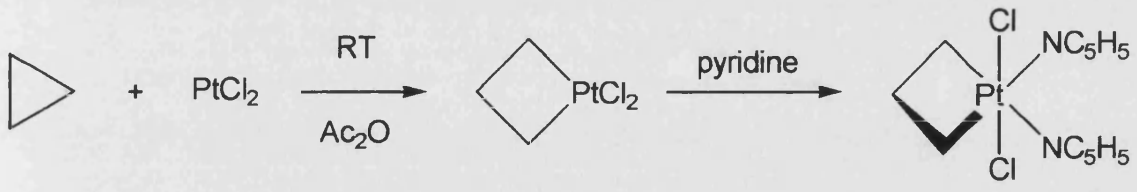

Scheme 5.15. - *Platinacyclobutane complex* ***(a)*** *and its bis(pyridine) derivative* ***(b)***

In an interesting case reported by McQuillin et al,[49] Zeise's Pt^{II} dimer reacts with cyclopropane to form tetrameric platina(IV)cyclobutanes, which upon addition of nitrogen donors provide the monomer in high yields. Unfortunately this process is limited in scope and reactions did not occur with cyclopropanes bearing electron withdrawing groups. It was shown that $[RhCl(CO)_2]_2$ inserts into the severely strained C-C bond of cubane **[Scheme 5.16.]**. In the case of biphenylenes, the reaction is not only driven by strain relief,

but also by formation of two strong M-C_{aryl} bonds. Eisch et al[42c] showed that the reactivity of nickel complexes with biphenylene increased with higher electron density on the metal $[Ni(cod)(bpy)] < [Ni(PPh_3)_4] < [Ni(PPh_3)_2(C_2H_4)] < [Ni(PEt_3)_4]$.

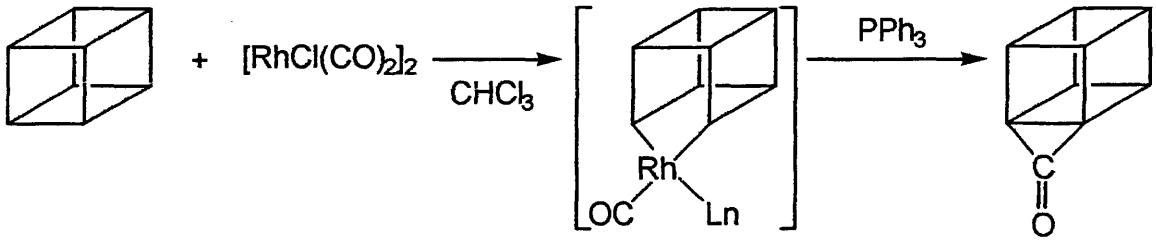

Scheme 5.16.

5.1.3.2.2. Metal insertion into an unstrained C-C bond.

In unstrained systems one cannot use the strain in the bond as a driving force for C-C activation. Therefore, a number of methodologies have been used to make C-C activation accessible.

a) Utilization of a carbonyl moiety to promote activation.

In an example reported by Suggs et al,[50] the α-keto C-C bond of 8-quinolinylalkyl ketone was activated by $[\{Rh(C_2H_4)_2Cl\}_2]$ **[Scheme 5.17.]**. This suggests that the C-C bond between a carbonyl atom and the carbon α to it was (relatively) weaker than other single bonds. It was also noted that the C-C bond points directly towards the metal centre, thus making the activation both thermodynamically and kinetically more feasible. Later work demonstrated the importance of the C=O bond, not only in weakening the C-C bond, but also in assisting the C-C cleavage, in a similar manner to the Baeyer-Villiger reduction of ketones. (as shown by formation of the tetrahedral intermediate [a] **[Scheme 5.17.]**).

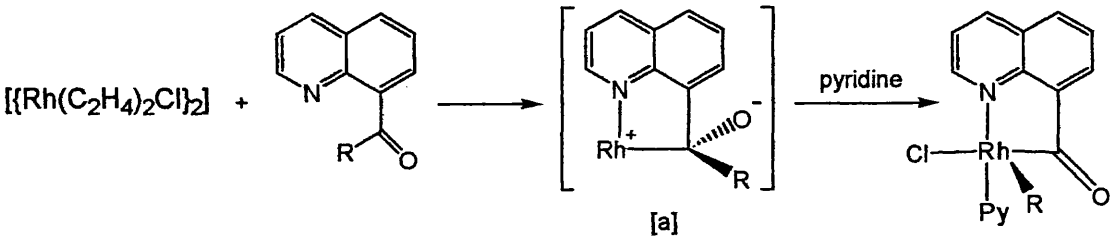

Scheme 5.17.

b) Aromatization promoted activation.

C-C bond cleavage in prearomatic systems can be achieved using aromaticity as a driving force. Eilbracht et al.[51] showed that C-C bond within tricarbonyliron complexes of 1,1-dialkyl-substituted spirocyclopentadienes were cleaved in boiling benzene, leading to π-cyclopentadienyl-σ-alkylcarbonyliron complexes **[Scheme 5.18.]**.

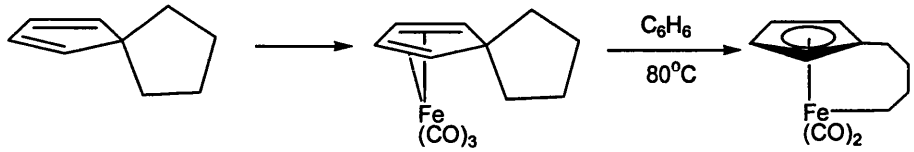

Scheme 5.18.

In another example an η^4-(*endo*-ethylcyclopentadienyl)molybdenum complex rearranged with breaking of a Cp-Et bond to give the η^5-(cyclopentadienyl) (ethyl)molybdenum complex upon generation of a vacant site on the metal **[Scheme 5.19.]**.[52] A number of variations of this reaction have been reported with iron,[53] manganese[54] and rhenium.[55]

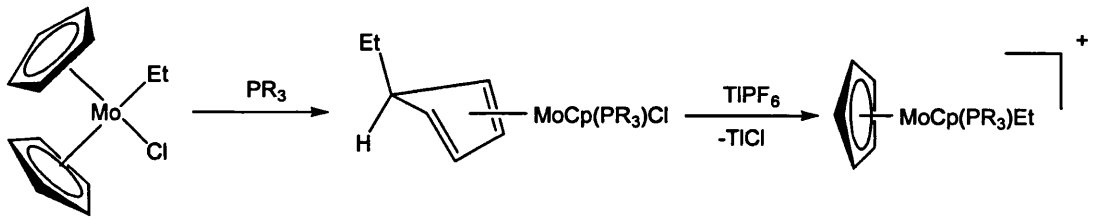

Scheme 5.19.

Crabtree et al.[56] reported C-C bond cleavage reactions in cationic 1,1-dialkyl-substituted cyclopentadienyliridium complexes. This occurred via a two step route leading to selective C-C bond breaking in disubstituted cyclopentanes. This work was extended to the use of cyclopentadienyl rings as a prearomatic system and led to the formation of **(a)** and **(b) [Scheme 5.20.]**, probably due to a reversible process during the cleavage/formation step.

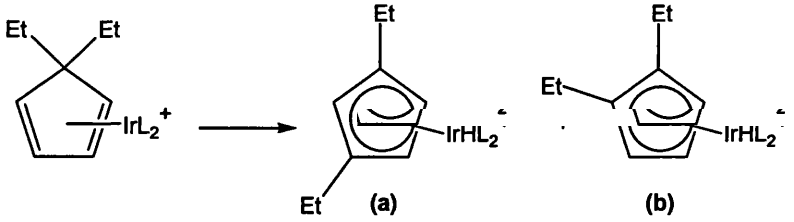

Scheme 5.20.

c) Promoted by agostic interactions.

Bennett and Spencer have demonstrated an interesting case of C-C cleavage in unsaturated cationic cobalt complexes that are stabilized by agostic interactions **[Scheme 5.21.]**.[57] In this process, the diene-hydride formed in the first step of the reaction is not stable, leading to the formation of a more stable product through an agostic interaction with a C-H bond on the ring. This eventually leads to a more stable product through the breaking of the C-C bond. Their attempt to extend this work to the C-C activation of six-membered rings was not successful, probably due to the stability of the C_6 ring and/or a poor accessibility of the C-C bond to the metal.

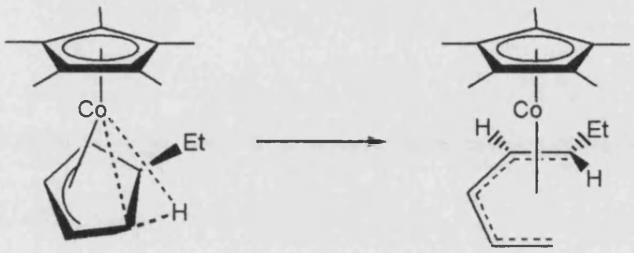

Scheme 5.21.

d) Cluster promoted activation.

In a very nice example reported by Suzuki et al,[58] C-C bond breaking occurs in a non-strained ordinary diene by reaction with a tri-ruthenium hydride cluster complex. In this process the Csp^2-Csp^3 bond of cyclopentadiene is cleaved by the ruthenium cluster to afford a ruthenacyclohexadiene, which rearranges to a 2-methylruthenacyclopentadiene **[Scheme 5.22.]**.

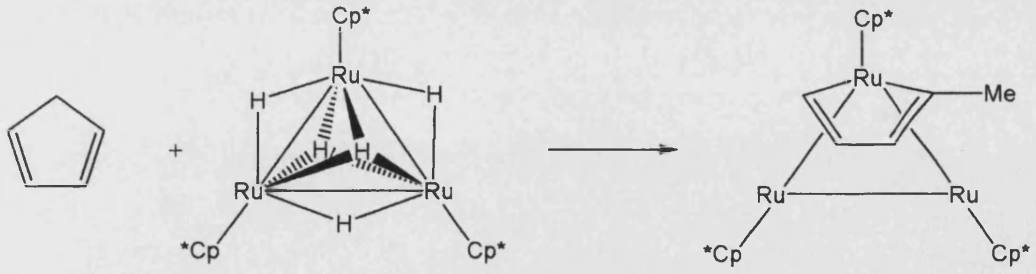

Scheme 5.22.

e) Utilization of pincer-type chelating ligands to promote activation.

One of the most interesting and well studied systems reported involves selective C-C activation using PCP and PCN pincer type ligands. Milstein et al.[59] designed a diphosphine pincer-type chelating ligand in order to observe selective cleavage of an alkyl group attached to an aromatic ring. Reaction of $[Rh(PPh_3)_4H]$ with the Ph-PCP ligand at

room temperature resulted in elimination of H_2 and formation of the kinetic C-H activation product. This can be reacted further by heating under hydrogen resulting in C-C activation and methane elimination **[Scheme 5.23.]**. Thermodynamic studies show that the C_{Me}-C_{aryl} bond in PCP ligand is much stronger than the C_{benzyl}-H bond [(BDE(C_6H_5-CH_3)= 426.5 ± 8 versus (BDE($C_6H_5CH_2$-H)= 368.7 ± 4 kJ mol^{-1}], indicating that the conversion of the C-H activation product into the C-C activation product is product controlled and that the strongest bond on the metal was formed by breaking the strongest bond in the substrate. Electronic perturbation of the ring by introduction of a methoxy group has no effect on the reaction rate or the product ratio suggesting that the C-C oxidative addition proceeds directly via a three-centred non polar transition state similar to that postulated for the C-H bond activation.

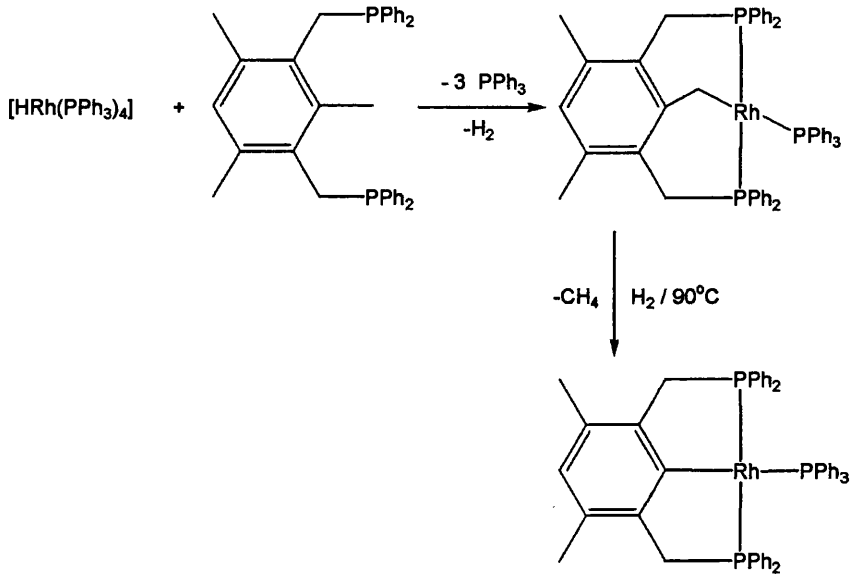

Scheme 5.23.

Reaction of a tri-butyl phosphine derivative of the PCP ligand leads to facile oxidative addition of the rhodium into one of the strong aryl-carbon bonds, yielding a C-C oxidative addition product **[Scheme 5.24.]**.[60]

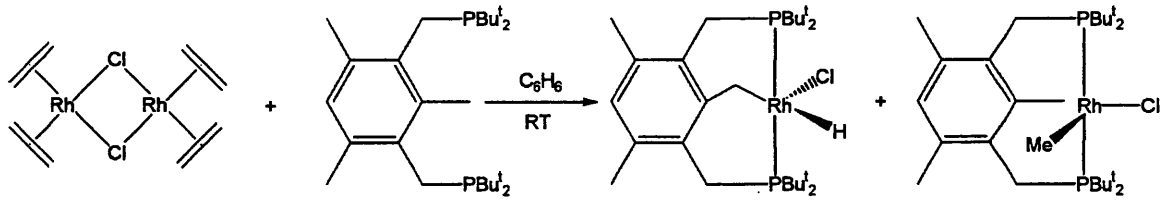

Scheme 5.24.

Subsequent work on a phosphine amine ligand derivative led to an easier reaction compared to the PCP derivative to give a C-C activated product. Rather than having to heat it up under hydrogen as in the phenylphosphine derivative, the reaction occurred in minutes at room temperature **[Scheme 5.25.]**.[61]

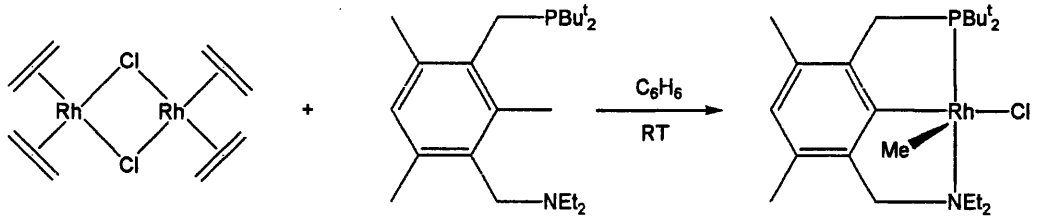

Scheme 5.25.

f). Miscellaneous types of C-C activation.

A variety of processes leading to C-C activation have been observed, such as C-C bond breaking in fullerenes, and electrochemically induced C-C activation of C_8H_8 in the pseudo-triple-decker complex $[Cp_2Ru_2(\mu\text{-cyclo-}C_8H_8)]$ **[Scheme 5.26.]**.[62]

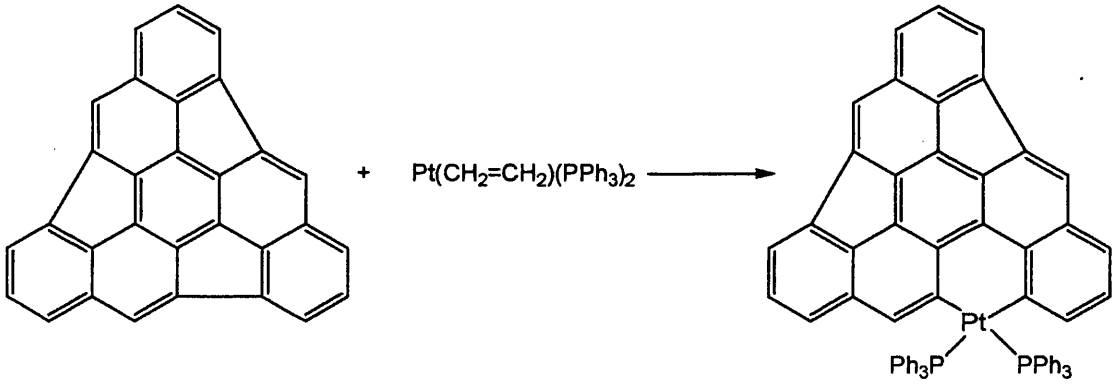

Scheme 5.26.

5.1.3.3. Catalytic reactions involving C-C bond cleavage.

Selective and efficient C-C activations set important goals in organometalic chemistry as much for the novelty of the reaction mechanism involved as the application it could lead to. Compared to the catalytic pathways developed through C-H activation, the field of catalytic C-C bond activation is undeveloped; nevertheless its potential applications to the petroleum industry attracts more and more research. This field of research has already been successfully described in major reviews and articles[37,39] and therefore we will go into little detail on the subject here. However we intend to give the reader an overview of the latest advances in this area. An early example was found when it was noted that tetraphenylene is formed quantitatively from biphenylene in the presence of

a catalytic amount of $Ni(cod)(PMe_3)_2$ **[Scheme 5.27.]**.[63]

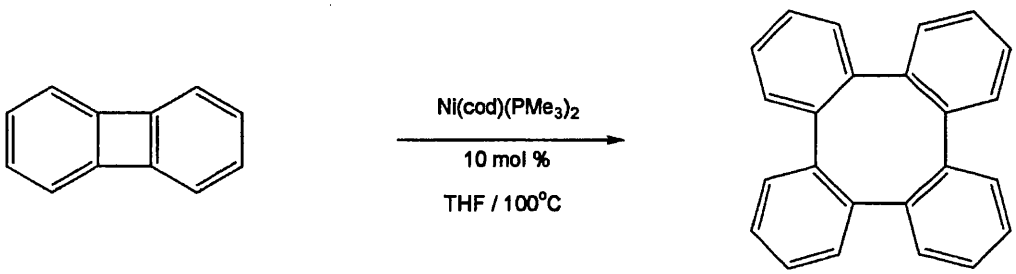

Scheme 5.27.

This research was recently extended by Jones et al to $Pt(PEt_3)_3$ and $Pd(PEt_3)_3$ and mechanistic studies described by them suggest a double oxidative addition of the biphenylene, leading to a bis-biphenylene M(IV) complex which finally generates the product **[Scheme 5.28.]**.[64]

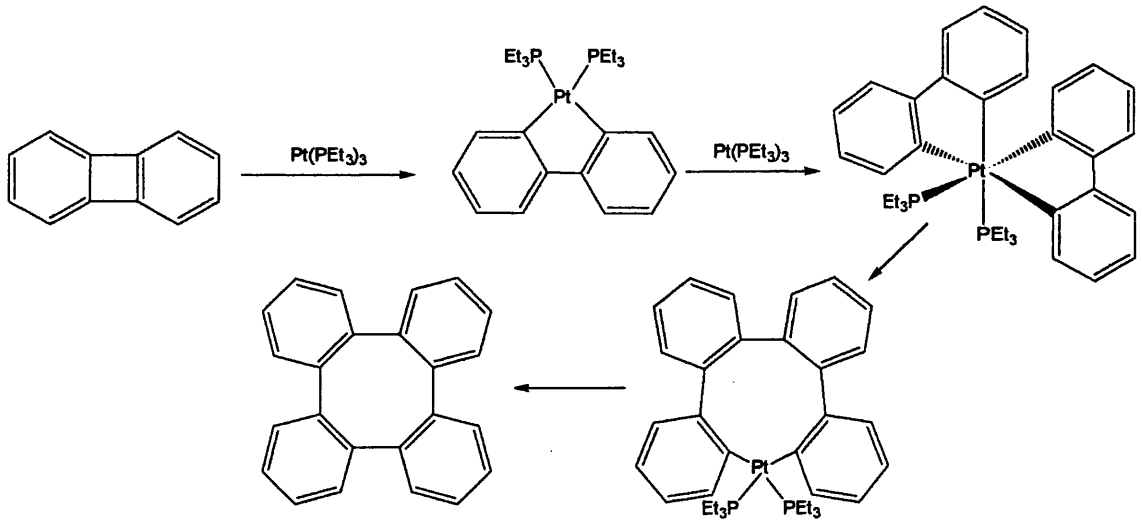

Scheme 5.28.

In another example, substituted phenols are synthesized by the Ni(0)-catalyzed ring opening of cyclobutanone under very mild conditions and subsequent [4+2] cycloaddition with alkynes **[Scheme 5.29.]**.[65]

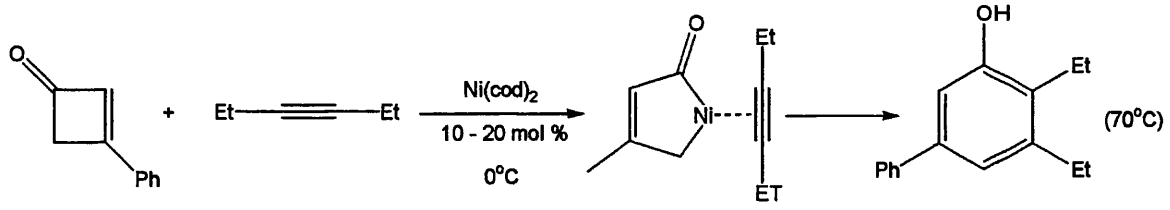

Scheme 5.29.

In a rather interesting example reported by Harayama et al. a six-membered allylic carbonate undergoes a palladium-catalyzed C-C bond cleavage to afford a dienic carbonyl compound **[Scheme 5.30.]**.[66]

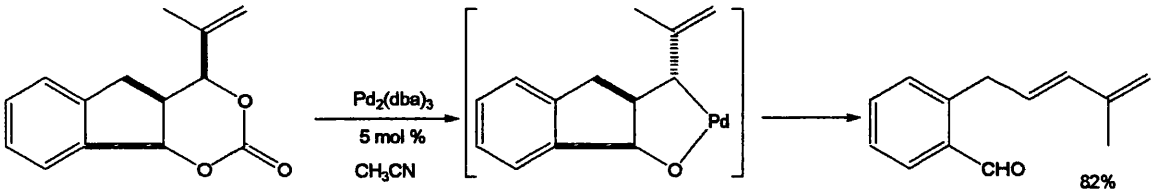

Scheme 5.30.

In this example, decarboxylation of the carbonate moiety provides the driving force for production of the intermediate five-membered hetero-palladacycle from which formal reductive cleavage takes place.

A very nice catalytic process allows conversion of a spirobutanone equipped with a second four membered ring to afford 2-cyclohexanone. The process is catalyzed by $[Rh(dppp)_2]Cl$ which successively cleaves two C-C bonds one by oxidative addition and the other by β-carbon elimination **[Scheme 5.31.]**.[67]

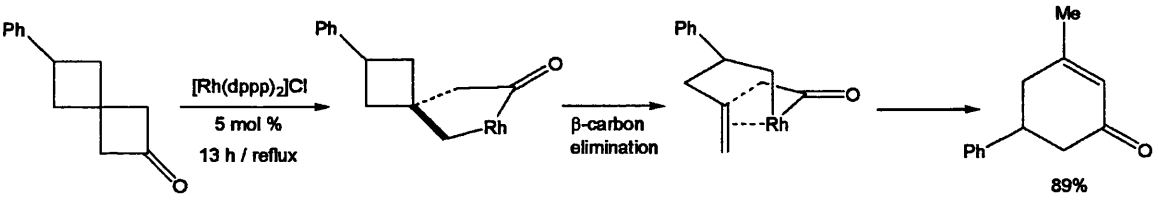

Scheme 5.31.

The cleavage of the diphosphine pincer ligand previously described was recently extended to catalytic applications. The methylene group was excised from the pincer ligand under hydrogen to afford the free bidentate C-C activated phosphine ligand, along with CH_4. This can be accomplished catalytically generating up to 106 turnovers in 3 days **[Scheme 5.32.]**.[68]

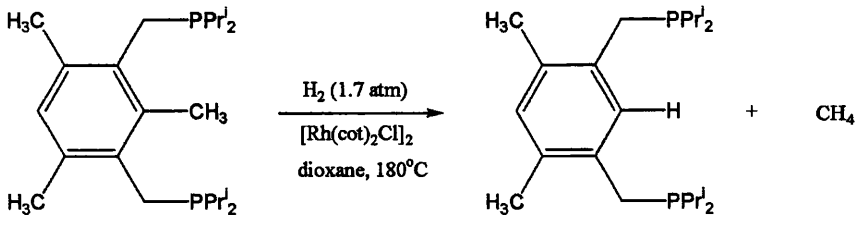

Scheme 5.32.

To summarise, C-C activation reactions are generally restricted to either strained systems or those used by Milstein and et al., which although unstrained, place the C-C bond in such a close proximity to the metal, that it has no other option than to break. In the result section now to be described, we demonstrate the first example of C-C bond activation of N-heterocyclic carbene ligands, a truly unstrained C-C cleavage.

5.2. Results and discussion.

5.2.1. Synthesis and reactivity of $Ru(IMes)(L)(CO)H_2$.

5.2.1.1. $Ru(PPh_3)_2(IMes)(CO)H_2$ (26)

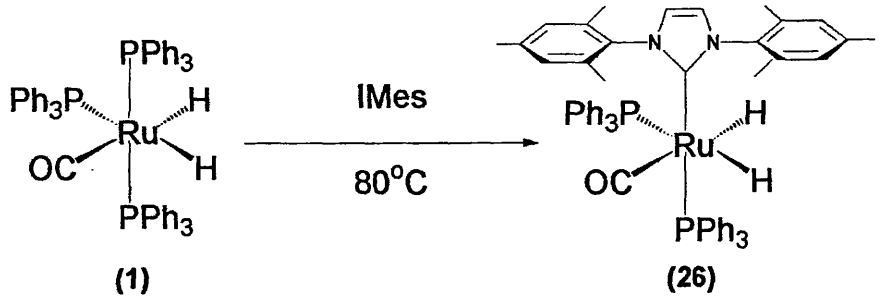

(1) (26)

Scheme 5.33.

Thermolysis of a benzene solution of $Ru(PPh_3)_3(CO)H_2$ with 3 equivalents of IMes **(25)** in toluene at 80°C for 14 days afforded $Ru(PPh_3)_2(IMes)(CO)H_2$ **(26) [Scheme 5.33.]**. The formation of **(26)** was monitored using $^{31}P\{^1H\}$ NMR spectroscopy **[Spectrum 5.1.]**. This showed depletion of the signals at 58.2 and 46.1 ppm from **(1)** and growth of two new doublets at 59.0 and 47.8 ppm for **(26)**. Complex **(26)** was isolated in a 65% yield by crystallization from benzene/ethanol and characterized by multinuclear NMR spectroscopy.

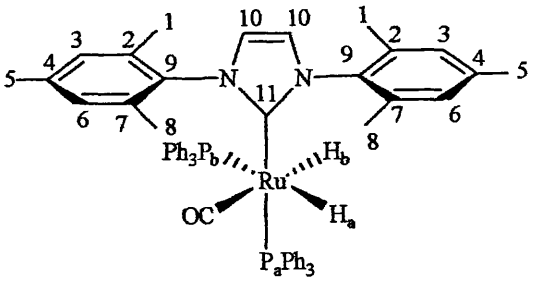

Figure 5.3. - *NMR assignment of the proton and carbon atom of (26)*

The hydride region showed two signals consistent with the presence of two hydrides *Ha* and *Hb*, sitting in different environments. Ru-*Hb* appears as a doublet of doublet of doublets at -6.36 ppm (J_{HPb} = 26.8, J_{HPa} = 23.6, J_{HHb} = 6.0 Hz) placing it *cis* to the two phosphorus ligands and *cis* to Ha. Ru-*Ha* appears as a doublet of doublet of doublets at -8.08 ppm (J_{HPb} = 81.2, J_{HPa} = 33.6, J_{HHb} = 6.0 Hz, 1H, H_a) demonstrating that it sits *trans* to P_b (indicated by the large coupling constant) and *cis* to P_a and H_b. There is no major influence on the chemical shift of the hydride resonances upon substitution of phosphine by IMes (c.f. hydride resonances for **(1)** at -6.53, -8.29 ppm).

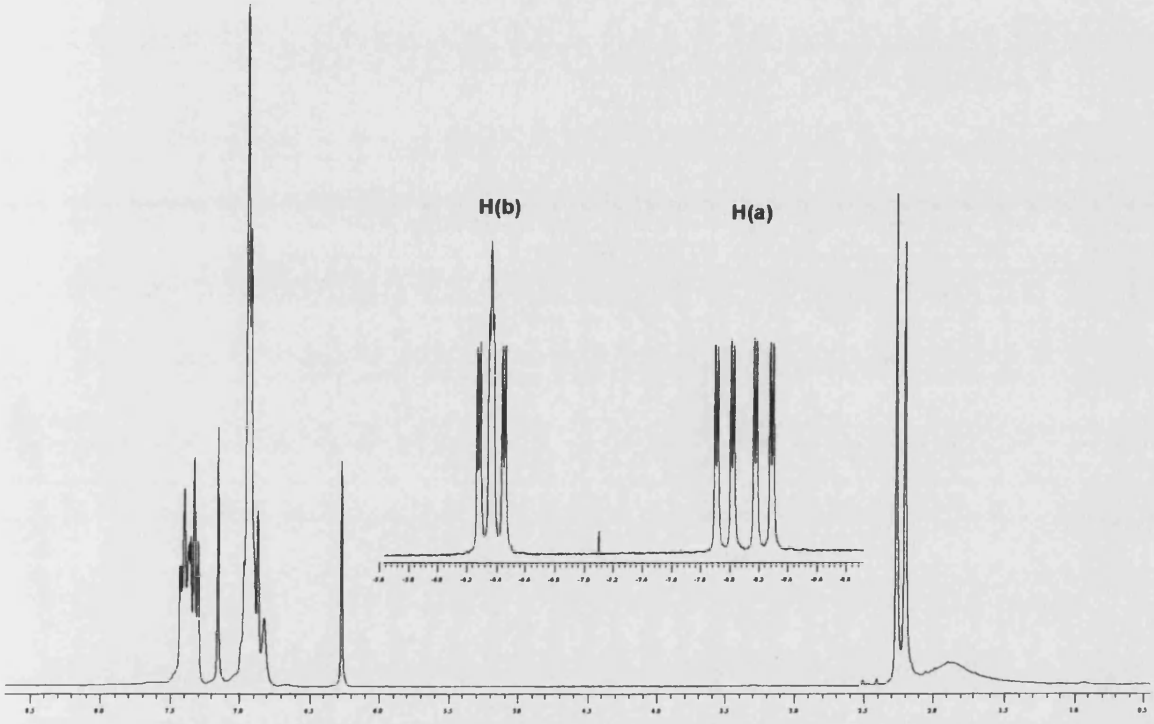

Spectrum 5.1. - *^{1}H NMR spectrum showing the formation of* ***(26)***.

The nature of P_a and P_b was determined unequivocally on the basis of selective decoupling of the phosporus signals from the hydride resonances. The proton NMR spectrum also exhibits characteristic signals validating the presence of a coordinated carbene on the complex. This is shown by three different methyl signals (H-*1*, H-*5*, H-*8*) at 2.26, 2.20, and 1.82 ppm, one signal for NCH=CHN (H-*10*) at 6.25 ppm and two different signals at 6.86 and 6.82 ppm for the IMes phenyl protons (H-*3*, H-*6*). In the $^{13}C\{^1H\}$ NMR spectrum, the Ru-CO carbon gives rise to a triplet at 205.2 ppm (J_{CP} = 8.8 Hz), *cis* to the two phosphorus ligands. The ruthenium carbene carbon (C-*11*) gives rise to a doublet of doublets at 197.7 ppm (J_{CPa} = 75.5, J_{CPb} = 6.7 Hz). The coupling constants indicate that (C-*11*) is *trans* to P_a (large coupling constant) and *cis* to P_b. The IR spectrum showed a single

band in the carbonyl region at 1937 cm^{-1}. The low value of ν_{CO} compared to that observed for **(1)** (1960 cm^{-1}) is consistent with a ruthenium species bearing a strongly σ-donating IMes ligand. Other examples in the literature have revealed a comparable influence in the shift of ν_{CO}.[69]

The difference in chemical shift between (H-*1*) and (H-*8*), as well as for (H-*3*) and (H-*6*), suggests that these are in a different environment in solution, probably due to a lack of free rotation a the N-boutC axial bond of the IMes ring as well as around the Ru-C bond.

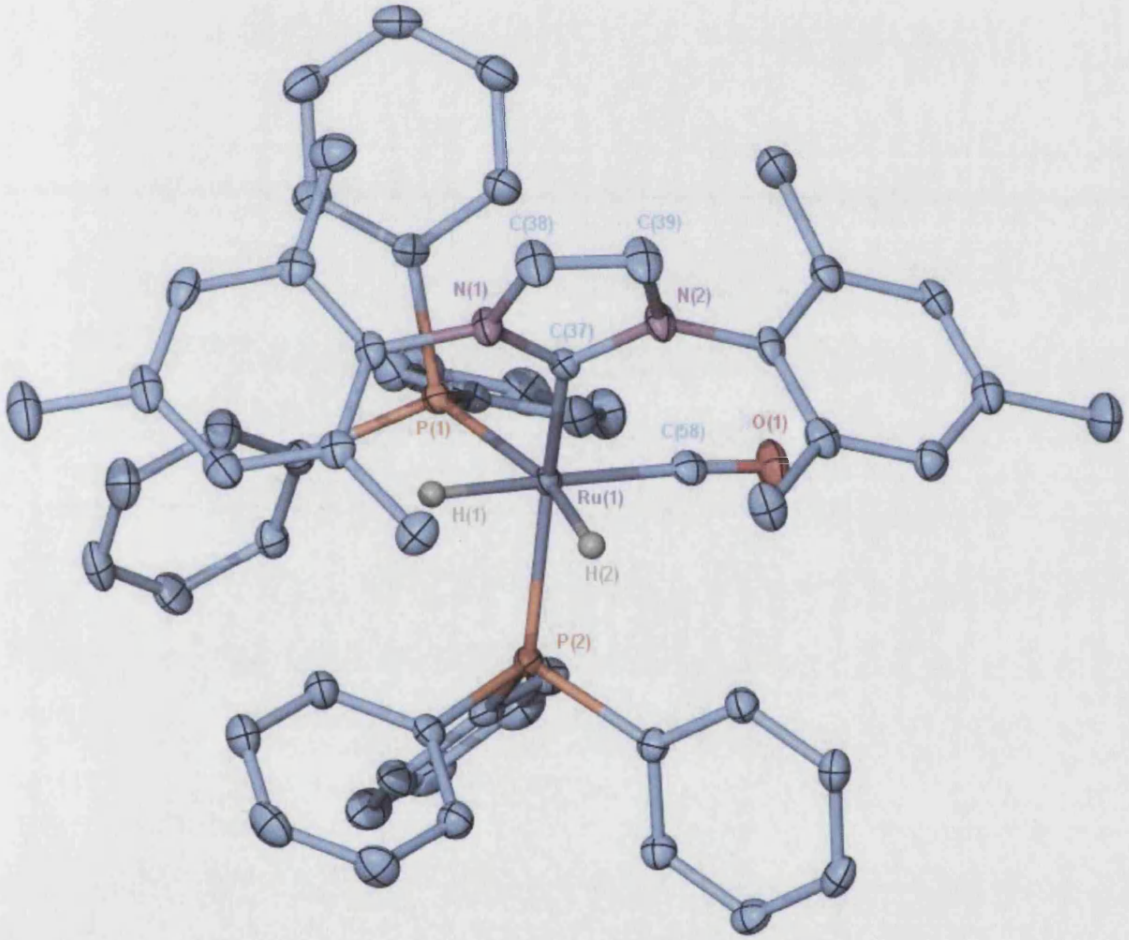

X-Ray 5.1: *X-ray structure of $Ru(PPh_3)_2(IMes)(CO)H_2$. The ellipsoids are represented at 50% of the occupancy, and the hydrogens (apart from hydrides) have been removed for clarity.*

The full molecular geometry of **(26)** was elucidated by X-ray crystallography **(X-Ray 5.1.)**; selected geometric data are given in **Table 5.1.**. The geometry around the ruthenium is distorted octahedral. The two triphenylphosphine ligands are *cis* to each other, the IMes ligand *trans* to one phosphine and *cis* to the other plus the carbonyl ligand is *cis* to both phosphines. The C(37)-Ru(1)-P(2) bond angle is smaller than expected for an octahedral complex with an angle of 146.33(5)° rather than 180°. This fact is reinforced by the larger than expected C(37)-Ru(1)-P(1) angle of 104.94(5)°. This effect is probably due to a combination of the electronic properties of the carbene moiety as well as the bulkiness of the carbene and the phosphine ligands as shown by a *side view* of the molecule **[Figure 5.4.]**. The interaction between the phosphine ligand *cis* to IMes forces the carbene and the remaining phosphine toward the hydride region, a less sterically crowded coordination site.

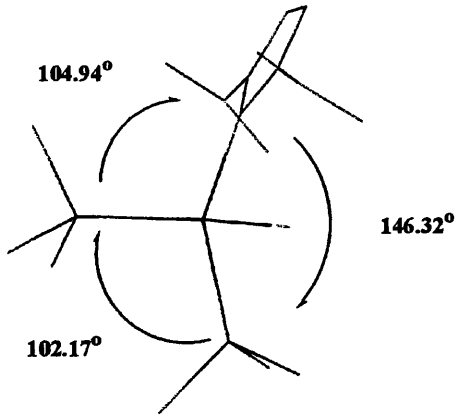

Figure 5.4. - *Side view of (26), the phenyl on the phosphines, and part of the Mes ligands are omitted for clarity.*

The Ru-P1 distance is significantly longer than the Ru-P2 bond length (2.3628 vs. 2.2985 (5) Å). The elongation of the Ru-P1 bond is due to the *trans* influence of a hydride group. This effect is observed in the structure of other hydride complexes such as **(1)** (2.4010(6) vs 2.3241(6)).[70] A structural comparison of **(26)** and **(1)** shows no influence from the carbene ligand upon the overall bond distances within the complexes as shown by the selected geometric data for **(1)** given in **Table 5.1.** (X-ray structure for **(1)** available in **[Figure 5.5.]**). Also very little effect is observed on the angular values in the complex.

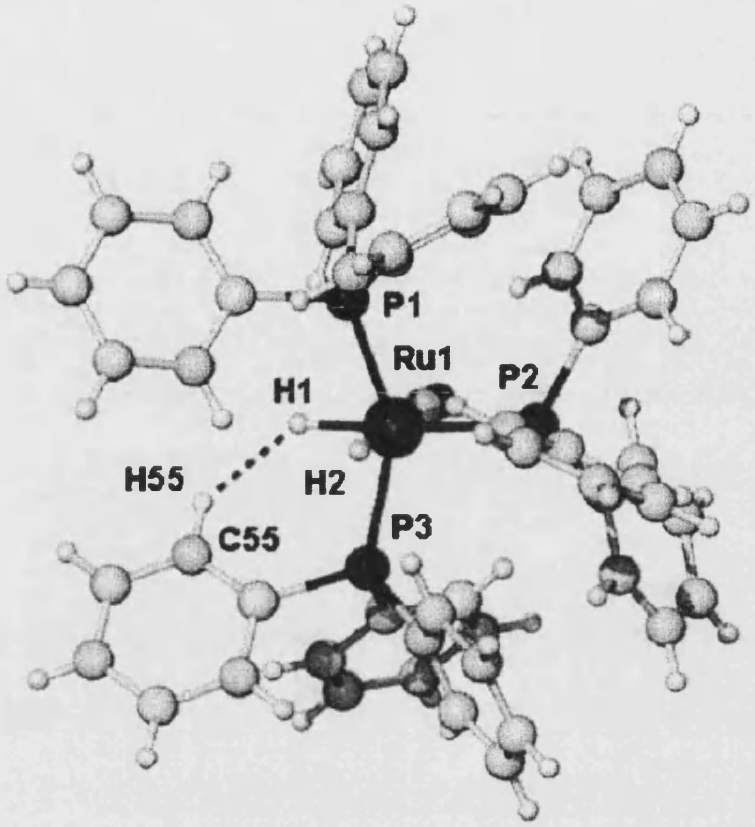

Figure 5.5. – *X-ray structure of (1).*[70]

(26)		(1)	
Selected Bond Lengths	**[Å]**		
Ru(1)-C(58)	1.9145(17)	Ru(1)-C(1)	1.893(3)
Ru(1)-P(2)	2.2985(5)	Ru(1)-P(1)	2.3241(6)
Ru(1)-P(1)	2.3628(4)	Ru(1)-P(2)	2.4010(6)
Ru(1)-C(37)	2.0956(17)	Ru(1)-P(3)	2.3111(7)
O(1)-C(58)	1.158(2)	C(1)-O(1)	1.155(3)
N(2)-C(37)	1.383(2)	N(1)-C(38)	1.388(2)
N(1)-C(37)	1.386(2)	N(2)-C(39)	1.384(2)
C(38)-C(39)	1.339(3)	Ru(1)-H(2)	1.65(3)
Ru(1)–H(1)	1.55(2) Å	Ru(1)-H(1)	1.59(3)
Ru(1)–H(2)	1.57(2) Å		

Selected Bond Angles	[°]		
C(58)-Ru(1)-C(37)	99.44(7)	C(1)-Ru(1)-P(1)	104.20(8)
C(37)-Ru(1)-P(2)	146.33(5)	C(1)-Ru(1)-P(2)	91.21(8)
C(37)-Ru(1)-P(1)	104.94(5)	C(1)-Ru(1)-P(3)	96.20(8)
C(58)-Ru(1)-P(2)	94.76(5)	P(1)-Ru(1)-P(2)	101.35(2)
C(58)-Ru(1)-P(1)	100.65(5)	P(1)-Ru(1)-P(3)	147.86(2)
P(2)-Ru(1)-P(1)	102.166(16)	P(2)-Ru(1)-P(3)	102.78(2)
H(1)–Ru(1)–H(2)	85.9(8)	H(1)-Ru(1)-H(2)	87(2)
C(37)-N(2)-C(39)	112.66(14)		
C(37)-N(1)-C(38)	111.97(14)		
N(2)-C(37)-N(1)	101.55(14)		

Table 5.1. - *Selected bond distances [Å] and bond angles [°] for (26) and, for comparison, complex (1).*

5.2.1.2. Synthesis and characterization of $Ru(PPh_3)_2(IMes')(CO)H$ (30)

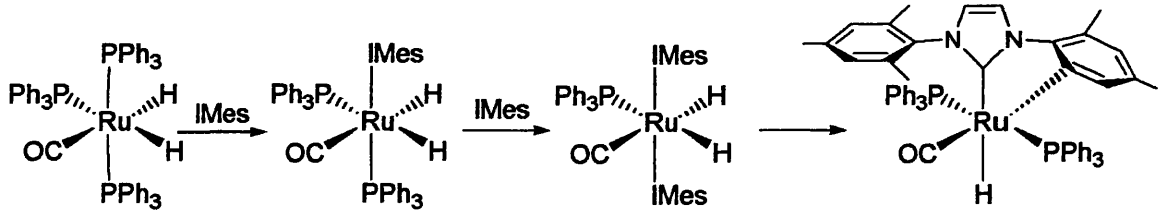

(30)

Scheme 5.34.

Continued heating of **(26)** for a further 2 days at 110 ° C afforded the C-C insertion product **(30)** resulting from cleavage of an Ar-CH_3 bond **[Scheme 5.34.]**. Complex **(30)** was isolated in a 96% yield by crystallization from benzene/ethanol and characterized by multinuclear NMR spectroscopy.

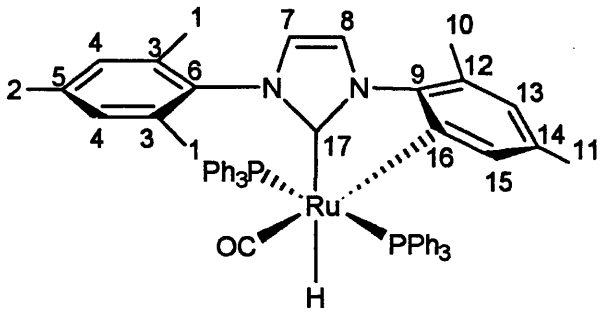

Figure 5.6. - *NMR assignment of the proton and carbon atoms of (30)*

The $^{31}P\{^1H\}$ NMR spectrum displayed a singlet resonance at δ 55.1 ppm. The Ru-H resonance appears as a triplet at -6.99 ppm (J_{HP} = 28.4 Hz) in the ^1H NMR spectrum **[Spectrum 5.2.]**, demonstrating that the complex contains two mutually *trans* phosphine ligands. The proton NMR spectrum also exhibits four different methyl signals for IMes ligand (H-*10*, H-*2*, H-*11*, H-*1*) in a 1:1:1:2 ratio, implying activation of one of the mesityl rings. This observation is confirmed by the presence of two inequivalent signals for the NCH=CHN moiety, H-*8* and H-*7*. Full assignment of the unactivated and activated ring protons in the two Mes groups was made by ^1H NOESY which shows an interaction between (H-*15*, H-*13*) and H-*11* **[Spectrum 5.2.]**, as well as between H-10 and (H-*8*, H-*13*). In the $^{13}C\{^1H\}$ NMR spectrum, the carbonyl moiety gives rise to a triplet at 207.4 ppm (J_{CP} = 10.0 Hz). The carbene carbon (C-*17*) is also a triplet (J_{CP} = 6.6 Hz), verifying that the complex contains two mutually *trans* phosphine ligands. Interestingly a triplet signal arises at 163.5 ppm (J_{CP} = 16.9 Hz); it is assigned unequivocally to the *ipso* carbon of the aryl group on the IMes ligand on the basis of ^{13}C PENDANT as well as ^{13}C-^1H HMQC and HMBC experiments.

The IR spectrum shows a single carbonyl band at 1914 cm^{-1} consistent with the proposed structure and showing the effect of the strongly σ-donating IMes ligand. The effect is enhanced by an increase of electron density on the metal from the C_5 orthometalated ring. This induces more backbonding from the metal to the Ru-CO and results in a decrease in the frequency of ν_{CO} for **(30)** in comparison to **(26)**.

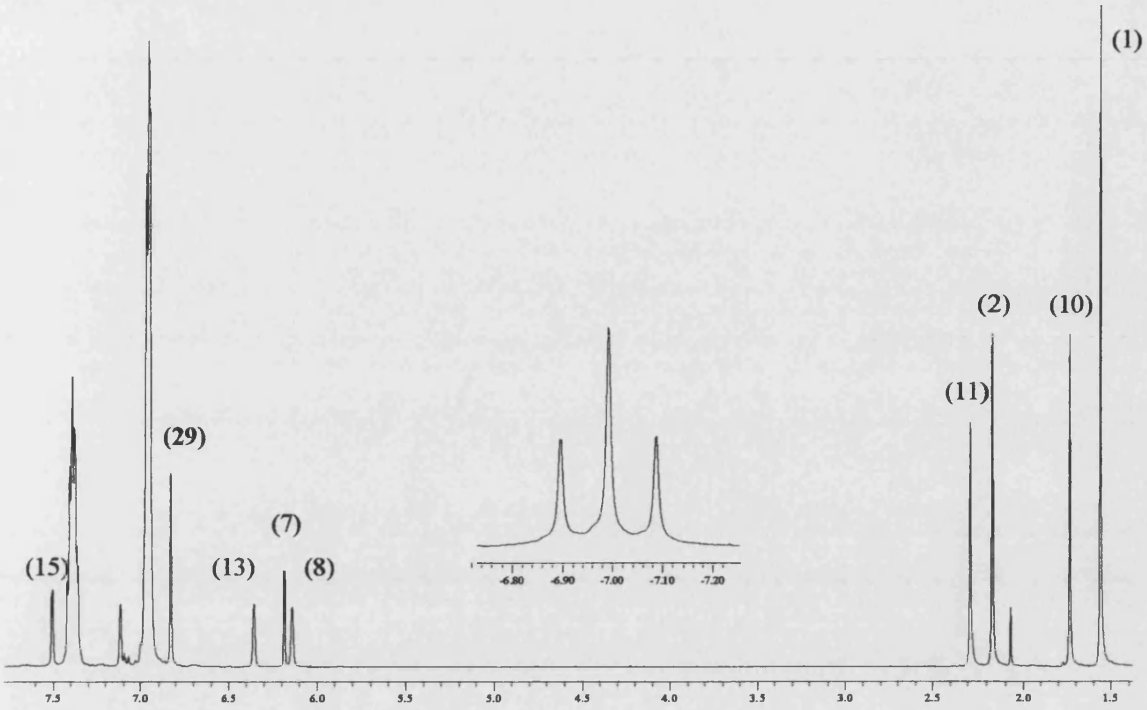

Spectrum 5.2. - *^{1}H spectrum of* ***(30)***

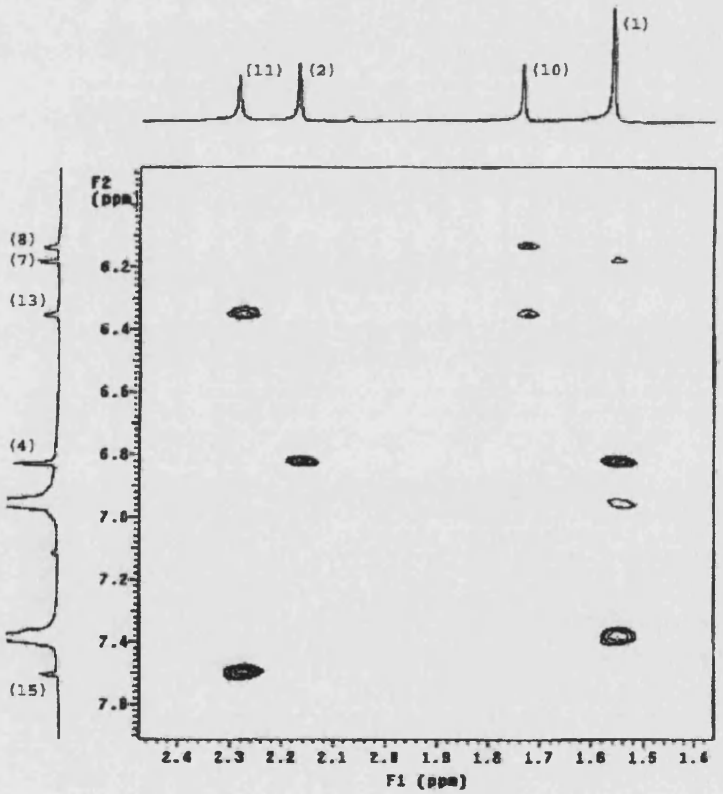

Spectrum 5.3. - *^{1}H-^{1}H NOESY spectrum of* ***(30)*** *indicating the loss of a methyl group on the IMes ligand. Only two -CH_3 groups interact through space to H(15) and H(13), instead of three -CH_3 which is the case for the free rotating mesityl ring.*

The full molecular geometry of **(30)** was elucidated by X-ray crystallography **[X-Ray 5.2.]**. Selected bond distances and bond angles are available in **Table 5.2.**.

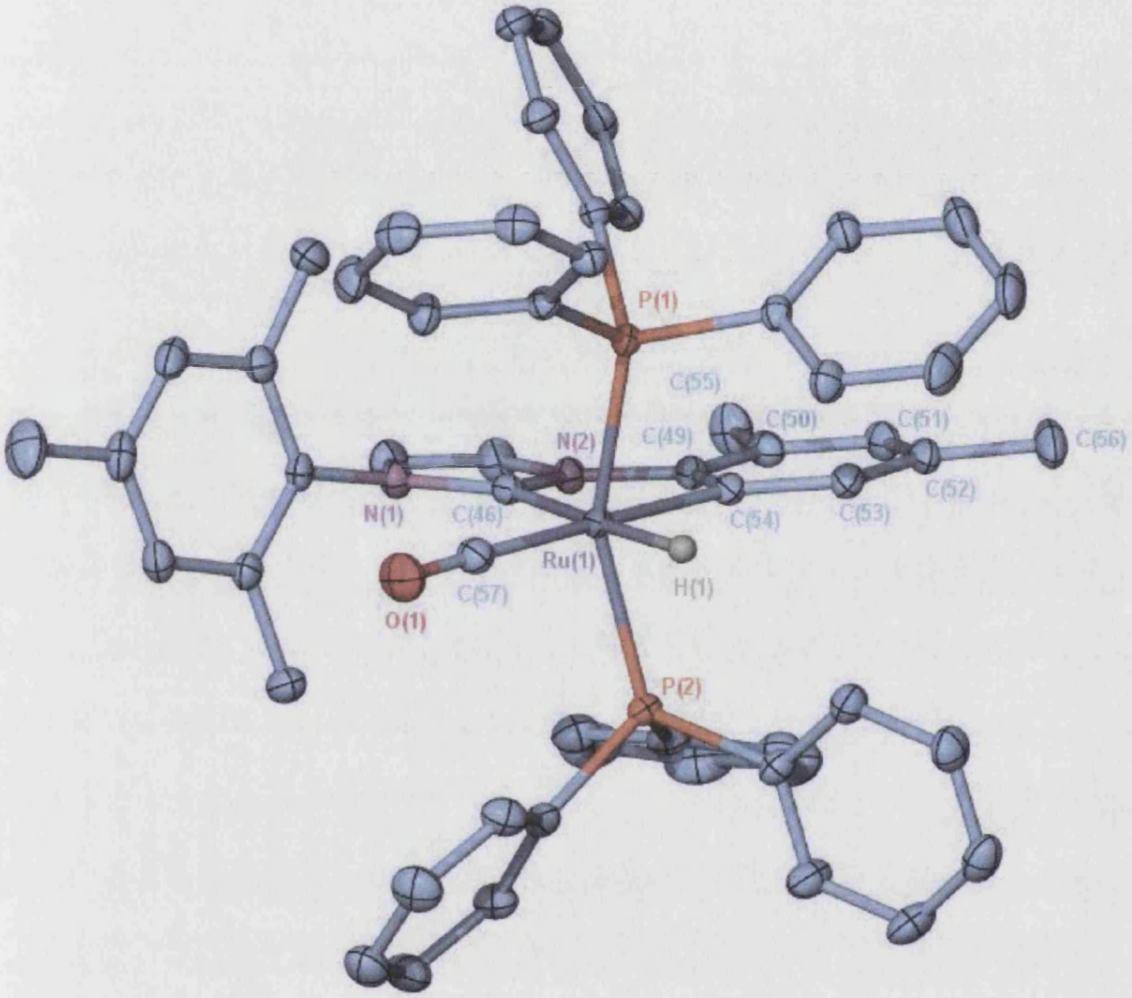

X-Ray 5.2. - *X-ray structure of Ru(IMes')(PPh$_3$)$_2$(CO)H. The ellipsoids are represented at 50% of the occupancy, and the hydrogens have been removed for clarity.*

Selected Bond Lengths	**[Å]**		
Ru(1)-C(57)	1.8908(13)	C(47)-C(48)	1.344(2)
Ru(1)-C(54)	2.1429(12)	C(49)-C(50)	1.4029(18)
Ru(1)-P(2)	2.3357(3)	C(50)-C(51)	1.399(2)
Ru(1)-C(46)	2.0746(12)	C(51)-C(52)	1.387(2)
Ru(1)-P(1)	2.3232(3)	C(52)-C(56)	1.5128(19)
O(1)-C(57)	1.1547(17)	C(49)-C(54)	1.4161(18)
N(2)-C(48)	1.3951(17)	C(50)-C(55)	1.511(2)
N(2)-C(46)	1.3741(16)	C(52)-C(53)	1.3945(18)
N(2)-C(49)	1.4376(16)	N(1)-C(37)	1.4394(16)
N(1)-C(46)	1.3673(16)	N(1)-C(47)	1.3928(17)
Selected Bond Angles	**[°]**		
C(57)-Ru(1)-C(46)	100.59(5)	P(1)-Ru(1)-P(2)	156.010(12)
C(46)-Ru(1)-C(54)	76.30(5)	C(46)-N(1)-C(47)	111.06(11)
C(46)-Ru(1)-P(1)	101.42(3)	C(46)-N(1)-C(37)	124.31(11)
C(57)-Ru(1)-P(2)	96.51(4)	C(46)-N(2)-C(49)	116.64(10)
C(54)-Ru(1)-P(2)	82.23(3)	C(46)-N(2)-C(48)	110.74(11)
C(57)-Ru(1)-C(54)	176.42(5)	N(1)-C(46)-N(2)	104.08(10)
C(57)-Ru(1)-P(1)	94.56(4)	C(47)-C(48)-N(2)	107.03(12)
C(54)-Ru(1)-P(1)	87.85(3)	C(48)-C(47)-N(1)	107.07(12)
C(46)-Ru(1)-P(2)	97.38(3)	N(2)-C(46)-Ru(1)	117.78(9)
C(49)-C(54)-Ru(1)	115.92(9)	C(54)-C(49)-N(2)	112.88(11)

Table 5.2. - *Selected bond distances [Å] and bond angles [°] for* ***(30)***.

The structure clearly shows that the ruthenium atom has inserted into one of the *ortho* Ar-CH_3 bonds of the IMes ligand to give a new Ru-C bond (2.1429(12) Å) which is an integral part of a five-membered metallacycle. The mesityl ring planes are approximately perpendicular to each other (torsion angle C(42)-C(37)-N(1)-C(47) = 101.1°) presumably to minimize interaction with the phosphines **[Figure 5.7.]**.

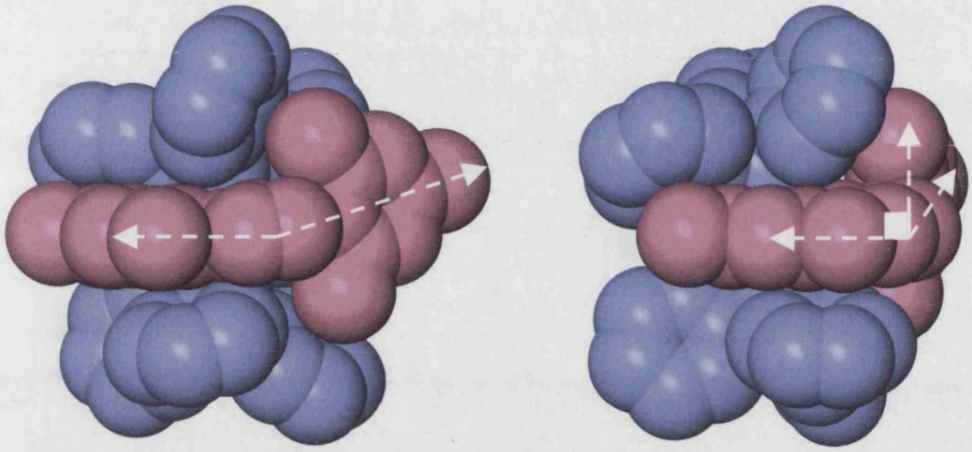

Figure 5.7. - *X-ray structure of* ***(30)*** *(with van der Waals radius) showing the interaction between the phosphine and the mesityl rings that forces the mesityl ring into a perpendicular position towards another. (NB: Phenyl ring are in blue, and mesityl ring are in pink).*

At the same time the mesityl rings appear to be bent, not through a rotation of the C-N bonds but rather from a slight reduction of the C(37)-N(1)-(I*) and C(49)-N(2)-(I*) angles (≅172° rather than 180°) **[Figure 5.8.]**. In fact, one would expect C(49), N(2), N(1), C(37) to be part of the same physical plane. One reason this is not the case could be due to the strong interaction of the bulky mesityl ring with the phenyl rings on the phosphine as suggested by the view **[Figure 5.7.]**. (NB: I* centre of the $N_1C_{47}C_{48}N_2C_{46}$).

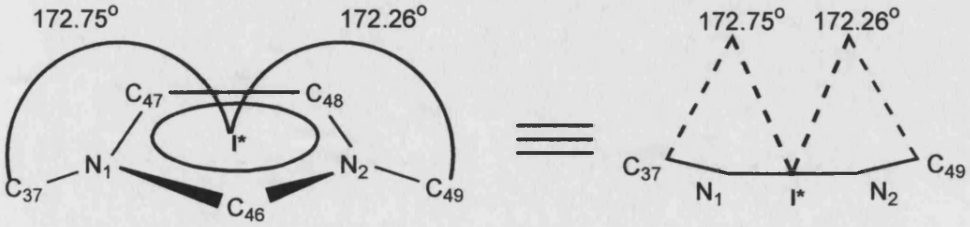

Figure 5.8. - *Bending of the phenyl rings out of the plane of the imidazolylidene ring (I* set as centre of the imidazolylidene ring for use of measurements)*

Futher studies of the C-C activated carbene ligand reveal other significant effects of the cyclometalation: the N(1)-C(46)-N(2) angle is more open than in the structure of **(26)** (104.08(10)° vs 101.55(14)°) and other related carbene complexes.[71] The C(46)-N(2)-C(49) angle is considerably smaller than its counterpart C(46)-N(1)-C(37) (116.64(10)° vs 124.31(11)°), and more generally the angles throughout the metallated ring testify to a relatively strained system **[Figure 5.9.]**. The bond distances within the C-C activated IMes system are affected very little by the activation process and remain comparable to the distances observed in **(26)** and other reported systems.[71] Nevertheless it is worth quoting some small differences in the imidazolylidene skeleton of **(30)** in comparison to **(26)**. In the non-metallated system, the N-C bond distances within the five membered are ring the same length (≅1.38 Å for **(26)**), whereas in this case the N-C bonds (N(1)-C(46) and N(2)-C(46)) are now smaller than the (N(1)-C(47) and N(2)-C(48) bonds (≅1.36 vs 1.39 Å), showing an increase in the double character of N(1)-C(46) and N(2)-C(46) **[Figure 5.9.]**. The ruthenium carbene bond distance remains comparable to the one observed in **(26)** and other related structures.[71] The ruthenium metallated carbon (Ru-C(54)) distance is slightly longer than other related metallated complexes (**e.g.** 2.120(5) Å for **(17)**).[72]

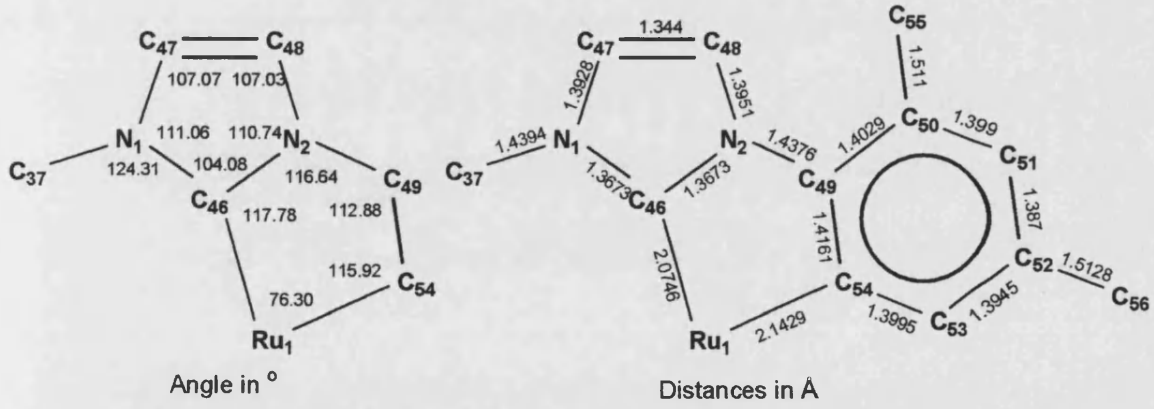

Figure 5.9. - *Significant bond distances and angles for the C-C activated IMes ring.*

In 1979 Lappert et al[73] reported the intramolecular C-H activation of bis(1,3-(4-methylphenyl)imidazol-2-ylidene) complexes of ruthenium leading to the formation of the structurally characterised species **(a)** and **(b) [Figure 5.10.]**. The bond distances and angles within the metallated ligands are comparable to the ones we observe for **(2) [Figure 5.9.]**. Bending of the carbene moiety is not observed in the Lappert examples. This is probably due to the presence of less bulky phosphine (PEt_3 compared to PPh_3).

The core structure of **(30)** is distorted octahedral with an attenuated P(1)-Ru-P(2) angle of only 156.010(12)°. This strain is likely to be electronic in origin as a similar distortion in related osmium hydrido-carbene complexes has been rationalized by enhanced π-back-donation to the *cis* carbene ligand,[74] but nevertheless this account has to be considered carefully as it is not observed in Lappert's structures. This could be because a smaller less bulky phosphine and carbene moiety are used, therefore minimizing the possible interaction between the phosphines and the carbene.

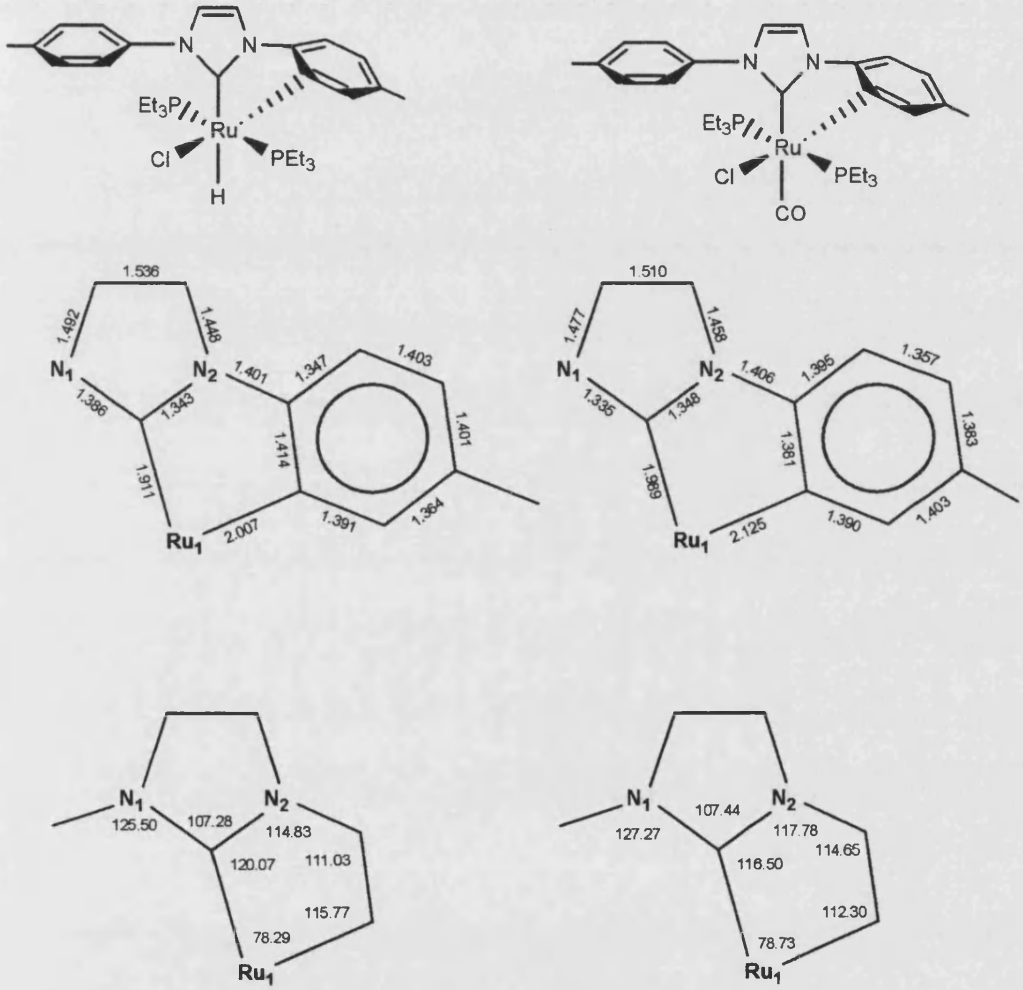

Figure 5.10. - *X-ray structures reported by Lappert et al., presenting structural similarities to* ***(30)****.*

5.2.1.3. Synthesis and characterization of Ru(IMes'')$(PPh_3)_2$(CO)H (31)

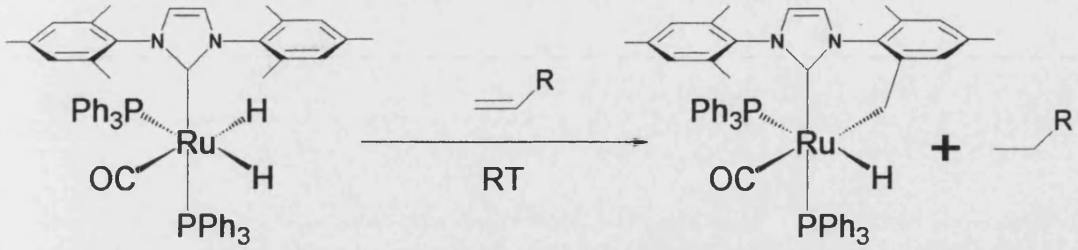

Scheme 5.35.

At no stage in the formation of the C-C activated complex could we detect any signals due to C-H activation as a result of $ArCH_2$-H cleavage. However, this process does occur quantitatively upon addition of 1 equivalent of CH_2=$CHSiMe_3$ to a C_6D_6 solution of **(26)** at room temperature to yield **(31)** in a 92% yield **[Scheme 5.35.]**.

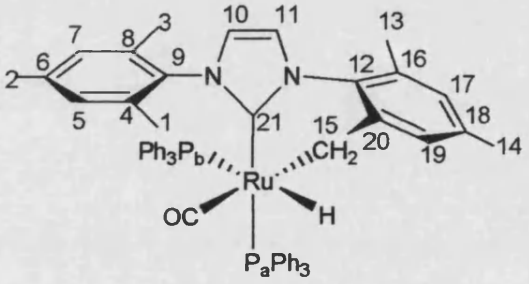

Figure 5.11. - *NMR assignment of the proton and carbon atom of (31)*

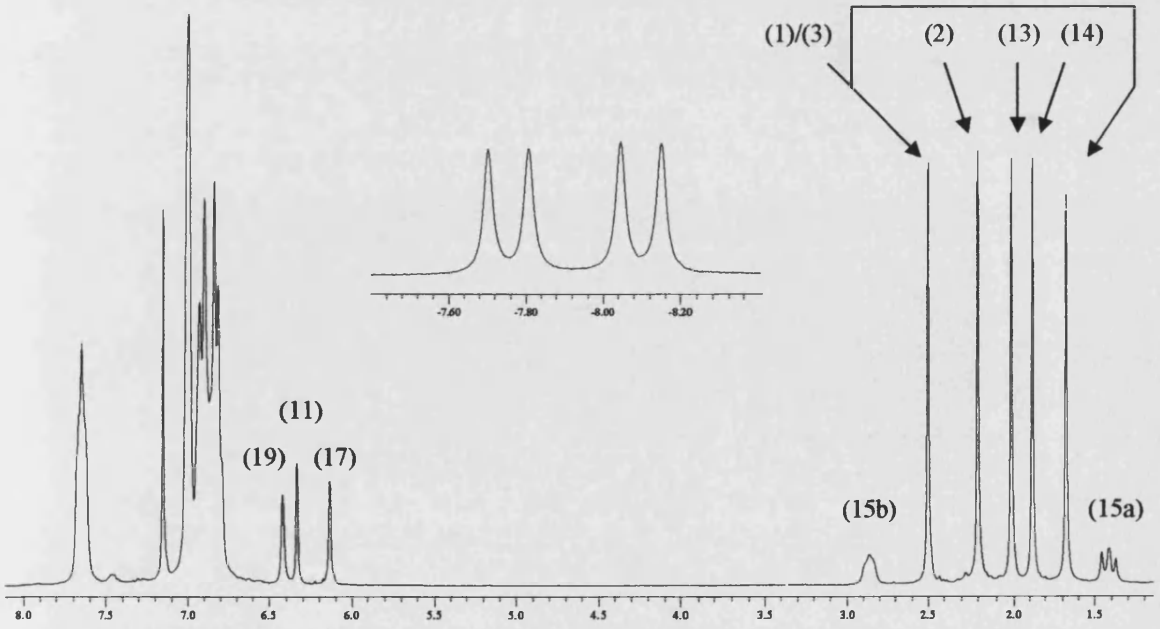

Spectrum 5.4. - *^{1}H NMR spectrum of (31)*

The $^{31}P\{^{1}H\}$ NMR spectrum of **(31)** shows two set of doublets at 53.7 (J_{PP} = 18.1 Hz, P_a) and 28.4 (J_{PP} = 18.1 Hz, P_b) ppm, while the ^{1}H NMR spectrum displays five different methyl signals (H-*1*, H-*2*, H-*3*, H-*13*, H-*14*) **[Spectrum 5.4.]**. This indicates a strong asymmetry in the IMes ligand, an observation reinforced by the presence of two signals at δ 2.76 and 1.35 ppm arising from the inequivalent protons of the Ru-CH_2Ar bond (H-15). ^{1}H-^{1}H COSY indicates that these two protons couple to each other **[Spectrum 5.6.]**, while the $^{31}P\{^{1}H\}$-^{1}H HETCOR spectrum also indicates that each phosphorus nucleus couples to only one Ru-CH_2Ar proton.

These experiments led us to observe that the P_a-H(15a) coupling is comparable to the H(15a)-H(15b) coupling since a broad triplet resonance is observed for H(15a). A broad resonance is observed for H(15b). These resolved upon cooling to 0°C into a broad doublet of doublet for H(15a) (J_{HaHb} =11.0 Hz, J_{PHa} = 11.6 Hz) and a broad unsymmetrical triplet for H(15b) (J = 9.6 Hz, J = 9.2 Hz) **[Spectrum 5.5.]**.

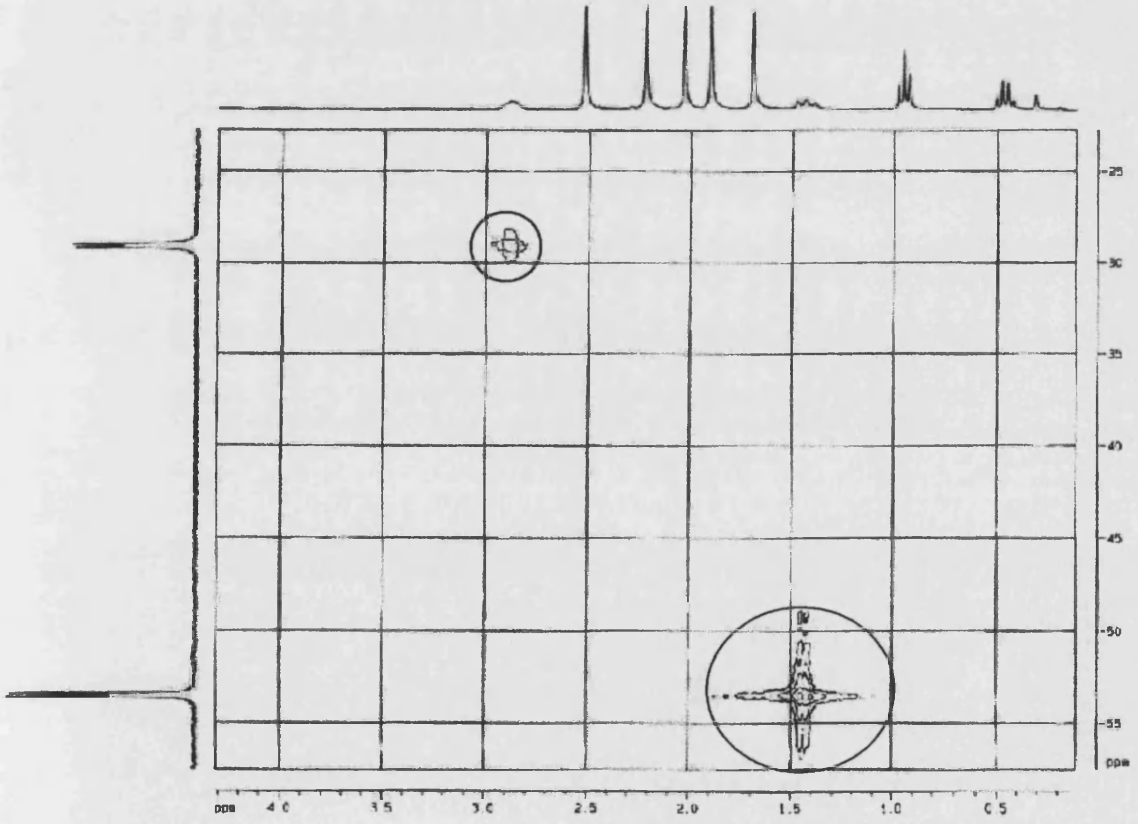

Spectrum 5.5. - *$^{31}P\{^{1}H\}$-^{1}H HETCOR spectrum of* ***(31)*** *indicating the correlation between P_a and H(15a) and P_b and H(15b).*

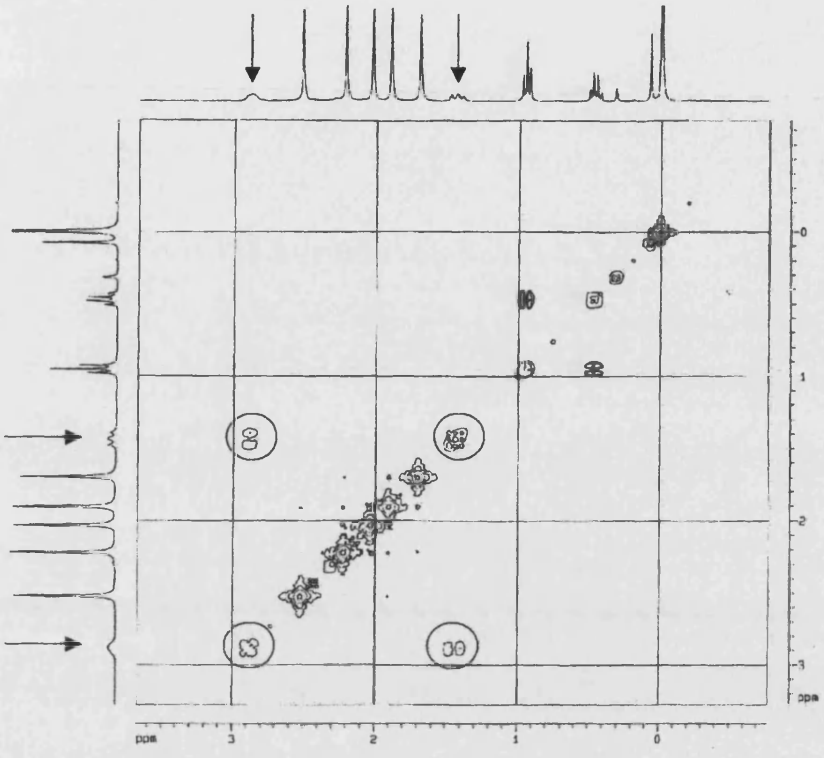

Spectrum 5.6. - *^{1}H-^{1}H COSY spectrum of (31) indicating the activation of a methyl group on the IMes ligand and showing the presence of coupling between H(15a) and H(15b).*

The hydride resonance appears as a doublet of doublets, with the magnitude of the coupling constants (J_{HP} = 102.4, 30.8 Hz) placing it *trans* and *cis* with respect to the two PPh_3 ligands **[Figure 5.11.]**. In the $^{13}C\{^{1}H\}$ NMR spectrum, the carbene carbon appears as broad doublet at 191.5 (J_{CPa} = 84.3 Hz). A broad singlet resonance at 149.3 ppm is assigned to the Ru-CH_2 carbon on the basis of ^{13}C PENDANT as well as ^{13}C-^{1}H HMQC and HMBC experiments. The IR vibrations of **(31)** (1955 (ν_{RuH}), 1919 (ν_{CO}) cm^{-1}) are shifted to lower frequency by comparison to **(26)**, but remain higher than observed for **(30)**, implying less back bonding from the metal to the carbonyl.

The full molecular geometry of **(31)** was elucidated by X-ray crystallography **[X-Ray 5.3.]**. Selected bond distances and bond angles are available in **Table 5.3.**

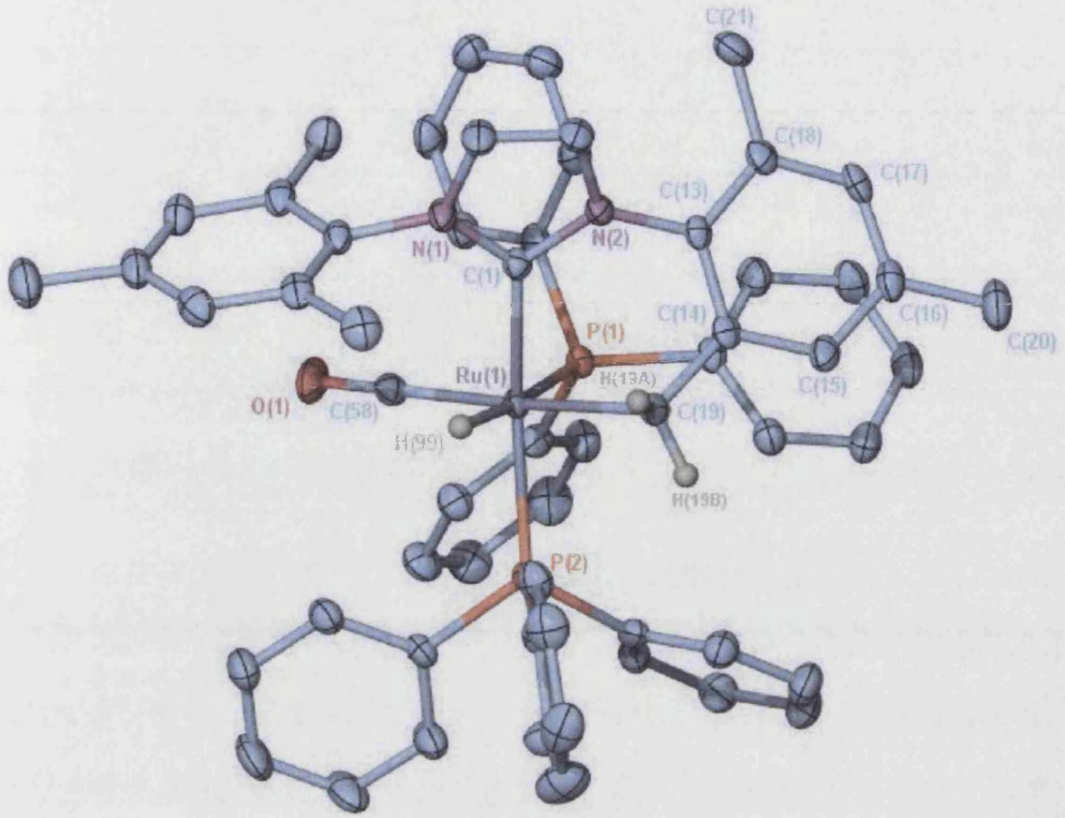

X-Ray 5.3. - *X-ray structure of Ru(IMes'')$(PPh_3)_2$(CO)H. The ellipsoids are represented at 50% of the occupancy, and the hydrogens have been removed for clarity.*

Selected Bond Lengths	**[Å]**		
Ru(1)-C(1)	2.0786(19)	N(2)-C(3)	1.391(3)
Ru(1)-C(58)	1.868(2)	C(14)-C(19)	1.485(3)
Ru(1)-C(19)	2.2346(19)	C(13)-C(14)	1.399(3)
Ru(1)-P(1)	2.4230(5)	C(14)-C(15)	1.399(3)
Ru(1)-P(2)	2.3521(5)	C(15)-C(16)	1.396(3)
Ru(1)-H(99)	1.60(2)	C(16)-C(20)	1.511(3)
O(1)-C(58)	1.155(2)	C(16)-C(17)	1.387(3)
N(1)-C(2)	1.393(3)	C(17)-C(18)	1.391(3)
N(2)-C(1)	1.381(2)	C(18)-C(21)	1.513(3)
N(2)-C(13)	1.436(2)	C(13)-C(18)	1.401(3)
N(1)-C(1)	1.372(3)	N(1)-C(4)	1.447(2)

Selected Bond Angles	[°]		
C(58)-Ru(1)-C(1)	94.42(8)	C(2)-N(1)-C(4)	120.67(16)
C(1)-Ru(1)-P(2)	155.71(5)	C(1)-N(2)-C(13)	124.70(16)
C(1)-Ru(1)-P(1)	98.88(5)	C(14)-C(19)-Ru(1)	113.01(13)
C(1)-Ru(1)-C(19)	78.79(7)	C(13)-C(14)-C(19)	120.20(17)
C(58)-Ru(1)-P(1)	86.61(6)	C(1)-N(2)-C(13)	124.70(16)
C(19)-Ru(1)-P(1)	101.10(5)	C(1)-N(1)-C(4)	127.60(16)
N(1)-C(1)-N(2)	102.66(16)	C(1)-N(2)-C(3)	111.42(16)
P(2)-Ru(1)-P(1)	102.096(17)	C(1)-N(1)-C(2)	111.71(16)
C(1)-N(1)-C(4)	127.60(16)	C(2)-N(1)-C(4)	120.67(16)
C(1)-N(2)-C(3)	111.42(16)	C(1)-N(2)-C(13)	124.70(16)
C(3)-N(2)-C(13)	123.78(16)	C(2)-C(3)-N(2)	107.13(17)
C(1)-N(1)-C(2)	111.71(16)	C(3)-C(2)-N(1)	107.01(18)

Table 5.3. - *Selected bond distances [Å] and bond angles [°] for (31)*

The X-ray structure of **(31)** shows a distorted octahedral geometry around ruthenium with a P(1)-Ru-P(2) angle of 102.096(17)°. The structure clearly shows that the ruthenium atom has inserted into one of the *ortho* $ArCH_2$-H bonds of the IMes ligand to give a new Ru-C bond (2.2346(19) Å) as an integral part of a six-membered metallacycle. The mesityl ring planes are in an eclipsed position where the activated ring rotates approximately 50° away from the plane (torsion angle C(14)-C(13)-C(4)-C(9) = 49.8°). This torsion of the ring is less than observed for **(30)** but remains comparable to other reported examples of intramolecular C-H activated IMes ligands such as reported by Nolan et al. for Rh(IMes)(IMes'')(Cl)(H)[75] (torsion angle C(35)-C(24)-C(27)-C(22) = 42.2°). As shown in **Figure 5.1.**, the IMes fragment in **(31)** has some typical feature as a result of the cyclometalation; the C(19)-C(14) of the *ortho* metallated C-H bond is slightly shorter than the other methyl bonds along the mesityl rings (1.485(3) vs 1.513(3) and (1.511(3)Å). However as already observed for **(30)** very little effect on the overall bond distances is seen within the structure of **(31)**. The main effect of the cyclometalation affects the angles within the IMes ligands, shown by the reduced C_{Ph}-N-C: angle (C(1)-N(2)-C(13) =

N(2)-C(13) = 124.70(16)°) after the formation of the 6-membered ring. The Ru-CO bonds are comparable to many examples reported in the literature, as well as to the structures described so far in this chapter.

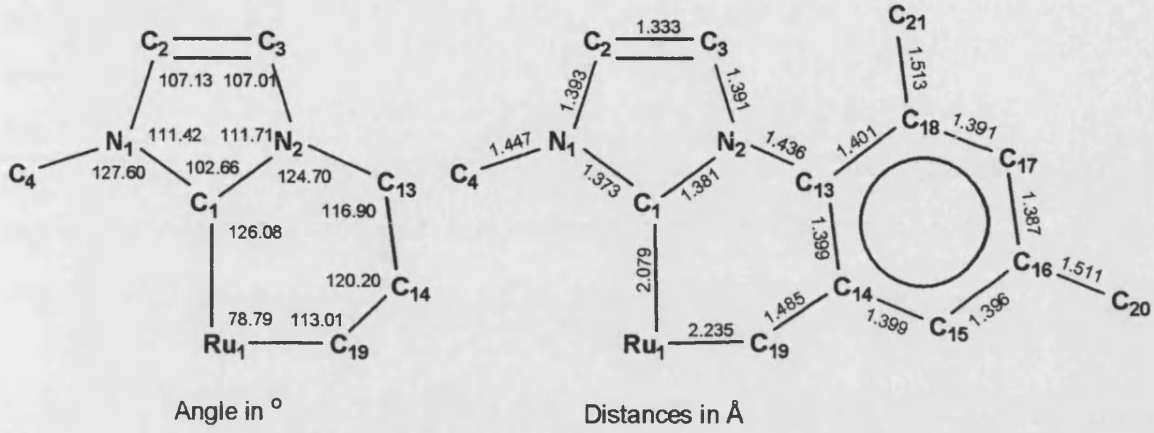

Figure 5.12. - *Significant bond distances and angles for the C-H activated IMes ring.*

The C(1)-Ru(1)-P(2) bond is severely bent (155.71(5)°) toward the C(19)-Ru(1)-H(1) region mainly due to the bulkiness of the phosphines. This idea is supported by the fact that this bending of the C(1)-Ru(1)-P(2) bond does not appear in the phosphine free C-H activated complexes of IMes **[Figure 5.12.]**. A second point to notice is the presence on a strongly bent imidazole ring relative to the Ru(1)-C(1) bond (γ = 14.38°) **[Chapter 5.2.3.]**.

5.2.1.4. Mechanistic studies of the C-C activation reaction.

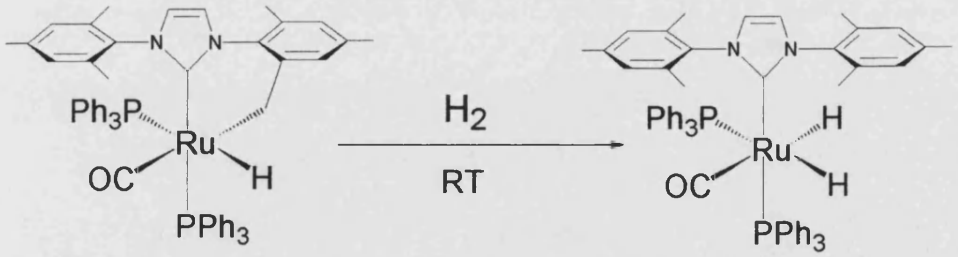

Scheme 5.36.

While **(30)** appears to be the thermodynamically favoured product in this system, efforts to convert the C-H activated species **(31)** into the C-C complex **(30)** proved unsuccessful. Reaction of **(31)** with 1 atm of H_2 led only to the reformation of **(26)** within 3 days at room temperature **[Scheme 5.36.]**.

The formation of **(30)** starting from **(26)** proceeds via the intermediacy of the bis carbene species $Ru(PPh_3)(IMes)_2(CO)H_2$ **(29) [Scheme 5.36., Spectrum 5.6.]** which, was characterised by $^{31}P\{^1H\}$ and ^1H NMR spectroscopy. Complex **(29)** shows a single phosphorus resonance at 47.3 ppm, and two distinctive doublet of doublets for the hydride groups in the proton NMR spectrum. One shows a *cis* coupling to phosphorus and to hydride (J_{HP} = 18.8, J_{HH} = 7.1 Hz), while the other displays *trans* splitting to phosphorus (J_{HP} = 93.5 Hz) and *cis* coupling to hydride (J_{HH} = 7.1 Hz). The species was further characterised by multinuclear 2-D experiments but could not be isolated due to its high reactivity.

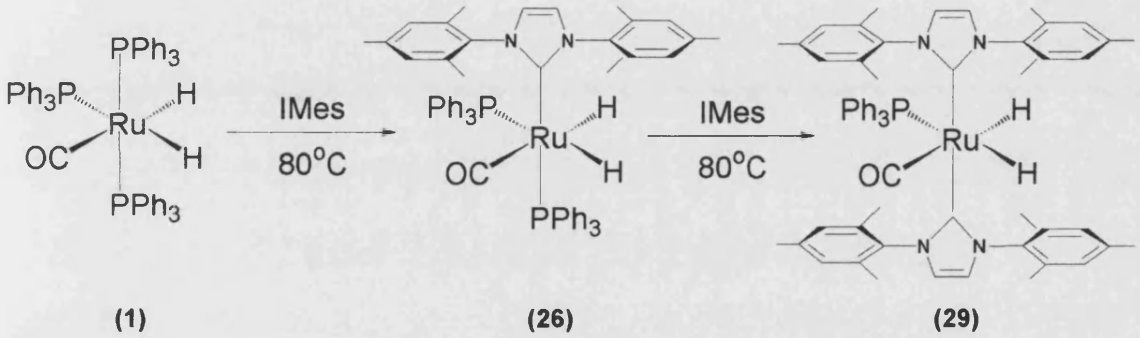

(1) **(26)** **(29)**

Scheme 5.35.

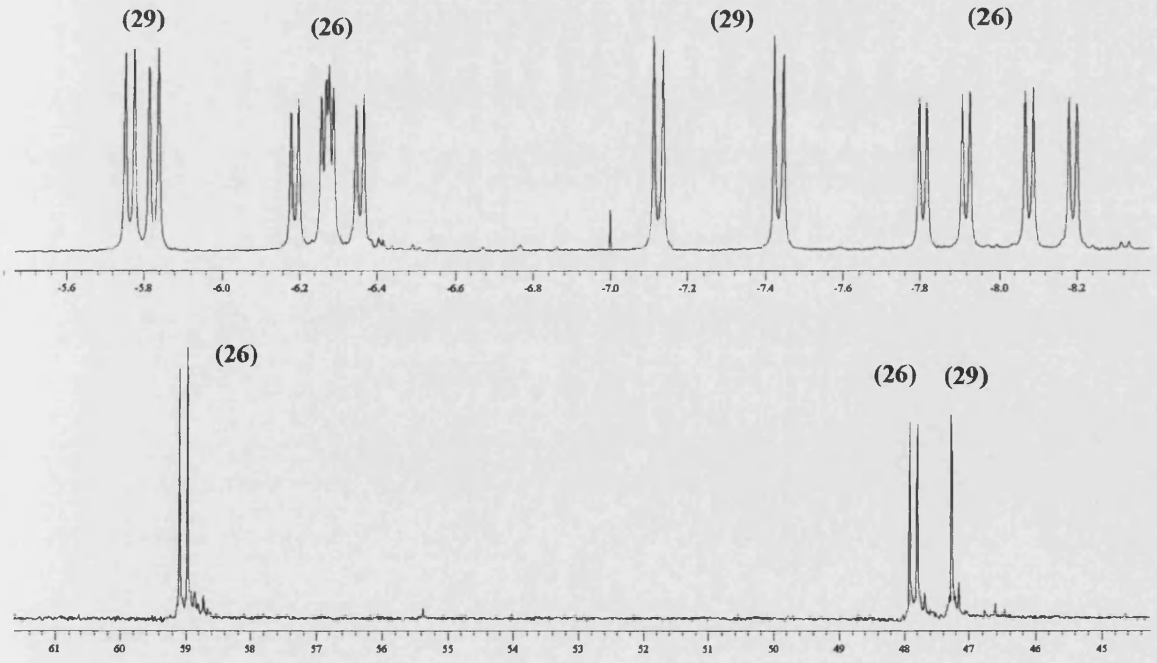

Spectrum 5.7. - *^1H and $^{31}P\{^1H\}$ NMR spectra showing the formation of* ***(29)****.*

Labeling experiments.

While the precise mechanism surrounding the formation of **(30)** has yet to be established, a number of observations show that the pathway is not straightforward. In particular, when the formation of **(30)** was performed in C_6D_6 and followed by ^1H and $^{31}P\{^1H\}$ NMR, extensive H/D exchange into both the hydride and the two PPh_3 ligands of the product **[Scheme 5.37.]** and into the *ortho* positions of free PPh_3 in solution **[Spectra 5.8.]** was detected.[76] These surprising results have led us to investigate the importance of these H-D exchange reactions and the various stages at which they occurred on the reaction pathway.

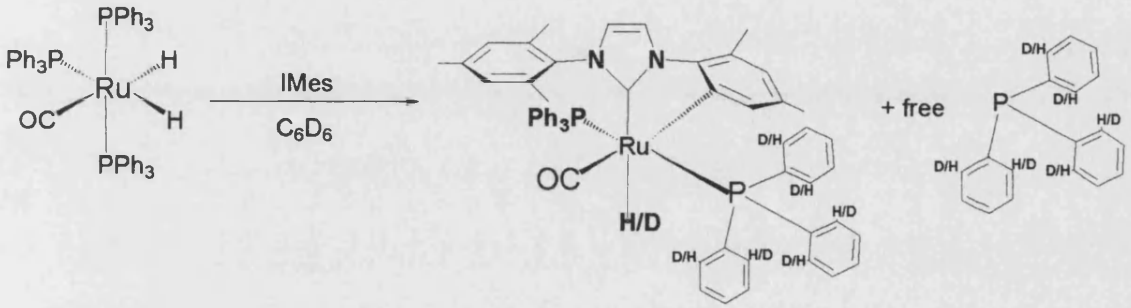

Scheme 5.37.

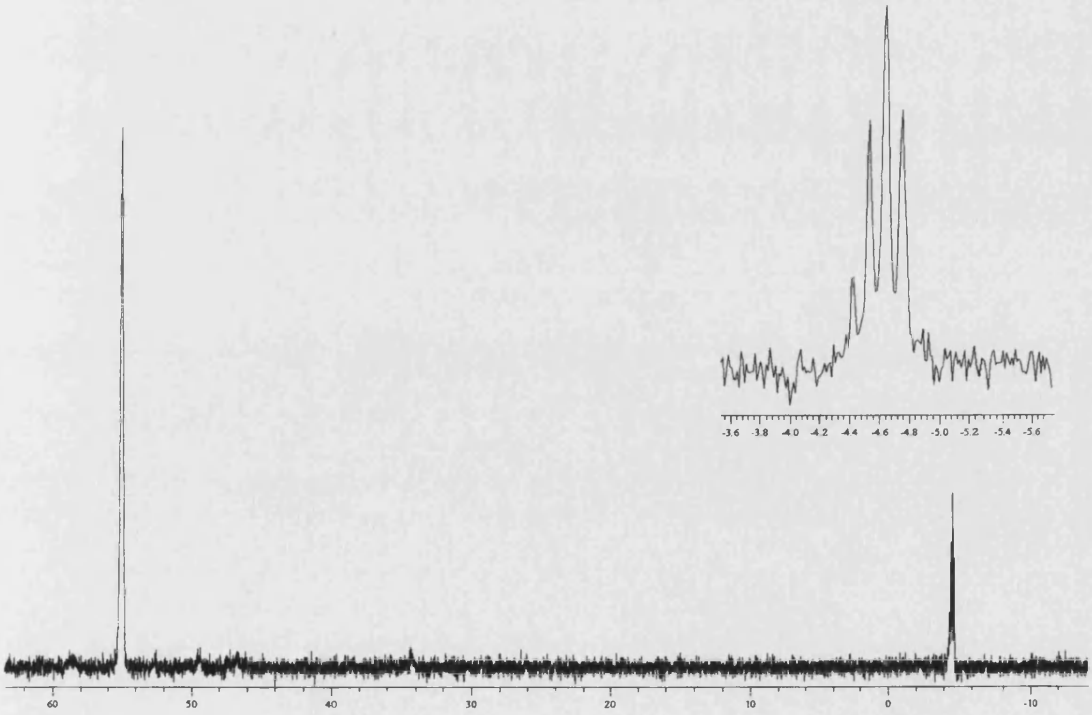

Spectrum 5.8. - *$^{31}P\{^1H\}$ spectrum showing extensive H/D exchange as shown in* ***Scheme 5.37.***

Thus, conversion of **(26)** exclusively to **(29)** in C_6D_6 at 80°C leads to no H/D exchange, while subsequent thermolysis of **(29)** at 110°C affords a mixture of H/D exchanged **(26)**, **(29)**, **(30)** and PPh_3 **[Scheme 5.38.]**.

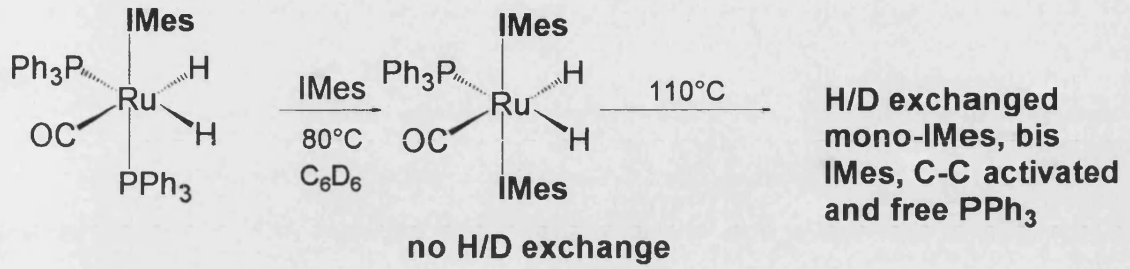

Scheme 5.38.

Upon reaction of **(26)** with D_2 at room temperature, **(26)**-HD and **(26)**-DH (50/50) were generated within 4 days, while a further 7 days afforded **(26)**-D_2 **[Scheme 5.39., Spectrum 5.9.]**. This process of H/D exchange, although not unusual, remains rare at room temperature.[77]

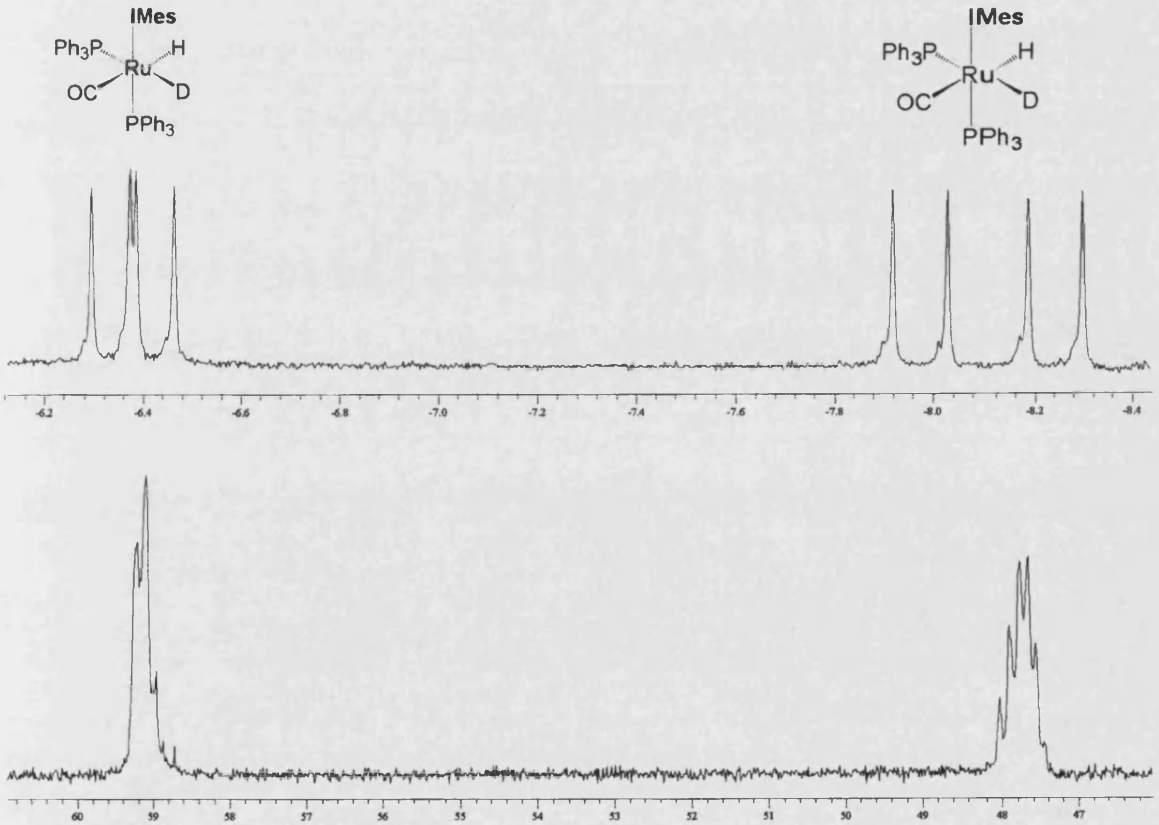

Spectrum 5.9. - *$^{31}P\{^1H\}$ and ^1H NMR spectra during the room temperature deuteration of* ***(26)*** *under D_2.*

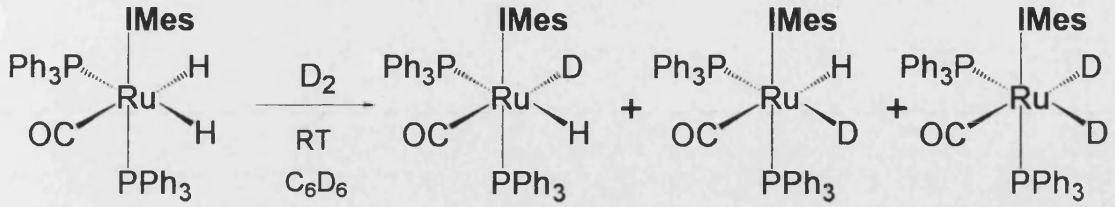

Scheme 5.39.

Subsequent reaction of **(26)**-D_2 with IMes at 80 °C in C_6D_6 gives **(29)**-H_2, **(29)**-HD, **(29)**-D_2 and exchanged PPh_3, while further heating of the mixture generated similar analogue of **(26)** (**(26)**-H_2, **(26)**-HD, **(26)**-D_2) **(Scheme 5.40., Spectrum 5.10.)**.

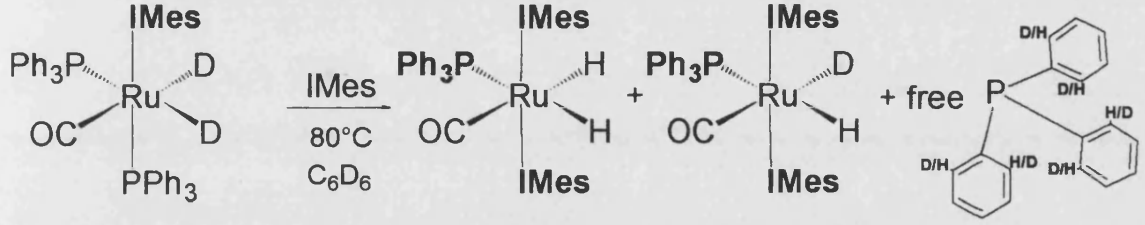

Scheme 5.40.

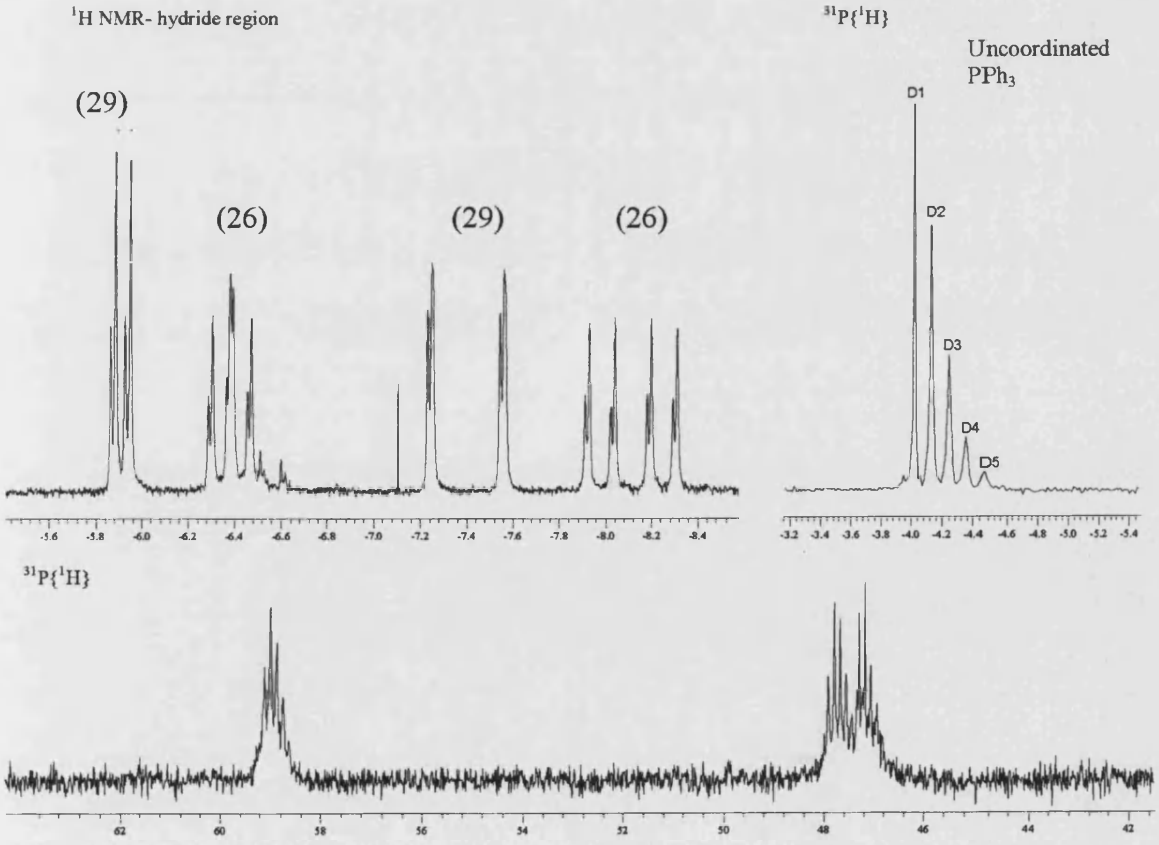

Spectrum 5.10. - *$^{31}P\{^1H\}$ and ^1H spectra showing extensive H/D exchange as shown in Scheme 5.38.*

These results suggest that PPh_3 activation is important in the conversion of **(26)** to **(29)**, that solvent activation subsequently occurs at higher temperature, and finally that there is a reversible reaction between **(26)** and **(29)**.

The experiments we have run show that the conversion of **(26)** to **(29)** and ultimately to **(30)** requires the presence of free IMes, even though the C-C activation product only contains one carbene ligand. In fact thermolysis of **(26)** in C_6D_6 in the absence of IMes resulted in only trace amounts of **(30)** being formed, along with **(26)**-HD, **(29)**-H_2, **(29)**-HD, **(1)** and **(1)**-HD.

Attempts to change the solvent used in the reaction to d^8 toluene resulted in extensive H/D being observed (under the same conditions). Surprisingly almost no H/D was observed when using d^8-thf even under the long reaction time required to form **(26)**. Further investigation of the influence of thf as a solvent for the reaction showed that **(26)** could be formed almost selectively in thf, whereas use of benzene or toluene inevitably resulted in a reasonable amount of **(30)** being formed. Therefore thf was chosen as a preferred solvent for the selective synthesis of **(26)**. The absence of H/D exchange observed in thf and the selective formation of **(26)**, indicates the importance of solvent activation in the pathway to C-C activation. This is currently under investigation by another student.

DFT calculations.

As proposed by Milstein and Martin and their co-workers, the oxidative addition of a C-C bond can start with a kinetically favoured C-H activation reaction prior to the thermodynamically favoured C-C activation process.[60,78] In order to see if C-H activation was on the pathway to C-C activation in these NHC complexes, DFT calculations[79] were performed by Dr Stuart Macgregor (Heriot-Watt University) with (2-methylphenyl)imidazol-2-ylidene and PH_3 as model ligands **[Figure 5.13.]**. Computed metal-ligand distances in **(x)**, **(y)**, and **(z)** (models of **(26)**, **(30)** and **(31)** respectively) were in good agreement with the experimentally determined values, although the angles at the metal centre (e.g. *cis*-P-Ru-P and *trans*-C_{IMes}-Ru-P) were underestimated as a consequence of using less sterically demanding ligands in the calculations. However, the small *trans*-P-Ru-P angle in **(30)** (156.0°) was reproduced in **(y)** (159.4°) confirming that electronic factors are responsible for this distortion. The computed energies show that while **(z)** (+H_2) is 47.3 kJ/mol higher in energy than **(x)**, **(y)** (+CH_4) is 31.4 kJ.mol^{-1} more stable than **(x)**.

These results confirm that the C-C activation species is indeed the thermodynamically preferred reaction product. Moreover, the higher energy of the C-H activation product supports the idea that this species does not lie on the formation pathway of the C-C activated complex. Further calculations on the bis carbene analogue of **(30)** are needed, along with a profile of the reaction pathway before the solution results can be fully rationalised.

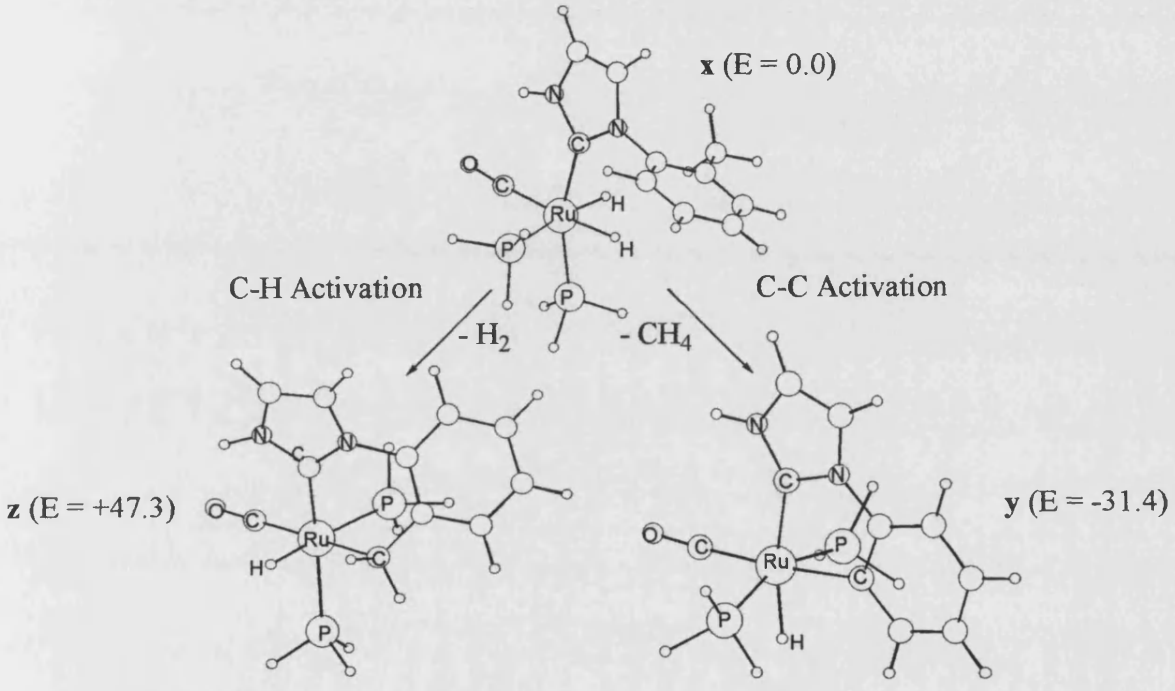

Figure 5.13. - *DFT calculations performed with the ADF program using the BP86 gradient-corrected functional. (Performed by Macgregor, S. A.; Heriot-Watt Univeristy. (**NB:** Relative energies in kcal.mol^{-1})*

5.2.2. Synthesis and characterization of Ru(L)(IMes'')(CO)H [L = dppp, arphos] and their C-H activation reactions.

5.2.2.1. Formation of Ru(dppp)(IMes)(CO)H_2 (27)

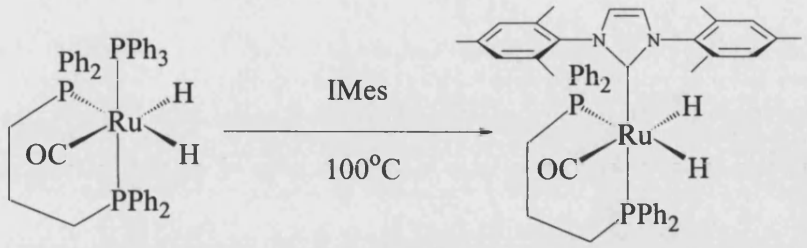

(8) (27)

Scheme 5.41.

The synthesis of Ru(dppp)(IMes)(CO)H_2 (dppp = $Ph_2P(CH_2)PPh_2$) was performed in a similar way to that for **(26) [Scheme 5.41.]**. Comparable reaction time was required, though this could be reduced by using Ru(dppp)($AsPh_3$)(CO)(H_2) as the precursor instead, bringing the synthesis time to 1 week at 110°C. Removal of solvent and washing with ethanol gave a white solid in a 73% yield. X-ray quality crystals were grown by layering a benzene solution of **(27)** with ethanol.

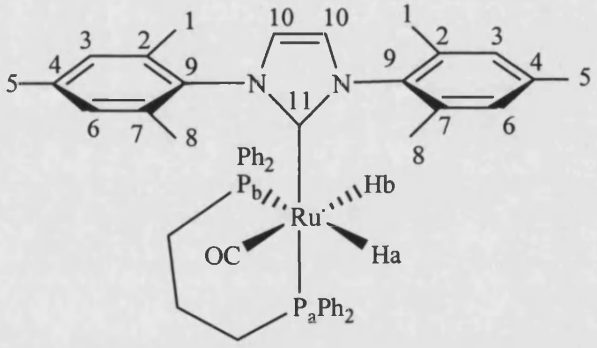

Figure 5.14. - *NMR assignment of the proton and carbon atom of (27)*

The formation of **(27)** was monitored using $^{31}P\{^1H\}$ NMR, which showed two new doublet signals at 40.6 and 28.1 ppm for **(27)**. The hydride region of the ^1H NMR spectrum showed the presence of two sets of signals consistent with the presence of two hydrides H_a and H_b. Ru-H_b appears as a doublet of doublet of doublets at -6.12 ppm (J_{HbPb} = 22.9, J_{HbPa} = 15.5, J_{HbHb} = 5.8 Hz) and Ru-H_a appears as a doublet of doublet of doublets at -7.07 ppm

spectrum, the carbonyl carbon gives rise to a triplet at 205.8 ppm (J_{CP} = 9.0 Hz) indicating that the carbonyl carbon is *cis* to two phosphorus nuclei, whereas the ruthenium carbene carbon (C-*11*) appears as a doublet of doublets at 195.5 ppm (J_{CPa} = 75.5, J_{CPb} = 7.5 Hz), indicating that (C-*11*) is *trans* to one phosphorus (large coupling constant) and *cis* to the other. The IR spectrum showed a single band in the carbonyl region at 1937 cm^{-1}.

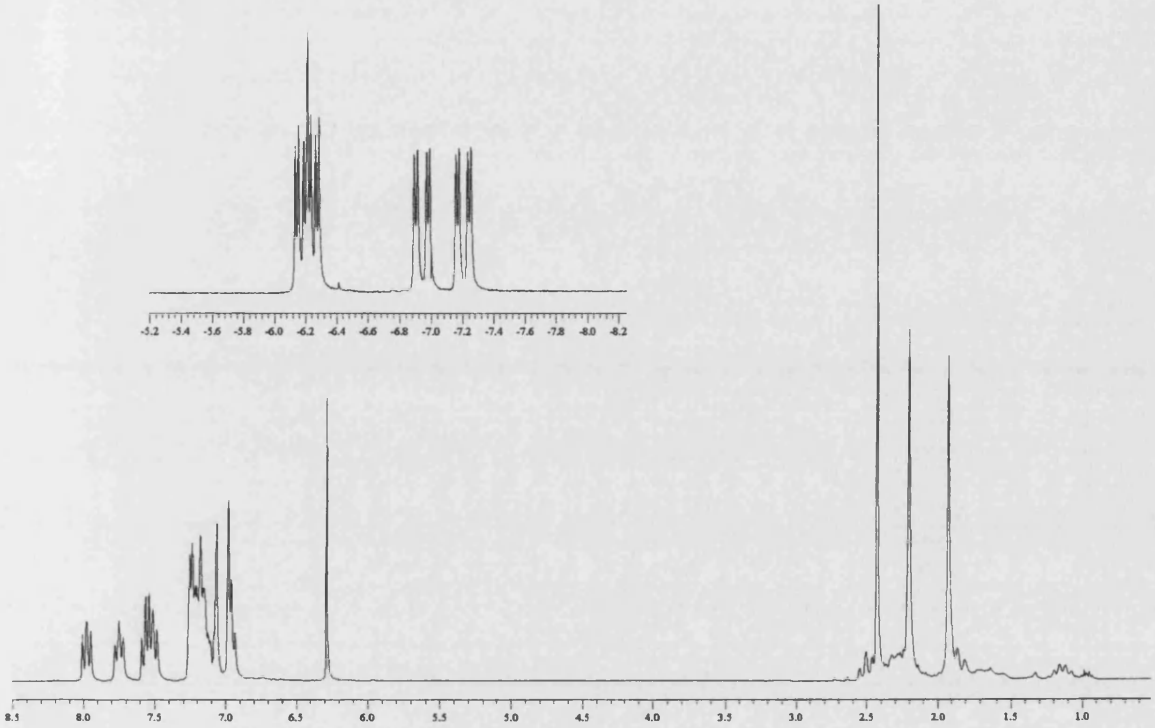

Spectrum 5.11. - *^1H NMR spectrum of (27)*

The full molecular geometry of **(27)** was elucidated by X-ray crystallography **[X-Ray 5.4.]**. Selected bond distances and bond angles are available in **Table 5.4.**. The ruthenium is centred at the base of a distorted octahedral structure with the IMes ligand *trans* to one phosphine of the dppp fragment and *cis* to the other. The two hydrides were freely refined and are shown to be *cis* to each other (H(1)–Ru(1)–H(2) = 83.2(10)°), one being *trans* to a phosphine ligand. The carbonyl ligand is in a *cis* position to both phosphine groups. The same structural features noted for **(26)** apply to the structure of **(27).** The structure is severely bent around the C(2)-Ru(1)-P(2) axis (158.78(4)) mainly due to the bulkiness of the phosphines, but it is no different to that previously observed in the structure of $Ru(dppp)(PPh_3)(CO)H_2$.[80a] Finally it is important to note that the carbene ligand is again out of Ru–C(2) axe with a Ru-C carbene bond **[Chapter 5.2.3.]**.

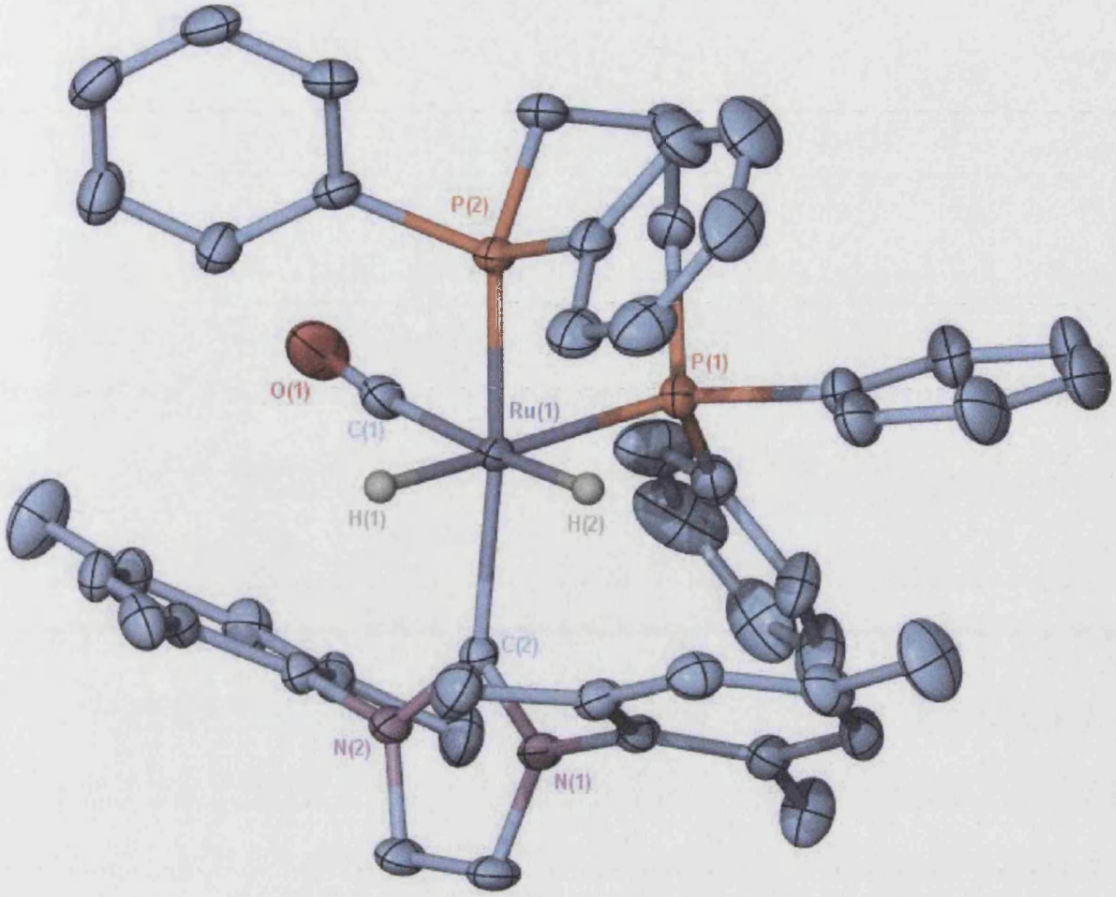

X-Ray 5.4 - *X-ray structure of Ru(dppp)(IMes)(CO)H_2. The ellipsoids are represented at 50% of the occupancy, and the hydrogens have been removed for clarity.*

Selected Bond Lengths	[Å]	Selected Bond Angles	[°]
Ru(1)-H(2)	1.589(14)	H(2)-Ru(1)-H(1)	83.2(10)
Ru(1)-H(1)	1.632(15)	C(2)-Ru(1)-P(2)	158.78(4)
Ru(1)-C(1)	1.9054(15)	C(1)-Ru(1)-P(1)	91.29(5)
Ru(1)-C(2)	2.0981(12)	C(2)-Ru(1)-P(1)	105.13(4)
Ru(1)-P(2)	2.2816(3)	P(2)-Ru(1)-P(1)	91.224(14)
Ru(1)-P(1)	2.3392(4)	C(1)-Ru(1)-C(2)	100.16(5)
O(1)-C(1)	1.1561(19)		

Table 5.4. - *Selected bond distances [Å] and bond angles [°] for (27).*

5.2.2.2. Formation of Ru(dppp)(IMes'')(CO)H (32)

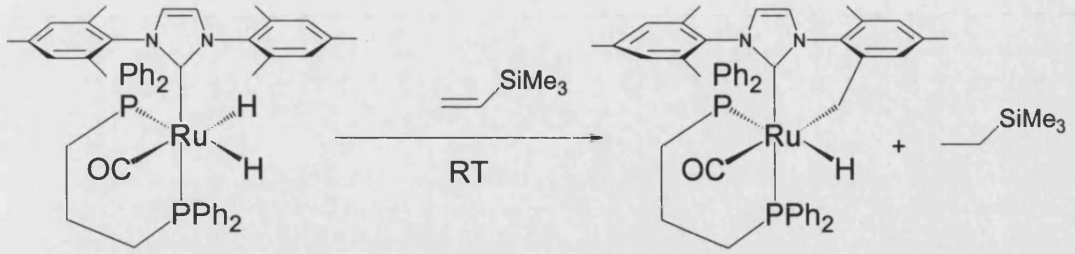

(27) (32)

Scheme 5.42.

Addition of 1 equivalent of CH_2=$CHSiMe_3$ to a C_6D_6 solution of **(27)** at 100°C for 24 hr resulted in dehydrogenation of the complex yielding **(32)** in an 89% yield **[Scheme 5.42.]**.

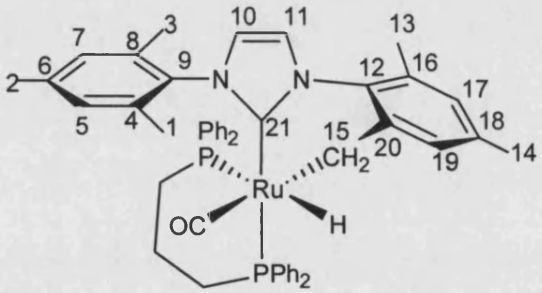

Figure 5.15. - *NMR assignment of the proton and carbon atom of (32)*

The formation of **(32)** was monitored using $^{31}P\{^1H\}$ NMR and showed two new sets of doublets for **(32)** at 39.6 and 15.2 ppm. The ^1H NMR spectrum displayed a single hydride resonance coupled to the two ^{31}P nuclei (J_{HP} = 102.6, 21.1 Hz) in a *trans* and *cis* orientation. The two inequivalent methylene protons appears as a doublet of doublets (J_{HH} = 10.8, J_{HP} = 14.2 Hz) and a broad triplet (J = 10.2 Hz) **[Spectrum 5.12.]**. In the $^{13}C\{^1H\}$ NMR spectrum, the carbonyl carbon gives rise to a triplet at 204.5 ppm (J_{CP} = 9.1 Hz) indicating that it lies *cis* to the two ends of the dppp ligand, while the ruthenium carbene carbon (C-21) gives rise to a doublet of doublets at 191.5 ppm (J_{CPa} = 82.3 Hz, J_{CPb} = 8.3 Hz). The IR spectrum showed a single band in the carbonyl region at 1920 cm^{-1}.

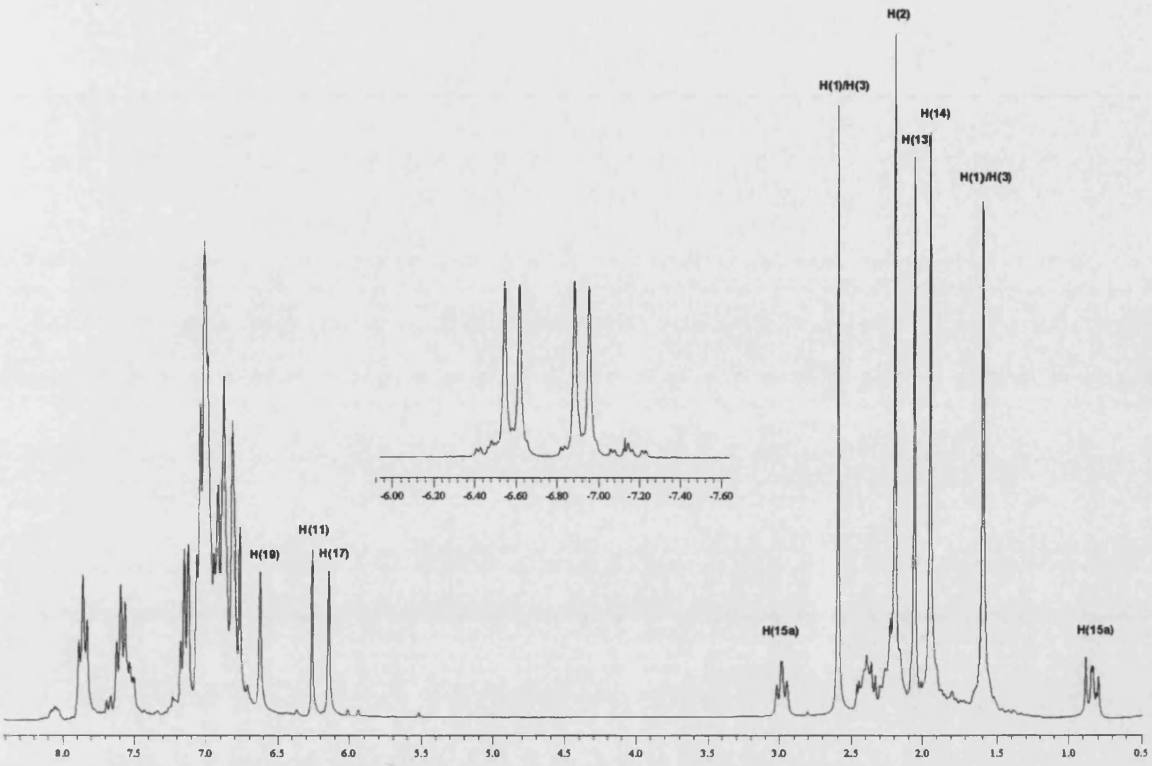

Spectrum 5.12. - *^{1}H spectrum NMR of (32).*

The full molecular geometry of **(32)** was elucidated by X-ray crystallography **[X-Ray 5.5.]**. Selected bond distances and bond angles are available in **Table 5.5.**. The ruthenium is centred at the base of a distorted octahedral structure with the IMes ligand *trans* to one phosphine of the dppp fragment and *cis* to the other. The hydride was freely refined (Ru(1)-H(99) = 1.62(2)) and shown to be in a *cis* position relative to one phosphorus atom and *trans* to the other.

The same points already elucidated in the structure of **(31)** apply to that of **(32)**. The structure is severely bent around the C(2)-Ru(1)-P(2) axis (159.73(5)°) mainly due to the bulkiness of the phosphine, and not much different (cf 155.71(5)°) to that already observed for **(31)**. It is important to notice that the carbene ligand is again out of the Ru-C(2) axe **[Chapter 5.2.3.]**.

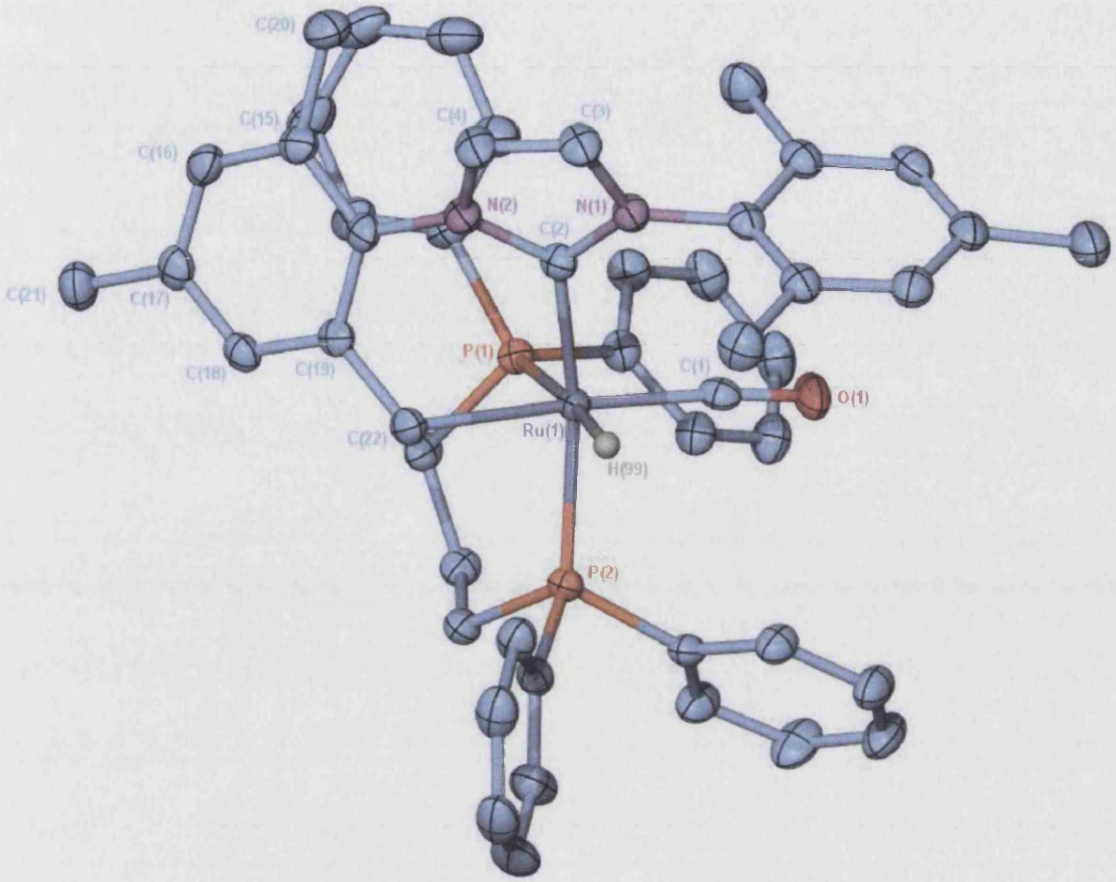

X-Ray 5.5 - *X-ray structure of Ru(IMes'')(dppp)(CO)H. The ellipsoids are represented at 50% of the occupancy, and the hydrogens have been removed for clarity.*

Selected Bond Lengths	**[Å]**	**Selected Bond Angles**	**[°]**
Ru(1)-H(99)	1.62(2)	C(2)-Ru(1)-P(2)	159.73(5)
Ru(1)-C(1)	1.864(2)	C(2)-Ru(1)-C(22)	81.13(7)
Ru(1)-C(2)	2.0827(19)	C(2)-Ru(1)-P(1)	102.59(6)
Ru(1)-C(22)	2.2258(19)	C(1)-Ru(1)-C(22)	169.58(8)
Ru(1)-P(2)	2.3108(5)	N(1)-C(2)-N(2)	102.90(16)
Ru(1)-P(1)	2.3673(5)	C(22)-Ru(1)-P(1)	93.38(5)
O(1)-C(1)	1.159(2)		

Table 5.5. - *Selected bond distances [Å] and bond angles [°] for (32).*

As shown in **Figure 5.16.**, very little difference is seen between the overall X-ray structures of the two C-H activated systems with either PPh_3 **(31)** or dppp **(32)** ligands. However the orientation of the C-H activated rings changes between the two structures, probably as a consequence of the variation in bulk between the PPh_3 and the dppp **[Table 5.6.]**. The effect from the bulk of the phosphine ligand is mainly seen in the C(19)-Ru(1)-P(1) and C(22)-Ru(1)-P(1) angles, showing the wider angle when a bulkier phosphine is used. When this is the case, the mesityl ring points away from the metal in order to minimize the interaction with the phosphine ligand.

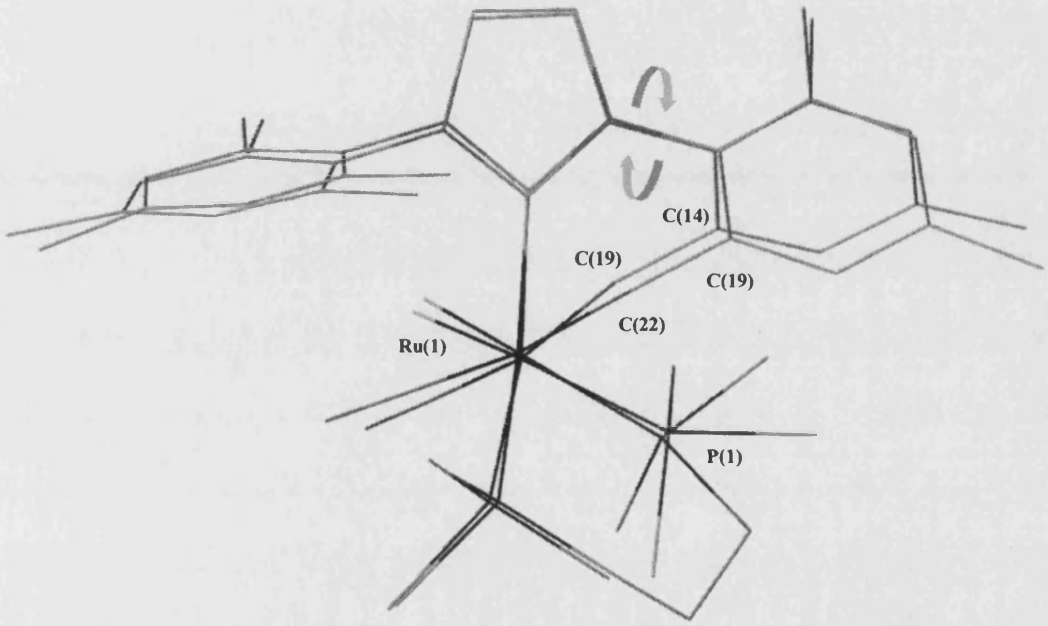

Figure 5.16. - *Overlapping of the X-Ray structure of (31) and (32).*

$Ru(PPh_3)(CO)(IMes')H$		**Ru(dppp)(CO)(IMes')H**	
C(19)-Ru(1)-P(1)	101.10(5)	C(22)-Ru(1)-P(1)	93.38(5)
C(1)-N(2)-C(13)-C(14)	43.8	C(2)-N(2)-C(14)-C(19)	45.5
C(14)-C(19)-Ru(1)	113.01(13)	C(19)-C(22)-Ru(1)	112.81(13)
C(13)-C(14)-C(19)	120.20(17)	C(14)-C(19)-C(22)	119.84(18)
C(14)-C(13)-N(2)	116.90(16)	C(19)-C(14)-N(2)	117.45(17)

Table 5.6. - *Selected bond distances and bond angles representing the main differences between (31) and (32).*

5.2.2.3. Formation of Ru(arphos)(IMes)(CO)H_2 (28)

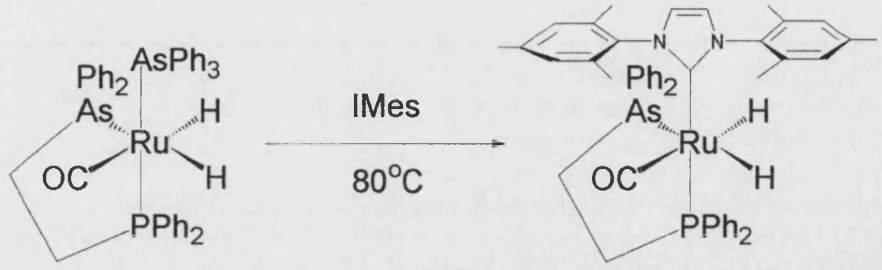

(11) **(28)**

Scheme 5.43.

Treatment of $Ru(AsPh_3)(arphos)(CO)H_2$ **(11)** (arphos = $Ph_2AsCH_2CH_2PPh_2$) with IMes at 80°C for 7 days gave $Ru(arphos)(IMes)(CO)H_2$ **(28)** in 73% yield **[Scheme 5.43.]**. The $^{31}P\{^1H\}$ NMR spectrum of **(28)** shows a signal at 88.7 ppm. The hydride region appears as two doublet of doublets at δ -7.44 (J_{HP} = 25.9, J_{HH} = 3.3 Hz) and δ -8.95 (J_{HP} = 25.9, J_{HH} = 3.3 Hz) **[Spectrum 5.13.]**. In the $^{13}C\{^1H\}$ NMR spectrum the carbonyl carbon gives rise to a doublet at 204.5 ppm (J_{CP} = 7.5 Hz), while a large doublet resonance for the Ru-IMes carbene carbon (J_{CP} = 78.4 Hz), places it *trans* to the phosphorus terminus of the arphos ligand. The IR spectrum displayed one band in the carbonyl region at 1914 cm^{-1}.

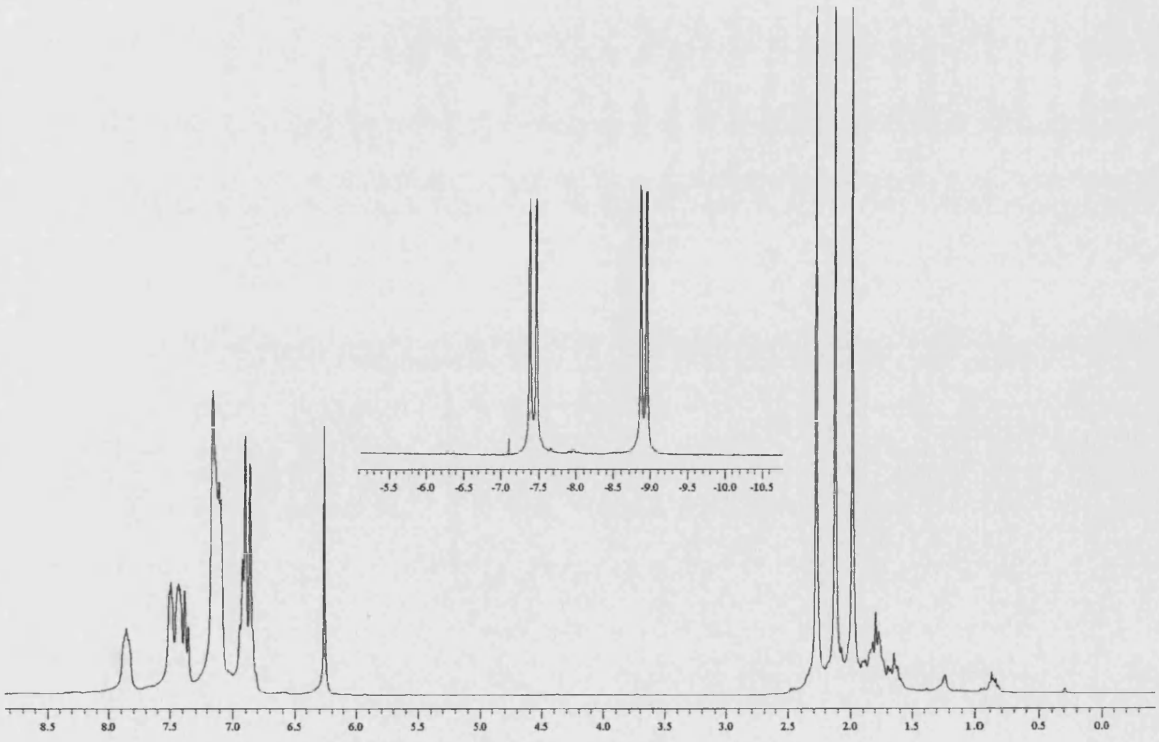

Spectrum 5.13. - *^1H NMR spectrum of (28)*

5.2.2.4. Formation of Ru(IMes'')(arphos)(CO)H (33)

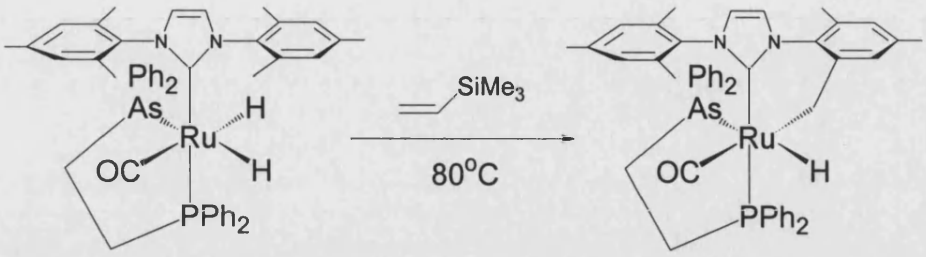

(28) (33)

Scheme 5.44.

Surprisingly, reaction of a C_6D_6 solution of **(28)** with CH_2=$CHSiMe_3$ at 80°C did not result in quantitative formation of the C-H activated product **(33)** as it was expected on the basis of the observed reactivity of **(26)** and **(27)** **[Scheme 5.44.]**. Careful analysis of the ^1H NMR of the reaction mixture showed formation of the hydrogenation product of $CH_3CH_2SiMe_3$ along with several products in the hydride region of the spectrum. In total five hydridic species were observed **[Spectrum 5.14.].** These proved to be the only products on the basis of the observed $^{31}P\{^1H\}$ spectrum and ^{31}P-^1H HETCOR spectrum. No free phosphine was observed at any stage of the reaction.

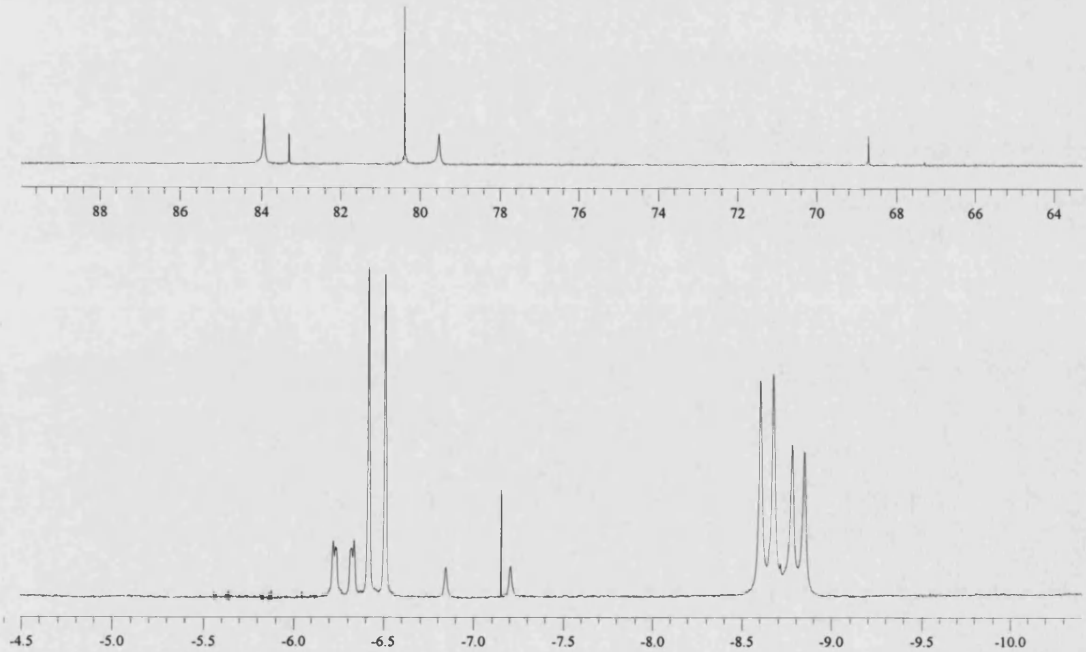

Spectrum 5.14. - *$^{31}P\{^1H\}$ and ^1H NMR spectra of reaction mixture resulting from the reaction of **(28)** with one equivalent of trimethylvinylsilane.*

Interestingly variation of the reaction conditions (i.e. reaction temperature, equivalents of alkene added) did not modify the ratio of the five hydride products. Although none of these species could be either isolated or fully characterised, it was possible on the basis of the NMR spectra (^{1}H-^{1}H COSY and ^{31}P-^{1}H HETCOR) to postulate formation of several C-H activated species. This reactivity was attributed to the hemi-labile nature of arphos.[80b]

5.2.3. Structural similarities observed in (26), (27), (30), (31) and (32).

In all the structurally characterised complexes reported in this chapter, the low-temperature X-ray data collection enabled the hydride ligands to be located from the Fourier difference map and their positional and thermal parameters refined freely to give Ru-H distances of 1.55(2) and 1.57(2) Å and an H-Ru-H angle of 85.9(8)° for **(26)** and 1.589(14), 1.632(15), and 83.24(10)° for **(27)**. Closer examination of intramolecular contacts reveals some very interesting features.

In the structure of **(27),** there is an intramolecular H···H interaction between the hydrido ligand H(2) and an adjacent *o*-C-H hydrogen (AFIX43 refined position) of a phenyl group on one of the phosphine ligands P(1). This H···H distance of 2.146 Å is significantly shorter than the sum of the van der Waals radii (2.4 Å). It has been suggested by Crabtree et al[81] that a d_{HH} cutoff of 2.2 Å be considered for significant attractive interactions. The Ru-H···H and H···H-C angles of 125.41° and 141.98° are not linear as a consequence of the steric demands of the coordination complex as a whole, however, the aryl ring C(39)-C(44) is clearly orientated in such a way as to bring about the relatively short H···H contact as shown by the almost flat torsion angles of C(39)-P(1)-Ru(1)-H(2) and Ru(1)-P(1)-C(39)-C(40) (6.3° and 2.2° respectively).

The second hydrido ligand, H(1), shows an H···H interaction of 2.146 Å with one of the *ortho* methyl hydrogen (AFIX 137 refined position on C(13)). This effect can be explained by two structural factors. In the first instance, a larger rotation of the mesityl ring C(5)-C(13) toward H(1) than for the other Mes ring of the carbene is observed, as shown by the rotation angle around the N-C_{Mes} bond (C(2)-N(1)-C(5)-C(10): 80.1°, C(2)-N(2)-C(14)-C(19): 84.3°). The second structural factor occurring for this interaction is presumably due to the combined electronic and steric interactions of both the phosphines and the carbene ligand as suggested by the angles γ (5.77°) and β (105.12°) which are defined in **Figure 5.17.**.

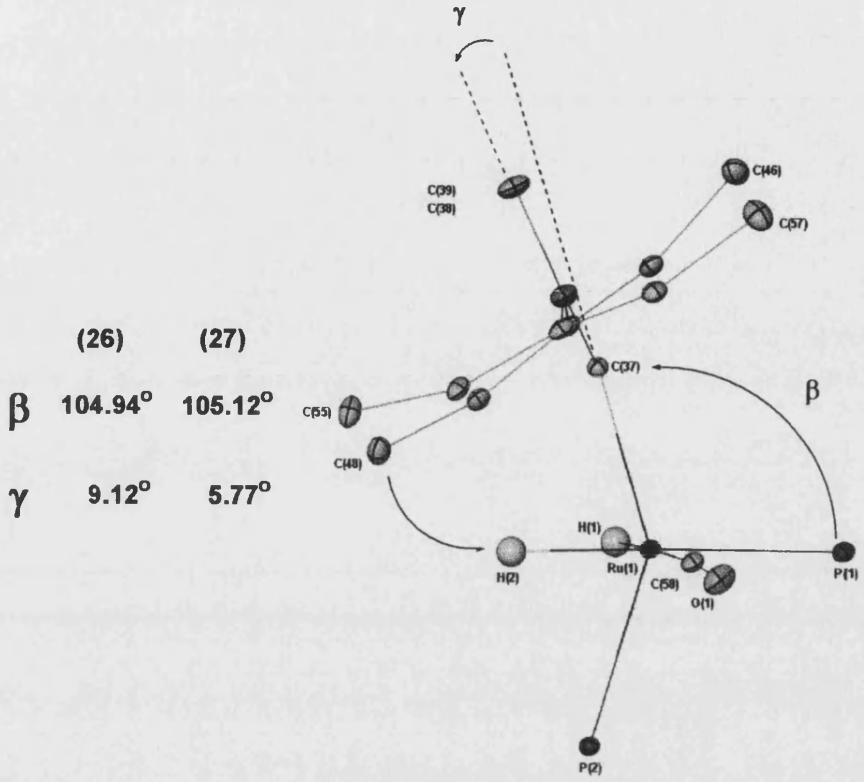

Figure 5.17. - *Simplified structure of (26) and (27) where the angles (γ) and (β) are put in context. The mesityl rings have been simplified for clarity. It is showed as well how twisted is the C(40)-C(48) Mes ring, compares to the C(51)-C(57) Mes ring, bringing C(48) CH_3 closer to H(2).* ***NB:*** *The same characteristics apply to* ***(27)****.*

The observation of these phenyl hydrogen-ruthenium hydride interactions has been observed by Junk et al[70] in the solid state structure of $Ru(PPh_3)_3(CO)H_2$. In order to determine if Ru-H···H-aryl + Ru-H···H_3C-C are common features in other ruthenium hydride systems, a survey of the Cambridge Crystallographic Database was performed.[70, 82-96] We limited our survey to values between 1.7 and 2.2 Å as any value lower than 1.7 Å falls into the domain of an agostic interaction.[30] **Graph 5.1.** reveals that there are many cases of ruthenium hydrido-phenyl interactions **[Table 5.7.]** with the crystallographically determined H···H distances ranging from 1.71 to 2.16 Å, the majority clustering around 2.06 Å **[Graph 5.1.]**. A plot of the Ru-H···H-Ph distance versus the Ru···C(Ph) distance shows the Ru···C(Ph) distance is relatively similar in such cases and is centred around 3.89 Å. As shown on **Graph 5.1.**, our examples fit in perfectly with the bulk of these determinations.

Complex	Ru-H--H-CH_2	Ru---CH_3	Reference
$Ru(PPh_3)_3(CO)H_2$	2.025	3.853	**70**
$[Ru(PPh_3)(PCy_3)(CH_3CN)_2(CO)H][BF_4]$	1.983	3.758	**82**
$Ru_2(PPh_3)_4(N_2)(H)(\mu\text{-}H)_3$	2.174	4.885	**83**
	2.174	3.663	
$[Ru(PPh_3)_2(\eta^6\text{-}C_7H_8)H][BPh_4]$	2.044	3.836	**84**
$Ru(AsPh_3)_2(CO)(BH_2(Pyrazol\text{-}1\text{-}yl))H$	1.987	3.890	**85**
$Ru(PPh_2Me)_3(CO)(Cl)H$	2.116	3.758	**86**
$R(PMe_3)_4(SPh)H$	1.787	3.849	**87**
$RuPCy_3(SiPh_3)H_2(H_2)(\mu\text{-}H)$	2.144	3.863	**88**
$\{Ru(PPh_3)_2\}(\mu\text{-}O_2CMe)_2(\mu\text{-}H)_2$	1.713	3.819	**89**
$[Ru(dppe)_2H(H_2)][BPh_4]$	2.111	3.782	**90**
	1.944	3.398	
$[Ru(C_P^*)(dppm)(H_2)][BF_4]$	2.116	3.868	**91**
	1.995	3.785	
$Ru(PPh_3)_2$(Ethane-1,2-bis(dimethylsilane)-H,H')H_2	2.194	3.839	**92**
$Ru(PPh_3)(dppp)(CO)H_2$	1.986	3.846	**80**
	1.899	3.763	

Table 5.7. - *Ru-H···H-Ph / Ru···C(Ph) distances in ruthenium hydrido complexes extracted from the Cambridge Crystallographic Database.*

While the observation of a Mes-CH_3 hydrogen-ruthenium hydride interaction has not been described previously, several examples of CH_3 hydrogen to ruthenium hydride interactions are apparent. These arise largely within hydrido-Ru-P^iPr_3 complexes, so one has to be cautious when using these as a true comparison with our NHC system.

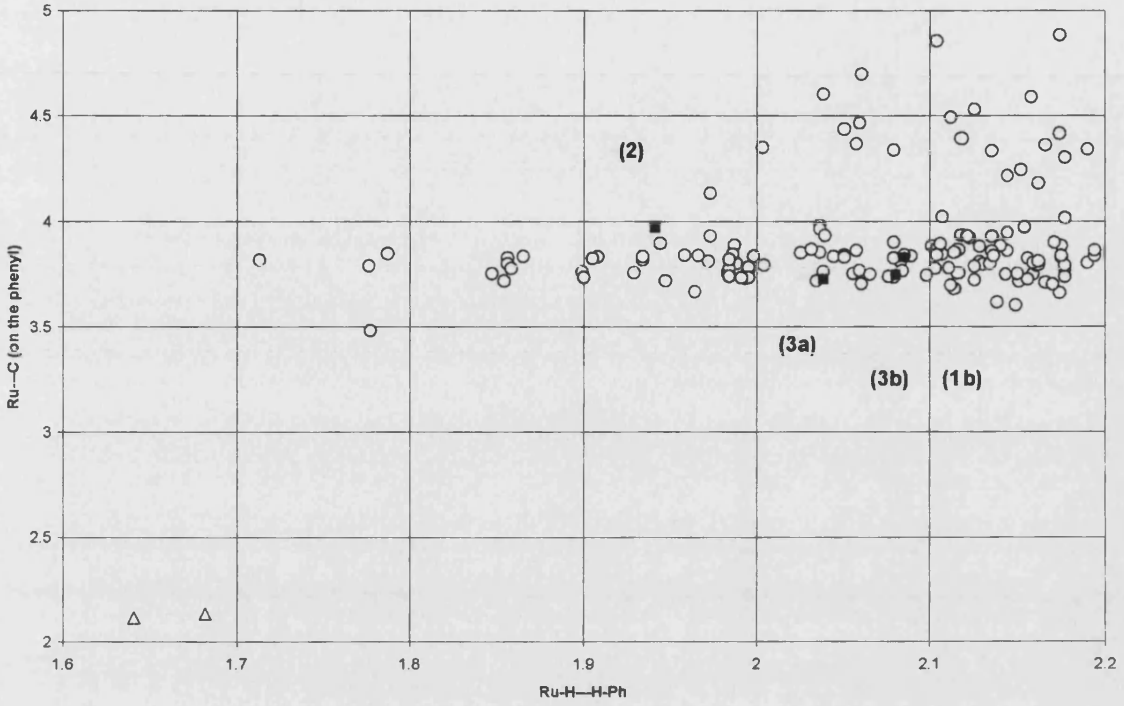

Graph 5.1. - *CCD survey[70, 83-97] plot of the Ru-H···H-Ph distance versus the Ru···C(Ph) distance: (Δ): Examples of agostic interaction[α]; (O): Reported X-ray structure where the intramolecular Ru-H···H-Ph is within 1.7 to 2.2 Å;(■):* ***(26), (27),(30), (31), (32).***

The results of this survey are shown in **Table 5.8.**. It stands out from these data that the mean value of a Ru-H···H-CH_2 interaction is ca. 2.07 Å with a Ru···CH_3 distance of 3.87 Å. By comparison, Ru(dppp)(IMes)(CO)H_2 shows rather longer distances (Ru-H···H-CH_2: 2.146 Å, Ru···CH_3: 4.033 Å). However, in the only reported example of an Ru(IMes)H complex available from the database (Ru(PCy_3)(IMes)(CO)HCl, the Ru-H···H-CH_2 distance is 2.905 Å (4.221 Å for Ru···CH_3), leaving the possibility of such an interaction taking place. More examples of hydrido ruthenium IMes complexes are needed before this kind of interaction becomes more than a postulate.

Complex	Ru-H---H-CH_2	Ru---CH_3	Reference
$Ru(PCy_3)(IMes)(CO)HCl$	2.905	4.211	**93**
$Ru(PCy_3)_2(\eta^2$–allyldimethylsilane)H_2	2.137	3.318	**94**
$Ru(PiPr_3)_2(bis(L_1)(H_2)H$	2.098	3.900	**95**
	2.197	3.863	
$Ru(PPh_3)_2(\eta$–$C_7H_8)H$	2.044	3.836	**96**
$[Ru(PEt_3)_2(Cp^*)(SH)H][BPh_4]$	1.987	3.890	**97**
$Ru(dmpe)_2$(N-methylindole)H	2.042	3.576	**98**
$[Ru(Cp^*)(iPrP(CH_2)_2PiPr)H_2][BPh_4]$	2.079	3.875	**99**
Ru(CO)(NCS)(6,6'-Dimethyl-2,2'-bipyridine)H	2.200	3.388	**100**
$Ru(PiPr_3)_2Cl_2H_2$	2.197	4.069	**101**
Ru(P(*t*-Bu)$_2$(CH_3))(CO)(F)(difluoromethylene)H	2.101	3.906	**102**
	2.112	3.924	
Ru(CO)(PCP)H	2.169	3.869	**103**
	2.043	3.780	
	1.926	3.819	
	2.150	3.843	
$[Ru(Cp^*)(iPr_2P(CH_2)_2PiPr_2)(L_2)H][BPh_4]$	2.106	3.841	**104**

L_1 = 3,5-bis(trifluoromethyl)(pyrazolyl)-borate-H,N)

L_2 = Methoxycarbonylethynyl

PCP = 2,6-bis(di-t-butylphosphidomethyl)phenyl-C,P,P'

Table 5.8. - *Ru-H···H-CH_2 / Ru···CH_3 distances in ruthenium hydrido.*

Similar H···H interactions have been observed in **(26)**, **(30)**, **(31)** and **(32)**. In **(30)**, the H···H interaction is observed between the hydride H(1) and one of the phenyl hydrogens H(20) (H(1)···H(20): 1.941 Å; Ru(1)···C(20): 3.793 Å). This interaction is optimized by pointing of the C(19)-C(24) phenyl toward the hydride as shown by two small torsion angles between the hydride and the phenyl hydrogen (H(1)-Ru(1)-P(2)-C(19) = 19.9°; Ru(1)-P(2)-C(19)-C(20) = 0.1°). In **(31)**, intramolecular H···H interaction is observed within the X-ray structure between H(41) and the hydride H(99) (H(99)···H(41):

2.038 Å; Ru(1)···C(41): 3.730 Å) This interaction is optimized by a pointing of the C(19)-C(24) phenyl toward the hydride as shown by two small torsion angles between the hydride and the phenyl hydrogen (H(99)-Ru(1)-P(2)-C(40) = 0.8°; Ru(1)-P(2)-C(40)-C(41) = 37.1°), and an another H···H interaction is observed between one of the IMes methyl proton H(12c) and the hydride H(99) (Hydride···H: 2.178 Å; Ru···C(Ph): 4.350 Å). Finally, there is an intramolecular H···H interaction in the X-ray structure of **(32)** between H(31) and the hydride H(99) (H(99)···H(31): 2.080 Å; Ru(1)···C(41): 3.751 Å); this interaction is optimized by pointing of the C(26)-C(31) phenyl toward the hydride as shown by two small torsion angles between the hydride and the phenyl hydrogen (H(99)-Ru(1)-P(2)-C(26) = 26.9°; Ru(1)-P(2)-C(26)-C(31) = 0.7 °).

In the structures of **(26)**, **(27)**, **(31)**, and **(32)** a recurrent structural factor is observed. This factor, described by the angle γ in **Figure 5.17.**, is observed in all the hydridic structures **[Table 5.9.]**. The peculiarity of this factor lies in the fact that it is unexpected that the Ru-C-imidazole angle would be anything other than 0°.

Structure	γ [°]
(26)	9.12
(27)	5.77
(31)	14.38
(32)	17.94

Table 5.9. - *Ru-H···H-CH_2 / Ru···CH_3 distances in ruthenium hydrido complexes.*

5.2.4. Reactivity of (26) and (30) toward CO insertion.

5.2.4.1. Ru(IMes)(CO)$_3$(PPh$_3$) (36)

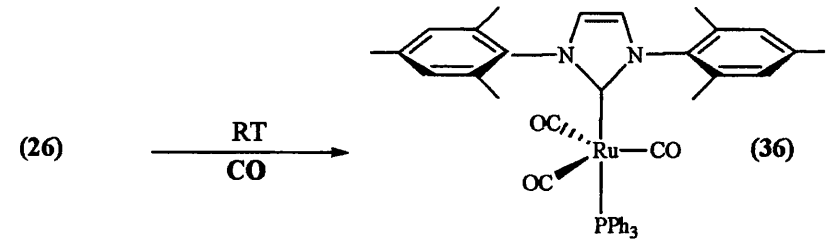

Scheme 5.45.

Ru(IMes)(PPh$_3$)$_2$(CO)H$_2$ was stirred under an atmosphere of CO in toluene for 12 hr at room temperature to afford **(36)** in a 77% isolated yield **[Scheme 5.45.]**. The $^{31}P\{^1H\}$ NMR spectrum of **(36)** showed a single resonance at 60.6 ppm. Examination of the $^{13}C\{^1H\}$ NMR spectrum of **(36)** showed a doublet resonance at 211.7 ppm (J_{C-P} = 16.6 Hz) for the three equivalent CO ligands and a doublet at 185.5 ppm (J_{C-P} = 64.9Hz) for the carbene carbon. The IR spectrum shows a single very intense band at 1889 cm^{-1}, the low frequency being consistent with a Ru^0 oxidation state.

The full molecular geometry of **(36)** was elucidated by X-ray crystallography **[X-Ray 5.6.]**. Selected bond distances and bond angles are available in **Table 5.10.** The structure displays a trigonal-bipyramidal geometry with the phosphine and carbene ligands in the axial sites. The **Ru-CO** distances are in the range of values reported by Chaudret et al[105] for Ru(CO)$_3$(PPh$_3$)$_2$. The Ru environment in **(36)** can be compared to those of similar ruthenium species **[Table 5.11.]** and to that of Os in Os(CO)$_3$(PPh$_3$)$_2$[106] and to Fe in Fe(CO)$_3$(P(OMe)$_3$)$_2$.[107] The most noticeable difference in these complexes is the OC-Ru-CO angle. In the Os complex, the ideal 120°C values are imposed by crystallographic symmetry and in the Fe complex, the C-Fe-C angles are equal to 120° in the 3σ limits. In the structure of **(36)** these have significantly different values of 120.66(12), 110.28(11) and 128.54(12). These unsymmetrical values are observed in similar complexes of ruthenium **[Table 5.11.]**.[105,108]

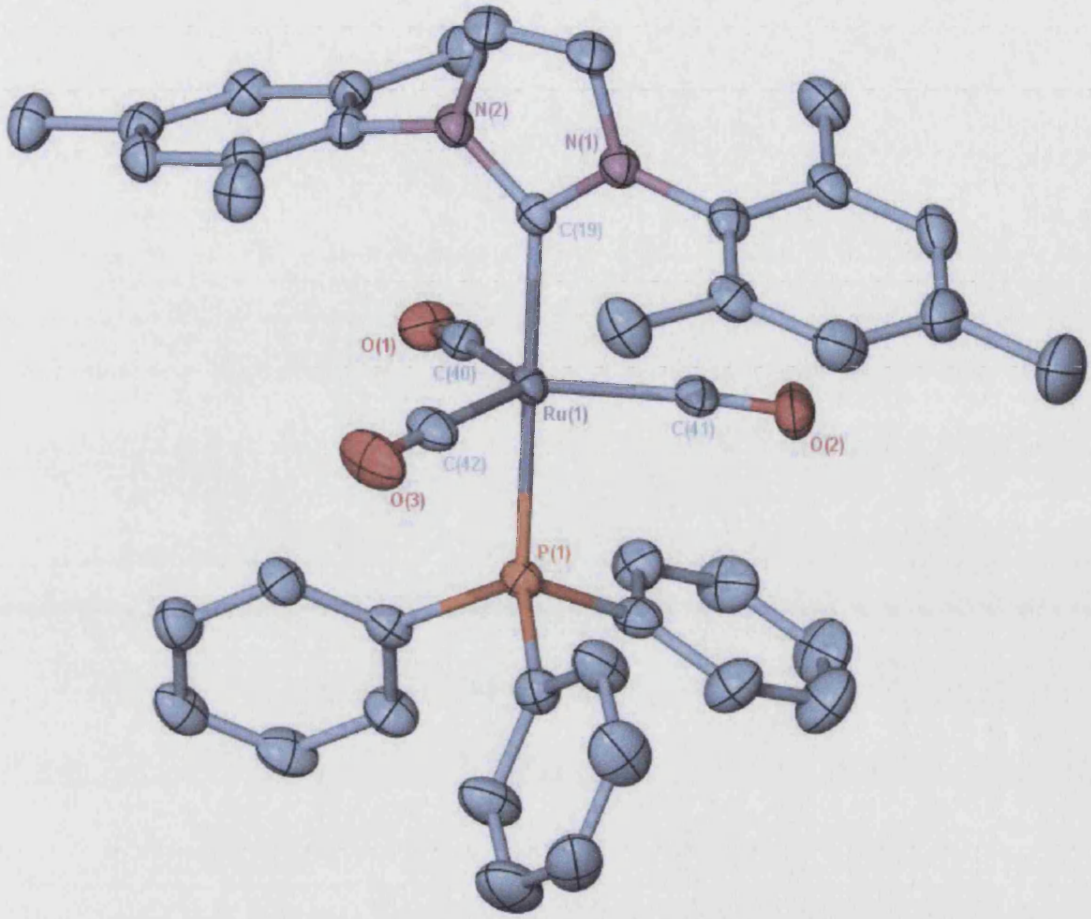

X-Ray 5.6. - *X-Ray structure of $Ru(PPh_3)(IMes)(CO)_3$. The ellipsoids are represented at 50% of the occupancy, and the hydrogens have been removed for clarity.*

Selected Bond Lengths	[Å]	Selected Bond Angles	[°]
Ru(1)-C(42)	1.906(3)	C(42)-Ru(1)-C(40)	120.66(12)
Ru(1)-C(41)	1.924(2)	C(40)-Ru(1)-C(41)	110.28(11)
Ru(1)-C(40)	1.918(3)	C(42)-Ru(1)-C(41)	128.54(12)
O(1)-C(40)	1.157(3)	C(19)-Ru(1)-P(1)	174.77(6)
O(2)-C(41)	1.156(3)	N(2)-C(19)-N(1)	102.70(19)
O(3)-C(42)	1.160(3)		
Ru(1)-C(19)	2.111(2)		
Ru(1)-P(1)	2.3340(6)		

Table 5.10. - *Selected bond distances [Å] and bond angles [°] for* ***(36)****.*

$Ru(CO)_3L_2$	Bonds [Å]			Angles [°]	
L	Ru-C	C-O	Ru-P	C-Ru-C	P-Ru-P
PPh_3	1.895 (10)	1.079 (10)	2.332 (2)	127.9 (4)	175.73 (7)
	1.880 (10)	1.138 (12)	2.330 (2)	117.3 (4)	
	1.925 (8)	1.138 (12)		114.7 (4)	
$P(Ph_2)(C_4H_3S)$	1.917 (2)	113.6 (2)	2.321 (5)	118.28 (6)	174.50 (2)
	1.92.6 (2)	114.5 (3)	2.321 (5)	123.45 (11)	
	1.92.6 (2)	114.5 (3)		118.28 (6)	

Table 5.11. - *Selected bond distances [Å] and bond angles [°] for various tricarbonyl complexes of ruthenium.*

The formation of **(36)** from **(26)** proceeds via the formation of a dicarbonyl intermediate $Ru(PPh_3)(IMes)(CO)_2H_2$ **(34) [Spectrum 5.16.]**. Addition of 1 atm ^{13}CO to a d^8-toluene solution of **(26)** in a resealable NMR tube rapidly afforded a species identified as **(34)**. This shows a singlet phosphorus resonance at 61.4 ppm while the proton spectrum displays a doublet at -6.53 (J_{HP} = 26.8 Hz) integrating as 2H relative to the methyls and the NCH=CHN signals of the IMes group **[Spectrum 5.16.]**. No attempt was made to isolate this intermediate species but NMR similarities with the other dicarbonyl dihydride complexes such as $Ru(PPh_3)_2(CO)_2H_2$ (^1H: δ -4.3ppm, J_{P-H}=23.5Hz) confirmed the identity. **(34)** then reacts further to afford **(36)**, as seen by a of the hydride resonance for **(34)**. There is ample precedent for this type of process.[109]

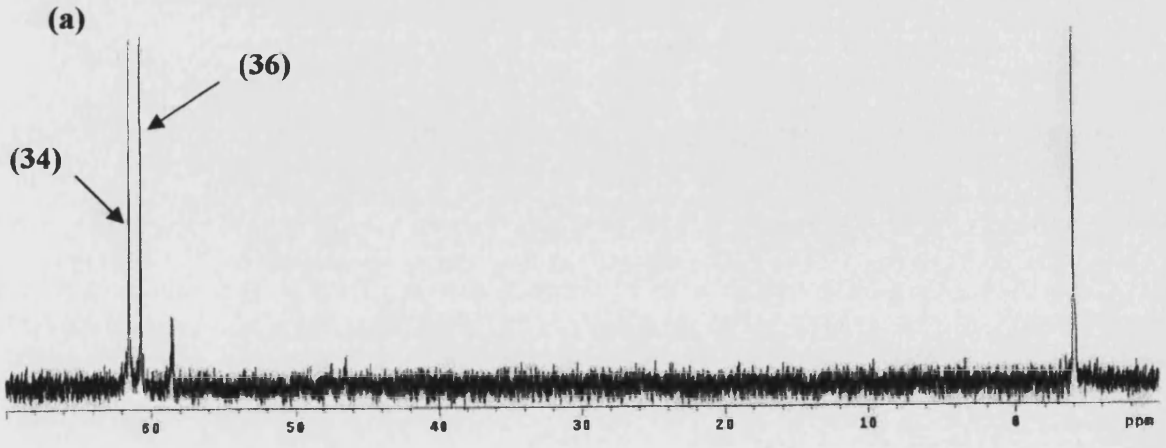

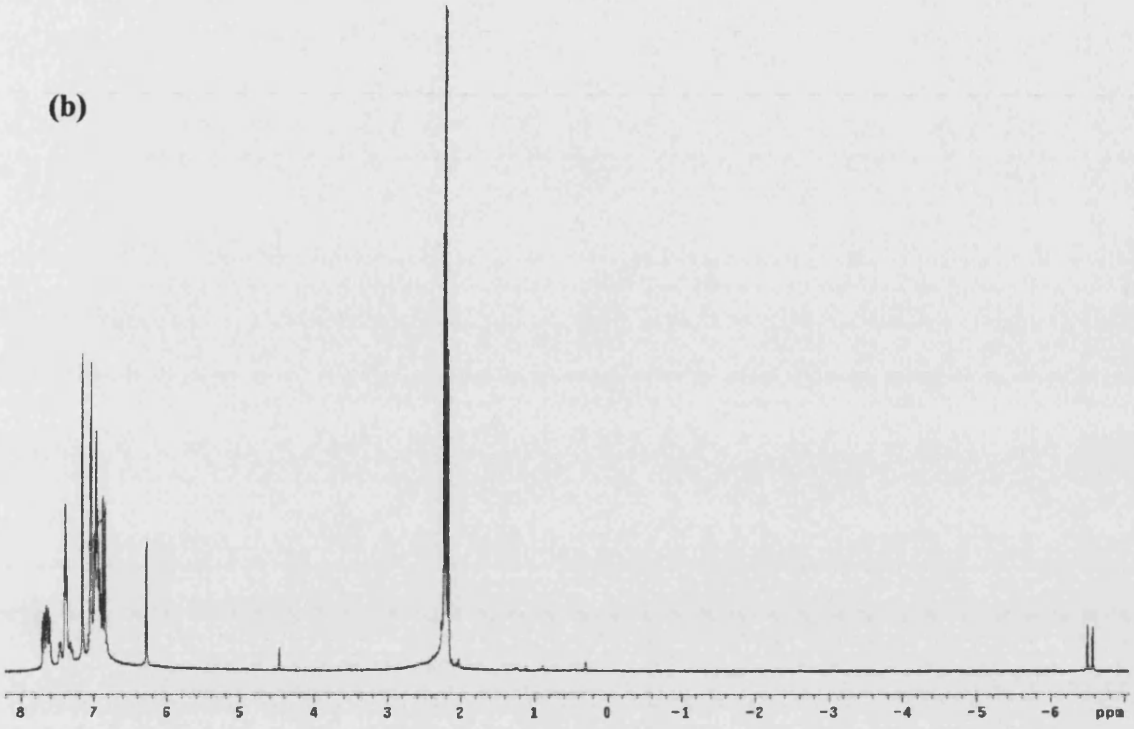

Spectrum 5.15. – ***(a)*** *$^{31}P\{^{1}H\}$ NMR spectrum of the reaction mixture of the reaction between* ***(26)*** *and CO, 5 min after CO admission. Showing rapid formation of* ***(34)*** *and* ***(36)****.* ***(b)*** *^{1}H NMR spectrum of* ***(34)****.*

5.2.4.2. Ru(IMes'-H)(CO)$_3$(PPh$_3$) (37)

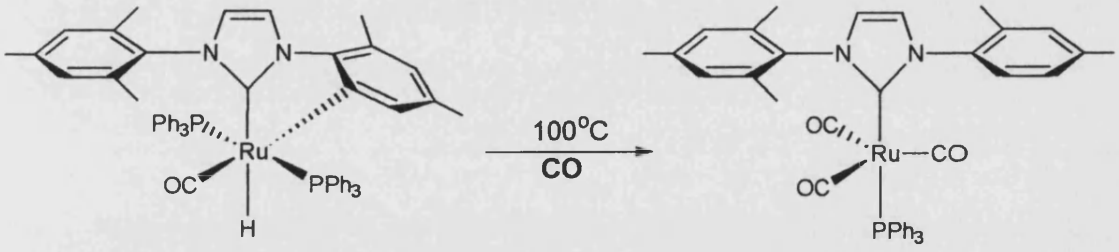

(30) **(37)**

Scheme 5.46.

In the same manner as seen for **(26)**, **(30)** reacts with CO to generate Ru(PPh$_3$)(IMes')(CO)$_3$. The reaction proceeds at a somewhat higher temperature (100°C) compared to the one described earlier and for a longer period of time (4 days) **[Scheme 5.46.]**. Nevertheless, **(37)** could be isolated in 71% yield. $^{31}P\{^{1}H\}$ NMR spectroscopy showed the expected singlet resonance at 65.5 ppm.

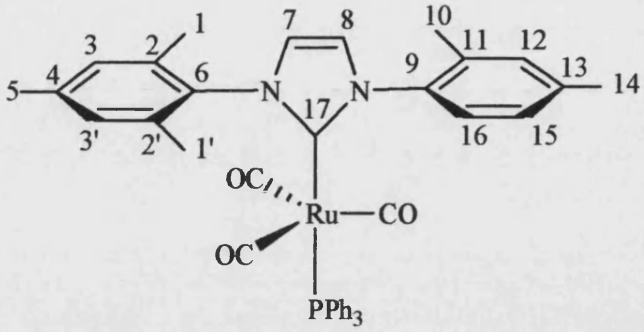

Figure 5.18. - *NMR assignment of the proton and carbon atoms of (37).*

The proton spectrum of (37) confirms the presence of an unsymmetrical carbene ligand on the complex **[Spectrum 5.16.]**. This is shown from the five methyl resonances at 2.27 (H-*14*), 2.20 (H-*5*), 2.13 (H-*10*), 2.10 (H-*1* or H-*1'*), and 2.09 (H-*1* or H-*1'*). The two backbone protons H-7 and H-8 appear to be inequivalent due to the asymmetry of the carbene and their resonances appear at 6.46 (J_{H-H} = 1.9 Hz), 6.24 (J_{H-H} = 1.83 Hz). The $^{13}C\{^1H\}$ shows a signal at 211.6 ppm (J_{C-P} = 16.18 Hz) with *cis* coupling to phosphine for the carbonyl resonance, and a signal at 185.8 ppm (J_{C-P} = 64.4 Hz) showing *trans* coupling to phosphine for the carbene carbon C-8. The IR spectrum shows two carbonyl bands at 1886 and 1864 cm^{-1}, instead of one in the case of related complexes. The two bands observed can be attributed to a lowering of the symmetry in **(37)** due to the unsymmetrical carbene moiety.

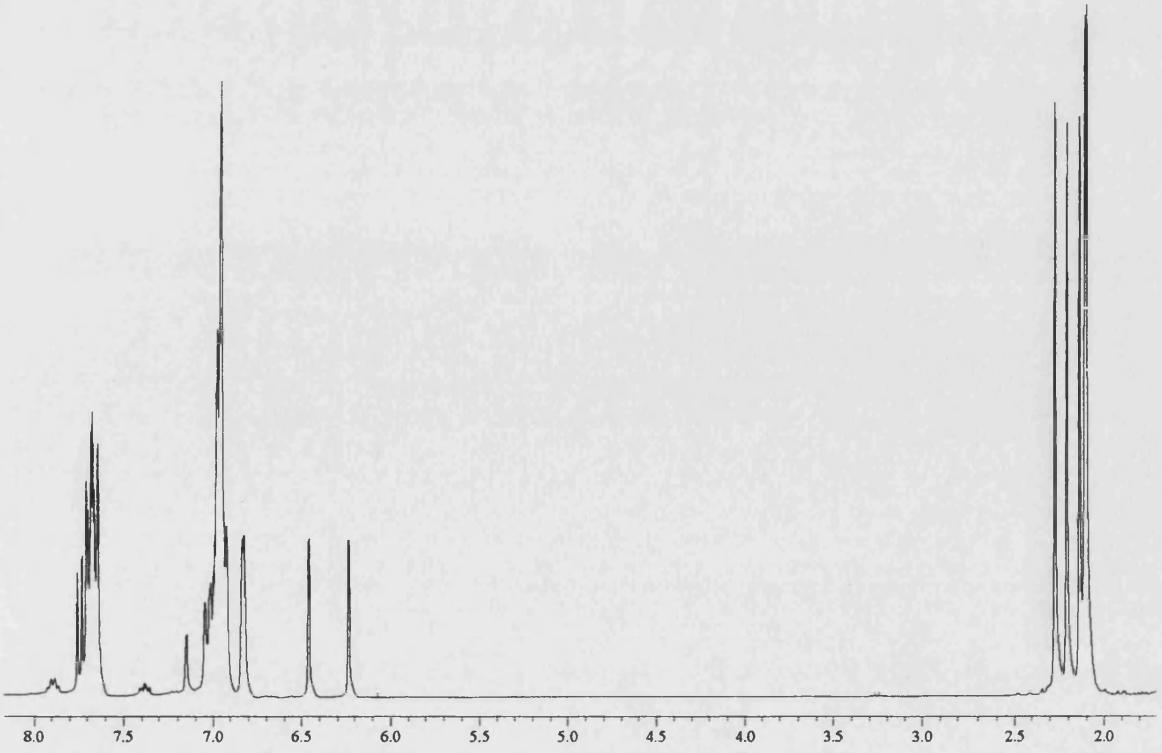

Spectrum 5.16. - *^1H NMR spectrum of (37)*

The full molecular geometry of **(37)** was elucidated by X-ray crystallography **[X-Ray 5.7.]**. Selected bond distances and bond angles are available in **Table 5.12.**. The structure of **(37)** has trigonal-bipyramidal geometry with the phosphine and carbene ligands at the apices. The Ru-C distances are within the range of expected values already seen for **(36)**, with the Ru-C(1-3) bond distances in the same range of values (~1.91 Å) and consequently the C-O bonds are of the same magnitude (~1.15 Å).

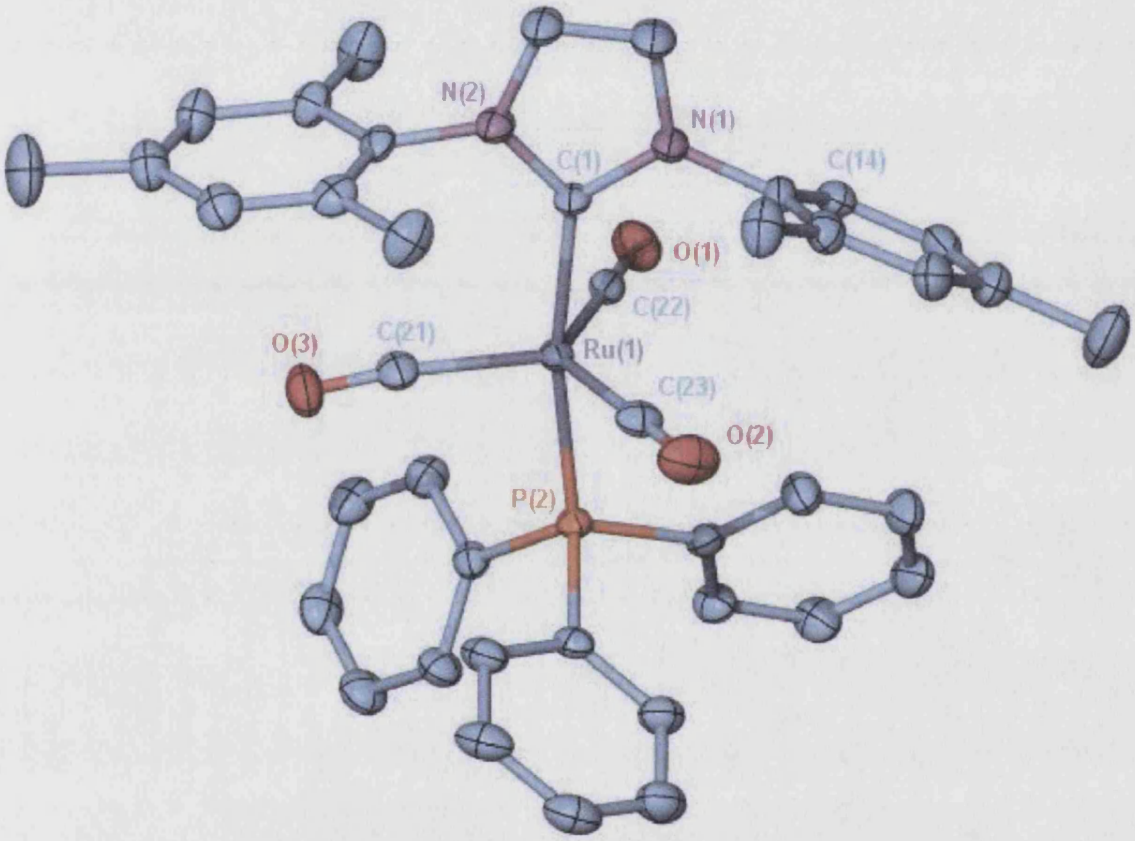

X-Ray 5.7. - *X-Ray structure of Ru(IMes')(CO)$_3$(PPh$_3$). The ellipsoids are represented at 50% of the occupancy, and the hydrogens have been removed for clarity.*

Selected Bond	(Å)	Selected Angle	(°)
Ru(1)-C(21)	1.910(2)	C(21)-Ru(1)-C(22)	115.96(10)
Ru(1)-C(22)	1.902(2)	C(23)-Ru(1)-C(22)	114.26(10)
Ru(1)-C(23)	1.934(2)	C(23)-Ru(1)-C(21)	129.60(10)
O(1)-C(21)	1.154(3)	C(**4**)-Ru(1)-P(1)	169.06(6)
O(2)-C(22)	1.150(3)	N(2)-C(**4**)-N(1)	103.48(17)
O(3)-C(23)	1.160(3)		
Ru(1)-C(1)	2.104(2)		
Ru(1)-P(2)	2.3282(5)		

Table 5.12. - *Selected bond distances [Å] and bond angles [°] for (37).*

The reaction pathway from **(30)** to **(37)** is quite slow and could be monitored easily by NMR spectroscopy. The reaction has been shown to proceed via the formation of a cyclometalated species **(35)** bearing two *cis* carbonyls and a hydride *trans* to the remaining phosphine ligand, which finally generates **(37)** **[Scheme 5.47.]**. In a first step loss of one of the phosphine ligands is observed by $^{31}P\{^{1}H\}$ NMR. This loss is probably due to the substitution by CO to generate the intermediate **(35a)**, which then isomerizes to **(35)**. **(35)** was seen as a perfectly stable intermediate and was characterized by $^{31}P\{^{1}H\}$, ^{1}H, and ^{31}P-^{1}H HETCOR NMR. The proton spectrum **[Spectra 5.17.]** of **(35)** is characterized by a doublet hydride resonance at δ -7.00 (J_{P-H} = 82 Hz) showing a *trans* coupling to phosphorus and by five inequivalent methyl resonances at 2.41, 2.38, 2.30, 2.21 and 1.47 ppm. Over time, depletion of the signal of **(35)** was observed with appearance of the final product **(37)**.

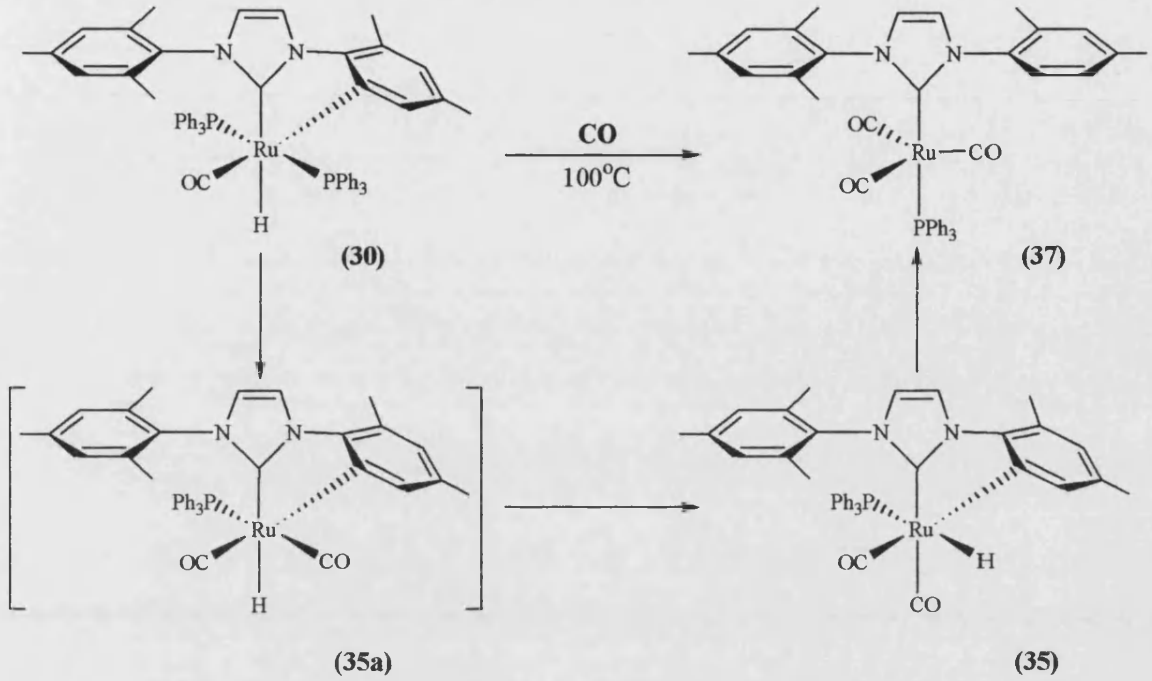

Scheme 5.47. - *Proposed reaction mechanism for the formation of (37).*

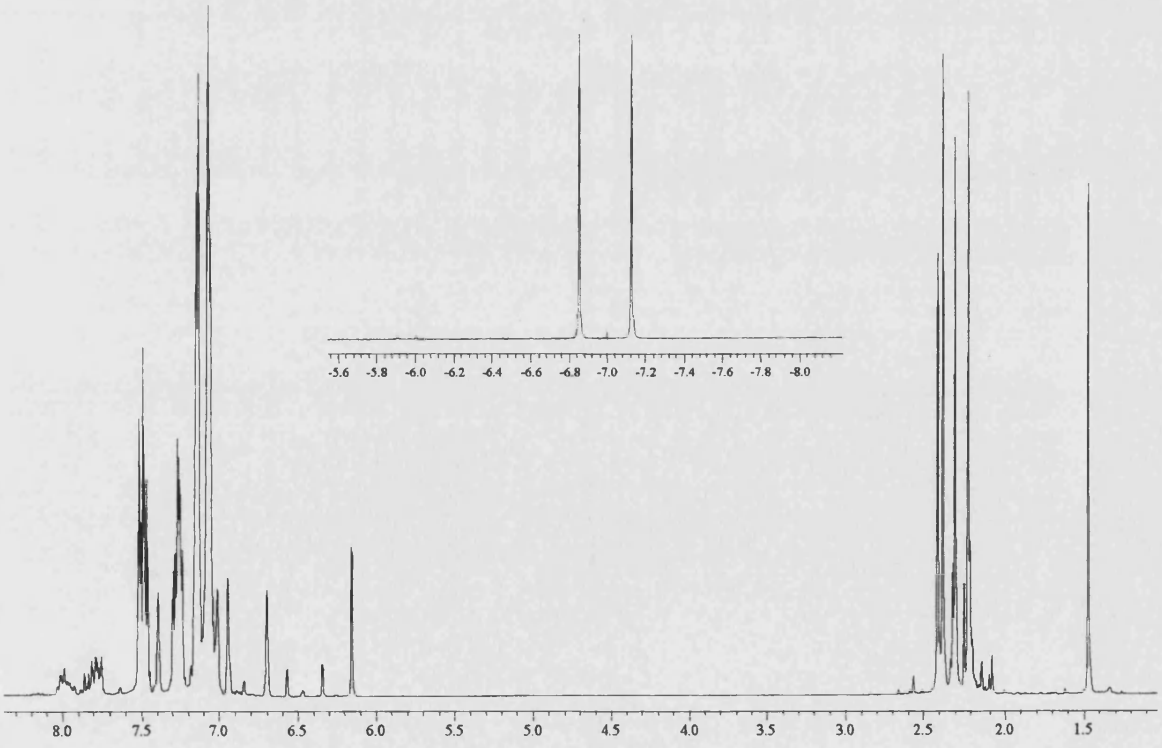

Spectrum 5.17. - *^{1}H NMR spectrum of (35)*

5.3. Conclusions

Thermolysis of **(1)** with IMes has been shown to afford **(26)** which could be isolated as a pure material. Thermolysis of **(26)** in the presence of IMes resulted in the formation of the biscarbene complex **(29)** prior to C-C activation of an Ar-CH_3 bond in one of the mesityl rings of the carbene ligand to afford **(30)**. Upon addition of alkene to a solution of **(26)**, C-H bond activation was observed instead. Extensive H/D exchange was observed on the pathway to C-C activation in d^6-benzene, while no similar H/D exchange and subsequent C-C bond activation was observed upon using d^8-THF under the same condition, suggesting the importance of solvent activation on the pathway to C-C activation. The thermodynamics of these C-C and C-H cleavage reactions have been probed using density functional theory, and it was shown that the C-C bond activation is thermodynamically more favourable than insertion into a C-H bond. Attempts to extend this study to related bidentate phosphine complexes led to the synthesis of **(27)**-(dppp) and **(28)**-(arphos), both showed no activity for C-C bond activation. It was found that **(27)** displayed similar reactivity to **(26)** toward C-H bond activation to afford **(31)** in the presence of alkene, while **(28)**, due to the hemilabile nature of arphos, resulted in several unisolated species. The use of bidentate phosphine has demonstrated the necessity of phosphine to come off in order for C-C activation to be observed. Finally the stoichiometric reactivity of **(26)** and **(30)** towards CO has been studied affording the tricarbonyl species **(36)** and **(37)**.

In conclusion, the first example of intramolecular C-C bond activation of an *N*-heterocyclic carbene has been demonstrated. At this stage the mechanism of this C-C activation has not yet been fully understood, but further investigations are currently in hand.

5.4. References

1. Gosalvi, L.; Adam, H.; Sunley, G. S.; Ditzel, E.; Haynes, A. J. Am. Chem. Soc., **2002**, *124*, 13597.
2. Noyori, R.; Ohkuma, T. *Angew. Chem. Int. Ed.*, **2001**, *10*, 10.
3. Su, R. Q.; Nguyen, V. N.; Mullen, T. E. *Topics in Catal.*, **2003**, *22*, 23.
4. Vora, K. P.; Lochow, C. F.; Miller, R. G. *J. Organomet Chem.*, **1980**, *192*, 257.
5. Hartung, J.; Greb, H. *J. Organomet. Chem.*, **2002**, *67*, 661.
6. See for example: Naota, T.; Takaya, H.; Murahashi, S.-I. *Chem. Rev.*, **1998**, *98*, 2599.
7. **(a)** Kakuishi, F.; Murai, S. "*Topics in Organometallic Chemistry*", ed. S. Murai, Springer-Verlag, Berlin, **1999**, 47. **(b)** Dyker, G. *Angew. Chem. Int. Ed.*, **1999**, *38*, 1698. **(c)** Trost, B. M.; Toste, F. D.; Pinkerton, A. B. *Chem. Rev.*, **2001**, *101*, 2067. **(d)** Ritleng, V.; Sirlin, C.; Pfeffer, M. *Chem. Rev.*, **2002**, *102*, 1731. **(e)** Shilov, A. E.; Shul'pin, G. B. *Chem. Rev.*, **1997**, *97*, 2879. **(f)**
8. **(a)** Allen, A. D.; Senoff, C. V. *J. Chem. Soc. Chem. Comm.*, **1965**, 621. **(b)** Hidai, M.; Mizobe, Y. *Chem. Rev.*, **1995**, 95, 1115. **(c)** Hay, P. J. "*Transition Metal Hydrides*", ed. A. Dedieu, VCH, New York, **1992**, 309.
9. **(a)** Shilov, A. E.; Shul'pin, G. B. *Chem. Rev.*, **1997**, *97*, 2879. **(b)** Dehand, J.; Pfeffer, M. *Coord. Chem. Rev.*, **1976**, *18*, 327. **(c)** Abicht, H. –P.; Issleib, K. *Ztschr. Chem.*, **1977**, *17*, 1. **(d)** Newkome, G. R.; Puckett, W. E.; Gupta, V. K.; Keifer, G. E., *Chem. Rev.*, **1986**, *86*, 451. **(e)** Evans, D. W.; Baker, G. R.; Newkome, G. R. *Coord. Chem. Rev.*, **1989**, *93*, 155.
10. **(a)** Kawano, H.; Tanaka, R.; Fujikawa, T.; Hiraki, K.; Onishi, M. *Chem. Lett.*, **1999**, 401. **(b)** Cole-Hamilton, D. J.; Wilkinson, G. *Nouv. Jour. Chim.*, **1976**, *1*, 141. (c) Stolzenberg, A. M.; Muetterties, E. L. *Organometallics*, **1985**, *4*, 1739.
11. **(a)** Chaudret, B. *J. Organomet. Chem.*, **1984**, *268*, C33. **(b)** Borowski, A. F.; Sabo-Etienne, S.; Christ, M. L.; Donnadieu, B.; Chaudret, B. *Organometallics*, **1996**, *15*, 1427.
12. Kliman, J. P.; Dubeck, M. *J. Am. Chem. Soc.*, **1963**, *85*, 1544.
13. **(a)** Gründemann, S.; Kovacevic, A.; Albrecht, M.; Faller, J. W.; Crabtree, R. H. *Chem. Commun.*, **2001**, 2274. **(b)** Danopoulos, A. A.; Winston, S.; Hursthouse, M. B. J. *Chem. Soc., Dalton Trans.*, **2002**, 2090. **(c)** Hitchcock, P. B.; Lappert, M. F.; Terreros, P. *J. Organomet. Chem.*, **1982**, *239*, C26.

14. **(a)** Ryabov, A. D. *Synthesis*, **1985**, 233. **(b)** Lewis, L. N. *J. Am. Chem. Soc.*, **1986**, *108*, 743. **(c)** Santra, P. K.; Saha, C. H. *J. Mol. Catal.*, **1987**, *39*, 279. **(d)** Bose, A.; Saha, C. H. *J. Mol. Catal.*, **1989**, *49*, 271 **(e)** Sokolov, V. I. *Pure Appl. Chem.*, **1983**, *55*, 1837.
15. **(a)** Shilov, A. E.; Shteinman, A. A. *Coord. Chem. Rev.*, **1977**, *24*, 97. **(b)** Deem, M. L. *Coord. Chem. Rev.*, **1986**, *74*, 101. **(c)** Ephritikhine, M. *Nouv. Jour. Chim.*, **1986**, *10*, 9. **(d)** Rabaa, H.; Saillard, J. -Y.; Hoffmann, R. *J. Am. Chem. Soc.*, **1986**, *108*, 4327.
16. Ryabov, A. D. *Chem. Rev.*; **1990**, *90*, 403.
17. Crabtree, R. *Chem. Rev.*, **1985**, *85*, 245.
18. Halpern, J. *Inorg. Chim. Acta.*, **1985**, *100*, 41.
19. Lavin, M.; Holt, E. M.; Crabtree, R. H. *Organometallics*, **1989**, *8*, 99.
20. Jones, W. D.; Feher, F. J. *J. Am. Chem. Soc.*, **1982**, *104*, 4240.
21. Jones, W. D.; Feher, F. J. *J. Am. Chem. Soc.*, **1985**, *107*, 620.
22. Cope, A. C.; Siekman, R. W. *J. Am. Chem. Soc.*, **1965**, *87*, 3272.
23. Cope, A. C.; Friedrich, E. C. *J. Am. Chem. Soc.*, **1968**, *90*, 909.
24. Ryabov, A. D.; Sakodinskaya, I. K.; Yatsimirsky, A. K. *J. Chem. Soc., Dalton Trans.*, **1985**, 2629.
25. 103-110-117-121
26. Rabinovich, D.; Parkin, G. *J. Am. Chem. Soc.*, **1990**, *112*, 5381.
27. Cole-Hamilton, D. J.; Wilkinson, G. *Nouv. Journ. Chim.*, **1976**, *1*, 141.
28. Diversi, P.; Jacoponi, S.; Ingrosso, G.; Laschi, F.; Lucherini, A.; Zanello, P. *J. Chem. Soc., Dalton Trans.*, **1993**, 35.
29. Albrecht, M.; Dani, P.; Lutz, M.; Spek, A. L.; van Koten, G. *J. Am. Chem. Soc.*, **2000**, *122*, 11822.
30. Toner, A. J.; Gründemann, S.; Clot, E.; Limbach, H.-H.; Donnadieu, B.; Sabo-Etienne, S.; Chaudret, B. *J. Am. Chem. Soc.*, **2000**, *122*, 6777.
31. Watson, P.L.; Roe, D.C.; *J. Am. Chem. Soc.*, **1982**, *104*, 6471.
32. Eshuis, J. J. W.; Tan, Y. Y.; Teuben, J. H.; Renkema, J. *J. Mol. Cat.*, **1990**, *62*, 277.
33. Eshuis, J. J. W.; Tan, Y. Y.; Meetsma, A.; Teuben, J. H. *Organometallics*, **1992**, *11*, 362.
34. Etienne, M.; Mathieu, R.; Donnadieu, B. *J. Am. Chem. Soc.*, **1997**, *119*, 3218.
35. Hartwig, J. F.; Bergman, R. O.; Andersen, R. A. *Organometallics*, **1991**, *10*, 3344.
36. McNeill, K.; Andersen, R. A.; Bergman, R. G. *J. Am. Chem. Soc.*, **1997**, *119*, 11.

37. Milstein, D.; Rybtchinski, B. *Angew. Chem. Int. Ed.*, **1999**, *38*, 870.

38. Crabtree, R. H.; Holt, E. M.; Lavin, M.; Morehouse, S. M. *Inorg. Chem.*, **1985**, *24*, 1986.

39. Murakami, M.; Ito, Y. "*Topics in Organometallic Chemistry*", ed. By S. Murai, Springer-Verlag, Berlin, **1999**, 97.

40. Tipper, C. H. F. *J. Chem. Soc.*, **1955**, 2045.

41. **(a)** Adams, D. M.; Chatt, J.; Guy, R.; Sheppard, N. *J. Chem. Soc.*, **1961**, 738. **(b)** Lenarda, M.; Ros, R.; Graziani, M.; Belluco, U. *J. Organomet. Chem.*, **1974**, *65*, 407. **(c)** Yarrow, D. J.; Ibers, J. A.; Lenarda, M.; Graziani, M. *J. Organomet. Chem.*, **1974**, *70*, 133. **(d)** Hoberg, J. O.; Larsen, R. D.; Jennings, P. W. *Organometallics*, **1990**, *9*, 1334. **(e)** Ikura, K.; Ryu, I.; Ogawa, A.; Sonoda, N.; Harada, S.; Kasai, N. *Organometallics*, **1991**, *10*, 528. **(f)** Hemond, R. C., Hughes, R. P.; Robinson, D. J.; Rheingold, A. L. *Organometallics*, **1988**, *7*, 2239.

42. **(a)** Atkinson, E. R.; Levins, P. L.; Dickelman, T. E. *Chem. Ind.*, **1964**, 934. **(b)** Ros, R.; Lenarda, M.; Pahor, N. B.; Calligaris, M.; Delisa, P.; Randaccio, L.; Graziani, M. *J. Chem. Soc. Dalton*, **1976**, 1937. **(c)** Cassar, L.; Eaton, P. E.; Halpern, J. *J. Am. Chem. Soc.*, **1970**, *92*, 3515.

43. **(a)** Gillard, R.D.; Keeton, M.; Mason, R.; Pilbrow, M. F.; Russell, D. R. *J. Organomet. Chem.*, **1971**, *33*, 247. **(b)** McQuillin, F. J.; Powell, K. G. *J. Chem Soc. Dalton*, **1972**, 2123

44. **(a)** Cassar, L.; Halpern, J. *J. Chem. Soc. Chem. Commun.*, **1970**, 1082. **(b)** Periana, R. A.; Bergman, R. G. *J. Am. Chem. Soc.*, **1986**, *108*, 7346. **(c)** Perthuisot, C.; Jones; V. D. *J. Am. Chem. Soc.*, **1994**, *116*, 3647.

45. Noyori, R.; Nishimura, T.; Takaya, H. *J. Chem. Soc. Chem. Commun.*, **1969**, 89.

46. Eisch, J. J.; Piotrowski, A. M.; Han, K. I.; Kruger, C.; Tsay, Y. H. *Organometallics*, **1985**, *4*, 224.

47. Lu, Z.; Jun, C. H.; de Gala, S. R.; Sigalas, M.; Eisenstein, O.; Crabtree, R. H. *J. Chem. Soc. Chem. Commun.*, **1993**, 1877.

48. Perthuisot, C.; Edelbach, B. L.; Zubris, D. L.; Jones, W. D. *Organometallics*, **1997**, *16*, 2016.

49. Jennings, P. W., Johnson, L. L. *Chem. Rev.*, **1994**, *94*, 2241.

50. Suggs, J. W.; Jun, C. H. *J. Am. Chem. Soc.*, **1986**, *108*, 4679.

51. Eilbracht, P.; Dahler, J. *Organometallics*, **1977**, ***135***, C23.

52. **(a)** Benfield, F. W. S.; Green, M. L. H. *J. Chem. Soc. Dalton Trans.*, **1974**, 1324. **(b)** Kang, J. W.; Moseley, K.; Maitlis, P. M. *J. Am. Chem. Soc.*, **1969**, *91*, 5970.

53. Eilbracht, P.; Dahler, P. *Chem. Ber.*, **1980**, *113*, 542.

54. Hemond, R. C.; Hughes, R. P.; Locker, H. B. *Organometallics*, **1986**, *5*, 2391.

55. Jones, W. D.; Maguire, J. A. *Organometallics*, **1987**, *6*, 1301.

56. **(a)** Crabtree, R. H.; Dion, R. P. *J. Chem. Soc. Chem. Commun.*, **1984**, 1260. **(b)** Crabtree, R. H.; Dion, R. P.; Gibboni, D. J.; McGrath, D. V.; Holt, E. M. *J. Am. Chem. Soc.*, **1986**, *108*, 7222.

57. **(a)** Bennett, M. A.; Nicholls, J. C.; Rahman, A. K. F.; Redhouse, A. D.; Spencer, J. L.; Willis, A. C. *J. Chem. Soc. Chem. Commun.*, **1989**, 1328. **(b)** Nicholls, J. C.; Spencer, J. L. *Organometallics*, **1994**, *13*, 1781.

58. Suzuki, H.; Takaya, Y.; Takemori, T.; Tanaka, M. *J. Am Chem. Soc.*, **1994**, *116*, 10779.

59. Gozin, M.; Weisman, A.; Ben-David, Y.; Milstein, D. *Nature*, **1993**, *364*, 699.

60. **(a)** Liou, S. Y.; Gozin, M.; Milstein, D. *J. Am. Chem. Soc.*, **1995**, *117*, 9774. **(b)** Rybtchinski, B.; Vigalok, A.; Ben-David, Y.; Milstein, D. *J. Am. Chem. Soc.*, **1996**, *118*, 12406.

61. Gandelman, M.; Vigalok, A.; Shimon, L. J. W.; Milstein, D. *Organometallics*, **1997**, *16*, 3981.

62. Shaltout, R. M.; Sygula, R.; Sygula, A.; Fronczek, F. R.; Stanley, G. G.; Rabideau, P. W. *J. Am. Chem. Soc.*, **1998**, *120*, 835.

63. Schwager, H.; Spyroudis, S.; Vollhardt, K. P. C. *J. Organomet. Chem.*, **1990**, *382*, 191.

64. Edelbach, B. L.; Lachicotte, R. L.; Jones, W. D. *J. Am. Chem. Soc.*, **1998**, *120*, 2843.

65. Huffman, M. A.; Liebeskind, L. S. *J. Am. Chem. Soc.*, **1991**, *113*, 2771.

66. Harayama, H.; Kuroki, T.; Kimura, M.; Tanaka, S.; Tamarn, Y. *Angew. Chem. Int. Ed. Engl.* **1997**, *36*, 2352.

67. Murakami, M.; Takahashi, K.; Amii, H.; Ito, Y. *J. Am. Chem. Soc.*, **1997**, *119*, 9307.

68. Liou, S. Y.; van der Boom, M. E.; Milstein, D. *Chem. Commun.*, **1998**, 687.

69. Kocher, C.; Herrmann, W. A. *J. Organomet. Chem.*, **1997**, *532*, 261.

70. Junk, P. C.; Steed, J. W. *J. Organomet. Chem.*, **1999**, *587*, 191.

71. Lee, H. M.; Smith, D. C., Jr.; He, Z.; Stevens, E. D.; Yi, C. S.; Nolan, S. P. *Organometallics,* **2001**, *20*; 794.

72. **(a)** Barrio, P.; Castarlenas, R.; Esteruelas, M. A.; Onate, E. *Organometallics,* **2001**, *20*, 2635. **(b)** Hartwig, J. F.; Bergman, R. G.; Andersen, R. A. *J. Am. Chem. Soc.*, **1991**, *113*, 3404. **(c)** Ozaa, F.; Yamagami, I.; Yamamoto, A. Yamamoto. *J. Organomet. Chem.*, **1994**, *473*, 265. **(d)** Guari, Y. Sabo-Etienne, Chaudret, B. *J. Am. Chem. Soc.*, **1998**, *120*, 4228.

73. Hitchcock, P. B.; Lappert, M. F.; Pye, P. L.; Thomas, S. *J. Chem. Soc. Dalton Trans.*, **1979**, 1929.

74. Gerard, H.; Clot, E.; Eisenstein, O. *New J. Chem.* **1999**, *23*, 495.

75. Huang, J.; Stevens, E. D.; Nolan, S. P. *Organometallics,* **2000**, *19*, 1194.

76. Jones, W. D.; Rosini, G. P.; Maguire, J. A. *Organometallics,* **1999**, *18*, 1754.

77. **(a)** Packett, D. L.; Trogler, W. C. *Inorg. Chem.*, **1988**, *27*, 1768. **(b)** Safarowic, F. J.; Bierdemann, D. J.; Keister, J. B. *J. Am. Chem. Soc.*, **1996**, *118*, 11805.

78. van der Boom, M. E.; Liou, S.-Y.; Ben-David, Y.; Gozin, M.; Milstein, D. *J. Am. Chem. Soc.*, **1998**, *120*, 13415.

79. Calculations used the ADF1999 program with the BP86 functional and incorporated a treatment of relativistic effects. No symmetry constraints were imposed. A triple-ζ-STO basis set was used for Ru and a double-ζ plus polarization STO basis set for all other atoms. The frozen core approximation was applied (Ru:3d; P:2p; C, N, O:1s). **(a)** Baerends, E. J.; Ellis, D. E.; Ros, P. *Chem. Phys.*, **1973**, *2*, 41. **(b)** te Velde, G.; Baerends, E. J. *J. Comput. Phys.*, **1992**, *99*, 84. **(c)** Fonseca Guerra, C.; Snijders, J. G.; te Velde, G.; Baerends, E. J. *Theor. Chem. Acc.*, **1998**, *99*, 391.

80. **(a)** Kawano, H.; Tanaka, R.; Fujikawa, T.; Hiraki, K.; Onishi, M. *Chem. Lett.*, **1999**, 401. **(b)** Jung, C. W.; Garrou, P. E. *Organometallics*, **1982**, *1*, 658.

81. Richardson, T. B.; de Gala, S.; Crabtree, R. H. *J. Am. Chem. Soc.*, *117*, **1995**, 12875.

82. Yi, C. S.; Lee, D. W.; He, Z.; Rheingold, A. L.; Lam, K. -C.; Concolino, T. E. *Organometallics*, **2000**, *19*, 2909.

83. Chaudret, B.; Devillers, J.; Poilblanc, R. *Organometallics*, **1985**, *4*, 1727.

84. Siedle, A. R.; Newmark, R. A.; Pignolet, L. H.; Wang, D. X. Albright, T. A. *Organometallics*, **1986**, *5*, 38.

85. Huh, S.; Kim, Y.; Park, T.–J.; Jun, M.-J. *Acta, Crystallogr., Sect. C (Cr. Str. Comm.)*, **1999**, *55*, 850.

86. Motevalli, M.; Hursthouse, M. B.; Barron, A. R.; Wilkinson, G. *Acta, Crystallogr., Sect. C (Cr. Str. Comm.)*, **1987**, *43*, 214.

87. Huang, J.; Li, C.; Nolan, S. P.; Petersen, J. L. *Organometallics*, **1998**, *17*, 3516.

88. Hussein, K.; Marsden, C. J.; Barthelat, J.-C.; Rodriguez, V.; Conejero, S.; Sabo-Etienne, B.; Chaudret, B. *Chem. Commun.*, **1999**, 1315.

89. Skapski, A. C.; Stephens, F. A. *J. Chem. Soc., Dalton, Trans.*, **1974**, 390.

90. Albinati, A.; Klooster, W. T.; Koetzle, T .F.; Fortin, J. B.; Ricci, J. S.; Eckert, J.; Fong, T. P.; Lough, A. J.; Morris, R. H.; Golombek, A. P. *Inorg. Chim. Acta.*, **1997**,*259*, 351.

91. Klooster, W. T.; Koetzle, T. F.; Guocchen Jia, Fong, T. P.; Morris, R. H.; Albinati, A. *J. Am. Chem. Soc.*, **1994**, *116*, 7677.

92. Delpesh, F.; Sabo-Etienne, S.; Daran, J.-C.; Chaudret, B.; Hussein, K.; Marsden, C. J.; Barthelat, J.-C. *J. Am. Chem. Soc.*, **1999**, *121*,6668.

93. Lee, H. M.; Smith Junior, D. C.; He, Z.; Stevens, E. D.; Nolan, S. P. *Organometallics*, **2001**, *20*, 794.

94. Delpech, F.; Sabo-Etienne, S.; Donnadieu, B.; Chaudret, B. *Organometallics*, **1998**, *17*, 4926.

95. Rodriguez, V.; Atheaux, I.; Donnadieu, B.; Sabo-Etienne, S.; Chaudret, B., *Organometallics*, **2000**, *19*, 2916.

96. Siedle, A. R.; Newmark, R. A.; Pignolet, L. H.; Wang, D. X.; T. A. Albright. *Organometallics*, **1986**, *5*, 38.

97. Cotot, A.; Tenerio, M. J.; Puerta, M. C.; Valerga, P. *Organometallics*, **1998**, *17*, 4392.

98. Hsu, G. C.; Kosar, W. P.; Jones, W. D. *Organometallics*, **1994**, *13*, 385.

99. de los Rios, I.; Tenorio, M. J.; Tenerio, M. J.; Puerta, M. C.; Valerga, P. *J. Am. Chem. Soc.*, **1996**, *15*, 4565.

100. Homanen, P.; Haukka, M.; Pakkanen, T. A.; Pursiainen, Laitinen, R. H. *Organometallics*, **1996**, *15*, 4081.

101. Grunwald, C.; Gevert, O.; Wolf, J.; Gonzalez-Herrero, P.; Werner, H. *Organometallics*, **1996**, *15*, 1960.

102. Huang, D.; Koren, P. R.; Folting, K.; Davidson, E. R.; Caulton, K. G. *J. Am. Chem. Soc.*, **2000**, *122*, 8916.

103. Gusev, D. G.; Dolgushin, F. M.; Antipin, M. Y. *Organometallics*, **2000**, *19*, 3429.

104. de los Rios, I.; Tenorio, M. J.; Puerta, M. C.; Valerga, P. *J. Am. Chem. Soc.*, **1997**, *119*, 6529

105. Dahan, F.; Sabo, S.; Chaudret, B. *Acta Cryst. Sec. C*, **1984**, *40*, 786.

106. Stalick, J. K.; Ibers, J. A. *Inorg. Chem.*, **1969**, *8*, 419.

107. Ginderow, P. A. *Acta. Cryst. Sec. B*, **1974**, *B30*, 2798.

108. Cenini, S.; Porta, F.; Pizzotti, M. *Inorg. Chim. Acta*, **1976**, *20*, 119. **(b)** Lee, C.-L.; Chisholm, J.; James, B.R.; Nelson, D.A.; Lilga, M.A. *Inorg. Chim. Acta*, **1986**, *30*, L7-L10.

109. **(a)** Mawby, R. J.; Perutz, R. N.; Whittlesey, M. K. *Organometallics*, **1995**, *14*, 3268. (b) Whittlesey, M. K.; Perutz, R. N.; Virrels, I. G.; George, M. W. *Organometallics*, **1997**, *16*, 268.

Chapter 6.

Bis N-heterocyclic carbene complexes of ruthenium.

6.1. Introduction.

Complexes containing bonds between late transition metals and heteroatoms such as nitrogen, oxygen and sulfur have been identified as playing key roles in both biological processes[1] (e.g. Fe-S in nitrogenase, Fe-OH in lipoxygenase) and catalytic reactions, such as alkene oxidation (Wacker process)[2] and hydroamination.[3] For second and third row metals, hard-soft acid-base (HSAB) theory predicts an energetic mismatch between the 'soft' metal and 'hard' anionic N and O ligands, which imparts the resulting metal alkoxo, hydroxo and amido complexes with exceptionally interesting physical and chemical properties.[4] For example, the hydroxo and parent amido complexes *trans*-$Ru(dmpe)_2(OH)H$ and *trans*-$Ru(dmpe)_2(NH_2)H$ display remarkable basicities (pK_a values of the aqua and ammonia complexes are ca. 22 and 32 respectively),[5] while C_2H_4 insertion into the Ir-OH bond in $Cp^*Ir(PMe_3)Ph(OH)$ occurs under unexpectedly mild conditions.[6]

In recent years, there has been an increase in the number of examples of well-characterised M-X (X = O, N) complexes, largely because of the development of more general and reliable routes to their synthesis.[7] This has allowed structure/bonding/reactivity relationships to be investigated along with the role of $p\pi$-$d\pi$ interactions, correlation of M-X and H-X bond strengths and fundamental chemical reactivity towards organic substrates to be studied in more detail.[8] Much of this work has utilised complexes containing carbocyclic rings (arene, cyclopentadienyl) and/or phosphines as ancillary ligands, and hence, the influence of steric and electronic factors on the chemistry of M-X bonds remains generally unexplored.

We have seen in **Chapter 5** that thermolysis of $Ru(PPh_3)_3(CO)H_2$ with IMes (IMes = bis(1,3-(2,4,6-trimethylphenyl)imidazol-2-ylidene) at > 100°C results in the unprecedented C-C bond activation of an unstrained sp^2-sp^3 hybridised C-C bond of the IMes ligand via the intermediate bis-carbene complex $Ru(IMes)_2(PPh_3)(CO)H_2$. In an attempt to find milder conditions for this transformation, we turned to the triphenylarsine precursor $Ru(AsPh_3)_3(CO)H_2$. This complex displayed remarkably different reactivity towards IMes than the phosphine analogue, affording under the same reaction conditions *trans*-dihydride ethanol and water complexes of ruthenium, devoid of arsine ligands and stabilised by the presence of two bulky NHC ligands. The Ru-OH_2 and the Ru-OHEt bonds prove reactive to a range of small molecules (CO, CO_2, CH_3CN) and provide a route to stable products containing Ru-O, Ru-N, Ru-S, Ru-F and Ru-Cl linkages. The results depicted in this chapter are consequential to the investigation of the chemistry of the

biscarbene complexes of ruthenium. These led to a large number of results being obtained due to the fascinating activity that these complexes displayed.

Interestingly there are very few bis-carbene complexes reported in the literature. Nevertheless, these examples cover a wide range of metal centres throughout the periodic classification involving metal such as metal such as Pd,[9] Ru,[10] Fe,[11] U,[12] Ni,[13,14] Pt,[14] Cu,[15] Ag,[15] Au,[16] and Hg,[17] Rh,[18] Y.[19] The first example of bis-carbene complexe was reported by Wanzlick and Öfele in 1968, with the synthesis of the mercury complex shown in **Scheme 6.1.**.[20]

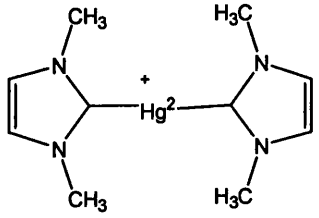

Scheme 6.1.

The first fully characterized bis-carbene complexes were reported by Arduengo et al in 1993 and involved the synthesis of bis-carbene complexes containing Ag, Cu, Au.[21] This work was later extended to Ni and Pt **[Scheme 6.2.]**.[22]

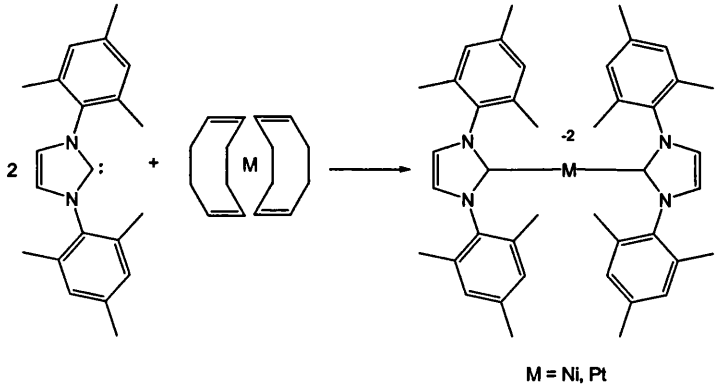

Scheme 6.2.

X-ray crystallography studies of these complexes have shown that a near linear geometry at the metal centre is observed, with a relative twist from coplanarity mainly due to the bulk of the mesityl ring.

Further examples reported by Herrmann et al describe the synthesis and catalytic use of a bis carbene complex of Pd.[23] The main difference with respect to the Arduengo examples lies in the *cis* stereochemistry of the carbenes **[Scheme 6.3.]**.

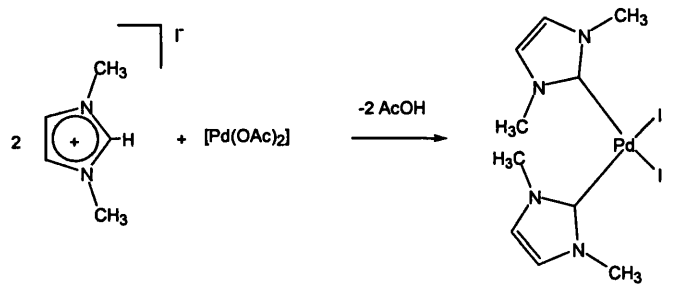

Scheme 6.3.

In another example reported by these a bis-carbene derivatives of the Grubbs catalyst has been isolated **[Scheme 6.4.]**.[24]

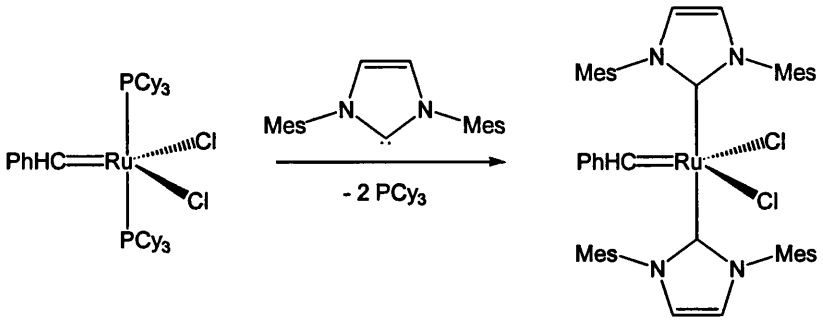

Scheme 6.4.

These display moderate catalytic activity toward ROMP and RCM, due to the steric effects and the poor lability of the carbene ligands.

Surprisingly, bis carbene complexes containing even bulkier carbenes were synthetised by Hermann et al[25] using the very bulky 1,3-Bis(adamantylimidazolin)-2-ylidene. In this case, a *trans* configutation of the carbenes was observed, due to the bulk of the adamantyl carbene **[Scheme 6.5.]**.

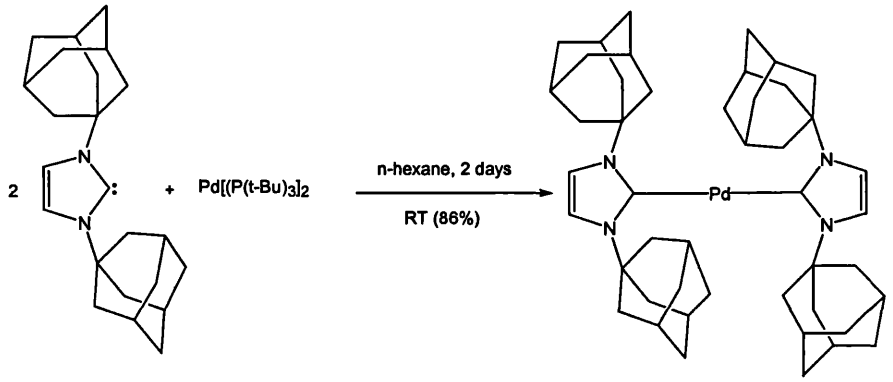

Scheme 6.5.

Here again catalytic activity was observed, and high TOF (1100) was reported for the Suzuki cross-coupling of aryl chlorides at room temperature under mild conditions.

To summarize, very little is known about transition metal bis-carbene complexes, and even less bis-carbene complexes of ruthenium have been fully characterised. Nevertheless amongst the very few examples reported, promising catalytic activities have been described for numerous reactions such the ROMP,[26] Suzuki cross coupling,[27] Heck coupling,[28] and atom transfer polymerization[29] just to name a few.

6.2. Results.

6.2.1. Synthesis of $Ru(IMes)_2(L)(CO)(H_2)$ [L = EtOH (39), H_2O (40), MeOH (41), *p*-$EtO(C_6H_4)OH$ (42)

6.2.1.1. Synthesis of $Ru(IMes)_2(EtOH)(CO)(H_2)$

The reaction of $Ru(AsPh_3)_3(CO)H_2$ **(9)** with 3-4 equivalents of IMes overnight at 70°C afforded a mixture of unreacted starting material and the bis-carbene complex $Ru(AsPh_3)(IMes)_2(CO)H_2$ **(38) [Spectrum 6.1.]**.

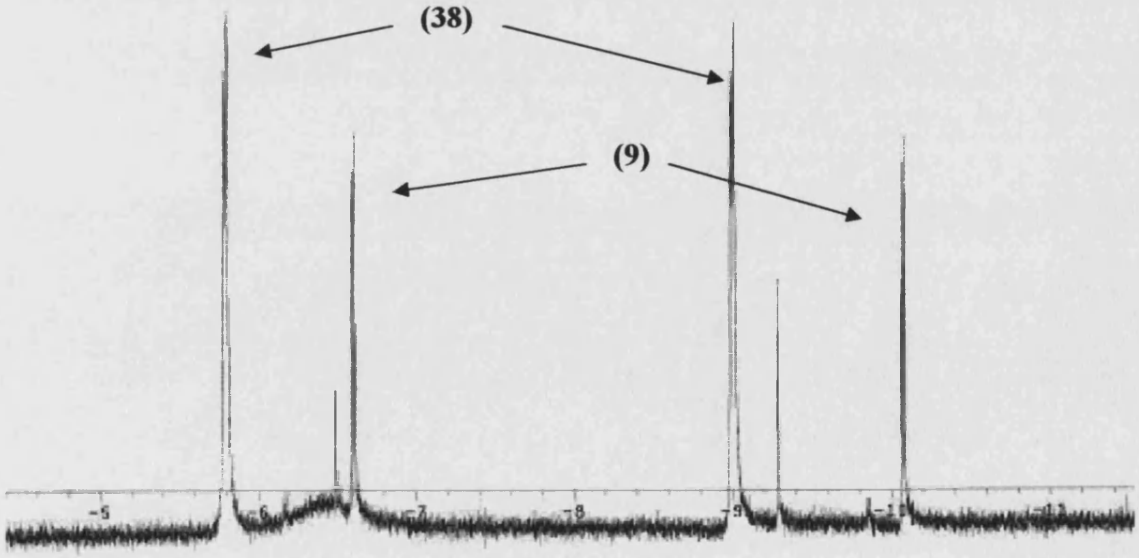

Spectrum 6.1. - *^1H spectrum of the formation of **(38)** upon reaction of **(9)** with IMes for 1 day at 70°C.*

None of the mono-substituted $Ru(AsPh_3)_2(IMes)(CO)H_2$ were detectable by ^1H NMR.

Prolonged heating for 4 days gave a solution containing only **(38)**, which displayed two doublets in the hydride region of the ^1H NMR spectrum (δ -5.71 and -8.93, J_{HH} = 5.9 Hz), consistent with the *cis*-RuH_2 stereochemistry shown in **Scheme 6.6.**, and a single methyl resonance (δ 2.15) integrating in a ratio of 1:1:36.

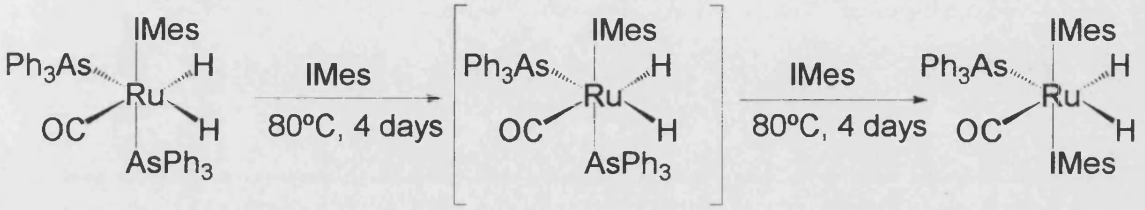

Scheme 6.6.

Two low field resonances at δ 202.8 and 197.1 in the $^{13}C\{^1H\}$ NMR spectrum were assigned to the presence of Ru-CO and Ru-C(carbene) respectively. Attempts to isolate this bis-carbene complex by crystallisation from ethanol gave instead $Ru(IMes)_2(CO)(EtOH)H_2$ **(39)**, in which the triphenylarsine ligand had been displaced by ethanol **[Scheme 6.7.]**. Complex **(39)** was isolated in 78% yield as an air-sensitive yellow microcrystalline solid **[Spectrum 6.2.]**.

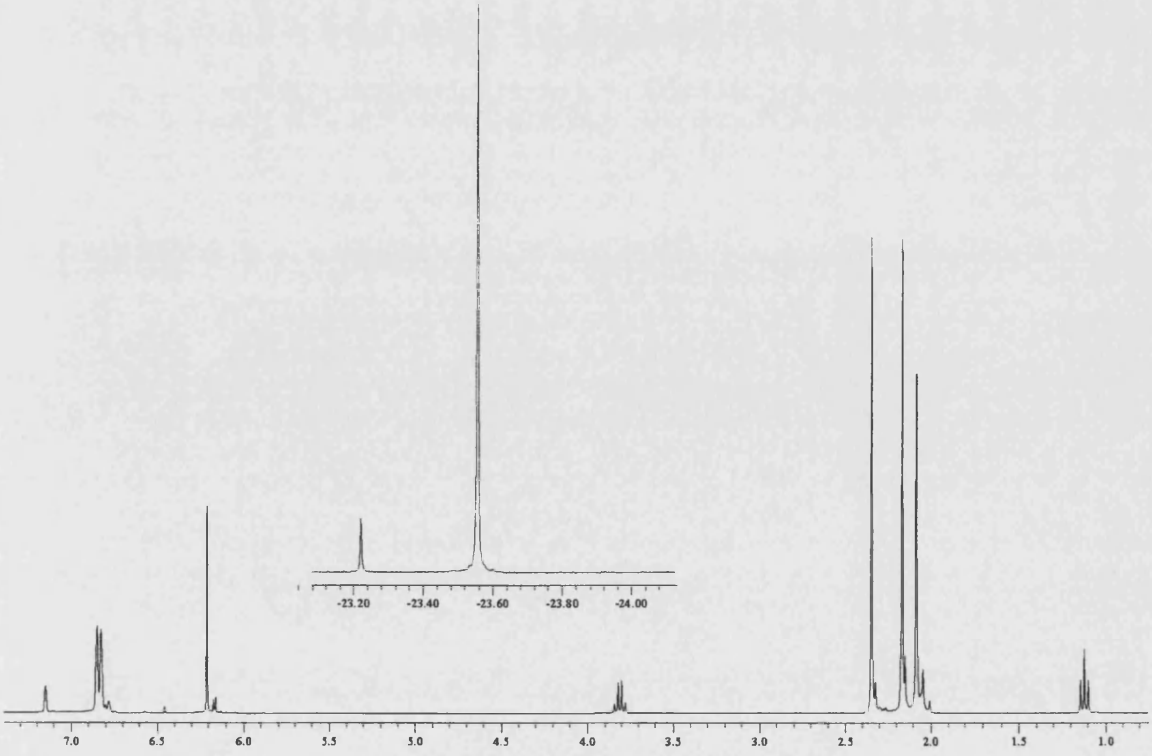

Spectrum 6.2. - *^1H spectrum of the reaction of $Ru(AsPh_3)_3(CO)H_2$*

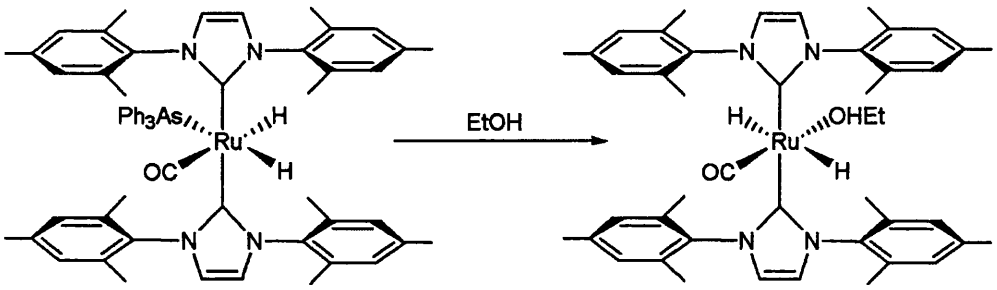

Scheme 6.7.

Clearly the formation of **(39)** from $Ru(AsPh_3)(IMes)_2(CO)H_2$ does not involve a simple substitution of arsine by ethanol since there is an isomerisation from *cis*-RuH_2 to *trans*-RuH_2 occuring. The ^1H NMR spectrum of **(39)** in C_6D_6 showed only one single high-field hydride resonance at δ -23.51, which integrated in a ratio of 2:2:3 with two signals at δ 3.81 (quartet, J_{HH} = 6.79 Hz) and 1.13 (triplet, J_{HH} = 6.69 Hz) for the coordinated ethanol **[spectrum 6.2.]**. The $^{13}C\{^1H\}$ NMR spectrum displayed two singlets at δ 69.7 and 23.3 for the Ru-HOEt group, while two low-field resonances at 197.9 and 205.6 ppm, were assigned to the Ru-C(IMes) and CO groups respectively. The IR spectrum of **(39)** contained a single ν(CO) absorption band at 1887 cm^{-1}, the low frequency presumably reflecting the presence of two strongly σ-donating IMes ligands.

The solid state structure of **(39)** was determined by X-ray crystallography and is shown in **X-Ray 6.1**. The geometry at the ruthenium centre **[Table 6.1.]** is close to octahedral with two *trans* IMes ligands (180.000(1)°) as seen already in the X-ray structure of the bis-adamantylcarbene complex of palladium.[25] The Ru(1)-C(2) / Ru(1)-C(13) bonds (2.087(5) / 2.071(13)) are comparable to the ones already observed in the structures described in **chapter 5** (c.f. **(26)** Ru-C(carbene) 2.0956(17)). The Ru(1)-C(1) appears to be longer than the observed in the structure of **(26)** (2.01(2) vs (2.0956(17)) whereas the C(1)-O(1) bond is smaller than observed in **(26)** (1.02(3) vs 1.155(3)). This elongation of the Ru-C bond and the shortening of the C-O triple bond can be seen in all the dihydride structures and will be explained in **Chapter 6.3.2.** of this chapter.

The 5-membered imidazole rings of the IMes ligands in **(39)** are twisted 32.3° from coplanarity. This, and the fact that the two sets of opposing phenyl rings are not equally spaced, is a feature that is observed to varying degrees in all of the other structurally characterised bis-carbene complexes reported in this chapter **[Chapter 6.3.2.]**.

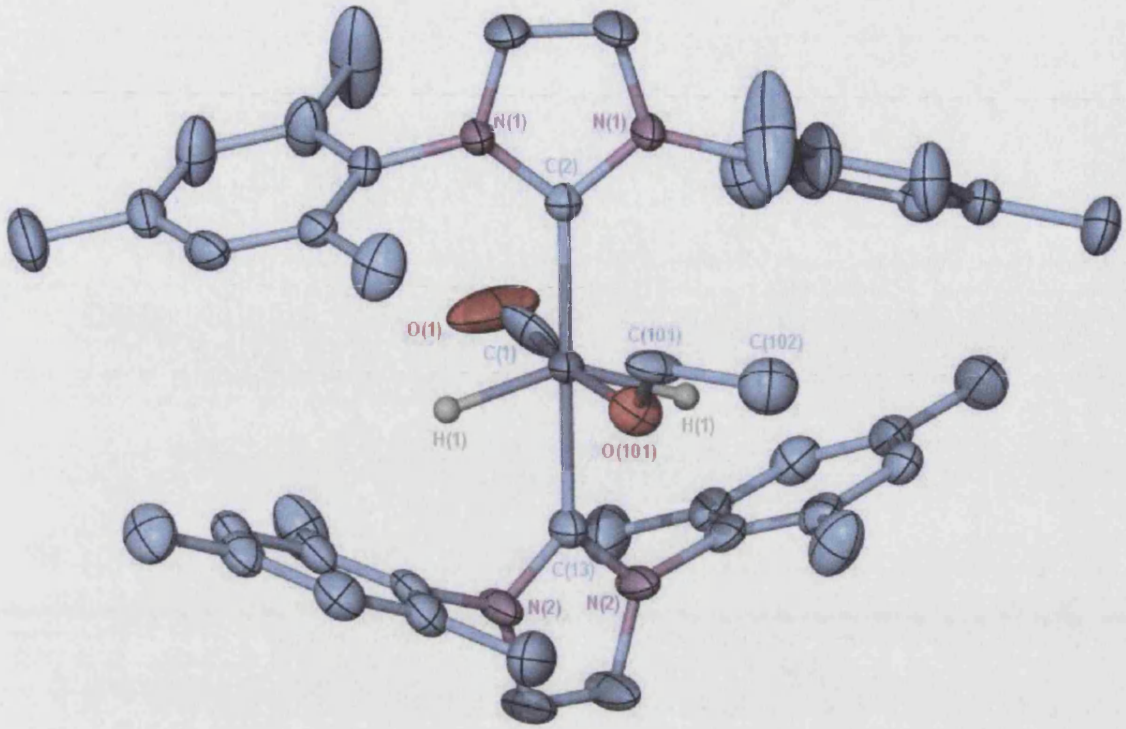

X-Ray 6.1. - *X-ray structure of* ***(39)****. Thermal ellipsoids are set at the 50% probability level. Hydrogen atoms (apart from hydrides) have been omitted for clarity.*

Selected Bond Lengths	**[Å]**		
Ru(1)-C(2)	2.087(5)	Ru(1)-C(1)	2.01(2)
Ru(1)-C(13)	2.071(6)	O(1)-C(1)	1.02(3)
Ru(1)-O(101)	1.881(10)	O(101)-C(101)	1.37(2)
Selected Bond Angles	**[°]**		
O(101)-Ru(1)-C(1)	16.2(4)	C(13)-Ru(1)-C(2)	180.000(1)
O(101)-Ru(1)-C(13)	83.4(3)	C(101)-O(101)-Ru(1)	135.2(9)
C(1)-Ru(1)-C(13)	90.8(6)	O(1)-Ru(1)-C(1)	165.4(19)
O(101)-Ru(1)-C(2)	96.6(3)	C(1)-Ru(1)-C(2)	89.2(6)

Table 6.1. - *Selected bond lengths [Å] and angles [°] for* $Ru(IMes)_2(CO)(EtOH)H_2$ ***(39)****.*

The most notable feature of the structure is the *trans* geometry of the two hydrides, which is an unusual orientation given the strong *trans* influence of hydride ligand. Indeed, few stable *trans*-dihydride complexes are known.[30]

In a recent example reported by Milstein et al.[30] thermal *cis* / *trans* isomerisation of the hydrides is observed showing that the *trans*-dihydride complex is thermodynamically more stable than the *cis*-dihydride complex.

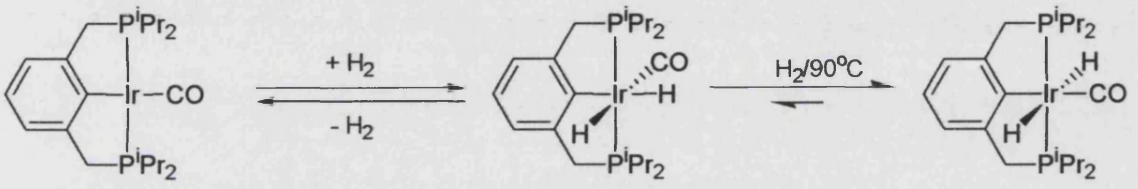

Scheme 6.8.

In the case of complexes $Pt(PR_3)_2H_2$ containing bulky phosphines (R = *t*-Bu, Cy, *t*-Bu_2Ph, *i*-Pr_3), the hydride ligands are forced to be *trans* to each other, while with the less bulky PMe_3, the electronically more favorable *cis*-$Pt(PMe_3)_2H_2$ is seen to be the major isomer in solution.[30] Thus, steric factors play a major role in the stabilization of four-coordinate platinum *trans*-dihydrides.

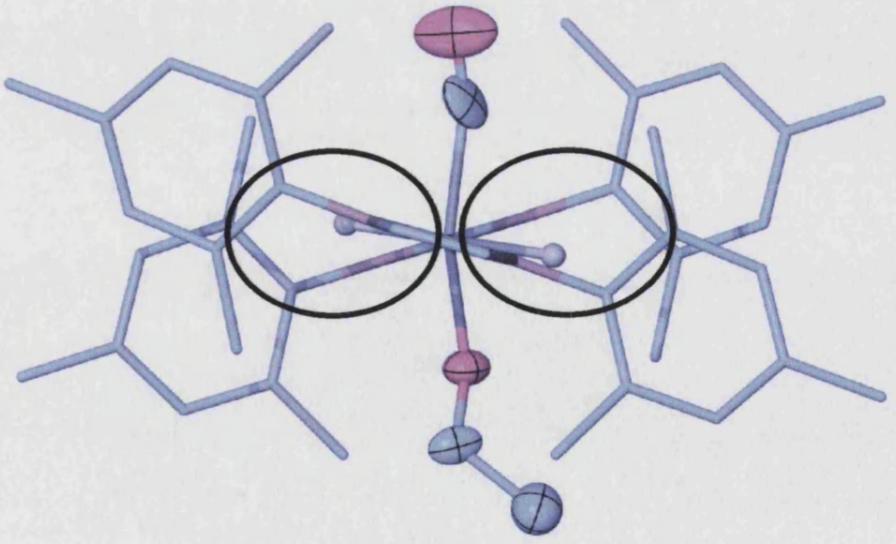

Figure 6.1. - *View of the X-ray structure of* ***(39)*** *down the C(2)-Ru-C(13) axis.*

In our system it is impossible not to take into account the bulkiness of the carbene ligands when trying to explain the mechanism involved into the formation of the *trans* hydride complex. In fact when viewing the X-ray structure along the C(2)-Ru-C(13) axis, it possible to see that the hydrides sit between the mesityl rings in order to allow the bulkier CO and EtOH to occupy the more accessible (less crowded) coordination sites **[Figure 6.1]**. Therefore, it is reasonable to assume that the mechanism of formation involves the formation of a 16e⁻ intermediate **[Scheme 6.9.]**, which provides an isomerisation step for the hydride and the generation of a vacant site *trans* to the carbonyl ligand.

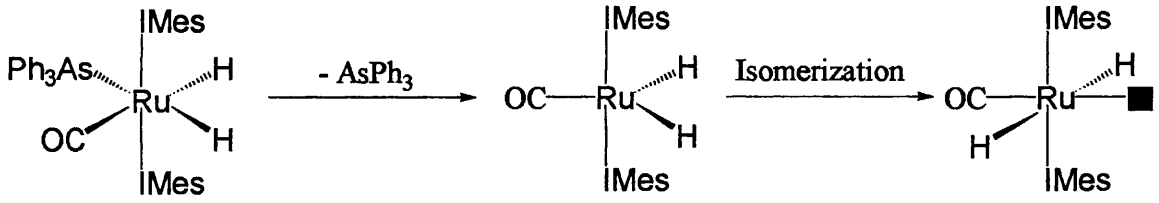

Scheme 6.9. - *Proposed mechanism for the formation of (39).*

While alcohol complexes of transition metals have been invoked in a number of catalytic hydrogenation reactions,[31] there are relatively few structurally characterised examples, the majority of these being cationic **[table 6.2]**.[32-34]

Compounds	Ru-O [Å]	[Ref]
$Ru(PPh_3)(nMePPh)(EtOH)Cl$	2.224(9)	**[32a]**
$[Ru(PCy_3)_2(CO)(MeOCNH)(iPrOH)H][BF_4]$	2.321(3)	**[33]**
[*mer*-RuOTf(CO)(NN'N)(HOEt)]OTf	2.159(2)	**[34]**
$[Cp(CO)_3W(HO^iPr)]^+OTf^-$	2.176(8)	**[32f]**

Table 6.2. - *Selected bond lengths [Å] in M-OHR complexes*

Interestingly the **Ru-OH(Et)** bond distances (Ru(1)-O(101): 1.881(10) Å) appears considerably shorter than observed in other related ethanol complexes **[Table 6.2]** and is closer to the Ru-O bond distances observed in ruthenium ethoxy complexes (1.898(7) for $[Ru(C_2H_5O)(NO)(NO_2)_2(C_6H_{16}N_2)]$,[35] and 1.983(4) for trans-{$Ru(OEt)_2$(anti-Me_8[16] aneS_4)}$^+$).[36]

6.2.1.2. Synthesis of $Ru(IMes)_2(H_2O)(CO)(trans\text{-}H_2)$

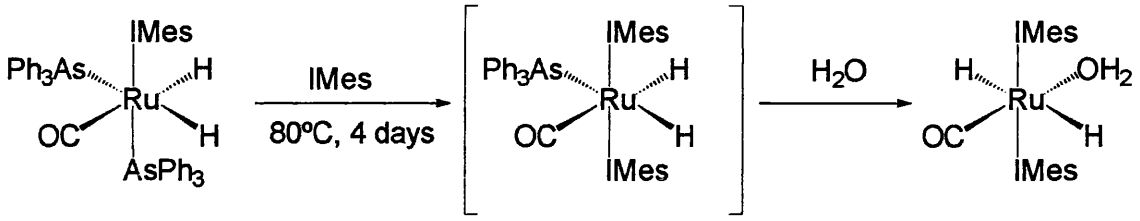

Scheme 6.10.

Replacement of ethanol by hexane as the crystallising solvent, afforded the aqua complex $Ru(IMes)_2(CO)(H_2O)H_2$ **(40)**, which was isolated in 37% yield **[Scheme 6.10.]**. This product presumably arose due to the presence of adventitious water, but all attempts to use more rigorously dry conditions led simply to lower yields of **(40)**. Moreover, when a mixture of hexane/H_2O (10/1 ratio) was used for crystallisation, yields of **(40)** in excess of 80% were isolated. Crystallisation with D_2O-saturated hexane gave $Ru(IMes)_2(CO)(D_2O)H_2$ **(2-D_2O)**. The spectroscopic features of **(40)** are similar to those of the ethanol complex. For example, in the ^1H NMR spectrum the hydride resonance was shifted by 0.36 ppm downfield relative to **(39)**. However more surprisingly perhaps, the carbonyl absorption bands come at quite different frequencies **(39)**, 1886 cm^{-1}; **(40)**, 1861 cm^{-1}). The ^1H NMR spectrum of **(40)** showed a broad resonance for the coordinated water at δ 0.93. This signal remained broad even upon cooling to -80°C, but disappeared upon shaking with D_2O.

An X-ray crystal structure determination of **(40)** showed the molecular geometry to be isostructural with that of **(39)** **[X- Ray 6.2]** with *trans* IMes and hydride ligands. The IMes rings are twisted 48° from coplanarity. No disorder was observed in the structure of **(40)**, although the hydrogen atoms on the bound water could not be reliably located. The Ru-OH_2 distance of 2.023(2) Å **[Table 6.3.]** appears significantly shorter than many reported ruthenium aqua complexes,[37] but remains in range of ruthenium aqua complexes **[Table 6.4.]**.

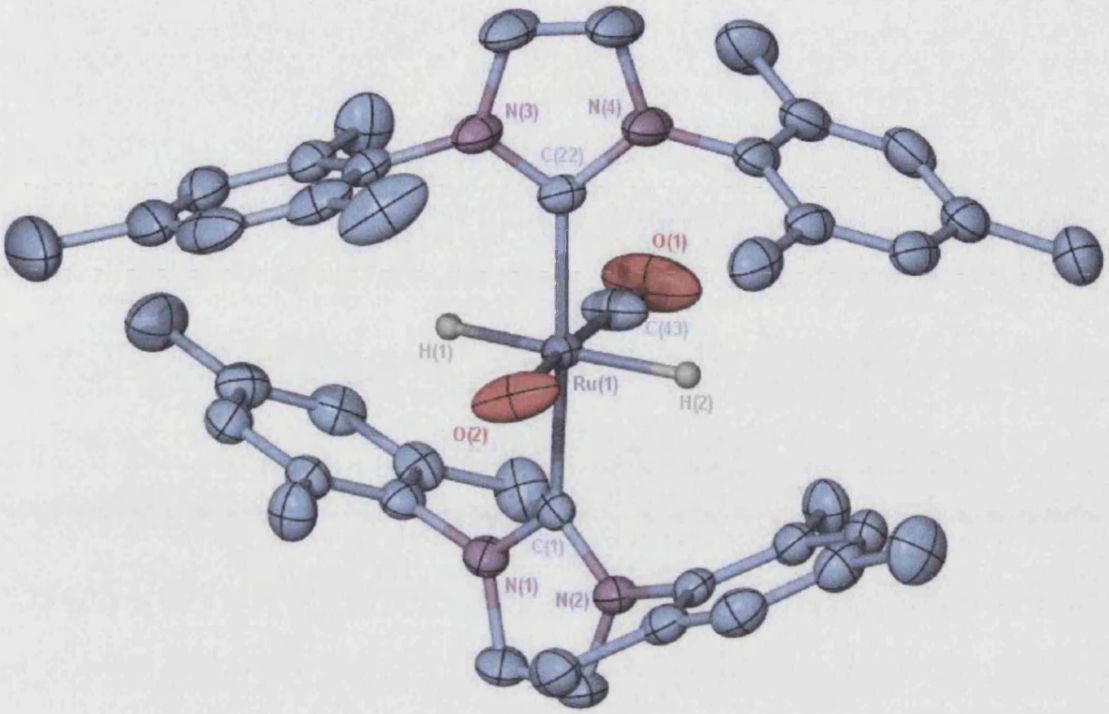

X-Ray 6.2. - *X-ray structure of* ***(40)****. Thermal ellipsoids are set at the 50% probability level. Hydrogen atoms (apart from hydrides) have been omitted for clarity.*

Selected Bond Lengths	**[Å]**		
Ru(1)-C(43)	1.798(3)	Ru(1)-O(2)	2.023(2)
Ru(1)-C(22)	2.066(2)	Ru(1)-C(1)	2.069(2)
O(1)-C(43)	1.165(3)		
Selected Bond Angles	**[°]**		
C(43)-Ru(1)-O(2)	174.90(13)	C(43)-Ru(1)-C(22)	91.25(11)
O(2)-Ru(1)-C(22)	88.19(9)	C(43)-Ru(1)-C(1)	93.23(11)
O(2)-Ru(1)-C(1)	87.43(9)	C(22)-Ru(1)-C(1)	175.43(9)

Table 6.3. - *Selected bond lengths [Å] and angles [°] for* $Ru(IMes)_2(CO)(H_2O)H_2$ ***(40)****.*

Compounds	Ru-O [Å]	[Ref]
$Ru(dppb)(Cl)_3(H_2O)$	2.216(5)	[38]
(R,R_P,S_{Ru})-[{η^6:η^1:η^1-(PArN*)}$Ru(OH_2)$]$^{2+}$	2.155(5)	[39]
$[Ru(dppe)(CO)(H_2O)_3][OSO_2CF_3]_2$	2.180(2) / 2.170(2) / 2.157(2)	[40]
trans-$[(CH_3)_2NH_2][Ru(C_2O_4)_2(H_2O)_2]\cdot 4H_2O$	2.041(3) / 1.994(3)	[41]

Table 6.4. - *Selected bond lengths [Å] in M-OH_2 complexes*

The structures of **(40)** and **(39)** are interesting from a coordination chemistry point of view. In fact, although water is regarded as a very common ligand in coordination chemistry, far fewer examples are known of organometallic aqua complexes, since a metal centre wants to be either "hard" or "soft", but not usually both at the same time.[42] It has been proposed that the ruthenium(II) oxidation state is particularly suited for bonding conventional organometallic ligands such as CO and, at the same time, binding to water.[43] Nevertheless there are only a few examples of neutral Ru-OH_2 complexes.

6.2.1.3. Synthesis of $Ru(IMes)_2(L)(CO)(H_2)$ [L = MeOH (41), *p*-$EtOC_6H_4OH$ (42)]

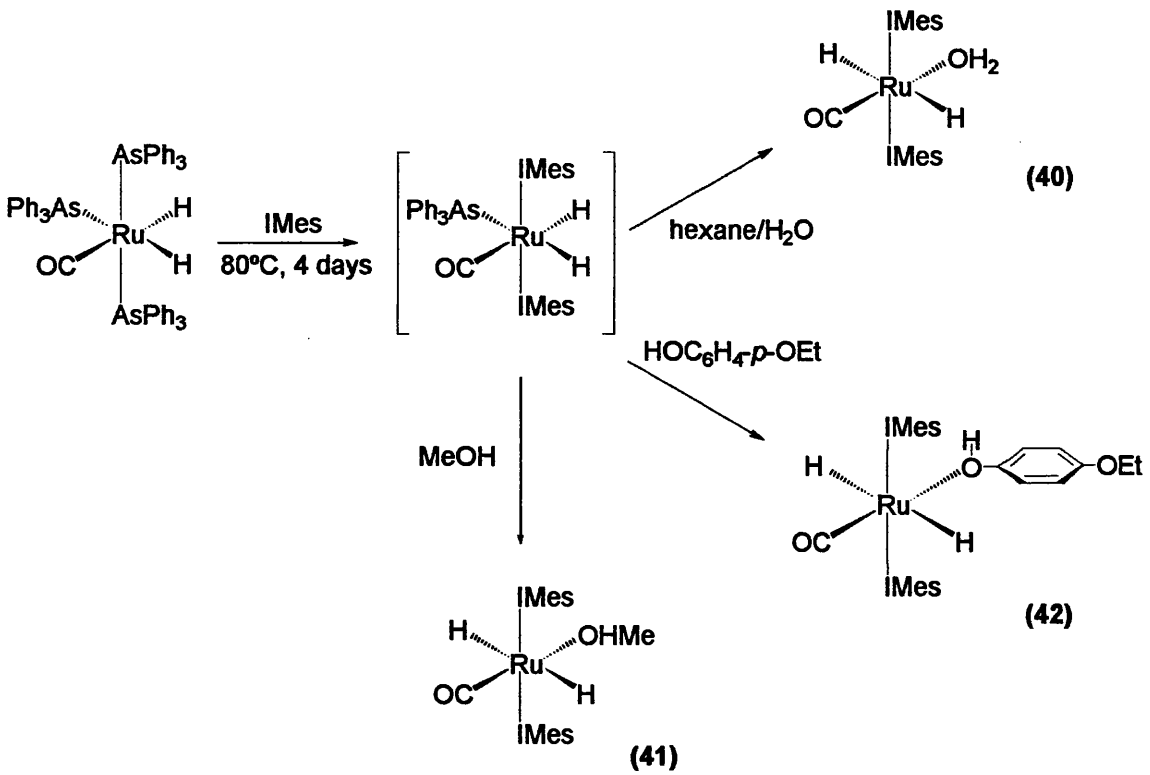

Scheme 6.11.

A similar synthesis could be made with MeOH and *p*-$EtOC_6H_4OH$ as ligands **[Scheme 6.11.]**. In the case of HOC_6H_4-*p*-OEt, the synthesis was done with addition of 1.2 equivalents of HOC_6H_4-*p*-OEt to an hexane solution of $Ru(AsPh_3)(IMes)_2(CO)H_2$. Complexes **(41)** and **(42)** were fully characterised by NMR and IR spectroscopies, and show similarities to **(39)** and **(40)** as shown in **[table 6.5.]**.

	(39)	**(40)**	**(41)**	**(42)**
^{1}H (ppm)	-23.51	-23.15	-23.79	-24.48
IR (cm^{-1})	1887	1861	1858	1881

Table 6.5.

In the ^{1}H spectrum of **(41),** a single resonance at 3.84 ppm was attributed to the coordinated methanol ligand. The ^{1}H spectrum of **(42)** displayed broad resonances for the *p*-$EtOC_6H_4OH$ moiety **[Spectrum 6.3.]**, these were resolved at 233 K into a triplet and a quartet for the O-CH_2CH_3 fragment (J_{HH} = 7.2 Hz), and two doublets for the C_6H_4 fragment (J_{HH} = 8Hz).

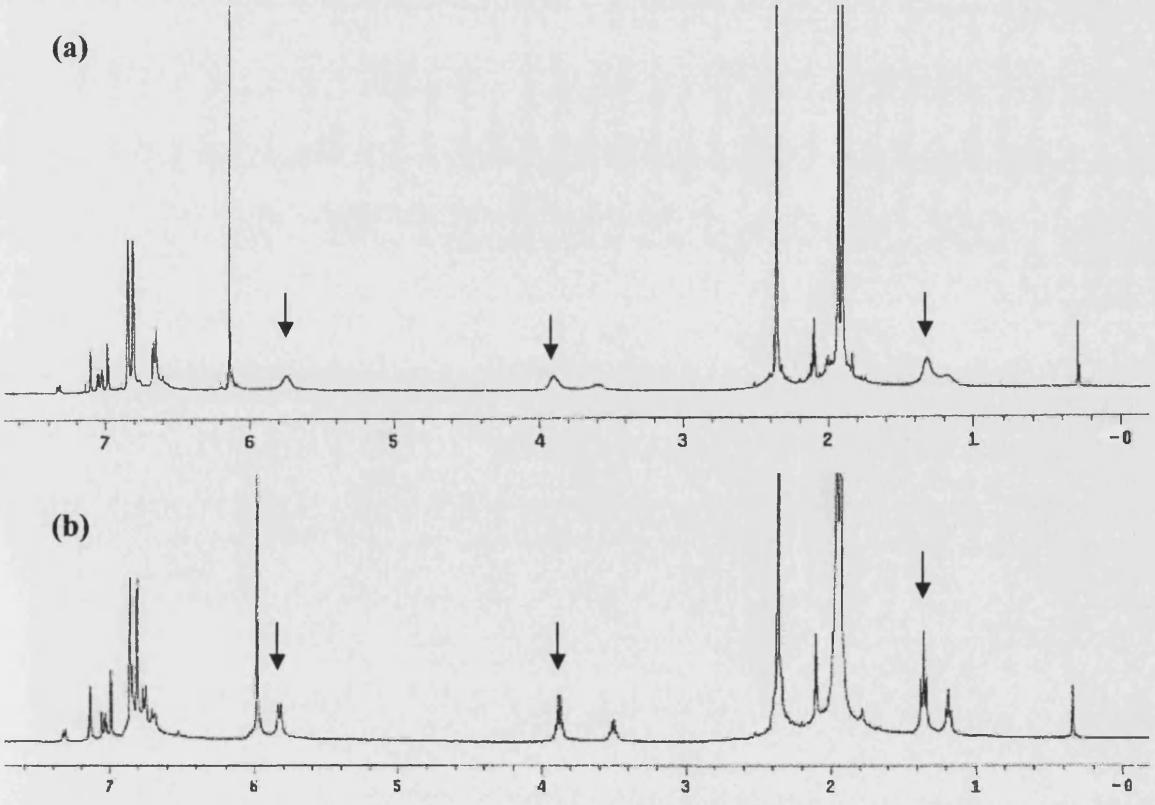

Spectrum 6.3. - *^{1}H NMR VT of* ***(42)****. **(a)** 273 K ; **(b)** 233 K. **NB:** The Minor species on the side of the triplet and quartet for* ***(42)*** *arise for free p-$EtOC_6H_4OH$.*

Although single crystals of **(41)** and **(42)** were obtained, they were of insufficient quality to facilitate good structural analysis by X-ray crystallography. However, the solid state structure of **(41)** served to confirm at least that the ruthenium was bonded to the phenolic oxygen rather than the oxygen of the ethoxy substituent **[X-Ray 6.3.]**.

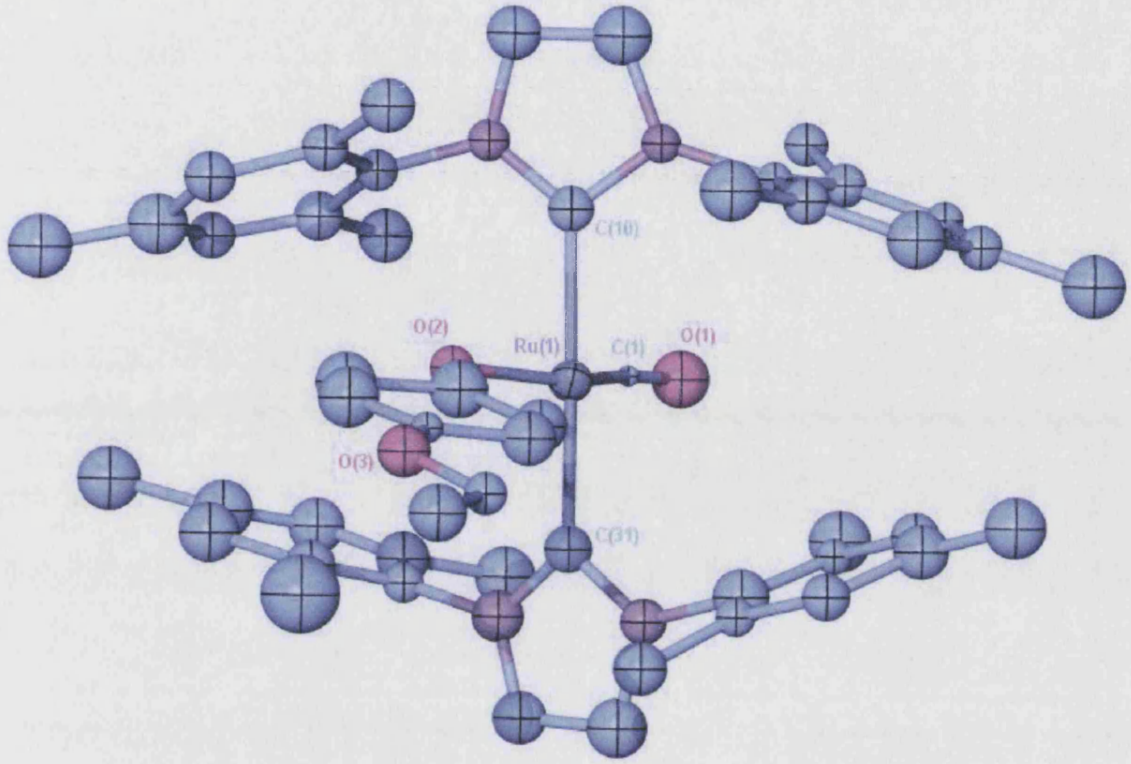

X-Ray 6.3. - *X-ray structure of (42) in the solid state.*

6.2.2. Thermolytic stability of (39) and (40).

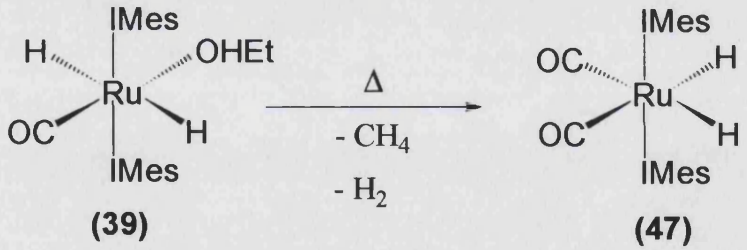

Scheme 6.12.

In order to investigate the stability of **(39)** and **(40)**, the reactivity of these towards thermal decomposition was probed. Surprisingly the aqua complex proved to be thermally stable even at 120°C, as evidenced by the lack of detectable change in the ^1H NMR spectrum at that temperature over 3 days. Thermolysis of **(39)** in C_6D_6 at 90°C for 2 weeks yielded the bis-carbene dihydride complex $Ru(IMes)_2(CO)_2H_2$ **(47)** resulting from decarbonylation of the coordinated ethanol **[Scheme 6.12.]**.[44] The ^1H NMR spectrum of

(47) contained a single hydride resonance at δ –6.53, shifted significantly downfield relative to that seen for **(39) [Spectrum 6.4.]**. The appearance of only one Ru-CO resonance (204.3 ppm) in the $^{13}C\{^1H\}$ NMR spectrum and two ν_{CO} bands in the IR spectrum (1973, 1936 cm^{-1}) indicate that **(47)** possesses a *trans, cis, cis*-stereochemistry.[45]

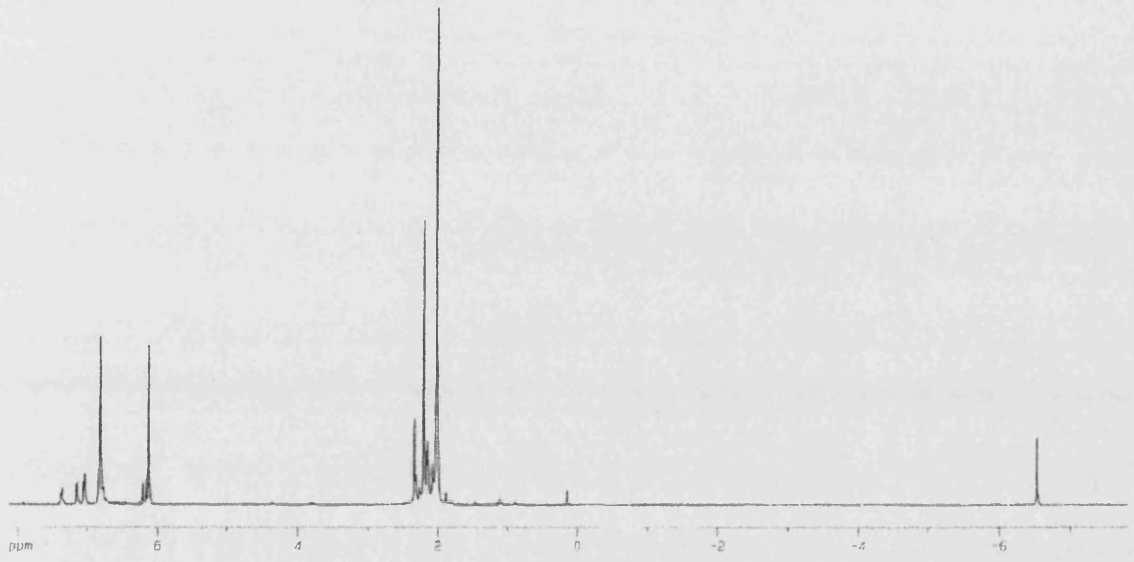

Spectrum 6.4. - *^1H NMR spectrum of (47).*

Although the mechanism for such a process was not investigated, few examples of intramolecular decarboxylation of alcohols have been reported,[46] which support the idea of the mechanism described in **Scheme 6.13.**. These processes have been mainly observed with hydride and dihydrogen complexes and involves formation of an alkoxy intermediate (either as an alkoxide dihydride via oxidative addition or as a alkoxo dihydrogen via protonation). An intramolecular protonation of the $Ru(RCH_2OH)H$ fragment is reasonable, as the acidity of alcohol coordinated on the metal is enhanced, and M-H can be a very effective proton acceptor as demonstrated by many examples of intramolecular and intermolecular protonations of M-H by R-O-H, R-S-H, and RR'N-H.[47]

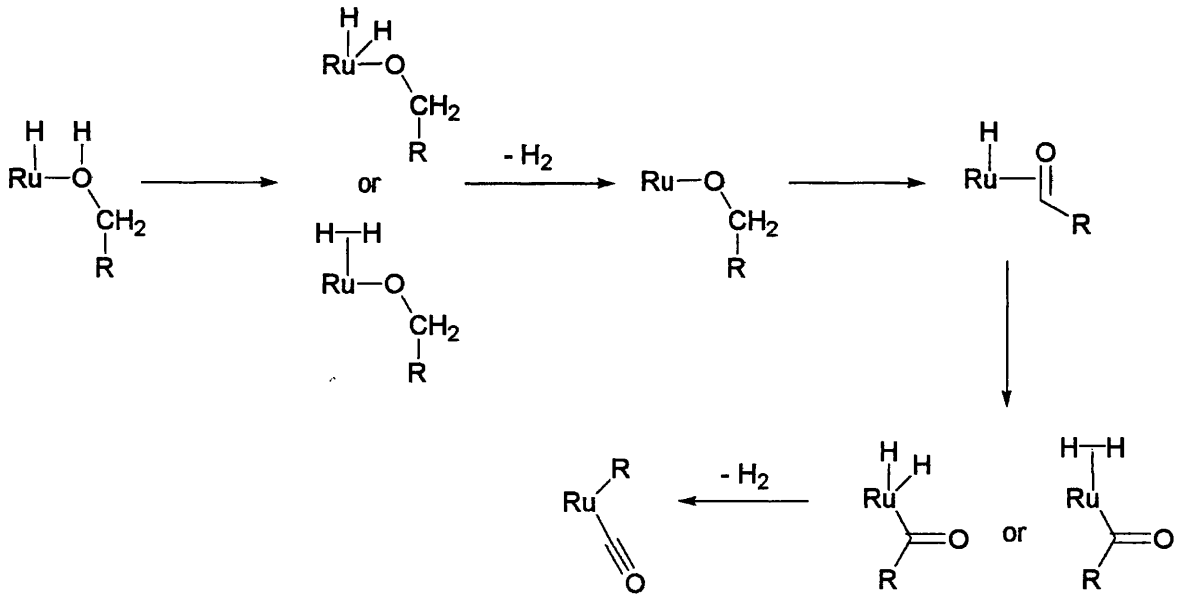

Scheme 6.13. - *Proposed mechanism for the formation of (40).*

The unexpected inactivity of **(40)** is unusual as one would have expected that the aqua compound would be more reactive would proceed as seen for **(39)** **[Scheme 6.14.]**. It is possible that this pathway is driven kinetically rather than thermodynamically in this case or that the thermodynamic barrier is very high.

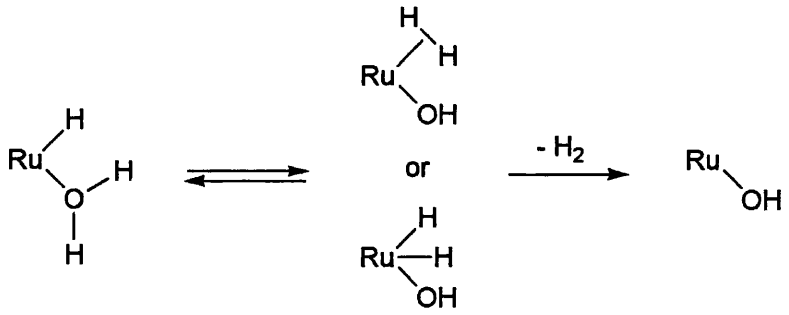

Scheme 6.14. - *Expected mechanism for the thermolysis reactivity of (40)*

6.2.3. Reaction of (39) and (40) with CO.

In order to further asses the reactivity of **(39)** and **(40)** it was decided to investigate their reactivity towards CO.

6.2.3.1. Characterisation of $Ru(IMes)_2(CO)_3$ (58)

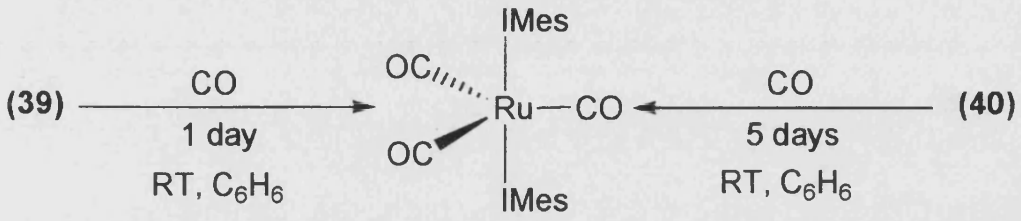

Scheme 6.15

Addition of CO to a solution of **(39)** at room temperature resulted in an immediate colour change from yellow to clear and then back to orange/yellow affording the ruthenium(0) complex, $Ru(IMes)_2(CO)_3$ **(58)**, over the course of one day **[Scheme 6.5]**. The spectroscopic features of **(58)** are consistent with a trigonal bipyramidal structure with three CO ligands in the equatorial plane.[48] The tricarbonyl complex was also identified as the final product upon addition of CO to solutions of the aqua complex **(40)**, although in this case, 5 days were required for the reaction to go to completion at room temperature **[Scheme 6.5]**.

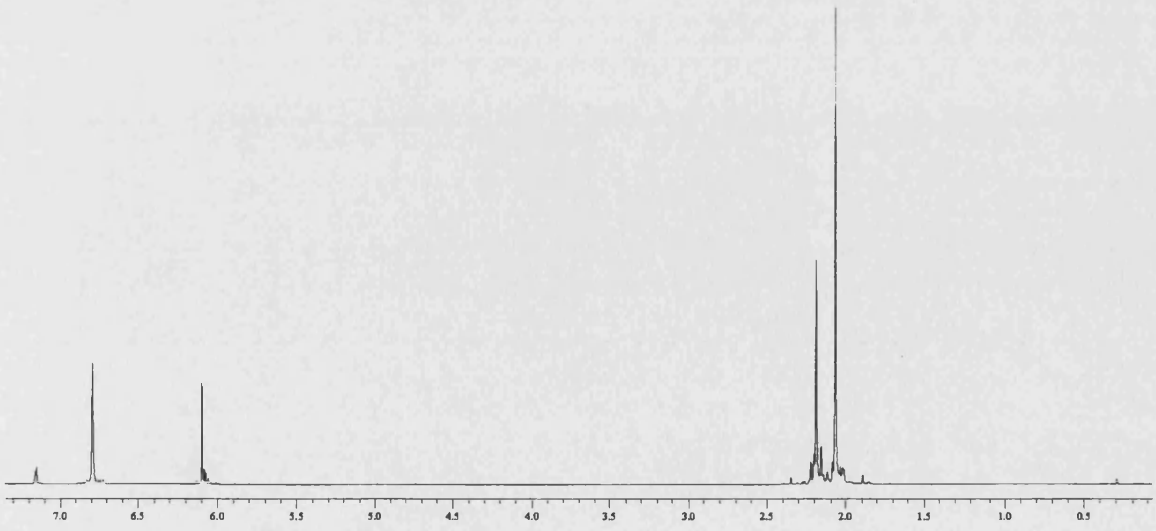

Spectrum 6.5. - *^1H spectrum of (58).*

The ^{1}H NMR spectrum of **(58)** shows just two sets of methyl resonances integrating in a ratio of 2:1 for the *ortho* and *para*-mesityl groups of the IMes ligands **[Spectrum 6.5.]**. The $^{13}C\{^{1}H\}$ NMR spectra displayed one very low field carbonyl resonance (217.6 ppm), which becomes very intense when ^{13}CO is used. Interestingly although a single IR absorption band was expected, solution IR of **(58)** showed two ν_{CO} absorption bands at 1875 and 1838 cm^{-1}. Meanwhile a solid state (Nujol) IR of the material displayed three ν_{CO} absorption bands at 1950, 1879 and 1829 cm^{-1}. This fact can only be explained by a lowering of the symmetry in **(58)**. Although clear sizeable crystals of **(58)** could be grown out of a solution of a benzene / hexane mixture, the X-ray data could not be processed. Even after repeated attempts.

6.2.3.2. Mechanism of formation of (58) in the reaction of (39) with CO.

The ultimate formation of $Ru(IMes)_2(CO)_3$ from the addition of CO to solutions of **(39)** or **(40)** implied a similar reaction pathway in both cases, although the different completion times suggested different stabilities and reactivity of intermediate species along the way.

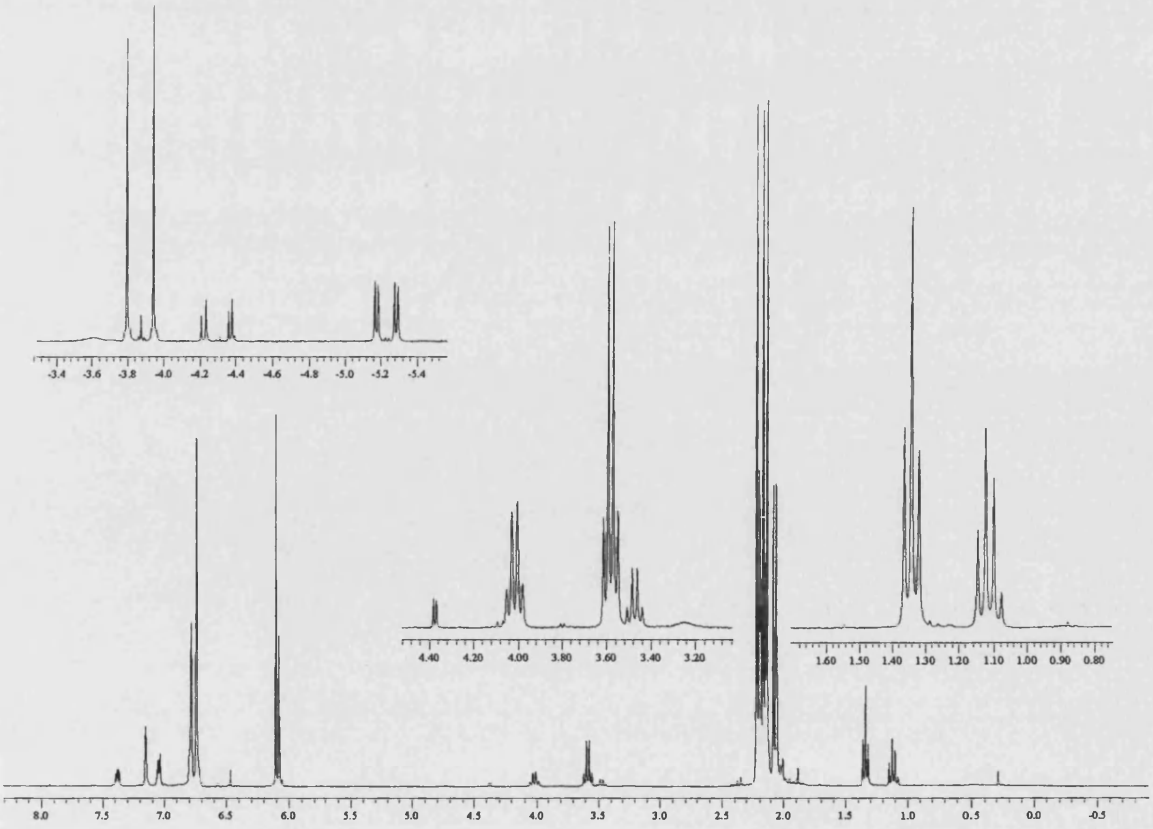

Spectrum 6.6. - *^{1}H spectrum of the reaction of (39) with CO after 1h.*

This was investigated in more detail by labelling experiments with ^{13}CO. The ^{1}H NMR spectrum recorded within 1 h of addition of ^{13}CO to a C_6D_6 solution of **(39)** showed the complete disappearance of the starting material and the formation of two new major hydride products with resonances at δ -3.88 (d, J_{HC} = 43.7 Hz) **(39')**, and -5.24 (dd, J_{HC} = 33.5, J_{HC} = 5.4 Hz) **(39'')**. Additionally, the ^{1}H NMR spectrum displayed two sets of ethoxide signals at 3.58 and 1.12 ppm (J_{HH} = 6.8 Hz) for **(39')** and 4.02 and 1.34 ppm (J_{HH} = 7.0 Hz) for **(39'')**. We propose that these signals arise from $Ru(IMes)_2(CO)_2(OEt)H$ **(39')** and the CO insertion product $Ru(IMes)_2(CO)_2(C(O)OEt)H$ **(39'')**[49] respectively **[Scheme 6.16., Spectrum 6.6.]**.

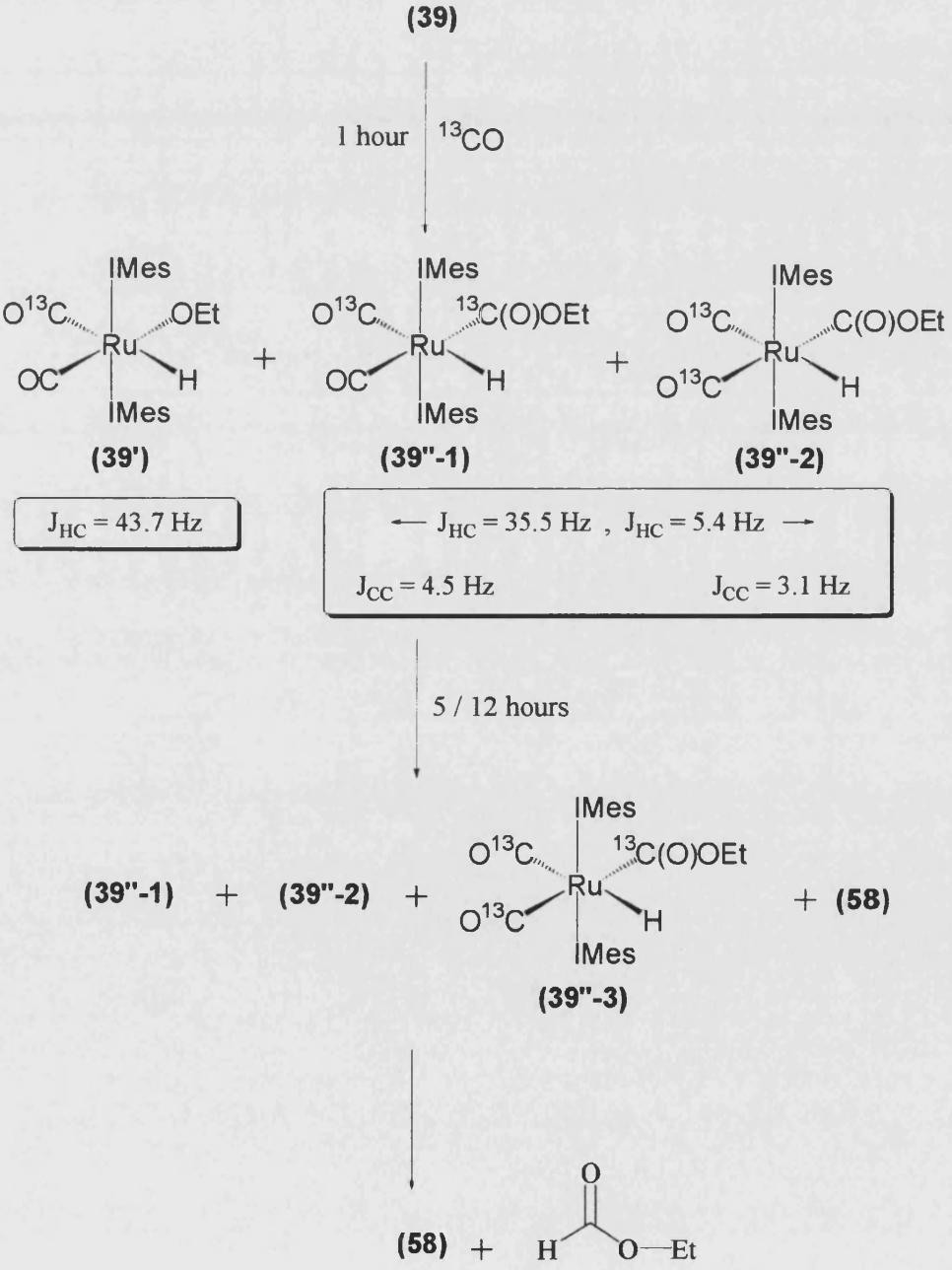

Scheme 6.16.

(39') and **(39'')** show a large ^{1}H-^{13}C coupling constant (30-45 Hz) which is consistent with ^{13}CO incorporation *trans* to Ru-H, while the small coupling constant value seen for **(39'')** is due to an equivalent *cis* coupling to either the Ru-$^{13}C(O)OEt$ ligand in **(39''-1)** or the *cis*-Ru-^{13}CO moiety in **(39''-2) [Scheme 6.16., Spectrum 6.7.]**.

The carbon spectrum at this stage of the reaction showed the formation of a single ^{13}C-enhanced CO resonance at δ 195.2 for **(39')**, and three ^{13}C-enriched doublet signals at δ 206.1 (J_{CC} = 3.1 Hz), 202.9 (J_{CC} = 4.5 Hz) and 198.5 (J_{CC} = 4.5 Hz) attributed to a mixture of **(39''-1)** and **(39''-2)**. (NB: Only three signals are observed due to the very small difference between the C-C coupling (cf. 3.1 Hz Vs 4.5 Hz).

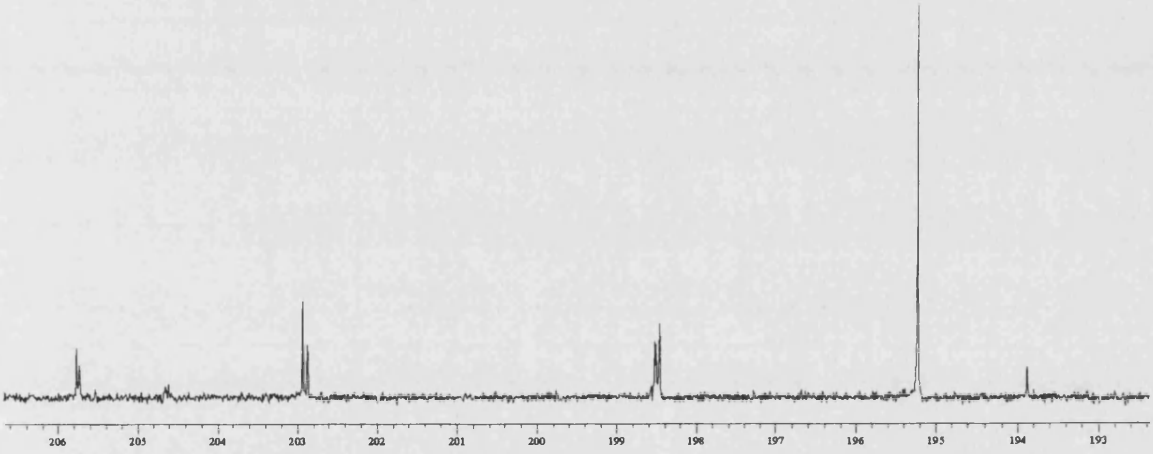

Spectrum 6.7. - *$^{13}C\{^{1}H\}$ NMR spectrum of the reaction of **(39)** with CO after 1h.*

HMQC showed ^{2}J coupling between the ^{13}C=O (δ 202.9) carbon and the protons on the CH_2 of the ethoxy group **[Spectrum 6.8.]**.

This fact added to the *cis*-coupling (4.5 Hz) observed for the signals at δ 202.9, and 198.5 is consistent with the presence of a coupled Ru-^{13}CO and Ru-$^{13}C(O)OEt$ groups giving $Ru(IMes)_2(^{13}CO)(CO)(^{13}C(O)OEt)H$ **(39''-1)**. Meanwhile the third resonance at δ 206.1 was attributed to a very small amount of $Ru(IMes)_2(^{13}CO)_2(C(O)OEt)H$ **(39''-2)** being formed.[50]

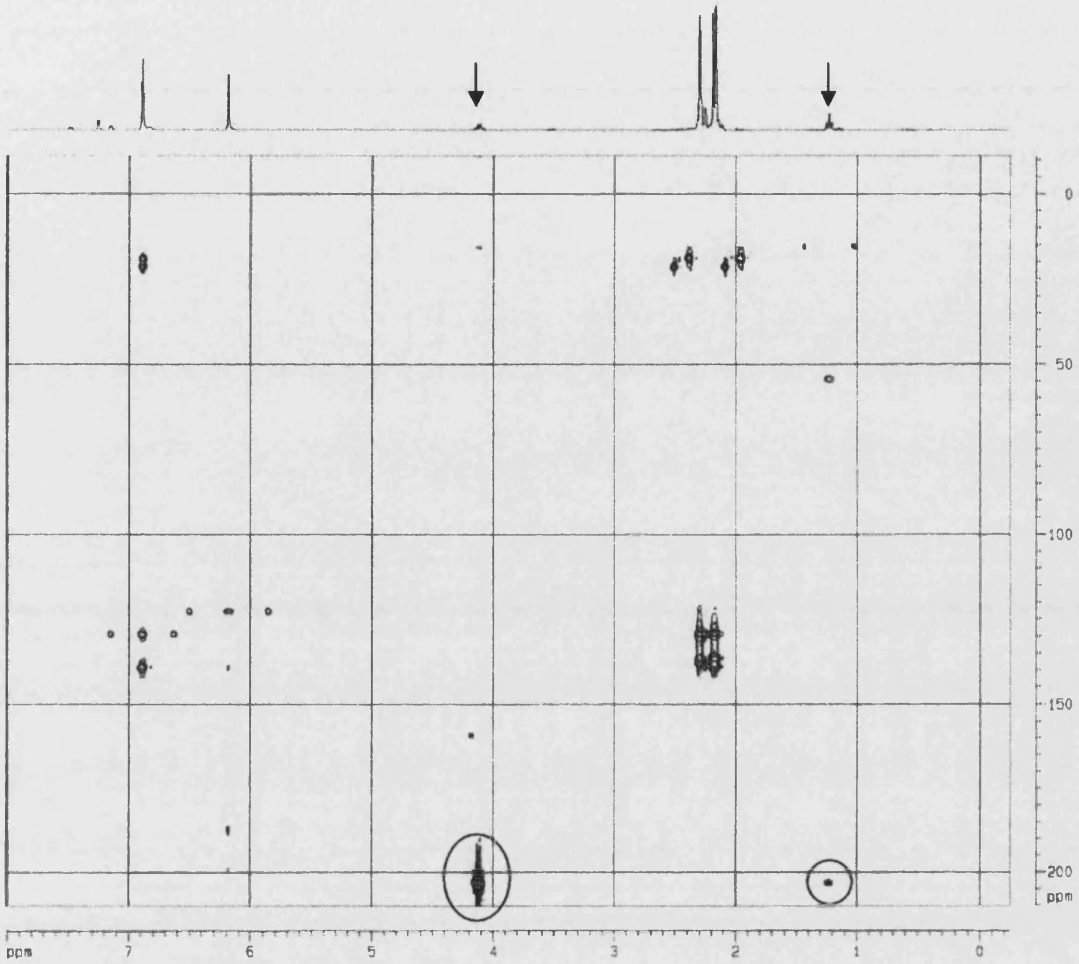

Spectrum 6.8. – HMQC spectrum

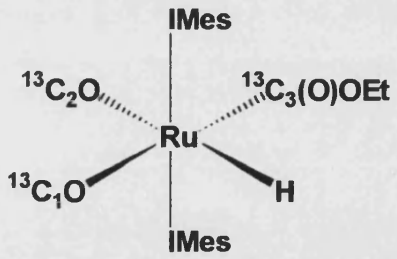

C1 = 206.1 ppm J_{C1-C2} = **3.1 Hz**

C3 = 202.9 ppm J_{C2-C3} = **4.5 Hz**

C2 = 198.5 ppm J_{C1-C3} = **33.5 Hz**

Scheme 6.17.

After 4 h at room temperature, the ^{1}H and $^{13}C\{^{1}H\}$ NMR showed almost complete conversion of **(39')** to **(39''-1),** and **(39''-2)** (a minute amount of ^{13}CO-labelled $Ru(IMes)_2(^{13}CO)_2(^{13}C(O)\text{-}OEt)H$ **(39''-3)** is produced, as shown by satellite doublet of doublets centred on C_1 and C_3 **[Scheme 6.17., Spectrum 6.9.]**, and a small amount of **(58)** is apparent in the $^{13}C\{^{1}H\}$ NMR spectrum **[Scheme 6.16., Spectrum 6.9.]**. Over longer time, $^{13}C\{^{1}H\}$ NMR spectroscopy simply showed a depletion of the **(39'')** labelled species **(39''-1, 39''-2, 39''-3)** and an increase in the amount **(58) [Spectrum 6.10.]**.

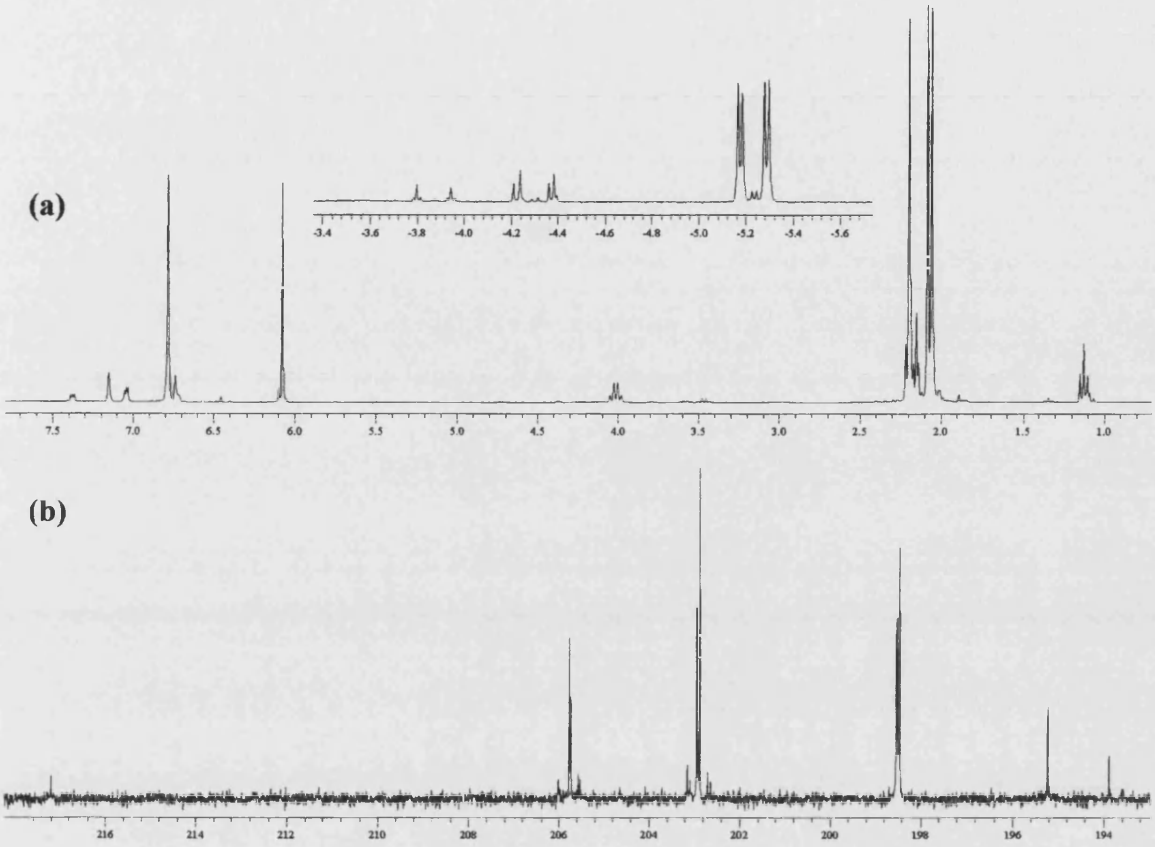

Spectrum 6.9. - *^{1}H **(a)** and $^{13}C\{^{1}H\}$ **(b)** spectra of the reaction of **(39)** with CO after 4h.*

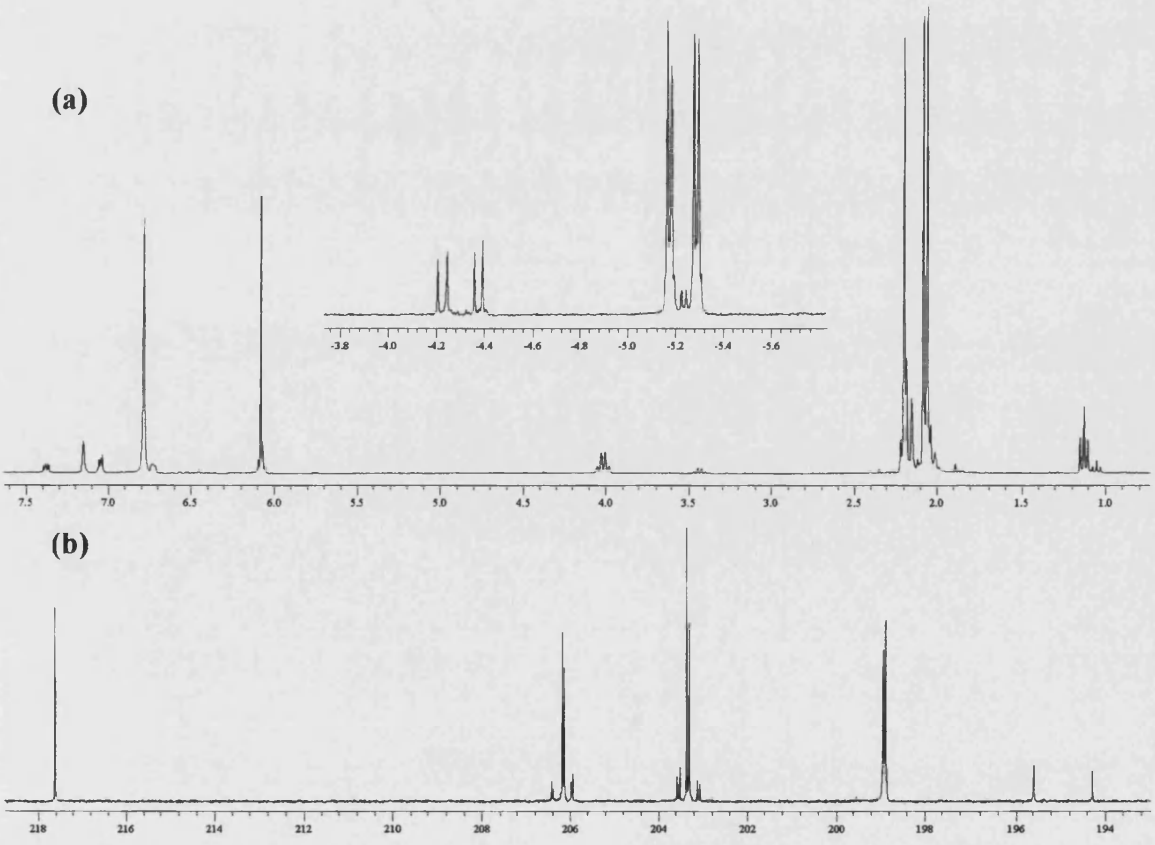

Spectrum 6.10. - *^{1}H **(a)** and $^{13}C\{^{1}H\}$ **(b)** spectra of the reaction of **(39)** with CO after 12h.*

6.2.3.3. Mechanism of the reaction of (40) with CO.

In an analogous manner to the reaction seen between CO and **(39)**, addition of 1 atm of CO to a C_6D_6 solution of **(40)** resulted in an instantaneous colour change from yellow to colourless. At this stage, the ^1H NMR spectrum of the colourless solution showed the presence of the hydroxy hydride complex $Ru(IMes)_2(CO)_2(OH)H$ **(48)** as the major species, along with a much smaller concentration of $Ru(IMes)_2(CO)_3$ **(58)**.

The hydroxy hydride complex displayed a single hydride resonance moved significantly to lower field (δ -4.27) relative to that for **(40)** **[Spectrum 6.11.]**, consistent with a loss of the *trans* H-Ru-H stereochemistry by insertion of a CO ligand. This shift to lower field is observed in all cases where a *cis*-$Ru(CO)_2(X)H$ unit is formed in reactions with CO.[51] The ^1H NMR spectrum of **(48)** also showed a broad hydroxyl resonance (δ -3.75) which sharpened to two 1:1 singlets with the hydride upon cooling to 203 K **[Spectrum 6.12]**.[6,52] The chemical shift of the hydroxyl proton in **(48)** is comparable to those reported for other late metal 18-electron hydroxy complexes as shown in **Table 6.5.**.

In order to investigate the mechanism of this process, the formation of **(48)** was repeated using ^{13}CO. The ^1H NMR spectrum recorded within 5 min of addition of ^{13}CO to a C_6D_6 solution of **(40)** showed the formation of **(48)** with a signal at δ -4.37 showing a *trans* coupling to ^{13}CO (J_{HC} = 43.6 Hz). The room temperature proved inconclusive in establishing that no ^{13}CO label was present *cis* to OH. Therefore a VT NMR was performed which showed no evidence for incorporation of ^{13}CO *cis* to the Ru-OH moiety **[Spectrum 6.12.]**.

Hydroxy hydrides remain an unusual class of compounds. Thus we decided to investigate the formation of **(48)** by deuterium labelling studies. As shown in **Scheme 6.18.**, $Ru(IMes)_2(CO)(D_2O)H_2$ **(40)**-D_2O was synthesised upon reaction of $Ru(AsPh_3)(IMes)_2(CO)H_2$ with D_2O. The ^1H NMR spectrum recorded after addition of CO to a C_6D_6 solution of **(40)**-D_2O displayed the expected hydride resonance at δ -4.27, but showed no OH peak, indicating the formation of $Ru(IMes)_2(CO)_2(OD)H$ **[Spectrum 6.13]**. This observation, together with the exclusive ^{13}CO incorporation *trans* to hydride described above, is consistent with the formation of the hydroxy hydride via proton transfer rather than oxidative addition of water **[Scheme 6.18.]**.[52,53,54]

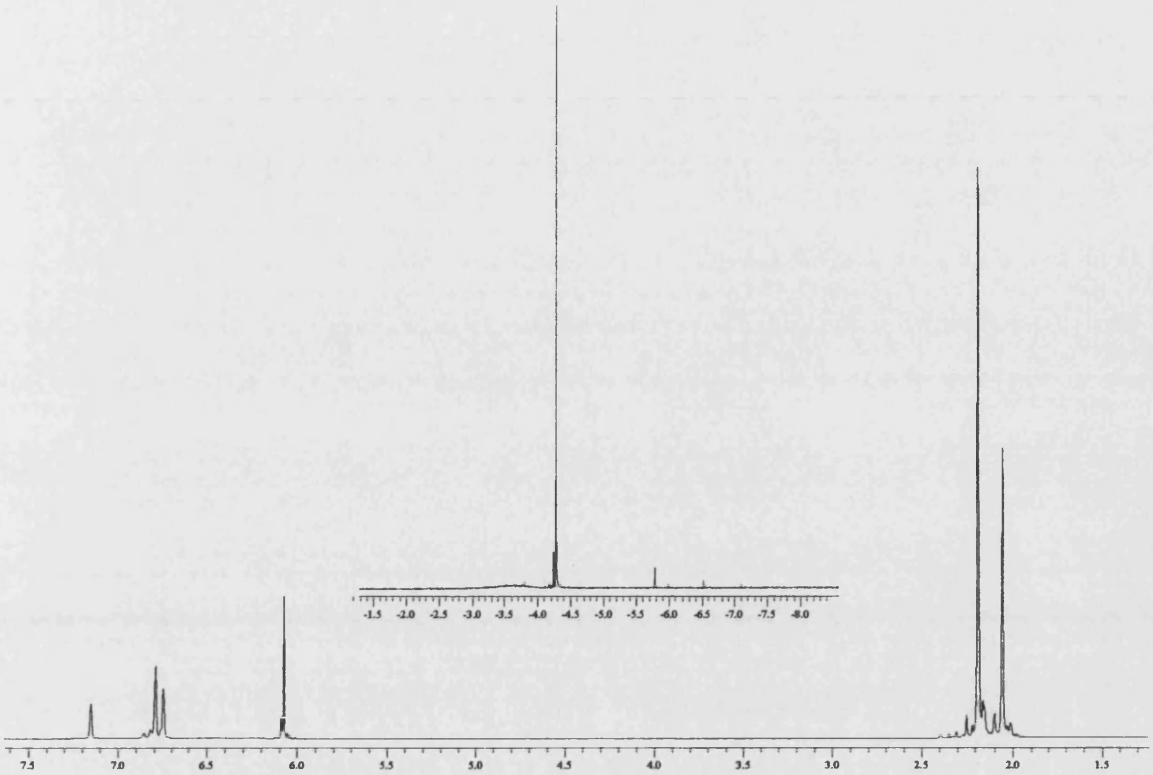

Spectrum 6.11. - *^{1}H spectrum of* ***(48)***.

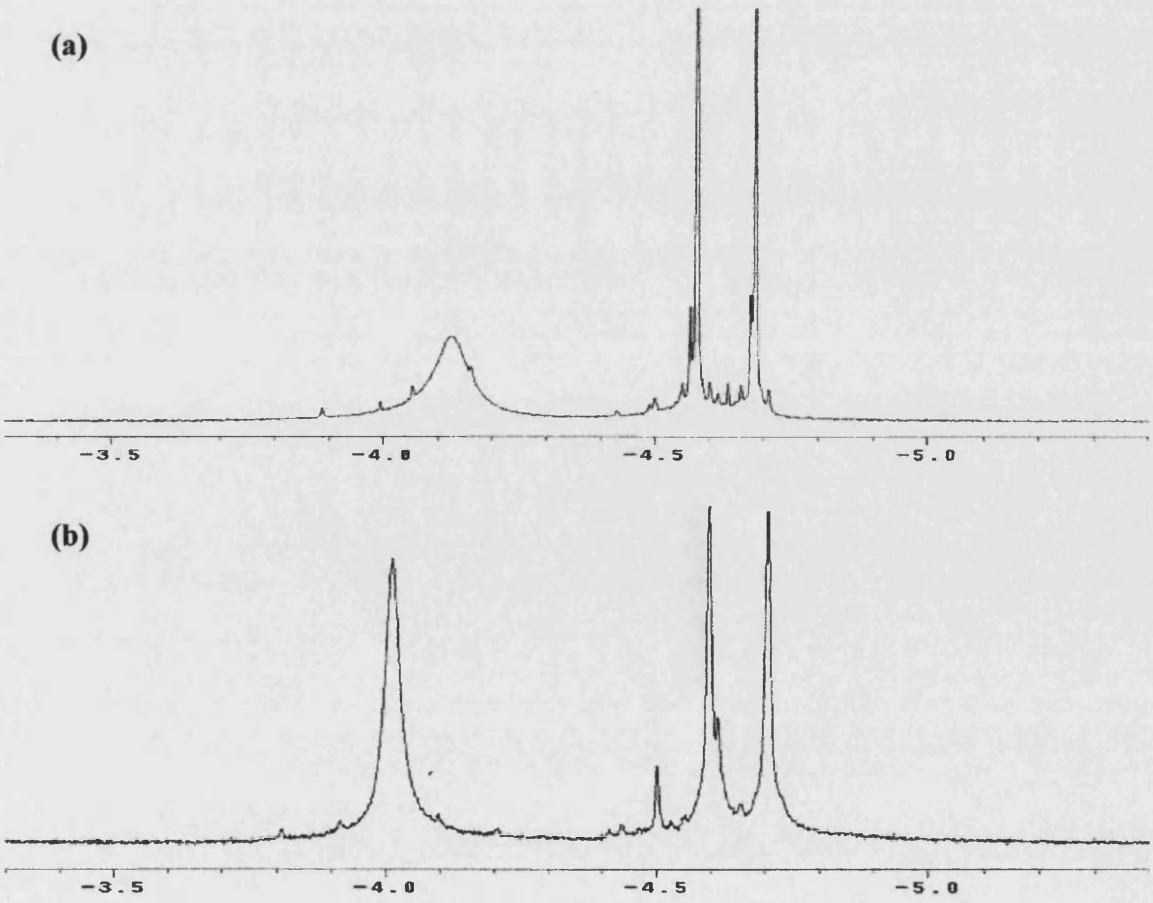

Spectrum 6.12. - *^{1}H NMR VT spectrum of* ***(48)***. ***(a)*** *273 K.* ***(b)*** *203 K.*

Compounds	δ (OH) / δ (H)	[Ref]
trans-Ru(dmpe)$_2$(OH)H,	-4.55 / -21.75	**[53a]**
cis-Ru(PMe$_3$)$_4$(OH)H	-4.64 / -8.31	**[53b]**
cis-Ru(PMe$_3$)$_4$(OH)Me	-3.79 / NA	**[53b]**
cis-Ru(PMe$_3$)$_4$(OH)H	-3.79 / -8.31	**[53b]**
cis-Ru(PMe$_3$)$_4$(OH)(Ph)	-4.47 / NA	**[54]**
cis-[Ir(PMe$_3$)$_4$(OH)H]$^+$	-1.40 / -11.19	**[55]**

Table 6.5.

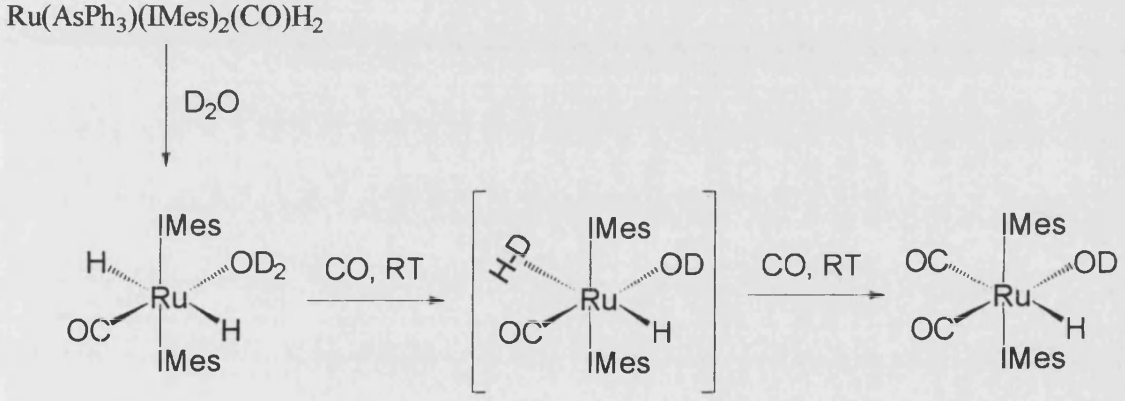

Scheme 6.18.

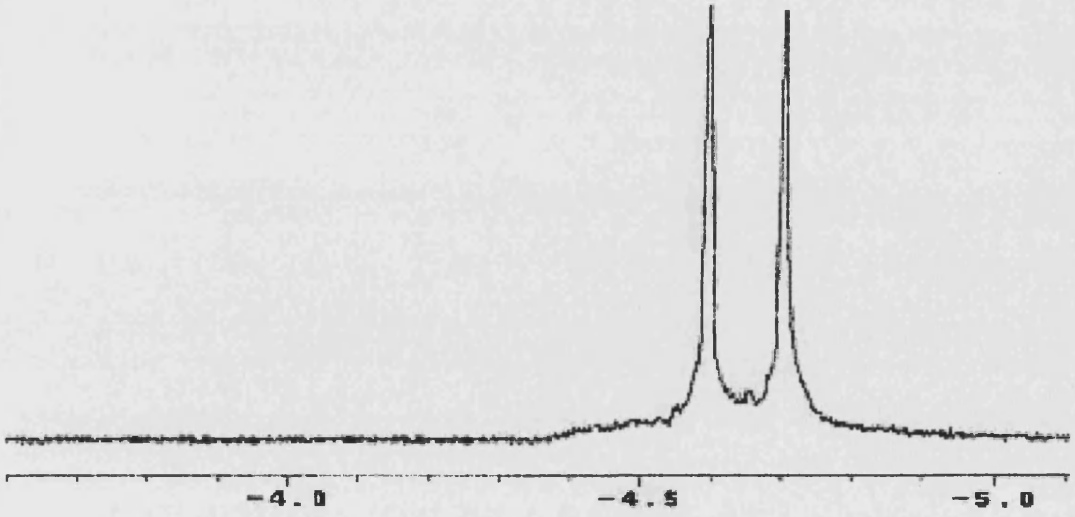

Spectrum 6.13. *^{1}H NMR spectrum of* ***(48)****-Ru^{13}(CO)(CO)****(OD)****H.*

Hence, we propose that the protonation of one of the strongly hydridic hydride ligands by the (acidic) coordinated water yields a putative dihydrogen hydroxy hydride

Hence, we propose that the protonation of one of the strongly hydridic hydride ligands by the (acidic) coordinated water yields a putative dihydrogen hydroxy hydride species, which readily dissociates H_2 in the presence of CO.[58] Additional evidence for this protonation pathway was revealed upon treatment of a C_6D_6 solution of **(40)** with an excess of D_2O. The intensity of the hydride signal readily depleted, as evidenced by the relative integrations of Ru-H:aryl:methyl signals (1:18:81 rather than the expected 1:4:18 recorded after 5 days at 50 °C), indicating Ru-H/D_2O exchange. ^1H NMR spectroscopy showed only traces of the hydride signal remaining. The pathway for this exchange process is shown in **Scheme 6.19.**, proceeding by the same dihydrogen (or hydrogen-deuterium) hydroxy hydride species **[Spectrum 6.14.]**. Proton NMR spectra recorded over the course of the reaction between **(40)** and D_2O also showed a smaller than expected integral for the NCH=CHN backbone protons of the IMes ligands, raising the likelihood of H/D exchange here also. H/D exchange into the backbone positions using D_2O has been reported in the free carbene ligand.[59]

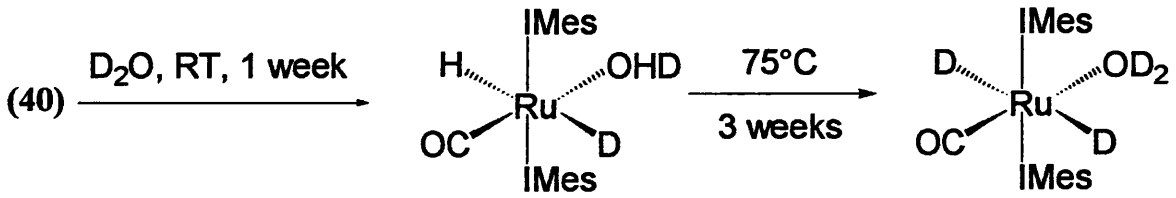

Scheme 6.19.

Due to the paucity of structurally characterised hydroxy hydride complexes,[54,56] the molecular structure of $Ru(IMes)_2(CO)_2(OH)H$ was confirmed by a single crystal X-ray structure determination as shown in **X-ray 6.4.**. Selected bond distances and angles are given in **Table 6.6.**. The complex has distorted octahedral geometry with a strained *trans* arrangement of both the IMes ligands (C(3)-Ru-C(24) = 167.94(8)°) and the hydroxo group *trans* to the carbonyl (C(2)-Ru-O(3) = 172.7(4)°). The Ru-O distance of 2.058(3) Å is significantly shorter than that seen in [*trans*-$Ru(dmpe)_2(OH)H.H_2O]_2$ (2.230(2) Å),[53a] presumably due to the greater *trans* influence of H compared to CO, but is globally in good agreement with various metal hydroxides reported in the literature as shown in **Table 6.7.**. The weaker *trans* influence of OH relative to hydride explains the two quite different Ru-CO distances found in the structure of **(48)** (1.966(3), 1.873(6) Å) **[See Chapter 6.3.]**.

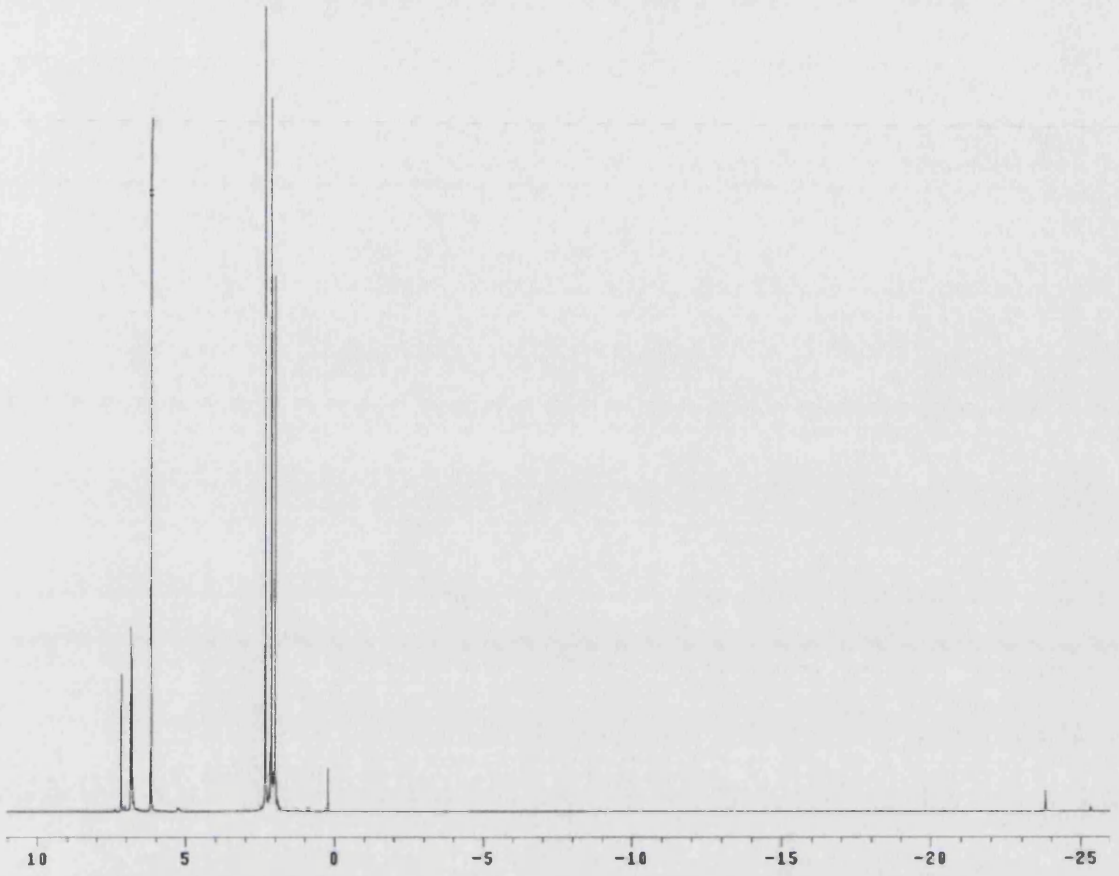

Spectrum 6.14. *^1H NMR spectrum of the reaction mixture from reaction of* ***(40)*** *with D_2O.*

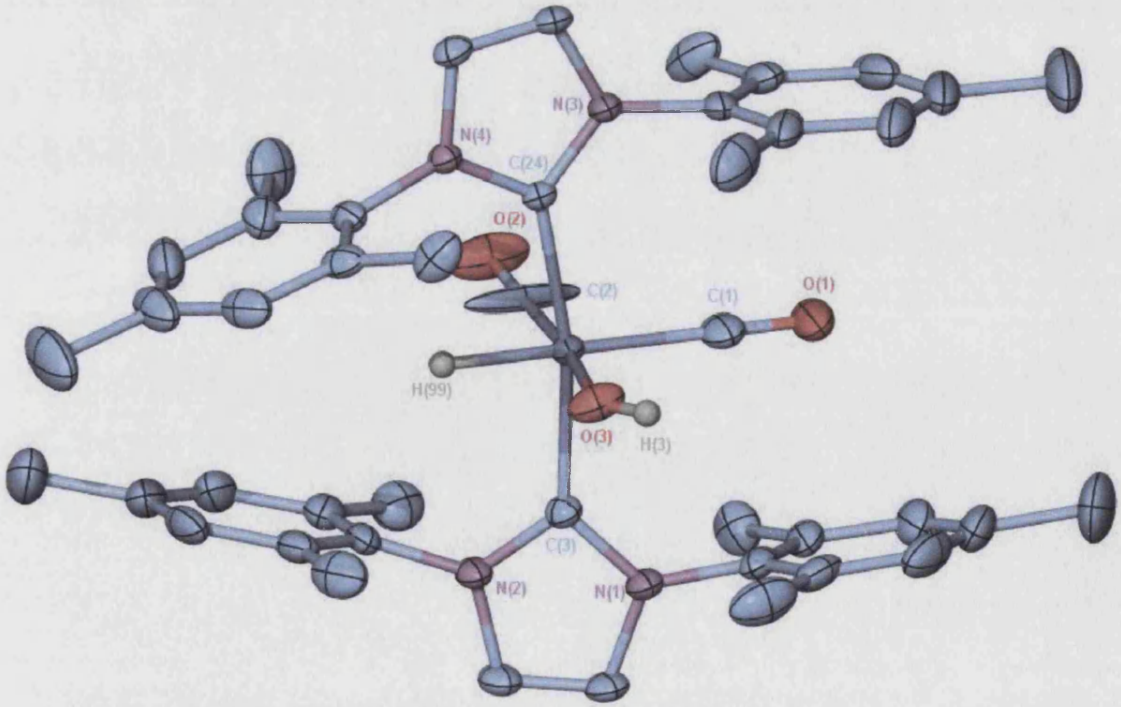

X-Ray 6.4. - *X-ray structure of* ***(48)****. Thermal ellipsoids are set at the 50% probability level. Hydrogen atoms (apart from hydride and hydroxide hydrogen's) have been omitted for clarity.*

Selected Bond Lengths	**[Å]**		
Ru(1)-C(2A)	1.931(14)	Ru(1)-C(2)	1.873(6)
Ru(1)-O(3)	2.058(3)	Ru(1)-C(1)	1.966(3)
Ru(1)-C(24)	2.101(2)	Ru(1)-O(3A)	2.10(2)
O(1)-C(1)	1.144(3)	Ru(1)-C(3)	2.113(2)
		O(2)-C(2)	1.207(7)
Selected Bond Angles	**[°]**		
C(2)-Ru(1)-C(2A)	150.5(6)	C(2A)-Ru(1)-C(1)	111.9(5)
C(2)-Ru(1)-C(1)	97.5(4)	C(2)-Ru(1)-O(3)	172.7(4)
C(2A)-Ru(1)-O(3)	22.8(4)	C(1)-Ru(1)-O(3)	89.44(15)
C(2A)-Ru(1)-O(3A)	154.5(6)	C(1)-Ru(1)-O(3A)	93.6(3)
O(3)-Ru(1)-O(3A)	174.9(4)	C(2A)-Ru(1)-C(24)	90.1(3)
C(2)-Ru(1)-C(24)	88.7(2)	O(3)-Ru(1)-C(24)	88.49(10)
C(1)-Ru(1)-C(24)	96.22(9)	C(2A)-Ru(1)-C(3)	82.5(3)
O(3A)-Ru(1)-C(24)	87.1(4)	O(3)-Ru(1)-C(3)	88.28(11)
C(2)-Ru(1)-C(3)	93.1(2)	C(24)-Ru(1)-C(3)	167.94(8)
C(1)-Ru(1)-C(3)	95.37(9)	O(3A)-Ru(1)-C(3)	95.5(4)

Table 6.6. - *Selected bond lengths [Å] and angles [°] for Ru(IMes)$_2$(CO)$_2$(OH)H* ***(48)***.

Compounds	**M-O [Å]**	**[Ref]**
trans-Ru(dmpe)$_2$(OH)H	2.230(2)	**[53c]**
Tp^{i}Pr$_2$Ru(dppe)(OH)	2.067(4)	**[53d]**
cis-Ru(PMe$_3$)$_4$(OH)(Ph)	2.168(3)	**[53e]**
cis-[Ir(PMe$_3$)$_4$(OH)H]$^+$	2.119(5)	**[53f]**

Table 6.7. - *Selected M-O bond distances in metal hydroxy complexes.*

The slower conversion of **(40)** to **(58)** compared to the formation of **(58)** from the ethanol complex **(39)**, prompted us to probe the mechanism of the reaction by ^{13}CO labelling in an attempt to identify any intermediates present. Thus, addition of ^{13}CO to **(40)** showed by $^{13}C\{^{1}H\}$ NMR spectroscopy at early times (5 h) only the hydroxy hydride complex **(48)** and a small amount of **(58)** **[Spectrum 6.15.]**. Over time (36 h) as **(48)** was depleted and **(58)** grew in, we also detected an additional minor product, which was identified as the η^1-bicarbonate complex $Ru(IMes)_2(CO)_2(OC(O)OH)H$ **(57)** **[Spectrum 6.16]**, on the basis of an alternative synthetic route as reported in **Chapter 6.2.5.2.**.

We therefore postulate that **(48)**, **(57)** and **(58)** are formed via the mechanism shown in **Scheme 6.20.**. The hydroxy hydride inserts ^{13}CO in an analogous way to $Ru(IMes)_2(CO)_2(OEt)H$, but the resulting $Ru(IMes)_2(CO)_2(C(O)OH)H$ species readily decarboxylates to give **(47)** and CO_2. The dihydride complex **(47)** then reacts with CO to afford **(58)**, while CO_2 inserts into the Ru-OH bond of **(48)** to yield the bicarbonate complex **(57)**. Although free $^{13}CO_2$ was not observed in the ^{13}CO labelled experiments, reaction of CO_2 with an isolated sample of the hydroxy hydride complex afforded **(57)** as the only product, giving strong support to the proposed scheme **(Chapter 6.2.5.2.)**. The initial formation of some $Ru(IMes)_2(CO)_3$ upon addition of CO to **(40)** implied that there must be a minor pathway to the tricarbonyl either directly from the water complex, or via the hydroxy hydride.

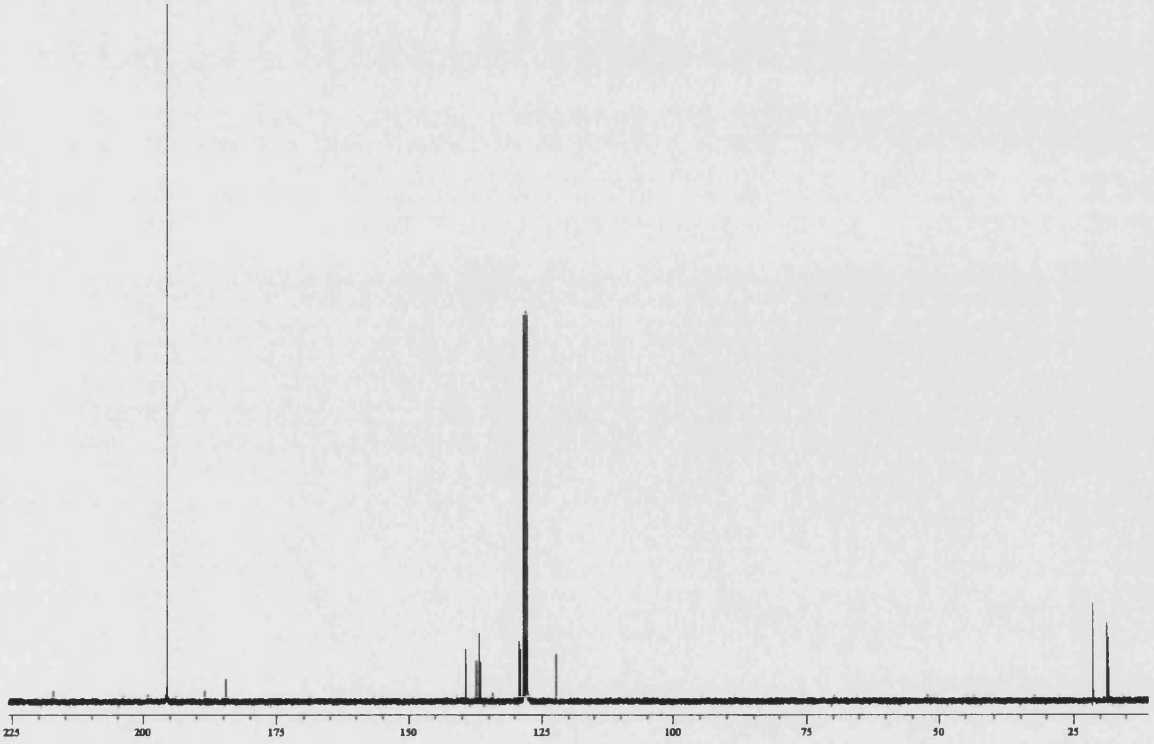

Spectrum 6.15. - *^{13}C spectrum of the reaction of **(40)** with CO after 5 h.*

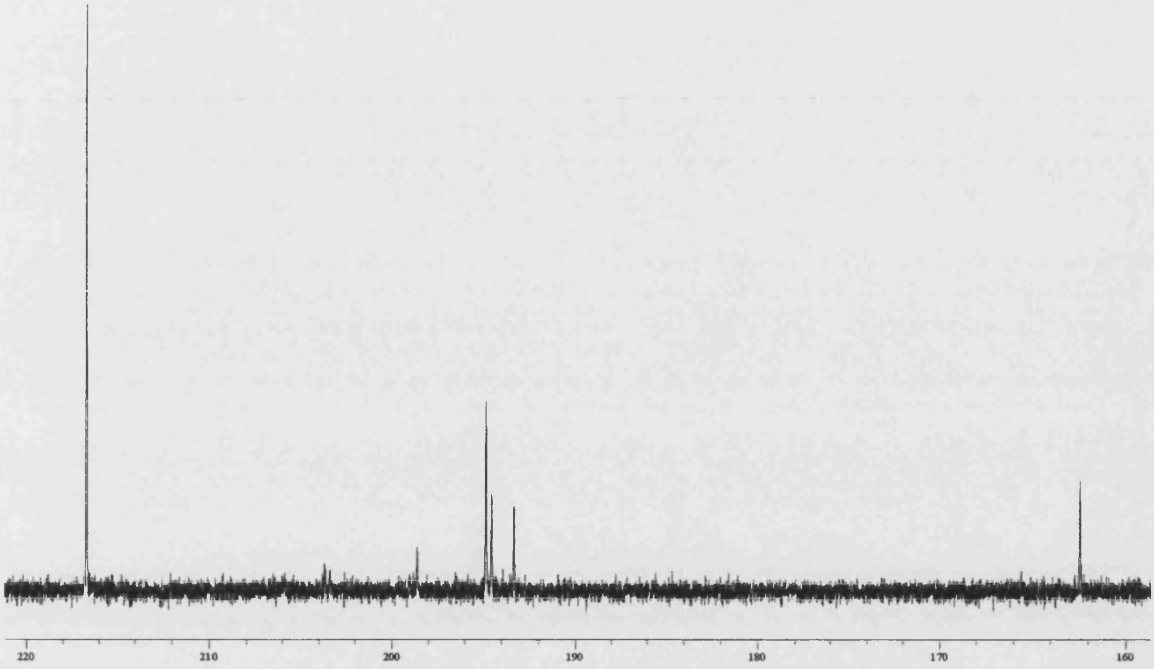

Spectrum 6.16. - *^{13}C spectrum of the reaction of **(40)** with CO after 36 h.*

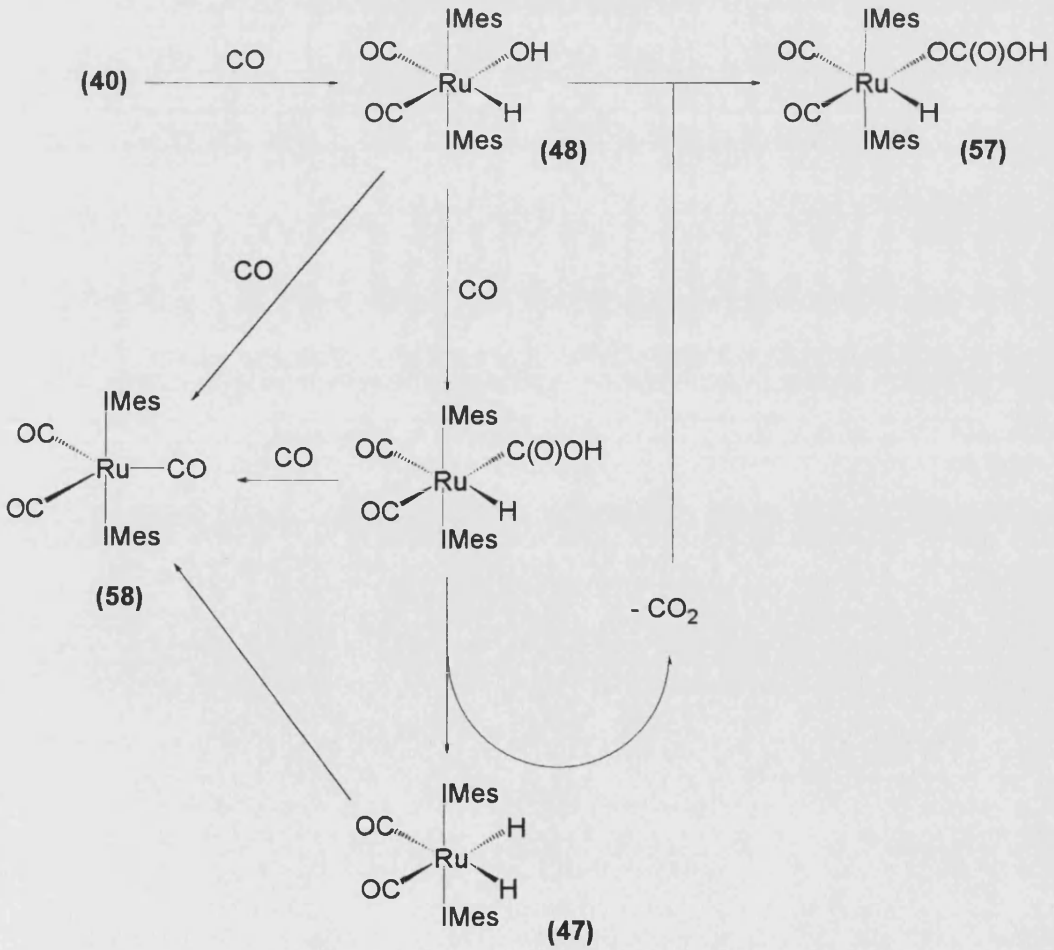

Scheme 6.20. - *Postulated mechanisms for the formation of **(58)** and side product **(57)** from the reaction of **(40)** with CO.*

6.2.4. Reaction of (39) and (40) with O-donor ligands.

The ^1H NMR spectrum of **(39)** in C_6D_6 recorded following addition of a 20-fold excess of water showed significant broadening of the hydride signal at δ -23.51 **[Spectrum 6.17.]**, but no broadening of the ethanol ligand nor any resonance for the aqua complex **(40)** was detected.

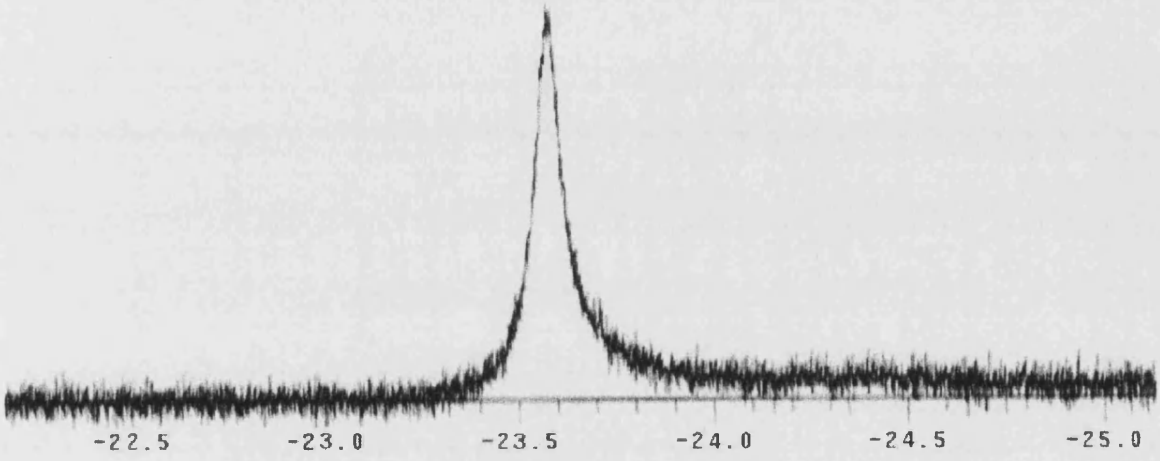

Spectrum 6.17. – *^1H NMR spectrum of the solution of **(39)** + H_2O. (Hydride region).*

In the same way, broadening of hydride signal was observed upon addition of EtOH to solutions of the aqua complex. These observations suggest either the presence of intermolecular M-H···H-OR hydrogen bonding interactions, examples of which have recently been reported,[47] or Ru-H/H-OR exchange. No reaction was seen upon the addition of DMSO or THF to benzene solutions of **(39)** or **(40)**. We assumed that donor ligand bulk was responsible for this lack of reaction.

6.2.5. Addition of CO_2 or HO_2C-(C_5H_4N) reactions to (39) and (40).

6.2.5.1. Characterisation of $Ru(IMes)_2(CO)(\kappa^2\text{-}O_2COR)H$ (R = H (54), Et (55), C_5H_4N) (56))

(54) **(55)**

Scheme 6.21.

The reaction of **(39, 40)** with dry CO_2 resulted in formation of $Ru(IMes)_2(CO)(\kappa^2\text{-}O_2COEt)H$ and $Ru(IMes)_2(CO)(\kappa^2\text{-}O_2COH)H$ respectively **[Scheme 6.21.]**.

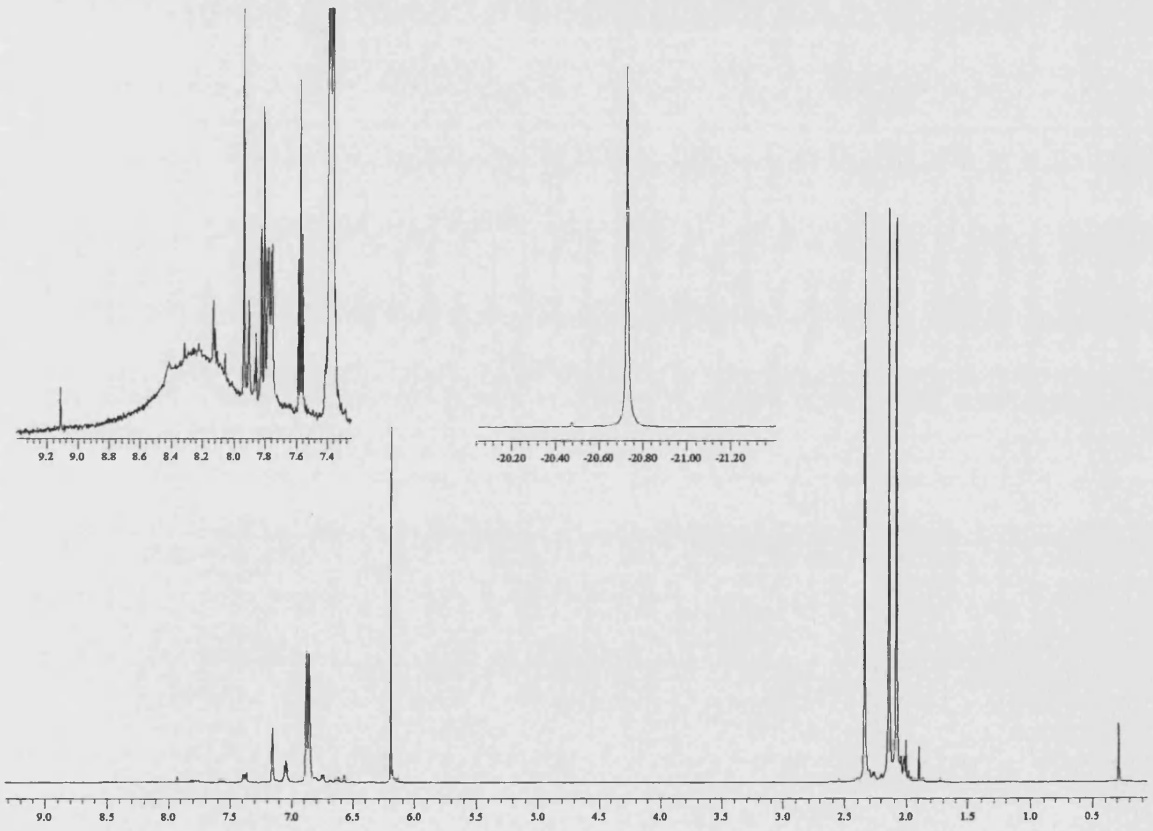

Spectrum 6.18. - *^1H NMR spectrum of (54).*

The ^{1}H NMR spectrum of **(54)** showed a hydride resonance at δ –20.73 and a broad OH signal for the bicarbonate ligand at δ 8.80 **[Spectrum 6.18.]**; The $^{13}C\{^{1}H\}$ displayed a carbonyl resonance at 207.4 ppm, a carbene carbon at 194.0 ppm, and a distinctive singlet for the bicarbonate carbon at 160.3 ppm.[60]

In the same way, **(39)** reacted with $^{13}CO_2$ in C_6D_6 to produce the partially soluble complex $Ru(IMes)_2(CO)(\kappa^2\text{-}O_2{}^{13}COEt)H$ **(55) [Scheme 6.21., Spectrum 6.19.]**. This displayed an hydride resonance for **(55)** at δ –18.84 and a coupled (doublet of quartets) methylene signal at δ 3.56 (J_{HH} = 6.8 Hz, J_{HC} = 2.4 Hz). The bicarbonate carbon appeared as a distinctive singlet at 158.7 ppm in the $^{13}C\{^{1}H\}$ NMR spectrum.[60]

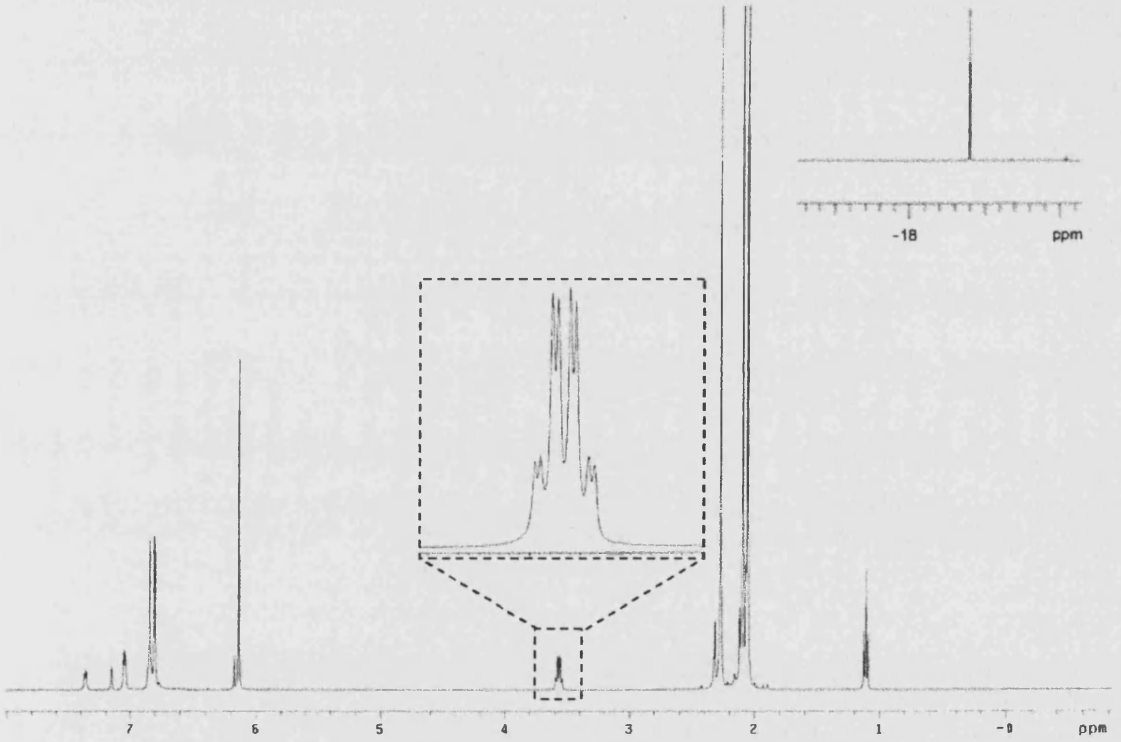

Spectrum of 6.19. - *^{1}H NMR spectrum of (55).*

The κ^2-coordination mode in both these compounds was revealed by the IR spectra, which contain symmetric OCO stretches at 1593 and 1598 cm^{-1} and stretching modes at 1453 and 1460 cm^{-1} for **(54)** and **(55)** respectively.[60,61]

All attempts to isolate crystals of **(54, 55)** suitable for X-ray crystallography proved unsuccessful. Nevertheless use of isonicotinic acid ($NC_5H_4CO_2H$) afforded the κ^2-isonicotinate complex $Ru(IMes)_2(CO)(\kappa^2\text{-}O_2CC_5H_4N)H$ **(56)** **[Scheme 6.22.]**.

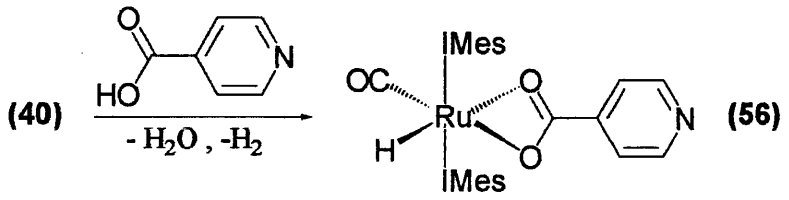

Scheme 6.22.

Similarly to **(54, 55)**, the ^1H NMR spectrum of **(56)** showed an hydride resonance at δ –18.49 and a distinctive resonance for the bicarbonate carbon atom at 172.2 ppm in the $^{13}C\{^1H\}$ NMR spectrum. As seen for **(54)** and **(55)**, the IR spectra displays a bands at 1596 cm^{-1} for symmetric OCO stretching of the κ^2-coordination mode, and at 1461 cm^{-1} for the asymmetric stretching modes.[60,61]

The κ^2-coordination mode in **(56)** was authenticated by an X-ray crystal structure determination **[X-Ray 6.5.]**. Selected geometric data are given in **Table 6.9.**. The $O_2CC_5H_4N$ ligand sits almost perfectly perpendicular to the IMes-Ru-IMes axis with the pyridyl ring twisted 7.8° out of the RuOCO plane. The Ru-O bond lengths (2.2763(16), 2.2921(14) Å) are long in comparison to the Ru-O distances in similar ruthenium carboxylate complexes **[Table 6.8.]**.

Compounds	Ru-O distance	[Ref]
$Ru(PPh_3)_2(CO)(MeOH)(OC(O)CF_3)_2$	2.139(6) / 2.101(7)	**[62]**
$Ru(PPh_3)_2(CO)_2(OC(O)Ph)_2$	2.086(5) / 2.083(7)	**[63]**
$Ru(PPh_3)_2(CO)_2(O_2CO)$	2.079(2)	**[64]**

Table 6.8. - *Selected Ru-O bond distances in carboxylate complexes of ruthenium.*

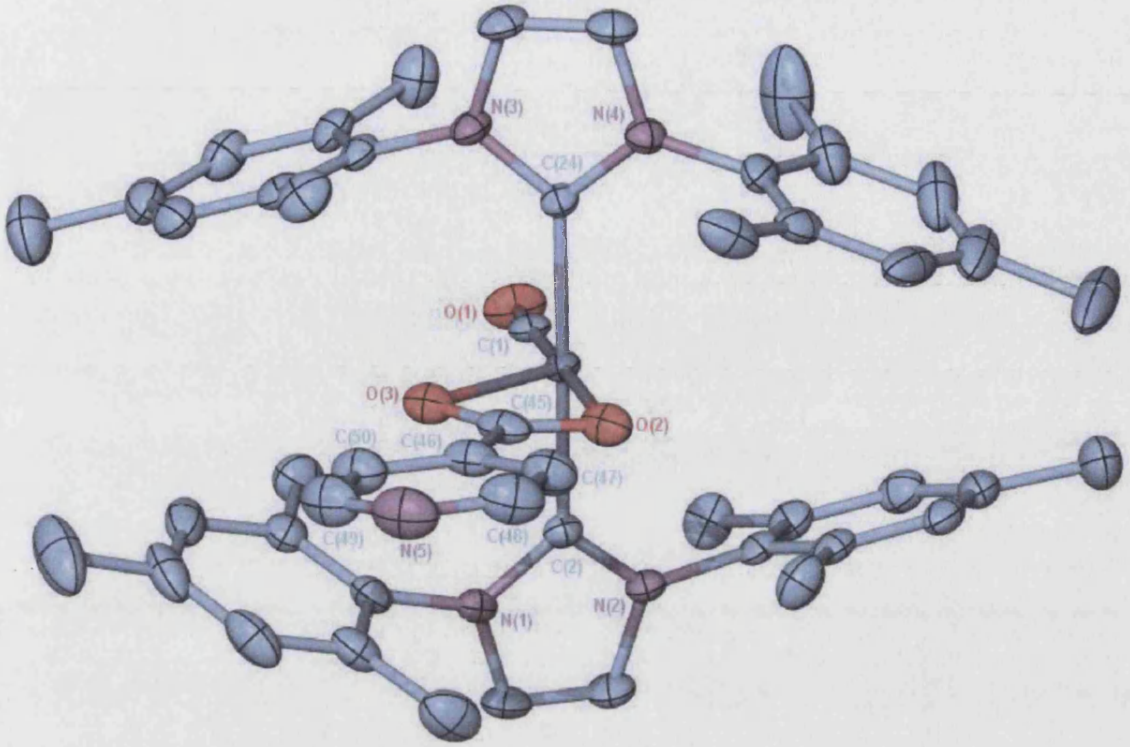

X-Ray 6.5. - *X-ray structure of* ***(56)****. Thermal ellipsoids are set at the 50% probability level. Hydrogen atoms have been omitted for clarity (The hydride could not be reliably located due to disorder within the complex).*

Selected Bond Lengths	**[Å]**		
Ru(1)-C(1A)	1.733(6)	Ru(1)-C(1)	1.803(3)
Ru(1)-C(2)	2.0897(18)	Ru(1)-C(24)	2.0962(18)
Ru(1)-O(2)	2.2763(16)	Ru(1)-O(3)	2.2921(14)
O(1)-C(1)	1.172(4)	O(2)-C(45)	1.264(3)
O(3)-C(45)	1.257(3)		
Selected Bond Angles	**[°]**		
C(1A)-Ru(1)-C(1)	56.7(3)	C(1A)-Ru(1)-C(2)	92.08(19)
C(1)-Ru(1)-C(2)	86.30(11)	C(1A)-Ru(1)-C(24)	87.76(19)
C(1)-Ru(1)-C(24)	92.63(11)	C(2)-Ru(1)-C(24)	178.82(8)
C(1A)-Ru(1)-O(2)	122.8(3)	C(1)-Ru(1)-O(2)	177.09(10)

C(2)-Ru(1)-O(2)	90.87(6)	C(24)-Ru(1)-O(2)	90.20(6)
C(1A)-Ru(1)-O(3)	175.26(18)	C(1)-Ru(1)-O(3)	123.12(12)
C(2)-Ru(1)-O(3)	92.63(6)	C(24)-Ru(1)-O(3)	87.53(6)
O(2)-Ru(1)-O(3)	57.67(6)	C(45)-O(2)-Ru(1)	90.48(14)
C(45)-O(3)-Ru(1)	89.94(13)		

Table 6.9. *Selected bond lengths [Å] and angles [°] for Ru(IMes)$_2$(CO)(κ^2-$O_2COC_5H_4N$))H.*

Although **(54-56)** are structurally related, differences in there synthesis suggest two different mechanisms in there formations. A common feature observed in the preparation of these later was formation of hydrogen gas during the synthesis. Although the mechanistic of the formation of **(54, 55)**, and **(56)** was not studied a proposed mechanism can be devised.

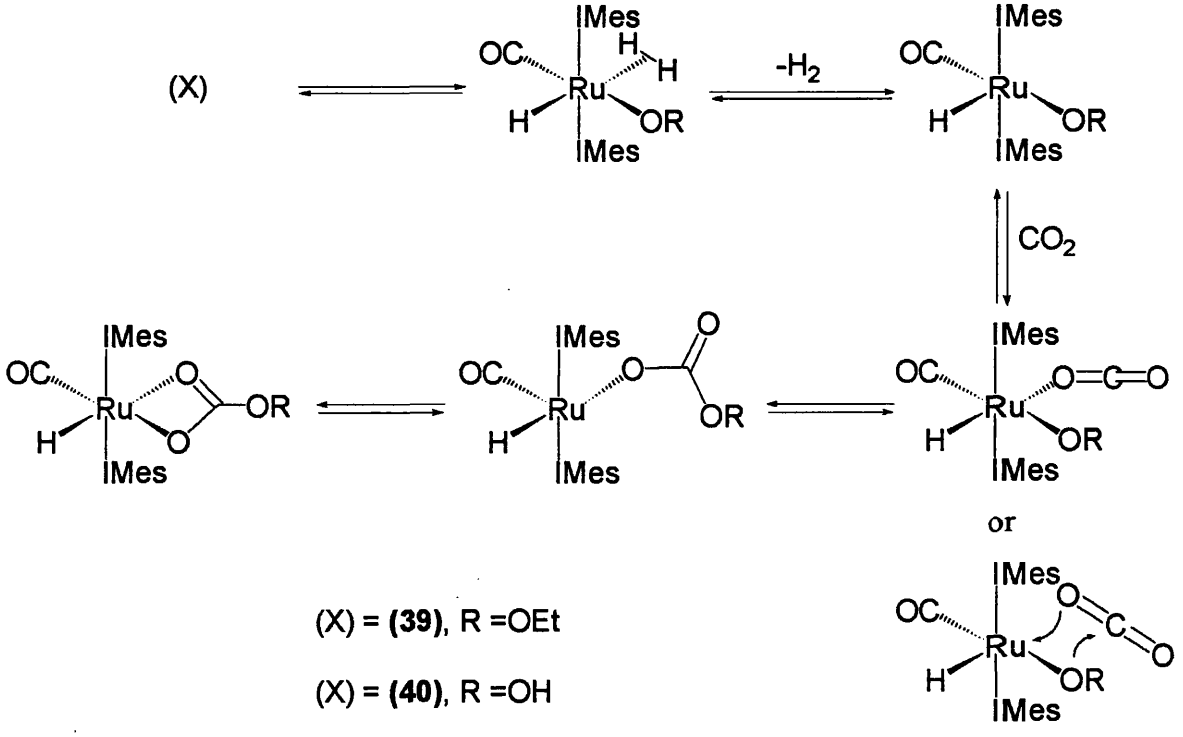

Scheme 6.23. - *Proposed mechanism for the formation of (54) and (55).*

In the reaction of **(39, 40)** with CO_2 proton transfer must occur in a first step to generate a vacant site (through a 16 e$^-$ species already postulated in the formation of **(48))** **[Scheme 6.23.]**. Which then insert CO_2 and proceed through to generate **(54, 55)**. The second part of this mechanism has already been described in many CO_2 insertion into M-H

bonds,[65] and Ab Initio MO study of the mechanism of CO_2 insertion into a Cu(I)-H bond has shown to proceed via charge transfer from the metal to the CO_2.[66] These observations easily extend to our system. Due to the coordinatively free lone pair orbital on the OR moiety lowering of the activation barrier of the insertion step readily occurs through a charge transfer interaction from the OR to CO_2 **[Scheme 6.23.]**.[66]

In the reaction of **(39, 40)** with isonicotinic acid it is possible that a first step substitution of the ROH (R = H, Et) occurs (as shown by the presence of the free ethanol in solution in the reaction of **(39)** with isonicotinic acid, followed by proton transfer to finally afford **(56) [Scheme 6.24.]**.

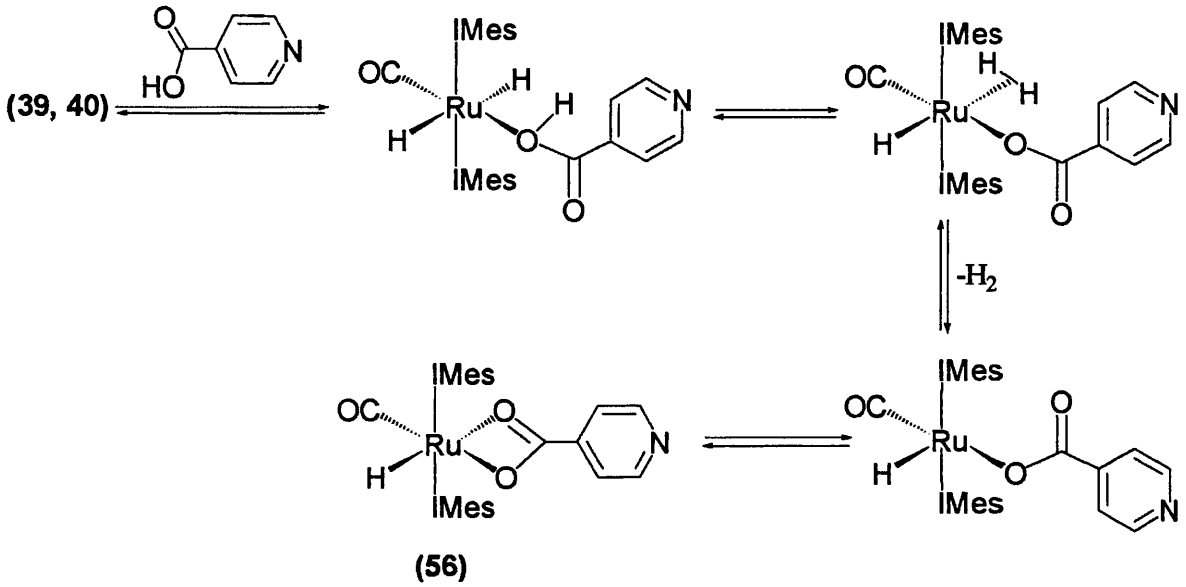

(56)

Scheme 6.24. - *Proposed mechanism for the formation of (56).*

6.2.5.2. Reactivity of (54), and (55) toward CO insertion.

The monodentate bicarbonate complex $Ru(IMes)_2(CO)_2(\eta^1\text{-}OC(O)OH)H$ **(57)** which was reported above as being formed as a minor product in the reaction of $Ru(IMes)_2(CO)_2(OH)H$ with CO, was isolated in nearly quantitative yield when CO was introduced into a C_6D_6 solution of **(54) [Scheme 6.25.]**. The NMR spectra of **(57)** showed characteristic features for this type of ligand binding, specifically a broad low field OH resonance in the ^1H NMR spectrum at δ 12.10 and a bicarbonate carbon signal at 162.8 ppm in the $^{13}C\{^1H\}$ NMR spectrum. The mode of bonding is also revealed by the appearance of the symmetric and asymmetric OCO stretching bands at 1605 and 1355 cm^{-1} in the IR spectrum.[52]

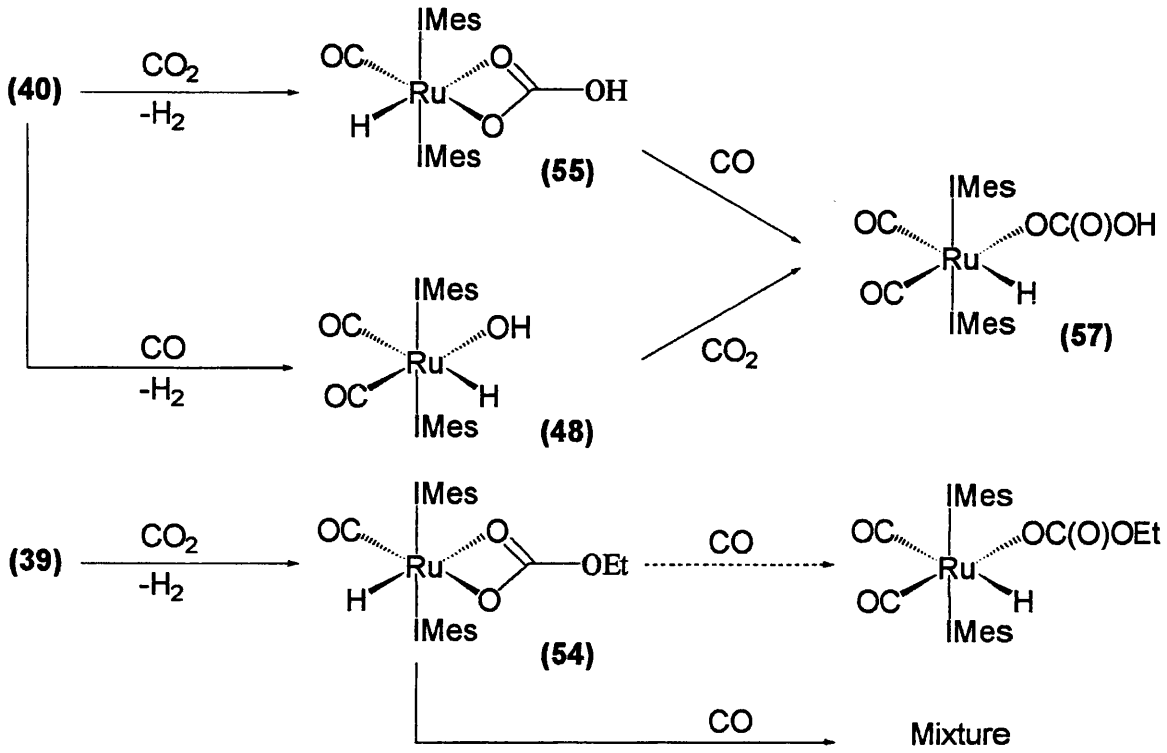

Scheme 6.25.

The X-ray crystal structure of **(57)** is shown in **X-Ray 6.6.1.** and selected bond lengths and angles are given in **Table 6.10.**.

The most significant feature of this structure is the molecular packing, which demonstrates the dimerisation of two molecules in the asymmetric unit via hydrogen bonding of the bicarbonate groups **[X-Ray 6.6.2.]**.[67] This mode of bonding has been observed before by McLoughlin et al. in 1999.[68] The Ru-O distances in **(57)** are 2.1344(18) and 2.1352(19) Å, while the Ru-CO bond lengths are significantly different due to the different *trans* influences exerted by -OC(O)OH and hydride. As in the other structurally characterised $Ru(IMes)_2(CO)_2(X)H$ complexes reported here, the *trans*-IMes ligands are somewhat strained as shown by the reduction in bond angles below 180° (C(25)-Ru(1)-C(4) 166.85(12)°, C(125)-Ru(2)-C(4) 167.66(12)°).

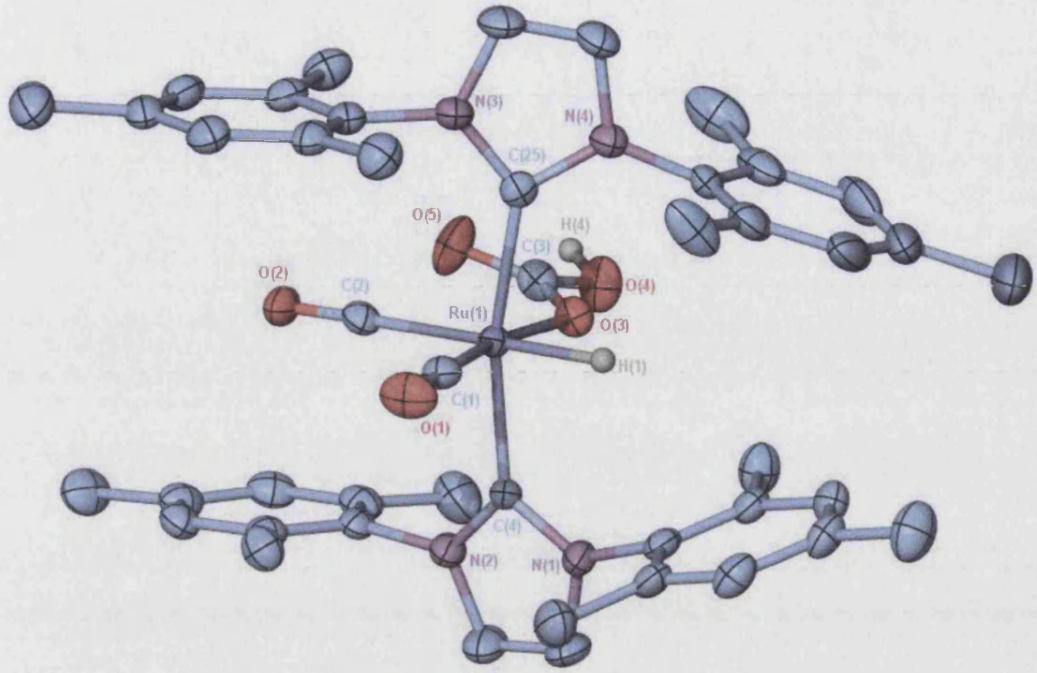

X-Ray 6.6. - *X-ray structure of* ***(57)****. Thermal ellipsoids are set at the 50% probability level. Hydrogen atoms have been omitted for clarity (apart from hydride and bicarbonate hydrogens*).

Selected Bond Lengths	**[Å]**		
Ru(1)-C(1)	1.818(3)	Ru(1)-C(2)	1.989(3)
Ru(1)-C(25)	2.110(3)	Ru(1)-C(4)	2.116(3)
Ru(1)-O(3)	2.1344(18)	Ru(2)-C(101)	1.820(3)
Ru(2)-C(102)	1.982(3)	Ru(2)-C(125)	2.112(4)
Ru(2)-C(104)	2.119(3)	Ru(2)-O(103)	2.1352(19)
O(1)-C(1)	1.164(3)	O(2)-C(2)	1.133(4)
O(3)-C(3)	1.278(3)	O(4)-H(4)	0.91(5)
O(4)-C(3)	1.348(3)	O(5)-C(3)	1.231(4)
O(5)-H(104)	1.58(5)	O(101)-C(101)	1.150(3)
O(102)-C(102)	1.145(3)	O(103)-C(103)	1.268(3)
O(104)-H(104)	1.04(5)	O(104)-C(103)	1.341(4)
O(105)-C(103)	1.237(3)	O(105)-H(4)	1.74(5)

Selected Bond Angles	[°]		
C(1)-Ru(1)-C(2)	93.08(13)	C(1)-Ru(1)-C(25)	95.33(13)
C(2)-Ru(1)-C(25)	94.53(13)	C(1)-Ru(1)-C(4)	90.82(13)
C(2)-Ru(1)-C(4)	96.73(12)	C(25)-Ru(1)-C(4)	166.85(12)
C(1)-Ru(1)-O(3)	171.69(11)	C(2)-Ru(1)-O(3)	94.52(10)
C(25)-Ru(1)-O(3)	87.43(10)	C(4)-Ru(1)-O(3)	84.94(10)
C(101)-Ru(2)-C(102)	94.89(14)	C(101)-Ru(2)-C(125)	89.48(13)
C(102)-Ru(2)-C(125)	97.78(12)	C(101)-Ru(2)-C(104)	93.12(13)
C(102)-Ru(2)-C(104)	94.02(12)	C(125)-Ru(2)-C(104)	167.66(12)
C(101)-Ru(2)-O(103)	170.19(12)	C(102)-Ru(2)-O(103)	94.71(10)
C(125)-Ru(2)-O(103)	87.22(10)	C(104)-Ru(2)-O(103)	88.22(10)
C(3)-O(3)-Ru(1)	125.23(19)	H(4)-O(4)-C(3)	106(3)

Table 6.10. - *Selected bond lengths [Å] and angles [°] for* $Ru(IMes)_2(CO)_2(\eta^1\text{-}OC(O)OH)H$.

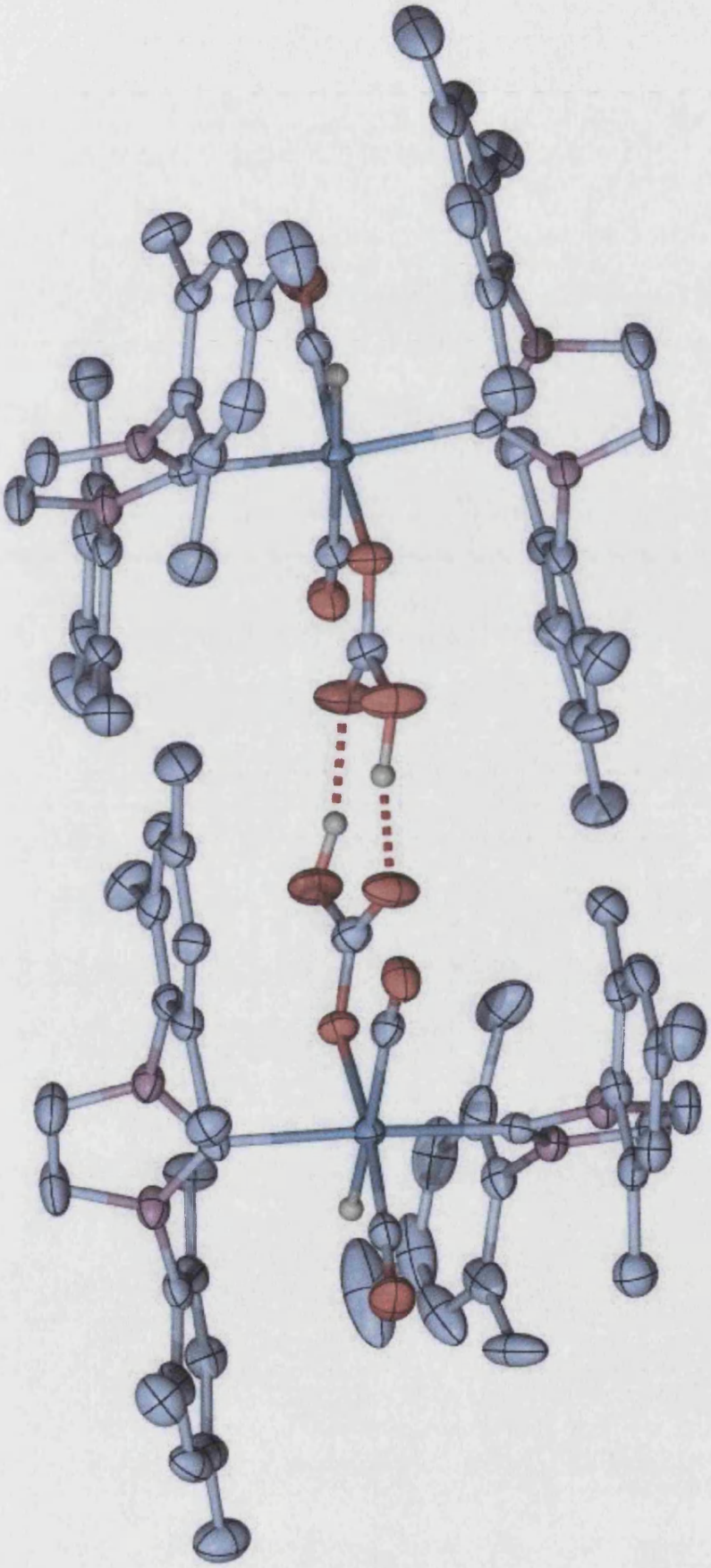

X-Ray 6.6.2 *Molecular structure of (57) showing the hydrogen bonding interaction between two molecules of the complexes trhough the carbonate linkages.*

6.2.6. Reaction of $Ru(IMes)_2(CO)(L)(H)_2$ (39, 40) with CH_3CH_2SH and H_2S.

6.2.6.1. Synthesis of $Ru(IMes)_2(CO)(CH_3CH_2CH_2SH)H_2$ (44).

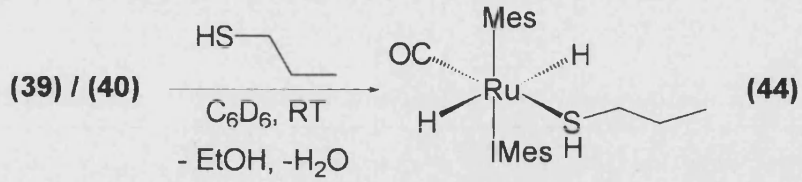

Scheme 6.26.

Propanethiol ($CH_3CH_2CH_2SH$) readily substituted at room temperature the coordinated solvent ligands (H_2O, EtOH) in both **(39)** and **(40)** to afford the same thiol dihydride product $Ru(IMes)_2(CO)(CH_3CH_2CH_2SH)H_2$ **(44) [Scheme 6.26.]**.[69] While we were unable to observe the S-H resonance in the ^1H NMR spectrum of **(44)**, the appearance of a single high-field hydride resonance (δ -23.77), similar to that seen for **(39 - 42)**, implied the presence of a 2-electron RSH ligand *trans* to CO.

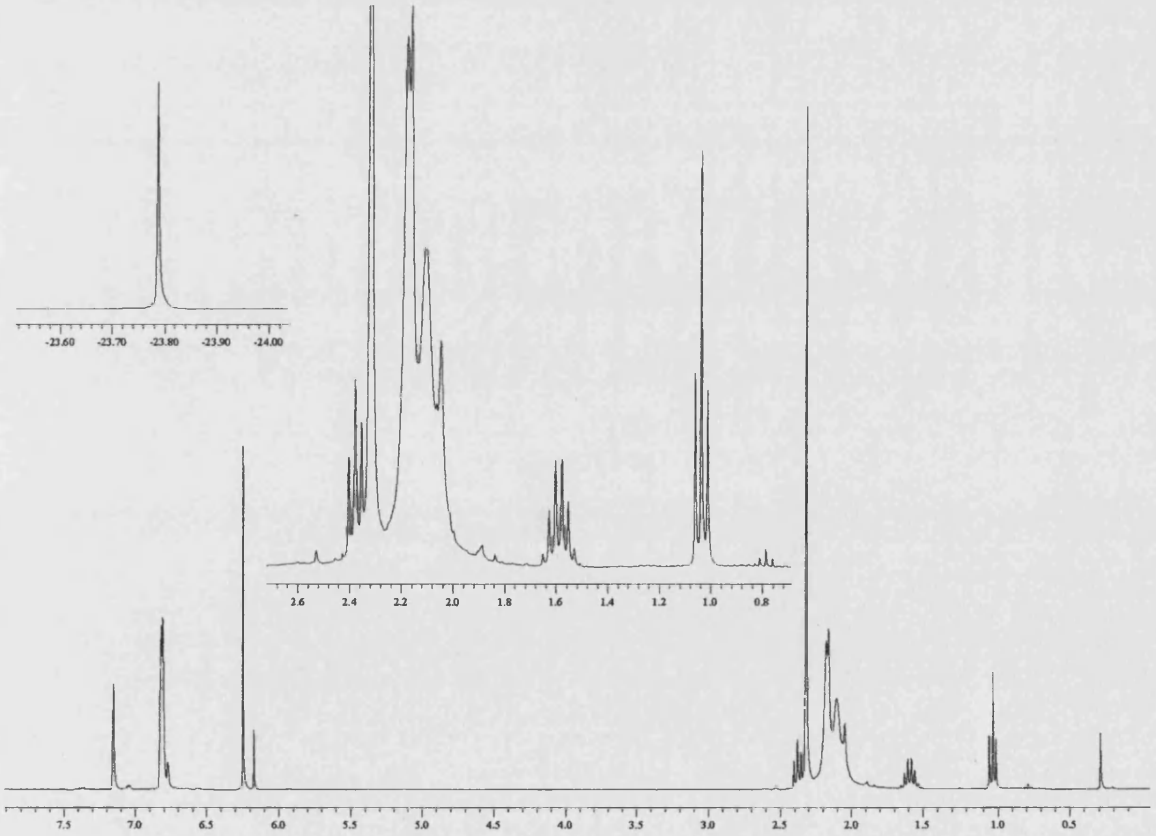

Spectrum 6.20. - *^1H NMR spectrum of (44).*

The ^1H NMR spectrum showed a large broadening of the methyl of the IMes moiety, presumably due to the interaction of the propanethiol ligand with the mesityl rings

of the carbene **[spectrum 6.20.]**. The coordinated thiol resonances are all shifted to lower field related to free $CH_3CH_2CH_2SH$. The IR spectrum of **(44)** displayed a ν_{CO} at 1883 cm^{-1}, similar to that observed for **(39 - 42)**.

The x-ray crystal structure of **(44) [X-Ray 6.7.]**, and the selected geometric data are given in **Table 6.12.**. The geometry at the ruthenium centre is very close to octahedral with a *trans*-C(5)-Ru-C(26) angle of 177.56(4)°. Disorder in the sulphur position (68:32) precluded a reliable location of the SH hydrogen atom. The occupancy levels implies that the Ru-S bond length is closer to the value of 2.3706(15) found for Ru-S(1); this distance is in line with other Ru(II) thiol complexes **[Table 6.11]**.[70]

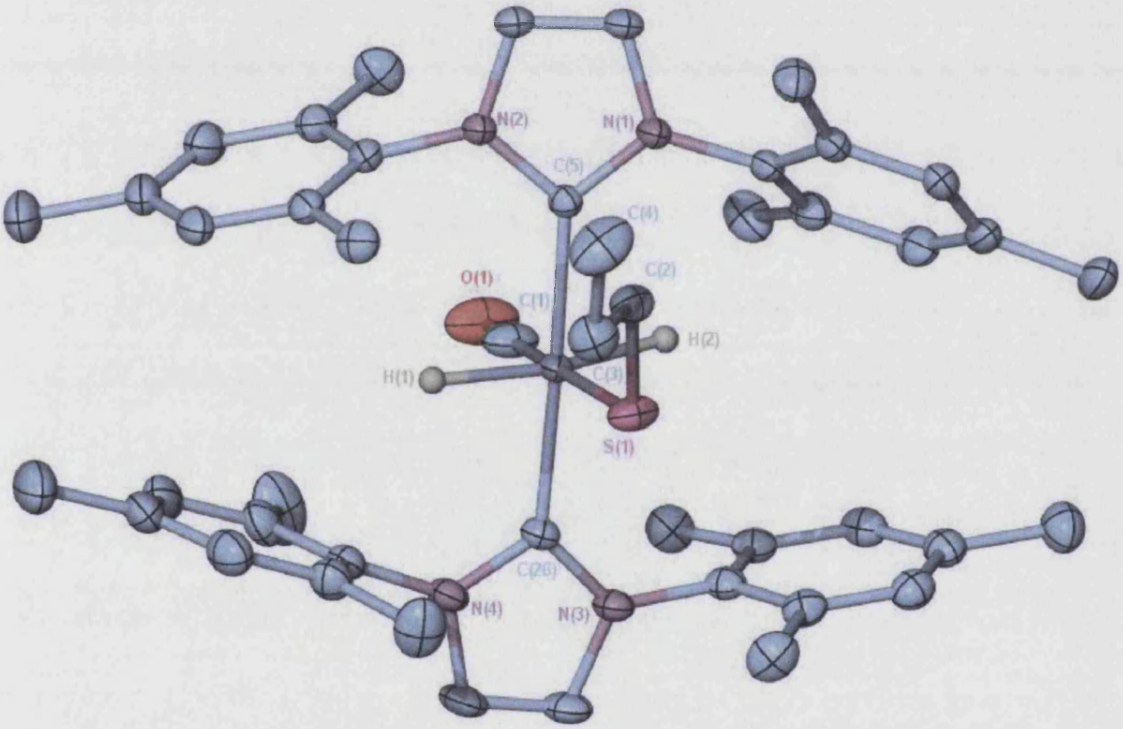

X-Ray 6.7. - *X-ray structure of **(44)**. Thermal ellipsoids are set at the 50% probability level. Hydrogen atoms have been omitted for clarity (apart from hydride).*

Compounds	Ru-S distance	S-C distance	[Ref]
$Ru(PPh_3)_2(Cp)(HSPr)$	2.377(2)	1.837(6)	**[70]**
$Ru(dppm)(Cp)(HS^tBu)$	2.371	1.870	**[71]**
$Ru(PPh_3)_2(Cp)(HS(CH_2)_2Ph)$	2.369	1.818	**[72]**

Table 6.11. - *Selected Ru-S and S-C bond distances in R-SH ruthenium complexes.*

Selected Bond Lengths	**[Å]**		
Ru(1)-C(1)	1.8258(14)	Ru(1)-C(5)	2.0874(11)
Ru(1)-C(26)	2.0917(11)	Ru(1)-S(1)	2.3706(15)
Ru(1)-S(1A)	2.425(3)	S(1)-C(2)	1.8401(19)
O(1)-C(1)	1.1578(18)		
Selected Bond Angles	**[°]**		
C(1)-Ru(1)-C(5)	87.91(5)	C(1)-Ru(1)-C(26)	90.32(5)
C(5)-Ru(1)-C(26)	177.56(4)	C(1)-Ru(1)-S(1)	173.27(6)
C(5)-Ru(1)-S(1)	95.23(5)	C(26)-Ru(1)-S(1)	86.71(5)
C(1)-Ru(1)-S(1A)	173.67(8)	C(5)-Ru(1)-S(1A)	96.11(8)
C(26)-Ru(1)-S(1A)	85.51(8)	S(1)-Ru(1)-S(1A)	10.85(6)
C(2)-S(1)-Ru(1)	114.80(8)		

Table 6.12. - *Selected bond lengths [Å] and angles [°] for Ru(IMes)$_2$(CO)(HSCH$_2$CH$_2$CH$_3$)H$_2$* ***(44)***.

6.2.6.2. Reactivity of (44) with CO.

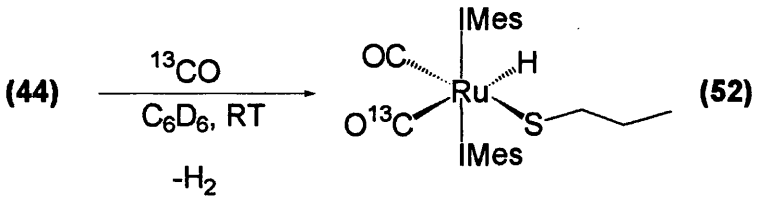

Scheme 6.27.

In line with reactions described for **(39, 40)** with CO, **(44)** reacts with CO at room temperature to generate a dicarbonyl complex, namely Ru(IMes)$_2$(CO)$_2$(SCH$_2$CH$_2$CH$_3$)H **(52)** **[Scheme 6.27.]**. Labelling experiments with ^{13}CO showed that the labelled CO is incorporated in the position *trans* to the hydride (J_{CH} = 36.6 Hz) **[Spectrum 6.21.]**.

The hydride signal for **(52)** was observed in the ^{1}H NMR spectrum at δ –4.47, while the resonances for the propyl chain (2.55, 2.26 and 1.57 ppm) were assigned on the basis of COSY spectroscopy **[Spectrum 6.22.]**. The IR spectrum shows three strong bands 2015, 1946, and 1890 cm^{-1} **[Chapter 6.3.1.]**.

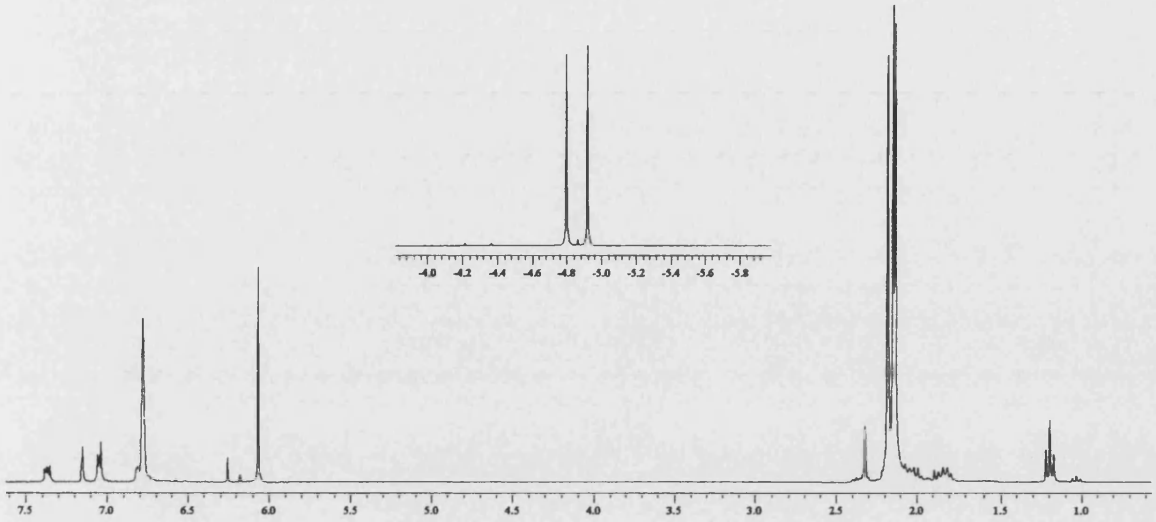

Spectrum 6.21. - *^{1}H NMR spectrum of (52).*

The structure of **(52)** was confirmed by X-ray diffraction, as shown in **X-Ray 6.8.**. Selected bond distances and angles for **(52)** are given in **Table 6.13.**. As in the structure of the hydroxy hydride **(48)**, the coordination geometry around the central ruthenium in **(52)** is distorted from a regular octahedron with highly bent *trans*-IMes-Ru-IMes and *cis*-$Ru(CO)_2$ angles (C(6)-Ru-C(27) 165.91(6)°, C(2)-Ru-C(1) 97.81(7)°). The two Ru-CO bond lengths exhibit significant differences (1.9546(18), 1.8629(17) Å), while the Ru-S distance at 2.4539(4) Å is comparable to that reported for other Ru(II) thiolate complexes **[Table 6.14.]**.[73-76]

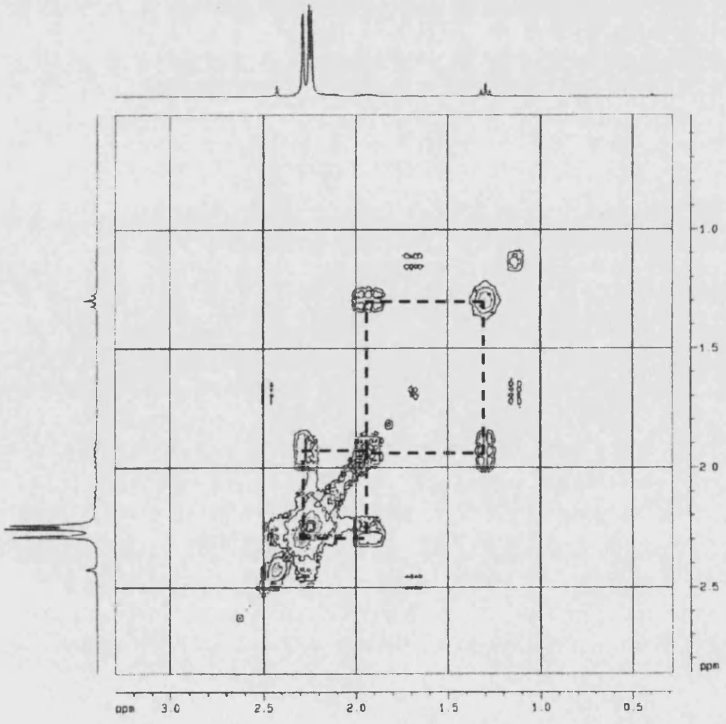

Spectrum 6.22. - *^{1}H - ^{1}H COSY spectrum (52).*

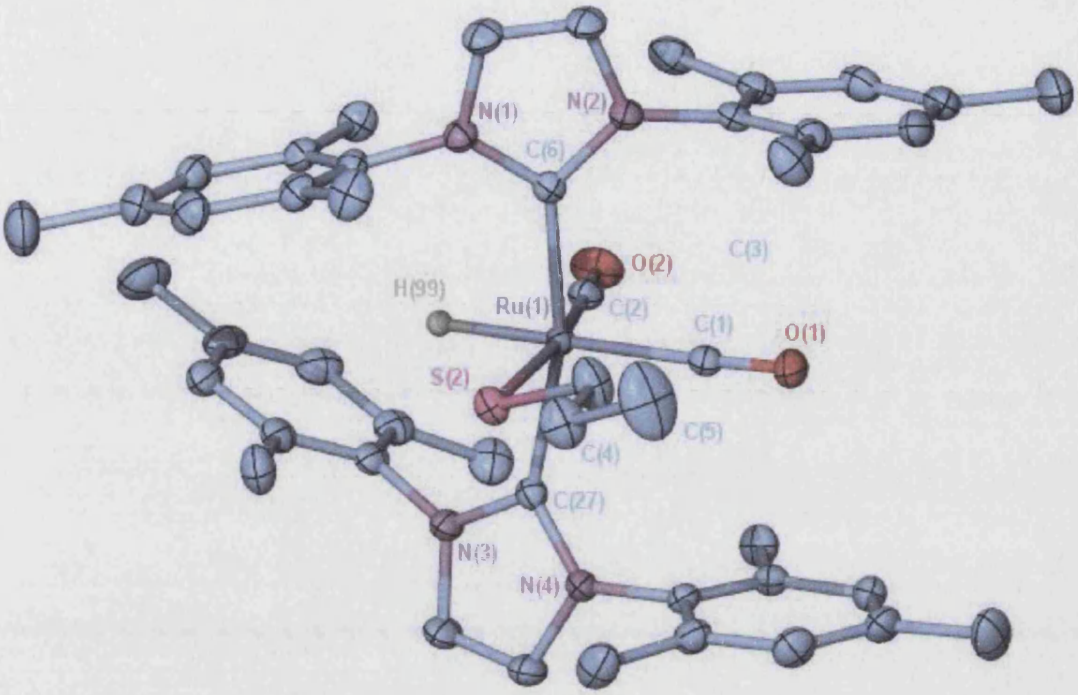

X-Ray 6.8. - *X-ray structure of* ***(52)****. Thermal ellipsoids are set at the 50% probability level. Hydrogen atoms have been omitted for clarity (apart from hydride).*

Selected Bond Lengths	**[Å]**		
Ru(1)-C(1)	1.9546(18)	Ru(1)-C(2)	1.8629(17)
Ru(1)-C(6)	2.1207(16)	Ru(1)-C(27)	2.1086(16)
Ru(1)-S(2)	2.4539(4)	O(1)-C(1)	1.142(2)
O(2)-C(2)	1.149(2)		
Selected Bond Angles	**[°]**		
C(2)-Ru(1)-C(1)	97.81(7)	C(1)-Ru(1)-C(27)	97.69(7)
C(2)-Ru(1)-C(27)	91.43(7)	C(2)-Ru(1)-C(6)	94.04(7)
C(1)-Ru(1)-C(6)	94.41(6)	C(27)-Ru(1)-C(6)	165.91(6)
C(1)-Ru(1)-S(2)	92.94(5)	C(2)-Ru(1)-S(2)	168.89(6)
C(6)-Ru(1)-S(2)	87.87(4)	C(27)-Ru(1)-S(2)	84.35(5)
O(1)-C(1)-Ru(1)	177.57(15)	C(3)-S(2)-Ru(1)	106.75(7)
O(2)-C(2)-Ru(1)	176.62(16)		

Table 6.13. *Selected bond lengths [Å] and angles [°] for $Ru(IMes)_2(CO)_2(SPr)H$.*

Compounds	Ru-S [Å]	[Ref]
$Ru(SPh)_2(DMPE)_2$	2.472(1) / 2.466(1)	[73]
cct-$RuH(SC_6H_4pMe)(CO)_2(PPh_3)_2$	2.458(1)	[74]
cct-$Ru(SC_6H_4pMe)_2(CO)_2(PPh_3)_2$	2.450(2) / 2.470(2)	[74]
$(\eta^6$-arene$)Ru(2,4,6\text{-}SC_6H_2(CHMe_2)_3)_2$	2.259(1)/2.339(1)	[75]

Table 6.14. *Selected bond lengths [Å] in Ru-S-C-R complexes.*

The high acidity of coordinated thiol ligands[76] combined with the instability of many thiol complexes[77] helps to explain the paucity of structurally characterised thiol complexes. The transformation of **(44)** into **(52)** upon reaction with CO is presumed to follow a similar protonation or hydrogen transfer pathway to that described above for the formation of $Ru(IMes)_2(CO)_2(OH)H$. Support for such a process comes from the work of James and co-workers[78] who have reported H/D exchange both Ru-SH and Ru-H in $Ru(PPh_3)_2(CO)_2(SH)H$ in CD_3OD doped C_6D_6 solutions.

In a logical step (*cf.* **(39, 40)** + CO_2) **(44)** was reacted with CO_2 (1 atm). No reaction was observed even upon heating to 120°C. This can be explained by the strong nature of the Ru-S bond in thiolate compounds, which prevent CO_2 insertion.[79] This point was demonstrated in 1995 by Bergman and co-workers who reported that the addition of p-thiocresol to a phenoxide complex led to quantitative formation of the arylthiolate complex at room temperature. They argued that the Ru-S bond was stronger that the Ru-O bond because of the soft Ru(2+) centre and its favourable coordination to the soft sulfur bond. Also the reaction was driven forward by the difference in E-H bond dissociation energies since in PhSH the S-H bond is weaker than the O-H bond by 3 kcal/mol.[80] Finally calorimetric studies by Nolan et al. have shown that formation of a Ru-S bond at the expense of a Ru-O bond can be viewed to be favoured by ca. 20 kcal mol^{-1}.[69]

6.2.6.3. Synthesis of $Ru(IMes)_2(H_2S)(CO)(H)_2$.

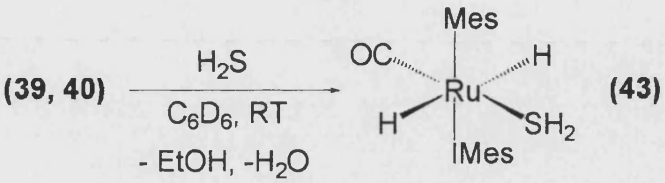

Scheme 6.28.

In the same manner of propanethiol, hydrogen sulfide (H_2S) readily substituted the coordinated solvent in both **(39, 40)** at room temperature to afford $Ru(IMes)_2(CO)(H_2S)H_2$ **(43) [Scheme 6.28.]**. In related H_2S complexes of ruthenium the ^1H resonance of the coordinated H_2S have been shown to occur at a relatively high frequency (broad singlet at 1.0 ppm for cis-$RuCl_2$(P-N)(PPh_3)(SH_2)[80] and singlet at 1.96 ppm for $Ru(SH_2)(PPh_3)('S_4')$[81] moreover in some cases the signal for these have even been shown to split upon cooling due to intramolecular coupling within the H_2S fragment as demonstrated for cis-$RuCl_2$(P-N)(PPh_3)(SH_2): 0.36ppm and 1.42ppm). In our system the H_2S resonance was readily detected in the ^1H NMR spectrum of **(43)** as a singlet peak at -0.58 integrating in a 1:2 ratio with the NCH=CHN protons (shifted to lower frequency from the free H_2S: 0.29 ppm) but these did not show any splitting upon cooling to lower temperature. The appearance of a single high-field hydride resonance (δ -24.47) testified to the *trans* hydride structure **[Spectrum 6.23.]**. Finally the IR spectrum of **(43)** displayed a ν_{CO} band at 1879 cm^{-1}, which is in a similar region as previously observed for **(39 - 42)**.

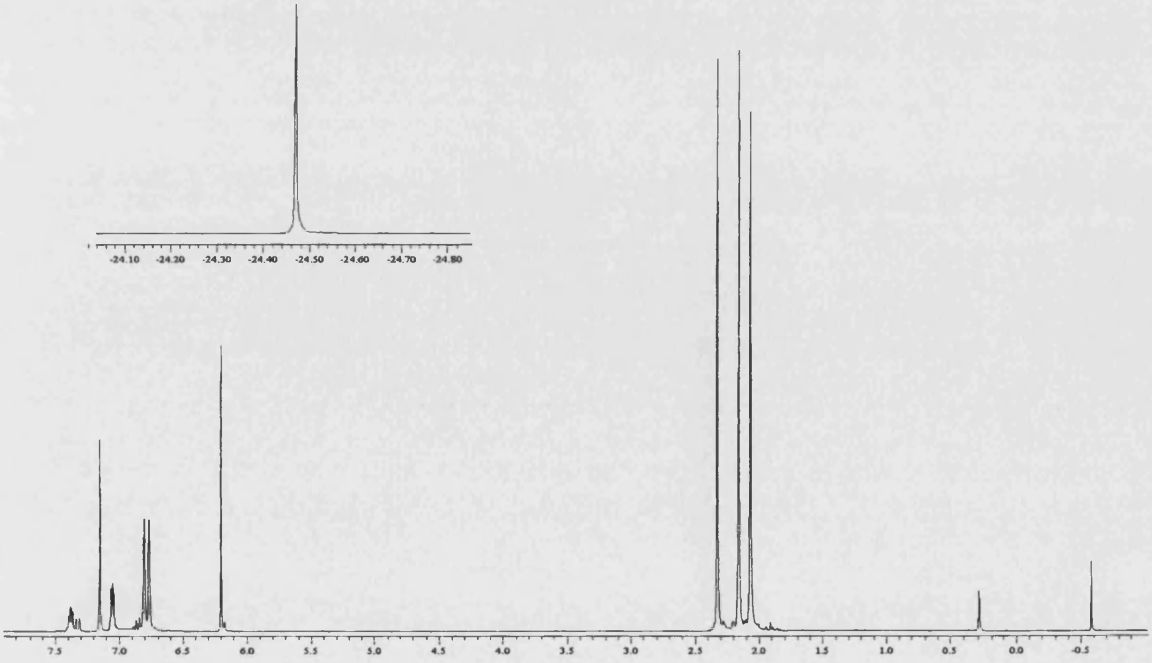

Spectrum 6.23. - *^1H NMR spectrum of (43).*

Deep orange crystals of **(43)** were grown out of a benzene/hexane mixture, and the structure of this later was confirmed by X-ray diffraction (30(2) K), as shown in **X-Ray 6.9,** and selected bond distances and angles for **(43)** are given in **Table 6.16.**. The asymmetric unit in this structure was seen to consist of 2 independent halves of the organometallic species. The carbene complexes are based on Ru1 and Ru2 respectively.

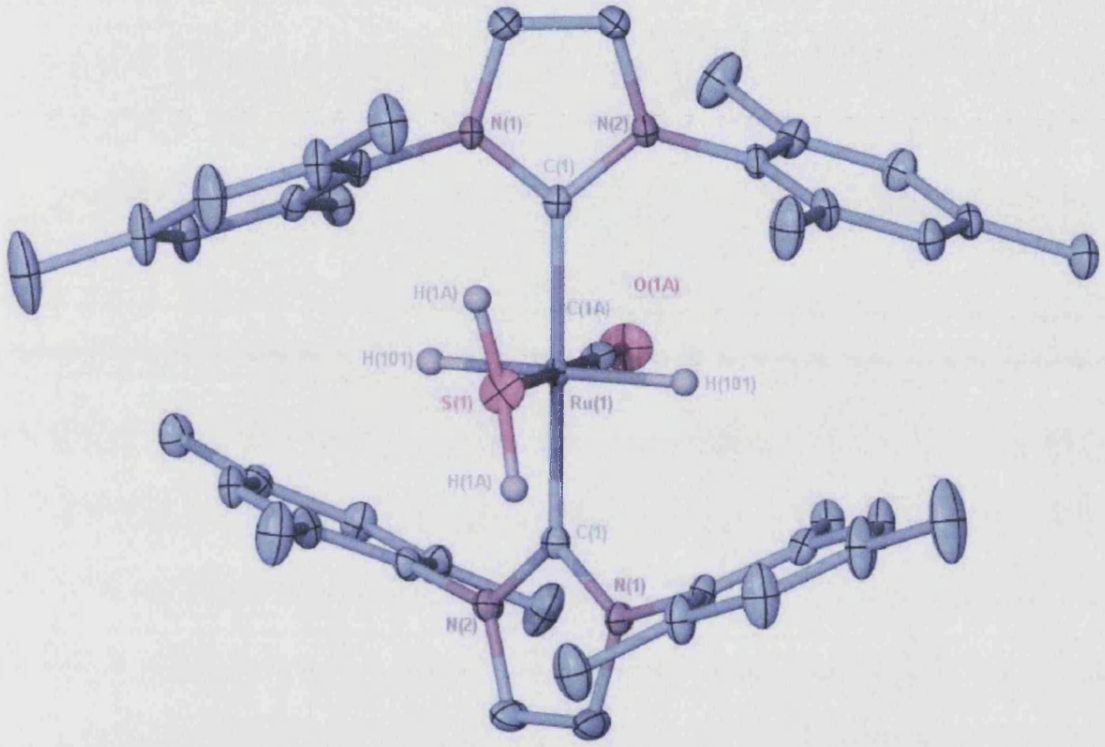

X-Ray 6.9. *X-ray structure of* ***(43)****. Thermal ellipsoids are set at the 50% probability level. Hydrogen atoms have been omitted for clarity (apart from hydride, and H_2S hydrogens).*

The first of these molecular fragments is positioned such that the central metal along with the CO and sulphur from the H_2S are located on a crystallographic 2-fold rotation axis, with the ligands disordered in a 1:1 ratio along this symmetry element. Nonetheless the partial hydrogens on the disulphide were readily located, as was the hydride hydrogen on the metal (H101). The second *bis* carbene molecule was also seen to be located on a 2-fold rotation axis, although in this instance, it was the metal plus the two hydrides which are located on the symmetry element. As in the previous fragment, the CO and H_2S ligands displayed 1:1 positional disorder. The geometry at the ruthenium centre is close to octahedral with two *trans* IMes ligands (180.000(1)°). The IMes ligands in **(43)** are twisted 52.2° from coplanarity. Disorder in the sulfur position of the two ruthenium fragment implies that the Ru-S bond length is closer to the value of 2.402(2) Å found for

Ru-S(1); this distance is in line with other Ru(II) H_2S complexes **[Table 6.15.]**, and is shorter than that of terminal mercapto complexes (average Ru-SH, 2.46 Å).[82] The length is shorter than that found in gaseous H_2S (1.33 Å) but is in the range reported for the Sellmann's complex (average 1.2 Å).[80,81]

The two mesityl rings appear to be twisted, resulting in some H···H interaction between the IMes-CH_2-H···HSH hydrogens, and the IMes-CH_2-H···H-Ru hydrogens. The shortest IMes-CH_2-H···HSH distances are 1.864 Å (H1A-H10B) and 1.939 Å (H3A-H31C) indicating some short H···H interactions. Related phenyl···mercapto hydrogen interaction have been detected, for example in $(PhMe_2P)_3Ru(\mu\text{-}SH)_3Ru(SH)(PMe_2Ph)_2$,[83] and implicated in HDS mechanisms.[84] In a same manner the shortest IMes-CH_2-H···HSH distances are 1.878 Å (H12C-H101) and 1.948 Å (H102-H33C) indicating some short H···H interactions.

Compounds	Ru-S [Å]	S-H	[Ref]
$Ru(PPh_3)'(SH_2)\ S_4$	2.399(5)	1.19 / 1.21	**[81]**
cis-$Ru(PPh_3)(P\text{-}N)(SH_2)Cl_2$	2.3503(3)	1.20(3) / 1.30(3)	**[80]**
cis-$Ru(PPh_3)(P\text{-}N)(SH_2)Br_2$	2.3333(1)	1.25(7) / 1.34(6)	**[80]**

Table 6.15. *Selected bond lengths [Å] for $Ru(H_2S)$ complexes.*

Selected Bond Lengths	[Å]		
Ru(1)-C(1A)	1.803(7)	Ru(1)-C(1B)	1.829(8)
Ru(1)-C(1)	2.0737(17)	Ru(1)-S(1)	2.402(2)
S(1)-H(1A)	1.200(2)	Ru(1)-S(2)	2.424(2)
Ru(2)-S(3)	2.4000(18)	Ru(2)-C(3A)	1.806(6)
S(3)-H(3A)	1.200(2)	Ru(2)-C(22)	2.0722(17)
C(1B)-O(1B)	1.117(8)		

Selected Bond Angles	[°]		
C(1A)-Ru(1)-C(1B)	180.000(1)	C(1A)-Ru(1)-C(1)	90.63(5)
C(1B)-Ru(1)-C(1)	89.37(5)	C(1)-Ru(1)-C(1)#1	178.73(9)
C(1A)-Ru(1)-S(1)	180.000(1)	C(3A)#2-Ru(2)-C(3A)	176.4(4)
C(1)-Ru(1)-S(1)	89.37(5)	C(3A)-Ru(2)-C(22)#2	89.8(2)
C(1)-Ru(1)-S(2)	90.63(5)	C(3A)-Ru(2)-C(22)	90.2(2)
C(22)#2-Ru(2)-C(22)	179.93(9)	C(22)#2-Ru(2)-S(3)	91.21(6)
C(3A)-Ru(2)-S(3)	178.0(2)	C(3A)#2-Ru(2)-S(3)#2	178.0(2)
C(22)-Ru(2)-S(3)	88.79(6)	C(22)#2-Ru(2)-S(3)#2	88.79(6)
C(22)-Ru(2)-S(3)#2	91.21(6)	S(3)-Ru(2)-S(3)#2	179.89(8)
C(3A)#2-S(3)-O(3B)#2	163.2(8)	O(3B)#2-S(3)-Ru(2)	169.6(5)
S(3)#2-C(3A)-Ru(2)	171.5(9)	O(3B)-C(3A)-Ru(2)	179.1(7)
		C(1A)-Ru(1)-C(1)	90.63(5)

Table 6.16. - Selected bond lengths [Å] and angles [°] for $Ru(IMes)_2(CO)_2(H_2S)H_2$.

6.2.6.4. Reactivity of (43) with CO.

As seen for **(42)**, **(43)** also reacts with CO at room temperature to generate $Ru(IMes)_2(CO)_2(SH)H$ **(49)** in high yield. Labelling experiments showed that the labelled ^{13}CO was incorporated *trans* to the hydride (J_{CH} = 36.1 Hz).

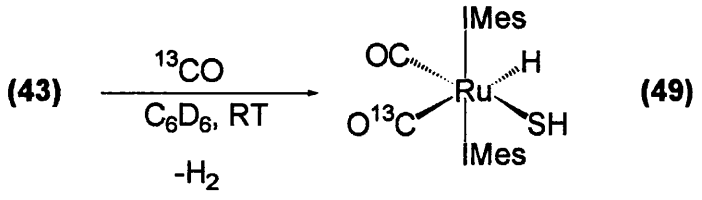

Scheme 6.29.

The hydride signal for **(49)** was observed in the ^1H NMR spectrum at δ -4.82, while the resonance for the SH appears as a broad signal at -3.15 ppm **[Spectrum 6.24.]**. The carbon NMR spectrum spectra displayed two carbonyl resonances at 203.15 and 197.45

ppm **[Spectrum 6.24.]**. The IR spectrum showed three strong bands between 2023-1892, with that at 1931 cm^{-1} (enhanced due to intensity stealing) **[Chapter 6.3.1.]**.

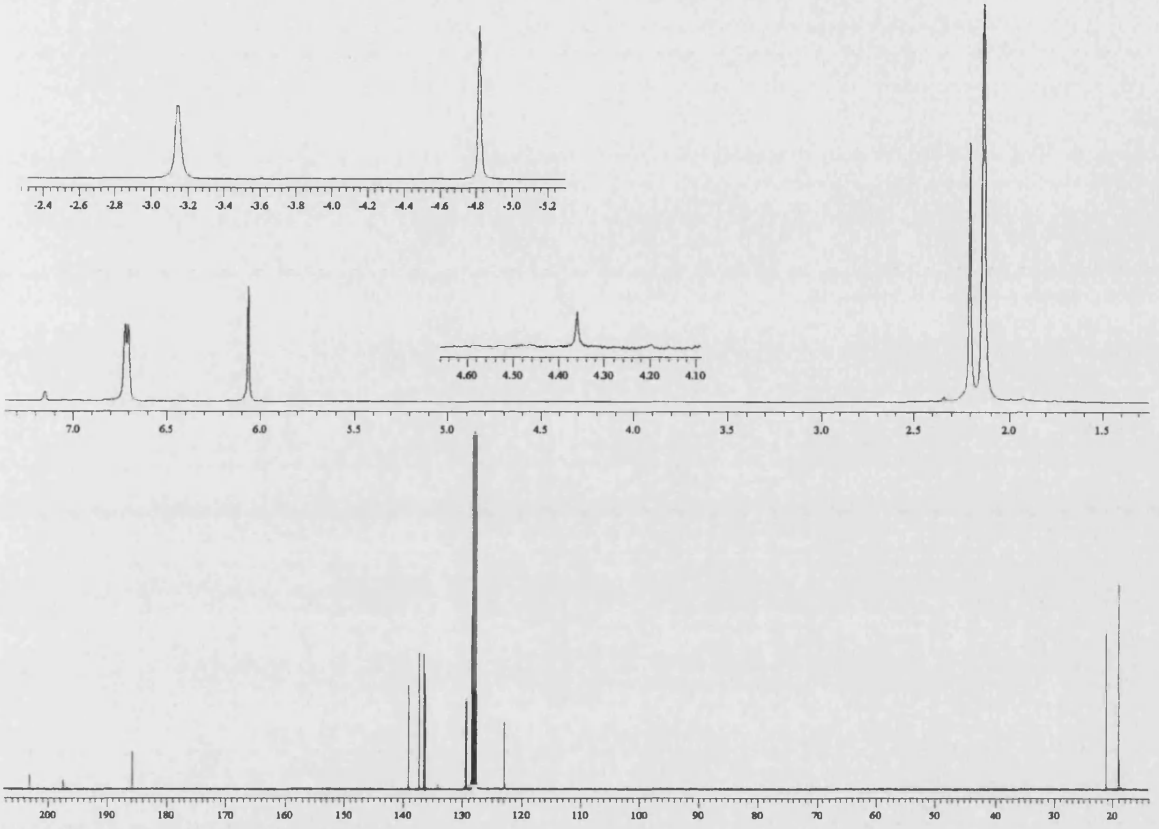

Spectrum 6.24. - *^{1}H and ^{13}C NMR spectrum of* ***(49)****.*

Pale yellow crystals were grown from a benzene solution of **(49)** layered with hexane. The structure of **(49)** was confirmed by X-ray diffraction **(X-Ray 6.10).** Selected bond distances and angles are given in **Table 6.17.** As in the structure of the hydroxy hydride **(48)**, the coordination geometry around the central ruthenium in **(49)** is distorted from a regular octahedron with highly bent *trans*-IMes-Ru-IMes and *cis*-$Ru(CO)_2$ angles (C(3)-Ru-C(24) 168.37 (6)°, C(2)-Ru-C(1) 95.7 (3)°). The two Ru-CO bond lengths exhibit significant differences (1.897(5), 1.9634 (18) Å), while the Ru-S distance at 2.4352(15) Å is comparable to that reported for other Ru(II) thiolate complexes **[Table 6.18.]**.[75] The extremely low temperature at which the structure was determined (30K) allowed the position of the hydrogen on the sulfur to be reliably located, as well as the hydride hydrogen. The S-H bond appears to be bent out of the Ru-S axis (Ru-S(1)-H(1A) = 101.00°).

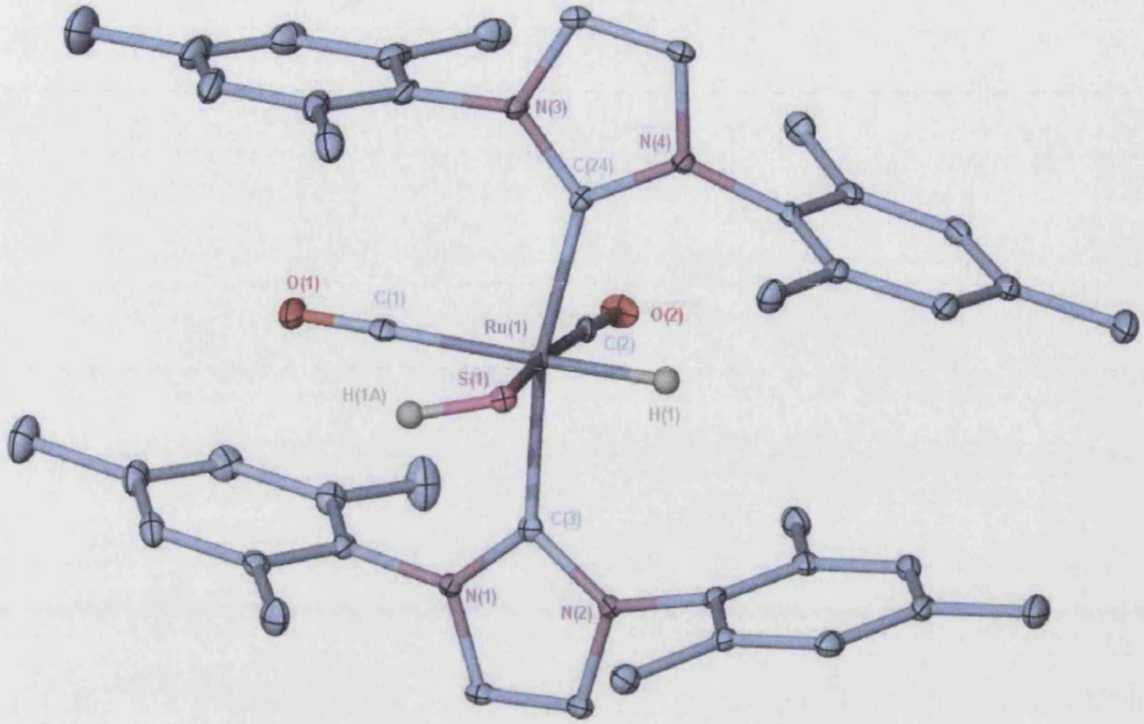

X-Ray 6.10. *X-ray structure of* ***(49)****. Thermal ellipsoids are set at the 50% probability level. Hydrogen atoms have been omitted for clarity (apart from hydride, and SH hydrogens).*

Selected Bond Lengths	**[Å]**		
Ru(1)-C(2)	1.897(5)	Ru(1)-C(1)	1.9634(18)
Ru(1)-C(3)	2.1165(16)	Ru(1)-C(24)	2.1069(16)
Ru(1)-S(1)	2.4352(15)	O(1)-C(1)	1.138(2)
O(2)-C(2)	1.182(5)		
Selected Bond Angles	**[°]**		
C(2)-Ru(1)-C(1)	95.7(3)	C(2)-Ru(1)-C(24)	90.8(3)
C(1)-Ru(1)-C(24)	96.43(7)	C(1)-Ru(1)-C(3)	95.12(7)
C(2)-Ru(1)-C(3)	89.5(3)	C(24)-Ru(1)-C(3)	168.37(6)
C(1)-Ru(1)-S(1)	90.98(8)	C(2)-Ru(1)-S(1)	173.2(3)
C(24)-Ru(1)-S(1)	87.31(7)	C(3)-Ru(1)-S(1)	91.14(7)

Table 6.17. - *Selected bond lengths [Å] and angles [°] for $Ru(IMes)_2(CO)_2(SH)H$.*

Compounds	Ru-S [Å]	S-H	[Ref]
cct-Ru $(SH)_2(CO)_2(PPh_3)_2$	2.470(2) / 2.418(2)	1.2(1) / 1.0(2)	**[82a]**
$Cp^*Ru(PEt_3)(SH)H_2$	2.411(6)	1.56	**[85]**
$CpRu(PPh_3)_2(SH)(CO)$	2.381(3)	N.A.	**[86]**

Table 6.18. - *Selected bond lengths [Å] for Ru(SH) complexes.*

6.2.6.5. Reactivity of (43) with H_2S.

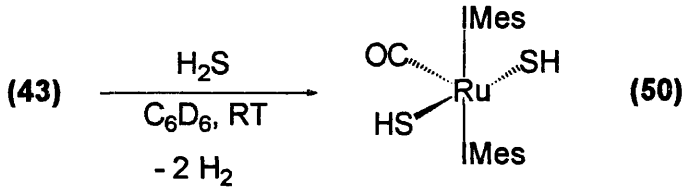

Scheme 6.30.

During the synthesis of **(43)** a significant colour change was observed for the solution from deep orange to deep purple when H_2S was present for extended reaction times. This was monitored by ^1H NMR, which showed depletion of the signals at -24.47 and 0.29 ppm and growth of a new signal at -1.00 ppm **[Spectrum 6.25.]**. VT NMR of the newly formed species revealed a bis-carbene structure while the ^1H NMR spectrum showed a 2:1 ratio of the SH protons with the NCH=CHN protons **[Spectrum 6.26.]**. These data are consistent with the formation of the 16 electron complex $Ru(IMes)_2(CO)(SH)_2$. The $^{13}C\{^1H\}$ NMR displayed a single carbonyl carbon signal at 202.8 and a carbene carbon at 192.7 ppm. The IR spectrum showed a low frequency ν_{CO} band at 1930 cm^{-1}.

The structure of **(50)** was confirmed by X-ray crystallography as the 16 e^- $Ru(IMes)_2(CO)(SH)_2$ **[X-Ray 6.10]**. Selected bond distances and angles for **(13)** are given in **Table 6.19.**. Thiolate hydrogens were located and refined without restraints.

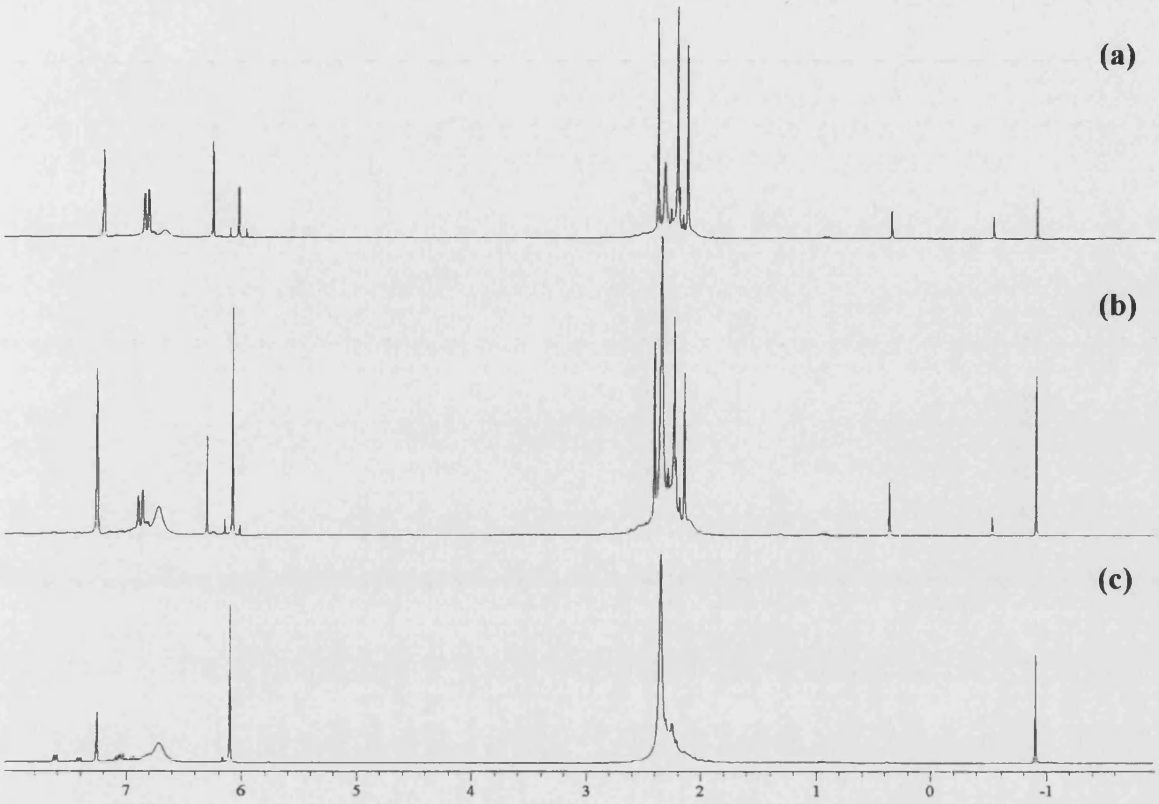

Spectrum 6.25. - *^{1}H NMR spectrum of the reaction described in* ***Scheme 6.30****.*. ***(a)*** *t = O 10 min;* ***(b)*** *t = 6 hour;* ***(c)*** *12 hour.*

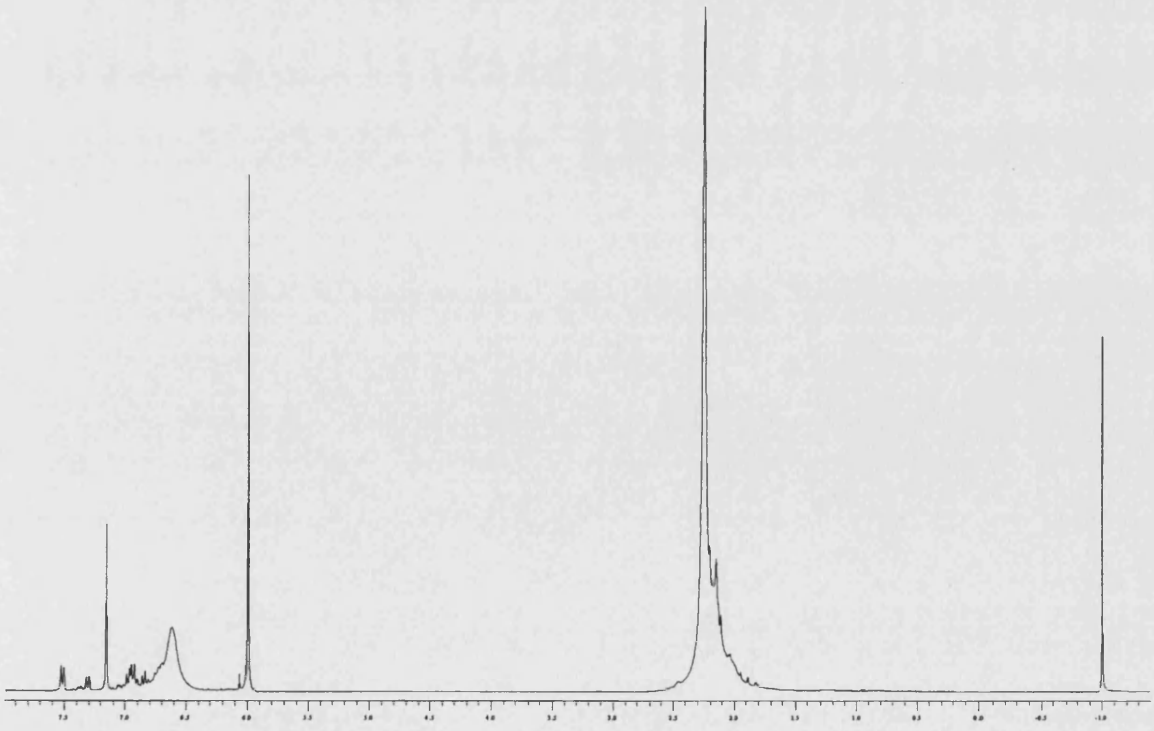

Spectrum 6.26. - *^{1}H NMR spectrum of* ***(50)****.*

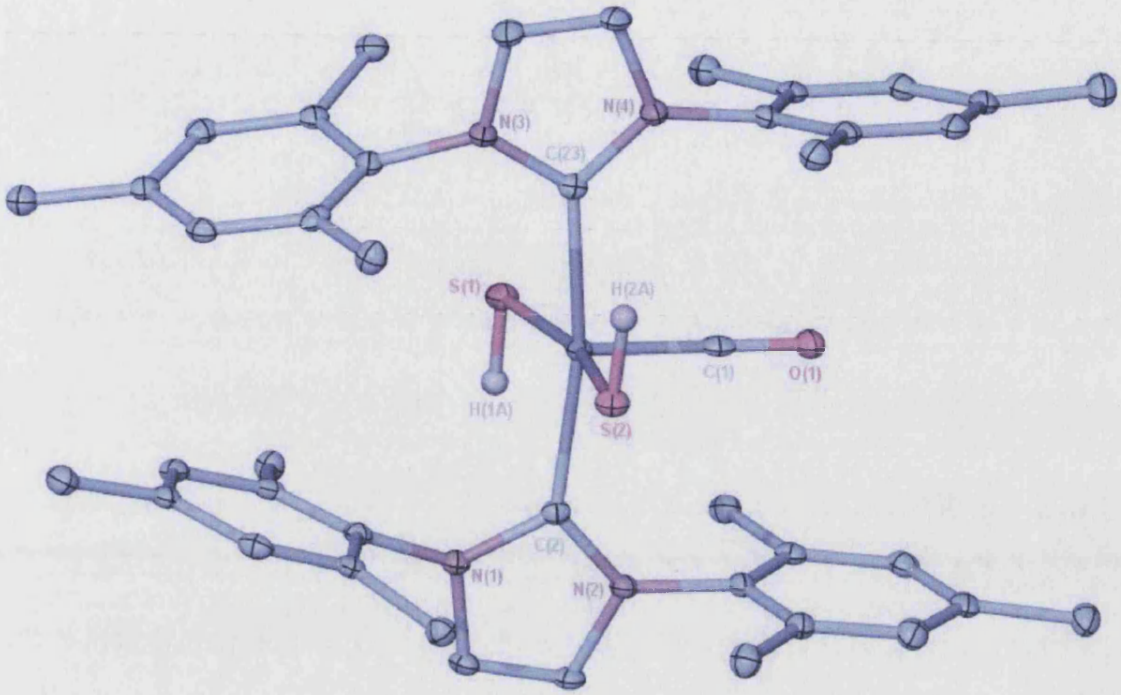

X-Ray 6.10. - *X-ray structure of* ***(50)****. Thermal ellipsoids are set at the 50% probability level. Hydrogen atoms have been omitted for clarity (apart from hydride and SH hydrogens).*

The coordination geometry around the central ruthenium in **(50)** is trigonal bipyramidal with the two SH moiety pointing *trans* towards one another (S(2)-Ru(1)-S(1) 166.203(19) Å). The Ru-S bonds appear to be noticeably smaller than in **(49)** (2.3764(5) / 2.3693(5) vs. 2.4352(15)) and in related compounds **[Table 6.18.]**. This can be seen as a direct effect of the electronic and steric nature of **(50)** and could results from π-donation filled orbital on the sulfur to the metal due to a lack of electron density. In a similar way, the Ru-CO displays unusual structural characteristics, the Ru-C bond is smaller than in **(49)** or **(51)** (1.773(2) vs 1.897(5), 1.9634(18)) and of any compounds described in this chapter, while the CO bond appears in line with these later (e.g. 1.166(2) vs. 1.165(3) for **(40)**). Due to the vacant orbital on the metal one would expect less electron backbonding from the metal to the carbonyl and therefore a longer Ru-C bond and a shorter CO bond, the unexpected Ru-C bond distances might be explained by electronic factor (trans effect of the vacant orbital) and structural factor (stacking of the IMes mesityl ring on the top of the carbonyl **[Figure 6.2.]**). Several unusual structural factors arise form the presence of a vacant site *trans* to the carbonyl as shown in **Figure 6.2.**

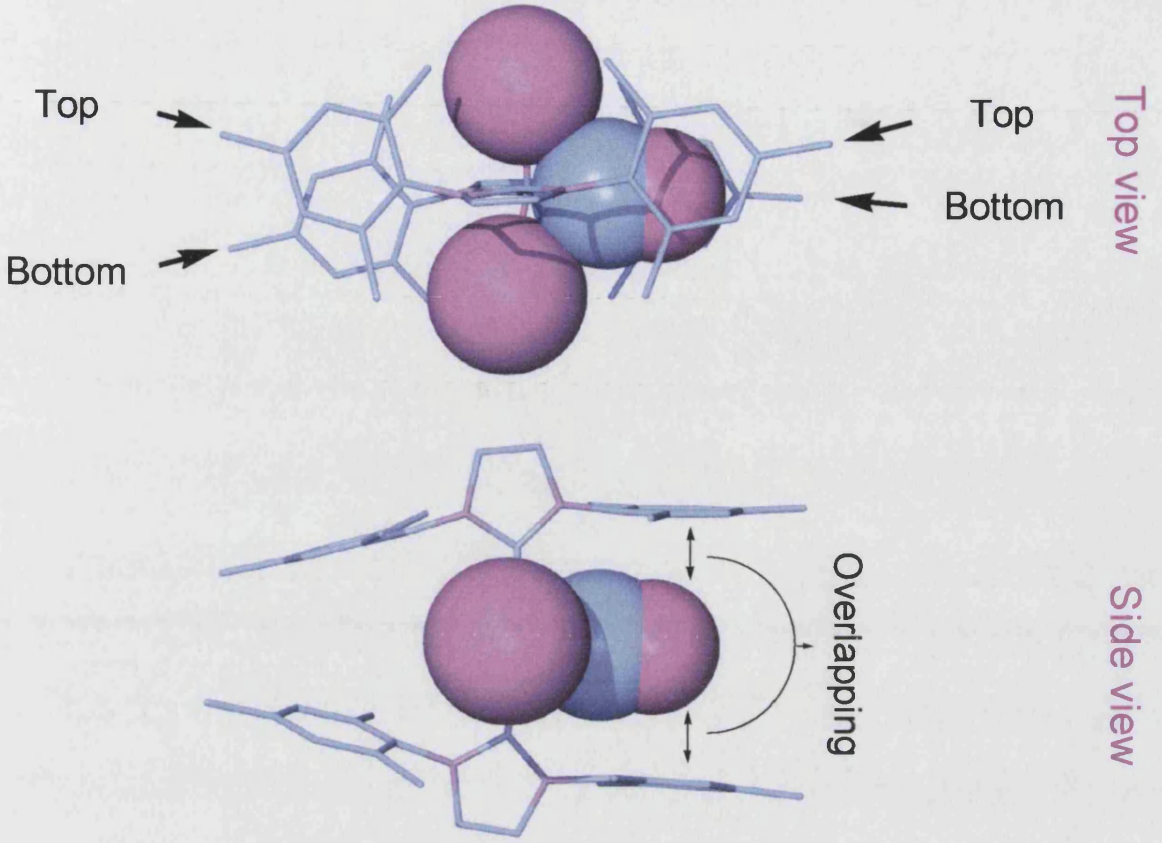

Figure 6.2. - *Top and side view of the X-ray structure of* ***(50)****. The top view shows the "V" shape bending of the IMes ligand, as well as the over lapping of the Mesityl rings on the top of the carbonyl. The side view shows the almost parallel mesityl ring on each side of the carbonyl.*

First the two phenyl rings on each side on the carbonyl appears to be almost parallel (NB: The planes of the two mesityl rings are rotated with respect to each other by 8.6°) and seat directly on the top of the carbonyl. The orientation seen for the carbene ligand is such that it keeps the CO ligand in the plane of the N heterocycle and therefore allow a face-on position of the mesityl rings. This factor is sterically more viable than these rings being face-on to the SH groups. Other possible explanations could arise from an attractive interaction - perhaps rather of the sort that makes C_6F_6 like to be face on to arenes as demonstrated by Marder et al..[87] Here the interaction would be a dipole/octupole rather than octupole-octupole (as in C_6F_6/C_6H_6).[88] The C(1)-Ru(1)-C(2) (94.76(8)) angle suggests that the mesityl rings are pressed hard against the carbonyl moiety since the carbene tilts towards the vacant site rather than the CO. The last peculiar factor occurring

in this structure as a result of steric congestion is the unusual bending of the IMes ligands in a "V" shape which can be seen demonstrated via two factors as shown on **Figure 6.3.**.

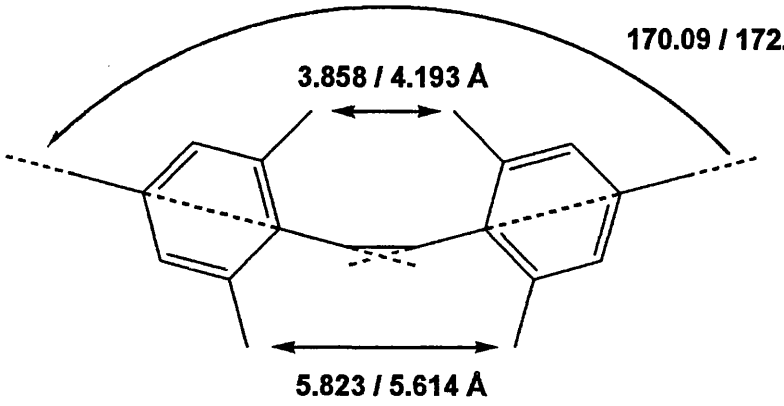

Figure 6.3. - *"V" shape bending of IMes ligands as consequence of the steric congestion around the metal.*

Selected Bond Lengths	**[Å]**		
Ru(1)-C(1)	1.773(2)	Ru(1)-C(23)	2.1086(18)
Ru(1)-C(2)	2.1097(18)	Ru(1)-S(2)	2.3693(5)
Ru(1)-S(1)	2.3764(5)	S(1)-H(20A)	5.9242
S(1)-H(11C)	6.1033	S(2)-H(43A)	5.4113
S(2)-H(34C)	5.8061	O(1)-C(1)	1.166(2)
Selected Bond Angles	**[°]**		
C(1)-Ru(1)-C(23)	95.37(8)	C(1)-Ru(1)-C(2)	94.76(8)
C(23)-Ru(1)-C(2)	169.86(7)	C(1)-Ru(1)-S(2)	94.85(6)
C(23)-Ru(1)-S(2)	88.30(5)	C(2)-Ru(1)-S(2)	91.23(5)
C(1)-Ru(1)-S(1)	98.94(6)	C(23)-Ru(1)-S(1)	90.10(5)
C(2)-Ru(1)-S(1)	87.94(5)	S(2)-Ru(1)-S(1)	166.203(19)
Ru(1)-S(1)-H(20A)	24.7	Ru(1)-S(1)-H(11C)	46.1
H(20A)-S(1)-H(11C)	34.1	Ru(1)-S(2)-H(43A)	26.8
Ru(1)-S(2)-H(34C)	30.9	H(43A)-S(2)-H(34C)	30.6

Table 6.19. - *Selected bond lengths [Å] and angles [°] for $Ru(IMes)_2(CO)(SH)_2$.*

Although the reaction mechanism for the formation of **(50)** was not probed, free H_2 gas in solution in C_6D_6 was observed in the ^1H NMR of the reaction mixture, leading to a proposed mechanism based on hydrogen transfer from the H_2S ligands to the *trans* hydride. As shown in **Scheme 6.31.**, on the basis of the observations and reactions studied so far, that it is realistic to assume that protonation of one of the strongly hydridic hydride ligands by the (very acidic) coordinated H_2S yields a putative dihydrogen hydrogen sulfate hydride species, which readily dissociates H_2 (observed by ^1H NMR during the reaction) in the presence of H_2S. Preliminary work on this mechanism has showed that **(50)** reacts back in the presence with H_2 to regenerate **(43)**. This process could readily be achieved backward and forward several times by adding H_2S to **(43)** or H_2 to **(50)** **[Spectrum 6.27.]**. Further work is currently at hand by mean of D_2 labelling studies.

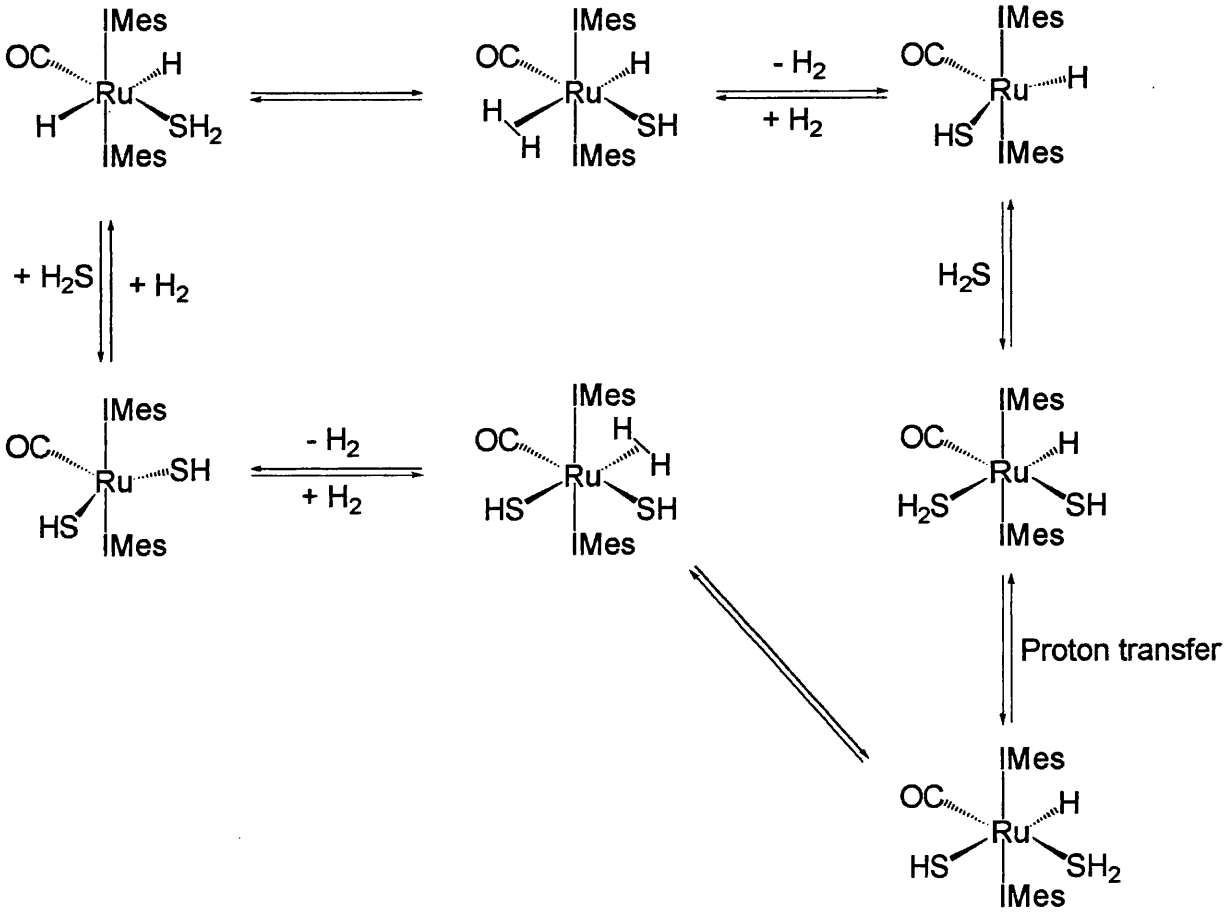

Scheme 6.31. - *Proposed mechanism for the formation of* **(50)**.

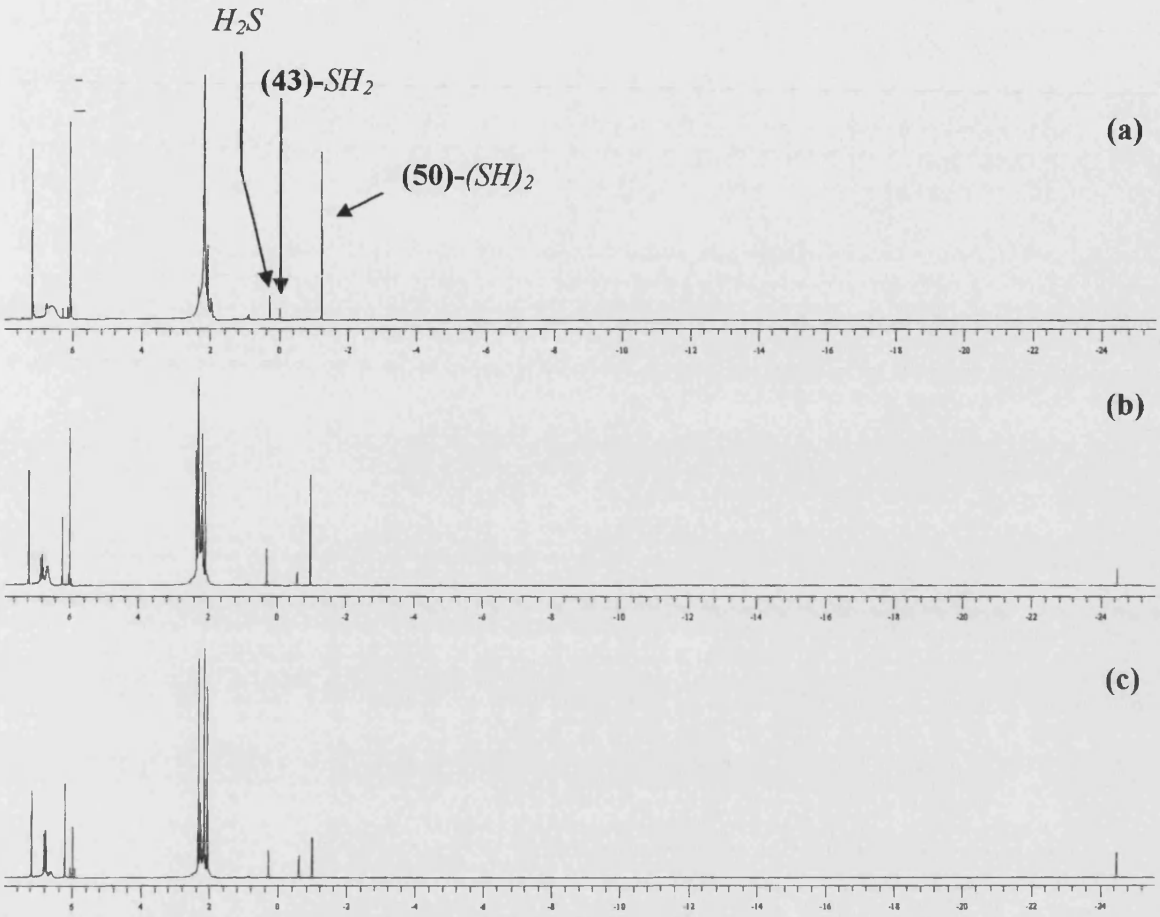

Spectrum 6.27. - *Addition of H_2 to* ***(50)****.* ***(a)*** *t = 0 s;* ***(b)*** *t = 1 h;* ***(c)*** *t = 6h.*

6.2.6.6. Reactivity of (50) with CO.

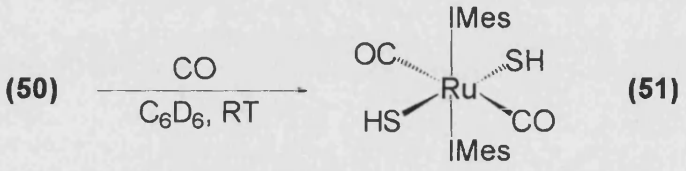

Scheme 6.32.

In order to access the reactivity of **(50)**, one atmosphere of CO gas was added to a C_6D_6 solution of **(50)**. Over the course of 1 hour the colour of the solution changed form purple to off yellow and a yellow precipitate was formed **[Scheme 6.32.]**. This process was monitored by ^1H NMR, and showed depletion of the signal at -1.00 ppm for the SH protons and growth of a new SH signal at δ -3.58 ppm **[Spectrum 6.28.]**. This new signal integrates in a 2:1 ratio of the SH protons with the NCH=CHN protons. The $^{13}C\{^1H\}$ NMR displayed a single carbonyl carbon signal at 199.4 and a carbene carbon at 183.5 ppm. The IR spectrum showed a ν_{CO} band at 1978 cm^{-1}. These data are consistent with the formation

of the 18 electron complex $Ru(IMes)_2(CO)_2(SH)_2$ **(51)**. This reaction can be explained due to the vacant orbital on **(50)** readily filled by the two donor electron CO ligand. **(51)** was easily isolated as a rather insoluble yellow material in a 86% yield.

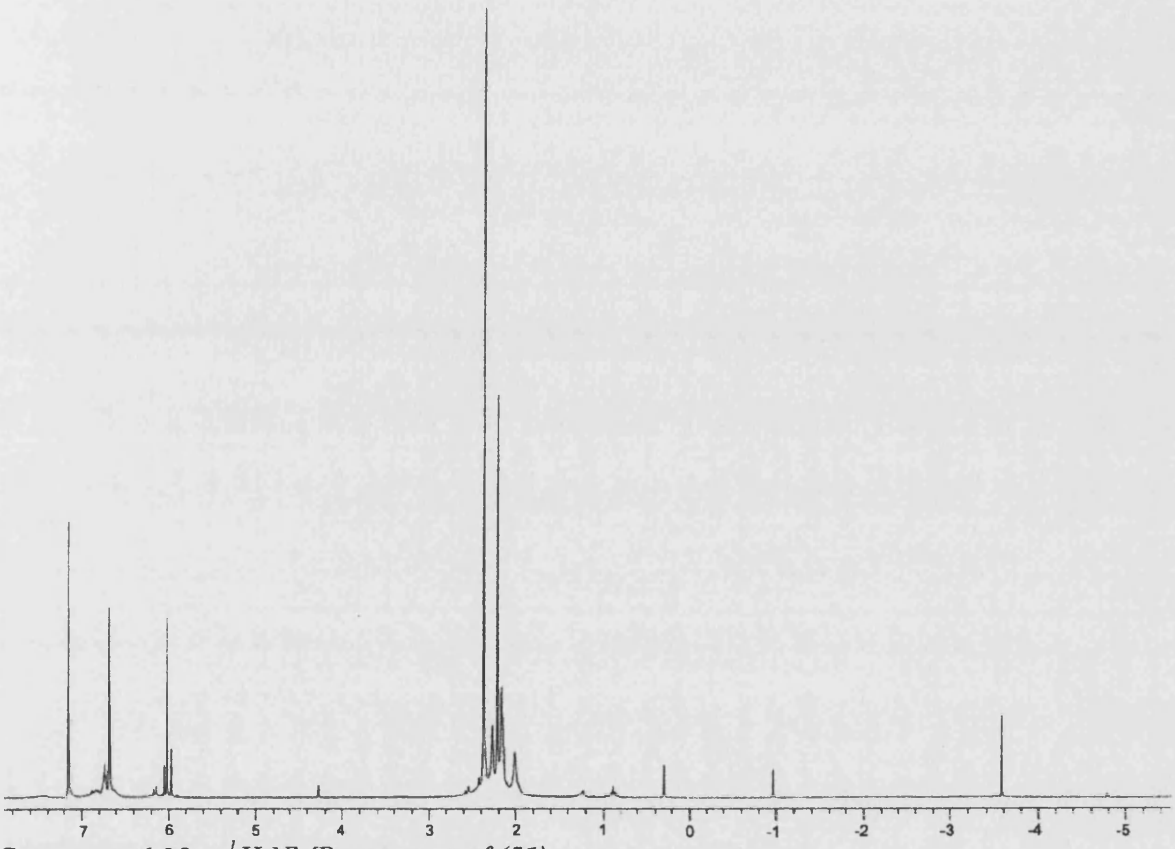

Spectrum 6.28. - *^1H NMR spectrum of (51).*

The structure of **(51)** was confirmed by X-ray crystallography **[X-Ray 6.11]**. Selected bond distances and angles for **(51)** are given in **Table 6.20.**. The coordination geometry around the central ruthenium in **(51)** close to regular octahedral due to the *trans* nature of the ligands (C(1)-Ru(1)-C(2): 173.67(10) °; C(3)-Ru(1)-C(24): 175.46(6) °; S(1)-Ru(1)-S(2): 178.862(19) °). The Ru-S bond (2.4440(5)Å) is in line with other reported thiolate complexes **[Table 6.18.]** and compares with **(49)** (2.4352(15)Å). The Ru-C in the carbonyl moiety is longer than for **(50)** (1.933(2) / 1.9388(18) vs. 1.773(2)Å). Which can be attributed to an increase π-back donation form the filled d-orbitals on the metal to the vacant π* orbital on the the carbonyl ligand resulting in a longer Ru-C bond and a shorter CO bond. Weak H-H interaction between the S-H and the methyl hydrogens are observed

(H2A-H12C : 1.607Å; H1-H33C: 1.773 Å). The peculiar feature of this structure lies in the *trans* nature of the carbonyl ligands, as in octahedral dicarbonyl complexes it is usual to find that the *cis*-dicarbonyl isomer is thermodynamically more stable than the corresponding *trans*-isomer. Very few *trans*-dicarbonyl complexes have been isolated and structurally characterised.[89]

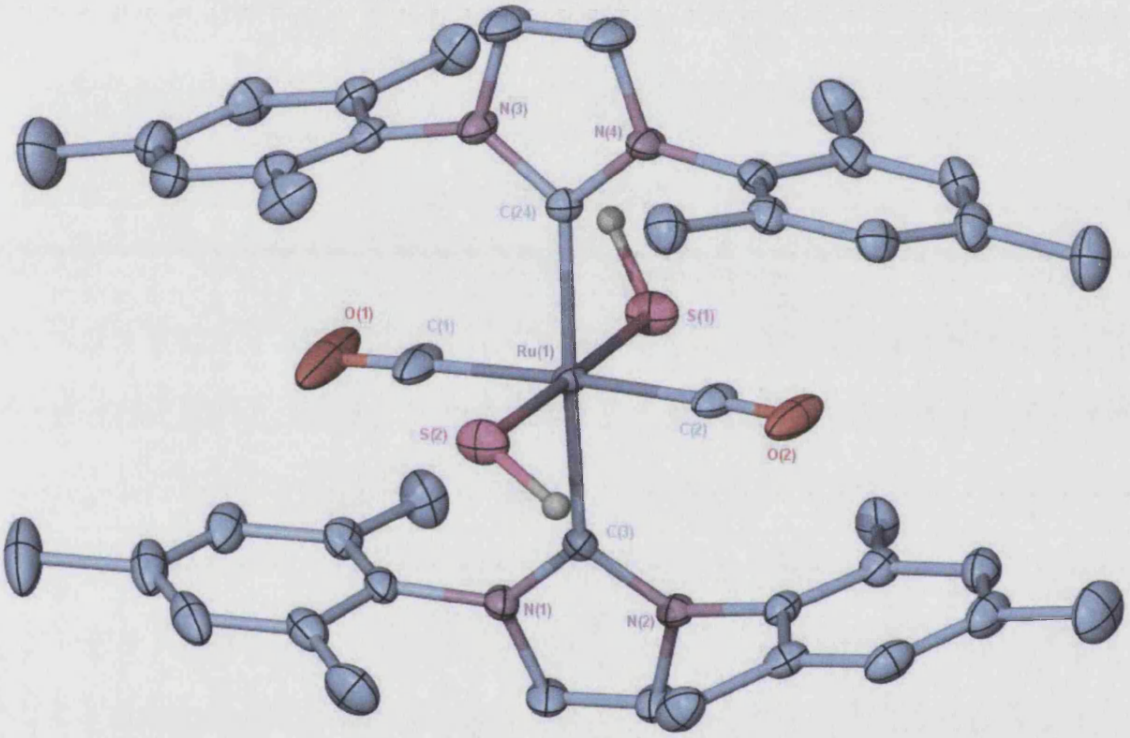

X-Ray 6.11. - *X-ray structure of* ***(51)****. Thermal ellipsoids are set at the 50% probability level. Hydrogen atoms have been omitted for clarity (apart from hydride and SH hydrogens).*

Selected Bond Lengths	**[Å]**		
Ru(1)-C(1)	1.933(2)	Ru(1)-C(2)	1.9388(18)
Ru(1)-C(3)	2.1704(16)	Ru(1)-C(24)	2.1716(16)
Ru(1)-S(1)	2.4440(5)	Ru(1)-S(2)	2.4478(5)
O(1)-C(1)	1.128(3)	O(2)-C(2)	1.133(2)
Selected Bond Angles	**[°]**		
C(1)-Ru(1)-C(2)	173.67(10)	C(1)-Ru(1)-C(3)	89.14(7)
C(2)-Ru(1)-C(3)	90.65(6)	C(1)-Ru(1)-C(24)	90.87(7)
C(2)-Ru(1)-C(24)	89.84(7)	C(3)-Ru(1)-C(24)	175.46(6)
C(1)-Ru(1)-S(1)	91.22(9)	C(2)-Ru(1)-S(1)	95.07(6)
C(3)-Ru(1)-S(1)	84.85(4)	C(24)-Ru(1)-S(1)	90.61(4)
C(1)-Ru(1)-S(2)	87.69(9)	C(2)-Ru(1)-S(2)	86.03(6)
C(3)-Ru(1)-S(2)	95.44(4)	C(24)-Ru(1)-S(2)	89.10(4)
S(1)-Ru(1)-S(2)	178.862(19)		

Table 6.20. - *Selected bond lengths [Å] and angles [°] for Ru(IMes)$_2$(CO)$_2$(SH)$_2$.*

Investigation of the process of formation of **(51)** has demonstrated the reversibility of this reaction. A C_6D_6 solution of **(51)** under 1 atm of CO would readily convert back to **(50)** within the course of an hour upon removal of the CO atmosphere under vacuum.[90] This process could be driven back and forward several times (up to 5 times have been observed) on a single sample without any decomposition or side product being observed. Moreover when dynamic vacuum was applied to a powder sample of **(51)**, slow fading from yellow to purple was observed suggesting CO loss in the solid state. This was verified by mean of IR experiments which showed slow formation of **(50)** after 24 hours under dynamic vacuum. Similarly formation of **(51)** from **(50)** slowly proceeded in the solid state under CO atmosphere. Further work is currently in hand in order to determine the kinetics and mechanism of this reaction.

6.2.7. Treatment of of (39) and (40) with N-donor ligands.

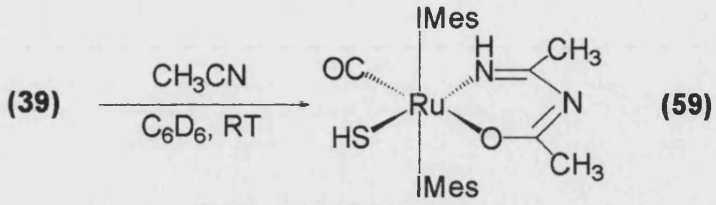

Scheme 6.33.

No reaction was observed upon treatment of **(39, 40)** with pyridine, *p*-anisidine, 2,4,6-trimethylpyridine, or *tert*-butyl isocyanide. Nevertheless, addition of four equivalents of acetonitrile to a C_6D_6 solution of **(39)** gave the *N*-imidoylimidato complex **(59)**, resulting from the coupling of two CH_3CN ligands in a head-to-tail manner with the Ru-OH_2 group **[Scheme 6.33.]**. The proton NMR spectrum of **(59)** showed two inequivalent methyl resonances (1.99, 1.52 ppm) and a singlet hydride resonance at δ -11.40 **[Spectrum 6.29.]**. A broad feature at δ 5.73 was assigned to the N-H group. The Ru-CO (210.3 ppm) and the Ru-C (191.4 ppm) were readily assigned in the $^{13}C\{^1H\}$ NMR spectrum. Whereas ^1H-^{13}C HMQC and HMBC experiments were used to assign two signals at 173.8 and 166.0 to the nitrile carbons. The IR spectrum displayed two bands at 1865 and 2016 cm^{-1} for the ν_{CO} and ν_{Ru-H} respectively.

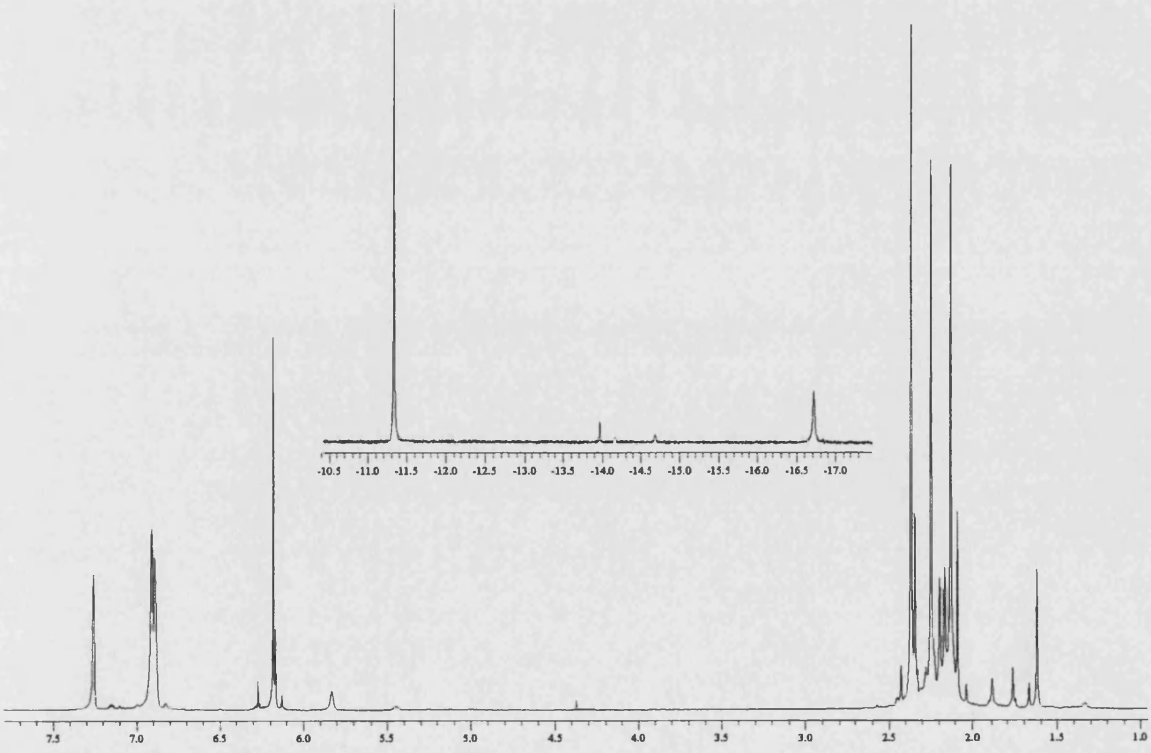

Spectrum 6.29. - *^1H NMR spectrum of (59).*

A single crystal of **(59)** suitable for X-ray diffraction was obtained from a toluene/hexane solution. A plot of the asymmetric unit is shown in **X-Ray 6.12.** while selected bond lengths and angles are given in **Table 6.21.**.

The *N*-imidoylimidato chelate ring is approximately flat, but not entirely planar. The maximum deviation from the least squares plane containing atoms Ru(1), N(5), C(2), N(6) and C(4) is 0.08 Å (for C(4)) while the perpendicular distance from O(2) to this plane is 0.28 Å. In this respect, the structure of **(59)** is a little different to the structure of $Ru(PPh_3)_2(CO)(NH{=}CRN{=}CRO)Cl$ (R = *p*- or *m*-tolyl), reported by Hiraki et al,[91] which contains the 6 atoms of the chelate on a plane within 0.06 Å. A comparison of the bond lengths **[Figure 6.4.]** in the structures also revealed significant differences. Most noticeable is the lengthening of the Ru-O and Ru-N bond distances in **(59)**, and the fact that Ru-O is now shorter than the Ru-N distance. However, lengthening of the Ru-O bond length in **(59)** compared to the Hiraki complex would be expected due to the presence of an hydride rather than a chloride in the *trans* position. Similar 6-membered ring oxa-aza metallacycles have been characterised for Zr, Ni and Cu.[92-94]

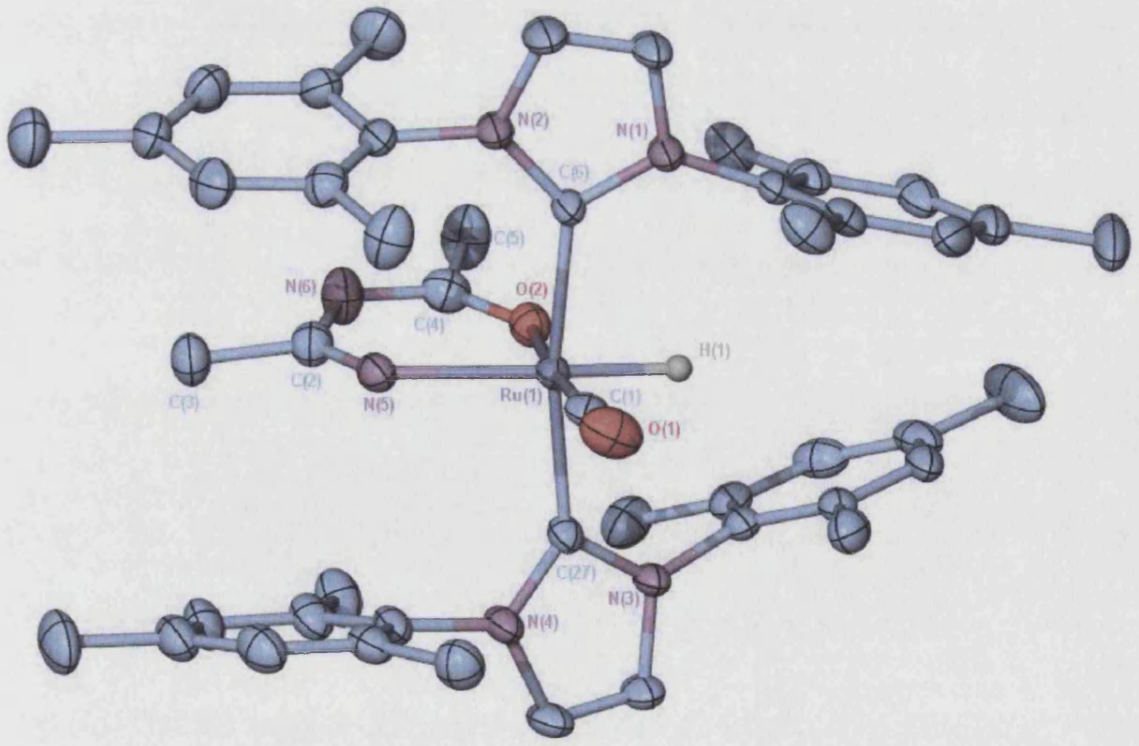

X-Ray 6.12. *X-ray structure of* ***(59)****. Thermal ellipsoids are set at the 50% probability level. Hydrogen atoms have been omitted for clarity (apart from hydride, and SH hydrogens).*

Selected Bond Length	**[Å]**		
Ru(1)-C(1)	1.828(3)	Ru(1)-C(27)	2.098(3)
Ru(1)-C(6)	2.107(3)	Ru(1)-O(2)	2.124(2)
Ru(1)-N(5)	2.173(2)	O(1)-C(1)	1.145(4)
O(2)-C(4)	1.250(4)	N(1)-C(6)	1.376(4)
N(1)-C(8)	1.385(4)	N(1)-C(9)	1.447(4)
N(2)-C(6)	1.376(4)	N(2)-C(7)	1.391(4)
N(2)-C(18)	1.442(4)	N(3)-C(27)	1.372(4)
N(3)-C(28)	1.391(4)	N(3)-C(39)	1.448(4)
N(4)-C(27)	1.373(4)	N(4)-C(29)	1.387(4)
N(4)-C(30)	1.447(4)	N(5)-C(2)	1.295(4)
N(6)-C(4)	1.339(4)	N(6)-C(2)	1.381(4)
C(2)-C(3)	1.506(4)	C(4)-C(5)	1.508(5)
Selected Bond Angles	**[°]**		
C(1)-Ru(1)-C(27)	90.27(12)	C(1)-Ru(1)-C(6)	89.03(12)
C(27)-Ru(1)-C(6)	170.28(11)	C(1)-Ru(1)-O(2)	174.31(11)
C(27)-Ru(1)-O(2)	89.61(10)	C(6)-Ru(1)-O(2)	90.13(10)
C(1)-Ru(1)-N(5)	104.90(12)	C(27)-Ru(1)-N(5)	93.46(10)
C(6)-Ru(1)-N(5)	96.09(10)	O(2)-Ru(1)-N(5)	80.79(9)
C(4)-O(2)-Ru(1)	129.3(2)	C(2)-N(5)-Ru(1)	129.5(2)
C(4)-N(6)-C(2)	121.5(3)	O(1)-C(1)-Ru(1)	178.0(3)
N(5)-C(2)-N(6)	126.1(3)	N(5)-C(2)-C(3)	121.6(3)
N(6)-C(2)-C(3)	112.4(3)	O(2)-C(4)-N(6)	130.3(3)
O(2)-C(4)-C(5)	114.6(3)	N(6)-C(4)-C(5)	115.1(3)

Table 6.21. - *Selected bond lengths [Å] and angles [°] for Ru(IMes)$_2$(CO)(NH=C(CH$_3$)N=C(CH$_3$)O)H* ***(59)***.

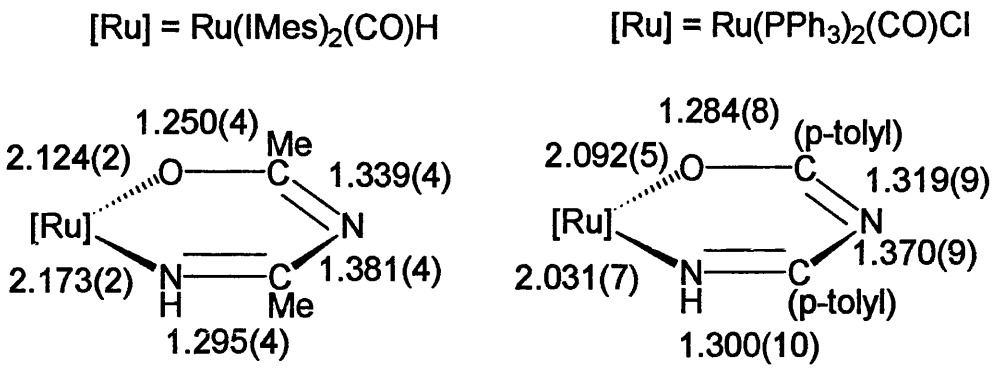

Figure 6.4. - *Comparison of bond lengths in the N-imidoylimidato complexes Ru(IMes)$_2$ (CO)(NH=C(CH$_3$)N=C(CH$_3$)O)H and Ru(PPh$_3$)$_2$(CO)(NH=C(p-tolyl)N=C(p-tolyl)O)Cl.*

The formation of $Ru(PPh_3)_2(CO)(NH{=}CRN{=}CRO)Cl$ was proposed to arise via nitrile hydration to give an intermediate amidato complex, which subsequently inserted a second nitrile to yield the final product following a 1,3-hydrogen shift. The presence of water was therefore vital to the formation of this metallacyclic complex. Although we have not probed the mechanism of the formation of **(59)**, a similar pathway would seem reasonable due to the availability of coordinated water in **(40)**. On the basis of the literature, two prospective pathway can be envisaged.[66,95,96] One route, involve a direct formation of **(59)** through a concerted mechanisms similar to those described for the CO_2 insertion into M-H bonds **[Scheme 6.34., Pathway (a)]**.[66] While a second route involve formation of a chelated amide intermediate.[95,96]

A spectrum recorded only two hours after the insertion of CH_3-CN shows formation of an intermediate **(59a)** showing an hydride resonance at -17.64 ppm **[Spectrum 2.30.]**. This signal is in the same region as observed for the $Ru(\kappa^2\text{-}O_2CO)$ reported in this chapter, suggesting similarities in structures around the ruthenium center. Thus we propose formation of a chelated amide such as $Ru(IMes)_2(CO)(\kappa^2\text{-}N,O\text{-}CMe)H$ **(59a)** which acts as an intermediate in the formation of **(59)**. Formation of these chelate amide complex is proposed to arise via interaction of an amide or a nitrile with a M-OH bond.[95] Subsequent reaction of **(59a)** with acetonitrile afford the final product **(59)**.

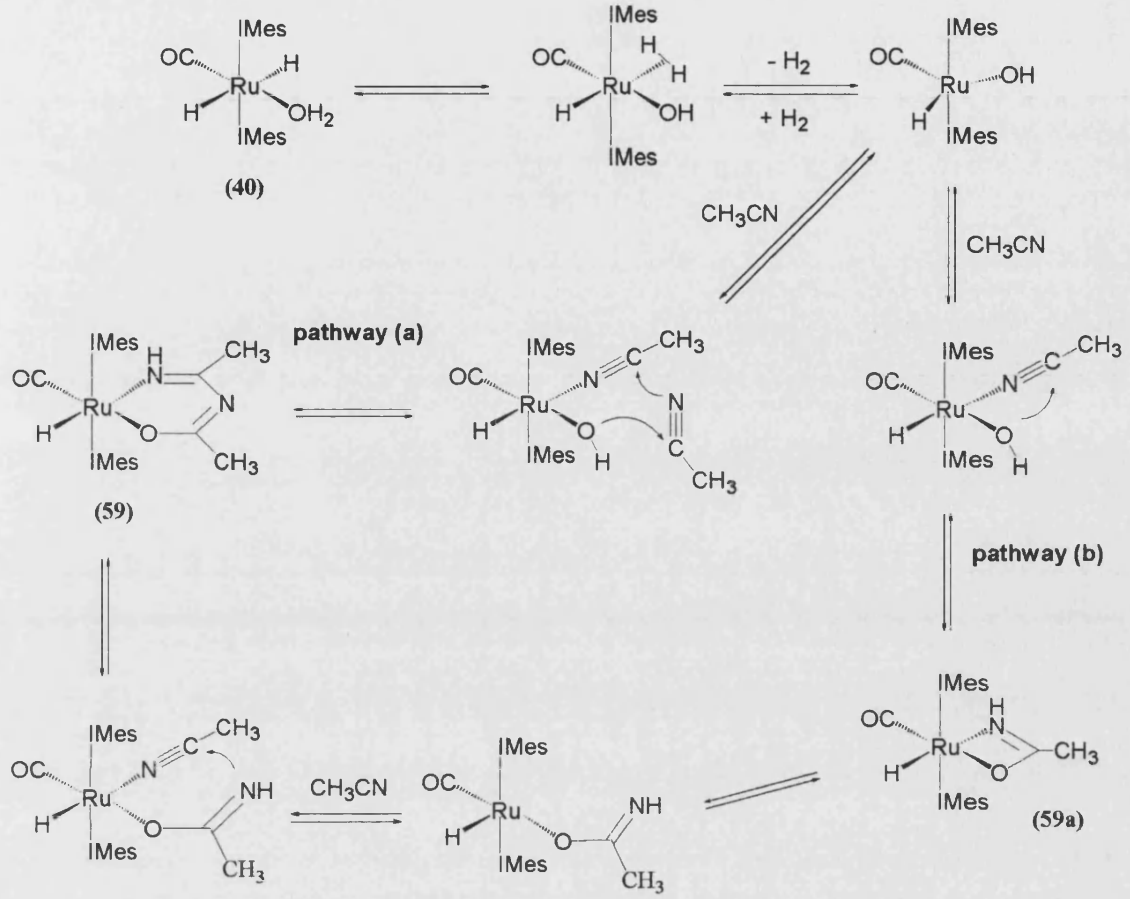

Scheme 6.34. - *Proposed mechanism for the formation of* ***(59)****.*

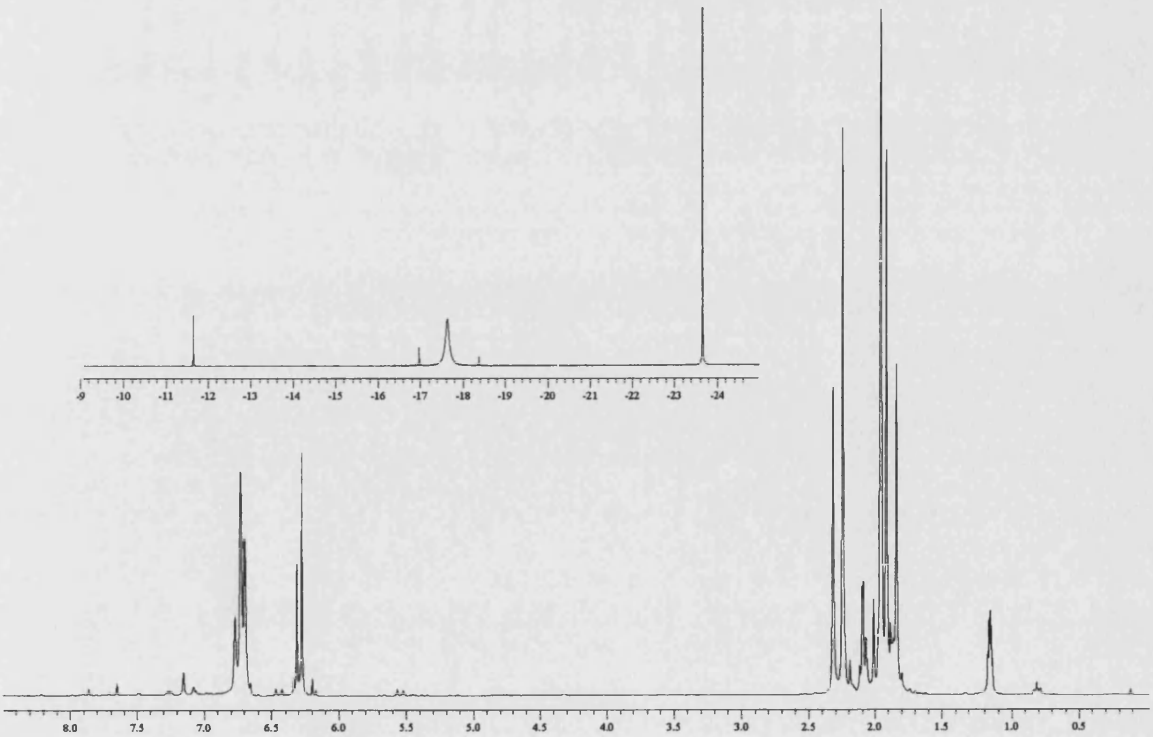

Spectrum 6.30. - *^{1}H NMR spectrum of* ***(59a)****.*

6.2.6. Reaction of (39) and (40) with C_6F_6 and C_6Cl_6.

6.2.6.1. Reaction of (39) and (40) with C_6F_6.

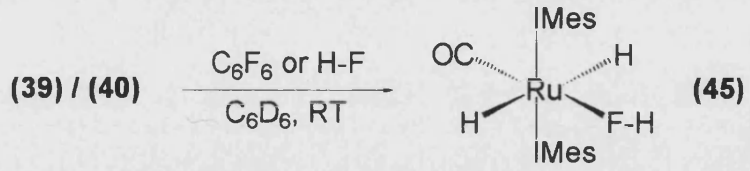

Scheme 6.35.

Upon the addition of 2 equivalents of C_6F_6 to a benzene solution of **(39)** or **(40)** a rapid colour change of the reaction mixture was observed. At this time a new *trans* hydride species was observed at -24.63 ppm **[Scheme 6.35., Spectrum 6.31.]**. The reaction was completed after 12 h and **(45)** could be isolated in an almost quantitative yield as a crystalline material (crystallisation was achieved by layering of the reaction mixture with hexane).

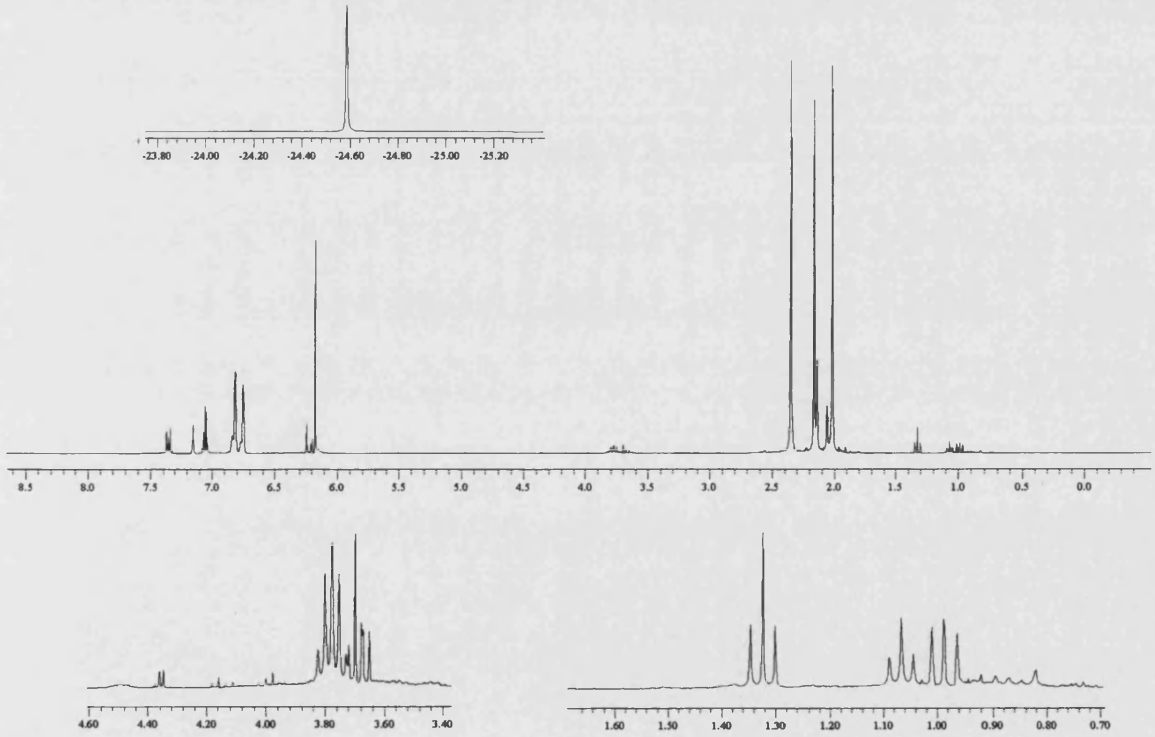

Spectrum 6.31. - *^{1}H NMR spectrum of (45).*

The ^{1}H and ^{13}C{^{1}H} NMR spectra of the isolated material revealed a new *trans* hydride species, similar to **(39-44)**. As the ^{1}H NMR spectrum showed, there was no evidence for any coordinated protio ligand, thus we opted for a fluorine derivative. The ^{19}F NMR spectrum displayed a broad signal at -208.49 ppm **[Spectrum 6.32]**. The chemistry of HF

complexes being really poor, very little chemistry is available on the subject, and amongst the very few M-HF characterised,[97-100] NMR characterisation remains dubious due to stabilization through hydrogen bonding. Nevertheless the ^{19}F NMR signal appears to be in line with H-F complexes stabilized by hydrogen bonding[100,101] and Ru-H-F-H[102] but remains considerably lower than any Ru-F[101] complexes. It has been shows that large F-H coupling occurs in the case of HF types of complexes (~440 Hz).[100] Unfortunately we were unable to observe either the F-H resonance in the ^{1}H NMR spectrum or the H-F coupling in the fluorine spectrum of **(45)**, even at very low temperature. Attempts to pull off the hydrogen on the fluorine by the use of strong base such as Et_3N, proton sponge, or PMe_3 proved to be impossible. The infra red spectra showed a single carbonyl band at 1872 cm^{-1} consistent with **(39-44)**.

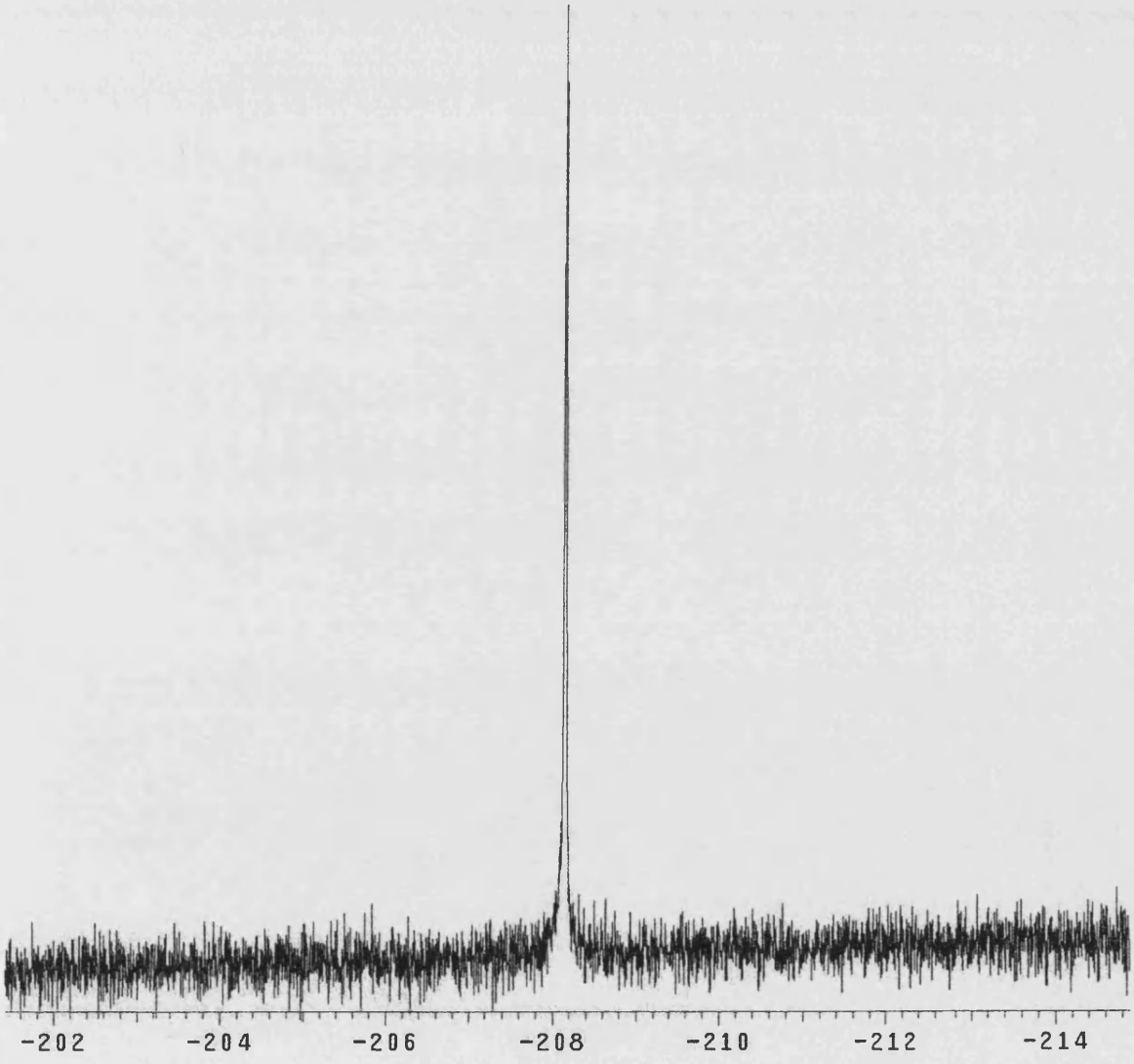

Spectrum 6.32. - *^{19}F NMR spectrum of complex **(45)**.*

Deep orange crystals were grown from a benzene solution of **(45)** layered with hexane and the structure of was confirmed by X-ray diffraction **[X-Ray 6.13.]**. Selected bond distances and angles for **(45)** are given in **Table 6.22.**. The coordination geometry around the central ruthenium in **(45)** is distorted from a regular octahedron with highly bent *trans*-IMes-Ru-IMes and was shown to be isostructural with that of all the bis-carbene *trans* hydrides seen so far. The IMes rings are twisted 47.3° from coplanarity, and a **Ru-F-H** distance of 2.0332(15) Å was observed. Unfortunately there are not any structural data available for such complexes. Nevertheless the HF nature of **(45)** will be discussed in **Part 6.3.2.**.

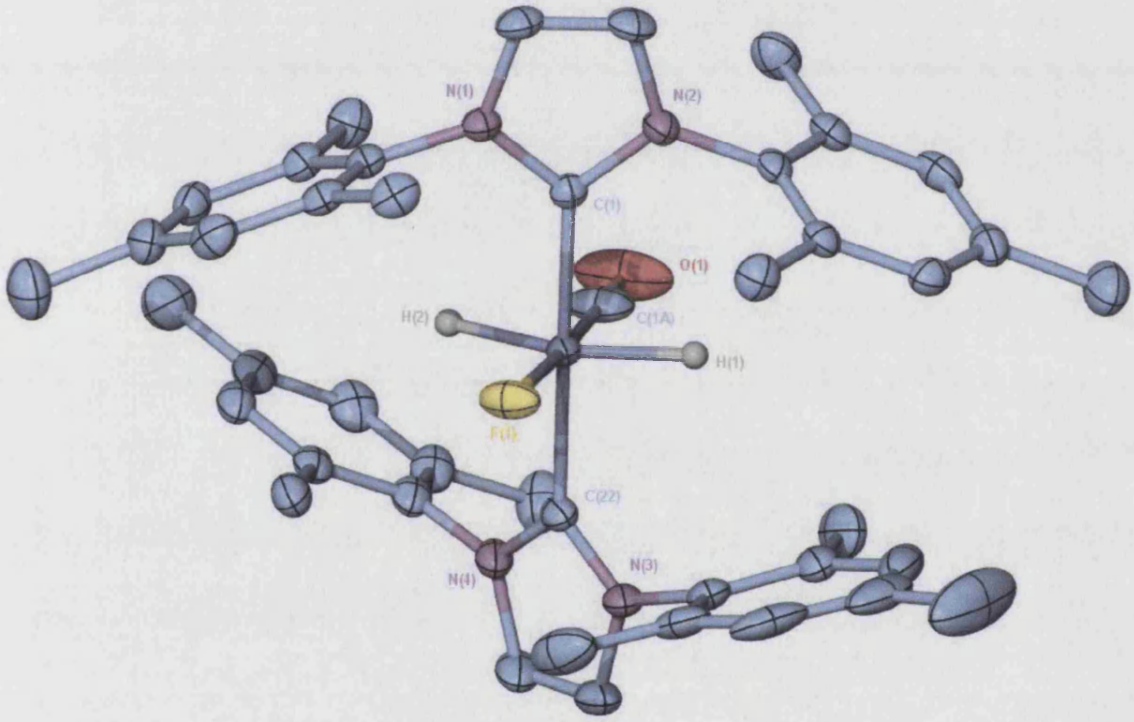

X-Ray 6.13. - *X-Seed drawing of the molecular structure of* ***(45)*** *in the solid state. Thermal ellipsoids are set at the 50% probability level. Hydrogen atoms are omitted for clarity (apart from the hydrides).*

Selected Bond Length	**[Å]**		
Ru(1)-C(1A)	1.784(3)	Ru(1)-F(1)	2.0332(15)
Ru(1)-C(1)	2.067(2)	Ru(1)-C(22)	2.073(2)
O(1)-C(1A)	1.170(4)		
Selected Bond Angles	**[°]**		
H(1)-Ru(1)-H(2)	152(2)	H(1)-Ru(1)-C(1A)	78.1(15)
H(2)-Ru(1)-C(1A)	74.3(19)	H(1)-Ru(1)-F(1)	105.8(15)
H(2)-Ru(1)-F(1)	101.7(19)	C(1A)-Ru(1)-F(1)	175.99(11)
H(1)-Ru(1)-C(1)	89.6(13)	H(2)-Ru(1)-C(1)	90.2(19)
C(1A)-Ru(1)-C(1)	92.69(11)	F(1)-Ru(1)-C(1)	86.67(8)
H(1)-Ru(1)-C(22)	90.2(13)	H(2)-Ru(1)-C(22)	91.8(19)
C(1A)-Ru(1)-C(22)	90.91(11)	F(1)-Ru(1)-C(22)	89.80(8)
C(1)-Ru(1)-C(22)	176.26(10)		

Table 6.22. Selected bond lengths [Å] and angles [°] for $Ru(IMes)_2(CO)(HF)H_2$ **(45)**.

Although the pathway to the formation of **(45)** was not been probed, several observations were made. In fact the synthesis of **(45)** could be made via a different route, by reacting **(39)** or **(40)** with a direct source of HF ($3H\text{-}F/NEt_3$). Secondly, when adding NEt_3 to **(45)** a chemical shift and broadening of the hydride was observed from δ -24.63 to -24.54 ppm and similarly for the fluorine signal shifting from δ -208.49 to -208.15 **[Spectrum 6.33.]**. A similar effect was observed upon reaction of **(45)** with a source of HF ($3H\text{-}F/NEt_3$), resulting in a shift of the hydride signal from δ -24.63 to -24.88, and a broadening of the signal; moreover a broad signal was observed on the proton at 12.14 ppm and a singular pattern was seen in the fluorine as seen in **Spectrum 6.34.** suggesting several hydrogen bonding patterns such as F-H···F-H or F-H···NEt_3.

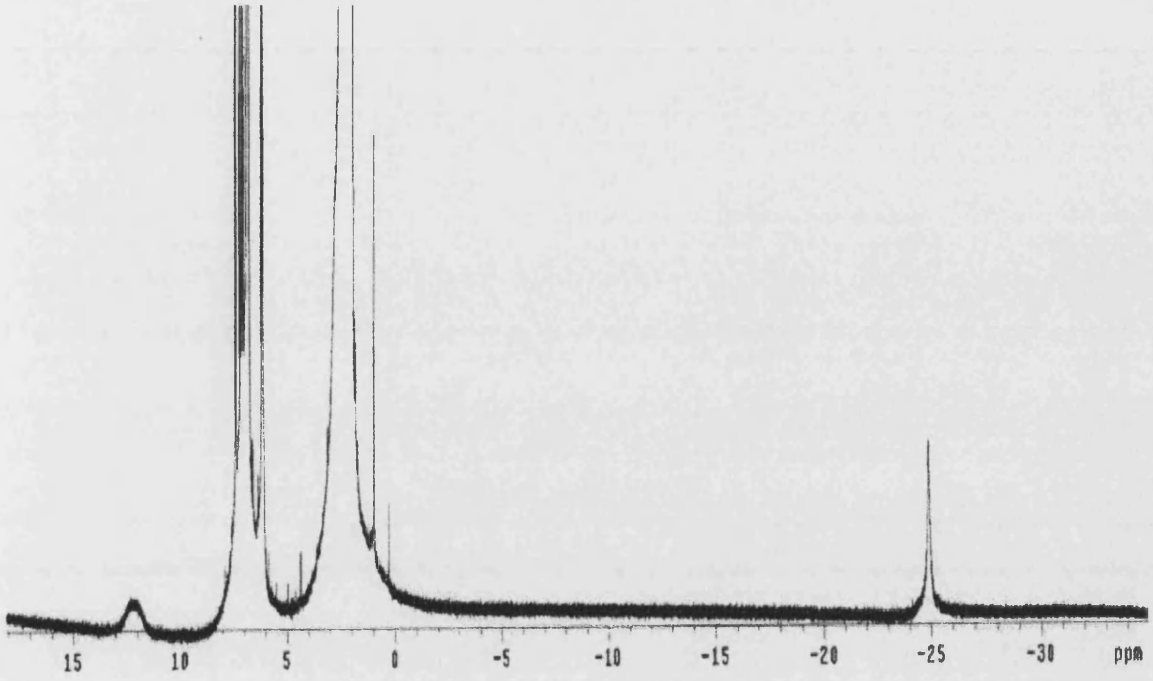

Spectrum 6.33. - *^{1}H NMR spectrum of the solution mixture of **(45)** and $3HF/NEt_3$.*

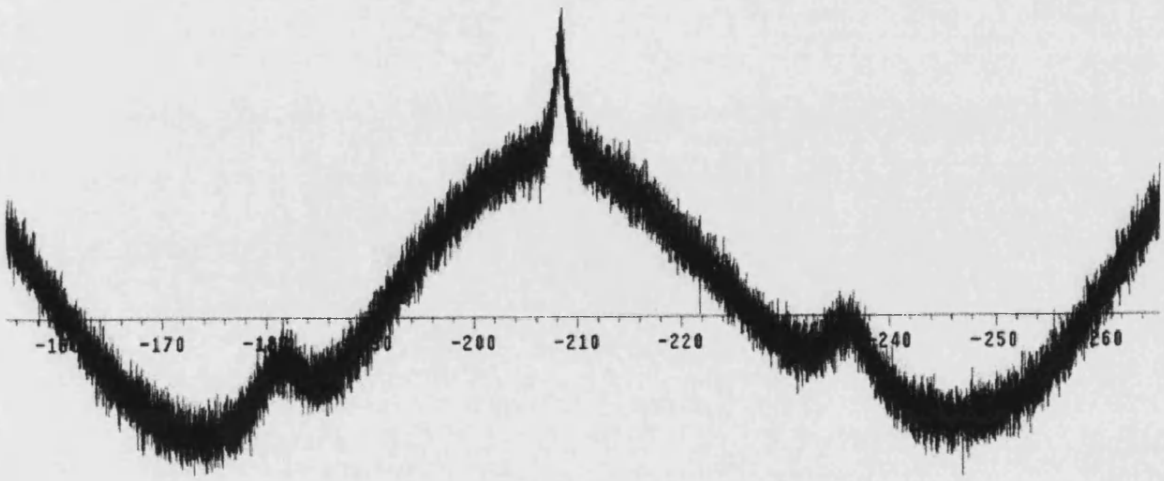

Spectrum 6.34. - *^{19}F NMR spectrum of the solution mixture of **(45)** and $3HF/NEt_3$.*

These are several interesting observations worth emphasising the NMR experiments conducted on the reaction mixture. Two major new species (C_6F_5OEt, *p*-$C_6F_4(OEt)_2$[103]) arising from the coupling of the ethanol ligand with C_6F_6 were observed and characterised by multinuclear / multidimentional NMR experiments **[Figure 6.5., Spectrum 6.35.]**, suggesting a similar pathway to the one observed so far as shown of **Scheme 6.36.** for the formation of **(45)**. (NB: Assignment of the fluorine signals have proven to be difficult due to over lapping of these later).

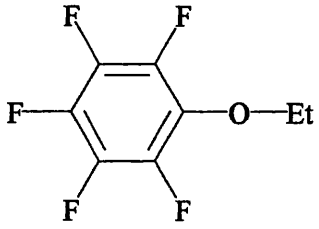

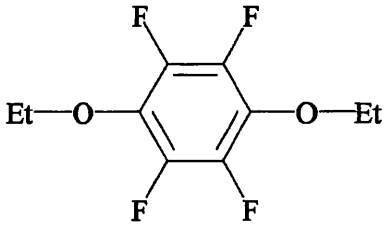

^{19}F	δ: -158.20(m) -164.91(m) -164.67(m)	
^{1}H	δ: 3.66 q (J_{HH} = 7.2 Hz, 2H, CH_2) 1.19 t (J_{HH} = 7.2 Hz, 3H, CH_3)	3.60 q (J_{HH} = 6.8 Hz, 2H, CH_2) 0.97 t (J_{HH} = 6.8 Hz, 3H, CH_3)
^{13}C	δ: 57.6 CH_2 21.6 CH_3	71.6 CH_2 15.5 CH_3

Figure 6.5. – *NMR shift assignments of the ethanol C_6F_6 coupling products.*

Spectrum 6.35. -

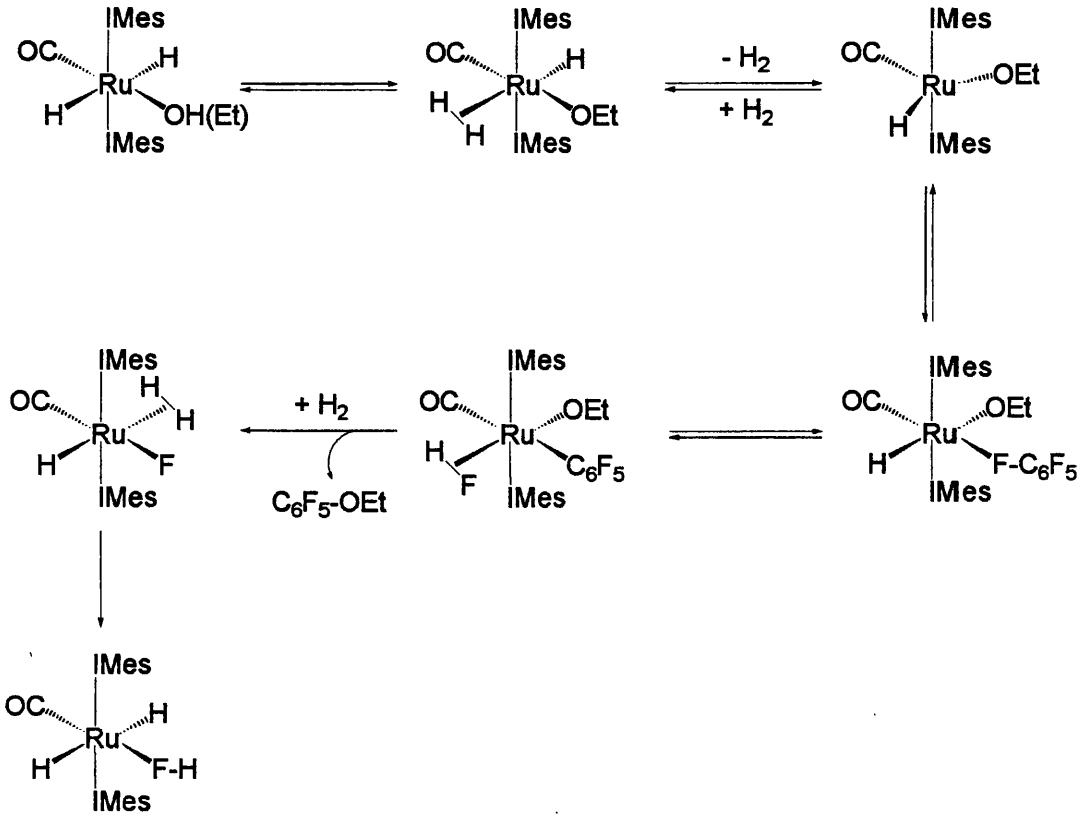

Scheme 6.36. - *Proposed mechanism for the formation of (45).*

6.2.6.2. Reaction of (45) with CO.

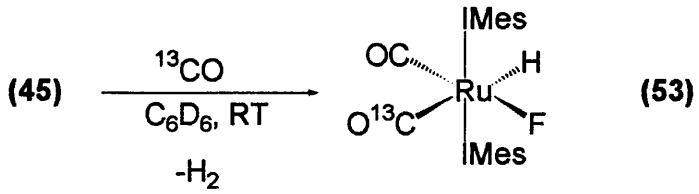

Scheme 6.36.

As seen for the previous dihydride isolated **(45)** reacts with CO at room temperature to generate the $Ru(IMes)_2(CO)_2(F)H$ **(53) [Scheme 6.36.]**. The hydride signal for **(53)** was observed in the ^1H NMR spectrum at δ -3.77 **[Spectrum 6.36.]** and labelling experiment showed that the labelled CO ends up in the position trans to the hydride (J_{HC} = 46.3 Hz), whereas the fluoride now seat *cis* to the hydride (J_{HF} = 6.4 Hz). The fluoride signal was observed at - 400 ppm on the ^{19}F NMR, as a broad singlet. The carbon spectra displayed two carbonyl carbon signal; at 205.1 (J_{CF} = 89.47Hz), 193.6 (J_{CF} = 9.55Hz) ppm. The IR spectrum shows three strong bands between 2001-1880 cm^{-1}, with that at 1938 cm^{-1} ($Ru(IMes)_2(^{13}CO)(CO)(F)H$ 1991, 1930, 1892 cm^{-1}) enhanced due to intensity stealing assigned to ν_{Ru-H} on the grounds of the observations made for **(53)**.

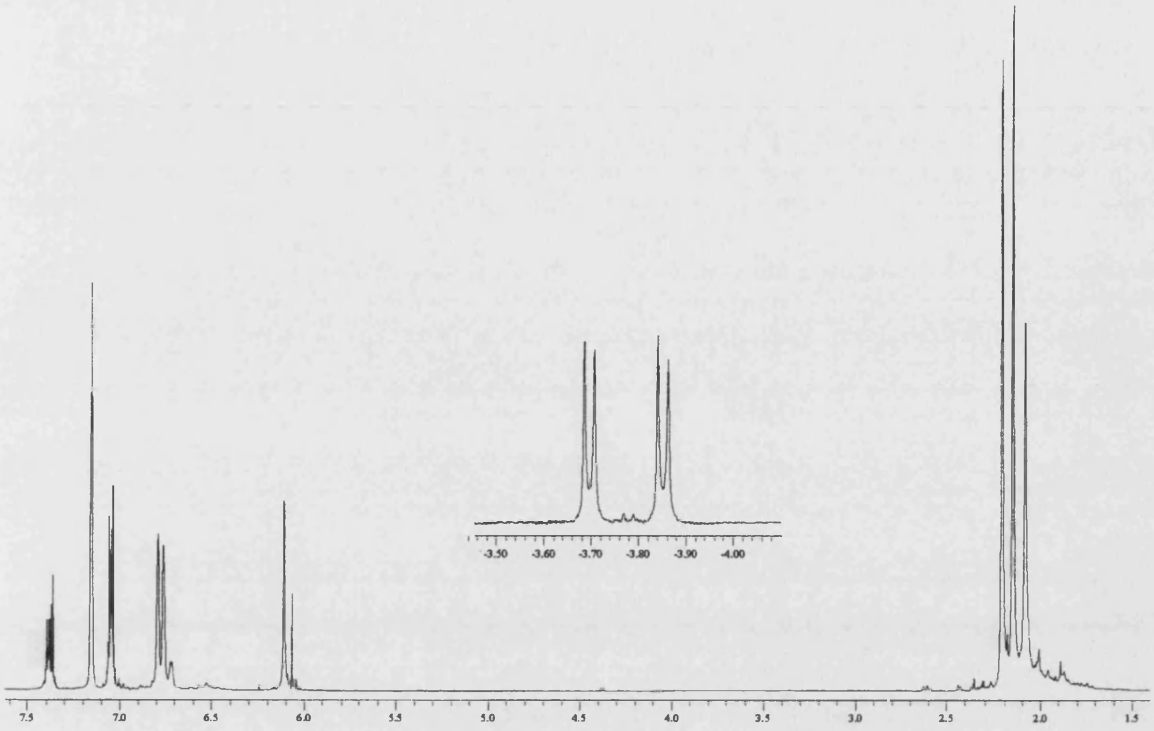

Spectrum 6.36. - *^{1}H NMR spectrum of (53)-^{13}CO.*

Light yellow crystals could be grown out of a benzene solution of **(53)** layered with hexane. The structure of **(53)** was confirmed by X-ray diffraction **[X-Ray 6.14.]**. Selected bond distances and angles for **(53)** are given in **Table 6.23.**. As in the structure of the hydroxy hydride **(48, 49. 52, 53)**, the coordination geometry around the central ruthenium in **(53)** is distorted from a regular octahedron with highly bent *trans*-IMes-Ru-IMes and *cis*-$Ru(CO)_2$ angles (C(3)-Ru-C(24) 167.67(6)°, C(2)-Ru-C(1) 96.14(18)°). The two **Ru-CO** bond lengths exhibit significant differences (1.890(6), 1.988(2) Å), while a distance of 2.019(5) Å for the Ru-F distance appears to be similar to the one than observed in other of Ru(II) fluoride complexes **[Table 6.24.]**.

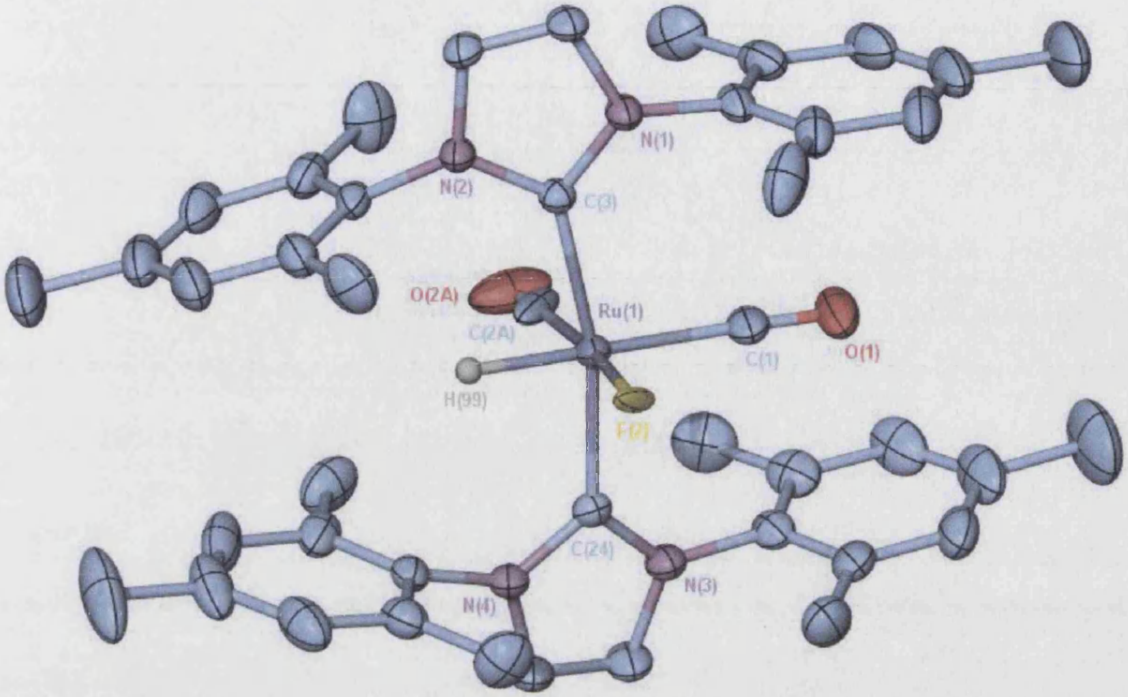

X-Ray 6.14. - *X-Seed drawing of the molecular structure of* ***(53)*** *in the solid state. Thermal ellipsoids are set at the 50% probability level. Hydrogen atoms have been omitted for clarity (apart from the hydride).*

Selected Bond Length	**[Å]**		
Ru(1)-H(99)	1.588(16)	Ru(1)-C(2)	1.890(6)
Ru(1)-C(1)	1.988(2)	Ru(1)-C(3)	2.0998(15)
Ru(1)-F(2A)	2.019(5)	O(2)-C(2)	1.115(8)
Ru(1)-C(24)	2.1074(16)	O(1)-C(1)	1.130(3)
Selected Bond Angles	**[°]**		
C(2)-Ru(1)-C(1)	96.14(18)	C(2)-Ru(1)-F(2A)	173.4(2)
C(1)-Ru(1)-F(2A)	90.03(15)	C(2)-Ru(1)-C(3)	88.06(17)
C(1)-Ru(1)-C(3)	96.33(7)	C(1)-Ru(1)-C(24)	95.66(7)
F(2A)-Ru(1)-C(3)	89.01(15)	F(2A)-Ru(1)-C(24)	88.12(15)
C(2)-Ru(1)-C(24)	93.50(18)	C(2A)-Ru(1)-C(24)	85.6(5)
		C(3)-Ru(1)-C(24)	167.67(6)

Table 6.23. - *Selected bond lengths [Å] and angles [°] for* $Ru(IMes)_2(CO)_2(F)H$ ***(53)***.

Compounds	Ru-F [Å]	[Ref]
$[Ru(dppp)_2F][PF_6]$	2.030	**[101]**
$Ru(dmpe)_2(F)(FHF)$	2.168(3) / 2.101(3)	**[104]**
$Ru(dppp)_2(F)_2$	2.071 / 2.058	**[101]**
$Ru(PPh_3)_2(CO)_2(F)_2$	2.011	**[105]**

Table 6.24. - *Selected bond lengths [Å] in Ru-F complexes*

Upon longer reaction time (36h) under ^{13}CO, formation of **(58)** was observed. This experiment was repeated upon reaction of a pure sample of **(53)** with CO and in a similar manner formation of **(58)** was observed suggesting two possible pathways as show on **Scheme 3.37**.

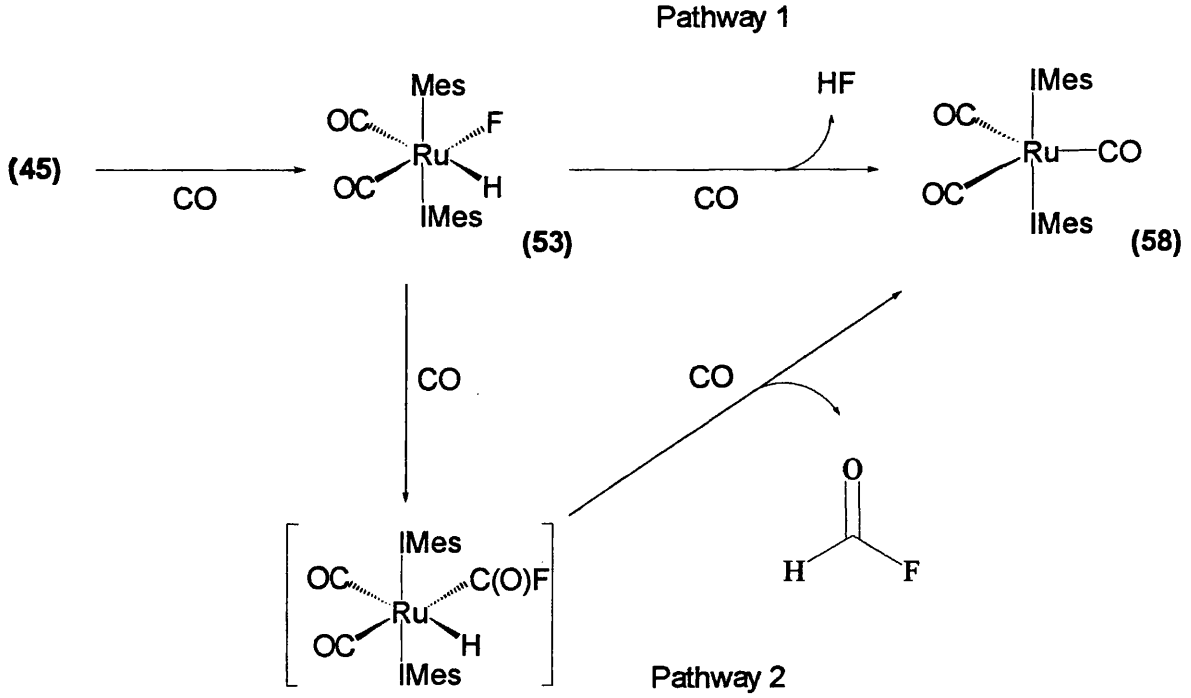

Scheme 3.37. - *Proposed reaction mechanism for the formation of (58) upon the reaction of (45) with CO.*

The first postulated pathway involves reductive elimination of HF **[Scheme 3.37., Pathway 1]**. Although very few and poorly characterised references are available in the literature for such a process,[106] it is backed up by various example of reductive elimination of HCl,[107] H_2O,[108] and HOR (R = CH_3, CH_2CH_3)[109] well described in the literature. Thus enabling the reductive elimination of HF as a possible pathway to **(58)**.

The second possible pathway originate form the observations made in the reaction of **(53)** with CO where we described the reaction of CO insertion into the Ru-OH bond, in a similar manner CO insertion into Ru-F bond has been reported previously by Brewer et al. to generate $M(PPh_3)_2(CO)_2((C=O)F)F$ (M = Ru, Os),[110] suggesting the possibility of the formation of **(58)** via CO insertion into the Ru-F bond **[Scheme 3.37., Pathway 2]**.

At this stage no definitive conclusion is to be made on either of these pathways due to the lack of mechanistic and spectroscopic information concerning the whole process.

6.2.6.3. Reaction of (39), (40) with C_6Cl_6.

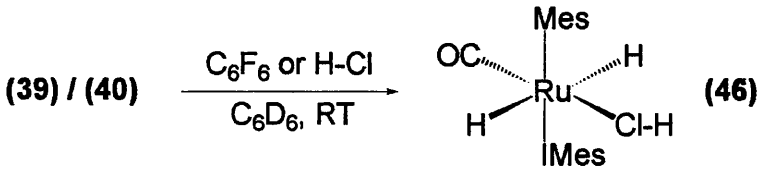

Scheme 3.38.

The reaction of **(39, 40)** with C_6F_6 could be extended to the use of C_6Cl_6, and addition of 2 equivalent of C_6Cl_6 to a benzene solution of **(39)** or **(40)** resulted in formation of $Ru(IMes)_2(CO)(Cl\text{-}H)H_2$ after 1 week at 50°C **[Scheme 3.38.]**. The ^1H NMR spectrum of **(46)** showed a *trans* hydride species with a hydride signal at -25.42 ppm **[Spectrum 6.37.]**. A single carbonyl band was observed in the IR spectrum at 1882 cm^{-1} in a similar region to **(39-46)**. However, both NMR and IR prove of limited use for further characterisation of $Ru(IMes)_2(CO)(HCl)H_2$. Fortunately, red crystals of **(46)** could be grown out of benzene/hexane solution.

The X-ray structure of **(46)** **[X-Ray 6.15.]** was recorded at 30 K, but showed disorder which prevented any hope of being able to observe the Ru-Cl-H hydrogen atom. Nevertheless, selected bond distances and angles for **(46)** are given in **Table 6.25.**. The coordination geometry around the central ruthenium in **(46)** is distorted from a regular octahedron with the IMes rings twisted 53.2° from coplanarity. The Ru-Cl-H distance is 2.0332(15) Å and noticeably, significantly shorter than 'conventional' Ru-Cl distances in, for example, *cis*-$Ru(PMePh_2)_3(CO)Cl_2$ (Ru-Cl: (*trans* to $PMePh_2$) 2.461(8), (*trans* to CO) 2.454(8) Å) and *trans*-$Ru(PMePh_2)_3(CO)Cl_2$ (Ru-Cl: 2.422(4), 2.423(3) Å).[111]

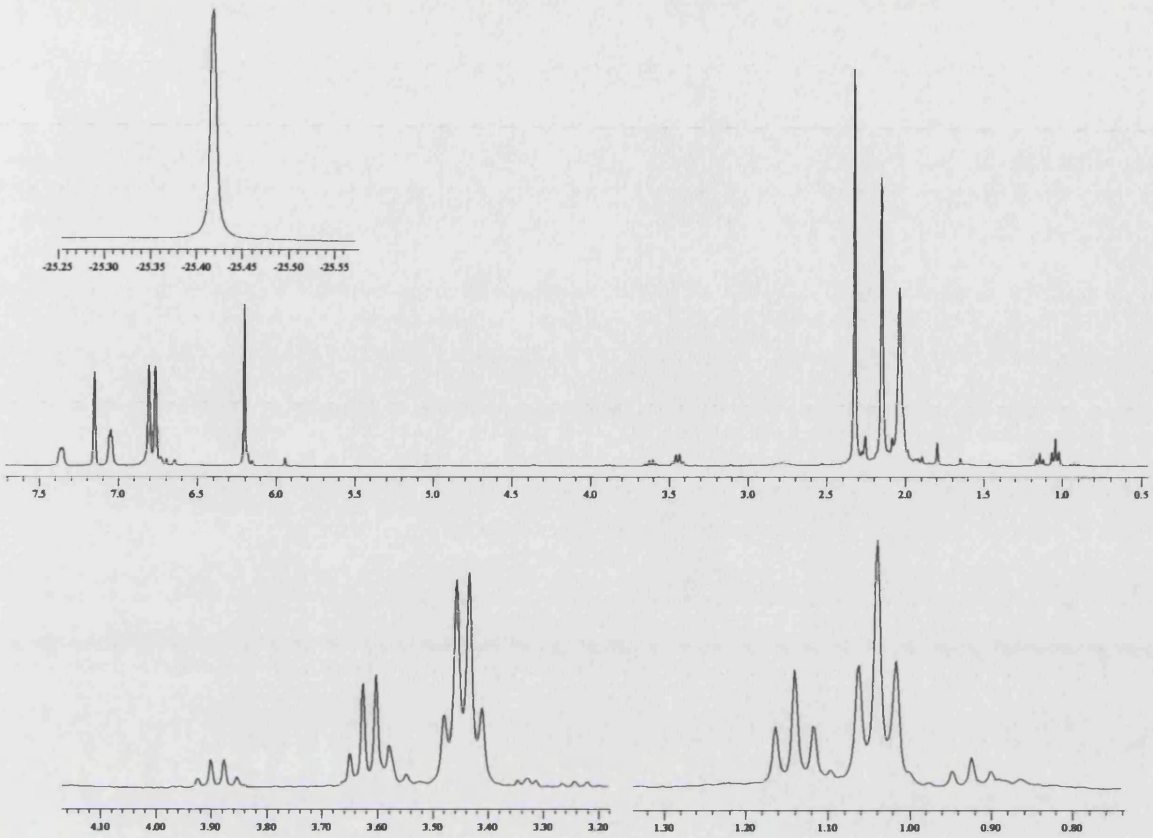

Spectrum 6.37. – *^{1}H NMR spectrum of the reaction mixture resulting from the formation of* ***(46)*** *by reaction of* ***(39)*** *with C_6Cl_6.*

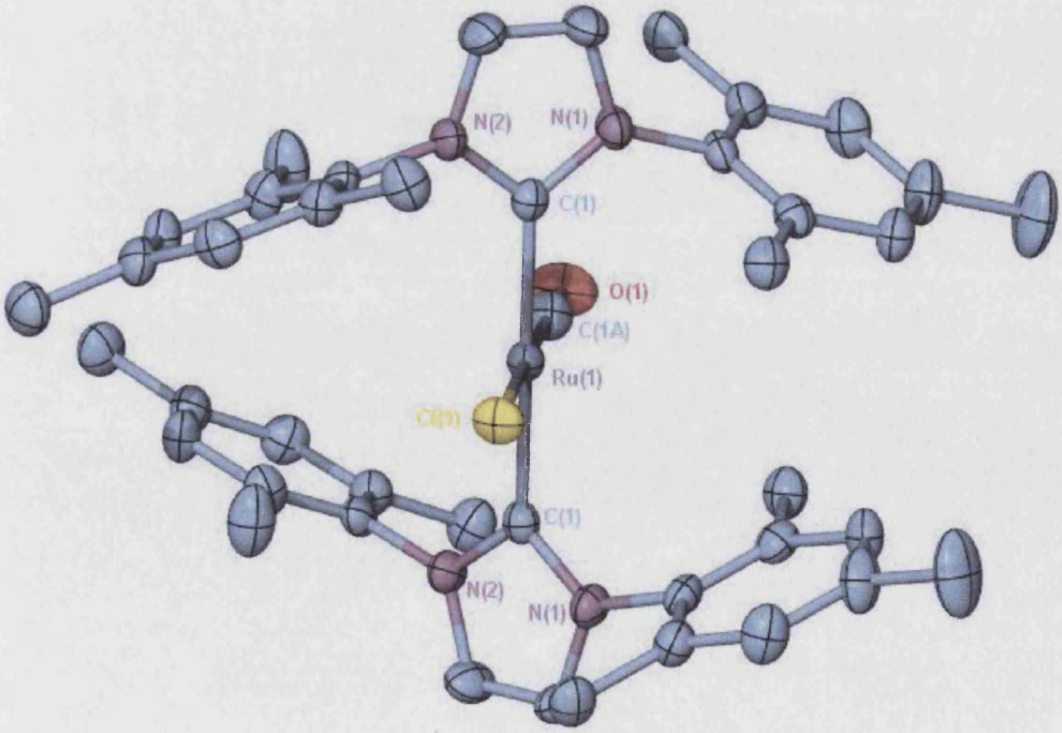

X-Ray 6.15. - *X-ray structure of* ***(46)****. Thermal ellipsoids are set at the 50% probability level. Hydrogen atoms have been omitted for clarity.*

Selected Bond Length	**[Å]**		
Ru(1)-C(1A)	1.776(12)	Ru(1)-Cl(1)	2.433(3)
Ru(1)-C(1)	2.075(3)	O(1)-C(1A)	1.189(13)
Selected Bond Angles	**[o]**		
C(1)-Ru(1)-C(1)	179.78(19)	C(1A)-Ru(1)-C(1)	89.1(5)
C(1A)-Ru(1)-Cl(1)	178.6(5)	C(1)-Ru(1)-Cl(1)	89.92(14)

Table 6.25. - *Selected bond lengths [Å] and angles [°] for $Ru(IMes)_2(CO)(HCl)H_2$ (46).*

As seen previously for **(46)** several new species coming from the coupling of the ethanol ligand with C_6Cl_6 were observed during the reaction of **(39)** with C_6Cl_6. These were characterised by multinuclear and multidimentional NMR experiments **(Figure 6.6.)**, suggesting a similar pathway to the one proposed for the formation of **(45)**.[112]

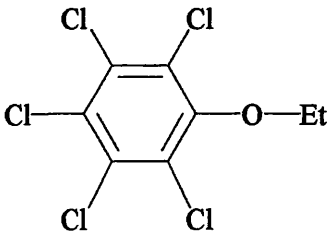

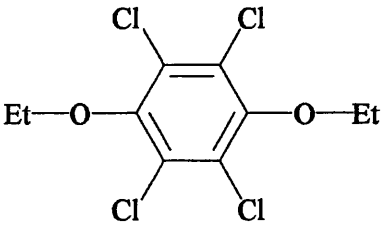

^1H	δ: 3.66 q (J_{HH} = 7.2 Hz, 2H, CH_2) 1.19 t (J_{HH} = 7.2 Hz, 3H, CH_3)	3.60 q (J_{HH} = 6.8 Hz, 2H, CH_2) 0.97 t (J_{HH} = 6.8 Hz, 3H, CH_3)
^{13}C	δ: 58.3 CH_2 18.4 CH_3	70.3 CH_2 15.8 CH_3

Figure 6.6. - *NMR shift assignments of the ethanol C_6Cl_6 coupling products.*

6.3 Discussion.

6.3.1. Spectroscopic analysis.

The complexes described in this chapter show very similar NMR spectra due to the symmetry brought about by the *trans*-IMes ligands. The proton spectra characteristically show 1 to 3 methyl resonances between 2.0 to 2.8 ppm, depending on the symmetry and the fluxionally within the complex. One resonance is always observed for the NCH=HCN protons (6.08 to 6.44 ppm), the average being around δ 6.15. As seen in **table 6.26.**, minute differences can be observed in the spectroscopic data of the trans-dihydride species.

Complex	Hydride (ppm)	Carbonyl carbon (ppm)	Carbene carbon (ppm)	IR (cm^{-1})
(39)	-23.51	205.6	197.9	1887
(40)	-23.15	206.4	198.6	1861
(41)	-23.79	205.0	197.0	1858
(42)	-24.48	205.5	194.9	1881
(43)	-23.77	203.1	197.5	1883
(44)	-24.47	202.8	192.7	1879
(45)	-24.63	206.0	196.3	1873
(46)	-25.42	202.4	195.5	1882

Table 6.26. - *Selected spectroscopic data for the trans-dihydride species.*

Similar trend is observed for the dicarbonyl species as seen in **table 6.27**. Interestingly in all these species three (instead of two) strong IR band are observed in the carbonyl region of the IR spectrum **[Spectrum 6.38.]**. This can be explained by an enhancement of the hydride signal due to intensity stealing and the ν_{Ru-H} could be assigned on the grounds of the observed shift to lower frequency of the other two bands upon ^{13}CO labelling **[Spectrum 6.38.]**.

Complex	Hydride (ppm)	Carbonyl carbon (ppm)	Carbene carbon (ppm)	IR (cm^{-1})
(48)	-3.75	204.2 / 188.9	184.8	2019 / 1924 / 1880
(49)	-4.82	203.1 / 197.4	185.8	2023 / 1931 / 1892
(52)	-4.47	202.9 / 199.0	186.6	2014 / 1946 / 1896
(53)	-3.80	205.1 / 193.6		1991 / 1930 / 1892
(57)	-4.30	206.2 / 194.8	185.0	2041 / 1965 / 1916
(39')	-3.88	/ 195.2		NA
(39'')	-5.24	206.1 / 198.5		NA

Table 6.27. - *Selected spectroscopic data for the cis-dicarbonyl species.*

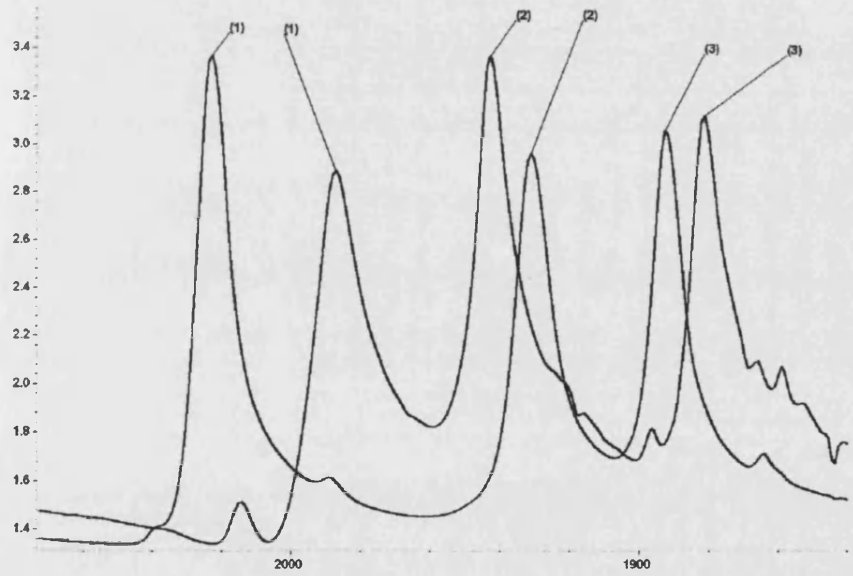

	(40)-CO	(40)-^{13}CO
(1)	2023	1987
(2)	1931	1943
(3)	1892	1881

Spectrum 6.38. - *Selected spectroscopic data for the cis-dicarbonyl species.*

6.3.2. Structural analysis.

While there a number of structurally characterised bis-carbene complexes reported in the literature,[113] only very few of these contain two IMes ligands.[114] A comparison of the crystallographically determined structures reported herein reveals some noteworthy trends.

In the first instance, the twist angle (θ_T) as defined in **Figure 6.7** varies across all compounds, from 18° in the propanethiol complex **(44)** to 53.2° for the H-Cl complex **(46)**. This is not unexpected, as unfavourable interactions between the *para*-methyl substituents on the mesityl rings might result if θ_T had a value of zero. The magnitude of the twist angle appears to be inversely proportional to the steric demand of the varying equatorial ligand in the *trans* dihydride complexes, as shown by the value of θ_T in **table 6.28**. It is therefore reasonable to assume that the carbene ligands act as rotating "umbrellas" for the ligand in the trans-position to the carbonyl, and can be considered as a structural evidence for the steric crowding around the metal centre.

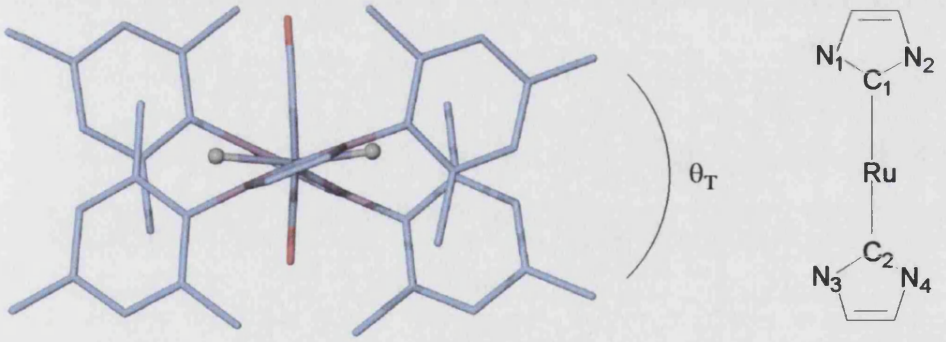

$\theta_T = 0.5\ [<N_1\text{-}C_1\text{-}C_2\text{-}N_3 + <N_2\text{-}C_1\text{-}C_2\text{-}N_4]$

Figure 6.7. - *Definition of the twist angle.*

Throughout the dihydride complexes, the IMes fragments in the molecule tend to be approximately axial with respect to the equatorial plane of the molecule (as defined by the metal centre, hydrides and ligand atoms bound to the metal) and this is reflected in the $C_{carbene}$-Ru-$C_{carbene}$ angles **[α; table 6.28]** for these compounds. Despite the inherent difficulty in locating hydrogen atoms from X–ray analysis, it is reasonable to say that the hydrides in all of these complexes are located in the 2 'pockets' **[Figure 6.7.]**, on either side

of the ruthenium, created by the IMes ligands, along a vector through the metal centre that bisects θ_T.

Complex	θ_T [°]	α [°]	Ru-C	C-O [Å]
(39)	32.3	180	1.824(7)	1.143(7)
(40)	48.0	174.90	1.798(3)	1.165(3)
(42)	27.6	178.05	1.826(18)	1.22(2)
(43)	18.2	177.56(4)	1.8258(14)	1.1578(18)
(44)	52.2	178.73(9)	1.803(7)	1.212(6)
(45)	47.3	176.26(10)	1.784(3)	1.170(4)
(46)	53.2	179.78(19)	1.776(12)	1.189(13)

Table 6.28. - *Selected bond angle and distances for the trans dihydride species.*

On the face of it, this pattern would seem to be reversed for the bis-carbonyl complexes where θ_T for the propanethiolate complex **(52)**, the monodentate bicarbonate complex **(57)**, the hydroxy hydride species **(48)**, the hydride fluoride **(53)** and the thiolate complex **(49)**, are correspondingly, 41.8, 39.0, 22.8°, 22.0° and 15.7° with the chelate **(59)** having a value of 26.4° **[Table 6.29.]** . In some structures the proximity between a *meta*-methyl carbon on the mesityl ring of one carbene to the centroid of the opposing aromatic ring on the second carbene might suggest the presence of some C–H•••π stabilisation, but this is a little tenuous given the inherent bulk of the carbenes themselves.

Complex	θ_T [°]	α [°]	Ru-C (cis)	Ru-C (trans)	C-O (cis)	C-O (trans)
(48)	22.8	167.94(8)	1.873(6)	1.966(3)	1.207(7)	1.144(3)
(49)	22.0	168.37(6)	1.897(5)	1.9634(18)	1.182(5)	1.138(2)
(52)	41.8	165.91(6)	1.8629(17)	1.9546(18)	1.149(2)	1.142(2)
(53)	15.7	167.67(6)	1.890(6)	1.988(2)	1.115(8)	1.130(3)
(57)	39.0	166.85(12)	1.818(3)	1.989(3)	1.164(3)	1.133(4)
(59)	26.4	170.28(11)	1.828(3)	NA	1.145(4)	NA

Table 6.29. - *Selected bond angle and distances for the cis dicarbonyl species.*

Comparative $C_{carbene}$–Ru–$C_{carbene}$ angles for the bis-carbonyl complexes **(48)**, **(49)**, **(52)**, **(53)**, **(57)** and the chelate compound **(59)** are considerably more acute at 167.94(8), 168.37(6), 165.91(6), 167.67(6), 166.85(12) and 170.28(11)° respectively. This is inevitable as one of the 'pockets' has to expand to accommodate a substituent considerably larger than a hydride in these four compounds, which results in concomitant compression of the of the mesityl rings enfolding the hydride. Asymmetry in the $N_{carbene}$-$C_{carbene}$-Ru angles strongly reflects this intramolecular elasticity with typical decreases of 3° on the hydride side of a carbene compared with the alternative angle in the same carbene. It is also striking that in these compounds, the pairs of aromatic rings that envelop individual pocketed coordination sites on the metal are almost mutually coplanar. Shortest distances between the carbons of one ring surrounding a carbonyl pocket and the least squares plane of the opposing ring range from 5.53 Å **(59)**, 5.72 Å **(48)**, 6.08Å **(57)** and 6.14 Å for **(52)**. Analysis of the superstructures for all compounds did not reveal any specific insight. Aromatic rings from neighbouring molecules in the lattice of **(39)** appear to stack, but an average distance between the carbons of one ring and the least squares plane of the other of 4.3 Å, suggests that this may largely be a packing effect.

HF nature of (45), HCl nature of (46).

The reaction of either aqua complex **(40)** or ethanol complex **(39)** with C_6F_6 or $Et_3N.3HF$ generates a complex that we believe would represent the first structurally characterised transition metal coordinated HF complex **[Table 6.30.]**. Crabtree and co-workers have spectroscopically characterised $Ir(H)(FH)(bq\text{-}H)(PPh_3)_2$, although the complex proved to be unstable above 210 K preventing structural characterisation. On the basis of our spectroscopic data for $Ru(IMes)_2(CO)(HF)H_2$, it is clear from the chemical shift in the ^{19}F NMR spectrum that it is not a terminal Ru-F species. Similarly, the carbonyl stretching frequency correlates well with other isolated *trans*-dihydride Ru(XH) species described in this chapter. On the basis of simple electron counting, we require a two-electron donor ligand in the position *trans* to CO to give an 18-electron complex. Although we have a number of X-ray structures covering a range of temperatures, we have not been able to resolve the hydrogen atom on the coordinated HF. There is no remaining electron density in the diffraction map ruling out a Ru-HF complex stabilized by solvent interaction. Unexpectedly, the Ru-F bond distance observed in **(40)** appears to be relatively short (2.0332(15) Å), and in line with bulk of measurements made for terminal ruthenium fluoride complexes, Further work, including a possible neutron defraction determination, is planned to resolve and prove the structure of **(40)**.

Compounds	M-F [Å]	[Ref]
$La(HF)_2(AsF_6)_3$	2.466(3)	**[115]**
$Pb(HF)(AsF_6)_2$	N.A (Powder Diff)	**[116]**
$Ir(H)(FH)(bq\text{-}NH_2)(PH_3)_2$	2.143 (DFT calcs)	**[117]**
$Ir(H)(FH)(bq\text{-}NH_2)(PPh_3)_2$	N.A.	**[118]**

Table 6.30. - *Selected bond lengths [Å] in M-FH complexes.*

Similar observations applies to **(46)**, although for this species there is less possibility that an hydrogen will be found due to the important electron density around the Cl atom (relatively to the hydrogen atom) which should prevent the hydrogen to be reliably located.

6.4. Conclusion.

Attempted crystallisation of $Ru(IMes)_2(AsPh_3)(CO)H_2$ by ROH (R = Me, Et, $EtOC_6H_4$) or hexane led to the isolation of $Ru(IMes)_2(CO)(ROH)H_2$ (R = Et **(39)**, Me **(41)**, EtOC6H4 **(42)**) and $Ru(IMes)_2(CO)(H_2O)H_2$ **(40)** respectively, all of which contain an unusual *trans* arrangement of the hydride ligands. Both **(39)** and **(40)** prove highly reactive towards a range of small molecules to afford Ru-X (X = heteroatom) complexes through either simple substitution processes (e.g. displacement of water by thiol, HF, H_2S and HCl) or via more complex reactions to give monohydride $Ru(IMes)_2(CO)_2(X)H$ compounds. Within the latter group, $Ru(IMes)_2(CO)_2(OH)H$ **(48)** and $Ru(IMes)_2(CO)_2(\eta^1\text{-}O_2COH)H$ **(57)** are of particular interest in that they represent rare examples of fully characterised hydroxy hydride and monodentate bicarbonate complexes. In all of the cases we have studied, reaction of the Ru-HOR (R = H, Et) bond occurs in preference to chemistry at the Ru-H ligand. Although full mechanistic studies of all the reactions described in this chapter have not been made, a general reaction pathway was observed for conversion of $Ru(CO)(XH)H_2$ to $Ru(CO)_2(X)H$ involving a hydrogen transfer from RuXH to Ru-H.

Of particular interest to us at the outset of this work was the likely stability of the Ru-X bonds. Caulton has shown the propensity of the coordinatively saturated iridium heteratom complexes $Ir(P^tBu_2Ph)_2(CO)(X)H_2$ to reductively eliminate H-X upon addition of CO is highly dependent upon X. Thus, for X = OC(O)OR and SPh, the 18-electron complex is metastable in the presence of CO, ultimately losing phosphine and HX to give 16-electron $Ir(P^tBu_2Ph)(CO)_2H$. When X = F or OPh, HX loss is almost instantaneous. These patterns of reactivity are governed by the π-donating ability of X (pπ-dπ interactions destabilise the 18-electron species and stabilise 16-electron complexes) and the strength of the H-X bond that is formed upon elimination. In the case of $Ru(IMes)_2(CO)_2(X)H$, we see some evidence for Ru-X reaction, though not via simple HX reductive elimination. Hence, although $Ru(IMes)_2(CO)_2(OH)H$ reacts with CO, the pathway involves a series of insertion and elimination processes leading to $Ru(IMes)_2(CO)_3$ as the final product. In conclusion, the presence of two bulky IMes ligands on Ru has been shown to help stabilise bonds to oxygen, nitrogen, sulphur, flurorine and chlorine. Further work is in progress to examine fully the reactivity of these linkages and to extend the scope to other X heteroatoms.

6.5. References.

1. Holm, R. H.; Kennepohl, P.; Solomon, E. I. *Chem. Rev.* **1996**, *96*, 2239
2. **(a)** Bäckvall, J. E.; Akermark, B.; Ljunggren, S. O. *J. Am. Chem. Soc.* **1979**, *101*, 2411. **(b)** Bäckvall, J. E.; Bjorkmann, E. E.; Pettersson, L.; Siegbahn, P. *J. Am. Chem. Soc.* **1984**, *106*, 4369. **(c)** Bäckvall, J. E.; Bjorkmann, E. E.; Pettersson, L.; Siegbahn, P. *J. Am. Chem. Soc.* **1985**, *107*, 7265.
3. **(a)** Müller, T. E.; Beller, M. *Chem. Rev.* **1998**, *98*, 675. **(b)** Johnson, J. S.; Bergman, R. G. *J. Am. Chem. Soc.* **2001**, *123*, 2923
4. Bryndza, H. E.; Tam, W. *Chem. Rev.* **1988**, *88*, 1163
5. Fulton, J. R.; Bouwkamp, M. W.; Bergman, R. G. *J. Am. Chem. Soc.* **2000**, *122*, 8799. Fulton, J. R.; Sklenak, S.; Bouwkamp, M. W.; Bergman, R. G. *J. Am. Chem. Soc.* **2002**, *124*, 4722.
6. Woerpel, K. A.; Bergman, R. G. *J. Am. Chem. Soc.* **1993**, *115*, 7888.
7. **(a)** Bergman, R. G. *Polyhedron* **1995**, *14*, 3227. (b) Sharp, P. R. *Comments Inorg. Chem.* **1999**, *21*, 85. **(c)** Sharp, P. R. *J. Chem. Soc., Dalton Trans.* **2000**, 2647. For recent examples, see: **(d)** Hartwig, J. F.; Andersen, R. A.; Bergman, R. G. *J. Am. Chem. Soc.* **1989**, *111*, 2717. **(e)** Hartwig, J. F.; Andersen, R. A.; Bergman, R. G. *Organometallics* **1991**, *10*, 1875. **(f)** Blum, O.; Milstein, D. *J. Am. Chem. Soc.* **1995**, *117*, 4582. **(g)** VanderLende, D. D.; Abboud, K. A.; Boncella, J. M. *Inorg. Chem.* **1995**, *34*, 5319. **(h)** Driver, M. S.; Hartwig, J. F. *J. Am. Chem. Soc.* **1995**, *117*, 4708. **(i)** Holland, P. L.; Andersen, R. A.; Bergman, R. G. *J. Am. Chem. Soc.* **1996**, *118*, 1092. **(j)** Boncella, J. M.; Eve, T. M.; Rickman, B.; Abboud, K. A. *Polyhedron* **1998**, *17*, 725. **(k)** Kaplan, A. W.; Ritter; J. C. M.; Bergman, R. G. *J. Am. Chem. Soc.* **1998**, *120*, 6828. **(l)** Mann, G.; Incarvito, C.; Rheingold, A. L.; Hartwig, J. F. *J. Am. Chem. Soc.* **1999**, *121*, 3224. **(m)** Matsuzaka, H.; Kamura, T.; Ariga, K.; Watanabe, Y.; Okubo, T.; Ishii, T.; Yamashita, M.; Kondo, M.; Kitagawa, S. *Organometallics* **2000**, *19*, 216. **(n)** Jayaprakash, K. N.; Gunnoe, T. B.; Boyle, P. D. *Inorg. Chem.* **2001**, *40*, 6481. **(o)** Tejel, C.; Ciriano, M. A.; Bordonaba, M.; López, J. A.; Lahoz, F. J.; Oro, L. A. *Inorg. Chem.* **2002**, *41*, 2348.
8 **(a)** Bryndza, H. E.; Fong, L. K.; Paciello, R. A.; Tam, W.; Bercaw, J. E. *J. Am. Chem. Soc.* **1987**, *109*, 1444. **(b)** Poulton, J. T.; Folting, K.; Streib, W. E.; Caulton, K. G. *Inorg. Chem.* **1992**, *31*, 3190. **(c)** Caulton, K. G. *New. J. Chem.* **1994**, *18*, 25. **(d)** Holland, P. J.; Andersen, R. A.; Bergman, R. G.; Huang, J.; Nolan, S. P. *J. Am. Chem. Soc.* **1997**, *119*, 12800. **(e)** Holland, P. L.; Andersen, R. A.; Bergman, R. G.

Comments Inorg. Chem. **1999**, *21*, 115. **(f)** Fulton, J. R.; Holland, A. W.; Fox, D. J.; Bergman, R. G. *Acc. Chem. Res.* **2002**, *35*, 44.

9. Bohm, V. P. W.; Gstottmayr, C. W. K.; Weskamp, T.; Herrmann, W. A. *J. Organomet. Chem.*, **2000**, *595*, 186.
10. **(a)** Hamilton, J. G.; Frenzel, U.; Kohl, F. J.; Weskamp, T.; Rooney, J. J.; Herrmann, W. A.; Nuyken, O. *J. Organomet. Chem.*, **2000**, *606*, 8. **(b)** Herrmann, W. A.; Kohl, F. J.; Weskamp, T. *Eur, Pat. Appl.*, **2000**, 16pp. **(c)** Weskamp, T.; Kohl, F. J.; Heiringer, W.; Gleich, D.; Herrmann, W. A. Angew. Chem., Int. Ed., **1999**, *38*, 2416.
11. Louie, J.; Grubbs, R. H. *Chem. Comm.*, **2000**, *16*, 1479.
12. Oldham, W. J. Jr.; Oldham, S. M.; Smith, W. H.; Costa, D. A.; Scott, B. L.; Abney, K. D. *Chem. Com.*, **2001**, *15*, 1348.
13. Herrmann, W. A.; Gerstberger, G.; Speigler, M. *Organomettalics*, **1997**, *16*, 2209.
14. Arduengo, A. J., III; Gamper, S. F.; Calabrese, J. C.; Davidson, F. *J. Am. Chem. Soc.*, **1994**, *116*, 4391.
15. Arduengo, A. J., III; Dias, H. V. R.; Calabrese, J. C.; Davidson, F. *Organometallics*, **1993**, *12*, 3405.
16. **(a)** Raubenheimer, H. G.; Cronje, S.; Rooyen, P. H. v.; Olivier, P. J. Toerien, J. G. *Angew. Chem., Int. Ed. Engl.*, **1994**, *33*, 672. **(b)** Kruger, G. J.; Olivier, P. J.; Lindeque, L.; Raubenheimer, H. G. *Acta Crystallogr.*, **1995**, *C51*, 1814. **(c)** Raubenheimer, H. G.; Lindeque, L.; Cronje, S. *J. Organomet. Chem.*, **1996**, *511*, 177.
17. Arduengo, A. J., III; Harlow, R. L.; Marshall, W. J.; Prakasha, T. K. *Heteroat. Chem.*, **1996**, *7*, 421.
18. Huang, J.; Stevens, E. D.; Nolan, S. P. *Organometallics*, **2000**; *19*, 1194.
19 Arduengo, A. J., III; Tamm, M.; McLain, S. J.; Calabrese, J. C.; Davidson, F.; Marshall, W. J. *J. Am. Chem. Soc.* **1994**, *116*, 7927.
20. Öfele, K. *J. Organomet. Chem.*, **1968**, *12*, P42.
21. Arduengo, A. J., III; Dias, H. V. R.; Calabrese, J. C.; Davidson, F. *Organometallics*, **1993**, *12*, 3405.
22. Arduengo, A. J., III; Gamper, S. F.; Calabrese, J. C.; Davidson, F. *J. Am. Chem. Soc.*, **1994**, *116*, 4391.

23. **(a)** Herrmann, W. A.; Elison, M.; Fischer, J.; Kocher, C.; Artus, G. R. J. *Angew. Chem., Int. Ed. Engl.* **1995**, *34*, 2371. **(b)** Herrmann, W. A.; Reisinger, C. P.; Spiegler, M. *J. Organomet. Chem.* **1998**, *557*, 93.

24. Weskamp, T.; Schattenmann, W. C.; Spiegler, M.; Herrmann,W. A. *Angew. Chem., Int. Ed. Engl.*, **1998**, 37, 2490.

25. Gstottmayr, C. W. K.; Bohm, V. P. W.; Herdtweck, E.; Grosche, M.; Herrmann, W. A. *Angew. Chem., Int. Ed.*, **2002**, *41*, 1363.

26. Frenzel, U.; Weskamp, T.; Kohl, F. J.; Schattenmann, W. C.; Nuyken, O.; Herrmann, W. A. *J. Organomet. Chem.*, **1999**, *586*, 263.

27. Andrus, M. B.; Song, C.; *Org. Lett.*, **2001**; *3*, 3761.

28. **(a)** Xu, L.; Chen, W.; Xiao, J.; *Organometallics*, **2000**, *19*, 1123 **(b)** Andrus, M. B.; Song, C.; Zhang, J. *Org. Lett.*, **2002**, *4*, 2079. **(c)** Selvakumar, K.; Zapf, A.; Beller, M. *Org. Lett.*, **2002**, *4*, 3031.

29. Louie, J.; Grubbs, R. H. *Chem. Commun.*, **2002**, 1479

30. **(a)** Shaw, B. L.; Uttley, M. F. *J. Chem. Soc., Chem. Commun.* **1974**, 918. **(b)** Yoshida, T.; Otsuka, S. *J. Am. Chem. Soc.*, **1977**, *99*, 2134. **(c)** Paonessa, R. S.; Trogler, W. C. *J. Am. Chem. Soc.*, **1982**, *104*, 1138. **(d)** Fryzuk, M. D.; MacNeil, P. A. *Organometallics*, **1983**, *2*, 682. **(e)** Rybtchinski, B.; Ben-David, Y.; Milstein, D. *Organometallics*, **1997**, *16*, 3786. **(f)** Li, S.; Hall, M. B. *Organometallics*, **1999**, *18*, 5682.

31. **(a)** Schrock, R. R.; Osborn, J. A. *J. Chem. Soc., Chem. Commun.*, **1970**, 567. **(b)** Crabtree, R. H.; Demou, P. C.; Eden, D.; Mihelcic, J. M.; Parnell, C. A.; Quirk, J. M.; Morris, G. E. *J. Am. Chem. Soc.*, **1982**, *104*, 6994. **(c)** Landis, C. R.; Halpern, J. *J. Am. Chem. Soc.*, **1987**, *109*, 1746. **(d)** Persson, B. A.; Larsson, A. L. E.; Le Ray, M.; Bäckvall, J. E. *J. Am. Chem. Soc.*, **1999**, *121*, 1645. **(e)** Laxmi, Y. R. S.; Bäckvall, J. E. *Chem. Commun.*, **2000**, 611. **(f)** Voges, M. H.; Bullock, R. M. *J. Chem. Soc., Dalton Trans.*, **2002**, 759.

32. ***Neutral alcohol complexes*: (a)** Viñas, C.; Nuñez, R.; Teixidor, F.; Kivekäs, R.; Sillanpää, R. *Organometallics* **1996**, *15*, 3850. **Cationic alcohol complexes: (b)** Agbossou, S. K.; Smith, W. W.; Gladysz, J. A. *Chem. Ber.*, **1990**, *123*, 1293. **(c)** Song, J.-S.; Szalda, D. J.; Bullock, R. M.; Lawrie, C. J. C.; Rodkin, M. A., Norton, J. R. *Angew. Chem., Int. Ed. Engl.*, **1992**, *31*, 1233. **(d)** Milke, J.; Missling, C.; Sünkel, K.; Beck, W. *J. Organomet. Chem.*, **1993**, *445*, 219. **(e)** Song, J.-S.; Szalda, D. J.; Bullock, R. M. *Organometallics*, **2001**, *20*, 3337. **(f)** Dell'Amico, D. B.;

Calderazzo, F.; Grazzini, A.; Labella, L.; Marchetti, F. *Inorg. Chim. Acta,* **2002**, *334*, 411.

33. Chae, S. Y.; Zhengjie He, I. A. G. *Organomettallics*, **2001**, *20*, 3641.

34. Abbenhuis, R. A. T. M.; del Rio, I.; Bergshoef, M. M.; Boersma, J.; Veldman, N.; Speck, A. L.; van Koten, G. *Inorg. Chem.*, **1998**, *37*, 1749.

35. Albores, P.; Chaia, Z. D.; Baraldo, L.; Castellano, E. E.; Piro, O. E. *Acta. Crystallogr., Sect. C. (Cr. Str. Commun.)*, **2002**, *58*, m235.

36. Yoshida, T.; Adachi, T.; Ueda, T.; Akao, H.; Tanaka, T.; Goto, T. *Inorg. Chim. Acta.*, **1995**, *231*, 95.

37. **(a)** Boniface, S. M.; Clark, G. R.; Collins, T. J.; Roper, W. R. *J. Organomet. Chem.* **1981**, *206*, 109. **(b)** Sun, Y.; Taylor, N. J.; Carty, A. J. *Inorg. Chem.* **1993**, 32, 4457.

38. Dinelli, L. R.; Batista, A. A.; Wohnrath, K.; Araujo, M. P.; Quieroz, S. L.; Bonfadini, M. R.; Oliva, G.; Nascimento, O.R.; Cyr, P. W.; MacFarlane, K. S.; James, B. R. *Inorg. Chem.*, **1999**, *38*, 5341.

39. **look in papers at home hopefully**

40. Mahon, M. F.; Whittlesey, M. K.; Wood, P. T. *Organometallics*, **1999**, *18*, 4068.

41. **look in papers at home hopefully**

42. **(a)** Eisen, M. S.; Haskel, A.; Chen, H.; Olmstead, M. H.; Smith, D. P.; Maestre, M. F.; Fish, R. H. *Organometallics,* **1995**, *14*, 2806. **(b)** Stebler-Rothlisberger, M.; Hummel, W.; Pittet, P.-A.; Burgi, H.-B.; Ludi, A.; Merbach, A. E. *Inorg. Chem.*, **1988**, *27*, 1358. **(c)** Kolle, U.; Flunkert, G.; Gorissen, R.; Schmidt, M. U.; Englert, U. *Angew. Chem., Int. Ed. Engl.*, **1992**, *31*, 440. **(d)** Ganja, E. A.; Rauchfuss, T. B.; Stern, C. L. *Organometallics*, **1991**, *10*, 270.

43. Kolle, U. *Coord. Chem. Rev.*, **1994**, *135/136*, 623.

44. **(a)** Cole-Hamilton, D. J.; Wilkinson, G. *Nouv. J. Chim.*, **1977**, *1*, 141. **(b)** Bruno, J. W.; Huffmann, J. C.; Caulton, K. G. *Inorg. Chim. Acta.*, **1984**, *89*, 167. **(c)** Van Der Sluys, L. S.; Kubas, G. J.; Caulton, K. G. *Organometallics,* **1991**, *10*, 1033. **(d)** Chen, Y.-Z.; Chan, W. C.; Lau, C. P.; Chu, H. S.; Lee, H. L.; Jia, G. *Organometallics,* **1997**, *16*, 1241.

45. The IR bands of **(47)** are moved to lower frequency than those in the related complex *trans,cis,cis*-$Ru(PMe_3)_2(CO)_2H_2$ containing strongly electron-donating trimethylphosphine ligands. Mawby, R. J.; Perutz, R. N.; Whittlesey, M. K. *Organometallics,* **1995**, *14*, 3268.

46. Van Der Sluys, L. S.; Kubas, G. J.; Caulton, K. G. *Organometallics*, **1991**, *10*, 1033.

47. **(a)** Shubina, E. S.; Belkova, N. V.; Krylov, A. N.; Vorontsov, E. V.; Epstein, L. M.; Gusev, D. G.; Niedermann, M.; Berke, H. *J. Am. Chem. Soc.*, **1996**, *118*, 1105. **(b)** Guari, Y.; Ayllon, J. A.; Sabo-Etienne, S.; Chaudret, B. *Inorg. Chem.*, **1998**, *37*, 640. **(c)** Messmer, A.; Jacobsen, H.; Berke, H. *Chem. Eur. J.*, **1999**, *5*, 3341.

48. Rossi, A. R.; Hoffmann, R. *Inorg. Chem.*, **1975**, *14*, 365.

49. **Reaction of M-OR with CO can lead to a range of products depending on the other ancillary ligands on the metal. CO insertion into M-OR:** **(a)** Bennett, M. A.; Robertson, G. B.; Whimp, P. O.; Yoshida, T. A. *J. Am. Chem. Soc.*, **1973**, *95*, 3028. **(b)** Bennett, M. A.; Yoshida, T. A. *J. Am. Chem. Soc.*, **1978**, *100*, 1750. (c) Michelin, R. A.; Napoli, M.; Ros, R. *J. Organomet. Chem.*, **1979**, *175*, 239. **(d)** Bryndza, H. E.; Kretchmar, S. A.; Tulip, T. H. *J. Chem. Soc., Chem. Commun.*, **1985**, 977. **(e)** Bryndza, H. E. *Organometallics*, **1985**, *4*, 1686. **(f)** Kim, Y.-J.; Osakabd, K.; Sugita, K.; Yamamoto, T.; Yamamoto, A. *Organometallics*, **1988**, *7*, 2182. **Insertion of CO into M-C rather than M-OR:** Hartwig, J. F.; Bergman, R. G.; Andersen, R. A. *J. Am. Chem. Soc.*, **1991**, *113*, 6499. **CO-induced reductive elimination:** Glueck, D. S.; Newman Winslow, L. J.; Bergman, R. G. *Organometallics*, **1991**, *10*, 1462.

50. Holland, P. L.; Andersen, R. A.; Bergman, R. G. *J. Am. Chem. Soc.*, **1996**, *118*, 1092.

51. **(a)** Heyn, R. H.; Macgregor, S. A.; Nadasdi, T. T.; Ogasawara, M.; Eisenstein, O.; Caulton, K. G. *Inorg. Chim. Acta* **1997**, *259*, 5. **(b)** Cooper, A. C.; Bollinger, J. C.; Huffman, J. C.; Caulton, K. G. *New J. Chem.* **1998**, *22*, 473.

52. Edwards, A. J.; Elipe, S.; Esteruelas, M. A.; Lahoz, F. J.; Oro, L. A.; Velero, C. *Organometallics*, **1997**, *16*, 3828.

53. **(a)** Burn, M. J.; Fickes, M. G.; Hartwig, J. F.; Hollander, F. J.; Bergman, R. G. *J. Am. Chem. Soc.*, **1993**, *115*, 5875. **(b)** Kaplan, A. W.; Bergman, R. G. *Organometallics*, **1997**, *16*, 1106.

54. **(a)** Stevens, R. C.; Bau, R.; Milstein, D.; Blum, O.; Koetzle, T. F. *J. Chem. Soc., Dalton Trans.*, **1990**, 1429. **(b)** Dorta, R.; Togni, A. *Organometallics*, **1998**, *17*, 3423. **(c)** Renkema, K. B.; Huffman, J. C.; Caulton, K. G. *Polyhedron*, **1999**, *18*, 2575. **(d)** Morales-Morales, D.; Lee, D. W.; Wang, Z.; Jensen, C. M. *Organometallics*, **2001**, *20*, 1144. **(e)** Dorta, R.; Rosenberg, H.; Shimon, L. J. W.;

Milstein, D. *J. Am. Chem. Soc.*, **2002**, *124*, 188. **(f)** Blum, O.; Milstein, D. *J. Am. Chem. Soc.*, **2002**, *124*, 11456.

55. Tani, K.; Iseki, A.; Yamagata, T. *Angew. Chem., Int. Ed.*, **1998**, *37*, 3381.

56. Hartwig, J. F.; Bergman, R. G.; Andersen, R. A. *J. Am. Chem. Soc.*, **1991**, *113*, 3404.

57. Milstein, D.; Calabrese, J. C.; Williams, I. D. *J. Am. Chem. Soc.*, **1986**, *108*, 6387.

58. **(a)** Crabtree, R. H.; Lavin, M.; Bonneviot, L. *J. Am. Chem. Soc.*, **1986**, *108*, 4032. **(b)** Jensen, C. M.; Trogler, W. C. *J. Am. Chem. Soc.*, **1986**, *108*, 723. **(c)** Leoni, P.; Sommovigo, M.; Pasquali, M.; Midollini, S.; Braga, D.; Sabatino, P. *Organometallics*, **1991**, *10*, 1038. **(d)** Kubas, G. J.; Burns, C. J.; Khalsa, G. R. K.; Van Der Sluys, L. S.; Kiss, G.; Hoff, C. D. *Organometallics*, **1992**, *11*, 3390. **(e)** Milet, A.; Dedieu, A.; Kapteijn, G.; van Koten, G. *Inorg. Chem.*, **1997**, *36*, 3223.

59. **(a)** Denk, M. K.; Rodezno, J. M. *J. Organomet. Chem.* **2000**, *608*, 122. (b) Denk, M. K.; Rodezno, J. M. *J. Organomet. Chem.* **2001**, *617-618*, 737.

60. Hossain, S. F.; Nicholas, K. M.; Teas, C. L.; Davis, R. E. *J. Chem. Soc., Chem. Commun.* **1981**, 268.

61. Nakamoto, K. *Infrared and Raman Spectra of Inorganic and Coordination Compounds*, 3rd ed.; Wiley: New York, 1978

62. **(a)** Ashworth, T. V.; Singleton, E. *J. Chem. Soc., Chem. Commun.* **1976**, 204. **(b)** Yoshida, T.; Thorn, D. L.; Okano, T.; Ibers, J. A.; Otsuka, S. *J. Am. Chem. Soc.* **1979**, *101*, 4212.

63. Dobson, A.; Moore, D. S.; Robinson, S. D.; Hursthouse, M. B.; New, L. *Polyhedron* **1985**, *4*, 1119.

64. Rotem, M.; Stein, Z.; Shvo, Y. *J. Organomet. Chem.* **1990**, *387*, 95.

65. **(a)** Field, L. D.; Lawrenz, E. T.; Shaw, W. J.; Turner, P. *Inorg. Chem.*, **2000**,*39*, 5632. **(b)** Whittlesey, M. K.; Perutz, R. N.; Moore, M. H. *Organometallics*, **1996**, *15*, 5166.

66. Sakaki, S.; Ohkubo, K. *Inorg. Chem.*, **1989**, *28*, 2583.

67. Dell'Amico, D. B.; Claderazzo, F.; Labella, L.; Marchetti, F. *J. Organomet. Chem.* **2000**, *596*, 144.

68. McLoughlin, M. A.; Keder, N. L.; Harrison, W. T. A.; Flesher, R. J.; Mayer, H. A.; Kaska, W. C. *Inorg. Chem.*, **1999**, *38*, 3223.

69. **(a)** Li, H. -C.; Nolan, S. P.; Peterson, J. L. *Organometallics*, **1998**, *17*, 3516. **(b)** Amarasekera, J.; Rauchfuss, T. B. *Inorg. Chem.* **1989**, *28*, 3875.

70. Conroy-Lewis, F. M.; Simpson, S. J. *J. Chem. Soc., Chem. Commun.*, **1991**, 388.

71. Park, H.; Minick, D.; Draganjac, M.; Cordes, A. W.; Hallford, R. L.; Eggleton, G. *Inorg. Chim. Acta.*, **1993**, *204*, 195.

72. Field, L. D.; Hambley, T. W.; Yau, B. C. K. *Inorg. Chem.*, **1994**, *33*, 2009.

73. Jessop, P. G.; Rettig, S. J.; Lee, C.-L.; James, B. R. *Inorg. Chem.*, **1991**, 30, *4617.*

74. Mashima, K.; Kaneyoshi, H.; Kaneko, S. -I.; Mikami, A.; Tani, K.; Nakamura, A. *Organometallics*, **1997**, *16*, 1016.

75. **(a)** Mura, P.; Olby, B. G.; Robinson, S. D. *J. Chem. Soc., Dalton Trans.* **1985**, 2101. **(b)** Mura, P.; Olby, B. G.; Robinson, S. D. *Inorg. Chim. Acta*, **1985**, *98*, L21. **(c)** Jessop, P. G.; Rettig, S. J.; Lee, C.-L.; James, B. R. *Inorg. Chem.* **1991**, *30*, 4617. **(d)** Field, L. D.; Hambley, T. W.; Yau, B. C. K. *Inorg. Chem.* **1994**, *33*, 2009. **(e)** Coto, A.; de los Ríos, I.; Jiménez Tenorio, M.; Puerta, M. C.; Valerga, P. *J. Chem. Soc., Dalton Trans.* **1999**, 4309.

76. **(a)** Treichel, P. M.; Rosenhein, L. D. *Inorg. Chem.* **1981**, *20*, 942. **(b)** Urban G.; Sunkel, K.; Beck, W. *J. Organomet. Chem.* **1985**, *290*, 329. **(c)** Treichel, P. M.; Schmidt, M. S.; Crane, R. A. *Inorg. Chem.* **1991**, *30*, 379. **(d)** Deeming, A. J.; Doherty, S.; Marshall, J. E.; Powell, J. L.; Senior, A. M. *J. Chem. Soc., Dalton Trans.* **1993**, 1093.

77. Jessop, P. G.; Rettig, S. J.; Lee, C.-L.; James, B. R. *Inorg. Chem.* **1991**, *30*, 4617.

78. Chisholm, M. H.; Davidson, E. R.; Huffman, C.; Quinlan, K. B. *J. Am. Chem. Soc.*, **2001**, *123*, 9652.

79. Burn, M. J.; Fickes, M. G.; Hollander, F. J.; Bergman, R. G. *Organometallics*, **1995**, *14*, 137.

80. Mudalige, D. C.; Ma, E. S.; Rettig, S. J. R.; James, B. R.; Cullen, W. R. *Inorg. Chem.*, **1997**, *36*, 5426.

81. **(a)** Sellmann, D.; Lechner, P.; Knoch, F.; Moll, M. *Angew. Chem., Int. Ed. Engl.*, **1991**, *30*, 552. **(b)** Sellmann, D.; Lechner, P.; Knoch, F.; Moll, M. *J. Am. Chem. Soc.*, **1992**, *114*, 922.

82. **(a)** Jessop, P. G.; Lee, C.-L.; Rastar, G.; James. B. R.; Lock, C. J. L.; Faggiani, R. *Inorg. Chem.*, **1992**, **31**, 4601. **(b)** Osakada, K.; Yamamoto, T.; Yamamoto, A. *Inorg. Chim. Acta.*, **1985**, *105*, L9.

83. Osakada, K.; Yamamoto, A.; Takenaka, A.; Sasada, Y. *Inorg. Chim. Acta.*, **1985**, *105*, L9.

84. Jessop, P. G.; Morris, R. H. *Inorg. Chem.* **1993**, *32*, 2236.

85. Coto, A.; Tenorio, J.; Puerta, C.; Valerga, P. *Organometallics*, **1998**, *17*, 4392.

86. Shaver, A.; Plouffe, P.-Y. *Inorg. Chem.*, **1994**, *33*, 4327.

87. Collings, J. C.; Roscoe, K. P.; Robins, E. G.; Batsanov, A. S.; Stimson, L. M.; Howard, J. A. K.; Clark, S. J. Marder, T. B. *New. J. Chem.*, **2002**, 26, 1740.

88. Collings, J. C.; Batsanov, A. S.; Howard, J. A. K. Marder, T. B. *Cryst. Eng.*, **2002**, *5*, 37.

89. Rickard, C. E. F.; Roper, W. R.; Williamson, A.; Wright, L. J. *Organometallics*, **2000**, *19*, 4344.

90. Shimada, M.; Harada, A.; Takahashi, S. *J. Chem. Soc., Chem. Comm.*, **1991**, 263.

91. **(a)** Hiraki, K.; Kinoshita, Y.; Kinoshita-Kawashima, J.; Kawano, H. *J. Chem. Soc., Dalton Trans.* **1996**, 291. **(b)** Hiraki, K.; Kinoshita, Y.; Ushiroda, H.; Koyama, S.; Kawano, H. *Chem. Lett.* **1997**, 1243

92. **(a)** Carney, M. J.; Walsh, P. J.; Hollander, F. J.; Bergman, R. G. *J. Am. Chem. Soc.* **1989**, *111*, 8751. **(b)** Carney, M. J.; Walsh, P. J.; Hollander, F. J.; Bergman, R. G. *Organometallics* **1992**, *11*, 761

93. Vart, J. C. J.; Bassi, I. W.; Calcaterra, M.; Pieroni, M. *Inorg. Chim. Acta* **1978**, *28*, 201.

94. Eberhardt, J. K.; Fröhlich, R.; Venne-Dunker, S.; Würthwein, E.-U. *Eur. J. Inorg. Chem.* **2000**, 1739.

95. Kim, J. H.; Britten, J.; Jik, C. *J. Am. Chem. Soc.*, **1993**, *115*, 3618.

96. Yeh, W. -Y.; Peng, S. M.; Liu, L.-K. *Inorg. Chem.*, **1993**, *32*, 2965.

97. Tramsek, M.; Lork, E.; Mews, R.; Zemva, B. *J. Fluorine. Chem.*, **2001**, *110*, 123.

98. den Reijer, C. J.; Worle, M.; Pregosin, P. S. *Organometallics*, **2000**, *19*, 309.

99. Mazej, Z.; Borrmann, K. L.; Zemva, B. *Inorg. Chem.*, **1998**, *37*, 5912.

100. Lee, D.-H.; Kwon, H. J.; Patel, B. P.; Liable-Sands, L. M.; Rheingold, A. L.; Crabtree, R. H. *Organometallics*, **1999**, *18*, 1615.

101. **(a)** Barthazy, P.; Hintermann, L.; Stoop, R. M.; Worle, M.; Mezzetti, A.; Togni, A. Helv. Chim. Acta. 1999, 82, 2448. **(b)** Barthazy, P.; Stoop, R. M.; Worle, M.; Togni, A.; Mezzetti, A. *Organometallics*, **2000**; *19*, 2844.

102. Jasim, N. A.; Perutz, R. N. *J. Am. Chem. Soc.*, **2000**, *122*, 8685.

103. **(a)** Cavalli, L. *J. Chem. Soc. Sect. B: Phys. Org.* **1967**, 384. **(b)** James, J. H.; Peach, M. E.; Williams, C. R. *J. Fluorine. Chem.*, **1985**, 27, 91.

104. Kirkham, M. S.; Mahon, M. F.; Whittlesey, M. K. *Chem. Commun.*, **2001**, 813.

105. Coleman, K. S.; Fawcett, J.; Holloway, J. H.; Hope, E. G.; Russell, D. R. *J. Chem. Soc., Dalton Trans.* **1997**, 3557.

106. Hughes, R. P.; Kovacik, I.; Lindner, D. C.; Smith, J. M.; Willemsen, S.; Zhang, D.; Guzei, I. A.; Rheingold, A. L. *Organometallics*, **2001**, *20*, 3190.

107. Geoffroy, G. L.; Hammond, G. S.; Gray, H. B. *J. Am. Chem. Soc.*, **1975**, *97*, 3933.

108. Darensbourg, M. Y.; Liaw, W. F.; Reibenspies, J. *Inorg. Chem.*, **1988**, *27*, 2555.

109. Newman, L. J.; Bergman, R. G. *J. Am. Chem. Soc.*, **1985**, *107*, 5314.

110. Brewer, S. A.; Coleman, K. S.; Fawcett, J.; Holloway, J. H.; Hope, E. G.; Russell, D. R.; Watson, P. G. *J. Chem. Soc., Dalton Trans.* **1995**, 1073.

111. Krassowski, D. W.; Nelson, J. H.; Brower, K. R.; Hauenstein, D.; Jacobson, R. A. *Inorg. Chem.*, **1988**, *27*, 4294.

112. Fausto R.; Eugene H. C.; Samuel D. *J. Am. Chem. Soc.*, **1959**, *81*, 4338.

113. **(a)** Hitchcock, P. B.; Lappert, M. F.; Pye, P. L. *J. Chem. Soc., Chem. Commun.* **1976**, 644. **(b)** Hitchcock, P. B.; Lappert, M. F.; Pye, P. L. *J. Chem. Soc., Dalton Trans.* **1978**, 826. **(c)** Weskamp, T.; Schattenmann, W. C.; Spiegler, M.; Herrmann, W. A. *Angew. Chem., Int. Ed.* **1998**, *37*, 2490. **(d)** Chaumonnot, A.; Donnadieu, B.; Sabo-Etienne, S.; Chaudret, B.; Buron, C.; Bertrand, G.; Metivier, P. *Organometallics* **2001**, *20*, 5614. **(e)** Grundemann, S.; Albrecht, M.; Kovacevic, A.; Faller, J. W.; Crabtree, R. H. *J. Chem. Soc., Dalton Trans.* **2002**, 2163.

114. **(a)** Arduengo, A. J., III; Dias, H. V. R.; Calabrese, J. C.; Davidson, F. *Organometallics* **1993**, *12*, 3405. **(b)** Arduengo, A. J., III; Gamper, S. F.; Calabrese, J. C.; Davidson, F. *J. Am. Chem. Soc.* **1994**, *116*, 4391.

115. $La(HF)_2(AsF_6)_3$

116. Tramsek, M. ; Lork, E. ; Mews, R. ; Zemva, B. *J. Fluorine. Chem.* **2001**, *110*, 123.

117. Clot, E.; Eisentstein, O.; Crabtree, R. H. *New J. Chem.* **2001**, *25*, 66.

118. Patel, B. P.; Crabtree, R. H. *J. Am. Chem. Soc.* **1996**, *118*, 13105.

Chapter 7

Experimental

7.1. General methods.

All manipulations were carried out under an argon atmosphere using standard Schlenk and high vacuum techniques or in an air and moisture free glovebox.

NMR solvents were purchased from Goss Scientific Ltd and were dried, degassed and stored under argon; d_6-benzene, d_8-toluene and d_8-tetrahydrofuran were vacuum transferred from purple solutions of potassium benzophenone ketyl; d_2-dichloromethane, d-chloroform, d_3-acetonitrile and d_6-dmso were vacuum transferred from CaH_2.

All solvents (unless otherwise stated) were distilled from purple solutions of sodium benzophenone ketyl (hexane, diethyl ether, toluene, benzene, tetrahydrofuran), Mg/I_2 (methanol, ethanol) or CaH_2 (triethylamine) and stored under argon. The ketone substrates were purchased from Aldrich; 2'-methylacetophenone and 4'-fluoroacetophenone were dried over 4 Å molecular sieves, vacuum transferred and stored under argon. 4-methoxy-acetophenone, acetophenone and benzophenone were stored in a glove box and used without further purification. The alkene substrates were purchased from Aldrich; triethoxyvinylsilane and trimethylvinylsilane were dried over 4 Å molecular sieves, vacuum transferred and stored under argon. Triphenylvinylsilane was stored in a glove box and used without further purification. Hexafluorobenzene was purchased from Aldrich, dried over 4 Å molecular sieves, vacuum transferred and stored under argon. $Et_3N.3HF$ and paraformaldehyde were purchased from Aldrich, stored in glove box and used without further purification. Ethene (Aldrich, 99.9%), D_2 (Aldrich, 99.8%), ^{13}CO (Cambridge Isotopes, 99%), $^{13}CO_2$ (Cambridge Isotopes, 99%) were used as received.

Physical and analytical measurements.

NMR spectra were recorded on JEOL EX 270, Bruker Avance 300 MHz or Varian Mercury 400 MHz NMR spectrometers. The ^1H NMR spectra were referenced to the chemical shifts of residual protio solvent resonances (d_5-benzene δ 7.15, d_7-toluene δ 2.10, d_7-tetrahydrofuran δ 3.60). The ^{13}C NMR spectra were referenced to d_6-benzene (δ 128.0), d_8-toluene (δ 21.1) and d_8-thf (δ 20.4). The ^{31}P NMR chemical shifts were referenced externally to 85% H_3PO_4 (δ 0.0). The ^{19}F NMR spectra were referenced to external $CFCl_3$ (δ 0.00). IR spectra were recorded as nujol mulls on a Nicolet NEXUS FTIR spectrometer. IR kinetic measurements were performed on a Nicolet Protégé 460 FTIR spectrometer. Elemental analyses were performed at the University of Bath. Gas chromatography was

carried out on a Fisons 8000 GC spectrometer.

7.2. Preparation of ruthenium precursors.

7.2.1. Preparation of ruthenium complexes bearing phosphine ligands.

7.2.1.1. Preparation of $Ru(PPh_3)_3(CO)H_2$ (1)

$Ru(PPh_3)_3(CO)H_2$ was prepared from a modified method in the literature.[1] A 500 ml three necked round bottomed flask equipped with a magnetic stirring bar, argon inlet, outlet bubbler and a reflux condenser was flame dried under vacuum and flushed with argon and then charged with triphenylphosphine (6.28 g, 24 mmol) followed by ~280 ml of ethanol. Before the preparation of the reflux, three Schlenk tubes were dried under vacuum and flushed with argon three times. (1) was charged with hydrated ruthenium trichloride (1.04 g, 4 mmol) and ~40 ml of ethanol; (2) was charged with aqueous formaldehyde (40 ml, 40% w/v solution) which was degassed by argon bubbling; (3) was charged with a ~40 ml of ethanol and potassium hydroxide (1.20 g, 20 mmol). Solutions (1), (2), (3) were quickly added in that order to the boiling ethanol solution of triphenylphosphine. The solution was heated under reflux for 25 min and then cooled in an ice bath. The resultant grey precipitate was washed with 50 ml of absolute ethanol, 50 ml of deionised water and 50 ml of absolute ethanol and 50 ml of hexane. The resultant crude product was dried under vacuum. (Yield 2.45 g). The crude powder was dissolved in warm benzene (NB: room temperature dissolution in benzene was used with a little increase in the volume of benzene used), and the solution filtered to remove insoluble solids. The benzene solution was passed through a neutral alumina column (neutral activity I; eluent benzene, 10 cm length x 5 cm i.d.) and then diluted by addition of 200 ml of methanol and then concentrated. The concentrated liquid was then put in a freezer for 2 hr to enforce the precipitation of $Ru(PPh_3)_3(CO)H_2$, and then filtered. The solid was washed with dry hexane (2x10 ml) and dried in vacuum for 2 hr, yielding 1.20 g (33%) of a white microcrystalline powder. ^1H NMR (C_6D_6, 400 MHz, 293 K): δ -6.53 (m, 1H, Ru-H_a, $J_{Pd\text{-}Ha}$=15.3 Hz, $J_{Pc\text{-}Ha}$=30.5 Hz, $J_{Ha\text{-}Hb}$ = 6.1 Hz), -8.29 (m, 1H, Ru-H_b, $J_{Pd\text{-}Hb}$=74.5 Hz, $J_{Pc\text{-}Hb}$=28.1 Hz, $J_{Ha\text{-}Hb}$=6.1 Hz); $^{31}P\{^1H\}$ NMR: δ 58.2 (d, $^2J_{P\text{-}P}$= 16.8 Hz), 46.1 (t, $^2J_{P\text{-}P}$= 16.8 Hz). IR(cm^{-1}): 1960(s) ($\nu_{Ru\text{-}CO}$), 1898(m) ($\nu_{Ru\text{-}H}$).

7.2.1.2. Preparation of $Ru(PPh_3)_2(CO)_2H_2$ (2)

$Ru(PPh_3)_2(CO)_2H_2$ was prepared using a modified route.[2]

a) Preparation of the tetrafluoroborate para-methoxyphenyl diazonium salt: The diazonium salt was prepared by a modification reported route.[3] The choice was made to substitute absolute ethanol for water as the reaction solvent, due to the highly solubility of the salt in water. In a beaker equipped with a magnetic stirring bar was added 30 ml of a 48% HBF_4 solution and 30 ml of absolute ethanol, then 12.31 g (0.1 mol) of *para*-anisidine was slowly added. The mixture was then cooled below 5°C by a salt/ice mixture. A solution of 6.90 g (0.1 mol) of $NaNO_2$ in 30 ml of absolute ethanol was slowly added so that the temperature did not exceed 278 K and stirring was continued for further 30 min until a white precipitate was completely formed. The salt was washed with 10 ml of cold ethanol, 20 ml of cold acetone and 10 ml of diethyl ether, and then placed in an ice-cooled Schlenk tube and carefully dried under partial vacuum. (CAUTION: EXPLOSIVE POWDER).

b) Preparation of the Arylazo derivative: A Schlenk tube equipped with a magnetic stirring bar was flame dried and charged with 1.00 g (1.41 mmol) of $Ru(PPh_3)_2(CO)_3$, 0.31 g (1.41 mmol) of diazonium salt and 20 ml of benzene. The mixture was then left stirring for 16 hr until an orange precipitate was formed. The solution was then removed via filter cannula and the solid material was washed with 3 x 5 cm^{-3} of benzene and 10 cm^{-3} of hexane, and then dried under vacuum. The compound was isolated as an orange powder (yield 1.08 g, 91%). IR (cm^{-1}): 2039 - 1970 ($\nu_{Ru\text{-}CO}$) (s).

c) Synthesis of *cis*-$Ru(PPh_3)_2(CO)_2H_2$: A Schlenk equipped with a magnetic stirring bar was flame dried and charged with 1.08 g (1.28 mmol) of the arylazo derivative, 0.89 g of $NaBH_4$ and 30 ml of ethanol. The mixture was left stirring over a period of 3 hr until the orange precipitate turned to a white creamy precipitate. The product was filtered off and washed with 3 x 5 ml of ethanol and 10 ml of n-hexane and then dried under vacuum. 0.61 g (70%) of an off-white powder was isolated. ^1H NMR (C_6D_6, 400 MHz, 293 K): δ -4.30 (t, 2H, Ru–H, $J_{P\text{-}H}$=23.5 Hz); IR(cm^{-1}): 2015(s) - 1970(s) ($\nu_{Ru\text{-}CO}$), 1870(m) - 1820(m) ($\nu_{Ru\text{-}H}$).

7.2.1.3. Preparation of $Ru(PPh_3)_3(CO)_2$ (3)

$Ru(PPh_3)_3(CO)_2$ was prepared by a modified route.[4] A Schlenk equipped with a magnetic stirring bar was flame dried and charged with 0.61 g (0.90 mmol) *cis*-$Ru(PPh_3)_2(CO)_2H_2$ and 7 equivalents (1.65 g) of triphenylphosphine in 30 ml of methanol. The mixture was heated and stirred at 363 K for 9 hr until the white creamy mixture turned to an orange suspension. The product was filtered off and washed with 3 x 5 ml of ethanol and 10 ml of n-hexane and dried under vacuum. 0.69 g (82%) of a creamy white powder was isolated. $^{31}P\{^1H\}$ NMR (C_6D_6, 400 MHz, 293 K): δ 51.0 (s). IR (cm^{-1}): 1895 (s) ($\nu_{Ru\text{-}CO}$).

7.2.1.4. Preparation of $Ru(PPh_3)_2(CO)_3$ (4)

$Ru(PPh_3)_2(CO)_3$ was prepared using a modified method in the literature.[5] A 500 ml three necked round bottomed flask equipped with a magnetic stirring bar, argon inlet, outlet bubbler and a reflux condenser was flame dried under vacuum and flushed with argon and then charged with triphenylphosphine (4.74 g, 18 mmol) followed by ~180 ml of 2-methoxyethanol. Before the preparation of the reflux, three Schlenk tubes were dried under vacuum and flushed with argon three times. (1) was charged with hydrated ruthenium trichloride (0.78 g, 3 mmol) and ~60 ml of cooled 2-methoxyethanol; (2) was charged with hot aqueous formaldehyde (60 ml, 40% w/v solution), which was degassed by argon bubbling; (3) was charged with a ~60 ml of hot 2-methoxyethanol and potassium hydroxide (1.20 g, 20 mmol). The contents of (1), (2) and (3) were rapidly added sequentially to the boiling ethanol solution of triphenylphosphine. The solution was heated under reflux for 2h and then cooled to room temperature. The resultant yellow microcrystalline precipitate was then washed with 100 ml of dried ethanol, 100 ml of degassed deionised water and 100 ml of dried ethanol and 100 ml of dried hexane. The resultant crude product was then dried under vacuum to afford 1.75 g (82%) of a yellow microcrystalline powder. $^{31}P\{^1H\}$ NMR (C_6D_6, 400 MHz, 293 K): δ 56.6 (s). IR (cm^{-1}): 1900 ($\nu_{Ru\text{-}CO}$).

7.2.1.5. Preparation of $Ru(PPh_3)_3Cl_2$ (5)

$Ru(PPh_3)_3Cl_2$ was prepared according to literature.[6] Typically a 500 ml, three necked, round bottom flask equipped with a magnetic stirring bar, an argon inlet, an outlet bubbler, and a reflux condenser was flame dried under vacuum and flushed with argon, and was charged with $RuCl_3$ (1.00 g, 3.80 mmol) followed by ~250 ml of methanol, and the solution refluxed under nitrogen for 5 mins. After cooling, triphenylphosphine was added

(6.00 g, 22.90 mmol) is added, and the solution is then refluxed under nitrogen for 3 hr. The complex precipitates from the hot solution as shiny black crystals. After the solution was left aside to cool down to room temperature, the isolated precipitate was washed 3 times with degassed ether, and then dried under vacuum. To give 2.54 g (70%) of product. The complex was used without any further purification or characterization.

7.2.1.6. Preparation of $Ru(PPh_3)_3(H)_2(H_2)$ (6)

$Ru(PPh_3)_3(H)_2(H_2)$ was prepared by a reported route.[7] A Schlenk tube equipped with a magnetic stirring bar was flame dried and charged with a solution of 0.76 g (0.85 mmol) of $Ru(PPh_3)_3Cl_2$ dissolved in 120 ml of a 4:3 mixture of H_2-saturated ethanol/benzene. Under a gentle stream of H_2, 0.14 g (3.75 mmol) of $NaBH_4$ dissolved in 10 ml of H_2-saturated ethanol was added dropwise to the ethanol/benzene solution. The red mixture rapidly changed to pink over the next 20 min. The mixture was stirred further to give a thick white precipitate over the next 2 hr. The filtrate was isolated by filtration with a filter cannula, washed with 3 x 5 ml of H_2-saturated ethanol and 10 ml of H_2-saturated n-hexane and then dried under vacuum to give a white powder. Yield 0.48 g, 63 %. ^1H NMR (C_6D_6, 400 MHz, 293 K): δ -6.96 (br s, 4H), 6.95-7.52 (m, 45H), $^{31}P\{^1H\}$ NMR: δ 58.5 (s). IR (cm^{-1}): 1946 (s) ($\nu_{Ru\text{-}CO}$).

7.2.1.7. Preparation of $Ru(PPh_3)_2(CO)[\eta^4\text{-}(CH_2{=}CH)Si(CH_3)_2]$ (7)

$Ru(PPh_3)_2(CO)[\eta^4\text{-}(CH_2{=}CH)Si(CH_3)_2]$ was prepared using a modified route.[8] A Schlenk tube equipped with a magnetic stirring bar was flame dried under vacuum and then charged with 0.50 g (0.55 mmol) of **(1)**, toluene (1 ml) and 118 µl (0.56 mmol) of triethoxyvinylsilane. The sealed Schlenk tube was heated at 120°C for 5~6 min. A quantitative yield of triethoxyethylsilane was formed. The Schlenk tube was then removed from the heating bath and cooled to room temperature. Dimethyldivinylsilane (125 µl, 0.53 mmol) was then injected into the solution, and the system put back into the heating bath for a further 10 min until solid material precipitated. The mixture was cooled to 10°C to enforce the precipitation of the solid material and 10ml of diethyl ether were added. The liquid phase was then removed via filter cannula and the resulting powder was washed three times with 10 ml of Et_2O. The solid was then dried under vacuum for 5h to give 0.34g (81%) of a light yellowish powder. The powder was dissolved in refluxing toluene (2-3 ml) and cooled to room temperature in an ice bath. Over the next 10 hr, transparent orange

crystals were formed. ^{1}H NMR (C_6D_6, 400 MHz, 293 K): δ 0.11 (s, 3H, CH_3), 0.94 (s, 3H, CH_3), 0.70 (br s, 1H); $^{31}P\{^{1}H\}$ NMR: δ 52.1 (s), IR (cm^{-1}): 1884 ($\nu_{Ru\text{-}CO}$). (NB: NMR: due to the high fluxionality of the vinyl protons, some of the resulting peaks were too broad to be seen.)

7.2.1.8. Preparation of $Ru(PPh_3)(dppp)(CO)H_2$ (8)

$Ru(PPh_3)(dppp)(CO)H_2$ was prepared using a modified route.[9] A Schlenk tube equipped with a magnetic stirring bar was flame dried and charged with 0.75 g (0.82 mmol) **(1)** and 0.36 g (0.87 mmol) dppp in 25 ml of toluene. The mixture was then refluxed for 1hr giving a dark brown solution. The toluene was removed under vacuum to leave a brown oil, which was when was diluted with 25 ml of methanol and stirred for 3h until a white precipitate was formed. The solution was then filtered via filter cannula and the resultant crude powder washed 3 times (10 ml of methanol and 10 ml of hexane) and then dried under vacuum. Yield 0.51g (77%). ^{1}H NMR (C_6D_6, 400 MHz, 293 K): δ -6.98 (m, 1H, Ru-H), -6.50 (m, 1H, Ru-H). $^{31}P\{^{1}H\}$ NMR: δ 59.9 (dd, $^{2}J_{P1\text{-}P3}$=228.1 Hz, $^{2}J_{P1\text{-}P2}$=23.4 Hz), 38.7 (dd, $^{2}J_{P3\text{-}P1}$=228.1 Hz, $J_{P3\text{-}P2}$=23.5 Hz), 29.25 (t, $^{2}J_{P1\text{-}P2}$=23.5 Hz). IR (cm^{-1}): 1932 ($\nu_{Ru\text{-}CO}$) (s), 1901 - 1832 ($\nu_{Ru\text{-}H}$) (m).

7.2.2. Preparation of ruthenium complexes bearing arsine ligands

7.2.2.1. Preparation of $Ru(AsPh_3)_3(CO)Cl_2$

$Ru(AsPh_3)_3(CO)Cl_2$ was prepared using a reported route from the literature.[10] The reaction was typically scaled up by a factor of 4 with no major changes made to the reported method. Typically, a 500 ml three necked round bottomed flask equipped with a magnetic stirring bar, argon inlet, outlet bubbler and a reflux condenser was flame dried under vacuum and flushed with argon and then charged with triphenylarsine (7.40 g, 24.2 mmol) followed by ~200 ml of 2-methoxyphenol. Before the preparation of the reflux, two Schlenk tubes were dried under vacuum and flushed with argon three times. (1) was charged with hydrated ruthenium trichloride (1.18 g, 4.52 mmol) and ~60 ml of 2-methoxyphenol; (2) was charged with aqueous formaldehyde (88 ml, 40% w/v solution) which was degassed by argon bubbling. (1) and (2) were quickly added in that order to the boiling ethanol solution of triphenylarsine. The mixture was heated under reflux for 2 hr during which the solution became pale orange. After cooling the solution was reduced in

volume to 80 ml before addition of 80 ml of cold methanol. The yellow precipitate which was formed was separated and washed with cold ethanol (2 x 50ml) and hexane (50ml). The resultant pure product was then dried under vacuum to give 4.10 g (81%) of a yellow microcrystalline powder. IR (cm^{-1}): 1949 ($\nu_{Ru\text{-}CO}$)

7.2.2.2. Preparation of $Ru(AsPh_3)_3(CO)H_2$ (9)

$Ru(AsPh_3)_3(CO)H_2$ was prepared using a modified route.[10] The reaction was scaled up (4x) with no major changes made to the reported route. Typically a 500 ml three necked round bottomed flask equipped with a magnetic stirring bar, argon inlet, outlet bubbler and a reflux condenser was flame dried under vacuum and flushed with argon. It was then charged with ethanol (200 ml), $Ru(AsPh_3)_3(CO)Cl_2$ (2.10 g, 1.77 mmol) and sodium borohydride (4.00 g, 105.57 mmol). The mixture was then brought to boiling and allowed to stir and reflux for 1.5 hr. After cooling, the tan slurry was washed 3 times with 100 ml of ethanol. The residue left was then pumped to dryness under vacuo and 100 ml of toluene was added to the residue for extraction. The mixture was then stirred for 30 min at 60°C and the solution was filtered through a filter cannula. Removal of the solvent under vacuo afforded a brown residue. To this residue was added 100 ml of ethanol and the mixture stirred for 10 min, during which time a white powder precipitated out. The powder was washed twice with 100 ml of ethanol, followed by 100 ml of hexane. The final product was then dried under vacuo to give 1.76 g (89 %) of a white powder. ^1H NMR (C_6D_6, 300 MHz, 293 K): δ -9.44 (d, 1H, J_{HH}=6.6 Hz), -9.92 (d, 1H, J_{HH}=6.6 Hz). IR (cm^{-1}): 1930 ($\nu_{Ru\text{-}CO}$), 1900 ($\nu_{Ru\text{-}H}$).

7.2.2.3. Preparation of $Ru(AsPh_3)(dppp)(CO)H_2$ (10)

$Ru(AsPh_3)(dppp)(CO)H_2$ was prepared using modified route.[11] A Schlenk tube equipped with a magnetic stirring bar was flame dried and charged with 0.750g (0.82 mmol) of **(9)**, 0.404 g (0.98 mmol, 1.2 eq) dppp in 25ml of toluene. The mixture was then refluxed 2 hr giving a dark brown solution. Toluene was removed under vacuum, leaving a brown oil, when was diluted with 25 ml of methanol were added to the oil and the mixture was stirred for 3h until a white precipitate was formed. The solution was removed via filter cannula and the resultant crude powder was washed with 3 times (10 ml of methanol, and 10 ml of hexane), and then dried under vacuum to afford 0.55g (79 %) of **(10)**. IR (cm^{-1}): 1934 ($\nu_{Ru\text{-}CO}$).

7.2.2.4. Preparation of $Ru(AsPh_3)(arphos)(CO)H_2$ (11)

$Ru(AsPh_3)(arphos)(CO)H_2$ (arphos = $Ph_2AsCH_2CH_2PPh_2$) was prepared using a modified route.[11] A Schlenk tube equipped with a magnetic stirring bar was flame dried and charged with 0.50 g (0.82 mmol) of **(9)** and 0.39 g (0.98 mmol, 1.2 equivalents) arphos in 25 ml of toluene. The mixture was then refluxed for 2 hr giving a dark brown solution. Toluene was removed under vacuum leaving a brown oil. 25 ml of methanol were added and the mixture was stirred for 3h until a white precipitate was formed. The solution was then filtered via filter cannula and the remaining crude powder washed 3 times with 10 ml of methanol and 10 ml of hexane. It was then dried under vacuum to afford 0.25 g (60.5 %) of **(11)**. ^1H NMR (C_6D_6, 400 MHz, 293 K): δ = -6.8 (dd, 1H, J_{HH} = 14.2 Hz, J_{PH} = 28.5 Hz), -7.2. (dd, 1H, J_{HH} = 14.2 Hz, J_{PH} = 28.5 Hz) IR (cm^{-1}): 1931 ($\nu_{Ru\text{-}CO}$).

7.3. Preparation of ruthenium complexes with relevance to the Murai reaction.

7.3.1. Synthesised, isolated and fully characterised complexes.

7.3.1.1. $Ru(PPh_3)_3(CO)(C_2H_4)$ (12)

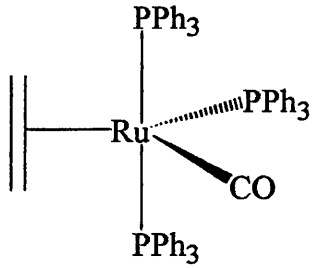

An ampoule fitted with a Teflon stopcock containing a solution of **(1)** (0.20 g, 0.22 mmol) in 2 ml toluene was freeze-pump-thaw degassed and placed under 1 atmosphere of ethene. The solution was heated at 120°C for 10 min, during which time the solution turned deep red. The mixture was cooled rapidly to room temperature and 20 ml ethene-saturated diethyl ether was added. After stirring for 15 min, a yellow precipitate formed. This was filtered off, washed with C_2H_4-saturated Et_2O (2 x 10 ml) and 10 ml hexane and pumped to dryness to leave a yellow powder in ca. 50% yield. Failure to use ethene-saturated solutions leads to depletion of product yields, typically to between 30-0%. Recrystallization from hot ethene-saturated toluene gave thin red plates suitable for X-ray crystallography. Analysis for $RuC_{57}H_{49}P_3O$ [found (calculated)]: C, 70.4 (72.52); H, 5.17 (5.23). Repeated analyses

consistently gave a low percentage of carbon. ^{1}H NMR (C_6D_6, 400 MHz, 293 K): δ 8.00–6.60 (br, 45H, PC_6H_5), 1.79 (br s, 4H, C_2H_4). ($C_6D_5CD_3$, 400 MHz, 203 K): δ 2.34 (br s, 2H, C_2H_4), 1.33 (br s, 2H, C_2H_4). $^{31}P\{^1H\}$ NMR (C_6D_6, 293 K): δ 48.4 (br s). ($C_6D_5CD_3$, 203 K): δ 45.6 (t, J_{PP} = 9.7 Hz), 49.3 (d, J_{PP} = 9.7 Hz). $^{13}C\{^1H\}$ (C_6D_6, 293 K): δ 214.1 (q, J_{PC} = 13.7 Hz, Ru-*C*O), 134.6 (br s), 128.7 (br s), 127.6 (br s), 29.8 (s, C_2H_4). ($C_6D_5CD_3$, 263 K): δ 213.4 (q, J_{PC} = 13.0 Hz, Ru-*C*O), δ 134.2 (br s), δ 129.3 (br s), δ 127.3 (br s), δ 29.4 (br s, C_2H_4), δ 25.7 (s, C_2H_4). ($C_6D_5CD_3$, 218 K): 213.3 (br t, J_{PC} = 20.1 Hz, Ru-*C*O), 30.0 (br s, C_2H_4), 28.6 (s, C_2H_4). IR (cm^{-1}): 1854 (ν_{CO}).

7.3.1.2. $Ru(PPh_3)_2(CO)(\eta^4\text{-}(CH_2{=}CH\text{-}CH{=}CH_2))$ (13)

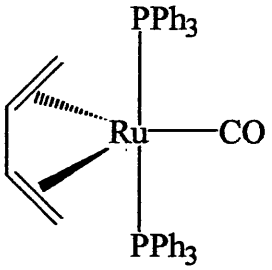

An ampoule fitted with a Teflon stopcock containing a solution of **(1)** (0.20 g, 0.22 mmol) in 2 ml toluene was freeze-pump-thaw degassed and placed under 1 atmosphere of ethene. The solution was heated at 120°C for 40 min, during which time the solution turned deep red. The solution was then cooled down to room temperature and the solvent was removed under vacuum, leaving a deep red residue. The residue was washed with 3 x 5 ml of hexane at -70°C (isopropanol/dry ice bath). The pure material was then dry under vacuum. Yield 0.18 g (85%). ^{1}H NMR (C_6D_6, 400 MHz, 293 K): δ 7.60–6.60 (br, 30H, PC_6H_5), 5.34 (br s, 1H, $CH_2{=}CH\text{-}CH{=}CH_2$), 5.00 (br s, 1H, $CH_2{=}CH\text{-}CH{=}CH_2$), 2.19 (br s, 1H, $CH_2{=}CH\text{-}CH{=}CH_2$), 1.22 (br s, 1H, $CH_2{=}CH\text{-}CH{=}CH_2$), -0.74 (br s, 2H, $CH_2{=}CH\text{-}CH{=}CH_2$). ($C_6D_5CD_3$, 400 MHz, 353 K): δ 5.11 (br s, 2H, $CH_2{=}CH\text{-}CH{=}CH_2$), 1.55 (br s, 2H, $CH_2{=}CH\text{-}CH{=}CH_2$), -0.75 (br t, 2H, $CH_2{=}CH\text{-}CH{=}CH_2$, $J_{P\text{-}H}$ = 7.2 Hz). ^{1}H NMR (C_6D_6, 400 MHz, 273 K): 5.42 (br s, 1H, $CH_2{=}CH\text{-}CH{=}CH_2$), 5.04 (br s, 1H, $CH_2{=}CH\text{-}CH{=}CH_2$), 2.25 (br m, 1H, $CH_2{=}CH\text{-}CH{=}CH_2$), 1.20 (br m, 1H, $CH_2{=}CH\text{-}CH{=}CH_2$), -0.74 (br q, 1H, $CH_2{=}CH\text{-}CH{=}CH_2$, J_{HP} = 6.0 Hz), -0.86 (br q, 1H, $CH_2{=}CH\text{-}CH{=}CH_2$, J_{HP} = 7.6 Hz). $^{31}P\{^1H\}$ NMR (C_6D_6, 293 K): δ 60.7 (br s), 47.8 (br s). $^{13}C\{^1H\}$ (C_6D_6, 293 K): δ 206.7 (pseudo t, J_{PC} = 10.4 Hz, Ru-*C*O), 139.0 (br s), 138.8 (br s), 137.1 (br s), 133.6 (br s), 128.5 (br s), 127.6 (br s), 89.3 (br s, $CH_2{=}CH\text{-}CH{=}CH_2$), 79.6 (br s, $CH_2{=}CH\text{-}CH{=}CH_2$), 44.4. (br s, $CH_2{=}CH\text{-}CH{=}CH_2$), 38.2 (br d, $CH_2{=}CH\text{-}CH{=}CH_2$, J_{PC} = 27.6 Hz), 37.9 (br s,

CH_2=CH-CH=CH_2). ($C_6D_5CD_3$, 253 K): δ 206.8 (br dd, J_{PC} = 13.5 Hz, J_{PC} = 6.0 Hz, Ru-*C*O), δ 88.8 (d, J_{PC} = 89.7 Hz, CH_2=CH-CH=CH_2), δ 79.6 (1:1:1 triplet, J_{PC} = 72.0 Hz, CH_2=CH-CH=CH_2), δ 44.8 (br m, CH_2=CH-CH=CH_2), δ 38.2 (s, CH_2=CH-CH=CH_2). IR (cm^{-1}): 1902 (ν_{CO}).

7.3.1.3. Ru(PPh_3)$_3$(*o*-$C_6H_4C(O)CH_3$)H (14)

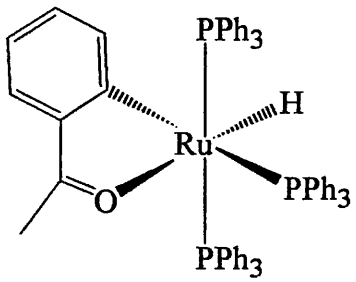

To a suspension of **(6)** (0.20 g, 0.22 mmol) in 5 ml thf was added an excess of acetophenone (366 μL, 3.1 mmol). The mixture was heated with stirring at 45°C for 12 hr. The solution was concentrated to yield an orange precipitate, which was filtered off, washed with hexane (3 x 10 ml) and dried *in vacuo*. Yield 0.18 g, 81%. Block shaped orange crystals were formed when thf solutions were left at room temperature for 2 weeks. Analysis for $RuC_{62}H_{52}P_3O.3.5$ thf [found (calculated)]: C, 72.8 (73.25); H, 5.78 (5.41). ^{1}H NMR (C_6D_6, 400 MHz, 293 K): δ 7.88-6.75 (m, 47H, PC_6H_5, C_6H_4), 6.30 (br t, J_{H-H} = 7.2 Hz), 6.45 (br t, J_{H-H} = 7.2 Hz), 1.36 (s, 3H, CH_3), -15.42 (dt, J_{PH} = 26.0 Hz, J_{PH} = 13.2 Hz, 1H, Ru-H). $^{31}P\{^1H\}$ NMR (C_6D_6, 293 K): δ 57.0 (d, J_{PP} = 23.1 Hz), 46.6 (t, J_{PP} = 23.1 Hz). $^{13}C\{^1H\}$ (C_6D_6, 293 K): δ 196.3 (s, Ru-O=*C*), 146.7 (s), 146.4 (s), 135.3-133.9 (m), 132.8 (s), 132.3 (s), 132.2 (s), 131.6 (s), 129.8 (s), 129.7 (s), 118.8 (s), 23.2 (s, CH_3). IR (cm^{-1}): 1940 (ν_{Ru-H}), 1574 ($\nu_{Ru-O=C}$).

7.3.1.4. Ru(PPh_3)$_3$(*p*-CH_3O-*o*-$C_6H_4C(O)CH_3$)H (15)

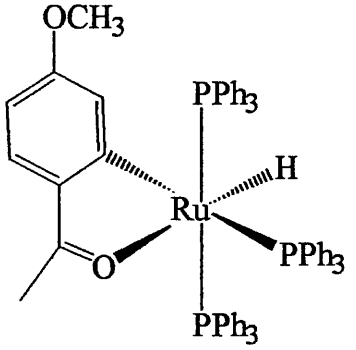

To a suspension of **(6)** (0.20 g, 0.22 mmol) in 5 ml thf was added an excess of *p*-

methoxyacetophenone (0.43 g, 3.10 mmol). The mixture was heated with stirring at 50°C for 12 hr. The solution was concentrated to yield an orange precipitate, which was filtered off, washed with hexane (3 x 10 ml) and dried *in vacuo*. Yield 0.17 g, 76%. Block shaped red crystals could be grown from a concentrated thf solution under argon in a sealed Schlenk tube at room temperature over 2 weeks. The compound proved to be too insoluble to be fully analysed by NMR. It was reacted with CO without any further characterisation **[see 7.3.1.6.]**.

7.3.1.5. $Ru(PPh_3)_2(o\text{-}C_6H_4C(O)CH_3)(CO)H$ (16)

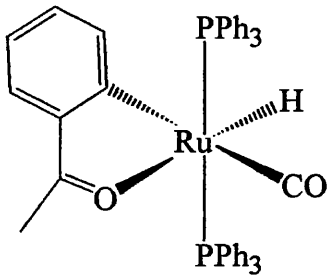

A benzene suspension (10 ml) of **(15)** (0.20 g, 0.20 mmol) was stirred under 1 atm of carbon monoxide for 30 min, during which time the colour changed from red to yellow. The solution was concentrated and hexane added (10 ml) to give a yellow precipitate. This was filtered off, washed with 2 x 10 ml hexane and dried *in vacuo*. Yield 0.12 g, 76%. Analysis for $RuC_{45}H_{38}P_2O_2$ [found (calculated)]: C, 69.4 (69.84); H, 4.87 (4.94). ^1H NMR (C_6D_6, 400 MHz, 293 K): δ 7.60 (br, 10H, C_6H_5), 7.57 (d, J_{HH} = 7.6 Hz, 1H, C_6H_4), 6.90 (br, 20H, C_6H_5), 6.88 (d, J_{HH} = 7.6 Hz, 1H, C_6H_4), 6.56 (t, J_{HH} = 7.6 Hz, 1H, C_6H_4), 6.49 (t, J_{HH} = 7.6 Hz, 1H, C_6H_4), 1.66 (s, 3H, CH_3), -14.29 (t, J_{PH} = 21.2 Hz, 1H, Ru-H). $^{31}P\{^1H\}$ NMR (C_6D_6, 293 K): δ 55.3 (s). $^{13}C\{^1H\}$ (C_6D_6, 293 K): δ 208.2 (s, Ru-O=*C*), 204.9 (t, J_{CP} = 12.8 Hz, Ru-*C*O), 202.9 (t, J_{CP} = 14.9 Hz, Ru-*C*), 145.9 (s), 144.9 (s), 135.7 (t, J_{CP} = 20.2 Hz), 134.4 (t, J_{CP} = 5.9 Hz), 130.3 (s), 130.2 (s), 129.0 (s), 120.2 (s), 24.0 (s, CH_3). IR (cm^{-1}): 1932 (ν_{Ru-H}), 1899 (ν_{CO}), 1583 ($\nu_{Ru-O=C}$).

7.3.1.6. $Ru(PPh_3)_2(p\text{-}CH_3O\text{-}o\text{-}C_6H_4C(O)CH_3)(CO)H$ (17)

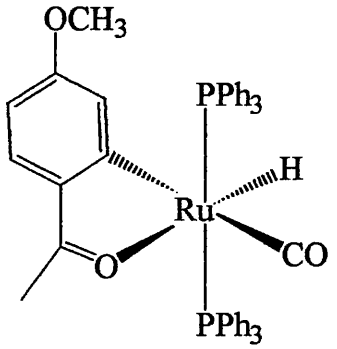

A benzene suspension (10 ml) of **(15)** (0.20 g, 0.20 mmol) was stirred under 1 atm of carbon monoxide for 30 min, during which time the colour changed from red to yellow. The solution was concentrated and hexane added (10 ml) to give a yellow precipitate. This was filtered off, washed with 2 x 10 ml hexane and dried *in vacuo*. Yield 0.13 g, 83%. ^{1}H NMR (C_6D_6, 400 MHz, 293 K): δ 7.65 (m, 10H, C_6H_5), 6.90 (m, 20H, C_6H_5), 6.91 (d, J_{HH} = 8.4 Hz, 1H, C_6H_4), 6.65 (br s, 1H, C_6H_3), 6.37 (br dd, J_{HH} = 8.4 Hz, J_{HH} = 2.4 Hz, 1H, C_6H_3), 3.03 (s, 3H, OCH_3), 1.69 (s, 3H, CH_3), -14.44 (t, J_{PH} = 22.0 Hz, 1H, Ru-H). $^{31}P\{^{1}H\}$ NMR (C_6D_6, 293 K): δ 56.2 (s). $^{13}C\{^{1}H\}$ (C_6D_6, 293 K): δ 208.5 (t, J_{CP} = 14.4 Hz, Ru-*C*O), 205.2 (t, J_{CP} = 13.9 Hz, Ru-*C*), 205.1 (s, Ru-*O*=*C*), 160.9 (s, *C*-OMe), 139.1 (s), 135.8 (t, J_{CP} = 20.3 Hz), 134.4 (t, J_{CP} = 5.9 Hz), 131.3 (s), 130.2 (s), 129.0 (s), 125.5 (s), 110.3 (s), 54.1 (s, OCH_3), 23.6 (s, CH_3). IR (cm^{-1}): 1919 (ν_{Ru-H}), 1912 (ν_{CO}), 1584 ($\nu_{Ru-O=C}$).

7.3.1.7. Ru(PPh$_3$)$_3$(*o*-NC$_4$H$_3$C(O)CH$_3$)H (18)

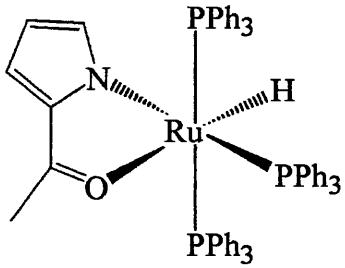

To a suspension of **(6)** (0.20 g, 0.22 mmol) in 5 ml thf was added an excess of 2-acetylpyrrole (0.34 g, 3.10 mmol). The mixture was heated with stirring at 50°C for 12 hr. The solution was concentrated to yield a pale yellow precipitate, which was filtered off, washed with hexane (3 x 10 ml) and dried *in vacuo*. Yield 0.20 g, 92 %. Block shaped red crystals could be grown from a concentrated thf solution under argon in a sealed Schlenk tube at room temperature over 2 weeks. Due to the insolubility of the product, it was characterised only by $^{31}P\{^{1}H\}$ NMR: 63.2 (t, J_{PP} = 29.1 Hz), 50.8 (d, J_{PP} = 29.1 Hz).

7.3.1.8. *cis*-Ru(PPh$_3$)$_2$(*o*-NC$_4$H$_3$C(O)CH$_3$)(CO)H (19)

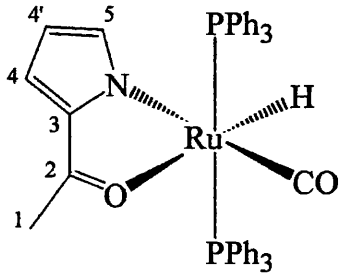

1) A benzene suspension (5 ml) of **(20)** (0.20 g, 0.26 mmol) was stirred at 110°C for 2 hr, during which time the suspension went in solution. The solution was concentrated and hexane added (10 ml) to give a white precipitate. This was filtered off, washed with 2 x 10 ml hexane and dried *in vacuo*. Yield 0.19 g, 95%.

2) In attempt to make $Ru(PPh_3)[Ph_2P(NC_4H_3C(O)CH_3](CO)H_2$, a Schlenk tube equipped with a magnetic stirring bar was flame dried and then charged with 0.50 g (0.51 mmol) **(1)**, 0.20 g (0.66 mmol, 1.2 equivalents) $NC_4H_3C(O)CH_3$ in 10 ml of toluene. The mixture was then refluxed for 2 hr giving a dark red solution. Toluene was removed under vacuum, leaving a dark red oil. 25 ml of methanol were then added to the oil and the mixture stirred for 3hr, until a pink/white precipitate was formed. The solution was then filtered via filter cannula and the resultant crude powder washed 3 times with 10 ml of methanol and 10 ml of hexane. Drying under vacuum afforded 0.18 g (43%) of product. Analysis for $RuC_{49}H_{43}P_2O_2N$ [found (calculated)]: C, 67.7 (67.70); H, 4.99 (4.88); N 1.90 (1.83). ^1H NMR (C_6D_6, 400 MHz, 293 K): δ 7.57 (br m, 10H, C_6H_5), 6.99 (br m, 20H, C_6H_5), 6.58 (br d, J_{HH} = 4.0 Hz, 1H, (4)), 6.51 (br s, (5)), 6.02 (dd, J_{HH} = 1.2 Hz, J_{HH} = 4.0 Hz, 1H, (4')), 1.67 (s, 3H, CH_3), -13.91 (t, J_{PH} = 20.4 Hz, 1H, Ru-H). $^{31}P\{^1H\}$ NMR (C_6D_6, 293 K): δ 48.2 (s). $^{13}C\{^1H\}$ (C_6D_6, 293 K): δ, 204.9 (t, J_{CP} = 13.0 Hz, Ru-*C*O), 188.5 (br s, Ru-O=*C*), 142.4 (s, (5)), 140.2 (s, (3)), 134.0 (t, J_{CP} = 21.0 Hz), 134.0 (t, J_{CP} = 6.0 Hz), 129.2 (s), 128.0 (s), 119.7 (s, (4)), 114.5 (s, (4')), 22.4 (s, CH_3). IR (cm^{-1}): 2037 (ν_{Ru-H}), 1927 (ν_{CO}), 1535 ($\nu_{Ru-O=C}$).

7.3.1.9. *trans*-$Ru(PPh_3)_2$(*o*-$NC_4H_3C(O)CH_3$)(CO)H (20)

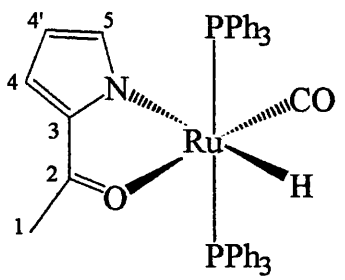

A benzene suspension (10 ml) of **(18)** (0.60 g, 0.60 mmol) was stirred under 1 atm

of carbon monoxide for 30 min, during which time the colour changed from pale yellow to colourless. The solution was concentrated and hexane added (10 ml) to give an off-white precipitate. This was filtered off, washed with 2 x 10 ml hexane and dried *in vacuo*. Yield 0.40 g, 87%. Analysis for $RuC_{49}H_{43}P_2O_2N$ [found (calculated)]: C, 67.5 (67.70); H, 4.94 (4.88); N 1.82 (1.83). ^1H NMR (C_6D_6, 400 MHz, 293 K): δ 7.66 (br m, 10H, C_6H_5), 6.99 (br m, 21H, C_6H_5, (5)), 6.69 (br d, J_{HH} = 3.6 Hz, 1H, (4)), 6.27 (dd, J_{HH} = 1.6 Hz, J_{HH} = 4.0 Hz, 1H, (4')), 1.42 (s, 3H, CH_3), -9.39 (t, J_{PH} = 20.8 Hz, 1H, Ru-H). $^{31}P\{^1H\}$ NMR (C_6D_6, 293 K): δ 48.5 (s). $^{13}C\{^1H\}$ (C_6D_6, 293 K): δ, 207.1 (t, J_{CP} = 13.5 Hz, Ru-*C*O), 188.2 (br s, Ru-O=*C*), 143.4 (s, (5)), 141.2 (s, (3)), 134.7 (t, J_{CP} = 21.1 Hz), 134.4 (t, J_{CP} = 6.1 Hz), 129.4 (s), 128.1(s),120.3(s, (4)), 115.2 (s, (4')), 21.8 (s, CH_3). IR (cm^{-1}): 1962 (ν_{Ru-H}), 1917 (ν_{CO}), 1536 ($\nu_{Ru-O=C}$)

7.3.1.10. Ru(PPh$_3$)$_2$(*o*-C$_6$H$_4$C(O)CH$_3$)(DMSO)H (21)

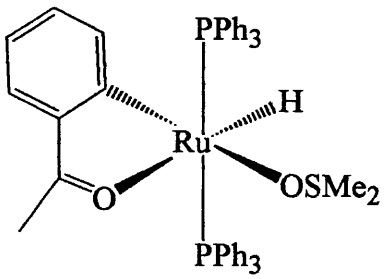

DMSO (29 μL, 0.40 mmol) was added to a toluene suspension (5 ml) of **(14)** (0.20 g, 0.20 mmol). The mixture was stirred for 30 min to give a homogeneous solution and then concentrated to ca. 1 ml. Addition of hexane (5 ml) and vigorous stirring for 5 min afforded a deep red oil. This operation was repeated twice more to give **(22)**, which was isolated as a light red powder upon drying *in vacuo* (0.16 g, 98%). Recrystallization from toluene/hexane afforded red needles suitable for X-ray diffraction. Analysis for $RuC_{45}H_{38}P_2O$.1.2 DMSO [found (calculated)]: C, 63.0 (63.34); H, 5.54 (5.62). ^1H NMR (C_6D_6, 400 MHz, 293 K): δ 7.80-6.90 (m, 30H, C_6H_5), 6.86 (br d, J_{HH} = 7.6 Hz, 1H, C_6H_4), 6.74 (br d, J_{HH} = 7.6 Hz, 1H, C$_6$H4), 6.38 (br t, J_{HH} = 7.2 Hz, 1H, C_6H_4), 6.12 (br t, J_{HH} = 6.8 Hz, 1H, C_6H_4), 2.09 (s, 6H, CH_3) 1.67 (s, 3H, CH_3), -15.30 (t, J_{PH} = 24.6 Hz, 1H, Ru-H). $^{31}P\{^1H\}$ NMR (C_6D_6, 293 K): δ 58.0 (s). $^{13}C\{^1H\}$ (C_6D_6, 293 K): δ 206.4 (s, Ru-O=C), 195.2 (t, J_{CP} = 15.8 Hz, Ru-C), 146.2 (s), 145.3 (s), 136.6 (t, J_{CP} = 19.1 Hz), 133.8 (t, J_{CP} = 5.8 Hz), 129.9 (s), 129.2 (s), 128.9 – 127.5 (m), 118.8 (s), 54.6 (s, CH_3), 23.7 (s, CH_3). IR (cm^{-1}): 1971 (ν_{Ru-H}), 1571 ($\nu_{Ru-O=C}$).

7.3.2. Complexes spectroscopically characterized.

To an NMR tube were added 80 mg (0.08 mmol) of **(1)**, 1 ml of C_6D_6 and two equivalents of $CH_2CHSiMe_3$ 18 μL (0.17 mmol). The tube was left in a water bath at 60°C for 12 hr, during which time the colour changed to deep red. A new product **(22)** was then analyzed by ^1H, $^{31}P\{^1H\}$, $^{31}P\{^1H\}$ COSY and $^{31}P\{^1H\}$-^1H HETCOR NMR experiments. The tube was then pumped to dryness for 12 hr to remove any traces of residual $CH_2CHSiMe_3$ and $CH_3CH_2SiMe_3$. Then 1 ml of C_6D_6 and 1.2 equivalents (11.6 mg, 0.096 mmol) of acetophenone were added. $^1H/^{31}P$ NMR spectra were then run every 6 hr in order to observe and characterize new species **(23)** and **(24)**. These were then analyzed by ^1H, $^{31}P\{^1H\}$, $^{31}P\{^1H\}$ COSY and $^{31}P\{^1H\}$-^1H HETCOR NMR experiments. At a set time of the reaction, 4 equivalents (relative to **(1)**) of CH_2=$CHSiMe_3$ were added to the reaction mixture.

$Ru(PPh_3)_2(PPh_2(o\text{-}C_6H_4))(CO)H$ (22)

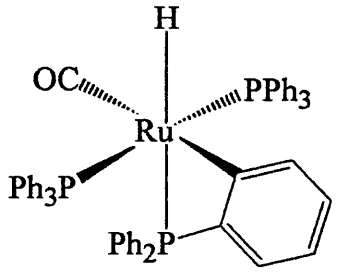

^1H NMR (C_6D_6): -8.35 (dt, J_{HPb} = 26.5, J_{HPa} = 83.4 Hz, 1H). $^{31}P\{^1H\}$ NMR (C_6D_6, 293 K): δ 52.8 (d, P_a, J_{PP} = 15.8 Hz), -34.7 (t, P_b, J_{PP} = 15.8 Hz).

***cis*-$Ru(PPh_3)_2(o\text{-}C_6H_4C(O)CH_3)(CO)H$ (23)**

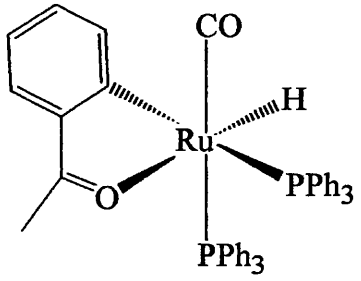

^1H NMR (C_6D_6): -5.84 (J_{HP} = 24.4 Hz, J_{HP} = 92.9 Hz). $^{31}P\{^1H\}$ NMR (C_6D_6, 293 K): δ 40.0 (d, J_{PP} = 18.5 Hz), 36.5 (d, J_{PP} = 18.5 Hz).

***trans*-$Ru(PPh_3)_2(o\text{-}C_6H_4C(O)CH_3)(CO)H$ (24)**

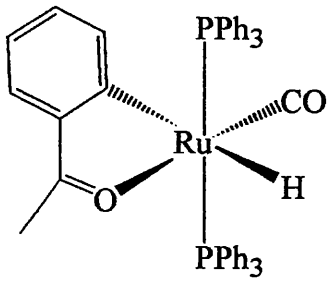

^{1}H NMR (C_6D_6): -3.26 (J_{HP} = 22.4 Hz).

7.4. Preparation of IMes and mixed N-heterocyclic carbene phosphine ruthenium complexes.

7.4.1. Synthesis of bis-(2,4,6-trimethylphenylimidazol-2-ylidene (25).[12]

7.4.1.1. Synthesis of glyoxal-bis-(2,4,6-trimethylphenyl)imine.

To a 1000 ml round bottomed flask were added 135.22 g (1.00 mol) of 2,4,6-trimethylphenylamine, 72.60 g of a 40% aqueous solution of glyoxal (0.50 mol) and 500 ml of undried but degassed ethanol. The mixture was stirred for 12 hr at room temperature, during which time a thick yellow precipitate formed. The precipitate was isolated by filtration and then washed three times with 50 ml of cold ethanol. The product was finally dried under vacuum for 6 hr or left to dry in air. Yield 212.00 g (73%). ^{1}H NMR ($CDCl_3$, 400 MHz, 293 K): δ 2.19 (s, 12H, *o*-CH_3), 2.32 (s, 6H, *p*-CH_3), 6.93 (s, 4H, *m*-CH), 8.13 (s, 2H, NCH=CHN). ^{13}C{^{1}H} ($CDCl_3$, 400 MHz, 293 K): δ 18.2 (s, *o*-CH_3), 20.7 (s, *p*-CH_3), 126.5 (s), 128.9 (s), 134.1 (s), 147.4 (s), 163.0 (s, NCH=CHN).

7.4.1.2. Synthesis of [IMes-H]$^+$Cl$^-$

To a toluene solution of bis-(2,4,6-trimethylphenyl)-diazabutadiene (19.3 g), 2.0 g of paraformaldehyde was added. The reaction mixture was heated to 100°C and then cooled to 40°C, after which time 16.5 ml HCl (4M in dioxane) was introduced. The reaction was maintained at 70°C for 5 hr and allowed to cool. The product was collected by filtration and washed with thf (15.6 g, 69 % w.r.t. diazabutadiene).

7.4.1.3. Synthesis of 1,3-bis-(2,4,6-trimethylphenyl)imidazol-2-ylidene (IMes, 25)

1,3-dimesitylimidazolium chloride (5.00 g, 14.00 mmol) was placed into a flame dried Schlenk tube and left under vacuum at 60°C for approximately 8 hr. After cooling to room temperature, potassium *tert*-butoxide (2.00 g, 18.00 mmol) was added and the mixture cooled to -70°C in an isopropanol/dry-ice bath, before 100 ml of thf were added to via cannula. With vigorous stirring, the mixture was allowed to warm to 0-5°C over 30 min, after which the reaction was warmed to room temperature and stirred for another 30 min. The solvent was then removed *in vacuo* and the residue pumped to dryness for up to 24 hr. (NB: complete dryness of the residue is crucial for the successful isolation of the final product). The residue was dissolved in toluene and the extract filtered through Celite. The filtrate was pumped down to a dry residue before 50ml of hexane were added. The mixture was stirred until a precipitate formed and cooled down to -30°C to enforce precipitation of **(25)** (Yield 3.26 g, 73 %). ^{1}H NMR (C_6D_6): δ 6.80 (s, 4H, *meta*-C*H*), 6.51 (s, 2H, im-*H*), 2.16 (s, 6H, *para*-CH_3), 2.14 (s, 12H, *ortho*-CH_3). ^{13}C {^{1}H} NMR (C_6D_6): δ 220.0 (s, im-C), 137.0-120.9 (m, *meta*-C, *ortho*-C, im-C=C), 21.7 (s, *para*-CH_3), 18.7 (s, *ortho*- CH_3).

7.4.1.4. $Ru(PPh_3)_2(IMes)(CO)H_2$ (26)

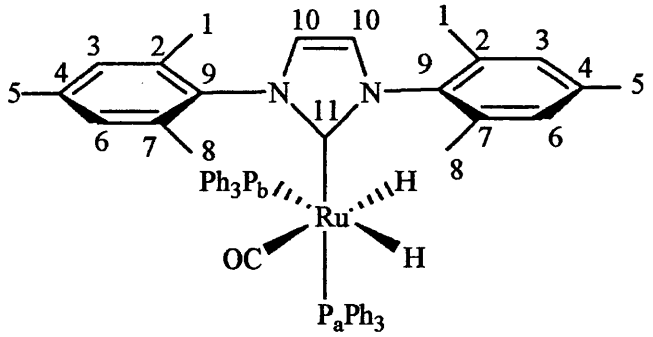

To a solution of 1.00 g **(1)** (1.09 mmol) in 30 ml toluene was added 1.00 g IMes (3.29 mmol) and the mixture heated to 80°C for 2 weeks. ^{31}P{^{1}H} NMR spectroscopy at this stage showed signals for **(26)** and residual **(1)**. Thermolysis for a further week afforded just **1**. Removal of solvent gave a dark oily residue; addition of 30 ml ethanol and stirring at room temperature gave a white solid. This was washed with ethanol (3 x 10 ml) and hexane (1 x 10 ml) to give 0.69 g of **(26)** (65% yield.). X-ray quality crystals were grown by layering a benzene solution with ethanol. Analysis for $RuC_{57}H_{49}P_3O$ [found (calculated)]: C, 72.4 (72.56); H, 5.88 (5.88); N, 2.93 (2.92). ^{1}H NMR (C_6D_6): δ 7.42–7.30 (m, 12H, PC_6H_5), 6.93 (m, 18H, PC_6H_5), 6.86 (br s, 2H, *H-3*), 6.82 (br s, 2H, *H-6*), 6.25 (br s, 2H, *H-10*), 2,26 (s, 6H, *H-5*), 2.20 (s, 6H, *H-1*), 1.82 (s, 6H, *H-8*), -6.36 (ddd, J_{HPb} =

26.8, J_{HPa} = 23.6, J_{HHb} = 6.0 Hz, 1H, H_b), -8.08 (ddd, J_{HPb} = 81.2, J_{HPa} = 33.6, J_{HHb} = 6.0 Hz, 1H, H_a). $^{31}P\{^1H\}$ NMR (C_6D_6, 293 K): δ 59.0 (d, P_a, J_{PP} = 14.8 Hz), 47.8 (d, P_b, J_{PP} = 14.8 Hz). $^{13}C\{^1H\}$ (C_6D_6): δ 205.2 (t, J_{CP} = 8.8 Hz, Ru-*C*O), 197.7 (dd, J_{CPa} = 75.5, J_{CPb} = 6.7 Hz, *C-11*), 142.2 (br d, PC_6H_5), 142.1 (br d, PC_6H_5), 140.1 (br s, C-*9*), 137.7 (br s, C-*2* or *7*), 134.6 (d, J_{CP} = 5.4 Hz, PC_6H_5), 134.4 (d, J_{CP} = 6.7 Hz, PC_6H_5), 129.4 (br s, C-*3* or *6*), 127.9 (s, PC_6H_5), 127.4 (d, J_{CP} = 8.4 Hz, PC_6H_5), 127.0 (d, J_{CP} = 8.9 Hz, PC_6H_5), 122.4 (br s, C-*10*), 21.4 (s, CH_3-*1*, *5* and *8*). IR (cm^{-1}): 1937 (ν_{CO}), 1987 (ν_{RuH}), 1872 (ν_{RuH}).

7.4.1.5. Ru(dppp)(IMes)(CO)H_2 (27)

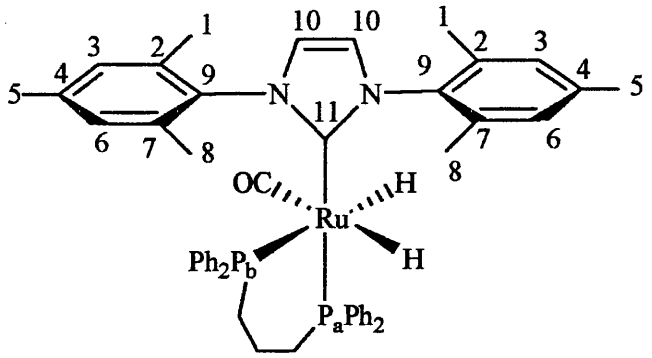

To a solution of 1.00 g **(8)** (1.24 mmol) in 30 ml toluene was added 1.11 g IMes (3.72 mmol) and the mixture heated to 100°C for 3 weeks. Removal of solvent gave a dark oily residue; addition of 30 ml ethanol and stirring at room temperature gave a white solid. This was washed with ethanol (3 x 10 ml) and hexane (1 x 10 ml) to give 0.77 g of **(27)** (73% yield.). X-ray quality crystals were grown by layering a benzene solution with ethanol. Analysis for $RuC_{49}H_{52}P_2N_2ORu$ [found (calculated)]: C, 69.6 (69.40); H, 6.14 (6.18); N, 3.26 (3.30). ^1H NMR (C_6D_6): δ 8.96-7.21 (m, 20H, PC_6H_5), 7.14 (br s, 2H, H-3), 7.06 (br s, 2H, H-6), 6.38 (br s, 2H, H-10), 2.59 (sex, J_{HH} = 12.0 Hz, 2H, PCH_2-CH_2), 2,51 (s, 6H, H-5), 2.29 (s, 6H, H-1), 2.01 (s, 6H, H-8), 1.94 (t, J_{HH} = 12.0 Hz, 2H, PCH_2-CH_2), 1.22 (sex, J_{HH} = 12.0 Hz, 2H, PCH_2-CH_2), -6.20 (ddd, J_{HPb} = 22.9, J_{HPa} = 15.5, J_{HHb} = 5.8 Hz, 1H, Hb), -7.07 (ddd, J_{HPb} = 79.4, J_{HPa} = 22.9, J_{HHb} = 5.8 Hz, 1H, Ha). $^{31}P\{^1H\}$ NMR (C_6D_6, 293 K): δ 40.6 (d, P_a, J_{PP} = 24.5 Hz), 28.1 (d, P_b, J_{PP} = 24.5 Hz). $^{13}C\{^1H\}$ (C_6D_6): δ 205.8 (br t, J_{CP} = 9.0 Hz, Ru-CO), 195.5 (dd, J_{CPa} = 75.5, J_{CPb} = 7.5 Hz, C-11), 148.6 (d, J_{CP} = 5.0 Hz, PC_6H_5), 148.5 (d, J_{CP} = 5.0 Hz, PC_6H_5), 145.3 (d, J_{CP} = 5.1 Hz, PC_6H_5), 144.7 (d, J_{CP} = 5.1 Hz, PC_6H_5), 141.5 (d, J_{CP} = 40.7 Hz, PC_6H_5), 140.3 (br s, C-9), 137.4 (s, C-2 or 7), 137.0 (s, C-2 or 7), 135.6 (d, J_{CP} = 15.1 Hz, PC_6H_5), 136.2 (s, C-4), 134.8 (d, J_{CP} = 26.4 Hz, PC_6H_5), 133.3 (d, J_{CP} = 12.2 Hz, PC_6H_5), 133.0 (d, J_{CP} = 12.3 Hz, PC_6H_5), 131.3 (d, J_{CP} = 9.1 Hz, PC_6H_5), 129.4 (s, C-3 or 6), 128.9 (s, C-3 or 6d), 121.4 (d, J_{CP} = 2.3 Hz, C-10),

34.9 (dd, J_{CP} = 5.9 Hz, J_{CP} = 24.8 Hz, PCH_2), 30.7 (d, J= 21.4 Hz, PCH_2), 21.4 (s, CH_3-5), 20.4 (br s, PCH_2-CH_2), 19.3 (s, CH_3-1 or 8), 18.7 (s, CH_3-1 or 8). IR (cm^{-1}): 1876 (ν_{CO}), 1968 (ν_{RuH}).

NB: The product could be synthesized using Ru(dppp)($AsPh_3$)(CO)H_2 and the reaction time was reduced to 1 week.

7.4.1.6. Ru(arphos)(IMes)(CO)H_2 (28)

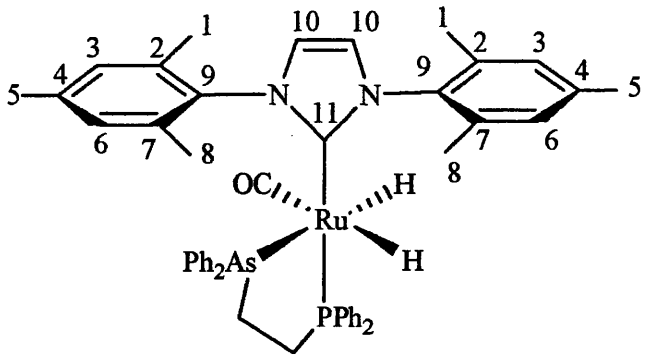

To a solution of 1.00 g **(11)** (1.22 mmol) in 30 ml toluene was added 1.10 g IMes (3.65 mmol) and the mixture heated to 100°C for 1 week. Removal of solvent gave a dark oily residue; addition of 30 ml ethanol and stirring at room temperature gave an off-white solid. This was washed with ethanol (3 x 10 ml) and hexane (1 x 10 ml) to give 0.74 g of **(28)** (69% yield.). X-ray quality crystals were grown by layering a benzene solution with ethanol. Analysis for $RuC_{48}H_{50}N_2PAsORu$ [found (calculated)]: C, 65.61 (65.67); H, 5.81 (5.74); N, 3.18 (3.19). ^1H NMR (C_6D_6): δ 7.90–7.35 (m, 10H, PC_6H_5), 7.2-6.9 (m, 10H, AsC_6H_5), 6.89 (br s, 2H, H-3), 6.87 (br s, 2H, H-6), 6.25 (br s, 2H, H-10), 2.27 (s, 6H, H-5), 2.12 (s, 6H, H-1), 1.98 (s, 6H, H-8), 1.79 (br, 2H, CH_2), 1.60 (br, 2H, CH_2) -7.44 (dd, J_{HPa} = 25.9, J_{HHb} = 3.3 Hz, 1H, H_a), -8.9 (dd, J_{HPa} = 25.9, J_{HHb} = 3.3 Hz, 1H, H_a). $^{31}P\{^1H\}$ NMR (C_6D_6, 293 K): δ 88.7 (s). $^{13}C\{^1H\}$ (C_6D_6): δ 204.5 (d, J_{CP} = 7.5 Hz, Ru-CO), 195.4 (d, J_{CPa} = 78.4 Hz, C-11), 144.3 (br d, J_{CP} = 3.2 Hz PC_6H_5), 141.4 (s, AsC_6H_5), 141.1 (s, AsC_6H_5), 141.0 (br, PC_6H_5), 140.2 (br s, C, 140.2 (s, C-9), 137.3 (s, C-4), 136.8 (s, C-2 or 7), 136.0 (s, C-2 or 7), 135.4 (d, J_{CP} = 12.6 Hz, PC_6H_5), 133.9 (s, AsC_6H_5), 132.8 (s, AsC_6H_5), 131.3 (d, J_{CP} = 10.5 Hz, PC_6H_5), 129.2 (s, C-3 or 6), 129.0 (s, C-3 or 6), 128.8 (s, PC_6H_5), 128.1 (s, AsC_6H_5), 127.9 (s, PC_6H_5), 127.4 (d, J_{CP} = 8.4 Hz, PC_6H_5), 127.1 (d, J_{CP} = 2.1 Hz, PC_6H_5), 121.3 (d, J_{CP} = 2.1 Hz, C-10), 33.9 (d, J_{CP} = 19.8 Hz, AsCH_2), 29.1 (d, J_{CP}= 23.2 Hz, PCH_2), 21.6 (s, CH_3-5), 19.7 (s, CH_3-1 or 8), 19.0 (s, CH_3-1 or 8). IR (cm^{-1}): 1914 (ν_{CO}), 1940 (ν_{RuH}), 1873 (ν_{RuH}).

7.4.1.7. $Ru(PPh_3)(IMes)_2(CO)H_2$ (29)

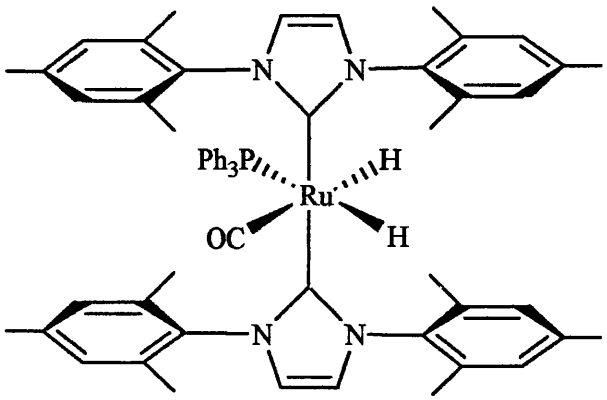

^1H NMR (C_6D_6): δ 7.33–7.25 (m, 15H, PC_6H_5), 6.94 (br s, 4H, IMes aryl), 6.79 (br s, 4H, IMes aryl), 6.09 (s, 4H, *HC=CH*), 2.35 (s, 12H, *para*-Me), 2.15 (s, 24H, *ortho*-Me), -5.89 (dd, J_{HP} = 18.8, J_{HH} = 7.1 Hz, 1H, Ru-H), -7.39 (dd, J_{HP} = 93.5, J_{HH} = 7.1 Hz, 1H, Ru-H). $^{31}P\{^1H\}$ NMR (C_6D_6): δ 47.3. Selected $^{13}C\{^1H\}$ NMR (C_6D_6): δ 205.9 (d, J_{CP} = 8.5 Hz, Ru-*C*O), 187.2 (d, J_{CP} = 6.8 Hz, Ru-$C_{carbene}$).

7.4.1.8. $Ru(PPh_3)_2(IMes')(CO)H$ (30)

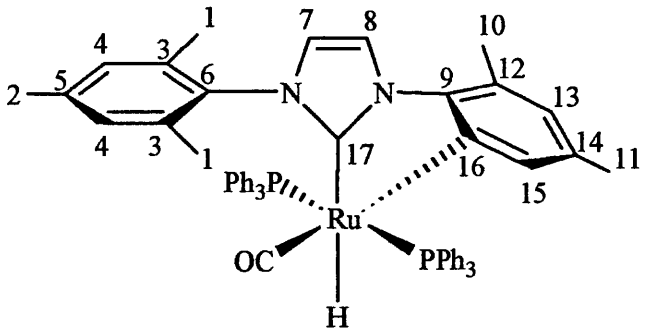

(1) (0.50 g, 0.55 mmol) was heated with 0.50 g IMes (1.65 mmol) in 20 ml toluene for 2 weeks at 110°C. $^{31}P\{^1H\}$ NMR spectroscopy showed formation of a single product, **(30)**. Removal of the solvent gave a dark oil, which was stirred in ethanol for 24 hr to afford a white precipitate. This was washed with ethanol (3 x 10 ml) and hexane (1 x 10 ml) to give 0.50g of **(30)** (96 % yield). X-ray quality crystals were grown by layering a benzene solution of **(30)** with hexane. Analysis for $RuC_{45}H_{38}P_2O_2$ [found (calculated)]: C, 72.8 (72.51); H, 5.53 (5.55); N, 2.96 (2.97). ^1H NMR ($C_6D_5CD_3$): δ 7.51 (d, J_{HH} = 1.6 Hz, 1H, *H-8*), 7.38-7.30 (m, 12H, PC_6H_5), 6.95-6.90 (m, 18H, PC_6H_5), 6.83 (s, 2H, *H-4*), 6.35 (br s, 1H, *H-13*), 6.19 (d, J_{HH} = 1.6 Hz, 1H, *H-7*), 6.14 (br s, 1H, *H-15*), 2.29 (s, 3H, CH_3-

10), 2.17 (s, 3H, C*H*$_3$-*2*), 1.73 (s, 3H, C*H*$_3$-*11*), 1.56 (s, 6H, C*H*$_3$-*1*), -6.99 (t, J_{HP} = 28.4 Hz, 1H, Ru-H). $^{31}P\{^1H\}$ NMR ($C_6D_5CD_3$): δ 55.1 (s). $^{13}C\{^1H\}$ ($C_6D_5CD_3$): δ 207.4 (t, J_{CP} = 10.0 Hz, Ru-CO), 202.8 (t, J_{CP} = 6.6 Hz, *C-17*), 163.5 (t, J_{CP} = 16.9 Hz, *C-16*), 146.5 (br, *C-9*), 146.0 (br, *C-15*), 138.8 (t, J_{CP} = 49.7 Hz, PC_6H_5), 138.3 (s, *C-5*), 136.9 (s, *C-3*), 134.4 (t, J_{CP} = 5.4 Hz, PC_6H_5), 130.9 (br, *C-14*), 129.2 (s, *C-4*), 128.4 (s, PC_6H_5), 128.3 (s, *C-6*), 128.2 (s, *C-13*), 127.3 (t, J_{CP} = 4.1 Hz, PC_6H_5), 121.0 (s, *C-7*), 120.2 (br , *C-12*), 118.4 (s, *C-8*), 23.1 (s, *C*H$_3$-*10*), 21.2 (s, *C*H$_3$-*2,11*), 18.5 (s, *C*H$_3$-*1*). IR (cm^{-1}): 1914 (ν_{CO}), 1854 (ν_{RuH}).

7.4.1.9 Ru(PPh$_3$)$_2$(IMes'')(CO)H (31)

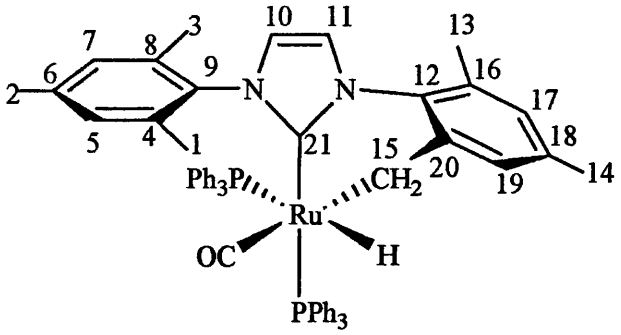

To a C_6D_6 solution of **(26)** (0.08 g, 0.08 mmol) in a Teflon capped resealable NMR tube was added one equivalent of trimethylvinylsilane (12 μl). After standing for 3 hr at room temperature, $^{31}P\{^1H\}$ NMR spectroscopy showed formation of **(31)** (98% conversion by NMR) and ethyltrimethylsilane. The solvent was removed *in vacuo* to give a yellow residue; this was dissolved in toluene (1 ml) and layered with hexane (4 ml) to give **(31)** as pale yellow crystals (0.07 g, 92% yield). Analysis for $RuC_{46}H_{44}P_2O_2$ [found (calculated)]: C, 72.3 (72.71); H, 5.60 (5.68); N, 2.89 (2.92). ^1H NMR ($C_6D_5CD_3$): δ 7.65-6.81 (m, 33H, C_6H_5 + *H-5, 7* and *10*), 6.42 (br s, 1H, *H-19*), 6.33 (br s, 1H, *H-11*), 6.14 (br s, 1H, *H-17*), 2.76 (br 't', 1H, J_{HH} = 10.8, J_{HPb} = 4.0 Hz, *H-15a*), 2.50 (s, 3H, C*H*$_3$-*1* or *3*), 2.21 (s, 3H, C*H*$_3$-*2*), 2.03 (s, 3H, C*H*$_3$-*13*), 1.88 (s, 3H, C*H*$_3$-*14*), 1.62 (s, 3H, C*H*$_3$-*1* or *3*), 1.35 ('t', 1H, J_{HH} = 10.8, J_{HPa} = 14.0 Hz, *H-15b*), -7.97 (dd, 1H, J_{HPa} = 102.4, J_{HPb} = 30.8 Hz, Ru-H). $^{31}P\{^1H\}$ NMR ($C_6D_5CD_3$): δ 53.7 (d, J_{PP} = 18.1 Hz, P_a), 28.4 (d, J_{PP} = 18.1 Hz, P_b). $^{13}C\{^1H\}$ ($C_6D_5CD_3$): δ 201.7 (br t, Ru-CO), 191.5 (br d, J_{CPa} = 84.3 Hz, *C-21*), 149.3 (br s, *C-14*), 140.9 (d, PC_6H_5), 140.5 (d, PC_6H_5), 138.9 (s, *C-9*), 138.5 (s, *C-6*), 138.1 (s, *C-4* or *8*), 136.9 (s, *C-4* or *8*), 136.3 (s, *C-12*), 135.1 (d, PC_6H_5), 135.0 (d, PC_6H_5), 134.4 (d, PC_6H_5), 134.3 (d, PC_6H_5), 134.2 (s, C-*18*), 129.6 (s, *C-5* or *7*), 129.5 (s, *C-5* or *7*), 128.9 (s, *C-19*), 128.7 (d, PC_6H_5), 128.3 (d, PC_6H_5), 128.0 (d, PC_6H_5), 127.9 (d, PC_6H_5), 127.9 (d,

PC_6H_5), 127.9 (d, PC_6H_5), 127.1 (s, *C-16*), 125.4 (s, *C-17*), 121.8 (br d, J_{CP} = 1.9 Hz, *C-10*), 121.4 (br d, J_{CP} = 2.3 Hz, *C-11*), 21.8 (s, CH_3-*14*), 21.7 (s, CH_3-*2*), 20.1 (s, CH_3-*13*), 20.1 (s, CH_3-*1* or *5*), 18.7 (s, CH_3-*5* or *1*), 12.1 (br d, J_{CP} = 7.8 Hz, CH_2-*15*). IR (cm^{-1}): 1955 (ν_{RuH}), 1919 (ν_{CO}).

7.4.1.10. Ru(dppp)(IMes'')(CO)H (32)

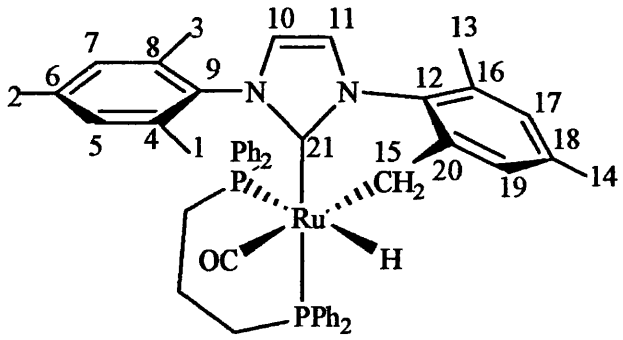

To a C_6D_6 solution of **(27)** (0.07 g, 0.077 mmol) in a Teflon capped resealable NMR tube were added 1.2 equivalents of trimethylvinylsilane (15 µl). After heating to 100°C for 24 hr, $^{31}P\{^1H\}$ NMR spectroscopy showed formation of **(32)** (98% conversion by NMR) and ethyltrimethylsilane. The solvent was removed *in vacuo* to give a yellow residue; this was dissolved in toluene (1 ml) and layered with hexane (4 ml) to give **(32)** as pale yellow crystals (0.05 g, 89%). Analysis for $RuC_{49}H_{50}P_2ORu$ [found (calculated)]: C, 69.6 (69.57); H, 5.94 (5.95); N, 2.88 (3.31). ^1H NMR ($C_6D_5CD_3$): δ 7.91-6.79 (m, 33H, C_6H_5 + H-5, 7 and 10), 6.66 (br s, 1H, H-19), 6.31 (d, 1H, J_{HH} = 2.1 Hz, H-11), 6.19 (br s, 1H, H-17), 3.02 (br 't', 1H, J = 10.2 Hz), 2.64 (s, 3H, CH_3-1 or 3), 2.24 (s, 3H, CH_3-2) 2.10 (s, 3H, CH_3-13), 1.99 (s, 3H, CH_3-14), 1.64 (s, 3H, CH_3-1 or 3), 0.88 (d, 1H, J_{HH} = 10.8, J_{HPa} = 14.2 Hz), -6.71 (dd, 1H, J_{HPa} = 102.6, J_{HPb} = 21.1 Hz, Ru-H). $^{31}P\{^1H\}$ NMR ($C_6D_5CD_3$): δ 39.6 (d, J_{PP} = 25.6 Hz, P_a), 15.2 (d, J_{PP} = 25.6 Hz, P_b). $^{13}C\{^1H\}$ ($C_6D_5CD_3$): δ 204.5 (t, J_{CPb} = 9.1 Hz, Ru-CO), 191.5 (dd, J_{CPa} = 82.3 Hz, J_{CPb} = 8.3 Hz, C-21), 154.7 (dd, J_{CP} = 9.8, J_{CP} = 1.8 Hz C-14), 142.3 (d, J_{CP} = 28.5 Hz), 141.6 (d, J_{CP} = 37.2 Hz), 138.6 (s, C-9), 138.2 (s, C-6), 137.2 (s, C-4 or 8), 136.4 (s, C-4 or 8), 136.1 (s, C-12), 134.4 (d, J_{CP} = 12.4 Hz, PC_6H_5), 133.9 (d, J_{CP} = 11.2 Hz, PC_6H_5), 133.8 (s, C-18), 133.3 (d, J_{CP} = 11.2 Hz, PC_6H_5), 133.0 (d, J_{CP} = 11.2 Hz, PC_6H_5), 132.0 (d, J_{CP} = 12.4 Hz, PC_6H_5) 129.4 (s, C-5 or 7), 129.2 (s, C-5 or 7), 128.9 (s, C-19), 128.3 (d, J_{CP} = 11.6 Hz, PC_6H_5), 128.0 (d, J_{CP} = 10.4 Hz, PC_6H_5), 127.9 (d, J_{CP} = 11.4 Hz, PC_6H_5), 127.9 (d, J_{CP} = 10.6 Hz, PC_6H_5), 127.9 (d, J_{CP} = 11.2 Hz, PC_6H_5), 126.8 (s, C-16), 125.0 (s, C-17), 120.9 (br d, J_{PC} =2.0 Hz, C-10), 120.2 (br d, J_{PC} = 2.6 Hz, C-11), 27.5 (br dt, J_{PC} = 25.5, PCH_2), 21.3 (s, CH_3-14), 21.0 (s,

CH_3-2), 20.9 (s, CH_3-13), 20.3 (br t, PCH_2CH_2) 19.7 (d, J_{CP} = 2.6 Hz, CH_2-15), 18.2 (s, CH_3-1 or 5), 10.7 (br dt, PCH_2),. IR (cm^{-1}): 1920 (ν_{CO})

7.4.1.11. Ru(arphos)(IMes'')(CO)H (33)

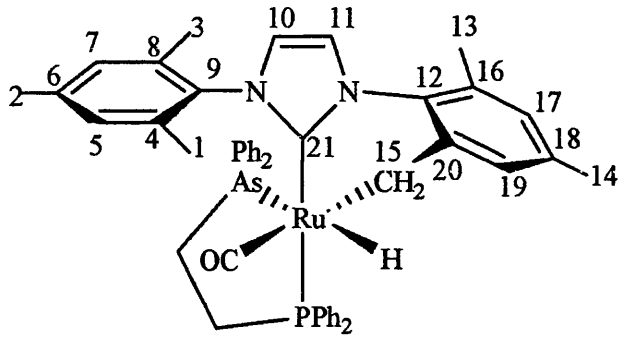

To a C_6D_6 solution of **(28)** (0.08 g, 0.091 mmol) in a Teflon capped resealable NMR tube were added 1.2 equivalents of trimethylvinylsilane (15 µl). After heating to 100°C for 24 hr, $^{31}P\{^1H\}$ NMR spectroscopy showed formation of several species (100% conversion by NMR) and ethyltrimethylsilane.

7.4.1.12. Ru(IMes)(PPh_3)$(CO)_2H_2$ (34)

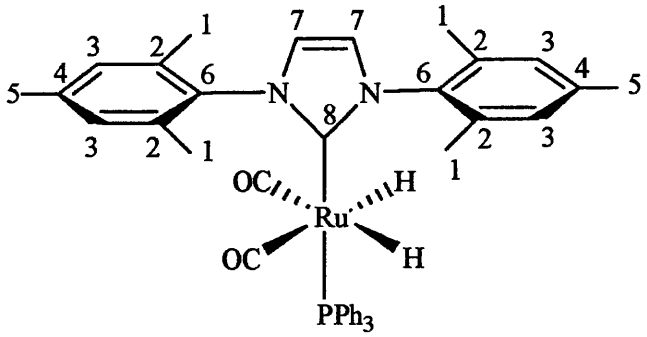

^1H NMR (C_6D_6, 400MHz): δ 7.42–6.80 (m, 19H, PC_6H_5,H-*3,6*), 6.27 (br s, 2H, CNC*H*=C*H*N), 2.20 (s, 12H, CH_3), 2.17 (s, 6H, CH_3), -6.53 (d, $J_{P\text{-}H}$ = 26.8 Hz, 1H). $^{31}P\{^1H\}$ NMR (C_6D_6, 293 K, 400MHz): δ 61.4 (s).

7.4.1.13 $Ru(PPh_3)(IMes')(CO)_2H$ (35)

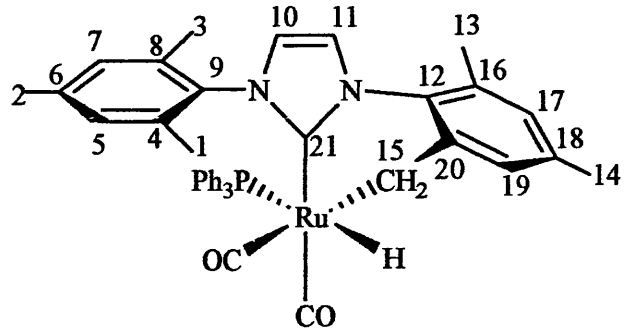

^1H NMR (C_6D_6, 400MHz): δ 7.65-7.01 (m, 33H, C_6H_5 + *H-5, 7* and *10*), 6.94 (br s, 1H, *H-19*), 6.69 (br s, 1H, *H-11*), 6.15 (br s, 1H, *H-17*), 2.41 (s, 3H, CH_3) 2.38 (s, 3H, CH_3), 2.30 (s, 3H, CH_3), 2.21 (s, 3H, CH_3), 1.47 (s, 3H, CH_3), -7.00 (d, J_{P-H} = 82.3 Hz, 1H). $^{31}P\{^1H\}$ NMR (C_6D_6, 293 K, 400MHz): δ 60.8 (s).

7.4.1.14. $Ru(PPh_3)(IMes)(CO)_3$ (36)

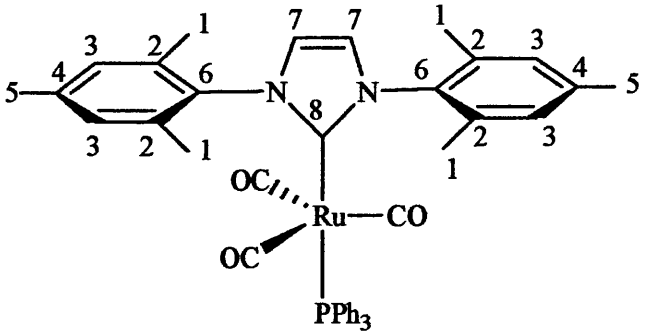

(26) (0.50 g, 0.52 mmol) was stirred under an atmosphere of CO in 20 ml toluene for 12 hr at room temperature. $^{31}P\{^1H\}$ NMR spectroscopy showed formation of a single product. Removal of solvent gave a dark-orange oily residue; addition of 3 ml of hexane and stirring at room temperature gave a yellow solid. This was washed with hexane (2 x 2 ml) and dried *in vacuo* to give 0.25g of **(36)** (62% yield.). NB: The yield could be improved by cooling the hexane at -40°C in an acetone/dry ice bath (Yield 0.31 g, 77%). X-ray quality crystals were grown by layering a benzene solution of **(36)** with hexane. Analysis for $RuC_{42}H_{49}N_2O_3P_1$ [found (calculated)]: C, 69.95 (69.98); H, 5.43 (5.45); N, 3.91 (3.88). ^1H NMR (C_6D_6): δ 7.72–7.65 (m, 9H, PC_6H_5), 6.96 (m, 6H, PC_6H_5, 4H, H-*3*, H-*6*) 6.26 (br s, 2H, H-*10*), 2.22 (s, 12H, CH_3), 2.16 (s, 6H, CH_3). $^{31}P\{^1H\}$ NMR (C_6D_6, 293 K): δ 60.6 (s). $^{13}C\{^1H\}$ (C_6D_6): δ 211.7 (d, J_{C-P} = 16.6 Hz, Ru-CO), 185.5 (d, J_{C-P} = 64.9 Hz, C-*8*), 138.7 (s), 138.5 (s), 138.1 (s), 137.5 (s), 137.9 (s), 136.4 (s), 134.4 (s),

134.3 (s), 134.2 (s), 134.0 (s), 129.4 (s), 128.8 (s), 128.7 (s), 128.5 (s), 127.9 (s), 122.9 (d, J_{PC} = 1.5 Hz, C-*7*), 21.2 (s, C-*5*), 18.7 (s, C-*1*). IR (cm^{-1}): 1878 (ν_{CO}), 1864 (ν_{CO})

7.4.1.15 $Ru(PPh_3)(IMes\text{-}H)(CO)_3$ (37)

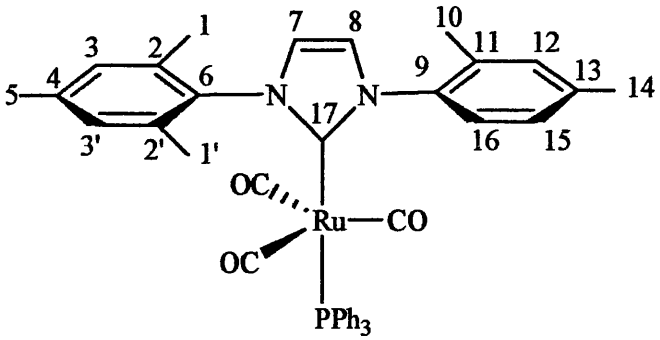

(30) (0.50 g, 0.62 mmol) was stirred under an atmosphere of CO in 10 ml toluene for 4 days at 100°C. $^{31}P\{^1H\}$ NMR spectroscopy showed formation of a single product. Removal of solvent gave a dark-orange oily residue; addition of 3 ml of hexane and stirring at room temperature gave a yellow solid. This was washed with hexane (2 x 2 ml), and dried *in vacuo* to give 0.27 g of **1** (58% yield.). NB: The yield could be improved by cooling the hexane at -40°C in an acetone/dry ice bath (yield 0.33 g, 71%). X-ray quality crystals were grown by layering a benzene solution of **(30)** with hexane. Analysis for $RuC_{41}H_{47}N_2O_3P_1$ [found (calculated)]: C, 65.86 (65.85); H, 6.29 (6.33); N, 3.74 (3.74). ^1H NMR (C_6D_6): δ 7.72–7.65 (m, 10H, PC_6H_5, H-*16*), 6.96 (m, 10H, PC_6H_5, 4H, H-*3,3'*, H-*12,15*), 6.46 (d, $J_{H\text{-}H}$ = 1.9 Hz, 1H, H-*7 or 8*), 6.24 (d, $J_{H\text{-}H}$ = 1.8 Hz, 1H, H-*7 or 8*), 2.27 (s, 3H, H-*14*), 2.20 (s, 3H, H-*5*), 2.13 (s, 3H, H-*10*), 2.10 (s, 3H, H-*1* or H-*1'*), 2.09 (s, 3H, H-*1* or *1'*). $^{31}P\{^1H\}$ NMR (C_6D_6, 293 K): δ 65.5 (s). $^{13}C\{^1H\}$ (C_6D_6): δ 211.6 (d, $J_{C\text{-}P}$ = 16.2 Hz, Ru-CO), 185.8 (d, $J_{C\text{-}P}$ = 64.4 Hz, C-*8*), 140.0 (s), 139.5 (s), 138.8 (s), 138.7 (s), 138.4 (s), 138.3 (s), 138.2 (s), 137.8 (s), 136.9 (s), 136.7 (s),135.7 (s), 134.7 (s), 134.6 (s), 134.6 (s), 134.4 (s), 132.1(s), 130.7 (s), 129.9 (d, $J_{C\text{-}P}$ = 1.4 Hz), 129.7 (d, $J_{C\text{-}P}$ = 2.0 Hz), 129.2 (s), 129.1 (s), 128.4 (s), 127.2 (s), 124.1 (d, $J_{C\text{-}P}$ = 2.3 Hz, C-*7 or 8*), 122.4 (d, $J_{C\text{-}P}$ = 2.3 Hz, C-*7 or 8*), 21.8 (s, C-*14* or *15*), 21.7 (s, C-*14* or *15*), 19.2 (s, C-10), 18.8 (s, C-*1* or *1'*), 18.7 (s, C-*1* or *1'*). IR (cm^{-1}): 1886 (ν_{CO}), 1864 (ν_{CO}).

7.5. Preparation of bis-carbene ruthenium complexes.

7.5.1. $Ru(AsPh_3)(IMes)_2(CO)H_2$ (38)

To a C_6D_6 solution of **(9)** (0.05 g, 0.045 mmol) in a Teflon capped resealable NMR tube were added 3 equivalents of IMes (43 mg, 0.142 mmol). After heating to 70°C for 1 hr, ^1H NMR spectroscopy showed formation of a single species showing two hydride signals at δ -5.71 and -8.93 (J_{HH} = 5.9 Hz).

7.5.2. $Ru(IMes)_2(CO)(EtOH)H_2$ (39)

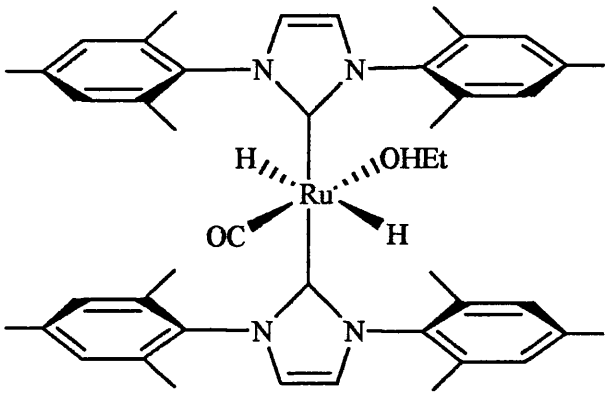

An ampoule fitted with a Teflon stopcock containing a solution of **(9)** (1.00 g, 0.95 mmol) in 20 ml toluene and 3 equivalents of IMes (0.87 g, 2.90 mmol) was heated at 75°C for 4 days, during which time the solution turned deep red. The mixture was cooled to room temperature and evaporated to dryness, leaving an oily dark brown residue. Ethanol (10 ml) was added to give a brown solution, which was stirred for 2 hr to give a yellow precipitate. This was filtered, washed with cold hexane (20 ml) and pumped to dryness to leave a yellow powder. A further batch of compound was isolated from the mother liquor. Yield 0.59 g, 78%. Analysis for $RuC_{45}H_{56}N_4O_2$ [found (calculated)]: C, 68.8 (68.75); H, 6.71 (7.18). ^1H NMR (C_6D_6, 400 MHz, 293 K): δ 6.85 (br s, 4H, $C_6H_2Me_3$), 6.83 (br s, 4H, $C_6H_2Me_3$), 6.20 (s, 4H, CNC*H*=C*H*N), 3.81 (q, J_{HH} = 6.8 Hz, 2H, OCH_2), 2.35 (s, 12H, CH_3), 2.17 (s, 12H, CH_3), 2.09 (s, 3H, CH_3), 1.13 (t, J_{HH} = 6.7 Hz, 3H, OCH_2CH_3), -23.51 (s, 2H, Ru-H). $^{13}C\{^1H\}$ (C_6D_6, 293 K): δ 205.6 (s, Ru-*C*O), 197.9 (s, Ru-*C*), 138.2 (s, N-*C*), 137.0 (s), 136.7 (s), 136.6 (s), 129.4 (s), 129.3 (s), 121.5 (s), 69.7 (s, OCH_2), 23.3 (s, OCH_2CH_3), 21.7 (s, CH_3), 19.2 (s, CH_3). IR (cm^{-1}): 1886 (ν_{CO}).

7.5.3. $Ru(IMes)_2(CO)(H_2O)H_2$ (40)

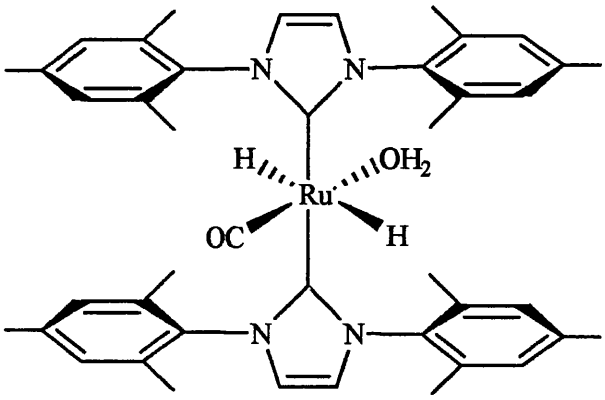

Isolation of the aqua complex was performed as reported for **(39)**, but using degassed, undried hexane (20 ml) rather than ethanol. Yield 0.58 g, 80%. Analysis for $RuC_{43}H_{52}N_4O_2$ [found (calculated)]: C, 68.7 (68.13); H, 6.49 (6.91); N, 7.44 (7.39). ^1H NMR (C_6D_6, 400 MHz, 293 K): δ 6.84 (br s, 4H, $C_6H_2Me_3$), 6.78 (br s, 4H, $C_6H_2Me_3$), 6.15 (s, 4H, CNC*H*=C*H*N), 2.34 (s, 12H, CH_3), 2.18 (s, 12H, CH_3), 2.05 (s, 3H, CH_3), 0.93 (s), -23.15 (s, 2H, Ru-H). $^{13}C\{^1H\}$ (C_6D_6, 293 K): δ 206.4 (s, Ru-*C*O), 198.6 (s, Ru-*C*), 138.1 (s, N-*C*), 137.2 (s), 136.9 (s), 136.5 (s), 129.3 (s), 129.2 (s), 121.4 (s), 21.9 (s, CH_3), 19.2 (s, CH_3), 19.1 (s, CH_3). IR (cm^{-1}): 1861 (ν_{CO}), 1818 (ν_{Ru-H}).

7.5.4. $Ru(IMes)_2(CO)(MeOH)H_2$ (41)

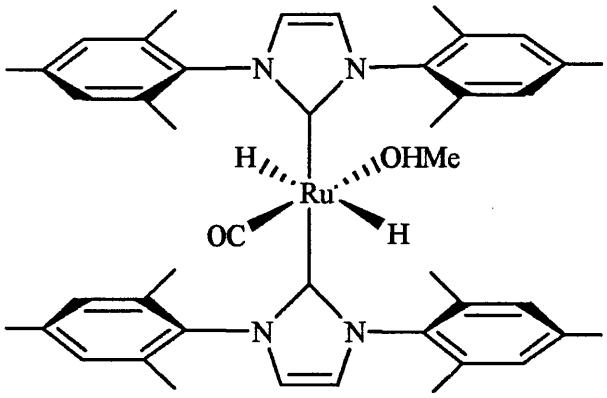

An ampoule fitted with a Teflon stopcock containing a solution of **(9)** (0.50 g, 0.48 mmol) in 20 ml toluene and 3 equivalents of IMes (0.44 g, 1.5 mmol) was heated at 80°C for 6 days, during which time the solution turned deep red. The mixture was cooled to room temperature and evaporated to dryness. Methanol (5 ml) was added the solution, which was stirred for 2 hr to give a yellow precipitate. This was filtered, washed with cold hexane (10 ml) and pumped to dryness to leave a yellow powder. Yield 0.16 g, 43%.

NMR (C_6D_6, 400 MHz, 293 K): δ 6.85 (br s, 4H, $C_6H_2Me_3$), 6.81 (br s, 4H, $C_6H_2Me_3$), 6.21 (s, 4H, CNC*H*=C*H*N), 2.34 (s, 12H, CH_3), 2.17 (s, 12H, CH_3), 2.07 (s, 3H, CH_3), -23.79 (s, 2H, Ru-H). $^{13}C\{^1H\}$ (C_6D_6, 293 K): δ 205 (s, Ru-*C*O), 197.0 (s, Ru-*C*), 137.8 (s, N-*C*), 136.7 (s), 136.5 (s), 136.2 (s), 128.9 (s), 121.1 (s), 63.7 (s, OCH_3), 21.3 (s, CH_3), 18.7 (s, CH_3), 18.6 (s, CH_3). IR (cm^{-1}): 1858 (ν_{CO}).

7.5.5. Ru(IMes)$_2$(CO)(*p*-EtO-C$_6$H$_4$OH)H$_2$ (42)

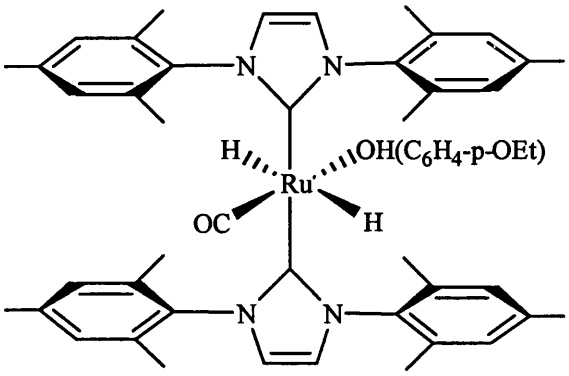

An ampoule fitted with a Teflon stopcock containing a solution of (**9**) (0.50 g, 0.47 mmol) in 20 ml toluene and 3 equivalents of IMes (0.43 g, 1.51 mmol) was heated at 75°C for 4 days, during which time the solution turned deep red. The mixture was cooled to room temperature and 1 equivalent of HOC_6H_4-*p*-OEt (0.07 g, 0.48 mmol) added. The mixture was stirred for 1 hr and then evaporated to dryness before addition of 10 ml of hexane. The compound crystallizes from cold solution of hexane as a yellow microcrystalline solid. Yield 0.31 g, 75%. Analysis for $RuC_{51}H_{60}N_4O_3$ [found (calculated)]: C, 70.4 (69.76); H, 6.80 (6.88); N, 5.52 (6.38). ^1H NMR (C_6D_6, 400 MHz, 293 K): δ 6.84 (br s, 4H, $C_6H_2Me_3$), 6.81 (br s, 4H, $C_6H_2Me_3$), 6.66 (br s, 2H, C_6H_4), 6.44 (br s, 2H, C_6H_4), 6.14 (s, 4H, CNC*H*=C*H*N), 3.90 (br s, 2H, OCH_2), 2.36 (s, 12H, CH_3), 1.93 (s, 12H, CH_3), 1.90 (s, 3H, CH_3), 1.31 (br s, 3H, OCH_2CH_3), -24.48 (s, 1H, Ru-H). $^{13}C\{^1H\}$ (C_6D_6, 293 K): δ 205.5 (s, Ru-*C*O), 194.9 (s, Ru-*C*), 137.8 (s, N-*C*), 137.4 (s), 136.9 (s), 136.2 (s), 129.5 (s), 129.4 (s), 121.9 (s), 116.0 (s), 64.0 (br s, OCH_2), 21.6 (s, CH_3), 18.9 (s, CH_3), 15.5 (s, OCH_2CH_3). IR (cm^{-1}): 1881 (ν_{CO}).

7.5.6. $Ru(IMes)_2(CO)(H_2S)H_2$ (43)

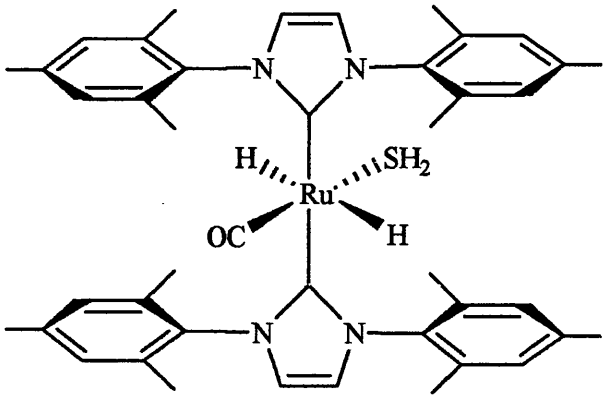

An ampoule fitted with a Teflon stopcock containing a solution of **(39)** (0.50 g, 0.64 mmol) in 5 ml toluene was freeze/pump/thaw degassed. To the mixture was admitted one atmosphere of H_2S and the mixture stirred for 2 min, during which precipitated an orange/yellow solid. The solution was then evaporated to dryness under vacuum. The ampoule was left pumping overnight to remove remaining traces of H_2S. The dry residue was then dissolved in a minimum amount of toluene and layered with hexane. The compound crystallizes as orange crystals. Yield 0.39 g, 79%. Analysis for $RuC_{43}H_{52}N_4OS.0.25C_6H_6$ [found (calculated)]: C, 67.4 (67.36); H, 6.49 (6.80); N, 7.06 (7.06). ^1H NMR (C_6D_6, 400 MHz, 293 K): δ 6.80 (br s, 4H, $C_6H_2Me_3$), 6.77 (br s, 4H, $C_6H_2Me_3$), 6.20 (s, 4H, CNC*H*=C*H*N), 2.32 (s, 12H, CH_3), 2.16 (s, 12H, CH_3), 2.08 (s, 12H, CH_3), -0.58 (s, 2H, SH_2), -24.47 (s, 2H, Ru-H). $^{13}C\{^1H\}$ (C_6D_6, 293 K): δ 202.6 (s, Ru-*C*O), 197.3 (s, C1), 137.6 (s, C3), 136.8 (s, C6), 136.0 (s, C4 or 4'), 135.7 (s, C4 or 4'), 121.8 (s), 21.2 (s, C8), 19.3 (s, C7 or C7'), 19.2 (s, CH_3, C7 or C7'). IR (cm^{-1}): 1879 (ν_{CO}).

7.5.7. $Ru(IMes)_2(CO)(HSCH_2CH_2CH_3)H_2$ (44)

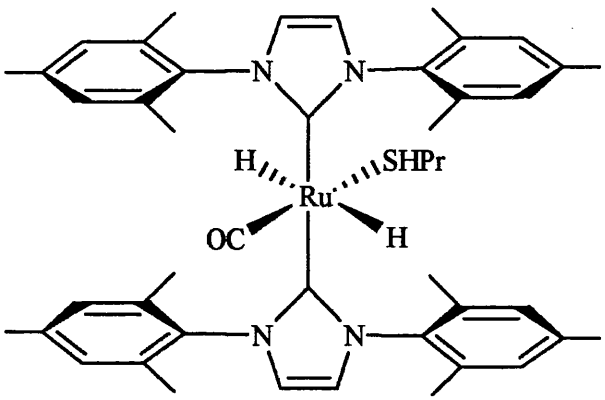

Two equivalents of 1-propanethiol (60 μl, 0.76 mmol) were added to a toluene

Removal of the solvent afforded a darkly coloured residue, which was dissolved in a minimum amount of toluene and layered with hexane to afford deep red crystals of **5** (Yield = 0.13 g, 40%). The mother liquor was evaporated to dryness and washed with 2 x 5 ml of hexane at -60°C and the precipitate dried *in vacuo* for 12h. An additional crop of material was isolated as a microcystalline orange solid (0.14 g, 43%). Analysis for $RuC_{46}H_{58}N_4OS$ [found (calculated)]: C, 68.0 (67.70); H, 6.77 (7.16); N, (6.86). ^1H NMR (C_6D_6, 400 MHz, 293 K): δ 6.81 (br s, 4H, $C_6H_2Me_3$), 6.77 (br s, 4H, $C_6H_2Me_3$), 6.25 (s, 4H, NC*H*=C*H*N), 2.38 (t, 2H, J_{HH} = 7.2 Hz, SCH_2), 2.32 (s, 12H, CH_3), 2.12 (br m, 24H, CH_3), 1.60 (m, J_{HH} = 7.2 Hz, 2H, CH_2), 1.04 (t, J_{HH} = 7.2 Hz, 3H, CH_2CH_3), -23.77 (s, 2H, Ru-H). $^{13}C\{^1H\}$ (C_6D_6, 293 K): δ 203.1 (s, Ru-*C*O), 197.5 (s, Ru-*C*), 137.1 (s, N-*C*), 136.6 (s, *C*-*p*-CH_3), 136.2 (s, *C*-*o*-CH_3), 129.5 (s, *m*-*C*H), 122.3 (s, N*C*H=*C*HN), 38.7 (s, SCH_2), 30.1 (s, SCH_2CH_2), 21.9 (s, *p*-*C*H_3), 20.2 (br s, *o*-*C*H_3), 15.2 (s, $SCH_2CH_2CH_3$). IR (cm^{-1}): 1883 (ν_{CO}).

7.5.8. $Ru(IMes)_2(CO)(HF)H_2$ (45)

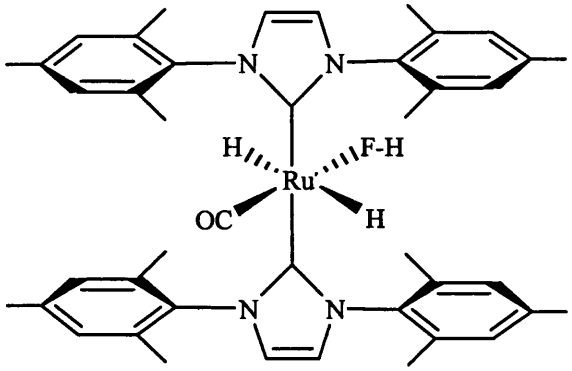

Two equivalents of C_6F_6 (0.238 µl, 1.28 mmol) were added to a toluene solution (5 ml) of **(39)** (0.50 g, 0.64 mmol) and the resulting solution stirred for 2 hr at room temperature, during which the solution turned deep orange. The solution was concentrated under vacuum to 2 ml and layered with 10 ml of hexane to afford deep orange crystals of compound. Yield 0.47 g (96%). Analysis for $RuC_{43}H_{51}N_4OF$ [found (calculated)]: C, 67.9 (67.95); H, 6.40 (6.76); N, 7.33 (7.37). ^1H NMR (C_6D_6, 400 MHz, 293 K): δ 6.81 (br s, 4H, $C_6H_2Me_3$), 6.75 (br s, 4H, $C_6H_2Me_3$), 6.17 (s, 4H, CNC*H*=C*H*N), 2.35 (s, 12H, CH_3), 2.01 (s, 12H, CH_3), -24.63 (s, 2H, Ru-H). ^{19}F NMR (C_6D_6, 400 MHz, 293 K): -208.49 (br s, F-H). $^{13}C\{^1H\}$ (C_6D_6, 293 K): δ 206.0 (d, J_{C-F} = 77.5 Hz, Ru-*C*O), 196.3 (d, J = 6.1Hz, Ru-*C*), 137.7 (s, N-*C*), 137.3 (s), 137.2 (s), 136.8 (s), 134.5 (s), 129.2 (s) 129.1 (s), 121.5

Ru-*C*), 137.7 (s, N-*C*), 137.3 (s), 137.2 (s), 136.8 (s), 134.5 (s), 129.2 (s) 129.1 (s), 121.5 (s), 21.9 (s, CH_3), 18.9 (d, J = 4.2 Hz, CH_3), 18.7 (d, J = 5.0 Hz, CH_3). IR (cm^{-1}): 1873 (ν_{CO}).

7.5.9. $Ru(IMes)_2(CO)(HCl)H_2$ (46)

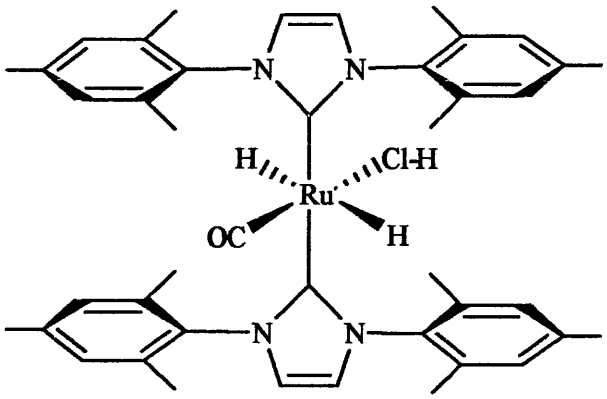

Two equivalents of C_6Cl_6 (0.36 g, 1.28 mmol) were added to a toluene solution (5 ml) of **(39)** (0.50 g, 0.64 mmol) and the resulting solution stirred for 1 week at 50°C, during which the solution turned deep orange. The solution was concentrated under vacuo to 2 ml, and layered with 10 ml of hexane to afford red crystals. Yield 0.44 g (89%). ^1H NMR (C_6D_6, 400 MHz, 293 K): δ 6.81 (br s, 4H, $C_6H_2Me_3$), 6.77 (br s, 4H, $C_6H_2Me_3$), 6.20 (s, 4H, CNC*H*=C*H*N), 2.33 (s, 12H, CH_3), 2.16 (s, 12H, CH_3), 2.05 (br s, 12H, CH_3), -25.33 (s, 2H, Ru-H). $^{13}C\{^1H\}$ (C_6D_6, 293 K): δ 202.4 (s, Ru-*C*O), 195.5 (s, Ru-*C*), 137.7 (s, N-*C*), 137.3 (s), 136.5 (brs), 134.5 (s), 129.4 (s) 129.3 (s), 122.0 (s), 21.7 (s, CH_3), 19.3 (s, CH_3), 19.2 (s, CH_3). IR (cm^{-1}): 1882 (ν_{CO}).

7.5.10. $Ru(IMes)_2(CO)_2H_2$ (47)

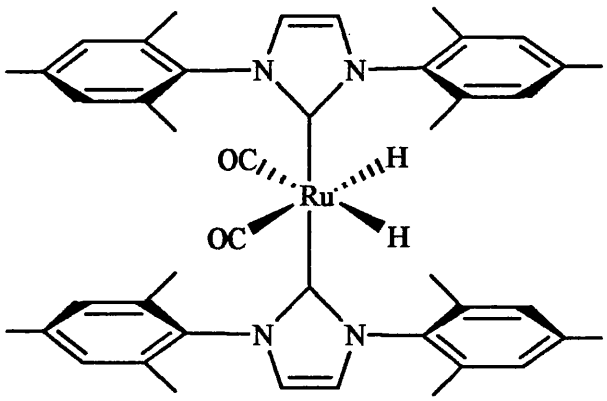

A toluene (2 ml) solution of **(39)** (0.20 g, 0.25 mmol) was stirred at 90°C for 2 weeks. The solution was then pumped to dryness and 1 ml of hexane was added. Stirring

for 1 hr gave a creamy white precipitate. The precipitation could be reinforced by cooling the mixture to -50°C. The precipitate was filtered off, washed twice with 1 ml of cold hexane and dried *in vacuo*. (NB: the compound is moderately soluble in hexane). Yield 0.13 g, 67%. Analysis for $RuC_{44}H_{50}N_4O_2$ [found (calculated)]: C, 68.5 (68.81); H, 6.28 (6.56); N, 7.20 (7.29). ^1H NMR (C_6D_6, 400 MHz, 293 K): δ 6.82 (s, 8H, $C_6H_2Me_3$), 6.12 (s, 4H, CNCH=CHN), 2.21 (s, 12H, CH_3), 2.02 (s, 24H, CH_3), -6.53 (s, 2H, Ru-H). $^{13}C\{^1H\}$ (C_6D_6, 293 K): δ 204.3 (s, Ru-CO), 192.5 (s, Ru-C), 139.6 (s, N-C), 137.3 (s), 136.3 (s), 134.1 (s), 128.9 (s), 121.0 (s) 21.2 (s, CH_3), 18.6 (s, CH_3). IR (cm^{-1}): 1974 (ν_{CO}), 1938 (ν_{CO}).

7.5.11. $Ru(IMes)_2(CO)_2(OH)H$ (48)

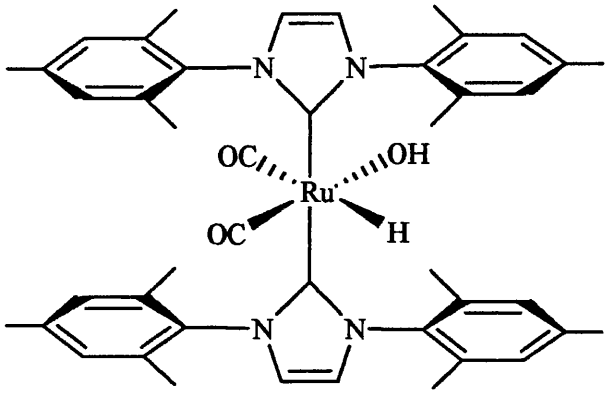

A toluene solution (5 ml) of **(40)** (0.20 g, 0.26 mmol) was stirred under 1 atm of carbon monoxide for 30 min, during which time the colour changed from pale orange to colourless. The solution was concentrated (3 ml) and layered with hexane (10 ml). Colourless crystals were isolated from the hexane solution during the next two days. These were filtered off, washed with 2 x 10 ml hexane and dried *in vacuo*. Yield 0.20 g, 95%. Analysis for $RuC_{44}H_{50}N_4O_3$ [found (calculated)]: C, 67.4 (67.41); H, 6.36 (6.43); N, 7.03 (7.14). ^1H NMR (C_6D_6, 400 MHz, 293 K): δ 6.75 (br s, 4H, $C_6H_2Me_3$), 6.74 (br s, 4H, $C_6H_2Me_3$), 6.08 (s, 4H, CNC*H*=C*H*N), 2.19 (s, 24H, CH_3), 2.07 (s, 12H, CH_3), -3.75 (br s, 1H, OH), -4.27 (s, 1H, Ru-H). $^{13}C\{^1H\}$ (C_6D_6, 293 K): δ 204.2 (s, Ru-*C*O), 188.9 (s, Ru-*C*O), 184.8 (s, Ru-*C*), 139.7 (s, N-*C*), 137.8 (s), 137.1 (s), 137.0 (s), 129.6 (s), 129.3 (s), 122.7 (s), 21.6 (s, CH_3), 19.0 (s, CH_3), 18.8 (s, CH_3). IR (cm^{-1}): 3426 (ν_{OH}), 2019 (ν_{CO}), 1880 (ν_{CO}), 1924 (ν_{Ru-H}).

7.5.12. $Ru(IMes)_2(CO)_2(SH)H$ (49)

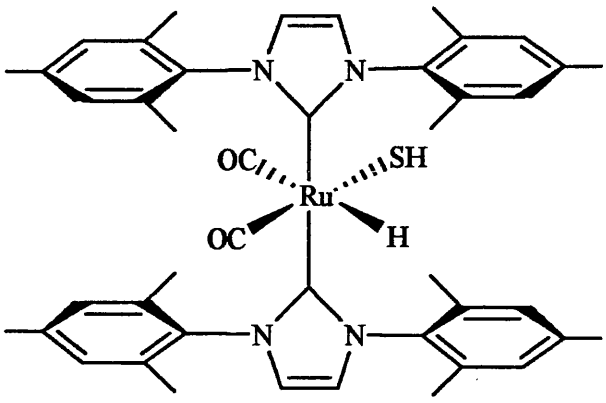

A toluene solution (5 ml) of **(43)** (0.20 g, 0.26 mmol) was stirred under 1 atm of carbon monoxide for 30 min, during which time the colour changed from pale orange to off-yellow. The solution was concentrated (3 ml) and layered with hexane (10 ml). Off-yellow crystals were isolated from the hexane solution during the next few days. These were filtered off, washed with 2 x 10 ml hexane and dried *in vacuo*. Yield 0.19 g, 91%. Analysis for $RuC_{44}H_{50}N_4O_2S_1$ [found (calculated)]: C, 65.7 (66.05); H, 6.17 (6.29); N, 6.86 (7.00). ^1H NMR (C_6D_6, 400 MHz, 293 K): δ 6.72 (br s, 4H, $C_6H_2Me_3$), 6.70 (br s, 4H, $C_6H_2Me_3$), 6.06 (s, 4H, CNC*H*=C*H*N), 2.20 (s, 12H, CH_3), 2.13 (s, 24H, CH_3), -3.15 (br s, 1H, SH), -4.82 (br s, 1H, Ru-H). $^{13}C\{^1H\}$ (C_6D_6, 293 K): δ 203.1 (s, Ru-*C*O), 197.4 (s, Ru-*C*O), 185.8 (s, C1), 139.12 (s, C3), 137.2 (s, C7), 136.4 (s, C4 or C4'), 136.3 (s, C4 or C4'), 129.4 (s, C5 or C5'), 129.3 (s, C5 or C5'), 122.8 (s, C2), 21.2 (s, C8), 19.0 (s, C7, C7'). IR (cm^{-1}): 2023, 1892 (νCO) and 1931 (νRu-H).

7.5.13. $Ru(IMes)_2(CO)(SH)_2$ (50)

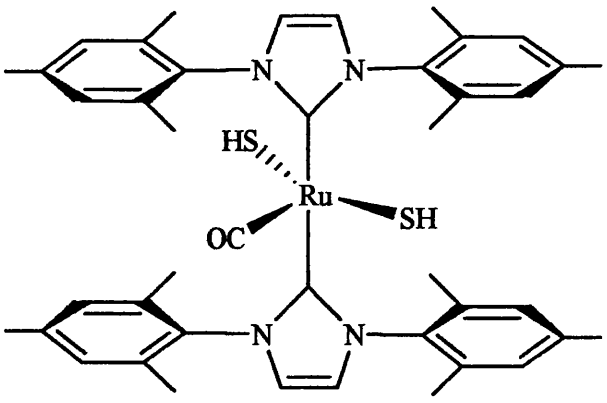

An ampoule fitted with a Teflon stopcock containing a solution of **(39)** (0.50 g, 0.64 mmol) in 5 ml toluene was freeze/pump/thaw degassed. To the mixture was admitted

of the mixture turned to purple. The solution was then evaporated to dryness under vacuo, and was left pumping overnight in order to remove any remaining traces of H_2S. The dry residue was then dissolved in a minimum amount of toluene and layered with hexane. The compound crystallizes as dark purple crystals. Yield 0.43 g, 84%. Analysis for $RuC_{43}H_{50}N_4O_1S_2$ [found (calculated)]: C, 64.0 (64.23); H, 6.14 (6.27); N, 6.79 (6.96). ^1H NMR (C_6D_6, 400 MHz, 293 K): δ 6.61 (v br s, 8H, $C_6H_2Me_3$), 5.99 (s, 4H, CNC*H*=C*H*N), 2.25 (vbr s, 48H, CH_3), -1.003 (s, 2H, SH). $^{13}C\{^1H\}$ (C_6D_6, 293 K): δ 202.8 (s, Ru-*C*O), 192.7 (s, C1), 137.6 (s, C3), 136.8 (br s, C6, C4, C4'), 124.18 (s, C2), 21.1 (s, C8), 19.8 (br s, C7, C7'), 19.2 (s, CH_3, C7 or C7'). IR (cm^{-1}): 1925 (ν_{CO}).

7.5.14. Ru(IMes)$_2$(CO)$_2$(SH)$_2$ (51)

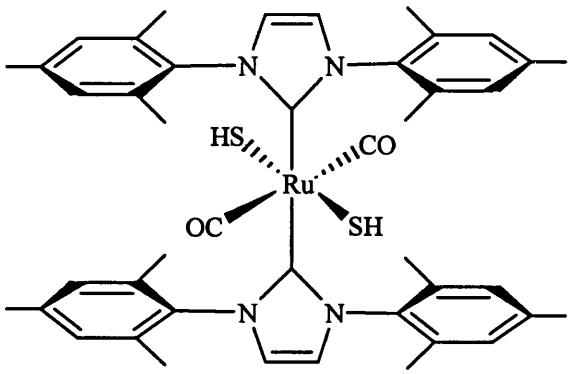

A toluene solution (5 mL) of **(50)** (0.20 g, 0.25 mmol) was stirred under 1 atm of carbon monoxide for 30 min, during which time the colour changed from purple to off-yellow and an off-white material precipitated. The solution was concentrated under a flow of CO; 10 ml of CO-saturated hexane were added to the mixture to enforce precipitation of the material. Off-yellow crystals could be grown by layering a toluene solution of **(51)** with hexane. (The crystallisation procedure was done under CO atmosphere). These were filtered off, washed with 2 x 10 ml hexane and dried under a stream of CO. Yield 0.18 g, 86 %. Attempts at CHN analysis repeatedly afforded low values, presumably due to the facile loss of CO from the product. Analysis for $RuC_{44}H_{50}N_4O_2S_2$ were not achieved due to the decomposition of the complex at high temperatures. ^1H NMR (C_6D_6, 400 MHz, 293 K): δ 6.68 (br s, 8H, $C_6H_2Me_3$), 6.02 (s, 4H, CNC*H*=C*H*N), 2.37 (s, 24H, CH_3), 2.21 (s, 12H, CH_3), -3.59 (br s, 2H, SH). $^{13}C\{^1H\}$ (C_6D_6, 293 K): δ 199.4 (s, Ru-*C*O), 183.7 (s, C1), 141.0 (s, C3), 139.0 (s, C4 or C4'), 138.5 (s, C4 or C4'), 137.6 (s, C7), 129.3 (s, C5 or C5'), 128.5 (s, C5, C5'), 124.6 (s, C2), 21.1 (s, C7, C7'), 19.5 (s, C8). IR (cm^{-1}): 1978 (ν_{CO}).

(ν_{CO}).

7.5.15. $Ru(IMes)_2(CO)_2(SCH_2CH_2CH_3)H$ (52)

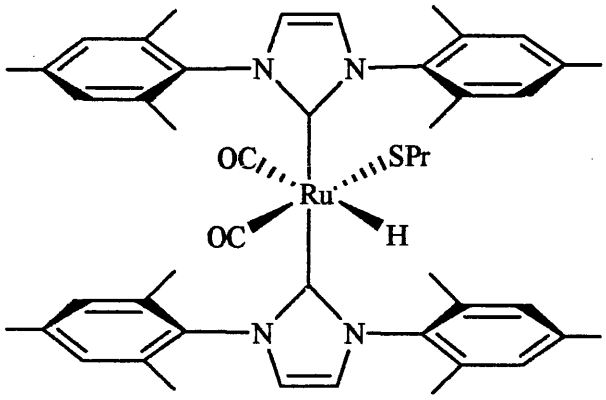

A hexane solution (5 ml) of **(44)** (0.10 g, 0.12 mmol) was stirred under 1 atm of CO for 30 min, during which time the colour changed from pale orange to colourless followed by precipitation of a white powder. The solvent was removed via cannula and the precipitate washed with 2 x 5 ml of cold hexane. The solid was then dissolved in a minimum amount of toluene and layered with hexane (10 ml). Colourless crystals were isolated by filtration, washed with hexane (2 x 10 ml) and dried *in vacuo*. Yield 0.10 g, 95%. Analysis for $RuC_{47}H_{56}N_4O_2S$ [found (calculated)]: C, 67.2 (67.03); H, 6.59 (6.70); N, 6.75 (6.65). ^1H NMR (C_6D_6, 400 MHz, 293 K): δ 7.15 (br s, 8H, $C_6H_2Me_3$), 6.44 (s, 4H, CNC*H*=C*H*N), 2.56 (s, 12H, CH_3), 2.55 (t, 2H, J_{HH} = 7.6 Hz, SCH_2), 2.53 (s, 12H, CH_3), 2.51 (s, 12H, CH_3), 2.26 (sex, J_{HH} = 7.6 Hz, 2H, CH_2), 1.57 (t, J_{HH} = 7.6 Hz, 3H, CH_2CH_3), -4.47 (s, 1H, Ru-H). $^{13}C\{^1H\}$ (C_6D_6, 293 K): δ 202.9 (s, Ru-*C*O), 199.0 (s, Ru-*C*O), 186.6 (s, Ru-*C*), 139.6 (s, N-*C*), 137.6 (s), 137.2 (s), 136.7 (s), 129.7 (s), 129.5 (s), 123.3 (s), 38.9 (s, SCH_2), 30.4 (s, CH_2), 21.8 (s, CH_3), 16.8 (s, CH_3), 16.5 (s, CH_3), 16.1 (s, CH_3). IR (cm^{-1}): 2014 (ν_{CO}), 1946 (ν_{Ru-H}), 1896 (ν_{CO}).

7.5.16. $Ru(IMes)_2(CO)_2(F)H$ (53)

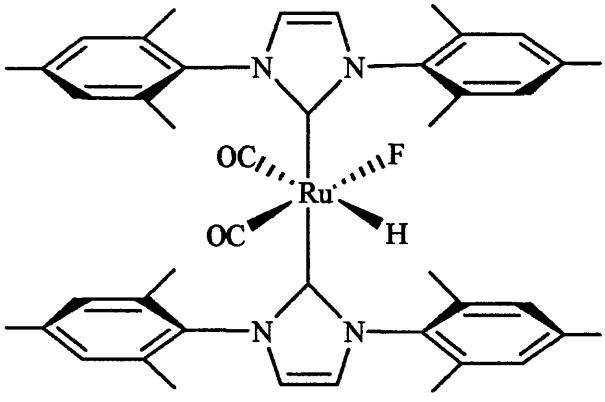

CO for 30 min, during which time the colour changed from pale orange to colourless followed by precipitation of a white powder. The solvent was removed via cannula, and the precipitate washed with 2 x 5 ml of cold hexane. The solid was then dissolved in a minimum amount of toluene and layered with hexane (10 ml). Colourless crystals were isolated by filtration, washed with hexane (2 x 10 ml) and dried *in vacuo*. Yield 0.19 g, 91%. ^{1}H NMR (C_6D_6, 400 MHz, 293 K): δ 6.75 (br s, 4H, $C_6H_2Me_3$), 6.72 (br s, 4H, $C_6H_2Me_3$), 6.07 (s, 4H, CNC*H*=C*H*N), 2.22 (s, 12H, CH_3), 2.16 (s, 12H, CH_3), 2.09 (s, 12H, CH_3), -3.80 (dd, J_{13C-H} = 46.4 Hz, J_{F-H} = 6.4 Hz, 1H, Ru-H). ^{19}F NMR (C_6D_6, 400 MHz, 293 K): -379.50 (s, F-H). ^{13}C{^{1}H} (C_6D_6, 293 K): δ 205.0 (s, Ru-*C*O), 193.6 (s, Ru-*C*O), 187.8 (s, Ru-*C*), 139.5 (s, N-*C*), 137.7 (s), 137.4 (s), 136.8 (s), 129.4 (s), 122.7 (s), 21.8 (s, CH_3), 19.0 (s, CH_3), 18.9 (s, CH_3), 18.8 (s, CH_3), 18.7 (s, CH_3). IR (^{13}CO labelled) (cm^{-1}): 1991 (ν_{CO}), 1930 (ν_{Ru-H}), 1880 (ν_{CO}).

7.5.17. Ru(IMes)$_2$(CO)(κ^2-O$_2$COH)H (54)

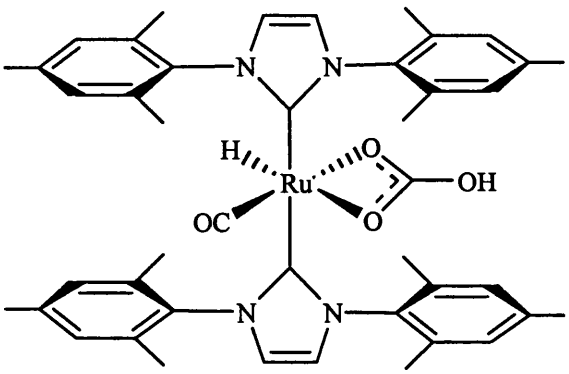

A toluene solution (5 ml) of **(40)** (0.10 g, 0.13 mmol) was stirred under 1 atm of carbon dioxide for 1 hr, during which the colour changed from yellow to colourless. The solvent was removed under vacuo and hexane (5 ml) was added. The resultant suspension was stirred at 0°C to enforce precipitation of an off-white powder. This was filtered, washed with cold hexane (2 x 5 ml), and dried under vacuo. Yield 0.08 g, 78%. Analysis for $RuC_{44}H_{50}N_4O_4$ [found (calculated)]: C, 66.3 (66.06); H, 6.39 (6.30); N, 7.01 (7.00). ^{1}H NMR (C_6D_6, 400 MHz, 293 K): δ 8.80 (br s, 1H, C-O*H*), 6.88 (br s, 4H, $C_6H_2Me_3$), 6.86 (br s, 4H, $C_6H_2Me_3$), 6.19 (s, 4H, CNC*H*=C*H*N), 2.34 (s, 12H, CH_3), 2.14 (s, 12H, CH_3), 2.08 (s, 3H, CH_3), -20.73 (s, 1H, Ru-H). ^{13}C{^{1}H} (C_6D_6, 293 K): δ 207.4 (s, Ru-*C*O), 194.0 (s, Ru-*C*), 160.3 (s, *C*-OH), 138.3 (s, N-*C*), 137.2 (s), 137.0 (s), 136.5 (s), 129.3 (s), 129.2 (s), 122.4 (s), 22.0 (s, CH_3), 19.3 (s, CH_3), 19.1 (s, CH_3). IR (cm^{-1}): 3416 (ν_{OH}), 1885 (ν_{CO}), 1593 (ν_{OCO}), 1453 (ν_{OCO}).

(s), 122.4 (s), 22.0 (s, CH_3), 19.3 (s, CH_3), 19.1 (s, CH_3). IR (cm^{-1}): 3416 (ν_{OH}), 1885 (ν_{CO}), 1593 (ν_{OCO}), 1453 (ν_{OCO}).

7.5.18. Ru(IMes)$_2$(CO)(κ^2-O$_2$COEt)H (55)

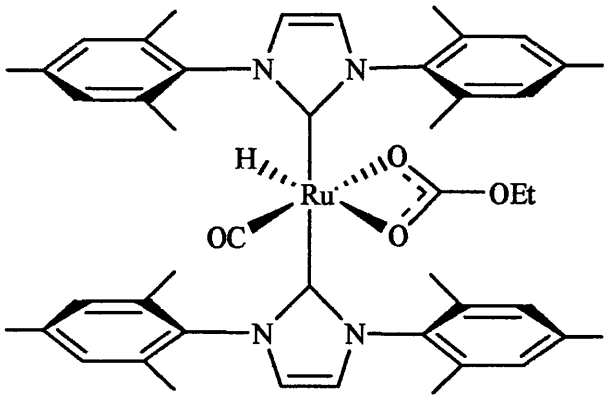

A toluene solution (5 ml) of **(39)** (0.10 g, 0.13 mmol) was stirred under 1 atm of carbon dioxide for 1 hr, during which the colour changed from yellow to colourless. The solvent was removed under vacuo and hexane (5 ml) was added. The resultant suspension was stirred at -40°C to enforce precipitation of an off-white powder. This was filtered, washed with cold hexane (2 x 5 ml), and dried under vacuo. Yield 0.08 g, 76%. ^{1}H NMR (C_6D_6, 400 MHz, 293 K): δ 6.84 (br s, 4H, $C_6H_2Me_3$), 6.80 (br s, 4H, $C_6H_2Me_3$), 6.13 (s, 4H, CNC*H*=C*H*N), 3.56 (dq, $J_{H\text{-}H}$ = 6.8 Hz, $J_{H\text{-}13C}$ = 2.4 Hz, 2H, $CH_2O^{13}CO_2$), 2.27 (s, 12H, CH_3), 2.09 (s, 12H, CH_3), 2.05 (s, 3H, CH_3), 1.12 (t, J_{HH} = 6.8 Hz, 3H, OCH_2-*CH_3*), -18.80 (s, 1H, Ru-H). ^{13}C{^{1}H} (C_6D_6, 293 K): δ 208.1 (s, Ru-*C*O), 194.1 (s, Ru-*C*), 158.7 (s, ^{13}*C*-O-Et), 138.7 (s, N-*C*), 137.4 (s), 137.1 (s), 136.2 (s), 129.3 (s), 129.0 (s), 122.4 (s), 60.6 (d, $J_{13C\text{-}C}$ = 1.3 Hz, $O_2{}^{13}$C-O-*CH_2*), 21.8 (s, CH_3), 19.2 (s, CH_3), 19.1 (s, CH_3), 15.9 (d, $J_{13C\text{-}C}$ = 2.7 Hz, OCH_2-*CH_3*). IR (cm^{-1}): 2096 (ν_H), 1884 (ν_{CO}), 1604 (ν_{OCO}), 1462 (ν_{OCO}).

7.5.19. Ru(IMes)$_2$(CO)(κ^2-O$_2$CC$_5$H$_4$N)H (56)

evaporated to dryness and the residue dissolved in a minimum amount of hexane. Slow concentration of the hexane solution afforded orange crystals (0.08 g) over two days. The remaining solution was cooled down to -60°C to enforce precipitation and yielded an additional 0.08 g as an orange powder. Yield 83%. Multiple attempts to record CHN analysis for $RuC_{49}H_{53}N_5O_3$ consistently gave unacceptably high %C and %N content. ^1H NMR (C_6D_6, 400 MHz, 293 K): δ 8.70 (d, J_{HH} = 5.6 Hz, 2H, C_5H_4N), 7.44 (d, J_{HH} = 5.6 Hz, 2H, C_5H_4N), 6.87 (br s, 4H, $C_6H_2Me_3$), 6.68 (br s, 4H, $C_6H_2Me_3$), 6.11 (s, 4H, NC*H*=C*H*N), 2.28 (s, 12H, CH_3), 2.03 (s, 12H, CH_3), 1.88 (s, 12H, CH_3), -18.49 (s, 1H, Ru-H). $^{13}C\{^1H\}$ (C_6D_6, 293 K): δ 208.0 (s, Ru-*C*O), 193.0 (s, Ru-*C*), 172.3 (s, -O*C*O), 149.5 (s, C_5H_4N), 141.7 (s, C_5H_4N), 138.3 (s, N-*C*), 136.9 (s, *C*-*o*-CH_3), 136.7 (s, *C*-*o*-CH_3), 136.6 (s, *C*-*p*-CH_3), 129.0 (s, *m*-*C*H), 128.8 (s, *m*-*C*H), 123.5 (s, C_5H_4N), 122.0 (s, NCH=*C*HN), 21.2 (s, *p*-CH_3), 18.6 (s, *o*-CH_3), 18.4 (s, *o*-CH_3). IR (cm^{-1}): 1886 (ν_{CO}), 1596 (ν_{OCO}), 1461 (ν_{OCO}).

7.5.20. Ru(IMes)$_2$(CO)$_2$(OC(O)OH)H (57)

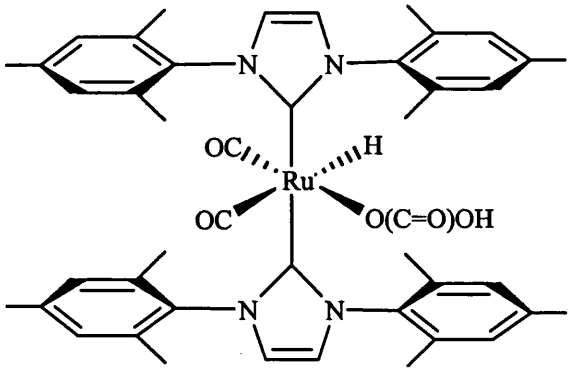

A toluene solution (5 ml) of **(48)** (0.20 g, 0.25 mmol) was stirred under 1 atm of carbon dioxide for 1 hr at room temperature. The solution was then concentrated (3 ml) and layered with hexane (10 ml). Colourless crystals were isolated from the hexane solution over the following two days. These were isolated, washed with 2 x 10 ml hexane and dried *in vacuo*. Yield 0.18 g, 86%. Analysis for $RuC_{45}H_{50}N_4O_5$ [found (calculated)]: C, 65.9 (65.28); H, 6.21 (6.09); N, 6.23 (6.77). ^1H NMR (C_6D_6, 400 MHz, 293 K): δ 12.10 (br s, 1H, OH), 6.87 (s, 8H, $C_6H_2Me_3$), 6.84 (s, 8H, $C_6H_2Me_3$), 6.09 (s, 4H, CNC*H*=C*H*N), 2.27 (s, 12H, CH_3), 2.18 (s, 12H, CH_3), 2.14 (s, 12H, CH_3), -4.30 (s, 1H, Ru-H). $^{13}C\{^1H\}$ (C_6D_6, 293 K): δ 206.2 (s, Ru-*C*O), 194.8 (s, Ru-*C*O), 185.0 (s, Ru-*C*), 162.8 (s, O*C*(O)OH), 138.7 (s, N-*C*), 137.3 (s), 136.7 (s), 136.5 (s), 129.3 (s), 129.2 (s), 122.9 (s), 21.6 (s, CH_3), 18.6 (s, CH_3), 18.5 (s, CH_3). IR (cm^{-1}): 2041 (ν_{CO}), 1965 (ν_{RuH}), 1916 (ν_{CO}), 1605 (ν_{OCO}), 1355 (ν_{OCO}).

and layered with hexane (10 ml). Colourless crystals were isolated from the hexane solution over the following two days. These were isolated, washed with 2 x 10 ml hexane and dried *in vacuo*. Yield 0.18 g, 86%. Analysis for $RuC_{45}H_{50}N_4O_5$ [found (calculated)]: C, 65.9 (65.28); H, 6.21 (6.09); N, 6.23 (6.77). ^{1}H NMR (C_6D_6, 400 MHz, 293 K): δ 12.10 (br s, 1H, OH), 6.87 (s, 8H, $C_6H_2Me_3$), 6.84 (s, 8H, $C_6H_2Me_3$), 6.09 (s, 4H, CNC*H*=C*H*N), 2.27 (s, 12H, CH_3), 2.18 (s, 12H, CH_3), 2.14 (s, 12H, CH_3), -4.30 (s, 1H, Ru-H). $^{13}C\{^1H\}$ (C_6D_6, 293 K): δ 206.2 (s, Ru-*C*O), 194.8 (s, Ru-*C*O), 185.0 (s, Ru-*C*), 162.8 (s, O*C*(O)OH), 138.7 (s, N-*C*), 137.3 (s), 136.7 (s), 136.5 (s), 129.3 (s), 129.2 (s), 122.9 (s), 21.6 (s, CH_3), 18.6 (s, CH_3), 18.5 (s, CH_3). IR (cm^{-1}): 2041 (ν_{CO}), 1965 (ν_{RuH}), 1916 (ν_{CO}), 1605 (ν_{OCO}), 1355 (ν_{OCO}).

7.5.21. Ru(IMes)$_2$(CO)$_3$ (58)

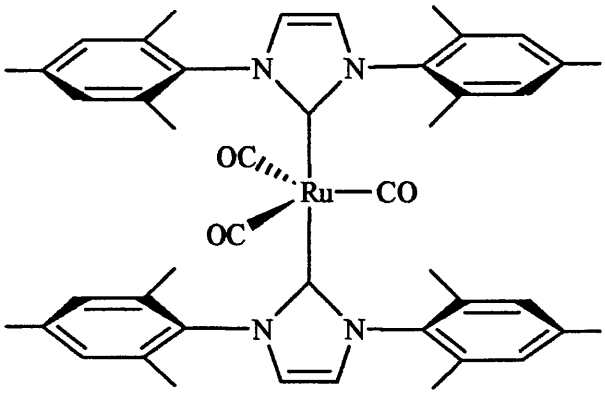

Introduction of one atmosphere of CO into a toluene solution (5 ml) of **(40)** (0.20 g, 0.26 mmol) gave a rapid colour change from pale orange to colourless. The solution was left to stir with CO for a total of 5 days, during which time the solution became deep orange. Removal of the solvent under vacuo afforded an orange residue. This was dissolved in a minimum amount of toluene and layered with hexane to yield **5** as orange crystals (0.20 g, 99%). Analysis for $RuC_{45}H_{48}N_4O_3$ [found (calculated)]: C, 68.7 (68.72); H, 5.09 (5.13); N, 7.06 (7.13). ^{1}H NMR (C_6D_6, 400 MHz, 293 K): δ 6.78 (s, 8H, $C_6H_2Me_3$), 6.10 (s, 4H, CNC*H*=C*H*N), 2.18 (s, 12H, CH_3), 2.05 (s, 24H, CH_3). $^{13}C\{^1H\}$ (C_6D_6, 293 K): δ 217.6 (s, Ru-*C*O), 186.8 (s, Ru-*C*), 138.9 (s, N-*C*), 137.9 (s), 137.1 (s), 129.5 (s), 123.4 (s), 21.6 (s, CH_3), 19.1 (s, CH_3). IR (cm^{-1}): 1950, 1879, 1830 (ν_{CO}).

7.5.22. Ru(IMes)$_2$(CO)(NH=C(CH$_3$)N=C(CH$_3$)O)H (59)

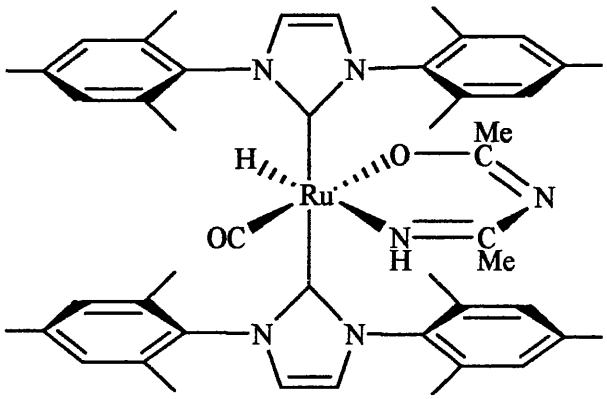

Acetonitrile (69 μL, 1.32 mmol) was added to a toluene solution (5 ml) of **(40)** (0.20 g, 0.26 mmol) and the mixture stirred for 6 days at room temperature. During this time the colour changed from pale orange to off-yellow. Removal of the solvent and addition of cold hexane gave **(59)** as a white microcrystalline solid. Crystals suitable for X-ray diffraction were isolated from a concentrated solution of toluene layered with hexane. Yield 0.20 g, 91%. Analysis for $RuC_{47}H_{56}N_6O_2$ [found (calculated)]: C, 67.2 (67.36); H, 6.97 (6.74); N, 9.38 (10.03). ^1H NMR (C_6D_6, 400 MHz, 293 K): δ 6.79 (s, 8H, $C_6H_2Me_3$), 6.08 (s, 4H, CNC*H*=C*H*N), 5.73 (s, 1H, NH), 2.27 (s, 6H, CH_3), 2.15 (s, 12H, CH_3), 2.03 (s, 12H, CH_3), 1.99 (s, 3H, N=CCH_3), 1.52 (s, 3H, N=CCH_3), -11.40 (s, 1H, Ru-H). $^{13}C\{^1H\}$ (C_6D_6, 293 K): δ 210.3 (s, Ru-*C*O), 191.4 (s, Ru-*C*), 173.8 (s, N=*C*CH_3), 166.0 (s, N=*C*CH_3), 139.0 (s, N-*C*), 136.6 (s), 136.1 (s), 128.9 (s), 128.8 (s), 122.2 (s), 31.6 (s, N=C*C*H_3), 28.2 (s, N=C*C*H_3), 21.4 (s, CH_3), 18.8 (s, CH_3), 18.7 (s, CH_3). IR (cm^{-1}): 1865 (ν_{CO}), 2016 (ν_{Ru-H}).

7.6. Experimental conditions for the study of candidates for the Murai reaction.

7.6.1. Probing of the reactivity of ruthenium complexes toward the Murai reaction.

Various precursors were synthesized and their reactivity probed for the Murai reaction. Typically an NMR tube fitted with a Youngs cap was charged with 0.01 mmol of catalyst precursor, 3.0 μl (0.04 mmol) of 2-methylacetophenone, 4.6 μl (0.04 mmol) of trimethylvinylsilane and 1 ml of d_6-benzene. The tube was then put in an oil bath at 100°C, unless otherwise stated. Both $^{31}P\{^1H\}$ and ^1H NMR spectra were recorded from t = 0, 15, 30, 60 and 120 min and then every 2 hr, up to two weeks in some cases. Activity of the catalyst was shown by **(a)** depletion of the $^{31}P\{^1H\}$ signal of the precursor and **(b)** growth of two new sets of signals in the ^1H spectrum for 2'-methyl-6'-[2-(triethoxysilyl)ethyl]acetophenone (δ = 2.6 and 0.94). The results for these measurements

are shown in **Table 7.1.**

Catalyst	Reaction	Murai Reaction
(1)	Y	**Y**
(10)	Y	**Y**
(4)	N	N
(3)	Y	**Y**
(2)	Y	**Y**
(8)	Y	N
(12)	Y	N
(6)	Y	**Y**
(7)	Y	**Y**
(13)	Y	**Y**
(14)	Y	**Y**
(15)	Y	**Y**
(17)	Y	**Y**
(21)	Y	**Y**
(20)	N	N
(22)	Y	**Y**
(26)	Y	**Y**

Table 7.1.

7.6.2. Catalytic activity of selected precursor under Murai conditions.

A 50 ml three necked round bottomed flask equipped with a magnetic stirring bar, argon inlet, outlet bubbler and reflux condenser was flame dried under vacuum and flushed with argon. It was then charged with complexes **(X) [table 7.2]** (0.04 mmol), 261 μL (2 mmol) of triethoxyvinylsilane, 420 μL (2 mmol) of 2'-methylacetophenone, 3 ml of toluene and 200 μL of dodecane as an internal reference. The reaction vessel was heated to

7.7. Experimental conditions for the NMR kinetic measurements.

Typically in an NMR tube fitted with a Youngs cap were added 35mgs (0.46 mmol) of **(21)** and 1 ml of d^8-toluene. The tube was sealed under an argon atmosphere, and the ^1H and the $^{31}P\{^1H\}$ NMR spectra of the mixture were recorded at room temperature. Then the tube was left aside while the NMR probe was warmed up to a set temperature (T(K) = 353, 358, 363, 368, 373), then the tube was quickly inserted and a ^1H NMR spectrum (10 ppm to -20 ppm) of the solution was recorded at a define time set.

7.8. Experimental conditions for the IR kinetic measurement.

The infrared catalytic experiments were all carried out using the same basic typical manipulation. All catalytic reactions employed a sample chamber, which was flushed constantly with a flow of nitrogen. In all cases the reactor contents were loaded inside of an inert atmosphere glove box under a nitrogen atmosphere and sealed before mounting in the reactor chamber. Background solvents were recorded by separate experiments taken at the temperature used in the catalytic experiment under nitrogen pressure. The reactor was always background / nitrogen purge tested before the experiment was continued. Spectra were measured every 32 seconds along the reaction, using a line resolution of 2 cm^{-1}.

Cell preparation:

Particular attention was made upon the preparation of the reaction solution under rigorous dry and degassed conditions. A flame dried ampoule was charged with 33.04 to 99.13 μmol of the inorganic ruthenium centred catalyst typically **(1)** which was then pumped dry for 30 minutes. Then 2 cm^{-3} of toluene was injected into the ampoule and the solution was freeze-pump-degassed. The ampoule was then loaded into a nitrogen-purged glovebox with 0.3 to 4 mmol of an aromatic ketone and an olefin. The infrared cell (CIR) was then filled via syringe and sealed.

Spectrometer preparation.

The CIR cell was then mounted in the spectrometer (N_2 purged) on a heating jacket linked to a temperature controller and ideally the cell was left standing there during one to

two hr prior to any experiment (to allow the spectrometer to be sufficiently purged from water and CO_2 interference). Then the infrared absorption spectrum of the solution was recorded using series software during 5 minutes prior to the beginning of the kinetic experiment. Finally the cell was heated to a known temperature and absorption spectrum of the solution was recorded time to time using the Nicolet Series software.

The Scanning was typically set up as the following:

Numbers of scans: 64 scs

Resolution: 2 cm^{-1}

Velocity of the Mirror: 1.2

Baseline: 1723.65-2128 cm^{-1}

Acquisition time: 3600 s to 72000 s.

7.10. References

1. **(a)** Ahmad, N.; Robinson, S. D.; Levinson, J. J.; Uttley, M. F. *Inorg. Synth.*, **1974**, *15*, 48. **(b)** Kakuichi, F.; Sekine, S; Tanaka, Y.; Kamatani, A.; Sonoda, M.; Chatani, S. Murai, *Bull. Chem. Soc. Jpn.*, 1995, **68**, 62. **(c)** Hallman, P. S., McGarvey, N.; Wilkinson, B. R. G. *J. Chem. Soc*, **1968**, 3143. **(d)** Ball, G.; Mann, B. E.; Brian, E. *J. Chem. Soc., Chem. Comm.*, **1992**, 561.
2. **(a)** Cenini, S.; Porta, F.; Pizzotti, M. *Inorg. Chim. Acta*, **1976**, *20*, 119. **(b)** Lee, C.-L.; Chisholm, J.; James, B. R.; Nelson, D. A.; Lilga, M. A. *Inorg. Chim. Acta*, **1986**, L7-L10.
3. Broxton, T. J.; Brunnett, J. F.; Park, C. H. *J. Org. Chem*, **1977**, *42*, 643.
4. Gaffney, T. R.; Ibers, J. A. *Inorg. Chem.*, **1982**, *21*, 2851.
5. Ahmad, N.; Robinson, S. D.; Levinson, J. J.; Uttley, M. F. *Inorg. Synth.*, **1974**, *15*, 50.
6. Hallman, P. S.; Stephenson, T. A.; Wilkinson, G. *Inorg. Synth.* **1970**, *12*, 237.
7. Van Der Sluys, L. S.; Kubas, G. J.; Caulton, K. G. *Organometallics*, **1991**, *10*, 1033.
8. Paulasaari, J. K.; Moiseeva, N.; Bau, R.; Weber, W. P. *J. Organomet. Chem.*, **1999**, *587*, 299.
9. Jung, C. W.; Garrou, P. E. *Organometallics*, **1982**, *1*, 658.

10. Harris, A. D.; Robinson, S. D. *Inorg. Chim. Acta*, **1980**, *42*, 25.

11. Kim, J-Y.; Jun, M-J. *Polyhedron*, **1996**, *15*, 3787.

12. Arduengo, A. J., III ; Krafczyk, R. ; Schmutzler, R. ; Craig, H. A. ; Goerlich, J. R. ; Marshall, W. J. ; Unverzagt, M. *Tetrahedron*, **1999**, *55*, 14523.